frontiers | Research Topics

Adenosine pathways in cancer immunity and immunotherapy

Edited by
Junjiang Fu, Ali Hafez El-Far, Luca Antonioli and Jamshid Hadjati

Published in
Frontiers in Immunology
Frontiers in Oncology

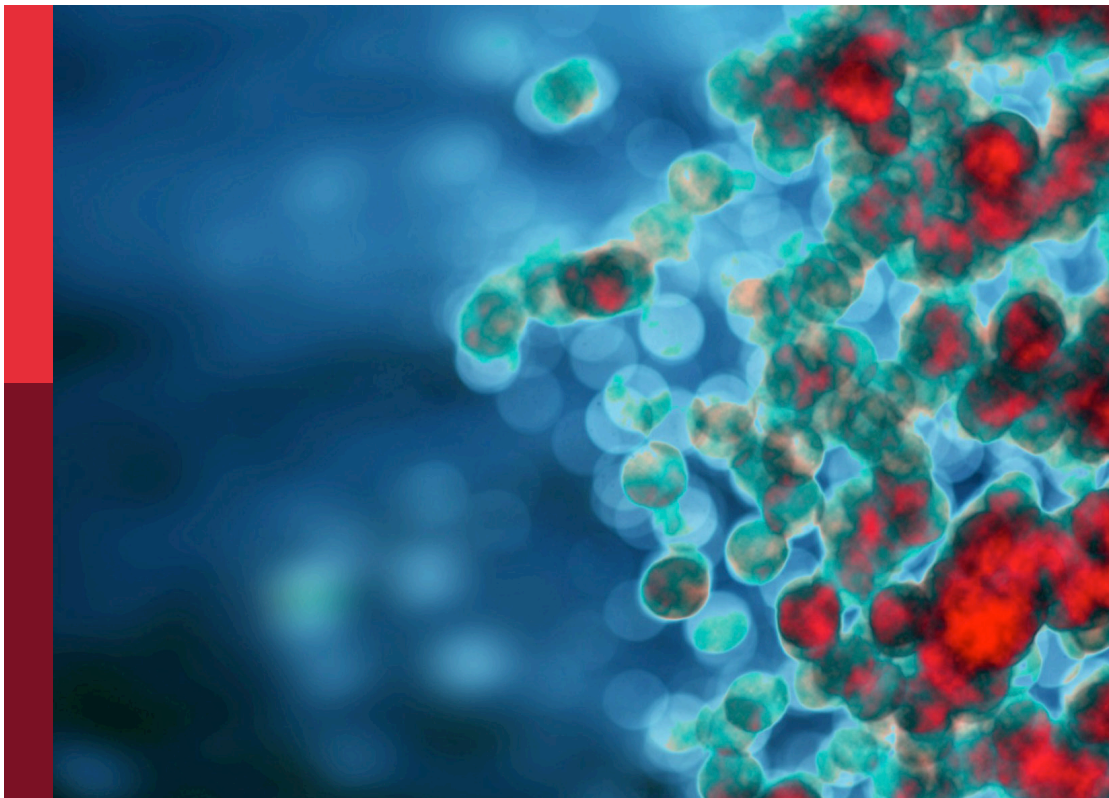

ISSN 1664-8714
ISBN 978-2-8325-3779-4
DOI 10.3389/978-2-8325-3779-4

About Frontiers

Frontiers is more than just an open access publisher of scholarly articles: it is a pioneering approach to the world of academia, radically improving the way scholarly research is managed. The grand vision of Frontiers is a world where all people have an equal opportunity to seek, share and generate knowledge. Frontiers provides immediate and permanent online open access to all its publications, but this alone is not enough to realize our grand goals.

Frontiers journal series

The Frontiers journal series is a multi-tier and interdisciplinary set of open-access, online journals, promising a paradigm shift from the current review, selection and dissemination processes in academic publishing. All Frontiers journals are driven by researchers for researchers; therefore, they constitute a service to the scholarly community. At the same time, the *Frontiers journal series* operates on a revolutionary invention, the tiered publishing system, initially addressing specific communities of scholars, and gradually climbing up to broader public understanding, thus serving the interests of the lay society, too.

Dedication to quality

Each Frontiers article is a landmark of the highest quality, thanks to genuinely collaborative interactions between authors and review editors, who include some of the world's best academicians. Research must be certified by peers before entering a stream of knowledge that may eventually reach the public - and shape society; therefore, Frontiers only applies the most rigorous and unbiased reviews. Frontiers revolutionizes research publishing by freely delivering the most outstanding research, evaluated with no bias from both the academic and social point of view. By applying the most advanced information technologies, Frontiers is catapulting scholarly publishing into a new generation.

What are Frontiers Research Topics?

Frontiers Research Topics are very popular trademarks of the *Frontiers journals series*: they are collections of at least ten articles, all centered on a particular subject. With their unique mix of varied contributions from Original Research to Review Articles, Frontiers Research Topics unify the most influential researchers, the latest key findings and historical advances in a hot research area.

Find out more on how to host your own Frontiers Research Topic or contribute to one as an author by contacting the Frontiers editorial office: frontiersin.org/about/contact

Adenosine pathways in cancer immunity and immunotherapy

Topic editors

Junjiang Fu — Southwest Medical University, China
Ali Hafez El-Far — Damanhour University, Egypt
Luca Antonioli — University of Pisa, Italy
Jamshid Hadjati — Tehran University of Medical Sciences, Iran

Citation

Fu, J., El-Far, A. H., Antonioli, L., Hadjati, J., eds. (2023). *Adenosine pathways in cancer immunity and immunotherapy*. Lausanne: Frontiers Media SA.
doi: 10.3389/978-2-8325-3779-4

Table of contents

frontiers | Frontiers in Immunology

TYPE Editorial
PUBLISHED 10 October 2023
DOI 10.3389/fimmu.2023.1298487

OPEN ACCESS

EDITED AND REVIEWED BY
Sandro Matosevic,
Purdue University, United States

*CORRESPONDENCE
Junjiang Fu
fujunjiang@swmu.edu.cn
Luca Antonioli
luca.antonioli@unipi.it
Ali H. El-Far
ali.elfar@damanhour.edu.eg

RECEIVED 21 September 2023
ACCEPTED 04 October 2023
PUBLISHED 10 October 2023

CITATION
Fu J, Antonioli L and El-Far AH (2023) Editorial: Adenosine pathways in cancer immunity and immunotherapy. *Front. Immunol.* 14:1298487. doi: 10.3389/fimmu.2023.1298487

Editorial: Adenosine pathways in cancer immunity and immunotherapy

Junjiang Fu[1*], Luca Antonioli[2*] and Ali H. El-Far[3*]

[1]Key Laboratory of Epigenetics and Oncology, the Research Center for Preclinical Medicine, Southwest Medical University, Luzhou, Sichuan, China, [2]Department of Clinical and Experimental Medicine, University of Pisa, Pisa, Italy, [3]Department of Biochemistry, Faculty of Veterinary Medicine, Damanhour University, Damanhour, Egypt

KEYWORDS

adenosine, cancer, immunity, immunotherapy, pathways

Editorial on the Research Topic
Adenosine pathways in cancer immunity and immunotherapy

Adenosine signalling represents a critical metabolic pathway involved in regulating tumour immunity, being co-opted by tumours to promote their growth, and impair immunity. Adenosine is produced at high tumour microenvironment (TME) levels in response to hypoxia. It is a broadly immunosuppressive metabolite that regulates innate and adaptive immune responses. Inhibition of adenosine-generating enzymes represents one strategy for promoting antitumor immunity by enhancing T cell and NK cell functionality and suppressing the pro-tumorigenic effects of myeloid cells and other immunoregulatory cells. Research into immunotherapeutic targeting various aspects of adenosine signalling is already underway, with several agents counteracting the adenosine axis have been developed. Pre-clinical studies have demonstrated anti-tumour activity alone and in combination with other immunotherapies, though more research is needed to understand their viability as a treatment option.

Extracellular adenosine activates cellular pathways through one of four known G-protein-coupled adenosine receptors: A_1, A_{2A}, A_{2B}, and A_3. The A_{2A} receptor is a high-affinity receptor expressed on T cells and natural killer T (NKT) cells, monocytes, macrophages, DCs, and natural killer (NK) cells. In contrast, the A_{2B} receptor is a relatively low-affinity receptor most highly expressed by macrophages and DCs (1). Many factors that favour adenosine generation-tissue disruption, hypoxia, ectonucleotidase expression, and inflammation-are highly characteristic of TME. Significant work has thus been done in targeting various aspects of tumour-associated adenosine signalling to enhance the immune response to malignancy (2).

Adenosine is an immunosuppressive metabolite produced at high levels within TME. Hypoxia, increased cell turnover, and expression of CD39 and CD73 are essential factors in adenosine production. Adenosine pathway blockade in immunotherapy for cancer is of great importance for cancer patients. Targeting of the adenosine pathway has generally focused on two primary aspects of immunosuppressive adenosine through (1) inhibition of adenosine production in the TME through targeting CD73 and CD39 and (2) the blockade of adenosine signalling through targeting the A_{2A} and A_{2B} receptors (3). Therefore,

targeting the A_{2B} receptor as an immunotherapeutic target in pancreatic cancer (Strickland et al.).

Combined with novel biomarkers, immune checkpoint inhibition may provide alternative pathways for treating chemotherapy-resistant triple-negative breast cancer (TNBC). Adenosine A_{2A} receptor is associated with aggressive clinical outcomes and reflects an immunosuppressive TME in human breast cancer. Also, zoledronate, the standard of care for high-risk early breast cancer patients, -induced growth inhibition and enhanced B and T lymphocyte infiltration into the orthotopic tumours with down-regulated CD73 (Petruk et al.). Because CD155 and CD73 expression was associated with a poor response to NAC and poor prognosis in this chemotherapy-resistant TNBC cohort, supporting additional immune checkpoint receptor inhibitor therapy (Cabioglu et al.).

Gastric cancer (GC) is one of the most common malignancies and a leading cause of cancer-related deaths worldwide. GC patients are usually in the advanced stage at first diagnosis and miss the best opportunity for treatment. The accumulation of extracellular adenosine inhibits the normal function of immune effector cells and facilitates the effect of immunosuppressive cells to enhance GC cell proliferation and migration. Wang et al. provided a comprehensive review that adenosine signalling can be an optimal target for GC immunotherapy.

The clinical benefit of immune checkpoint blockade in cancer therapy and the promising preclinical activity of adenosine pathway blockade is pivotal for cancer therapy. Several agents that block distinct targets along the adenosinergic pathway are presently in early-phase clinical trials.

Zohair et al. found that A_{2A} receptor could be a promising therapeutic target to overcome immune evasion prevailing within the TME of breast cancer patients. We encourage researchers to investigate the blockage of natural bioactive compounds to adenosine pathways in preclinical and clinical phases due to their safety, margine, and anticancer benefits.

Author contributions

JF: Writing – original draft, Writing – review & editing. LA: Writing – review & editing. AE-F: Writing – original draft, Writing – review & editing.

Acknowledgments

The authors are thankful to the contributors to this Research Topic and the Editorial support of the Journal.

Conflict of interest

The authors declare that the research was conducted in the absence of any commercial or financial relationships that could be construed as a potential conflict of interest.

Publisher's note

References

1. Cekic C, Linden J. Purinergic regulation of the immune system. *Nat Rev Immunol* (2016) 16:177–92. doi: 10.1038/NRI.2016.4

2. Blay J, White TD, Hoskin DW. The extracellular fluid of solid carcinomas contains immunosuppressive concentrations of adenosine. *Cancer Res* (1997) 57:2602–5.

3. Leone RD, Emens LA. Targeting adenosine for cancer immunotherapy. *J Immunother Cancer* (2018) 6:57. doi: 10.1186/s40425-018-0360-8

frontiers | Frontiers in Immunology

TYPE Review
PUBLISHED 16 September 2022
DOI 10.3389/fimmu.2022.1027838

OPEN ACCESS

EDITED BY
Junjiang Fu,
Southwest Medical University, China

REVIEWED BY
Jiao Wang,
Purdue University, United States
Muhammad Ikram Ullah,
Al Jouf University, Saudi Arabia

*CORRESPONDENCE
Xiangjian Chen
wz1370@126.com
Linyong Du
dulinyong@qq.com

SPECIALTY SECTION
This article was submitted to Cancer Immunity and Immunotherapy, a section of the journal Frontiers in Immunology

RECEIVED 25 August 2022
ACCEPTED 05 September 2022
PUBLISHED 16 September 2022

CITATION
Wang J, Du L and Chen X (2022) Adenosine signaling: Optimal target for gastric cancer immunotherapy. *Front. Immunol.* 13:1027838. doi: 10.3389/fimmu.2022.1027838

Adenosine signaling: Optimal target for gastric cancer immunotherapy

Junqing Wang[1], Linyong Du[2*] and Xiangjian Chen[1*]

[1]School of the 1St Clinical Medical Sciences, Wenzhou Medical University, Wenzhou, China, [2]Key Laboratory of Laboratory Medicine, Ministry of Education of China, School of Laboratory Medicine and Life Science, Wenzhou Medical University, Wenzhou, China

Gastric cancer (GC) is one of the most common malignancy and leading cause of cancer-related deaths worldwide. Due to asymptomatic or only nonspecific early symptoms, GC patients are usually in the advanced stage at first diagnosis and miss the best opportunity of treatment. Immunotherapies, especially immune checkpoint inhibitors (ICIs), have dramatically changed the landscape of available treatment options for advanced-stage cancer patients. However, with regards to existing ICIs, the clinical benefit of monotherapy for advanced gastric cancer (AGC) is quite limited. Therefore, it is urgent to explore an optimal target for the treatment of GC. In this review, we summarize the expression profiles and prognostic value of 20 common immune checkpoint-related genes in GC from Gene Expression Profiling Interactive Analysis (GEPIA) database, and then find that the adenosinergic pathway plays an indispensable role in the occurrence and development of GC. Moreover, we discuss the pathophysiological function of adenosinergic pathway in cancers. The accumulation of extracellular adenosine inhibits the normal function of immune effector cells and facilitate the effect of immunosuppressive cells to foster GC cells proliferation and migration. Finally, we provide insights into potential clinical application of adenosinergic-targeting therapies for GC patients.

KEYWORDS

gastric cancer, CD39, CD73, adenosine, immunotherapy

Abbreviations: GC, gastric cancer; ICI, immune checkpoint inhibitor; AGC, advanced gastric cancer; GEPIA, Gene Expression Profiling Interactive Analysis; EGC, early gastric cancer; HER2, human epidermal growth factor receptor 2; CAR, T-cell chimeric antigen receptor-modified T cell; CTLA-4, cytotoxic T lymphocyte-associated antigen 4; PD-1/PD-L1, programmed cell death receptor 1/programmed cell death ligand 1; OS, overall survival; PFS, progression-free survival; eAMP, extracellular adenosine monophosphate; eADP, extracellular adenosine diphosphate; eATP, extracellular adenosine triphosphate; TME, tumor microenvironment; NK, natural killer cell; Tregs, regulatory T cells; DC, dendritic cell.

Introduction

Gastric cancer (GC) is a major source of global cancer mortality with limited treatment options and poor patient survival. It is the fourth most commonly occurring cancer in men and the seventh in women (1). For patients with early gastric cancer (EGC) and low risk of lymph node metastasis, endoscopic submucosal dissection (ESD) or radical surgical resection alone is potentially curative (2, 3). Unfortunately, due to no apparent symptom or only indigestion-like clinical manifestations, such as inappetence, gastroesophageal reflux, and belching, patients with EGC often miss the best treatment opportunity because of negligence (2). Although endoscopic screening significantly increases the detection of EGC and improves prognosis (4). Skill among endoscopists varies greatly, and numerous patients are still missed for various reasons (5). As the disease progresses, hemorrhage, perforation, obstruction, cachexia, and other symptoms of advanced cancer gradually appear. GC is already in the advanced stage once detected in patients, which has a poor ending due to ineffective therapies and multiple resistance (6). Therefore, accurately diagnosing EGC and effectively treating advanced gastric cancer (AGC) patients who have lost the chance of radical surgical resection are two serious health problems all over the world.

For the patients who are suffering from GC, the treatments are mainly surgical excision, chemotherapy, targeted therapy, immunotherapy, and other comprehensive strategies (7). Among them, radical gastrectomy with D2 lymphadenectomy, with or without neoadjuvant therapy, is the only potentially curative treatment option (8). However, increasing numbers of studies have shown that surgery cannot benefit patients with unresectable AGC and post-operative complication is a negative predictor of long-term survival outcomes for them (9). Systemic chemotherapy with multiple drug regimens is the main therapy choice to further prolong the survival of post- or non-operative AGC patients (10). Despite relevant progress, the impact of chemotherapy on AGC patients' survival is still unsatisfactory, especially patients with multiple distant metastases (1). Additionally, as an emerging, attractive, and effective treatment, targeted therapy has shown promising effects in a part of GC patients, even if the beneficiary degree not definite (11). As the most common target in GC, the frequency of human epidermal growth factor receptor 2 (HER2) overexpression ranges from 4.4% to 53.4%, with a mean of 17.9% (12). Coupled with drug resistance developed during treatment, management of AGC patients by targeted therapy remains a challenge. Despite new therapeutic options, AGC remains associated with a poor prognosis compared with other cancers, on account of inactive immunogenicity and vast heterogeneity represent a barrier to disease management (13, 14).

Immunotherapies, especially immune checkpoint inhibitors (ICIs) and chimeric antigen receptor-modified T (CAR T) cell therapies, have been used continuously for decades, as lifesaving procedures for millions of patients with hematological malignancy (15). As the most extensively used ICIs at present, checkpoint inhibitor-based immunotherapies that target the cytotoxic T lymphocyte-associated antigen 4 (CTLA-4) and the programmed cell death receptor 1/programmed cell death ligand 1 (PD-1/PD-L1) pathway have achieved impressive success in the treatment of different cancer types (16). Nevertheless, there still exists various challenges that have severely limited the clinical application of immunotherapies in AGC, for instance, the ineffectiveness and serious side effects (6). For AGC patients, anti-CTLA-4 and anti-PD-1/PD-L1 monoclonal antibodies cannot acquire satisfactory curative effect without the assistance of other cancer treatments (17–20). Some clinical trials have shown positive effects on overall response and disease control in combination with ICIs and other therapies, yet responses are slight and heterogeneous (17). Therefore, it is urgent to explore a more effective immunotherapy method to prolong the survival of AGC patients.

In this review, we find that CD73 is the most important immune checkpoint affecting the prognosis of GC patients by analyzing the Gene Expression Profiling Interactive Analysis (GEPIA) database. In addition, we also describe the mechanism of CD39-CD73-adenosine signaling pathway in immune regulation of cancers and discuss its role in the occurrence and development of GC. At the end of the article, we also put forward some prospects about treating GC with the help of targeting CD39-CD73-adenosine axis.

CD73 is an optimal target for GC immunotherapy

ICI, especially inhibition of PD-1/PD-L1 axis, is a new standard of immunotherapy in the treatment of advanced or metastatic GC and is represented in various combinations with and without other treatments within clinical trials (21). However, its curative effect is related to individual differences to a certain degree. For example, in a randomized, open-label, phase 3 trial (NCT02370498), the PD-1/PD-L1 blockade cannot significantly improve overall survival (OS) and progression-free survival (PFS) versus paclitaxel for PD-L1-positive GC (all $P > 0.6$) (22). In another phase 3 randomized clinical trial (NCT02494583), the PD-1/PD-L1 blockade plus chemotherapy was not superior to chemotherapy for OS (12.3 vs. 10.8 months; HR, 0.85; 95% CI, 0.62-1.17; $P = 0.16$) (19). Collectively, the immunotherapy of GC needs a more appropriate immune checkpoint to obtain superior efficacy.

To further confirm which target plays the most indispensable role in GC, we input 20 common immune checkpoint-related genes into the GEPIA server for in-depth analysis (Table 1). Among them, we found that 9 genes were confirmed to have significant differential expression in GC (Figure 1). Moreover, the expression levels of PDCD1 (encode PD-1), CD274 (encode PD-L1), and CTLA-4 genes in GC not change compared with adjacent tissues, which was consistent with the above-mentioned treatment results.

Furthermore, we investigated whether the expression of various immune checkpoint-related genes was correlated with prognosis in GC patients (Figure 2). The results of GEPIA analysis showed that only the high expression of NT5E (encode CD73) is more likely to encounter GC patients death earlier and shorten survival time ($p<0.05$). Additionally, with the help of immunohistochemistry, single-sample gene set enrichment analysis and flow cytometry, extensive related studies have reported that CD73 expression is upregulated in GC which is proved to be an independent adverse prognosticator for the patients (61–63).

Ecto-5'-nucleotidase (NT5E), also known as CD73, is a cytomembrane protein linked to the cell membrane *via* a glycosylphosphatidylinositol (GPI) anchor that regulates the conversion of extracellular adenosine monophosphate (eAMP) to adenosine contributing to immunosuppression (64). CD39, also termed ectonucleoside triphosphate diphosphohydrolase-1 (ENTPD1), catalyzes the hydrolysis of extracellular adenosine triphosphate (eATP) and adenosine diphosphate (eADP) into eAMP to provide raw materials for CD73 (65). As the end product of CD39-CD73 axis, adenosine mediates immunosuppression within the tumor microenvironment (TME) through triggering adenosine receptors on the membrane surface, including A1R (encoded by ADORA1), A2AR (encoded by ADORA2A), A2BR (encoded by ADORA2B), and A3R (encoded by ADORA3) (66).

Based on these, we analyzed the associations between 20 common immune checkpoint-related genes and survival contribution in GC by GEPIA database. In general, compared with other immune checkpoints, CD73 showed the most obvious detrimental role in GC patients (Figure 3A). In addition, according to the analysis of corresponding genes expression and the TNM stage, we also found that the expression of CD39 and CD73 was higher in GC patients with clinic stage II, stage III, or stage IV than that in stage I, which revealed that these upregulated genes might be associated with tumor progression positively (Figure 3B). However, the role of adenosine receptors in GC patients still needs to be further evaluated (Figure 3C).

Taken together, the CD39-CD73-adenosine signaling pathway, as the most important immune checkpoint in GC, mediates the immunosuppressive mechanism by which tumors escape immunosurveillance and impede anti-tumor immunity within the TME. Thereinto, CD73 is an optimal target for the immunotherapy of GC.

The CD39-CD73-adenosine signaling pathway in cancers

eATP and immune response

Under normal circumstances, ATP is almost exclusively present inside cells as the main energy currency, participating in virtually all biological processes (67). eATP, as an extracellular messenger, is set by both passive and active release mechanisms and degradation processes (68, 69). Measurement of eATP levels in different biological context reveals that healthy tissues present very low levels (10–100 nanomoles per liter) of this nucleotide in the pericellular space, while in sites of tissue damage, inflammation, hypoxia, ischemia or TME it can reach high levels (100–500 micromoles per liter) to promote inflammatory responses (Figure 4) (70, 71).

There are two families of P2 purinergic receptors (P2Rs) for eATP: ATP-gated ion channels known as P2X receptors (P2X1-7) and G protein–coupled P2Y receptors (P2Y1, P2Y2, P2Y4, P2Y6, P2Y11b, P2Y12, P2Y13, P2Y14c) (69). Among them, the P2X7 receptor (P2X7R), as the most structurally and functionally distinct P2R subtype, appears to be a main player in host-tumor cell interactions because of involvement in apoptotic, inflammatory, and tumor progression pathways (72, 73). During innate immune responses, the key role of P2X7R is to activate the assembly of nucleotide-binding domain (NOD) like receptor protein 3 (NLRP3) inflammasome rapidly, which could consecutively facilitate caspase-1 meditated maturation and release of the pro-inflammatory cytokines interleukin-1β and interleukin-18 to participate in both defense and inflammatory responses (74, 75). For adaptive immune responses, eATP signals *via* P2X7R to boost the activation, proliferation, and chemotaxis of immune cells with consequent stimulation of $CD8^+$ and $CD4^+$ T cell mediated anti-tumor responses (74, 76, 77). The production of pro-inflammatory cytokines, such as interleukin-1β and interleukin-18, are involved in the activation of B and NK cells (78). Additionally, the stimulation of P2X7R inhibits the tissue-specific immunosuppressive potential of regulatory T cells (Tregs) and facilitated their conversion to T helper 17 (Th17) cells during chronic inflammation (79). On the contrary, P2X7R antagonism increases Tregs and reduces clinical and histological graft-versus-host disease in a humanized mouse model (80). Overall, eATP can provide a variety of strategies to enhance the ability to eliminate malignant cells.

The CD39-CD73-adenosine axis

The human body always keeps a delicate balance between injury and repair to avoid overcorrection. Over time eATP becomes less inflammatory or even anti-inflammatory due to

TABLE 1 The characteristics of 20 immune checkpoint-related genes.

Gene Names	Protein Names	Subcellular Location	Normal Tissue Specificity	Cancer Types	Function	References
SIGLEC15	sialic acid-binding Ig-like lectin 15	plasma membrane	macrophage and/or dendritic cells of spleen and lymph nodes	lymphoma, leukemia, thyroid cancer, and renal cell cancer	TAM-associated Siglec-15 has a potent immune suppressive effect on T-cell responses	(23, 24)
VTCN1	V-set domain-containing T-cell activation inhibitor 1	plasma membrane	activated T- and B-cells, monocytes, and dendritic cells	breast cancer, ovarian cancer, and renal cell cancer	negatively regulates T-cell-mediated immune response by inhibiting T-cell activation, proliferation, cytokine production and development of cytotoxicity	(25, 26)
HHLA2	human endogenous retrovirus-H long terminal repeat-associating protein 2	plasma membrane	colon, kidney, testis, B-cells, and dendritic cells	colorectal cancer, pancreatic cancer, and gastric cancer	inhibits $CD8^+$ T and NK cell function and killing	(27, 28)
FGL2	fibroleukin	extracellular region and exosome	cytotoxic T-cells	leukemia and lymphoma	induces $CD8^+$ T cell apoptosis to limit T cell immunity through the inhibitory Fc receptor FcγRIIB	(29, 30)
ENTPD1	ectonucleoside triphosphate diphosphohydrolase 1 (CD39)	plasma membrane	activated lymphoid cells and endothelial tissues	glioma, gastric cancer, and renal cell cancer	hydrolyzes eATP and eADP into eAMP to provide raw materials for CD73	(31, 32)
PVR	poliovirus receptor (CD155)	cytoplasm, cell surface and extracellular space	widely expressed	esophageal carcinoma, adrenocortical carcinoma, and colon carcinoma	provides tumors with a mechanism of immunoevasion from NK cells	(33, 34)
CD24	signal transducer CD24	cell surface	B-cells	Breast cancer, colorectal cancer, and gastric cancer	regulates the proliferation of B-cells and prevents their terminal differentiation into antibody-forming cells	(35, 36)
CD200	OX-2 membrane glycoprotein	cell membrane	widely expressed	pheochromocytoma, paraganglioma and renal cell cancer	inhibits T-cell proliferation	(37, 38)
TNFRSF14	tumor necrosis factor receptor superfamily member 14 (CD270)	cell membrane	lung, spleen, and thymus	melanoma, lymphoma, and lung cancer	synergistically inhibits the function of lymphocytes with BTLA	(39, 40)
LGALS9C	galectin-9C	cytosol and nucleus	widely expressed	head and neck squamous cell carcinoma, and colorectal cancer	interacts with multiple molecules to regulate immune cells proliferation and death	(41, 42)
NT5E	5'-nucleotidase (CD73)	cell membrane	activated lymphoid cells and endothelial tissues	thyroid cancer, gastric cancer, sarcoma, and glioma	hydrolyzes eAMP into immunosuppressive adenosine	(43, 44)
LAG3	lymphocyte activation gene 3 protein (CD223)	cell membrane and extracellular region	activated T-cells and NK cells	leukemia and testicular germ cell tumors	negatively regulates the proliferation, activation, effector function and homeostasis of both $CD8^+$ and $CD4^+$ T-cells	(45, 46)
TIGIT	T-cell immunoreceptor with immunoglobulin and ITIM domains	cell membrane	T-cells and NK cells	leukemia and lung adenocarcinoma	suppresses T-cell activation by promoting the generation of mature immunoregulatory dendritic cells	(47, 48)
C10orf54	V-type immunoglobulin domain-containing suppressor of T-cell activation (VISTA)	cell membrane	placenta, spleen, plasma blood leukocytes, and lung	leukemia and pancreatic cancer	immunoregulatory receptor which inhibits the T-cell response	(49, 50)
BTLA	B- and T-lymphocyte attenuator (CD272)	cell membrane	lymph node	lymphoma and leukemia	inhibitory receptor on lymphocytes that negatively regulates antigen receptor signaling	(51, 52)
PDCD1	programmed cell death protein 1 (PD-1)	cell membrane	induced at programmed cell death	lymphoma, melanoma, and lung cancer	plays a critical role in induction and maintenance of immune tolerance	(53, 54)

(Continued)

TABLE 1 Continued

Gene Names	Protein Names	Subcellular Location	Normal Tissue Specificity	Cancer Types	Function	References
CD276	CD276 antigen	cell membrane	peripheral blood lymphocytes or granulocytes	sarcoma, glioma, lung cancer, and prostate cancer	inhibits T-cell-mediated immune response and NK cell-mediated lysis	(55, 56)
CTLA4	cytotoxic T-lymphocyte protein 4	cell membrane, Golgi apparatus, cytoplasm	widely expressed	lymphoma, leukemia melanoma, and lung cancer	inhibitory receptor acting as a major negative regulator of T-cell responses	(57, 58)
CD274	programmed cell death 1 ligand 1 (PD-L1)	cell membrane, nucleoplasm, and extracellular exosome	lung, heart, placenta, and kidney	lymphoma, melanoma, and lung cancer	as a ligand for the inhibitory receptor PD-1, modulates the activation threshold of T-cells and limits T-cell effector response	(53, 54)
CD47	leukocyte surface antigen CD47	cell surface and extracellular exosome	widely expressed	leukemia, ovarian cancer, lung cancer, and pancreatic cancer	prevents maturation of immature dendritic cells and inhibits cytokine production by mature dendritic cells	(59, 60)

TAM, tumor-associated macrophage; NK, natural killer cell; eAMP, extracellular adenosine monophosphate; eADP, extracellular adenosine diphosphate; eATP, extracellular adenosine triphosphate; ITIM, immunoreceptor tyrosine-based inhibitory motif.

the recruitment of Tregs and induction of ectoenzymes such as CD39 and CD73 (Figure 4) (69). As the critical components of the extracellular adenosinergic pathway, CD39 converts eATP and eADP to eAMP, and then CD73 converts eAMP to immunosuppressive adenosine (81). Moreover, another pathway generating adenosine involves participation of extracellular nicotinamide adenine dinucleotide (NAD^+), CD38, CD203a, and CD73 (82). Like CD39 and CD73,

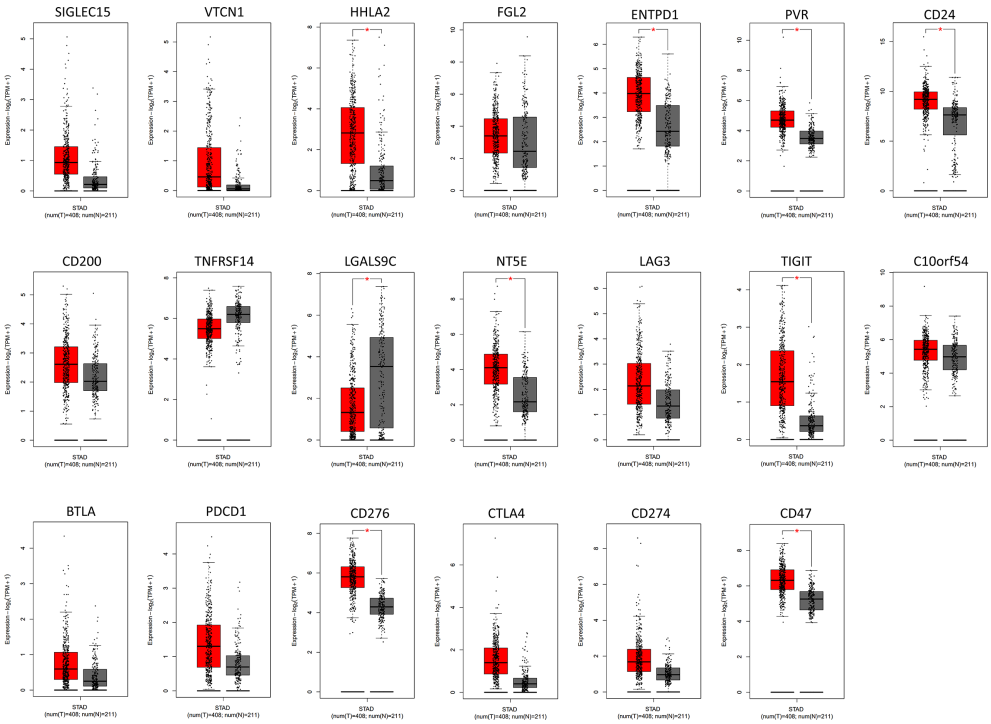

FIGURE 1
The analysis of immune checkpoint-related genes expression in GC by GEPIA database. The results revealed that 9 genes were confirmed to have significant differential expression in GC compared to the normal tissues. Among them, higher expression was observed in HHLA2, ENTPD1, PVR, CD24, NT5E, TIGIT, CD276, and CD47 and lower expression was observed in LGALS9C. Red color represents tumor tissue (n=408), and gray color represents normal tissue (n=211). STAD, stomach adenocarcinoma. * $P < 0.05$.

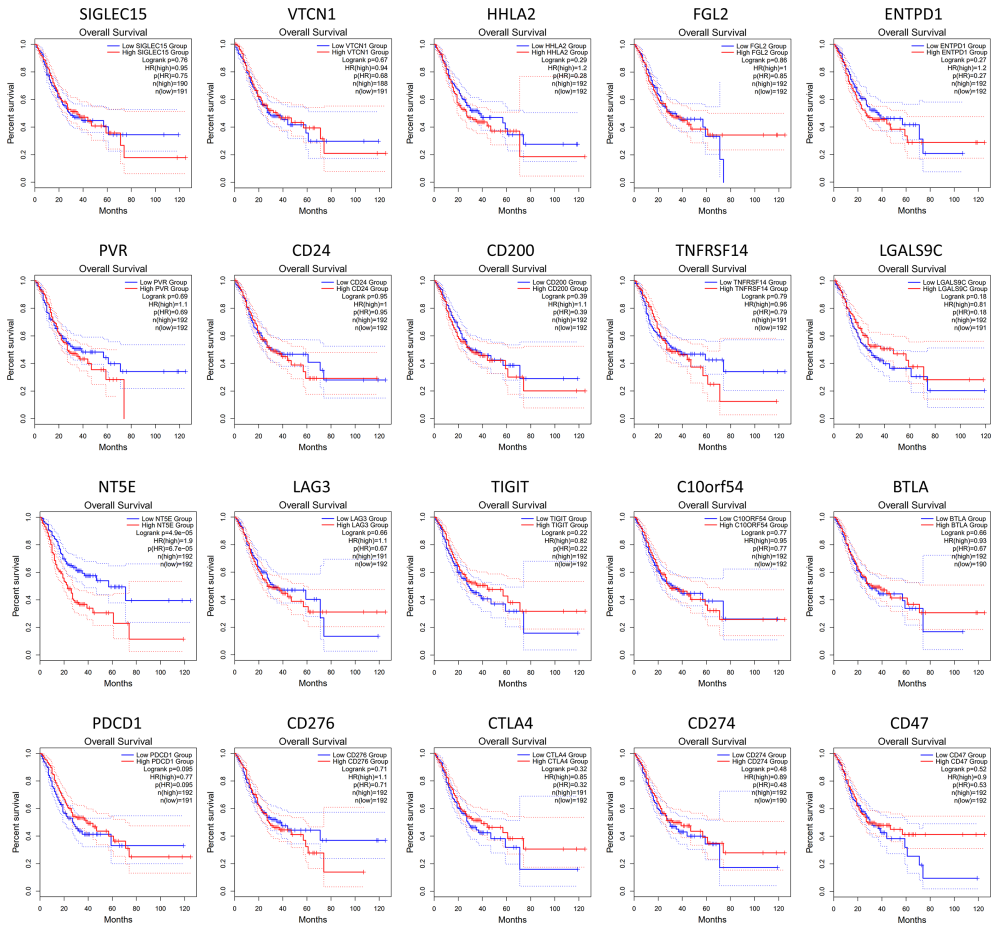

FIGURE 2
Kaplan-Meier survival curves comparing the high and low expression of immune checkpoint-related genes in GC by GEPIA database. The results showed that only the high expression of NT5E (encode CD73) was correlated with poor prognosis of GC patients ($p<0.05$). The red line indicates the high expression group of genes (n=192) and the blue line represents the low expression group of genes (n=191).

alkaline phosphatase (ALP) and prostatic acid phosphatase (PAP) also can catalyze the conversion of eATP to adenosine (83, 84). Furthermore, the high concentration of intracellular adenosine can be transported outside the cell *via* equilibrative nucleoside transporters (ENTs) and concentrative nucleoside transporters (CNTs) to maintain balance (85).

The levels of extracellular adenosine are regulated by adenosine-converting enzymes such as adenosine kinase (ADK) and adenosine deaminase (ADA). Among them, ADK adds the residue of phosphoric acid to adenosine and converts it into AMP and ADA separates an amino group from adenosine with the formation of inosine (86). However, in the TME, high concentrations of adenosine binding to the corresponding receptors to inhibit the activation and expansion of various immune cells and promote the immune escape of cancers (86). The four known subtypes of adenosine receptors (A1R, A2AR, A2BR, and A3R), all of which are G-protein coupled receptors (GPCRs), have distinct expression patterns and mediate diverse signaling pathways (87). Regarding the respective role of adenosine receptors, it has been demonstrated that among the four subtypes, adenosine binding to A2AR and A2BR causes an increase in intracellular cyclic adenosine monophosphate (cAMP) and consequently the functional inhibition of immune cells, while A1R and A3R activation leads to tumor growth, cell proliferation and survival in some cases (88–90).

Immunosuppressive adenosine and TME

Adenosine accumulated in the TME is a major cause of immunosuppression (Figure 4). As the main force to eliminate malignant cells, the impairment of $CD8^+$ T cells function and metabolic fitness are mediated by the A2AR/PKA/mTORC1 pathway as the main axis, due to the persistent high

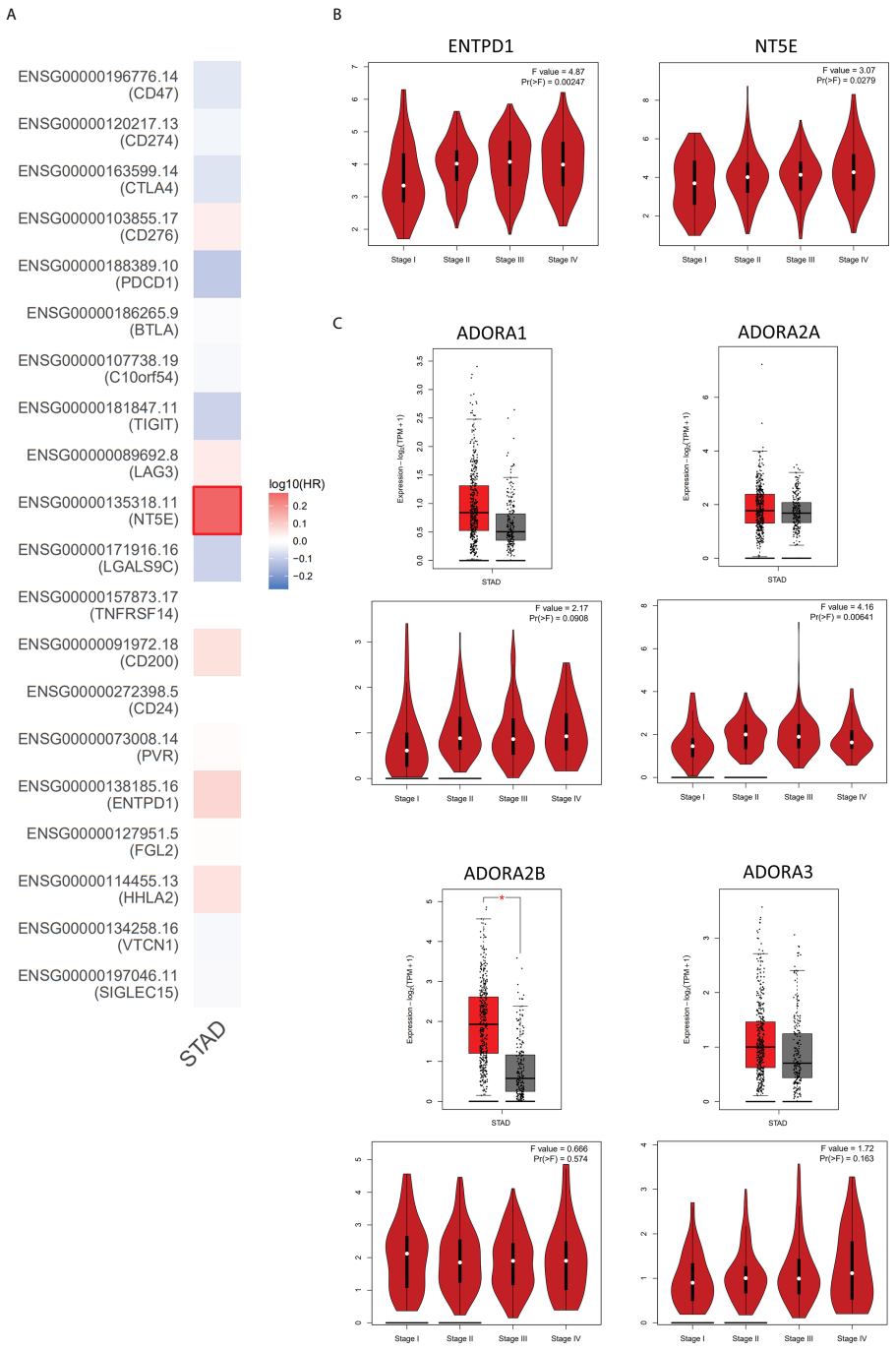

FIGURE 3
The analysis of adenosinergic pathway-related genes expression in GC by GEPIA database. **(A)** The risk assessment of 20 common immune checkpoint-related genes affecting the prognosis of GC patients. By comparing the survival contribution of multiple genes *via* Mantel-Cox test, we found that NT5E (encode CD73) showed the most obvious detrimental role in GC patients (n=383). **(B)** The expression levels of ENTPD1 and NT5E in different tumor stages of GC. With the progression of GC, the expression of ENTPD1 and NT5E also increased. **(C)** The expression levels of adenosine receptors in GC patients. The analysis showed that only ADORA2B expression (encode A2BR) increased in GC compared to the normal tissues and only ADORA2A (encode A2AR) was positively correlated with the progression of GC. Red color represents tumor tissue (n=408), and gray color represents normal tissue (n=211). STAD, stomach adenocarcinoma; HR, hazard ratio. * $P < 0.05$.

concentration of adenosine (91). Blocking the interaction of receptor with adenosine by a small-molecule A2AR antagonist can increase the recruitment of $CD8^+$ T cells into the tumor and broaden the circulating T cell repertoire (92). Similarly, existing studies also indicate that immunosuppressive adenosine can impair the parenchymal $CD4^+$ T cell and B cell response and infiltration (93, 94). Although NK cells rarely infiltrate cancers, their presence in tumor biopsies has been shown to positively associate with increased survival (95). As an intrinsic negative regulator of NK-cell maturation and anti-tumor immune responses, A2AR-mediated adenosine signaling can obviously limit tumor-infiltrating NK cells proliferation and activation (96). At the interface between the innate and adaptive immune system, dendritic cells (DCs) play key roles in inflammation and tumor immunity (97). However, adenosine and cAMP signaling can not only prevent DC maturation and development of effector functions but also skew DC differentiation towards a tolerogenic phenotype with defective $CD8^+$ T cell priming capacity (98).

Extensive literature shows that eATP-mediated activation of purinergic receptor is necessary for the maturation and release of interleukin-1β by activated macrophages (99). Nevertheless, adenosine generated by eATP likely contributes to the differentiation and recruitment of tumor-associated macrophages (TAMs) which further amplify adenosine-dependent immunosuppression *via* additional ectonucleotidase activity of cancer cells (100). Myeloid-derived suppressor cells (MDSCs) are considered to be an important contributor to the immunosuppressive TME and thus an obstacle for many cancer immunotherapies. The metabolite adenosine plays a vital role in MDSCs mobilization through several mechanisms to inhibit T cell functions and promote cancer progression (101). In addition, elevated adenosine upregulates CD73 on cancer associated fibroblasts (CAFs) *via* A2BR-mediated pathway, thereby inciting the adenosine-A2BR-CD73 feedforward circuitry, which further augments immunosuppression by activating the non-redundant adenosine-A2AR pathway in immune cells to inhibit immune activation (102). For mesenchymal stromal cells (MSCs), the modulation of the adenosine overall promotes a more aggressive phenotype of cancers and more serious immunosuppressive function (103). Recently, Abhishek Tripathi et al. found a strong correlation between CD73, CD39 and A2AR expression, and Treg gene expression signature. Adenosine activates the high-affinity A2AR receptor, which in turn inhibits infiltrating NK cells and cytotoxic T lymphocytes (CTLs) activity and increases Tregs

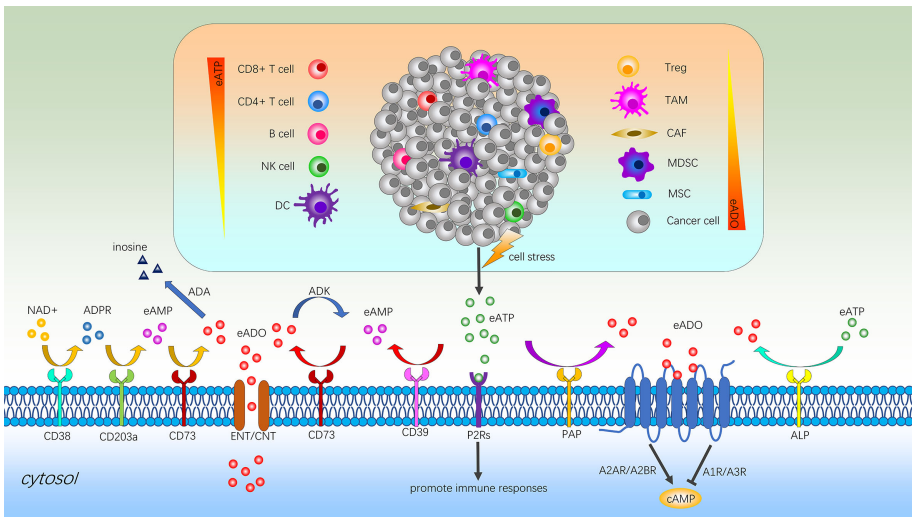

FIGURE 4
Immune regulation of adenosine signaling in the TME. Cell stress promotes eATP production and contributes to chronic inflammation *via* P2Rs. Within the TME, accumulated eATP can be degraded to ADO by the sequential action of the ectonucleotidases CD39 and CD73 or other alternative pathways such as ALP or PAP-mediated process. In addition, the sequential catabolism of NAD^+ by CD38, CD203a and CD73 also can generate ADO and the high concentration of intracellular ADO can be transported outside the cell *via* ENTs or CNTs to maintain balance. The bioavailability of extracellular ADO is regulated by adenosine-converting enzymes such as ADK and ADA, which converts ADO into AMP and inosine respectively. High concentrations of ADO binding to adenosine receptors to inhibit the activation of immune cells and stimulate immunosuppressive cells to promote the immune escape of cancers. eATP, extracellular adenosine triphosphate; eAMP, extracellular adenosine monophosphate; NK cell, natural killer cell; DC, dendritic cell; Treg, regulatory T cell; TAM, tumor-associated macrophage; CAF, cancer associated fibroblast; MDSC, myeloid-derived suppressor cell; MSC, mesenchymal stromal cell; ADO, adenosine; NAD^+, nicotinamide adenine dinucleotide; ADPR, adenosine diphosphate ribose; ADA, adenosine deaminase; ADK, adenosine kinase; ENT, equilibrative nucleoside transporter; CNT, concentrative nucleoside transporter; P2Rs, P2 purinergic receptors; PAP, prostatic acid phosphatase; ALP, alkaline phosphatase; cAMP, cyclic adenosine monophosphate.

proliferation to further promote immunosuppression (104). Beyond the task of providing an immune-tolerant TME by helping to determine the activity of immune and inflammatory cells, the adenosine system directly regulates cancer growth and metastatic dissemination through specific receptors that are expressed on cancer cells (105).

Overall, in the context of cancer, the accumulation of extracellular adenosine inhibits the normal function of immune effector cells and facilitate the effect of immunosuppressive cells to foster malignant cells proliferation and migration.

Adenosine signaling in GC

Extracellular release of the central cellular energy metabolite ATP has although evolved as a natural signal for cellular distress, immunogenic cell death (ICD) and the recruitment and activation of immune cells (106). Ectonucleotidases which up-regulated in many types of cancer, such as CD39 and CD73, rapidly metabolize eATP to immunosuppressive adenosine, thereafter exacerbating immunosuppression in the TME (107).

Similar to other malignancies, the expression of CD39 and CD73 is synergistically increased in GC, causing a poor outcome for patients (61, 108). Under the dysfunction of mitochondria, GC cells preferentially utilize both glycolytic and pentose phosphate pathways rather than electron transport chains to desperately generate ATP, classically recognized as the Warburg effect, to provide substrates for adenosine production (109). Importantly, CD73 is also a hypoxia-responsive gene and promotes the Warburg effect of GC dependent on its enzyme activity to further amplifying adenosine signal transduction (110). Immunosuppressive adenosine can enhance the stemness of GC to resist treatment and promote the expression of epithelial-mesenchymal transition-associated genes to stimulate GC cell invasion and metastasis *via* interaction with A2AR and subsequent activation of the PI3K/AKT/mTOR pathway (111, 112). Furthermore, pathway and gene set enrichment analysis of transcriptome data revealed the modulation role of adenosine in RICS/RhoA signaling, which subsequently inhibited phosphorylation of LIMK/cofilin and promoted β-catenin activation to induce metastasis of GC (63).

Long-term accumulation of adenosine in GC helps to establish the immunosuppressive TME and promote tumor development through its interaction with tumor parenchyma and stromal cells (113). For immune cells, tumor-associated Tregs express more CD39 and CD73 in GC tissue. They also can decompose eATP to adenosine and in turn not only induce apoptosis and inhibit the proliferation of $CD8^+$ T cells through the A2AR pathway but also prevent the infiltration of effector T cells into the TME (114, 115). Moreover, Hanyuan Liu et al. found that CD73 high expression GC showed a specific microenvironment with more $CD8^+$ T cell infiltration *via* recruiting 902 GC patients to examine CD73 expression and immune contexture, but these $CD8^+$ T cells displayed a dysfunctional phenotype for anti-tumor immunity (62). As a bypass pathway for adenosine production, restraining the conversion of NAD^+ to adenosine can improve the function of effector $CD8^+$ T cells and induce the apoptosis of GC cells simultaneously (116).

Though lots of systemic and in-depth researches on the role of the CD39-CD73-adenosine axis in diseases have been implemented, such as cardiovascular diseases, autoimmune disease, gut inflammation, and other cancers, immune checkpoint therapy targeting adenosine pathway in GC is still in the early phase (113, 117–119). With the use of small molecule inhibitors and monoclonal antibodies targeting adenosine pathway, an increasing number of clinical trials designed for GC treatment are ongoing, yet few successful experiences have been identified thus far (Table 2). Therefore, further exploration is still needed to complement the deficiencies of this immunotherapy method for GC patients.

Prospects

The considerable heterogeneity and immunosuppressive TME represent major obstacles to accurate diagnosis and effective treatment in GC patients, leading to ineffective immunotherapy (120). For tumor heterogeneity, the molecular classification of GC extends the potential for personalized treatments to benefit each patient and fulfill the concept of precision medicine (121). The development of GC is a complex process displaying polytropic cell and molecular landscape within the TME, which supports tumor growth, metastasis, and recurrence, and function as the soil for gastric tumorigenesis (122). There is increasing evidence that reprogrammed energy metabolism contributes to the development of tumor suppressive immune microenvironment and influences the course of GC (123).

As a common metabolite, immunosuppressive adenosine has been intensively studied in many benign and malignant diseases, nevertheless, few researchers are currently exploring this avenue in GC. Although the efficacy of multiple small-molecule antagonists and antibodies of CD39-CD73-adenosine signaling pathway are being verified in a variety of diseases, deficiencies such as inefficacy and excessive inflammation cannot be ignored. Based on both, further research should mainly focus on the following aspects to obtain better curative effect:

Develop new drugs targeting adenosine pathway with higher specificity, less side effect and better efficacy.

Adenosine signaling, as one of the key components in regulating normal immune responses, induces immune tolerance to prevent an overreaction with self and the

TABLE 2 The clinical trials of blocking adenosine signaling in patients with advanced solid tumors.

Target	Status	Drug names	Combination	Trial phase	Clinical trial number
CD39	Recruiting	SRF617	Gemcitabine Albumin-Bound Paclitaxel Pembrolizumab	Phase 1	NCT04336098
	Active	TTX-030	Nab-paclitaxel Gemcitabine	Phase 1	NCT04306900
	Recruiting	ES002023	None	Phase 1	NCT05075564
	Not yet recruiting	ES014	None	Phase 1	NCT05381935
	Recruiting	JS019	None	Phase 1	NCT05374226
	Not yet recruiting	PUR001	None	Phase 1	NCT05234853
CD73	Recruiting	IPH5301	Chemotherapy Trastuzumab	Phase 1	NCT05143970
	Recruiting	PT199	Anti-PD-1 monoclonal antibody	Phase 1	NCT05431270
	Recruiting	Sym024	Anti-PD-1 monoclonal antibody	Phase 1	NCT04672434
	Active	LY3475070	Pembrolizumab	Phase 1	NCT04148937
	Not yet recruiting	HLX23	None	Phase 1	NCT04797468
	Recruiting	AK119	Anti-PD-1/CTLA-4 bispecific antibody	Phase 1	NCT04572152
	Recruiting	IBI325	Anti-PD-1 monoclonal antibody	Phase 1	NCT05119998
	Terminated	GS-1423	mFOLFOX6 Regimen	Phase 1	NCT03954704
	Not yet recruiting	JAB-BX102	Anti-PD-1 monoclonal antibody	Phase 2	NCT05174585
	Active	MEDI9447	Anti-PD-L1 monoclonal antibody	Phase 1	NCT02503774
	Recruiting	INCA00186	Anti-PD-1 monoclonal antibody	Phase 1	NCT04989387
	Recruiting	TJ004309	None	Phase 2	NCT05001347
	Completed	BMS-986179	Anti-PD-1 monoclonal antibody	Phase 2	NCT02754141
A2AR	Not yet recruiting	ILB2109	None	Phase 1	NCT05278546
	Recruiting	EOS100850	None	Phase 1	NCT05117177
	Recruiting	M1069	None	Phase 1	NCT05198349
A2BR	Not yet recruiting	TT-4	None	Phase 2	NCT04976660

development of autoimmune disease (124). Due to the clinical experience with adenosine pathway inhibitors in oncology is limited, long-term exposure to these drugs and their association with other anti-tumor treatments could potentially lead to the emergence of systemic multiorgan toxicity (125). Therefore, the development of new drugs should also pay attention to its safety.

Simultaneously target multiple adenosinergic pathway components to acquire synergistic efficacy.

Multiple pathways can contribute to the production of adenosine, some of them by traditional CD39/CD73-dependent mechanisms, others by alternative pathways. In order to disrupt the adenosine production, Nathalie Bonnefoy et al. generated two antibodies, IPH5201 and IPH5301, targeting human membrane-associated and soluble forms of CD39 and CD73, respectively, and efficiently blocking the hydrolysis of immunogenic ATP into immunosuppressive adenosine. Their results suggested that the concomitant blockade of both CD39 and CD73 immunosuppressive enzymes can limit adenosine-mediated T cell inhibition, thereby enhancing anti-tumor immunity (126). Similarly, the simultaneous inhibition CD39 and CD73 cell surface ectonucleotidases by small molecular inhibitors can enhance the mobilization of bone marrow residing stem cells by decreasing the extracellular level of adenosine (127). In addition, co-targeting CD73 and A2AR strategy is also a promising novel therapeutic strategy for future hepatocellular carcinoma management (128). More interestingly, the alternative pathways can compensate the lack of adenosine production when the CD39/CD73/adenosine axis is blocked (129). Hence, a strong rationale exists for combining several inhibitions with the aim of more completely blunting adenosine production and signaling, but no similar research has been conducted on GC. It is worth noting that the combination therapy may improves the treatment outcome but it also carries more side-effect burden.

Combine adenosinergic pathway inhibitors with other cancer treatments.

Systemic immunosuppression greatly affects the chemotherapeutic anti-tumor effect. CD39 cell-surface

expression and activity is increased in patients with acute myeloid leukemia (AML) upon chemotherapy compared with diagnosis, and enrichment in CD39-expressing blasts is a marker of adverse prognosis in the clinic (130). Furthermore, extracellular vesicles from B cells through CD39 and CD73 vesicle-incorporated proteins hydrolyze eATP from chemotherapy-treated tumor cells into adenosine, thus impairing $CD8^+$ T cell responses (131). As receptor for adenosine signaling, elevated A2AR expression was also detected in recurrent tumor tissues with induction chemotherapy (132). These phenomena offer a preclinical proof for the administration of adenosine signaling inhibitors in combination with chemotherapy in cancers, possibly including GC. Notably, the addition of HER2-targeted therapies to first-line chemotherapy has improved the OS of patients with HER2-positive GC, and has become the standard-of-care treatment for this group of patients (133). In breast cancer, high levels of CD73 gene expression are associated significantly with poor clinical outcome and promote resistance to HER2 antibody therapy (134). However, whether inhibitors of adenosinergic signaling pathway can be used to increase the efficacy of HER2-targeted therapy in GC needs to be further demonstrated. Various forms of immunotherapy are proving to be effective at restoring T cell-mediated immune responses that can lead to marked and sustained clinical responses, especially ICIs and CAR T-cell therapy. However, the efficacy of various immunotherapies for solid tumor is still mediocre because of immunosuppression in the TME. Hypoxia and cell damage, as common phenomena in solid tumors, are strongly linked to hallmarks of cancers and facilitate the production of immunosuppressive adenosine. The studies revealed that targeted blockade of CD73 can enhance the therapeutic activity of anti-PD-1 and anti-CTLA-4 monoclonal antibodies and may thus potentiate therapeutic strategies targeting ICIs for colorectal cancer, breast cancer, and prostate cancer (126, 135). Previous studies have shown that adenosine generated by tumor cells potently inhibits CAR T-cell responses through activation of A2AR. Therefore, using either A2AR antagonists or genetic targeting of A2AR using short hairpin RNA can profoundly increase CAR T-cell efficacy, particularly when combined with PD-1 blockade (136). In addition, disrupting A2AR gene in human CAR T-cell with CRISPR-Cas9 increased the anti-tumor function and prevented the exhaustion of CAR T-cells (137). Mechanistically, human A2AR-edited CAR T-cells are significantly resistant to adenosine-mediated transcriptional changes, resulting in enhanced production of cytokines including interferon-γ and tumor necrosis factor-α, and increased expression of JAK-STAT signaling pathway associated genes (138). The purpose of combination therapy is to combine separate mechanisms of action that will make malignant cells more sensitive to therapeutic agent and acquire better curative effect, but no similar research has been conducted on GC.

Promote adenosine metabolism to attenuate the immunosuppressive ability of TME

In addition to the above methods, accelerating the metabolism of adenosine within TME also can restore an anti-tumor immune competence. Emanuele Sasso et al. encoded adenosine deaminase (ADA)into an oncolytic targeted herpes virus to improve enzyme secretion for the metabolism of adenosine, and the clearance of adenosine within the TME reversed HER2-positive breast cancer resistance to trastuzumab (139).

Conclusion

The growth and progression of solid tumors are strongly affected by adenosine metabolic changes and interplay with the TME that sustain tumor development and immune escape. We explored the expression pattern and prognostic value of common immune checkpoints in GC patients *via* GEPIA database. Compared with other targets, adenosinergic pathway plays an indispensable role in the occurrence and development of GC, especially CD73. The components of adenosinergic pathway on both GC cells and immune cells sustains immunosuppressive TME by affecting multiple aspects of the immune response. Furthermore, some emerging antagonists of adenosinergic pathway show therapeutic potential in the preliminary studies of other malignancies. Therefore, these findings uncovered a mechanism by which immunosuppressive adenosine participates in the immune tolerance of GC, implying the potential of adenosinergic pathway as a therapeutic target or predictive marker for GC patients. However, On the basis of the limited evidence available as of now, elaborate clinical evaluation is further warranted to confirm whether the adenosinergic-targeting therapies are suitable for GC patients.

Author contributions

J-QW: writing of original manuscript. L-YD: revision of the manuscript. X-JC: language modification of the manuscript. All authors contributed to the article and approved the submitted version.

Funding

This work was supported by Wenzhou Science & Technology Bureau Foundation (Grant No. Y2020144 to X-JC) and National Natural Science Foundation of China under (Grant No. 81902151 to L-YD).

Acknowledgments

All authors contributed to the conception of the study and the preparation and approval of the paper.

Conflict of interest

The authors declare that the research was conducted in the absence of any commercial or financial relationships that could be construed as a potential conflict of interest.

Publisher's note

References

1. Sexton RE, Al Hallak MN, Diab M, Azmi AS. Gastric cancer: A comprehensive review of current and future treatment strategies. *Cancer Metastasis Rev* (2020) 39(4):1179–203. doi: 10.1007/s10555-020-09925-3

2. Li GZ, Doherty GM, Wang J. Surgical management of gastric cancer: A review. *JAMA Surg* (2022) 157(5):446–54. doi: 10.1001/jamasurg.2022.0182

3. Ngamruengphong S, Ferri L, Aihara H, Draganov PV, Yang DJ, Perbtani YB, et al. Efficacy of endoscopic submucosal dissection for superficial gastric neoplasia in a Large cohort in north America. *Clin Gastroenterol Hepatol* (2021) 19(8):1611–9.e1. doi: 10.1016/j.cgh.2020.06.023

4. Li WQ, Qin XX, Li ZX, Wang LH, Liu ZC, Fan XH, et al. Beneficial effects of endoscopic screening on gastric cancer and optimal screening interval: A population-based study. *Endoscopy* (2021) 54(9):848–58. doi: 10.1055/a-1728-5673

5. He X, Wu L, Dong Z, Gong D, Jiang X, Zhang H, et al. Real-time use of artificial intelligence for diagnosing early gastric cancer by magnifying image-enhanced endoscopy: A multicenter diagnostic study (with videos). *Gastrointest Endosc* (2022) 95(4):671–8.e4. doi: 10.1016/j.gie.2021.11.040

6. Jin X, Liu Z, Yang D, Yin K, Chang X. Recent progress and future perspectives of immunotherapy in advanced gastric cancer. *Front Immunol* (2022) 13:948647. doi: 10.3389/fimmu.2022.948647

7. Zhu X, Su T, Wang S, Zhou H, Shi W. New advances in nano-drug delivery systems: Helicobacter pylori and gastric cancer. *Front Oncol* (2022) 12:834934. doi: 10.3389/fonc.2022.834934

8. Bausys A, Mazeikaite M, Bickaite K, Bausys B, Bausys R, Strupas K. The role of prehabilitation in modern esophagogastric cancer surgery: A comprehensive review. *Cancers (Basel)* (2022) 14(9):2096. doi: 10.3390/cancers14092096

9. Li Z, Bai B, Zhao Y, Yu D, Lian B, Liu Y, et al. Severity of complications and long-term survival after laparoscopic total gastrectomy with D2 lymph node dissection for advanced gastric cancer: A propensity score-matched, case-control study. *Int J Surg* (2018) 54(Pt A):62–9. doi: 10.1016/j.ijsu.2018.04.034

10. Jiang H, Cui J, Chu H, Xu T, Xie M, Jing X, et al. Targeting Il8 as a sequential therapy strategy to overcome chemotherapy resistance in advanced gastric cancer. *Cell Death Discovery* (2022) 8(1):235. doi: 10.1038/s41420-022-01033-1

11. Li H, Huang H, Zhang T, Feng H, Wang S, Zhang Y, et al. Apatinib: A novel antiangiogenic drug in monotherapy or combination immunotherapy for digestive system malignancies. *Front Immunol* (2022) 13:937307. doi: 10.3389/fimmu.2022.937307

12. Zhu Y, Zhu X, Wei X, Tang C, Zhang W. Her2-targeted therapies in gastric cancer. *Biochim Biophys Acta Rev Cancer* (2021) 1876(1):188549. doi: 10.1016/j.bbcan.2021.188549

13. Myer NM, Shitara K, Chung HC, Lordick F, Kelly RJ, Szabo Z, et al. Evolution of predictive and prognostic biomarkers in the treatment of advanced gastric cancer. *J Cancer Res Clin Oncol* (2022) 148(8):2023–43. doi: 10.1007/s00432-021-03902-1

14. Kumar V, Ramnarayanan K, Sundar R, Padmanabhan N, Srivastava S, Koiwa M, et al. Single-cell atlas of lineage states, tumor microenvironment, and subtype-specific expression programs in gastric cancer. *Cancer Discovery* (2022) 12(3):670–91. doi: 10.1158/2159-8290.Cd-21-0683

15. Finck AV, Blanchard T, Roselle CP, Golinelli G, June CH. Engineered cellular immunotherapies in cancer and beyond. *Nat Med* (2022) 28(4):678–89. doi: 10.1038/s41591-022-01765-8

16. Havel JJ, Chowell D, Chan TA. The evolving landscape of biomarkers for checkpoint inhibitor immunotherapy. *Nat Rev Cancer* (2019) 19(3):133–50. doi: 10.1038/s41568-019-0116-x

17. Högner A, Moehler M. Immunotherapy in gastric cancer. *Curr Oncol* (2022) 29(3):1559–74. doi: 10.3390/curroncol29030131

18. Myint ZW, Goel G. Role of modern immunotherapy in gastrointestinal malignancies: A review of current clinical progress. *J Hematol Oncol* (2017) 10(1):86. doi: 10.1186/s13045-017-0454-7

19. Shitara K, Van Cutsem E, Bang YJ, Fuchs C, Wyrwicz L, Lee KW, et al. Efficacy and safety of pembrolizumab or pembrolizumab plus chemotherapy vs chemotherapy alone for patients with first-line, advanced gastric cancer: The keynote-062 phase 3 randomized clinical trial. *JAMA Oncol* (2020) 6(10):1571–80. doi: 10.1001/jamaoncol.2020.3370

20. Li S, Gao J, Xu Q, Zhang X, Huang M, Dai X, et al. A signature-based classification of gastric cancer that stratifies tumor immunity and predicts responses to pd-1 inhibitors. *Front Immunol* (2021) 12:693314. doi: 10.3389/fimmu.2021.693314

21. Takei S, Kawazoe A, Shitara K. The new era of immunotherapy in gastric cancer. *Cancers (Basel)* (2022) 14(4):1054. doi: 10.3390/cancers14041054

22. Shitara K, Özgüroğlu M, Bang YJ, Di Bartolomeo M, Mandalà M, Ryu MH, et al. Molecular determinants of clinical outcomes with pembrolizumab versus paclitaxel in a randomized, open-label, phase iii trial in patients with gastroesophageal adenocarcinoma. *Ann Oncol* (2021) 32(9):1127–36. doi: 10.1016/j.annonc.2021.05.803

23. Wang J, Sun J, Liu LN, Flies DB, Nie X, Toki M, et al. Siglec-15 as an immune suppressor and potential target for normalization cancer immunotherapy. *Nat Med* (2019) 25(4):656–66. doi: 10.1038/s41591-019-0374-x

24. Sun J, Lu Q, Sanmamed MF, Wang J. Siglec-15 as an emerging target for next-generation cancer immunotherapy. *Clin Cancer Res* (2021) 27(3):680–8. doi: 10.1158/1078-0432.Ccr-19-2925

25. Podojil JR, Miller SD. Potential targeting of B7-H4 for the treatment of cancer. *Immunol Rev* (2017) 276(1):40–51. doi: 10.1111/imr.12530

26. John P, Wei Y, Liu W, Du M, Guan F, Zang X. The B7x immune checkpoint pathway: From discovery to clinical trial. *Trends Pharmacol Sci* (2019) 40(11):883–96. doi: 10.1016/j.tips.2019.09.008

27. Rieder SA, Wang J, White N, Qadri A, Menard C, Stephens G, et al. B7-H7 (Hhla2) inhibits T-cell activation and proliferation in the presence of tcr and Cd28 signaling. *Cell Mol Immunol* (2021) 18(6):1503–11. doi: 10.1038/s41423-020-0361-7

28. Wei Y, Ren X, Galbo PMJr., Moerdler S, Wang H, Sica RA, et al. Kir3dl3-Hhla2 is a human immunosuppressive pathway and a therapeutic target. *Sci Immunol* (2021) 6(61):eabf9792. doi: 10.1126/sciimmunol.abf9792

29. Nimmerjahn F. Keeping T-he killers at bay *Via* fcγriib. *Immunity* (2020) 52(1):9–11. doi: 10.1016/j.immuni.2019.12.012

30. Morris AB, Farley CR, Pinelli DF, Adams LE, Cragg MS, Boss JM, et al. Signaling through the inhibitory fc receptor fcγriib induces Cd8(+) t cell apoptosis to limit T cell immunity. *Immunity* (2020) 52(1):136–50.e6. doi: 10.1016/j.immuni.2019.12.006

31. Moesta AK, Li XY, Smyth MJ. Targeting Cd39 in cancer. *Nat Rev Immunol* (2020) 20(12):739–55. doi: 10.1038/s41577-020-0376-4

32. Li XY, Moesta AK, Xiao C, Nakamura K, Casey M, Zhang H, et al. Targeting Cd39 in cancer reveals an extracellular atp- and inflammasome-driven tumor immunity. *Cancer Discovery* (2019) 9(12):1754–73. doi: 10.1158/2159-8290.Cd-19-0541

33. Freed-Pastor WA, Lambert LJ, Ely ZA, Pattada NB, Bhutkar A, Eng G, et al. The Cd155/Tigit axis promotes and maintains immune evasion in neoantigen-expressing pancreatic cancer. *Cancer Cell* (2021) 39(10):1342–60.e14. doi: 10.1016/j.ccell.2021.07.007

34. Kučan Brlić P, Lenac Roviš T, Cinamon G, Tsukerman P, Mandelboim O, Jonjić S. Targeting pvr (Cd155) and its receptors in anti-tumor therapy. *Cell Mol Immunol* (2019) 16(1):40–52. doi: 10.1038/s41423-018-0168-y

35. Wang X, Liu M, Zhang J, Brown NK, Zhang P, Zhang Y, et al. Cd24-siglec axis is an innate immune checkpoint against metaflammation and metabolic disorder. *Cell Metab* (2022) 34(8):1088–103.e6. doi: 10.1016/j.cmet.2022.07.005

36. Barkal AA, Brewer RE, Markovic M, Kowarsky M, Barkal SA, Zaro BW, et al. Cd24 signalling through macrophage siglec-10 is a target for cancer immunotherapy. *Nature* (2019) 572(7769):392–6. doi: 10.1038/s41586-019-1456-0

37. Xiong Z, Ampudia Mesias E, Pluhar GE, Rathe SK, Largaespada DA, Sham YY, et al. Cd200 checkpoint reversal: A novel approach to immunotherapy. *Clin Cancer Res* (2020) 26(1):232–41. doi: 10.1158/1078-0432.Ccr-19-2234

38. Choueiry F, Torok M, Shakya R, Agrawal K, Deems A, Benner B, et al. Cd200 promotes immunosuppression in the pancreatic tumor microenvironment. *J Immunother Cancer* (2020) 8(1):e000189. doi: 10.1136/jitc-2019-000189

39. Malissen N, Macagno N, Granjeaud S, Granier C, Moutardier V, Gaudy-Marqueste C, et al. Hvem has a broader expression than pd-L1 and constitutes a negative prognostic marker and potential treatment target for melanoma. *Oncoimmunology* (2019) 8(12):e1665976. doi: 10.1080/2162402x.2019.1665976

40. Mintz MA, Felce JH, Chou MY, Mayya V, Xu Y, Shui JW, et al. The hvem-btla axis restrains T cell help to germinal center b cells and functions as a cell-extrinsic suppressor in lymphomagenesis. *Immunity* (2019) 51(2):310–23.e7. doi: 10.1016/j.immuni.2019.05.022

41. Yang R, Sun L, Li CF, Wang YH, Yao J, Li H, et al. Galectin-9 interacts with pd-1 and Tim-3 to regulate T cell death and is a target for cancer immunotherapy. *Nat Commun* (2021) 12(1):832. doi: 10.1038/s41467-021-21099-2

42. Giovannone N, Liang J, Antonopoulos A, Geddes Sweeney J, King SL, Pochebit SM, et al. Galectin-9 suppresses b cell receptor signaling and is regulated by I-branching of n-glycans. *Nat Commun* (2018) 9(1):3287. doi: 10.1038/s41467-018-05770-9

43. Targeting Cd73 may improve immunotherapy efficacy in glioblastoma. *Cancer Discovery* (2020) 10(2):175. doi: 10.1158/2159-8290.Cd-rw2020-005

44. Young A, Ngiow SF, Barkauskas DS, Sult E, Hay C, Blake SJ, et al. Co-Inhibition of Cd73 and A2ar adenosine signaling improves anti-tumor immune responses. *Cancer Cell* (2016) 30(3):391–403. doi: 10.1016/j.ccell.2016.06.025

45. Crunkhorn S. Understanding Lag3 effects on T cells. *Nat Rev Drug Discovery* (2022) 21(6):416. doi: 10.1038/d41573-022-00083-5

46. Mullard A. Lag3 pushes immuno-oncology's leading edge. *Nat Rev Drug Discovery* (2022) 21(3):167–9. doi: 10.1038/d41573-022-00036-y

47. Mullard A. Immuno-oncology target tigit attracts a new contender. *Nat Rev Drug Discovery* (2021) 20(8):576. doi: 10.1038/d41573-021-00123-6

48. Banta KL, Xu X, Chitre AS, Au-Yeung A, Takahashi C, O'Gorman WE, et al. Mechanistic convergence of the tigit and pd-1 inhibitory pathways necessitates Co-blockade to optimize anti-tumor Cd8(+) T cell responses. *Immunity* (2022) 55 (3):512–26.e9. doi: 10.1016/j.immuni.2022.02.005

49. Huang X, Zhang X, Li E, Zhang G, Wang X, Tang T, et al. Vista: An immune regulatory protein checking tumor and immune cells in cancer immunotherapy. *J Hematol Oncol* (2020) 13(1):83. doi: 10.1186/s13045-020-00917-y

50. ElTanbouly MA, Zhao Y, Nowak E, Li J, Schaafsma E, Le Mercier I, et al. Vista is a checkpoint regulator for naïve T cell quiescence and peripheral tolerance. *Science* (2020) 367(6475):eaay0524. doi: 10.1126/science.aay0524

51. Kennedy R, Klein U. A T cell-b cell tumor-suppressive axis in the germinal center. *Immunity* (2019) 51(2):204–6. doi: 10.1016/j.immuni.2019.07.006

52. Jones A, Bourque J, Kuehm L, Opejin A, Teague RM, Gross C, et al. Immunomodulatory functions of btla and hvem govern induction of extrathymic regulatory T cells and tolerance by dendritic cells. *Immunity* (2016) 45(5):1066–77. doi: 10.1016/j.immuni.2016.10.008

53. Goodman A, Patel SP, Kurzrock R. Pd-1-Pd-L1 immune-checkpoint blockade in b-cell lymphomas. *Nat Rev Clin Oncol* (2017) 14(4):203–20. doi: 10.1038/nrclinonc.2016.168

54. Jiang X, Wang J, Deng X, Xiong F, Ge J, Xiang B, et al. Role of the tumor microenvironment in pd-L1/Pd-1-Mediated tumor immune escape. *Mol Cancer* (2019) 18(1):10. doi: 10.1186/s12943-018-0928-4

55. Kanchan RK, Doss D, Khan P, Nasser MW, Mahapatra S. To kill a cancer: Targeting the immune inhibitory checkpoint molecule, B7-H3. *Biochim Biophys Acta Rev Cancer* (2022) 1877(5):188783. doi: 10.1016/j.bbcan.2022.188783

56. Yang S, Wei W, Zhao Q. B7-H3, a checkpoint molecule, as a target for cancer immunotherapy. *Int J Biol Sci* (2020) 16(11):1767–73. doi: 10.7150/ijbs.41105

57. Du X, Tang F, Liu M, Su J, Zhang Y, Wu W, et al. A reappraisal of ctla-4 checkpoint blockade in cancer immunotherapy. *Cell Res* (2018) 28(4):416–32. doi: 10.1038/s41422-018-0011-0

58. Rowshanravan B, Halliday N, Sansom DM. Ctla-4: A moving target in immunotherapy. *Blood* (2018) 131(1):58–67. doi: 10.1182/blood-2017-06-741033

59. Feng M, Jiang W, Kim BYS, Zhang CC, Fu YX, Weissman IL. Phagocytosis checkpoints as new targets for cancer immunotherapy. *Nat Rev Cancer* (2019) 19 (10):568–86. doi: 10.1038/s41568-019-0183-z

60. Logtenberg MEW, Scheeren FA, Schumacher TN. The Cd47-sirpα immune checkpoint. *Immunity* (2020) 52(5):742–52. doi: 10.1016/j.immuni.2020.04.011

61. Jiang T, Xu X, Qiao M, Li X, Zhao C, Zhou F, et al. Comprehensive evaluation of Nt5e/Cd73 expression and its prognostic significance in distinct types of cancers. *BMC Cancer* (2018) 18(1):267. doi: 10.1186/s12885-018-4073-7

62. He X, Gu Y, Cao Y, Hu B, Fang H, Fei Y, et al. Impact of intratumoural Cd73 expression on prognosis and therapeutic response in patients with gastric cancer. *Eur J Cancer* (2021) 157:114–23. doi: 10.1016/j.ejca.2021.08.006

63. Xu Z, Gu C, Yao X, Guo W, Wang H, Lin T, et al. Cd73 promotes tumor metastasis by modulating Rics/Rhoa signaling and emt in gastric cancer. *Cell Death Dis* (2020) 11(3):202. doi: 10.1038/s41419-020-2403-6

64. Liu Z, Wu X, Wang Q, Li Z, Liu X, Sheng X, et al. Cd73-adenosine a(1)R axis regulates the activation and apoptosis of hepatic stellate cells through the plc-Ip(3)-Ca(2+)/Dag-Pkc signaling pathway. *Front Pharmacol* (2022) 13:922885. doi: 10.3389/fphar.2022.922885

65. Nagate Y, Ezoe S, Fujita J, Okuzaki D, Motooka D, Ishibashi T, et al. Ectonucleotidase Cd39 is highly expressed on atll cells and is responsible for their immunosuppressive function. *Leukemia* (2021) 35(1):107–18. doi: 10.1038/s41375-020-0788-y

66. Franco R, Rivas-Santisteban R, Navarro G, Reyes-Resina I. Adenosine receptor antagonists to combat cancer and to boost anti-cancer chemotherapy and immunotherapy. *Cells* (2021) 10(11):2831. doi: 10.3390/cells10112831

67. Takenaka MC, Robson S, Quintana FJ. Regulation of the T cell response by Cd39. *Trends Immunol* (2016) 37(7):427–39. doi: 10.1016/j.it.2016.04.009

68. Kepp O, Bezu L, Yamazaki T, Di Virgilio F, Smyth MJ, Kroemer G, et al. Atp and cancer immunosurveillance. *EMBO J* (2021) 40(13):e108130. doi: 10.15252/embj.2021108130

69. Linden J, Koch-Nolte F, Dahl G. Purine release, metabolism, and signaling in the inflammatory response. *Annu Rev Immunol* (2019) 37:325–47. doi: 10.1146/annurev-immunol-051116-052406

70. de Andrade Mello P, Coutinho-Silva R, Savio LEB. Multifaceted effects of extracellular adenosine triphosphate and adenosine in the tumor-host interaction and therapeutic perspectives. *Front Immunol* (2017) 8:1526. doi: 10.3389/fimmu.2017.01526

71. Garcia-Jacobo RE, Bergamin LS, Vultaggio-Poma V, Thorstenberg ML, Tarantini M, García-Hernández MH, et al. The purinergic landscape of type 2 diabetes mellitus. *Molecules* (2022) 27(6):1838. doi: 10.3390/molecules27061838

72. Di Virgilio F, Sarti AC, Falzoni S, De Marchi E, Adinolfi E. Extracellular atp and P2 purinergic signalling in the tumour microenvironment. *Nat Rev Cancer* (2018) 18(10):601–18. doi: 10.1038/s41568-018-0037-0

73. McCarthy AE, Yoshioka C, Mansoor SE. Full-length P2x(7) structures reveal how palmitoylation prevents channel desensitization. *Cell* (2019) 179 (3):659–70.e13. doi: 10.1016/j.cell.2019.09.017

74. Cao F, Hu LQ, Yao SR, Hu Y, Wang DG, Fan YG, et al. P2x7 receptor: A potential therapeutic target for autoimmune diseases. *Autoimmun Rev* (2019) 18 (8):767–77. doi: 10.1016/j.autrev.2019.06.009

75. Zhang T, Tsutsuki H, Islam W, Ono K, Takeda K, Akaike T, et al. Atp exposure stimulates glutathione efflux as a necessary switch for Nlrp3 inflammasome activation. *Redox Biol* (2021) 41:101930. doi: 10.1016/j.redox.2021.101930

76. Ahn Y, Seo J, Lee EJ, Kim JY, Park MY, Hwang S, et al. Atp-P2x7-Induced inflammasome activation contributes to melanocyte death and Cd8(+) T-cell trafficking to the skin in vitiligo. *J Invest Dermatol* (2020) 140(9):1794–804.e4. doi: 10.1016/j.jid.2019.12.035

77. Scott BM, Gutiérrez-Vázquez C, Sanmarco LM, da Silva Pereira JA, Li Z, Plasencia A, et al. Self-tunable engineered yeast probiotics for the treatment of inflammatory bowel disease. *Nat Med* (2021) 27(7):1212–22. doi: 10.1038/s41591-021-01390-x

78. Kaplanski G. Interleukin-18: Biological properties and role in disease pathogenesis. *Immunol Rev* (2018) 281(1):138–53. doi: 10.1111/imr.12616

79. Schenk U, Frascoli M, Proietti M, Geffers R, Traggiai E, Buer J, et al. Atp inhibits the generation and function of regulatory T cells through the activation of

purinergic P2x receptors. *Sci Signaling* (2011) 4(162):ra12–ra. doi: 10.1126/scisignal.2001270

80. Cuthbertson P, Geraghty NJ, Adhikary SR, Casolin S, Watson D, Sluyter R. P2x7 receptor antagonism increases regulatory T cells and reduces clinical and histological graft-Versus-Host disease in a humanised mouse model. *Clin Sci (Lond)* (2021) 135(3):495–513. doi: 10.1042/cs20201352

81. Yang R, Elsaadi S, Misund K, Abdollahi P, Vandsemb EN, Moen SH, et al. Conversion of atp to adenosine by Cd39 and Cd73 in multiple myeloma can be successfully targeted together with adenosine receptor A2a blockade. *J Immunother Cancer* (2020) 8(1):e000610. doi: 10.1136/jitc-2020-000610

82. Horenstein AL, Chillemi A, Zini R, Quarona V, Bianchi N, Manfredini R, et al. Cytokine-induced killer cells express Cd39, Cd38, Cd203a, Cd73 ectoenzymes and P1 adenosinergic receptors. *Front Pharmacol* (2018) 9:196. doi: 10.3389/fphar.2018.00196

83. Jackson EK, Cheng D, Verrier JD, Janesko-Feldman K, Kochanek PM. Interactive roles of Cd73 and tissue nonspecific alkaline phosphatase in the renal vascular metabolism of 5'-amp. *Am J Physiol Renal Physiol* (2014) 307(6):F680–5. doi: 10.1152/ajprenal.00312.2014

84. Alarcón S, Toro M, Villarreal C, Melo R, Fernández R, Ayuso Sacido A, et al. Decreased equilibrative nucleoside transporter 1 (Ent1) activity contributes to the high extracellular adenosine levels in mesenchymal glioblastoma stem-like cells. *Cells* (2020) 9(8):1914. doi: 10.3390/cells9081914

85. Aherne CM, Collins CB, Rapp CR, Olli KE, Perrenoud L, Jedlicka P, et al. Coordination of Ent2-dependent adenosine transport and signaling dampens mucosal inflammation. *JCI Insight* (2018) 3(20):e121521. doi: 10.1172/jci.insight.121521

86. Zhulai G, Oleinik E, Shibaev M, Ignatev K. Adenosine-metabolizing enzymes, adenosine kinase and adenosine deaminase, in cancer. *Biomolecules* (2022) 12(3):418. doi: 10.3390/biom12030418

87. Sek K, Mølck C, Stewart GD, Kats L, Darcy PK, Beavis PA. Targeting adenosine receptor signaling in cancer immunotherapy. *Int J Mol Sci* (2018) 19 (12):3837. doi: 10.3390/ijms19123837

88. Muller-Haegele S, Muller L, Whiteside TL. Immunoregulatory activity of adenosine and its role in human cancer progression. *Expert Rev Clin Immunol* (2014) 10(7):897–914. doi: 10.1586/1744666x.2014.915739

89. Mazziotta C, Rotondo JC, Lanzillotti C, Campione G, Martini F, Tognon M. Cancer biology and molecular genetics of a(3) adenosine receptor. *Oncogene* (2022) 41(3):301–8. doi: 10.1038/s41388-021-02090-z

90. Gao ZG, Jacobson KA. A(2b) adenosine receptor and cancer. *Int J Mol Sci* (2019) 20(20):5139. doi: 10.3390/ijms20205139

91. Mastelic-Gavillet B, Navarro Rodrigo B, Décombaz L, Wang H, Ercolano G, Ahmed R, et al. Adenosine mediates functional and metabolic suppression of peripheral and tumor-infiltrating Cd8(+) T cells. *J Immunother Cancer* (2019) 7 (1):257. doi: 10.1186/s40425-019-0719-5

92. Fong L, Hotson A, Powderly JD, Sznol M, Heist RS, Choueiri TK, et al. Adenosine 2a receptor blockade as an immunotherapy for treatment-refractory renal cell cancer. *Cancer Discovery* (2020) 10(1):40–53. doi: 10.1158/2159-8290.Cd-19-0980

93. Amaral EP, Machado de Salles É, Barbosa Bomfim CC, Salgado RM, Almeida FM, de Souza PC, et al. Inhibiting adenosine receptor signaling promotes accumulation of effector Cd4+ T cells in the lung parenchyma during severe tuberculosis. *J Infect Dis* (2019) 219(6):964–74. doi: 10.1093/infdis/jiy586

94. Zhou SN, Zhang N, Liu HH, Xia P, Zhang C, Song JW, et al. Skewed Cd39/Cd73/Adenosine pathway contributes to b-cell hyperactivation and disease progression in patients with chronic hepatitis b. *Gastroenterol Rep (Oxf)* (2021) 9 (1):49–58. doi: 10.1093/gastro/goaa048

95. Neo SY, Yang Y, Record J, Ma R, Chen X, Chen Z, et al. Cd73 immune checkpoint defines regulatory nk cells within the tumor microenvironment. *J Clin Invest* (2020) 130(3):1185–98. doi: 10.1172/jci128895

96. Young A, Ngiow SF, Gao Y, Patch AM, Barkauskas DS, Messaoudene M, et al. A2ar adenosine signaling suppresses natural killer cell maturation in the tumor microenvironment. *Cancer Res* (2018) 78(4):1003–16. doi: 10.1158/0008-5472.Can-17-2826

97. Perez CR, De Palma M. Engineering dendritic cell vaccines to improve cancer immunotherapy. *Nat Commun* (2019) 10(1):5408. doi: 10.1038/s41467-019-13368-y

98. Challier J, Bruniquel D, Sewell AK, Laugel B. Adenosine and camp signalling skew human dendritic cell differentiation towards a tolerogenic phenotype with defective Cd8(+) T-cell priming capacity. *Immunology* (2013) 138(4):402–10. doi: 10.1111/imm.12053

99. Zumerle S, Calì B, Munari F, Angioni R, Di Virgilio F, Molon B, et al. Intercellular calcium signaling induced by atp potentiates macrophage phagocytosis. *Cell Rep* (2019) 27(1):1–10.e4. doi: 10.1016/j.celrep.2019.03.011

100. Montalbán Del Barrio I, Penski C, Schlahsa L, Stein RG, Diessner J, Wöckel A, et al. Adenosine-generating ovarian cancer cells attract myeloid cells which differentiate into adenosine-generating tumor associated macrophages - a self-amplifying, Cd39- and Cd73-dependent mechanism for tumor immune escape. *J Immunother Cancer* (2016) 4:49. doi: 10.1186/s40425-016-0154-9

101. Groth C, Hu X, Weber R, Fleming V, Altevogt P, Utikal J, et al. Immunosuppression mediated by myeloid-derived suppressor cells (Mdscs) during tumour progression. *Br J Cancer* (2019) 120(1):16–25. doi: 10.1038/s41416-018-0333-1

102. Yu M, Guo G, Huang L, Deng L, Chang CS, Achyut BR, et al. Cd73 on cancer-associated fibroblasts enhanced by the a(2b)-mediated feedforward circuit enforces an immune checkpoint. *Nat Commun* (2020) 11(1):515. doi: 10.1038/s41467-019-14060-x

103. Pietrobono D, Giacomelli C, Marchetti L, Martini C, Trincavelli ML. High adenosine extracellular levels induce glioblastoma aggressive traits modulating the mesenchymal stromal cell secretome. *Int J Mol Sci* (2020) 21(20):7706. doi: 10.3390/ijms21207706

104. Tripathi A, Lin E, Xie W, Flaifel A, Steinharter JA, Stern Gatof EN, et al. Prognostic significance and immune correlates of Cd73 expression in renal cell carcinoma. *J Immunother Cancer* (2020) 8(2):e001467. doi: 10.1136/jitc-2020-001467

105. Antonioli L, Blandizzi C, Pacher P, Haskó G. Immunity, inflammation and cancer: A leading role for adenosine. *Nat Rev Cancer* (2013) 13(12):842–57. doi: 10.1038/nrc3613

106. Draganov D, Lee PP. Purinergic signaling within the tumor microenvironment. *Adv Exp Med Biol* (2021) 1270:73–87. doi: 10.1007/978-3-030-47189-7_5

107. Mao C, Yeh S, Fu J, Porosnicu M, Thomas A, Kucera GL, et al. Delivery of an ectonucleotidase inhibitor with ros-responsive nanoparticles overcomes adenosine-mediated cancer immunosuppression. *Sci Transl Med* (2022) 14(648): eabh1261. doi: 10.1126/scitranslmed.abh1261

108. Cai XY, Wang XF, Li J, Dong JN, Liu JQ, Li NP, et al. High expression of Cd39 in gastric cancer reduces patient outcome following radical resection. *Oncol Lett* (2016) 12(5):4080–6. doi: 10.3892/ol.2016.5189

109. Nakachi S, Okamoto S, Tamaki K, Nomura I, Tomihama M, Nishi Y, et al. Impact of anti-diabetic sodium-glucose cotransporter 2 inhibitors on tumor growth of intractable hematological malignancy in humans. *BioMed Pharmacother* (2022) 149:112864. doi: 10.1016/j.biopha.2022.112864

110. Cao X, Zhu Z, Cao Y, Hu J, Min M. Cd73 is a hypoxia-responsive gene and promotes the warburg effect of human gastric cancer cells dependent on its enzyme activity. *J Cancer* (2021) 12(21):6372–82. doi: 10.7150/jca.62387

111. Shi L, Wu Z, Miao J, Du S, Ai S, Xu E, et al. Adenosine interaction with adenosine receptor A2a promotes gastric cancer metastasis by enhancing Pi3k-Akt-Mtor signaling. *Mol Biol Cell* (2019) 30(19):2527–34. doi: 10.1091/mbc.E19-03-0136

112. Liu G, Yang S, Liu Y, Xu Y, Qiu H, Sun J, et al. The adenosine-A2a receptor regulates the radioresistance of gastric cancer *Via* Pi3k-Akt-Mtor pathway. *Int J Clin Oncol* (2022) 27(5):911–20. doi: 10.1007/s10147-022-02123-x

113. Shi L, Yang L, Wu Z, Xu W, Song J, Guan W. Adenosine signaling: Next checkpoint for gastric cancer immunotherapy? *Int Immunopharmacol* (2018) 63:58–65. doi: 10.1016/j.intimp.2018.07.023

114. Shi L, Feng M, Du S, Wei X, Song H, Yixin X, et al. Adenosine generated by regulatory T cells induces Cd8(+) T cell exhaustion in gastric cancer through A2ar pathway. *BioMed Res Int* (2019) 2019:4093214. doi: 10.1155/2019/4093214

115. Sundström P, Stenstad H, Langenes V, Ahlmanner F, Theander L, Ndah TG, et al. Regulatory T cells from colon cancer patients inhibit effector T-cell migration through an adenosine-dependent mechanism. *Cancer Immunol Res* (2016) 4(3):183–93. doi: 10.1158/2326-6066.Cir-15-0050

116. Liu HY, Wang FH, Liang JM, Xiang YY, Liu SH, Zhang SW, et al. Targeting nad metabolism regulates extracellular adenosine levels to improve the cytotoxicity of Cd8+ effector T cells in the tumor microenvironment of gastric cancer. *J Cancer Res Clin Oncol* (2022). doi: 10.1007/s00432-022-04124-9

117. Sutton NR, Bouïs D, Mann KM, Rashid IM, McCubbrey AL, Hyman MC, et al. Cd73 promotes age-dependent accretion of atherosclerosis. *Arterioscler Thromb Vasc Biol* (2020) 40(1):61–71. doi: 10.1161/atvbaha.119.313002

118. Knight JS, Mazza LF, Yalavarthi S, Sule G, Ali RA, Hodgin JB, et al. Ectonucleotidase-mediated suppression of lupus autoimmunity and vascular dysfunction. *Front Immunol* (2018) 9:1322. doi: 10.3389/fimmu.2018.01322

119. Kulkarni N, Meitei HT, Sonar SA, Sharma PK, Mujeeb VR, Srivastava S, et al. Ccr6 signaling inhibits suppressor function of induced-treg during gut inflammation. *J Autoimmun* (2018) 88:121–30. doi: 10.1016/j.jaut.2017.10.013

120. Zhang M, Hu S, Min M, Ni Y, Lu Z, Sun X, et al. Dissecting transcriptional heterogeneity in primary gastric adenocarcinoma by single cell rna sequencing. *Gut* (2021) 70(3):464–75. doi: 10.1136/gutjnl-2019-320368

121. Ichikawa H, Nagahashi M, Shimada Y, Hanyu T, Ishikawa T, Kameyama H, et al. Actionable gene-based classification toward precision medicine in gastric cancer. *Genome Med* (2017) 9(1):93. doi: 10.1186/s13073-017-0484-3

122. Zhang H, Yang M, Wu X, Li Q, Li X, Zhao Y, et al. The distinct roles of exosomes in tumor-stroma crosstalk within gastric tumor microenvironment. *Pharmacol Res* (2021) 171:105785. doi: 10.1016/j.phrs.2021.105785

123. Zhao L, Liu Y, Zhang S, Wei L, Cheng H, Wang J, et al. Impacts and mechanisms of metabolic reprogramming of tumor microenvironment for immunotherapy in gastric cancer. *Cell Death Dis* (2022) 13(4):378. doi: 10.1038/s41419-022-04821-w

124. Nakahama T, Kawahara Y. Adenosine-to-Inosine rna editing in the immune system: Friend or foe? *Cell Mol Life Sci* (2020) 77(15):2931–48. doi: 10.1007/s00018-020-03466-2

125. Allard B, Allard D, Buisseret L, Stagg J. The adenosine pathway in immuno-oncology. *Nat Rev Clin Oncol* (2020) 17(10):611–29. doi: 10.1038/s41571-020-0382-2

126. Perrot I, Michaud HA, Giraudon-Paoli M, Augier S, Docquier A, Gros L, et al. Blocking antibodies targeting the Cd39/Cd73 immunosuppressive pathway unleash immune responses in combination cancer therapies. *Cell Rep* (2019) 27 (8):2411–25.e9. doi: 10.1016/j.celrep.2019.04.091

127. Adamiak M, Bujko K, Brzezniakiewicz-Janus K, Kucia M, Ratajczak J, Ratajczak MZ. The inhibition of Cd39 and Cd73 cell surface ectonucleotidases by small molecular inhibitors enhances the mobilization of bone marrow residing stem cells by decreasing the extracellular level of adenosine. *Stem Cell Rev Rep* (2019) 15(6):892–9. doi: 10.1007/s12015-019-09918-y

128. Ma XL, Shen MN, Hu B, Wang BL, Yang WJ, Lv LH, et al. Cd73 promotes hepatocellular carcinoma progression and metastasis *Via* activating Pi3k/Akt signaling by inducing Rap1-mediated membrane localization of P110β and predicts poor prognosis. *J Hematol Oncol* (2019) 12(1):37. doi: 10.1186/s13045-019-0724-7

129. Wang Y, Copeland J, Shin M, Chang Y, Venton BJ. Cd73 or Cd39 deletion reveals different mechanisms of formation for spontaneous and mechanically stimulated adenosine and sex specific compensations in atp degradation. *ACS Chem Neurosci* (2020) 11(6):919–28. doi: 10.1021/acschemneuro.9b00620

130. Aroua N, Boet E, Ghisi M, Nicolau-Travers ML, Saland E, Gwilliam R, et al. Extracellular atp and Cd39 activate camp-mediated mitochondrial stress response to promote cytarabine resistance in acute myeloid leukemia. *Cancer Discovery* (2020) 10(10):1544–65. doi: 10.1158/2159-8290.Cd-19-1008

131. Zhang F, Li R, Yang Y, Shi C, Shen Y, Lu C, et al. Specific decrease in b-Cell-Derived extracellular vesicles enhances post-chemotherapeutic Cd8(+) T cell responses. *Immunity* (2019) 50(3):738–50.e7. doi: 10.1016/j.immuni.2019.01.010

132. Ma SR, Deng WW, Liu JF, Mao L, Yu GT, Bu LL, et al. Blockade of adenosine A2a receptor enhances Cd8(+) T cells response and decreases regulatory T cells in head and neck squamous cell carcinoma. *Mol Cancer* (2017) 16(1):99. doi: 10.1186/s12943-017-0665-0

133. Oh DY, Bang YJ. Her2-targeted therapies - a role beyond breast cancer. *Nat Rev Clin Oncol* (2020) 17(1):33–48. doi: 10.1038/s41571-019-0268-3

134. Turcotte M, Allard D, Mittal D, Bareche Y, Buisseret L, José V, et al. Cd73 promotes resistance to Her2/Erbb2 antibody therapy. *Cancer Res* (2017) 77 (20):5652–63. doi: 10.1158/0008-5472.Can-17-0707

135. Allard B, Pommey S, Smyth MJ, Stagg J. Targeting Cd73 enhances the antitumor activity of anti-Pd-1 and anti-Ctla-4 mabs. *Clin Cancer Res* (2013) 19 (20):5626–35. doi: 10.1158/1078-0432.Ccr-13-0545

136. Beavis PA, Henderson MA, Giuffrida L, Mills JK, Sek K, Cross RS, et al. Targeting the adenosine 2a receptor enhances chimeric antigen receptor T cell efficacy. *J Clin Invest* (2017) 127(3):929–41. doi: 10.1172/jci89455

137. Li N, Tang N, Cheng C, Hu T, Wei X, Han W, et al. Improving the anti-solid tumor efficacy of car-T cells by inhibiting adenosine signaling pathway. *Oncoimmunology* (2020) 9(1):1824643. doi: 10.1080/2162402x.2020.1824643

138. Giuffrida L, Sek K, Henderson MA, Lai J, Chen AXY, Meyran D, et al. Crispr/Cas9 mediated deletion of the adenosine A2a receptor enhances car T cell efficacy. *Nat Commun* (2021) 12(1):3236. doi: 10.1038/s41467-021-23331-5

139. Gentile C, Finizio A, Froechlich G, D'Alise AM, Cotugno G, Amiranda S, et al. Generation of a retargeted oncolytic herpes virus encoding adenosine deaminase for tumor adenosine clearance. *Int J Mol Sci* (2021) 22(24):13521. doi: 10.3390/ijms222413521

frontiers | Frontiers in Immunology

TYPE Original Research
PUBLISHED 02 December 2022
DOI 10.3389/fimmu.2022.1052717

OPEN ACCESS

EDITED BY
Ali Hafez El-Far,
Damanhour University, Egypt

REVIEWED BY
Lili Yang,
Ronald Reagan UCLA Medical Center, United States
Beatriz Martín-Antonio,
University Hospital Fundación Jiménez Díaz, Spain

*CORRESPONDENCE
Cheng Qian
cqian8634@gmail.com
Junjie Shen
junjiesh@gmail.com

SPECIALTY SECTION
This article was submitted to Cancer Immunity and Immunotherapy, a section of the journal Frontiers in Immunology

RECEIVED 24 September 2022
ACCEPTED 14 November 2022
PUBLISHED 02 December 2022

CITATION
Li W, Zhu X, Xu Y, Chen J, Zhang H, Yang Z, Qi Y, Hong J, Li Y, Wang G, Shen J and Qian C (2022) Simultaneous editing of TCR, HLA-I/II and HLA-E resulted in enhanced universal CAR-T resistance to allo-rejection. *Front. Immunol.* 13:1052717. doi: 10.3389/fimmu.2022.1052717

Simultaneous editing of TCR, HLA-I/II and HLA-E resulted in enhanced universal CAR-T resistance to allo-rejection

Wuling Li[1,2], Xiuxiu Zhu[1,2], Yanmin Xu[3], Jun Chen[3], Hongtao Zhang[3], Zhi Yang[3], Yanan Qi[3], Juan Hong[3], Yunyan Li[3], Guixue Wang[1,4], Junjie Shen[3]* and Cheng Qian[1,2]*

[1]Key Laboratory for Biorheological Science and Technology of Ministry of Education, College of Bioengineering, Chongqing University, Chongqing, China, [2]Center for Precision Medicine of Cancer, Chongqing Key Laboratory of Translational Research for Cancer Metastasis and Individualized Treatment, Chongqing University Cancer Hospital, Chongqing, China, [3]Chongqing Key Laboratory of Gene and Cell Therapy, Institute of Precision Medicine and Biotechnology, Chongqing Precision Biotech Co., Ltd., Chongqing, China, [4]Key Laboratory for Biorheological Science and Technology of Ministry of Education, State and Local Joint Engineering Laboratory for Vascular Implants, Bioengineering College of Chongqing University, Chongqing, China

Introduction: The major challenge for universal chimeric antigen receptor T cell (UCAR-T) therapy is the inability to persist for a long time in patients leading to inferior efficacy clinically. The objective of this study was to design a novel UCAR-T cell that could avoid the occurrence of allo-rejection and provide effective resistance to allogeneic Natural Killer (NK) cell rejection, together with the validation of its safety and efficacy *ex vivo* and *in vivo*.

Methods: We prepared T-cell receptor (TCR), Human leukocyte antigen (HLA)-I/II triple-edited (TUCAR-T) cells and evaluated the anti-tumor efficacy ex vivo and in vivo. We measured the resistance of exogenous HLA-E expressing TUCAR-T (ETUCAR-T) to NK rejection by using an enhanced NK. Furthermore, we established the safety and efficacy of this regimen by treating Nalm6 tumor-bearing mice with a repeated high-dose infusion of ETUCAR-T. Moreover, we analyzed the effects of individual gene deficiency CAR-T on treated mice and the changes in the transcriptional profiles of different gene-edited T cells *via* RNA-Seq.

Results: Data showed that HLA-II editing didn't impair the anti-tumor efficacy of TUCAR-T ex vivo and in vivo and we found for the first time that HLA-II deficiency could facilitate the persistence of CAR-T. Contrastively, as the most commonly eliminated target in UCAR-T, TCR deficiency was found to be a key disadvantageous factor for the shorter-term anti-tumor efficacy *in vivo*. Our study demonstrated ETUCAR-T could effectively resist allogeneic NK rejection *ex vivo* and *in vivo*.

Discussion: Our research provided a potential and effective strategy for promoting the persistence of UCAR-T cells in clinical application. And it reveals the potential key factors of the poor persistence of UCAR-T along with new insights for future development.

KEYWORDS

universal CAR, CRISPR/Cas9, ETUCAR-T, natural killer cell, HLA-E

Introduction

Revolutionary advances in cancer treatment by chimeric antigen receptor T-cell (CAR-T) therapy have been achieved, especially in hematological malignancies (1). Hundreds of preclinical and clinical trials on CAR-T therapy have been conducted worldwide. Up to now, six CAR-T products have been approved by the Food and Drug Administration (FDA) for the clinical treatment of hematological tumors. Nevertheless, this therapy has not been widely applied in cancer treatment due to the high cost and the long time consumption of individualized manufacturing in the production of autologous CAR-T cells. The development of off-the-shelf universal CAR-T (UCAR-T) therapy is considered as an attractive direction. However, UCAR-T therapy also faces the challenges of uncertain gene-editing operation regimes and a wide gap in clinical efficacy compared to traditional unedited autologous CAR-T.

By now, the reported strategies for UCAR-T therapy are based on the combination of knocking out the T-cell receptor (TCR) and clearing lymphocytes by the CD52 monoclonal antibody or simultaneously eliminating β2 microglobulin (B2M) and/or programmed cell death protein 1 (PD-1) by means of zinc finger nucleases (ZFNs) and transcription activator-like effector nucleases (TALENs) as well as clustered regularly interspaced short palindromic repeats/Cas9 protein (CRISPR/Cas9) (2). CRISPR/Cas9 is considered as a more favorable selection because of the superiority in single-target and higher editing efficiency. Since the first clinical study on UCAR-T therapy, which started in 2015, reported the achievement of molecular remission within 28 days in two cases of infantile leukemia (3), increasing clinical studies focusing on UCAR-T therapy have ensued (4, 5).

HLA-II molecules, which are mainly expressed on the surface of antigen-presenting cells (APCs), play an important role in organ transplantation. In the field of UCAR, Kagoya et al. found that HLA-II expression on activated T cells would rise to a varying level, by up to 50% (6). Importantly, our prior clinical studies also found that up to 90% of HLA-II was detected in ready-to-infuse autologous CAR-T. The inconsistent HLA-II^{pos} may be attributed to the different activation and stimulation approach during T-cell production. However, both findings support the necessity of HLA-II elimination (6). We then restrained the expression of HLA-II by editing the class II transactivator (CIITA) with CRISPR/Cas9 (7) and successfully obtained TCR/HLA-I/HLA-II triple-deficiency UCAR-T (TUCAR-T) cells. Interestingly, HLA-II deficiency was found to improve rather than attenuate the efficacy of CAR-T cells. Furthermore, we exogenously delivered an HLA-E gene, a member of HLA-I family, and generated ETUCAR-T that could escape from the attack of host NK cells (8, 9). The safety and efficacy of ETUCAR-T cells were fully tested both *ex vivo* and *in vivo*, and the results of multiple dosing in mice have been provisionally provided as a reference for clinical application.

Despite the improvements in several aspects, our data suggested that ETUCAR-T showed unsatisfactory persistence in NOD.CgPrkdcscidIl2rgtm1Sug/JicCrl (NOG) mice. We thus further investigated and obtained some novel insights about the differential impacts of the deficiencies of TCR, HLA-I, and HLA-II on CAR-T cells by whole transcriptional profiling using RNA-seq. To sum up, discoveries in our research provided significant evidence for revealing the key factors affecting UCAR-T function and provided us with new countermeasures for UCAR-T therapy in the future.

Abbreviations: CAR-T, chimeric antigen receptor T cell; UCAR-T, universal chimeric antigen receptor T cell; DUCAR-T, conventional TCR and HLA-I double gene–edited universal chimeric antigen receptor T cell; TUCAR-T, TCR, HLA-I/II triple gene–edited universal chimeric antigen receptor T cell; ETUCAR-T, TCR, HLA-I/II triple gene–edited universal chimeric antigen receptor T cell with an exogenous expression of HLA-E; NK, NK cells isolated from the peripheral blood of a healthy donor; NK^{mbIL15}, NK with an exogenous expression of membrane-bound IL15; NR4A3, nuclear receptor subfamily 4 group A member 3; EGR3, early growth response 3; POLR2L, NA polymerase II, I, and III subunit L; GvHD, xenogeneic graft-versus-host disease; GvHR, graft-versus-host reaction; HvGR, host-versus-graft reaction.

Materials and methods

Cells and culture conditions

PBMCs were isolated from healthy volunteer donors using a human peripheral blood lymphocyte separation solution (TBDscience Tianjin, China). Primary human T cells were isolated by the Pan T Cell Isolation Kit, human (Miltenyi Biotech, Bergisch Gladbach) and stimulated with Dynabeads^{TM} CD3/CD28 (Invitrogen, USA) at a density of 2×10^6 cells/ml in an immunocell medium (TBDscience Tianjin, China) with 10% fetal bovine serum (FBS) (Biological Industries Beit-Haemek, Israel), 50 IU/ml IL7, 50 IU/ml IL15, and 50 IU/ml IL21 (Peprotech, USA). Dynabeads were removed with a magnetic holder at 2~3 days after activation. CAR-T cells were cryopreserved at day 9 postactivation in a lab-created cryoprotectant for injection at 1×10^8 cells per vial. NK cells were isolated from PBMCs using human CD56 MicroBeads (Miltenyi Biotech, Bergisch Gladbach) and LS Columns (Miltenyi Biotech, Bergisch Gladbach) by the manufacturer's instructions (Miltenyi Biotech, Bergisch Gladbach) and cultured at a density of 1×10^6 cells/ml in an immunocell medium (TBDscience Tianjin, China) supplemented with 10% FBS (Biological Industries, Israel), 50I U/ml IL18 and 50 IU/ml IL2 (Peprotech, USA). NK was transduced with a lentiviral expression of membrane-bound IL15 at 2 ~ 3 days of activation, and experiments were performed at 9 days of NK activation.

All cell lines were STR-fingerprinted and validated to be mycoplasma-free by PCR. The human acute lymphoblastic leukemia cell line $CD19^+$ Nalm6, human chronic myeloid leukemia cell line $CD19^-$ K562, and human carcinoma cell line A549 were purchased from ATCC (Virginia, USA). The A549 cell line was transduced with CD19 antigen in the Pcdh vector using the lentiviral vector to create a new $CD19^+$ A549 cell line. Nalm6 and K562 cell lines were transduced with Luc-2A-GFP in the Pcdh vector using the lentiviral to create the new cell line Nalm6-Luc-GFP. Nalm6 and K562 were cultured in RPMI 1640 (Gibco, USA), and 293T and A549 were cultured in DMEM (Gibco, USA). All cell lines were cultured with a medium supplemented with 10% FBS and 100 IU/ml penicillin/streptomycin (Beyotime Shanghai, China).

Generation of constructs

CD19 CAR was synthesized and/or amplified by PCR as published based on sequencing information and subcloned into a lentiviral vector (10). Mutant HLA-E was a fusion protein consisting of a codon-optimized signal peptide of β2-microglobulin (Genscript, Nanjing, China) and HLA-E Cdna Open Reading Frame (ORF) Clone in Cloning Vector, Human (Sinobiological, China). The following primers were used in overlap PCR: β2-microglobulin forward (5′-GCTCTAGAATGAGCAGAAGCGT-3′) and reverse (5′-TACTTCAAGGAGTGGGAGCCCATGCTAGGAATTCGCTTCC-3′), HLA-E Cdna ORF forward (5′-GGCTCCCACTCCTT GAAGTATTTCCACACTTCCGTGTCCC-3′) and reverse (5′-GGGTGTACATTACAAGCTGT-3′).

Flow cytometry

Flow cytometry (FCM) results were acquired on a LSRFortessa™ (Becton, Dickinson and Company, USA) or Quanteon (Agilent, USA) and analyzed by FlowJo_v10.6.2 or NovoExpress 1.4.1. Non-transduced T cells (Ctrl-T) and isotype antibodies were used as controls. The Human Leukocyte Antigen (HLA)-DR antibody is used to detect HLA-II expression levels on the cell surface, and the β2-microglobulin or HLA class I antibody is used to detect HLA-I expression levels on the cell surface. Information on the antibodies used in this study is shown in the Supplementary Material. CD3, HLA-I, and HLA-DR triple-negative UCAR-T cells were isolated by the flow cytometry instrument FACSAria III (BD) on day 7 postactivation.

Clustered regularly interspaced short palindromic repeats design

The following genome targeting sequences were used in the study: TRAC: 5′-AGAGTCTCTCAGCTGGTACA-3′, B2M: 5′-GGCCGAGATGTCTCGCTCCG-3′, CIITA: 5′-GATATTGGCATAAGCCTCCC-3′. Primary human T cells were transduced with the CD19 CAR lentivirus at 24 h of activation and electroporated using 4D-NucleofectorTM X (Lonza, Germany) with RNP that was separately mixed by Cas9 protein (Gibco, USA) and chemically synthesized no-annealing-needed sgRNA (Genscript, China, bearing 2′-O-methyl at three first and last bases, 3′ phosphorothioate-modified bounds between three first and last bases) at a 1:1:1:3 mole ratio for 10–15 min at room temperature at 48 h postactivation.

Lentivirus production

Lentiviruses were collected from the supernatants of 293T cells transduced with the lentivirus vector and helper plasmids (PMD2.G, pMDLg/Prre, and Prsv-Rev) as we described previously (11). After harvesting the supernatant, the lentivirus was mixed with 50% Polyethylene Glycol (PEG) and 4M NaCl at a 6:2:1 ratio and centrifuged at 10,000 × g at 4°C for 1 h. The supernatant was discarded following centrifugation, and the precipitate was dissolved in an appropriate volume of saline. For all experiments related to lentiviral transduction, the multiplicity of infection used was 2 MOI.

On-target and predicted off-target Sanger sequencing

The genome of UCAR-T cells from three healthy donors was extracted, the on-targets or predicted off-targets fragments were amplified separately with their corresponding primers, and the fragments were ligated to the T vector (Takara, Japan) for sequencing. The on-target and predicted off-target primers for PCR amplified are listed in Supplementary Experimental Methods.

Luciferase-based Cytotoxic T Lymphocyte (CTL) assay

In a 96-well, U-bottom plate (NEST, USA), CAR-T cells (effectors) and Nalm6-Luc-GFP (targets) or K562-Luc-GFP (targets) were cultured together at 37°C for 24 h at various effector- to-target ratios (E:T or E/T); the targets were 1×10^4/well. Supernatants were harvested for cytokine secretion detection following the centrifugation of the plate. Avoiding the unequal transduction of CAR-positive in T cells, non-transduced Ctrl-T cells were supplemented to adjust both the number of CAR^+ T cells, and the total number of T cells remained consistent in all groups. The substrate was added with the DPPIV-Glo™ Protease Assay (Promega, USA) and immediately centrifuged and detected. The results are reported

as the percentage of killing based on the luciferase activity in the wells with tumor cells but without T cells [% killing=100−((RLU from well with effector and target cell coculture)/(RLU from well with target cells) ×100)].

Real-time cell analysis CTL assay

A cytotoxicity assay to test CAR-T cells with adherent target cells was operated using an electrical impedance–based approach, namely, xCELLigence real-time cell analysis (RTCA) SP/MP Analyzer (Roche, Switzerland). The cell index represents the relative change of the cell proliferation rate for several days of continuous monitoring. Firstly, the baseline measurement was operated by adding 50 µl of DMEM per well to E-plates (Roche, Switzerland). Then, 100 µl of DMEM containing 1×10^4 $CD19^{+/-}$ A549 target cells were added in E-plates per well, and electrical impedance was measured throughout the cultivation period with 15 min intervals throughout the culture period until the target cells were in logarithmic growth (total time: 12 h). Next, CAR-T cells (effectors) were plated at a 1:1 E/T ratio in E-plates in a volume of 100 µl per well, following by discarding 50 µl of the medium. Negative control was described above.

ELISA assays

The incubation supernatant was stored at -80°C. Samples were diluted in an appropriate ratio (the standard curve ranges from 30 to 300 pg/ml), and each sample was assayed in duplicate or triplicate using an IFN gamma Human Uncoated ELISA Kit (Invitrogen, USA). Data analysis was conducted according to the related protocol and algorithm by Varioskan LUX (Thermo Fisher Scientific). All data were within the range of the calibrated curves.

Allogeneic rejection analyzed

Donor CAR-T cells were cocultured with freshly isolated allogeneic PBMCs at the specified E/T ratios in a 200 µl RPMI 1640 medium supplemented with 10% FBS in U-bottomed, 96-well plates. To generate primed alloreactive T cells in a host-versus-graft reaction (HvGR), donor CAR-T cells were treated with mitomycin C (BioVision, USA) in 10 µg/ml and then stained with the 2 mM CellTrace CFSE Cell Proliferation Kit (CFSE) (Thermo Fisher Scientific), mixed with fresh allogeneic PBMCs that were stained with a 2 mM CellTrace Violet Cell Proliferation Kit (CTV) (Thermo Fisher Scientific) at a 1:1 ratio. Cell stimulation was analyzed by FCM on day 0 and 7 days later. On the contrary, fresh allogeneic PBMCs were treated with mitomycin C (BioVision, USA) in 10 µg/ml mixed with donor CAR-T cells at a 1:1 ratio in an RPMI 1640 medium supplemented with 10% FBS in a graft-versus-host reaction (GvHR).

Mouse xenograft studies

The Nalm6 tumor model established: 8~10-week-old NOG mice line NOD. Cg-PrkdcscidIl2rgtm1Sug/JicCrl (GemPharmatech, China) was transplanted intravenously with 5×10^5 Nalm6-Luc-GFP tumor cells in the tail vein. CAR-T cells (2×10^6, activation for 9 days) were infused 3 days later. Euthanasia was administered when necessary. In Figures 3F, G and Figures S2E, F, tumors were established in NOG mice (n = 3 per group) by the intravenous injection of 5×10^5 Nalm6- Luc-GFP cells on day -3. Beginning on day 0, UCAR-T cells (2×10^6) were infused with a single injection. Ctrl-T cells were injected as the control group. NK^{mbIL15} was injected 6 h before UCAR-T cell injection; the same volume of saline was injected into the T-cell-only infusion groups. The ratio of NK^{mbIL15}: UCAR-T is 1:1 (by total cell count). All mice passed the qualifying quarantine a week before the experiment was conducted. To evaluate the development of xenogeneic graft-versus-host disease (GvHD), T-cell infused mice were monitored at least three times a week for clinical symptoms. In parallel, we have followed the proper previous reports of the performance of xenograft GvHD in mice (12).

Real-time PCR

Blood samples or the spleen and bone marrow were obtained according to the trial procedure for CAR copy number detection. Genomic DNA was extracted from the samples using a QIAamp DNA Blood Mini Kit (Qiagen, Germany) and following the protocol as per instructions. We applied SYBR and TaqMan probes for qPCR in an ABI QuantStudio (Thermo Fisher Scientific). For CAR copy number detection, the TaqMan primers of forward 5′-CAGAAGAAGAAGAAGGAGGATGTG-3′ and reverse 5′- TACTCCTCTCTTCGTCCTAGATTG -3′ were used. The probe used was 5′-FAM- CTGAGAGTGAAGTTC-3′. The TaqMan method was performed in accordance with the published protocol (10). PCBP2 was used as a control, and a correction factor (CF) was generated to correct for the DNA copy number. DNA samples from healthy donors were detected as negative controls. A lower limit of quantification (LLOQ) of five copies per microliter of genomic DNA was determined.

Total RNA was extracted from cells using the RNeasy Mini Plus Kit (Qiagen, Germany) following the instructions and was reverse-transcribed to cDNA by PrimeScript RT reagents (TaKaRa, Japan). The following primers were used: NR4A3 forward 5′-GCAAG GGCTTTTTCAAGAGAACA-3′ and reverse 5′-TTTGG AAGGCAGACGACCTC-3′, EGR3 forward 5′-TGCTATGA CCGGCAAACTCG-3′ and reverse 5′-CCGATGTCCATT

ACATTCTCTGT-3′, CD70 forward 5′-GTCACTTGGGTG GGACGTAG-3′ and reverse 5′-GATGGATACGTAGCTGCC CC-3′, POLR2L forward 5′-TACGCTGCTTCACTTGTGGC-3′ and reverse 5′-AGCGCATCCCCC TCGGT-3′, ID2 forward 5′-ATCCTGTCCTTGCAGGCTTC-3′ and reverse 5′-ACCGCTT ATTCAGCCACACA-3′, FHL2 forward 5′-TCAGTG CAAAAAGCCCATCAC-3′ and reverse 5′-GCAGTAGG CAAAGTCATCGC-3′, HSPA5 forward 5′-GGACCAC CTACTCCTGCGTC-3′ and reverse 5′-TCAAAGACCGTGTTC TCGGG-3′.

RNA-seq

Total RNA was extracted from cells using the RNeasy Mini Plus Kit (Qiagen, Germany) on day 9 of activation, followed by fragmentation into small pieces with a fragment buffer at an appropriate temperature. The RNA library was constructed by the MGIEasy RNA Directional Library Preparation Kit (MGI, China) prior to standard quality control for sequencing *via* the BGIseq500 platform (BGI, China). The fastq files were preprocessed using fastp <0.23.1>, and gene alignments were performed using the software sTAR <2.7.9a> to Human GRCh38 (hg38); then, gene expression was calculated using HTSeq software. Differential gene analysis was obtained by DESeq2 < v1.4.5>, and the entry criteria for differential genes was (padj < 0.1 and abs(log2FoldChange)>=1).

Statistical analysis

Statistical analyses were performed with GraphPad Prism 8.0 software using one-way ANOVA with Tukey's correction for multiple comparisons, paired or unpaired Student's *t*-tests (two-tailed), and the log-rank (Mantel–Cox) test as appropriate and indicated in each figure. Significant differences were marked on figure legends as *≤0.05, **≤0.01, ***≤0.001, and ****≤0.0001. Two biological replicates at least per experiment, each of which has at least three technical replicates. Experiments with a single biological replicate are *in vivo* experiments.

Results

Efficient generation of triple gene–edited universal chimeric antigen receptor T cell with CRISPR/Cas9

Off-the-shelf CAR-T cells using a gene-editing technique to obtain TCR^{neg} and/or $HLA\text{-}I^{neg}$ have been extensively reported (13, 14), and relative clinical trials have been conducted (4, 5, 15). As a common gene cluster that mediates acute immune rejection in organ transplantation (16, 17), HLA-II had not drawn sufficient attention in UCAR-T applications. This could be attributed to the low basal expression level of HLA-II in resting T cells. Nonetheless, we have noticed in our previous human clinical studies that HLA-DR was highly presented in autologous CAR-T cells for reinfusing (Figure S1A). Further exploration revealed that the expression of HLA-DR molecules increased along with the continued activation of T cells, rising up to 90% on day 9 (Figure 1A). Considering this hazard, we aimed to obtain a new UCAR-T cell by eliminating HLA-II, in addition to the elimination of TCR and HLA-I, which was expected to be more resistant to the rejection of the host (Figures S1B, C). The CIITA is the master regulator of MHC II expression, which could potentially lead to the accelerated rejection of infused allogeneic T cells (18); CIITA disruption produced a high level of HLA-II deficiency (7). Accordingly, a guide RNA (gRNA) targeting the exon3 of the CIITA gene was designed (Figure 1B). Based on our previously reported CD19-targeted CAR (10), we further utilized sgRNA in complex with Cas9 protein (RNP), which was a newly emerging technique with less cellular toxicity for industrial demands after plasmids and viruses. RNP complexes were obtained by incubating sg-TRAC, sg-B2M, and sg-CIITA with Cas9 protein at a molar ratio of 1:1:1:3.

Compared with a continuous high expression of HLA-DR on unedited activated CAR-T cells (Figure 1C), over 99% of the CAR-T cells lost CD3, 99% lost HLA-I, and 98% lost HLA-II (Figures S1D, E). We also excluded the potential effect of the electroporation stimulus on the expression of HLA-II (Figure S1F). The successful elimination of HLA-II on TUCAR-T was further confirmed by continuing the low expression of HLA-II upon T-cell activation (Figure 1C). The occurrence of insertions or deletions (indels) in the targeting region of the CIITA gene were established by clonal sequencing (Figure S1G). Importantly, there was no predicted off-target events observed in tested TUCAR-T cells (Table S1). The mixed lymphatic reaction (MLR) assays were then performed by mixing TUCAR-T donor cells and host PBMCs from allogeneic healthy volunteers, and our data showed that TUCAR-T cells did not induce detectable allogeneic rejection both in GvHR and HvGR compared to unedited CAR-T (Figures 1D, E).

Triple gene–edited universal chimeric antigen receptor T cell has comparable antitumor efficacy with unedited chimeric antigen receptor T cell *in vivo* but exhibited less persistence

To test whether CRISPR/Cas9 gene editing would affect the efficacy of CAR-T cells, CD19-specific cytotoxicity and the corresponding interferon-gamma (IFN-γ) secretion of TUCAR-T cells were examined. The results showed that TUCAR-T cells exhibited comparable cellular efficacy in

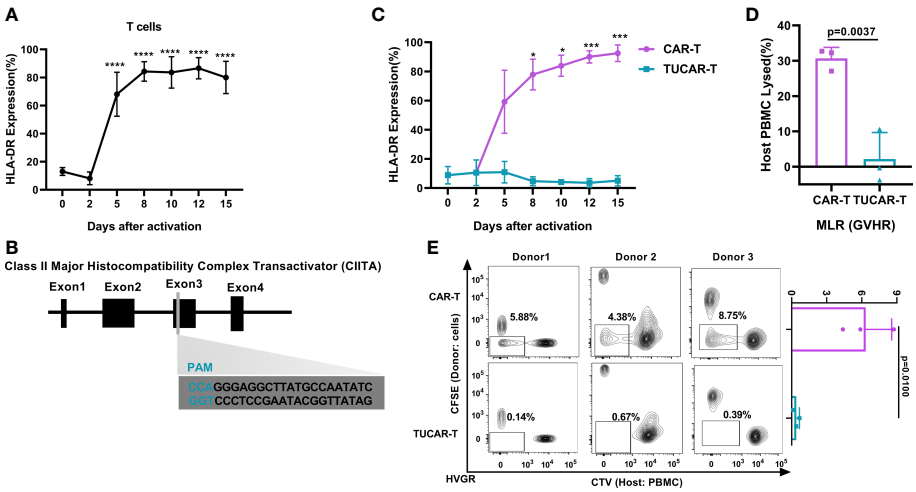

FIGURE 1
Efficient and specific editing of triplex genes in primary T cells. **(A)** HLA-DR was expressed continuously with the activation of T cells (n = 3). **(B)** Schematic diagram of the designed sgRNA targeting the human CIITA. **(C)** HLA-DR gene expression monitoring in TUCAR-T and unedited CAR-T cells with continued activation (n = 3). **(D)** (n = 3) and **(E)** (n = 3) Alloreactivities between donor TUCAR-T cells and PBMCs from the allogeneic donor were analyzed by the MLR assay. In GvHR, we showed the percentages of host PBMCs that died by rejection lysis **(D)**. In HvGR, the cells in the box represented host PBMCs proliferating from allogeneic CAR-T cell stimulation **(E)**. All data represent the mean ± SD with individual donors. Statistical significance was determined using one-way ANOVA with Dunnett's correction for multiple comparisons **(A)**, two-way ANOVA with Sidak's correction for multiple comparisons **(C)**, and two-tailed, paired or unpaired Student's *t*-test **(D, E)**. Significances of $p \leq 0.05$ are indicated by 1 asterisk (*), $p \leq 0.001$ are indicated by 3 asterisks (***), $p \leq 0.0001$ are indicated by 4 asterisks (****).

killing $CD19^+$ Nalm6-Luc-GFP tumor cells to unedited CAR-T cells *ex vivo* (Figure 2A). Both TUCAR-T and unedited CAR-T were effective in controlling tumor growth within 3 weeks of treatment for Nalm6 tumor-bearing mice. However, TUCAR-T failed to keep the effect afterward, while unedited CAR-T worked much better (Figure 2B). Consistently, CAR-T cells were undetectable in peripheral blood, the spleen, and bone marrow in the TUCAR-T group but were persistent in the unedited CAR-T group (Figure 2C). These results indicated that there was still a certain gap in persistence between TUCAR-T and unedited CAR-T cells.

A previous study had shown that TCR and HLA-I double-edited UCAR-T (DUCAR-T) had comparable antitumor efficacy with unedited CAR-T *in vivo* (14). We thus wondered whether the compromised *in vivo* efficacy of TUCAR-T cells could be due to the knockout of CIITA. To test this conjecture, DUCAR-T cells were produced by the electroporation transduction of the sg-TRAC and sg-B2M RNP mixture. Both TUCAR-T and DUCAR-T showed robust tumor cell lytic capacity and equivalent IFN-γ secretion *ex vivo* (Figure 2D). Furthermore, they showed equivalent antitumor capability (Figure 2E), similar levels of the CAR copy number in blood on day14 after CAR-T injection (Figure 2F), and comparable survival rates in Nalm6 tumor-bearing mice (Figure 2G). All these demonstrated that knocking out CIITA in addition to TRAC and B2M did not affect the antitumor ability and persistence of CAR-T cells.

Introduction of HLA-E into exogenous HLA-E expressing triple gene–edited universal chimeric antigen receptor T cell avoided rejection from host NK cells

The recognition of HLA-I by receptors on the surface of NK cells is an important mechanism of immune protection in organisms (8). Therefore, the CD52 monoclonal antibody is commonly adopted for lymphatic clearance prior to the infusion of HLA-I eliminated UCAR-T in clinic to help TUCAR-T cells escape from the rejection of host NK cells, while avoiding lymphatic clearance with anti-CD52 antibodies, which has many adverse effects in clinic. A fusion protein B2M and HLA-E, a non-classical conservative member of HLA-I family, was exogenously constructed to compensate for the elimination of HLA-I (Figures 3A, B). Recently, Guo had reported that the introduction of a mutated HLA-E or HLA-G in CAR-T cells along with HLA-I deficiency could help to avoid such rejection (19). However, the study failed to provide *in vivo* evidence to demonstrate its efficacy, and the mutation design of HLA-E was neither uncovered (19). Another report published excellent research in this area but only directly demonstrated *ex vivo* that UCAR-T could resist NK rejection effectively (20). In this study, we introduced mutants at the signal peptide region of wild-type B2M in fusion protein B2M and HLA-E to avoid recognition and cleavage by CRISPR-Cas9 targeting B2M. We confirmed that mutated HLA-E was successfully coexpressed with CAR on the surface of cells (Figure 3C).

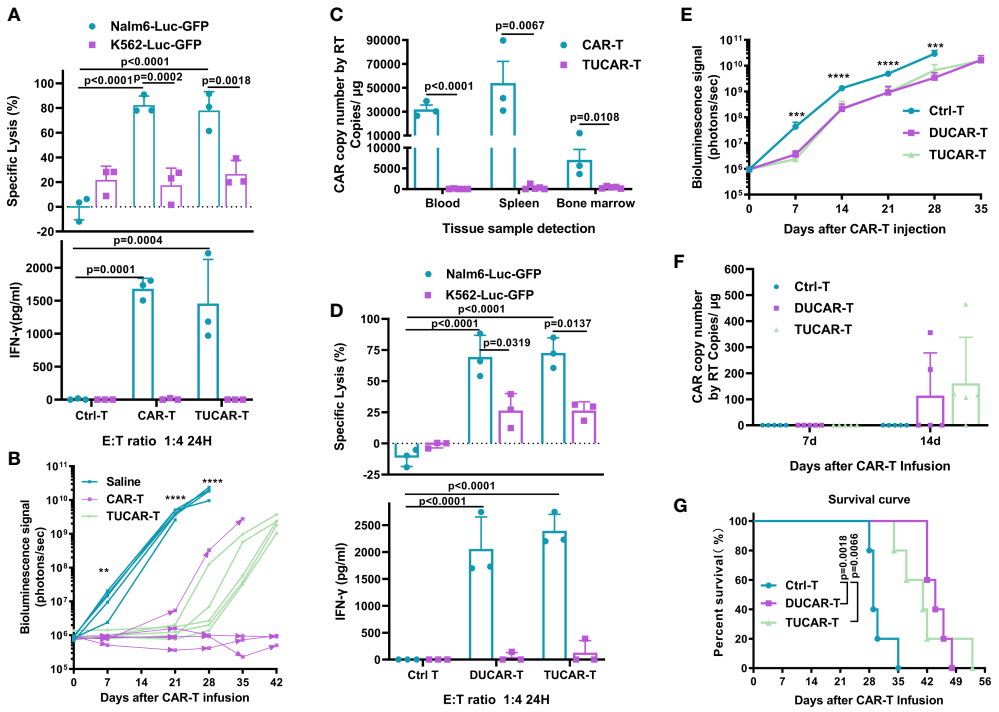

FIGURE 2
TUCAR-T has comparable antitumor efficacy *in vivo* with unedited CAR-T cells but exhibited less persistency. **(A)** (Top) Cytotoxicity of CAR-T and TUCAR-T cells was assessed by measuring the percentage of tumor cell lysis using the luciferase assay. (Bottom) IFN-γ release was analyzed by ELISA (n=3). **(B)** BLI of mice receiving different treatments (n=5). **(C)** Peripheral blood, spleen, and bone marrow from Nalm6-bearing NOG mice treated with different CAR-T cells were obtained on day 42 after CAR-T infusion for the presence of the copies of the CAR transgene by RT-PCR (BBz) (TUCAR-T: n=5, CAR-T: n=3). **(D)** (Top) Cytotoxicity of DUCAR-T and TUCAR-T cells was assessed by measuring the percentage of tumor cell lysis using the luciferase assay. (Bottom) IFN-γ release was analyzed by ELISA (n=3). **(E)**, BLI from each group of mice (n = 5). **(F)**, Peripheral blood from Nalm6-bearing NOG mice treated were obtained on day 7 and 14 for the presence of copies of the CAR transgene by and RT-PCR (BBz) after CAR-T cell injection (n = 5). **(G)**, Survival curve of mice (n=5). All data represent the mean ± SD. Statistical significance was determined with two-tailed, unpaired Student's *t*-test **(C)** and one-way ANOVA with Tukey's correction for multiple comparisons **(A, B, D, E, F)**, or the log-rank (Mantel–Cox) test **(G)**. Significances of $p \leq 0.01$ are indicated by 2 asterisks (**), $p \leq 0.001$ are indicated by 3 asterisks (***), $p \leq 0.0001$ are indicated by 4 asterisks (****).

To verify the protective role played by the expression of HLA-E, we used an armed NK that expresses membrane-bound IL15 (NK^{mbIL15}) to enhance the function of NK (Figures S2A–C) (21). First, UCAR-T cells were cocultured with NK^{mbIL15}. Approximately 20% of TUCAR-T was lysed by NK^{mbIL15}, while the ETUCAR-T expression of additional HLA-E was successfully escaped from killing (Figure 3D). Furthermore, we assessed the tumor-killing function of ETUCAR-T in the presence of NK^{mbIL15} to emulate the circumstances of CAR-T infused into patients. First, we confirmed that the efficacy of TUCAR-T against Nalm6 tumor cells was significantly attenuated in the presence of NK^{mbIL15}. Then, after HLA-E was introduced, the antitumor efficacy of ETUCAR-T remained and performed as well as unedited CAR-T and exogenously introduced HLA-E CAR-T(ECAR-T) (Figure 3E). Therefore, the expression of mutated HLA-E indeed endowed UCAR-T with the ability to resist alloimmune rejection mediated by NK. We then performed *in vivo* assessment by the coinfusion of ETUCAR-T or TUCAR-T at a 1:1 ratio with NK^{mbIL15} into Nalm6 tumor-bearing mice. We demonstrated beforehand in the tumor model that NK^{mbIL15} did not exhibit a specific antitumor activity (Figure S2D). Consistent with the *ex vivo* results, the antitumor efficacy of ETUCAR-T-treated mice was maintained (Figures 3F, S2E), while the antitumor efficacy of TUCAR-T-treated mice was decreased significantly (Figures 3G, S2F). These findings indicated that exogenously constructing an HLA-E could help UCAR-T cells escape from the cell lysis of host NK and benefit for cell persistence *in vivo*. Our data thus offer an additional possibility for universal CAR clinical applications.

Multiple infusions of high dose of exogenous HLA-E expressing triple gene–edited universal chimeric antigen receptor T cell could be used as a clinical indication for dosing

Given that UCAR-T cells have an inferior clinical efficacy in comparison to unedited autologous CAR-T, we then further tested

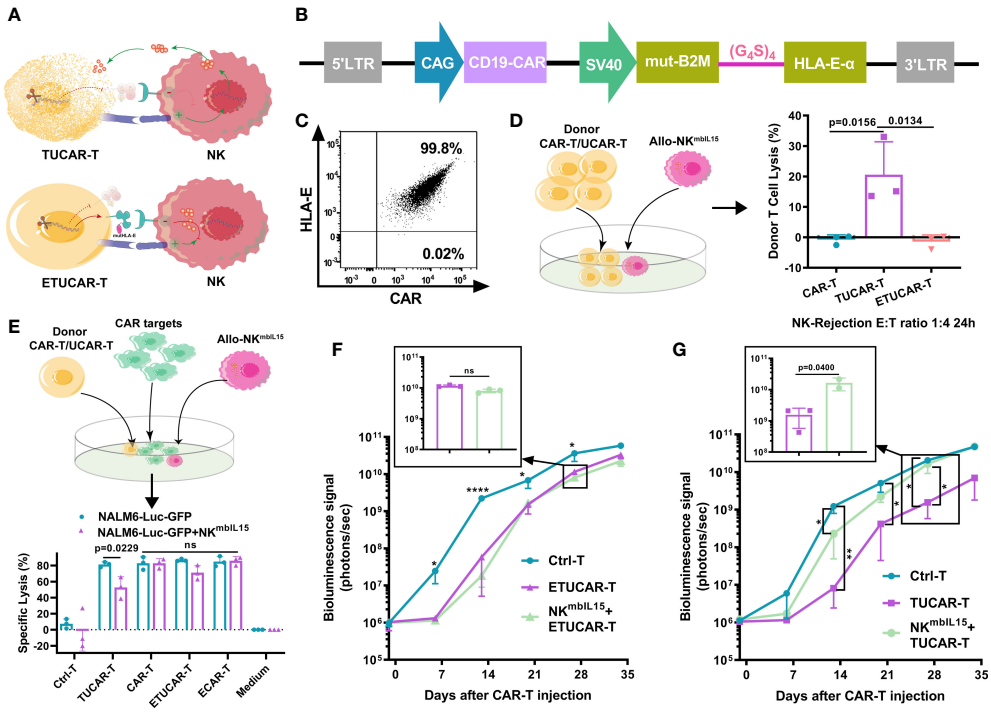

FIGURE 3
The HLA-E helps UCAR-T cells to escape the lysis induced by NK cells *in vivo* **(A)**, Schematic representation of HLA-I deficient TUCAR-T cells attacked by NK cells. **(B)**, Schematic design of the ECAR constructs. **(C)**, The representative data of HLA-E and CAR coexpressed on T cells by FCM. **(D)** (Left) Schematic of the model setup for UCAR-T cells rejected by NK^{mbIL15}. (Right) TUCAR-T cells were lysed by NK^{mbIL15}; NK^{mbIL15} and donor UCAR-T cells were mixed at a 1:4 ratio for 24 h (n = 3). **(E)** (Top) Schematic diagram of the simulated cell killing *in vivo* with Allo-NK^{mbIL15}. (Bottom) Cytotoxicity of ETUCAR-T and TUCAR-T cells was assessed by measuring the percentages of tumor cell lysis using the luciferase assay (n = 3). The tumor cell lysis ratio is 1:4 by the effective cell count; the allo-rejection cell lysis ratio is 1:1 by the total cell count. **(F, G)** BLI from each group of mice (n = 3). All data represent the mean ± SD. Statistical significance was determined with two-tailed, unpaired Student's *t*-test **(E)** or one-way ANOVA with Tukey's correction for multiple comparisons **(D, F, G)**. Significances of $p \leq 0.05$ are indicated by 1 asterisk (*), $p \leq 0.01$ are indicated by 2 asterisks (**), $p \leq 0.0001$ are indicated by 4 asterisks (****). Significance of $p > 0.05$ are indicated by nonsignificant (ns).

whether we could overcome this disadvantage by increasing the dosage and frequency of infusions in mice (Figure 4A). Furthermore, the UCAR-T transfusion dose was tended as more than three times the autologous CAR-T in clinical trials (1, 22). Nalm6 tumor-bearing mice were established by inoculating Nalm6 and were treated with a single dose of ETUCAR-T or unedited ECAR-T and a single high dose of $ETUCAR\text{-}T^{HD}$ or multiple high doses of $M\text{-}ETUCAR\text{-}T^{HD}$. Thereafter, peripheral blood was collected every 7 days to detect the existence of CAR-T. As we predicted, the increased dose and times of infusion significantly enhanced the antitumor efficacy and prolonged the survival of tumor-bearing mice (Figures 4B–D). More importantly, daily observation and weight measurement showed that no accidental death or obvious weight loss was observed in mice treated with a repeated high dose of CAR-T (Figures 4E, S3). Thus, this indicated that the dosage regimen was safe and effective for treatment. Unfortunately, even though the $M\text{-}ETUCAR\text{-}T^{HD}$ exhibited better antitumor efficacy, the mice suffered tumor recurrence on day28, approximately 2 weeks after the last treatment (Figure 4C). This phenomenon was consistent with the absence of CAR-T cells at this time point (Figure 4F). In contrast, the unedited ECAR-T showed higher persistence accompanied by the significant weight loss of mice (Figures 4E, F). In conclusion, these results prospectively offered some useful information for the future clinical application of off-the-shelf CAR-T cells. Aiming to advance the clinical use of UCAR-T products and explore the causes and solutions to the industry's dilemma based on this foundation, the data would serve as an important guideline for clinical trials that need to be done in a short time to facilitate the drug development process in a quicker manner.

T-cell receptor deficiency in universal chimeric antigen receptor T cell is the primary factor for the inferior efficacy

Other research has indicated that the antitumor efficacy of CAR-T cells was correlated with viability, proliferative capacity,

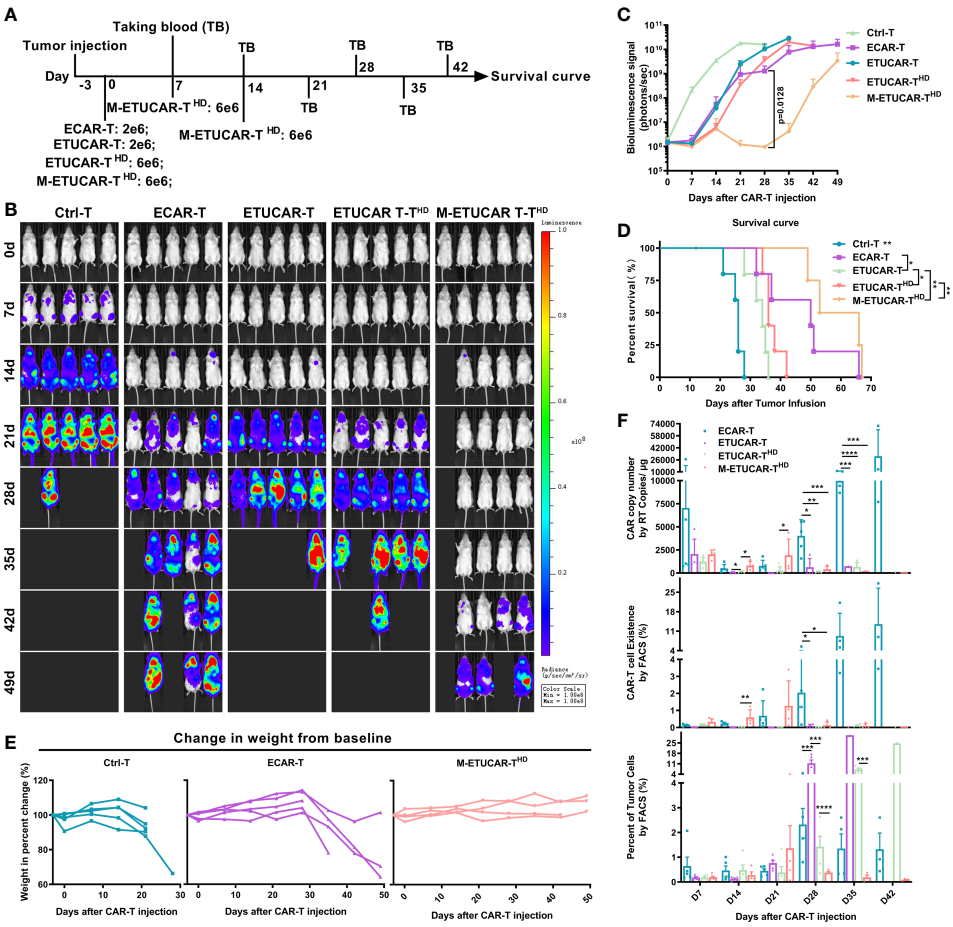

FIGURE 4
Improve efficacy by increasing the dosage and frequency of CAR-T infusion. **(A)**, Animal experimental timeline. All cells were cryopreserved (off the self). Here, the dose of cryopreserved cells was double the conventional dose (2×10^6). **(B, C)** BLI from each group of mice (n = 5); the high-dose ETUCAR-T^{HD} was three times conventional dosing (2×10^6) reinfusion, the three times conventional dosing for multiple reinfusion group (M-ETUCAR-T^{HD}). **(D)**, Survival curve of mice (n=5 per group). **(E)** Weight loss monitoring of mice receiving Ctrl-T (left), ECAR-T (center), or M-ETUCAR-T^{HD} (right) cell treatment (n = 5). **(F)**, Peripheral blood from mice receiving different treatments were obtained every 7 days for the presence of the copies of the CAR transgene by RT-PCR (BBz) (top) and the Fluorescence-activated Cell Sorting (FACS) assay (CD45(+)/CD3 (+) CAR-T cells) (center) and the presence of tumor cells (bottom) (n = 5). All data represent the mean ± SD. Statistical significance was determined by one-way ANOVA with Tukey's correction for multiple comparisons **(C, F)**, or the log-rank (Mantel–Cox) test **(D)**. Parts of the statistical significance in C were not marked.

T-cell subset distribution, and the CD4/CD8 ratio and could be represented by the expression of exhaustion markers (23–27). Before comparing these indicators, we first excluded the effects of electric shock operation on T cells by a comparative experiment (Figure S4). We found that ETUCAR-T was equivalent to unedited ECAR-T in the proliferative capacity and distribution of cell subpopulations or cell exhaustion (Figures 5A–F). In addition, representative data showed that they had similar efficacy, which was demonstrated by tumor cell lysis and IFN-γ secretion at different E/T ratios (Figure 5G).

With these results, neither the HLA-II deficiency nor the CAR-T subset distribution reflected the key issue, which was responsible for the inferiority of UCAR-T efficacy. To further unravel the crucial factor affecting the efficacy of UCAR-T, we then focused on TCR and HLA-I, the other two genes eliminated in UCAR-T. Despite the fact that the primary function of TCR had been mimicked or replaced by our CAR gene, the endogenous TCR was reported to be involved in many important biological processes (28–32), and HLA-I has also been proven to participate in a diverse range of ways in T cells (31, 32). We thus performed a series of *ex vivo* and *in vivo* comparative studies to explore the differences between the individual or triplex gene-edited CAR-T cells and the unedited CAR-T (Figure 5H). We firstly compared the *ex vivo* antitumor capacity of CAR-T utilizing an exogenous construct of $CD19^{+/-}$ A549 by a real-time cell analysis (RTCA) system, which could

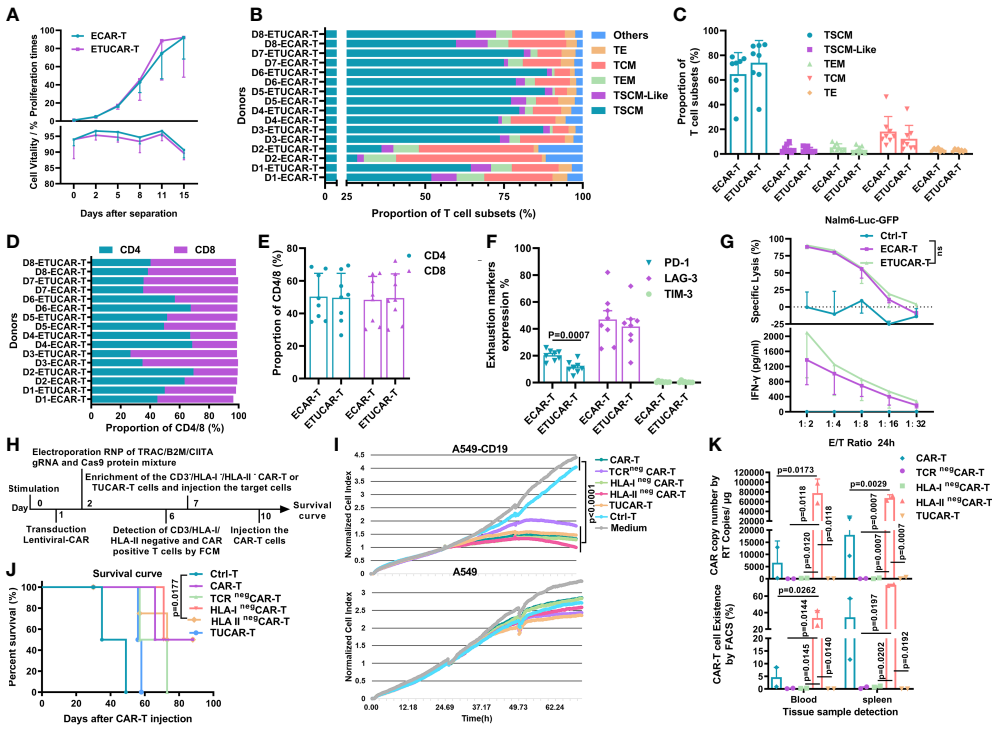

FIGURE 5
TCR deficiency in UCAR-T cells is the primary factor leading to inferior efficacy compared to unedited CAR-T cells. **(A)**, Comparison of the ETUCAR-T and unedited ECAR-T cell proliferation times (top) and viability (bottom) *ex vivo* (n = 3). **(B, C)**, T-cell subset distributions (n=8). The classification criteria are as shown in Figure S4. **(D, E)**, Proportion of CD4/CD8 T cells (n = 8). **(F)**, Cell surface expression of exhaustion markers, programmed cell death protein 1 (PD-1), lymphocyte activation gene-3 (LAG3), and T-cell immunoglobulin and mucin domain-containing protein 3 (TIM-3) (n = 8). **(G)**, Representative data of cell lysis (top) and IFN-γ secretion (bottom) in different E/T ratios (n=3). All data represent the mean ± SD. Statistical significance was determined with two-tailed, unpaired Student's *t*-test. **(H)**, Flow chart of the generation of UCAR-T cells and the time nodes of other experiments. **(I)**, Cytotoxicity of different UCAR-T cells was assessed by measuring the normalized cell index using RTCA (n = 3). **(J)**, Survival curve of mice (n = 4). **(K)**, Peripheral blood and spleen from mice treated with CAR-T cells was obtained on day 30 for the presence of copies of the CAR transgene by RT-PCR (BBz) (top) and the Fluorescence-activated Cell Sorting (FACS) assay (CD45 (+)/CD3(+) CAR-T cells) (bottom). Data from two mice were shown. All data represent the mean ± SD. Statistical significance was determined by two-way ANOVA with Tukey's correction for multiple comparisons **(A)** or two-tailed, unpaired Student's *t*-test **(C, E, F)**, log-rank (Mantel–Cox) test **(J)**, or one-way ANOVA with Tukey's correction for multiple comparisons **(G, I, K)**.

provide a real-time and informative view of CAR-T killing capacity continuously (33). The data showed that all tested CAR-T exhibited robust and indistinguishable antitumor efficacy *ex vivo* (Figure 5I). Next, we further explored their therapeutic efficacy and CAR-T persistence *in vivo*. We found that HLA-I or HLA-II elimination did not affect the antitumor efficacy of CAR-T, and these groups showed the comparable survival rate to the unedited CAR-T (Figure 5J). Of note, the deficiency of TCR showed the worst therapeutic effect (Figure 5J). In contrast, the CAR-T persistence result revealed a different landscape. The HLA-II^{neg} group showed a markedly high number of CAR-T persistence in blood and spleen after 30 days of treatment, followed by the unedited group, and CAR-T cells were undetectable in either the TCR^{neg} or HLA-I^{neg} group (Figure 5K). Collectively, the result suggested that the deficiency of both TCR and HLA-I caused poor CAR-T persistence, but, different from HLA-I, which did not impair the survival rate of treated mice, TCR deficiency was more likely the primary factor leading to the inferior efficacy of UCAR-T.

Poor efficacy of universal chimeric antigen receptor T cell is associated with a unique transcriptional profile in the absence of T-cell receptor

So far, targeting the TCR and HLA-I is the dominant scheme of research on UCAR-T therapeutic strategies. However, the corresponding change of the transcriptional profiles of gene editing is little known. We thus explored the global transcriptional profiles of TCR, HLA-I, or HLA-II deficiency T cells as well as unedited control T cells from two independent donors to investigate the key genes responding to the poor efficacy of ETUCAR-T. Firstly, the overview of the differential

gene expression profile hinted that, unlike TCR^{neg} T, the unedited Ctrl-T and HLA-II^{neg} T were much closer (Figure 6A), which implied that HLA-II deficiency had less impact on T cells compared to the other two genes. Furthermore, we verified the dramatic downregulation of gene-editing related genes, including TCR spliceosomes in TCR^{neg} T and B2M in HLA-I^{neg} T, as well as HLA-II isoforms or its invariant peptide chain CD74 in HLA-II^{neg} T, respectively, and all of them in ETUCAR-T. Of note, previous studies have shown that NR4A3 and EGR3 are critical in T-cell survival and differentiation (34–39), but they both showed obvious downregulation in TCR^{neg} T compared to the others (Figures 6A, B). These findings may explain the poor *in vivo* efficacy of both TCR^{neg} CAR-T and TUCAR-T, compared to unedited CAR-T (Figures 5J, K). Considering the outstanding performance of the *in vivo* persistence of HLA-II^{neg} CAR-T, we analyzed the differences between HLA-I^{neg} T and others. We interestingly found that CD70 and POLR2L were significantly upregulated in the HLA-II^{neg} group (Figures 6A, C). CD70 has been known to positively regulate T-cell proliferation (40), whereas the upregulation of POLR2L could also promote T-cell expansion (41). Together, the upregulation of them may facilitate the proliferation and persistence of HLA-II^{neg} CAR-T *in vivo*. Additionally, we noticed that both genes in HLA-I^{neg} were consistent with their TCR^{neg}, which might be related to undetectable CAR-T persistence in HLA-I^{neg} (Figure 6A).

To explore the comprehensive impact on genes edited in ETUCAR-T, we further analyzed the altered transcriptional profiles compared with CAR-T expressing HLA-E alone. There were 209 upregulated and 244 downregulated genes in ETUCAR-T (Figures 6D, E). Moreover, we found a subset of significantly upregulated genes involved in controlling cellular functions, including the negative regulation of cell proliferation such as ID2, LATS2, and PTCH1; the negative regulation of transcription including FHL2, the positive regulation of cell proliferation such as PRKCZ and ERBB3; and the positive regulation of glycolytic processes as PFKFB2 (Figures 6F, G). These genes may collectively result in the weakened persistence of ETUCAR-T cells *in vivo*. We also compared the gene panel of ETUCAR-T with TUCAR-T to further to investigate the effects

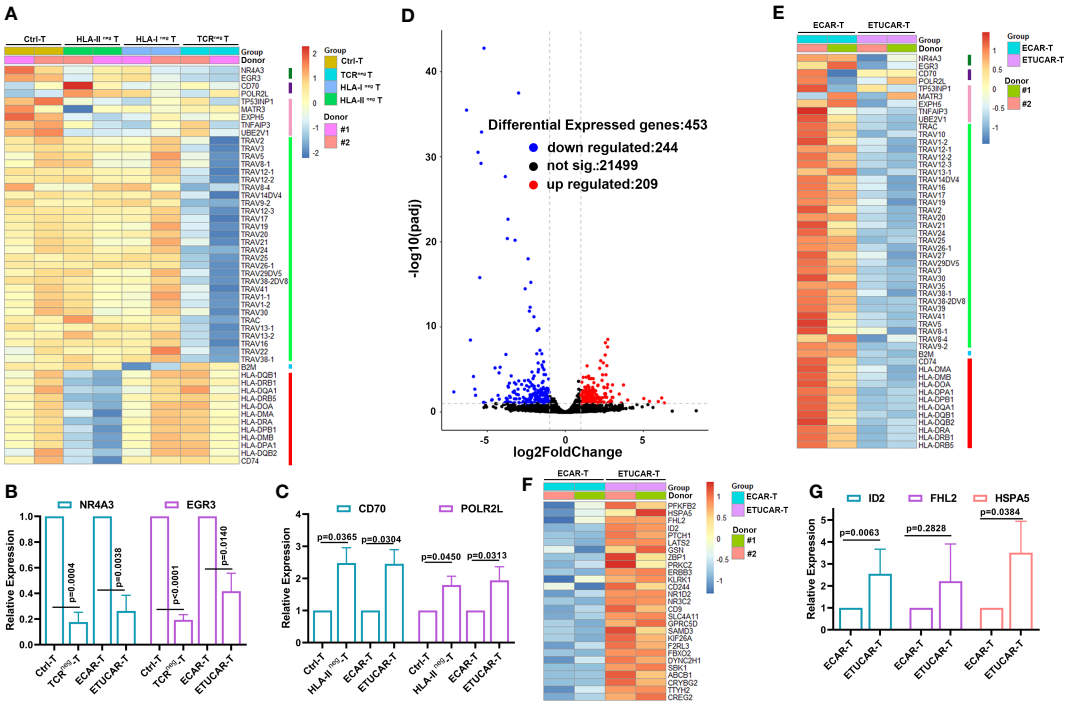

FIGURE 6
Poor efficacy of ETUCAR-T cells is associated with a unique transcriptional profile. **(A)**, Differential expression gene among Ctrl-T cell transduction with Cas9 protein, TCR^{neg} T, HLA-I^{neg} T, and HLA-II^{neg} T cells was analyzed by RNA sequencing. Heat map of differential expression gene between Ctrl-T and single-gene-deficiency T cells (n = 2). **(B, C, G)**, RT-PCR results for analyzing the expression of representative differential expression genes in T cells (n = 3). **(D)**, Volcano diagram of differential expression genes of ETUCAR-T cells compared with unedited ECAR-T cells (n = 2). **(E)**, Downregulation expression genes between ECAR-T transduction with Cas9 protein and ETUCAR-T cells were analyzed by RNA sequencing (n = 2). **(F)**, Upregulation expression genes between ECAR-T transduction with Cas9 protein and ETUCAR-T cells were analyzed by RNA sequencing (n = 2). Data represent the mean ± SD. Statistical significance was determined with two-tailed, unpaired Student's *t*-test. Cells were collected after being activated for 9 days. Differential gene entry criteria were (padj < 0.1 and abs (log2FoldChange)≥ 1).

of expressing HLA-E and got a similar transcriptional pattern (Figure S5). This suggested that the expression of HLA-E was safe and HLA-E was not the crucial factor for the impaired function of CAR-T. In the summary of these results, the simultaneous editing of all three genes on T cells produced a double-edged result, which reminded us that what we have seen through our experiments was only the tip of the iceberg of the effects of gene editing, and additional information needs to be further explored in-depth. Briefly, these results highlighted the necessity of identifying the potential safety risks of the multiple impacts produced by gene deficiencies when utilizing gene-edited cells as therapeutic transplants in the future.

Discussion

Allogeneic universal CAR-T therapy has been continuously researched and explored for the benefit of cancer patients who failed to meet the criteria of traditional autologous CAR-T (2). However, the clinical results of universal CAR-T-cell therapy did not reach a parallel level to the autologous CAR-T therapy (4, 5, 15). Currently, the recognized contributors of the struggle for the field have been focusing on poor UCAR-T expansion and survivability *in vivo* (4).

It is known that the risk of HvGR and GvHR in allografts is a key determinant of success, and HLA matching is an important consideration in assessing these risks. Up to now, clinical regimens pay main attention to the elimination of HLA-I, whereas HLA-II was neglected. Herein, we designed a novel universal CAR-T cell called ETUCAR-T, which is designed using CRISPR/Cas9 to eliminate TCR, HLA-I, and HLA-II and incorporates exogenous expression of HLA-E simultaneously. On one hand, ETUCAR-T was more tolerant to host rejection owing to the absence of main MHC molecules. On the other hand, the presentation of HLA-E could assist them to escape the recognition and lysis from allogeneic NK. Multiple infusions of high-dose ETUCAR-T cells in tumor-bearing mice showed no obvious safety issue, suggesting that this regimen was relatively safe and feasible. It was noteworthy that on the research journey of UCAR-T, for the first time, we found that the critical factor for the poor efficacy was the TCR deficiency, and we also found that the HLA-II-knockout improved the persistence of CAR-T *in vivo*. We also revealed the possible key molecules with the RNA-seq analysis of the individual or comprehensive impact of these edited genes.

On the other hand, in this article, no significant difference in antitumor efficacy or T-cell persistence *ex vivo* and *in vivo* were found between reported DUCAR-T and our TUCAR-T, which had the additional elimination of HLA-II (Figure 2F). Intriguingly, we found that HLA-II^{neg} CAR-T cells showed superior efficacy and well persistence *in vivo* than TCR^{neg} or HLA-I^{neg} CAR-T (Figure 5). Beyond that, the whole transcriptional profile of HLA-II^{neg} T cells is much more similar with unedited Ctrl-T cells (Figure 6A). Again, these results supported the necessity and feasibility of HLA-II elimination. It has been suggested that HLA-II expression on T cells could mediate apoptosis through a variety of intracellular signaling pathways (42). Owing to the highly polymorphic characteristics of the HLA-II gene, it was a relatively feasible way to obtain HLA-II-deficient cells by the knockout of CIITA. In addition, previous studies indicated that the DNA methylation of CIITA promoter III in T cells had a great potential for HLA-II deficiency (42), which may bring a new choice for HLA-II elimination. Furthermore, we verified the necessity of HLA-E presence for UCAR-T cells in resisting rejection by allogeneic NK cells both *ex vivo* and *in vivo*. Nonetheless, subsequent clinical trials are essential to validate the role of the exogenous expression of mutant HLA-E in UCAR-T therapy.

With a similar RNP gene-editing scheme, we have successfully produced CD19-targeting UCAR-T cells that could be applied to at least 10 patients by our clinical manufacturing methods. With the rapid development of RNA vaccines in recent years, the large-scale production of RNA has become more sophisticated; thus, this may further support the wide usage of RNP-based gene-editing strategies. Equally important, the data from allogeneic rejection tests and the evaluations of high-dose antitumor infusion demonstrated that simultaneously editing three genes was still safe and feasible. Some researchers in industry now begin to engage in this practice, and our data could provide some support in this area. There is also a trend in the field to conduct gene editing by transducing a single RNA consisting of multiple sgRNAs or siRNAs in a tandem fashion. In addition, the production of RNP complexes manufactured directly by bacteria may become an industry trend (43). However, we should mention that the safety of gene-editing technology remains highly controversial (44). Currently, we have difficulty in claiming whether a large number of gene transcriptional profile changes (Figure 6) are caused by gene editing itself or the genes being edited, and whether it is a superimposed effect of both. The two early-starting UCAR-T teams have been urgently suspended by the FDA for safety issues like the occurrence of a clinically lethal event and a report of a chromosomal abnormality in a patient, respectively. These reminded us that more far-reaching impacts caused by gene editing in UCAR-T therapies should be explored in-depth to uncover.

It is well known that endogenous TCR is non-essential for CAR function exertion in CAR-T therapy; nonetheless, in almost all UCAR-T studies reported to date, it has been eliminated by gene editing as a key gene involved in GvHR. Previously published reports barely investigated the irreversible effects of TCR deficiency on T cells; the statements reported to date were in dispute (28, 45). In contrast to Yang (28), as with Stenger (45), our study found that the TCR deficiency contributed to the poor survivability of CAR-T cells, and the lack of effectors would

result in the failure of effectively controlling the tumor *in vivo*. It should be noted that the role of TCR deficiency on T-cell persistence might be amplified in a mice model. It had been reported that human TCR could cross-react with MHC molecules in mice, to which T-cell expansion and persistence may benefit (46). We indeed found that some of the mice receiving unedited CAR-T cells developed xenogeneic GvHD at the experiment endpoint. We thus could not exclude the possibility that the inferior persistence of TCR editing CAR-T was a consequence of the elimination of such cross-reaction from mice. Accordingly, better applicable models are needed for the evaluation of treatment efficacy in future studies.

With further exploration, TCR deficiency was found to lead to significant transcriptional profile changes, including the downregulation of NR4A3 and EGR3. NR4A3 is a member of the nuclear receptor subfamily 4, which has been identified as a downstream gene of TCR signaling (34). Previous studies have reported that the NR4A family is essential for maintaining immune homeostasis (36), and NR4A3 regulates Treg cell development (35). EGR3 is a member of the zinc-finger transcription factor in the early growth response gene family that is involved in the development of T cells (37). Previous findings suggested that the EGR3 gene defect in mice accelerated T-cell death as it is involved in the regulation of T-cell antigen recognition (39). Moreover, it has been shown that the lack of EGR2 and EGR3 in lymphocytes led to a fatal autoimmune syndrome and decreased the proliferation of antigen receptor–induced B and T cells (38). For the next investigations, we will systematically validate the functions of these genes to further elucidate the molecular mechanisms involved and reassess the safety risks of gene editing in future studies.

In summary, we have constructed a more effective UCAR-T and provided some new insights into the gene editing of off-the-shelf UCAR-T therapy. Current research on UCAR-T therapy mainly focuses on hematological tumors, such as targeting CD19, CD20, and BCMA while it focuses less on solid tumors, such as targeting NKG2DL and GD2 (2). Actually, UCAR-T would have great advantages in treatment of other diseases that only require short-term effects, such as systemic lupus erythematosus and cardiac disease (47, 48). Joel et al. developed a CAR-T cell for the generation of transient antifibrosis by the lipid nanoparticle (LNP) delivery of CAR's mRNA *in vivo* and showed that treatment with modified mRNA-targeted LNPs reduced fibrosis and restored cardiac function after injury (48). Comparing the early stage of the *in vivo* manufacture of CAR-T, we believe that UCAR-T could serve the same purpose in the treatment of such diseases. In the flood of UCAR-T against tumors, what we need to do first is to address the poor persistence of UCAR-T, pay attention to the safety risks, and struggle on the development of safe and effective clinical application regimens. We have obtained some hints from RNA-Seq analysis, and with this information, we intend to explore the manifestations of immune rejection–related genes' absence in the signal pathway of T-cell proliferation and apoptosis. Next, we need to determine the effects of gene editing using CRISPR/Cas9 on cells by comparing the knockout of other genes that are irrelevant to T-cell immune rejection. Additionally, to avoid safety issues that gene editing may bring, we have also focused on non-editing methods for UCAR preparation to acquire inspiration for developing more safe and effective products. For instance, taking advantage of induced pluripotent stem cells, CAR-T can be generated from genomic background–defined clones to overcome the safety issues of gene editing (49). More interestingly, a recent study has successfully prepared universal CAR-T cells by utilizing the mechanism where HIV-1-infected host cells evaded the host immune response by regulating membrane trafficking and achieved the downregulation of MHC-I (50); a combination almost perfectly illustrates the wonders of the life sciences. Up to now, most of the studies in the UCAR industry have been devoted to the development of new products, ignoring the potential pitfalls of gene editing and the genes being edited themselves. In the principle of safety first, we need to pay more attention to mechanism studies, which are indispensable for collaboratively driving the clinical application of the off-the-shelf CAR-T industry.

Data availability statement

The original contributions presented in the study are publicly available. This data can be found in the NCBI Sequence Read Archive database (Accession: PRJNA905653).

Ethics statement

The animal study was reviewed and approved by China Council on Animal Care and Chongqing Precision Biotech Co., Ltd. protocol for animal use.

Author contributions

CQ, JS. and WL contributed to the conception and design, collection and assembly of data, data analysis and interpretation, manuscript writing. XZ, YX performed part of the experiments, discussed the data. JC performed the animal experiments. YL prepared CAR-T cells clinical samples. GW provided suggestions for statistical analysis in data analysis. HZ, ZY, YQ, JH discussed the data and final approval of manuscript. All authors contributed to the article and approved the submitted version.

Funding

This work was supported by the Major Program of National Natural Science Foundation of China (91959206), Major international (regional) joint research project (82120108019), Key Projects of Ministry of Science and Technology of China (SQ2020YFF0401839).

Acknowledgments

We would like to gratefully acknowledge all healthy donors who provided peripheral blood for *ex vivo* and *in vivo* studies. We are grateful to Dr. Mengzhu Wang and Dr. Yukang Huang for their helpful suggestions on the manuscript and Mr. Jiabing Ma for the expert advice on the figures. We thank Dr. Huailong Xu for the help with RNA-Seq data analysis.

Conflict of interest

Chongqing Precision Biotech Co., Ltd. is a biotechnology company focused on research and development of tumor cellular immunotherapy. JS, YX, HZ, JC, ZY, YQ, JH, YL, are full-time employees of Chongqing Precision Biotech Co., Ltd. CQ is the chief scientist of this company.

The remaining authors declare that the research was conducted in the absence of any commercial or financial relationships that could be construed as a potential conflict of interest.

Publisher's note

Supplementary material

The Supplementary Material for this article can be found online at: https://www.frontiersin.org/articles/10.3389/fimmu.2022.1052717/full#supplementary-material

References

1. Lee DW, Kochenderfer JN, Stetler-Stevenson M, Cui YK, Delbrook C, Feldman SA, et al. T Cells expressing CD19 chimeric antigen receptors for acute lymphoblastic leukaemia in children and young adults: a phase 1 dose-escalation trial. *Lancet* (2015) 385:517–28. doi: 10.1016/S0140-6736(14)61403-3

2. Lin H, Cheng J, Mu W, Zhou J, Zhu L. Advances in universal CAR-T cell therapy. *Front Immunol* (2021) 12:744823–23. doi: 10.3389/fimmu.2021.744823

3. Qasim W, Zhan H, Samarasinghe S, Adams S, Amrolia P, Stafford S, et al. Molecular remission of infant b-ALL after infusion of universal TALEN gene-edited CAR T cells. *Sci Transl Med* (2017) 9:eaaj2013. doi: 10.1126/scitranslmed.aaj2013

4. Listed NA. Sending CAR T cells after T-cell malignancies. *Cancer Discovery* (2020) 10:754. doi: 10.1158/2159-8290.CD-NB2020-039

5. Hu Y, Zhou Y, Zhang M, Ge W, Li Y, Yang L, et al. CRISPR/Cas9-engineered universal CD19/CD22 dual-targeted CAR-T cell therapy for Relapsed/Refractory b-cell acute lymphoblastic leukemia. *Clin Cancer Res* (2021) 27:2764–72. doi: 10.1158/1078-0432.CCR-20-3863

6. Kagoya Y, Guo T, Yeung B, Saso K, Anczurowski M, Wang CH, et al. Genetic ablation of HLA class I, class II, and the T-cell receptor enables allogeneic T cells to be used for adoptive T-cell therapy. *Cancer Immunol Res* (2020) 8:926–36. doi: 10.1158/2326-6066.CIR-18-0508

7. Abrahimi P, Chang WG, Kluger MS, Qyang Y, Tellides G, Saltzman WM, et al. Efficient gene disruption in cultured primary human endothelial cells by CRISPR/Cas9. *Circ Res* (2015) 117:121–28. doi: 10.1161/CIRCRESAHA.117.306290

8. Braud VM, Allan DS, O'callaghan CA, Söderström K, D'andrea A, Ogg GS, et al. HLA-e binds to natural killer cell receptors CD94/NKG2A, b and c. *Nature* (1998) 391:795–99. doi: 10.1038/35869

9. Gornalusse GG, Hirata RK, Funk SE, Riolobos L, Lopes VS, Manske G, et al. HLA-e-expressing pluripotent stem cells escape allogeneic responses and lysis by NK cells. *Nat Biotechnol* (2017) 35:765–72. doi: 10.1038/nbt.3860

10. Heng G, Jia J, Li S, Fu G, Wang M, Qin D, et al. Sustained therapeutic efficacy of humanized anti-CD19 chimeric antigen receptor T cells in Relapsed/Refractory acute lymphoblastic leukemia. *Clin Cancer Res* (2020) 26:1606–15. doi: 10.1158/1078-0432.CCR-19-1339

11. Zhang C, Wang Z, Yang Z, Wang M, Li S, Li Y, et al. Phase I escalating-dose trial of CAR-T therapy targeting CEA(+) metastatic colorectal cancers. *Mol Ther* (2017) 25:1248–58. doi: 10.1016/j.ymthe.2017.03.010

12. Naserian S, Leclerc M, Thiolat A, Pilon C, Le Bret C, Belkacemi Y, et al. Simple, reproducible, and efficient clinical grading system for murine models of acute graft-versus-Host disease. *Front Immunol* (2018) 9:10. doi: 10.3389/fimmu.2018.00010

13. Poirot L, Philip B, Schiffer-Mannioui C, Le Clerre D, Chion-Sotinel I, Derniame S, et al. Multiplex genome-edited T-cell manufacturing platform for "Off-the-Shelf" adoptive T-cell immunotherapies. *Cancer Res* (2015) 75:3853–64. doi: 10.1158/0008-5472.CAN-14-3321

14. Ren J, Liu X, Fang C, Jiang S, June CH, Zhao Y. Multiplex genome editing to generate universal CAR T cells resistant to PD1 inhibition. *Clin Cancer Res* (2017) 23:2255–66. doi: 10.1158/1078-0432.CCR-16-1300

15. Li S, Wang X, Yuan Z, Liu L, Luo L, Li Y, et al. Eradication of T-ALL cells by CD7-targeted universal CAR-T cells and initial test of ruxolitinib-based CRS management. *Clin Cancer Res* (2021) 27:1242–46. doi: 10.1158/1078-0432.CCR-20-1271

16. Colvin RB, Cohen AH, Saiontz C, Bonsib S, Buick M, Burke B, et al. Evaluation of pathologic criteria for acute renal allograft rejection: reproducibility, sensitivity, and clinical correlation. *J Am Soc Nephrol* (1997) 8:1930–41. doi: 10.1681/ASN.V8121930

17. Strehlau J, Pavlakis M, Lipman M, Shapiro M, Vasconcellos L, Harmon W, et al. Quantitative detection of immune activation transcripts as a diagnostic tool in kidney transplantation. *Proc Natl Acad Sci U.S.A.* (1997) 94:695–700. doi: 10.1073/pnas.94.2.695

18. Yang M, Liu L. MHC II gene knockout in tissue engineering may prevent immune rejection of transplants. *Med Hypotheses* (2008) 70:798–801. doi: 10.1016/j.mehy.2007.08.009

19. Guo Y, Xu B, Wu Z, Bo J, Tong C, Chen D, et al. Mutant B2M-HLA-E and B2M-HLA-G fusion proteins protects universal chimeric antigen receptor-modified T cells from allogeneic NK cell-mediated lysis. *Eur J Immunol* (2021) 51:2513–21. doi: 10.1002/eji.202049107

20. Jo S, Das S, Williams A, Chretien AS, Pagliardini T, Le Roy A, et al. Endowing universal CAR T-cell with immune-evasive properties using TALEN-gene editing. *Nat Commun* (2022) 13:3453. doi: 10.1038/s41467-022-30896-2

21. Baginska J, Viry E, Paggetti J, Medves S, Berchem G, Moussay E.Janji B. The critical role of the tumor microenvironment in shaping natural killer cell-mediated anti-tumor immunity. *Front Immunol* (2013) 4:490. doi: 10.3389/fimmu.2013.00490

22. Ma JS, Kim JY, Kazane SA, Choi SH, Yun HY, Kim MS, et al. Versatile strategy for controlling the specificity and activity of engineered T cells. *Proc Natl Acad Sci U.S.A.* (2016) 113:E450–8. doi: 10.1073/pnas.1524193113

23. Morrot A. Human stem memory T cells (T(SCM)) as critical players in the long-term persistence of immune responses. *Ann Transl Med* (2017) 5:120. doi: 10.21037/atm.2017.02.28

24. Golubovskaya V, Wu L. Different subsets of T cells, memory, effector functions, and CAR-T immunotherapy. *Cancers (Basel)* (2016) 8:36. doi: 10.3390/cancers8030036

25. Wherry EJ. T Cell exhaustion. *Nat Immunol* (2011) 12:492–99. doi: 10.1038/ni.2035

26. Turtle CJ, Hanafi LA, Berger C, Hudecek M, Pender B, Robinson E, et al. Immunotherapy of non-hodgkin's lymphoma with a defined ratio of CD8+ and CD4+ CD19-specific chimeric antigen receptor-modified T cells. *Sci Transl Med* (2016) 8:355ra116. doi: 10.1126/scitranslmed.aaf8621

27. Fraietta JA, Lacey SF, Orlando EJ, Pruteanu-Malinici I, Gohil M, Lundh S, et al. Determinants of response and resistance to CD19 chimeric antigen receptor (CAR) T cell therapy of chronic lymphocytic leukemia. *Nat Med* (2018) 24:563–71. doi: 10.1038/s41591-018-0010-1

28. Yang Y, Kohler ME, Chien CD, Sauter CT, Jacoby E, Yan C, et al. TCR engagement negatively affects CD8 but not CD4 CAR T cell expansion and leukemic clearance. *Sci Transl Med* (2017) 9:eaag1209. doi: 10.1126/scitranslmed.aag1209

29. Lanzavecchia A, Iezzi G, Viola A. From TCR engagement to T cell activation: a kinetic view of T cell behavior. *Cell* (1999) 96:1–4. doi: 10.1016/S0092-8674(00)80952-6

30. Smith-Garvin JE, Koretzky GA, Jordan MS. T Cell activation. *Annu Rev Immunol* (2009) 27:591–619. doi: 10.1146/annurev.immunol.021908.132706

31. Rudolph MG, Stanfield RL, Wilson IA. How TCRs bind MHCs, peptides, and coreceptors. *Annu Rev Immunol* (2006) 24:419–66. doi: 10.1146/annurev.immunol.23.021704.115658

32. Marrack P, Scott-Browne JP, Dai S, Gapin L, Kappler JW. Evolutionarily conserved amino acids that control TCR-MHC interaction. *Annu Rev Immunol* (2008) 26:171–203. doi: 10.1146/annurev.immunol.26.021607.090421

33. Cerignoli F, Abassi YA, Lamarche BJ, Guenther G, Santa Ana D, Guimet D, et al. *In vitro* immunotherapy potency assays using real-time cell analysis. *PloS One* (2018) 13:e0193498. doi: 10.1371/journal.pone.0193498

34. Bending D, Prieto Martín P, Paduraru A, Ducker C, Marzaganov E, Laviron M, et al. A timer for analyzing temporally dynamic changes in transcription during differentiation *in vivo*. *J Cell Biol* (2018) 217:2931–50. doi: 10.1083/jcb.201711048

35. Won HY, Hwang ES. Transcriptional modulation of regulatory T cell development by novel regulators NR4As. *Arch Pharm Res* (2016) 39:1530–36. doi: 10.1007/s12272-016-0803-z

36. Hiwa R, Nielsen HV, Mueller JL, Mandla R, Zikherman J. NR4A family members regulate T cell tolerance to preserve immune homeostasis and suppress autoimmunity. *JCI Insight* (2021) 6:e151005. doi: 10.1172/jci.insight.151005

37. Lazarevic V, Zullo AJ, Schweitzer MN, Staton TL, Gallo EM, Crabtree GR, et al. The gene encoding early growth response 2, a target of the transcription factor NFAT, is required for the development and maturation of natural killer T cells. *Nat Immunol* (2009) 10:306–13. doi: 10.1038/ni.1696

38. Li S, Miao T, Sebastian M, Bhullar P, Ghaffari E, Liu M, et al. The transcription factors Egr2 and Egr3 are essential for the control of inflammation and antigen-induced proliferation of b and T cells. *Immunity* (2012) 37:685–96. doi: 10.1016/j.immuni.2012.08.001

39. Collins S, Lutz MA, Zarek PE, Anders RA, Kersh GJ, Powell JD. Opposing regulation of T cell function by egr-1/NAB2 and egr-2/Egr-3. *Eur J Immunol* (2008) 38:528–36. doi: 10.1002/eji.200737157

40. Ramming A, Thümmler K, Schulze-Koops H, Skapenko A. Homotypic T-cell/T-cell interaction induces T-cell activation, proliferation, and differentiation. *Hum Immunol* (2009) 70:873–81. doi: 10.1016/j.humimm.2009.08.003

41. Liu Y, Jia W, Li J, Zhu H, Yu J. Identification of survival-associated alternative splicing signatures in lung squamous cell carcinoma. *Front Oncol* (2020) 10:587343. doi: 10.3389/fonc.2020.587343

42. Holling TM, Schooten E, Van Den Elsen PJ. Function and regulation of MHC class II molecules in T-lymphocytes: of mice and men. *Hum Immunol* (2004) 65:282–90. doi: 10.1016/j.humimm.2004.01.005

43. Qiao J, Li W, Lin S, Sun W, Ma L, Liu Y. Co-Expression of Cas9 and single-guided RNAs in escherichia coli streamlines production of Cas9 ribonucleoproteins. *Commun Biol* (2019) 2:161. doi: 10.1038/s42003-019-0402-x

44. Yip BH. Recent advances in CRISPR/Cas9 delivery strategies. *Biomolecules* (2020) 10:839. doi: 10.3390/biom10060839

45. Stenger D, Stief TA, Kaeuferle T, Willier S, Rataj F, Schober K, et al. Endogenous TCR promotes *in vivo* persistence of CD19-CAR-T cells compared to a CRISPR/Cas9-mediated TCR knockout CAR. *Blood* (2020) 136:1407–18. doi: 10.1182/blood.2020005185

46. Hess NJ, Brown ME, Capitini CM. GVHD pathogenesis, prevention and treatment: Lessons from humanized mouse transplant models. *Front Immunol* (2021) 12:723544. doi: 10.3389/fimmu.2021.723544

47. Jin X, Xu Q, Pu C, Zhu K, Lu C, Jiang Y, et al. Therapeutic efficacy of anti-CD19 CAR-T cells in a mouse model of systemic lupus erythematosus. *Cell Mol Immunol* (2021) 18:1896–903. doi: 10.1038/s41423-020-0472-1

48. Rurik JG, Tombácz I, Yadegari A, Méndez Fernández PO, Shewale SV, Li L, et al. CAR T cells produced *in vivo* to treat cardiac injury. *Science* (2022) 375:91–6. doi: 10.1126/science.abm0594

49. Themeli M, Kloss CC, Ciriello G, Fedorov VD, Perna F, Gonen M, et al. Generation of tumor-targeted human T lymphocytes from induced pluripotent stem cells for cancer therapy. *Nat Biotechnol* (2013) 31:928–33. doi: 10.1038/nbt.2678

50. Dirk BS, Pawlak EN, Johnson AL, Van Nynatten LR, Jacob RA, Heit B, et al. HIV-1 nef sequesters MHC-I intracellularly by targeting early stages of endocytosis and recycling. *Sci Rep* (2016) 6:37021. doi: 10.1038/srep37021

frontiers | Frontiers in Immunology

TYPE Review
PUBLISHED 08 December 2022
DOI 10.3389/fimmu.2022.1079181

OPEN ACCESS

EDITED BY
Ali Hafez El-Far,
Damanhour University, Egypt

REVIEWED BY
Pouya Safarzadeh Kozani,
Guilan University of Medical Sciences, Iran
Enrico Maffini,
University of Bologna, Italy

*CORRESPONDENCE
Xin Kang
honghuikangxin@163.com

SPECIALTY SECTION
This article was submitted to Cancer Immunity and Immunotherapy, a section of the journal Frontiers in Immunology

RECEIVED 25 October 2022
ACCEPTED 24 November 2022
PUBLISHED 08 December 2022

CITATION
Chen X, Li P, Tian B and Kang X (2022) Serious adverse events and coping strategies of CAR-T cells in the treatment of malignant tumors. *Front. Immunol.* 13:1079181. doi: 10.3389/fimmu.2022.1079181

Serious adverse events and coping strategies of CAR-T cells in the treatment of malignant tumors

Xiujin Chen, Peng Li, Bin Tian and Xin Kang*

Department of Orthopedics, Honghui Hospital, Xi'an Jiaotong University, Xi'an, China

Chimeric antigen receptor T (CAR-T) cells technology has been successfully used in the treatment of B cell-derived hematological tumors and multiple myeloma. CAR-T cells are also being studied in a variety of solid tumors. Current clinical reports on CAR-T cells in the treatment of malignant tumors are abundant. The tumor-killing activity of CAR-T cells and the unique adverse effects of CAR-T cells have been confirmed by many studies. There is evidence that serious adverse events can be life-threatening. CAR-T cells therapy is increasingly used in clinical settings, so it is important to pay attention to its serious adverse events. In this review, we summarized the serious adverse events of CAR-T cells in the treatment of malignant tumors by reading literature and searching relevant clinical studies, and discussed the management and treatment of serious adverse events in an effort to provide theoretical support for clinicians who deal with such patients.

KEYWORDS

CAR-T, serious adverse events, lymphoma, leukemia, multiple myeloma, solid tumor, CRS, ICANS

1 Introduction

Immunotherapy has become a mainstay of cancer treatment, in addition to standard surgery, chemotherapy and radiation (1). The discovery of tumor-mediated immunosuppression and its relationship to malignant tumor progression laid the foundation for the application of T cells therapy strategies (2). Thus, gene-edited T cells immunotherapy has been rapidly developed in recent years. Chimeric antigen receptor T cells (CAR-T) are genetically reprogrammed T cells that express antibody fragments that bind specifically to tumor-surface antigens (3). The mechanism of tumor killing is that CAR-T cells bind to tumor antigens and induce a potent antitumor immune response (4, 5). Recently, CD19-targeting CAR-T cells have shown significant efficacy in patients with relapsed/refractory (R/R) CD19+ B cell malignancies (6–10). Targeting BCMA or CD22

CAR-T cells has also demonstrated potent antitumor activity in clinical studies of multiple myeloma and acute lymphoblastic leukemia (11–15). Moreover, CAR-T cells are being studied in solid tumors, although they have shown limited efficacy so far (16–21).

Immune system activation-related toxicities have been shown in clinical studies involving CAR-T cells (22). The toxic symptoms experienced after CAR-T cells therapy are mainly caused by cytokine release syndrome (CRS) and immune effector cell associated neurotoxicity (ICANS) (23). Currently, although the safety profile of CAR-T cells therapy is generally acceptable, the incidence of serious adverse events (SAEs) is high among clinical trials using CAR-T cells (24–26). Therefore, it is crucial to systematically evaluate the toxicity characteristics and life-threatening potential of CAR-T cells therapies. In this article, we downloaded CAR-T cells related clinical study data from the Clinical Trials Database (www.clinicaltrials.gov). In combination with published clinical studies, the clinical manifestations of SAEs of CAR-T cells in the treatment of solid and hematological tumors were summarized. Finally, the management and treatment measures of SAEs were discussed to lay a theoretical foundation for the better application of CAR-T cells in clinical practice.

2 Clinical presentation of SAEs associated with CAR-T cells therapy

Clinicians should be aware of the serious and potentially fatal toxicity associated with CAR-T cells therapy, although they hold promise for the treatment of certain cancers (27). In this study, 24 clinical studies (1208 cases) in hematological tumors and 7 clinical studies (92 cases) in solid tumors were downloaded from the clinical trial database (www.clinicaltrials.gov), and the trial results data were available for all the downloaded clinical studies (Table 1–4). In addition, the data of SAEs from the included clinical studies were analyzed, and the occurrence of SAEs in the treatment of malignant tumors with CAR-T cells was systematically summarized in combination with the relevant published literature. Numerous clinical studies have shown that CAR-T cells can cause SAEs in the treatment of both hematological and solid tumors (Figure 1). The SAEs can affect any organ system of the body, and can develop into multiple organ failure in severe cases, endangering life.

2.1 SAEs of CAR-T cells in the treatment of hematological tumors

2.1.1 Immune system toxicities

This study found that 141 patients (11.67%) had immune system SAEs, and the incidence of SAEs from high to low was the CRS (137 cases), graft versus host disease (2 cases), etc (Table 2). As a result of the high production of cytokines during CAR-T cells therapy, CRS is the most common SAEs of immune system (28). It was found that 128 cytokines may be closely related to CRS, among which IL6, IFN-γ, TNF-α, ICAM-1, VCAM-1, VEGFA and other important factors may be the key factors to predict CRS (29). Additionally, it causes SAEs throughout the body in a variety of systems (30). Cytokines are a double-edged sword in the process of CAR-T cells therapy, which can stimulate immune cells to kill tumor cells while also causing damage to normal organs of the body (31, 32).

Z. Ying et al. (33)conducted a meta-analysis involving 27 studies (1687 patients) to evaluate the safety of CD19-targeted CAR-T cells in patients with diffuse large B-cell lymphoma (DLBCL). Severe CRS and severe neurotoxicity were found in 6% (95%CI: 3-10%) and 16% (95%CI: 10-24%), respectively. Moreover, studies have shown that neurological SAEs are associated with CRS (34, 35). This suggests that CRS may contribute to neurological adverse events. Furthermore, M. Shao et al. (36) retrospectively analyzed the adverse events of 37 R/R MM patients treated with BCMA-targeted CAR-T cells. All of the 37 patients had CRS, and 34 (91%) had at least one coagulation parameter abnormality. The values of coagulation parameters were positively correlated with the severity of CRS, as well as with the levels of cytokines such as IL-6, IL-10 and IFN-γ. The findings suggest that these factors may play an important role in CRS-related coagulopathy as well as a connection between coagulopathy and CRS. In addition, J. Zhou et al. (37) retrospectively analyzed 133 patients with R/R lymphoma who received CAR-T cells therapy. Studies have found that severe neutropenia, anemia, and thrombocytopenia frequently occur after CAR-T cells infusion. Further studies found that both neutropenia and severe thrombocytopenia in severe patients were associated with the incidence of CRS and the levels of associated inflammatory factors. The above studies all reflect that CRS is an adverse events and a initiating factor causing various SAEs.

2.1.2 Nervous system toxicities

In this study, 244 patients (20.20%) developed nervous system SAEs. The incidence of clinical symptoms from high to low was encephalopathy (94 cases), speech impairment (33 cases), seizure (24 cases), somnolence (20 cases), confusion (11 cases), syncope (8 cases), and brain oedema (8 cases), headache (8 cases), etc (Table 2). The most common life-threatening neurological adverse event is encephalopathy, probably due to the significant effects of CAR-T cells on cerebral vessels. Secondly, the high incidence of severe speech complications found in this study suggests that the language center may also be an easy target for CAR-T cells. Seizures are also very common, indicating that CAR-T cells disrupt brain neuronal electrical activity.

TABLE 1 The incidence of clinically serious adverse events of CAR-T in hematological tumors.

NCT Number	Conditions	Interventions	Characteristics	countrys	Adverse event assessment criteria	Enrollment	All-Cause Mortality (n/Total)	Serious adverse events (n/Total)	Other (Not Including Serious) Adverse Events(n/Total)
NCT03958656	Myeloma;Multiple Myeloma	Anti-Signaling; lymphocytic activation molecule F7 (SLAMF7); chimeric antigen receptor(CAR) T cells	Phase 1	United States	CTCAE v5.0	10	0/10	3/10	10/10
NCT03287804	Multiple Myeloma	AUTO2	Phase 1 Phase 2	United Kingdom	CTCAE v4.0	11	8/11	6/11	11/11
NCT03289455	B-cell Acute Lymphoblastic Leukemia	AUTO3 (CD19/22 CAR-T cells	Phase 1 Phase 2	United Kingdom	CTCAE v5.0	15	9/15	6/15	15/15
NCT00924326	Primary Mediastinal B-cell Lymphoma; Diffuse, Large B-cell; Lymphoma	Anti-CD19-CAR-T cells	Phase 1 Phase 2	United States	CTCAE 3.0	46	2/46	29/46	46/46
NCT03019055	Lymphoma;Non-Hodgkin, Lymphoma, B-Cell; Small Lymphocytic Lymphoma	CAR-20/19-T cells	Phase 1	United States	CTCAE v4.0	22	0/22	22/22	22/22
NCT02659943	Lymphoma;B-Cell, Lymphoma, Non-hodgkins	Anti-CD19-CAR-T cells	Phase 1	United States	CTCAE v5.0	21	0/21	17/21	21/21
NCT02794246	Multiple Myeloma	Anti-CD19-CAR-T cells	Phase 2	United States	CTCAE v4.03	6	0/6	2/6	1/6
NCT01747486	Relapsed or Refractory CLL or SLL	Anti-CD19-CAR-T cells	Phase 2	United States	CTCAE v4.0	42	12/42	32/42	35/42
NCT02215967	Myeloma-Multiple Myeloma	Anti- BCMA-CAR-T cells	Phase 1	United States	CTCAE 4.0	26	0/26	13/26	26/26
NCT02535364	Acute Lymphoblastic Leukemia	Anti-CD19-CAR-T cells	Phase 2	United States	CTCAE v4.0	38	24/38	23/38	38/38
NCT01593696	B Cell Lymphoma, Leukemia	Anti-CD19-CAR-T cells	Phase 1	United States	CTCAE v4.0	53	29/53	14/53	53/53
NCT01593696	Recurrent Plasma Cell Myeloma	BCMA CAR-T Cells	Phase 1	United States	CTCAE v4.0	25	7/25	21/25	25/25
NCT01593696	Lymphoma; Lymphoma, Large B-Cell, Diffuse; Lymphoma, Extranodal NK-T Cell;Lymphoma, T-Cell,Peripheral	Anti-CD30 CAR-T Cells	Phase 1	United States	CTCAE v5.0	22	0/22	10/22	22/22
NCT03318861	Relapsed/Refractory Multiple Myeloma	BCMA-CAR-T cells(KITE-585)	Phase 1	United States	CTCAE v 4.03	14	7/14	1/14	14/14
NCT01593696	ALL;B Cell Lymphoma; Leukemia;Large	Anti-CD19-CAR-T cells	Phase 1	United States	CTCAE v 4.0	53	29/53	14/53	53/53

(Continued)

10.3389/fimmu.2022.1079181

TABLE 1 Continued

NCT Number	Conditions	Interventions	Characteristics	countrys	Adverse event assessment criteria	Enrollment	All-Cause Mortality (n/Total)	Serious adverse events (n/Total)	Other (Not Including Serious) Adverse Events(n/Total)
	CellLymphoma; Non-Hodgkin Lymphoma								
NCT03624036	Relapsed/Refractory Chronic Lymphocytic Leukemia and Relapsed/Refractory Small Lymphocytic Lymphoma	Anti-CD19-CAR-T cells(KTE-X19)	Phase 1	United States	CTCAE v 5.0	16	3/16	7/16	16/16
NCT02030847	Patients With B Cell ALL, Relapsed or Refractory	CD19-CAR-T	Phase 2	United States	CTCAE v 4.0	30	30/30	30/30	30/30
NCT02614066	Relapsed/Refractory Bprecursor Acute Lymphoblastic Leukemia	Anti-CD19 CAR-T Cells	Phase 1 Phase 2	United States	CTCAE v 4.0	125	65/125	80/125	125/125
NCT03761056	B-cell Lymphoma	anti-CD19 CAR-T	Phase 2	United States, Australia and France	CTCAE v5.0	40	6/40	18/40	40/40
NCT01865617	Recurrent Adult Acute Lymphoblastic Leukemia;Recurrent Chronic Lymphocytic Leukemia;Recurrent Diffuse Large B-Cell Lymphoma Recurrent Mantle Cell Lymphoma	anti-CD19 CAR-T	Phase 1 Phase 2	United States	CTCAE v 4.0	197	115/197	189/197	196/197
NCT02348216	B-Cell Lymphoma; Transformed Follicular Lymphoma (TFL)	anti-CD19 CAR-T	Phase 1 Phase 2	United States	CTCAE v 4.0	292	115/292	153/292	292/292
NCT02926833	Refractory Diffuse Large B Cell Lymphoma	anti-CD19 CAR-T	Phase 1 Phase 2	United States	CTCAE v 4.0	34	11/34	23/34	34/34
NCT02706405	B Cell Lymphoma	anti-CD19 CAR-T	Phase 1	United States	CTCAE v 4.03	29	13/29	19/29	29/29
NCT03568461	Follicular Lymphoma	anti-CD19 CAR-T	Phase 2	United States	CTCAE v 4.03	97	7/97	42/97	94/97

All clinicaltrials can be downloaded from www.clinicaltrials.gov (accessed October 02, 2022).

Neurotoxicity caused by CAR-T cells, also known as ICANS, is the primary cause of these complications (38). Similarly, studies have demonstrated that the most common ICANS with CAR-T cells include encephalopathy, headache, tremor, dizziness, aphasia, delirium, insomnia, and anxiety (39, 40). L. Lv et al. (41)explored the safety of CAR-T cells for central nervous system lymphoma (CNSL). A total of 63 patients were included in 8 studies in the meta-analysis, and the incidence of grade 3 or above neurotoxicity was found to be 12%. Besides, A. Gajra et al. (42) investigated adverse neurologic events associated with

TABLE 2 Summary of clinical serious adverse events of CAR-T in hematological tumors(Patients Number/symptom).

NCT Number (Patients Number)	General complications	Infections and infestations	Cardiac complications	Nervous system complications	Immune system complications	Blood and lymphatic system complications	Respiratory, thoracic and mediastinal complications	Gastrointestinal complications	Vascular complications
NCT03287804 (11)	2/Pyrexia	1/Lung infection	1/Acute myocardial infarction	1/Hedache			1/Dyspnoea		
NCT03289455 (15)	1/Pyrexia	1/Cellulitis		1/Encephalopathy;1/Seizure		3/Anaemia;3/ Neutropenia; 3/ Thrombocytopenia;2/ Febrile neutropenia			
NCT00924326 (46)	3/Fever	1/Pneumonia	2/Arrhythmia. Supraventricular tachycardia;1/ Supraventricular and nodal arrhythmia;1/ Atrial fibrillation;1/Left ventricular systolic dysfunction	12/Speech impairment; 10/ Confusion; 9/Somnolence, depressed level of consciousness; 4/Neuropathy,motor; 2/Seizure; 2/ Ataxia;2/Cognitive disturbance; 1/ CNS cerebrovascular ischemia;1/ Encephalopathy		6/Febrile neutropenia; 1/Lymphopenia	4/Hypoxia; 2/Dyspnea	1/Colitis;2/Dysphagia	5/Hypotension;2/ Thrombosis
NCT03338972 (25)	11/fever	1/lung infection;1/ upper respiratory infection			1/CRS	8/febrile neutropenia; 2/neutropenic fever		1/nausea	1:hypotension
NCT02535364 (38)	1/Asthenia; 1/Pyrexia	2/Sepsis;1/ Bacteraemia	1/Atrial fibrillation; 1/Myocardial infarction	8/Encephalopathy; 5/Brain oedema; 2/Seizure	8/CRS	1/Febrile neutropenia		1/Neutropenic colitis;1/Abdominal pain	
NCT03049449 (22)	2/Fever	3/Sepsis	3/Sinus tachycardia	1/Encephalopathy		1/Anemia	1/Dyspnea; 1/Hypoxia	1/Diarrhea; 1/Nausea	4/Hypotension
NCT03318861 (14)	1/Chest pain						1/Hypoxia		
NCT01593696 (53)	3/Fever		3/Sinus tachycardia;2/ Left ventricular systolic dysfunction; 1/Cardiac arrest; 1/Heart failure	4/Nervous system complications; 2/Seizure; 1/Dysphasia; 1/ Headache; 1/Hydrocephalus; 1/Somnolence	9/CRS		2/Hypoxia; 1/Pulmonary edema; 1/Respiratory failure		2/Hypotension;1/ Hypertension
NCT03624036 (16)	2/Pyrexia; 1/Malaise	1/Sepsis; 1/Systemic candida	1/Tachycardia	1/Aphasia; 1/Confusional state	4/CRS			1/Abdominal pain	3/Hypotension;1/ Embolism
NCT02030847 (30)		3/Sepsis;2/ Pneumonia;1/ Meningitis;1/ Staphylococcal infection		1/Haemorrhage intracranial; 1/ Headache;1/Seizure	21/CRS	1/Febrile neutropenia	1/Hypoxia	1/Constipation	

(Continued)

10.3389/fimmu.2022.1079181

TABLE 2 Continued

NCT Number (Patients Number)	General complications	Infections and infestations	Cardiac complications	Nervous system complications	Immune system complications	Blood and lymphatic system complications	Respiratory, thoracic and mediastinal complications	Gastrointestinal complications	Vascular complications
NCT02614066 (125)	20/Pyrexia;2: Fatigue; 1:Chills; 1:Multiple organ dysfunction syndrome;1:Face oedema	9/Bacteraemia;7/ Sepsis;6/ Pneumonia;1/ Cellulitis	9/tachycardia;1/ Cardiomyopathy	15/Encephalopathy;7/Aphasia;5/ Seizure;2/Cerebrovascular accident;1/Immune effector cell-associated neurotoxicity syndrome;1/Brain oedema; 1/ Facial paralysis 1/Headache	1/Drug hypersensitivity;1/ Graft versus host disease;	6/Febrile neutropenia; 2/Pancytopenia;2/ Disseminated intravascular coagulation; 1/Cytopenia; 1/Neutropenia	13/Hypoxia;5: Respiratory failure; 4:ARDS;3/ Dyspnoea;1/ Pulmonary embolism	2/Colitis;2/Ileus;1/ Diarrhoea;1/Gastritis	31/Hypotension;1/ Hypertension;1/ Shock
NCT03019055 (22)	1/Fever;1/Multi-organ failure	1/Upper respiratory infection		1/Nervous system complications - Other, specify	5/CRS	4/Blood and lymphatic system complications; 1/Febrile neutropenia	1/Pleural effusion; 1/Pneumonitis	1/Diarrhea	
NCT03761056 (40)	3/Pyrexia;2/Non-cardiac chest pain	3/infection;1/Covid-19;1/Covid-19 pneumonia;1/ Cytomegalovirus infection reactivation	1/Atrial fibrillation; 1/ Sinus bradycardia; 1/ Supraventricular tachycardia	5/Encephalopathy;1/ Neurotoxicity;1/Dysarthria;1/ Memory impairment; 1/ Haemorrhage intracranial		1/Anaemia;1/ Neutropenia	1/Acute pulmonary oedema	1/Abdominal pain	1/Hypertension;1/ Hypotension
NCT01865617 (195)	17/Fever;3/Multi-organ failure	9/Infections and infestations-Other, specify;6/Lung infection; 3/Sepsis	3/Atrial fibrillation; 3/ Sinus tachycardia; 2/ Cardiac arrest; 2/Heart failure; 2/Left ventricular systolic dysfunction	18/Encephalopathy;4/Seizure; 4/ Depressed level of consciousness;2/Edema cerebral;2/Nervous system complications;1/Dysphasia	41/CRS	132/Febrile neutropenia; 2/Disseminated intravascular coagulation;	8/Respiratory failure;6/ Hypoxia;3/Pleural effusion; 3/ Pulmonary edema;2/ARDS;1/ Dyspnea	2/Abdominal pain;2/ Nausea	34/Hypotension
NCT02659943 (21)	1/Fever	1/Lung infection	1/Cardiac arrest; 1/Sinus tachycardia	3/Syncope;1/Encephalopathy;1/ Tremor		1/Anemia;1/ Neutrophil count decreased	3/Hypoxia	2/Diarrhea;1/ Abdominal pain; 1/ Ileus	6/Hypotension
NCT02348216 (292)	25/Pyrexia	7/Lung infection; 3/ Bacteraemia;2/ Adenovirus infection;2/Covid-19; 1/Covid-19 pneumonia	4/Atrial fibrillation; 4/ Cardiac arrest; 2/Atrial flutter; 2/Cardiac failure	29/Encephalopathy;10/Aphasia;8/ Somnolence;5/Seizure;3/ Headache;3/Syncope;2/Depressed level of consciousness; 2/ Haemorrhage intracranial; 1/ Immune effector cell-associated neurotoxicity syndrome;		12/Febrile neutropenia; 5/Neutropenia;5/ Pancytopenia;2/ Thrombocytopenia; 2/Bone marrow failure	7/Hypoxia;2/ Acute respiratory failure; 2/Pleural effusion	3/Abdominal pain;3/ Pancreatitis;2/ Dysphagia	13/Hypotension
NCT02926833 (34)	3/Pyrexia;1/ Multiple organ dysfunction syndrome;1/ Localised oedema	1/Lung infection; 1/Sepsis	1/Supraventricular tachycardia	10/Encephalopathy;2/Seizure;1/ Aphasia	1/ Haemophagocytic lymphohistiocytosis	2/Anaemia;1/ Neutropenia;1/ Febrile neutropenia	3/Hypoxia;1/ Respiratory failure; 1/Pleural effusion	1/Abdominal pain;1/ Diarrhoea;1/ Obstruction gastric	2/Hypotension

(Continued)

10.3389/fimmu.2022.1079181

TABLE 2 Continued

NCT Number (Patients Number)	General complications	Infections and infestations	Cardiac complications	Nervous system complications	Immune system complications	Blood and lymphatic system complications	Respiratory, thoracic and mediastinal complications	Gastrointestinal complications	Vascular complications
NCT02215967 (25)	2/Fever	2/Lung infection; 2/ Upper respiratory infection	4/Sinus tachycardia; 1/ Supraventricular tachycardia	1/Encephalopathy		1/Disseminated intravascular coagulation	6/Dyspnea;3/ Hypoxia	2/Diarrhea	6/Hypotension
NCT02706405 (29)	5/Fever;1/Multi-organ failure	1/Bacteremia	2/Sinus tachycardia	2/Encephalopathy;1/Somnolence	9/CRS	3/Febrile neutropenia	1/Dyspnea;1/ Pleural effusion	2/Abdominal pain;1/ Duodenal hemorrhage	1/Hypotension
NCT03958656 (10)	1/Fever		2/Sinus tachycardia		1/CRS				
NCT03568461 (97)	3/Pyrexia	8/Pneumonia;6/ encephalitis;1/ Bacteraemia;1/ COVID-19;1/ COVID-19 pneumonia; 1/Lower respiratory tract infection;1/Sepsis	1/Ventricular fibrillation	2/Encephalopathy;1/Headache;1/ Immune effector cell-associated neurotoxicity syndrome;1/ Syncope	19/CRS;1/Graft versushost disease in gastrointestinal tract	6/Febrile neutropenia; 2/Neutropenia;1/ Anaemia	2/Pleural effusion; 1/Acute respiratory failure;1/ Dyspnoea;1/ Pneumothorax	1/Gastrointestinal ulcer;1/Nausea;1/ Vomiting;1/Stomatitis	
NCT02794246 (6)		1/Upper respiratory infection			1/CRS				
NCT01747486 (42)	10/Pyrexia;1/ Fatigue	2/Pneumonia;2/ Upper respiratory tract infection; 1/Sepsis		1/Encephalopathy;1/Syncope	18/CRS	8/Febrile Neutropenia	1/Hypoxia;1/ Pneumonitis;1/ Pulmonary oedema	1/Abdominal Pain;1/ Diarrhoea	

All clinicaltrials can be downloaded from www.clinicaltrials.gov (accessed October 02, 2022).

10.3389/fimmu.2022.1079181

TABLE 3 The incidence of clinical serious adverse events of CAR-T in solid tumors.

NCT Number	Conditions	Interventions	Characteristics	Country	Adverse event assessment criteria	Enrollment/ n	All-Cause Mortality (n/Total)	Serious adverse events (n/ Total)	Other (Not Including Serious) Adverse Events(n/ Total)
NCT02664363	Glioblastoma; Gliosarcoma	EGFRvIII CAR-T cells	Phase 1	United States	CTCAE v5.0	3	3/3	1/3	3/3
NCT03330834	Advanced Lung Cancer	PD-L1 CAR-T cells	Phase 1	China	CTCAE v4.0	1	1/1	1/1	1/1
NCT01454596	Malignant Glioma; Glioblastoma; Brain Cancer; Gliosarcoma	EGFRvIII CAR-T cells	Phase 1 Phase 2	United States	CTCAE v4.0	18	1/18	2/18	18/18
NCT01583686	Cervical Cancer; Pancreatic Cancer; Ovarian Cancer; Mesothelioma; Lung Cancer	Anti-mesothelin CAR-T cells	Phase 1 Phase 2	United States	CTCAE v4.0	15	1/15	5/15	15/15
NCT01218867	Metastatic Cancer; Metastatic Melanoma; Renal Cancer	Anti-VEGFR2 CAR-T cells	Phase 1 Phase 2	United States	CTCAE v3.0	22	1/22	5/22	21/22
NCT02761915	Relapsed or Refractory Neuroblastoma	Genetic/1RG-CAR-T cells	Phase 1	United Kingdom	CTCAE v4.0	12	6/12	5/12	12/12
NCT02706392	Hematopoietic and Lymphoid Cell Neoplasm; Malignant Solid Neoplasm; Metastatic Lung Non-Small Cell Carcinoma; Metastatic Triple-Negative Breast Carcinoma; Recurrent Acute Lymphoblastic Leukemia; Recurrent Mantle Cell Lymphoma; Refractory Chronic Lymphocytic Leukemia	ROR1 CAR-T cells	Phase 1	United States	CTCAE v4.0	21	12/21	17/21	21/21

All clinicaltrials can be downloaded from www.clinicaltrials.gov (accessed October 02, 2022).

TABLE 4 Summary of clinical serious adverse events of CAR-T in solid tumors(Patients Number/symptom).

NCT Number (Patients Number)	General complications	Infections and infestations	Nervous system complications	Immune system complications	Blood and lymphatic system complications	Respiratory, thoracic and mediastinal complications	Gastrointestinal complications	Vascular complications
NCT03330834 (1)						1/1interstitial pneumonia disease		
NCT02664363 (3)	1/Generalized muscle weakness		1/Confusion					
NCT01583686 (15)					1/Anemia 1/Platelet count decreased;2/ Lymphocyte count decreased	1/Hypoxia	1/Constipation	
NCT01218867 (22)	1/Pain;3/ALT, SGPT (serum glutamic pyruvic transaminase);3/AST, SGOT (serum glutamic oxaloacetic transaminase);3/Bilirubin (hyperbilirubinemia)	1/Infection				2/Hypoxia	1/Nausea;1/Vomiting	
NCT01454596 (18)	1/Multi-organ failure					1/Dyspnea (shortness of breath);1/Hypoxia		
NCT02706392 (21)	13/Fever 1/Non-cardiac chest pain;1/Myalgia		1/Encephalopathy	3/CRS	3/Febrile neutropenia	2/Dyspnea 3/Hypoxia 1/Respiratory failure		3/Hypotension
NCT02761915 (12)	1/Pain;5/Pyrexia	1/Post procedural cellulitis;1/ Pseudomonal bacteraemia;1/ Pseudomonal sepsis;1/Urinary tract infection			1/Febrile neutropenia;	1/Laryngeal haemorrhage		

All clinicaltrials can be downloaded from www.clinicaltrials.gov (accessed October 02, 2022).

10.3389/fimmu.2022.1079181

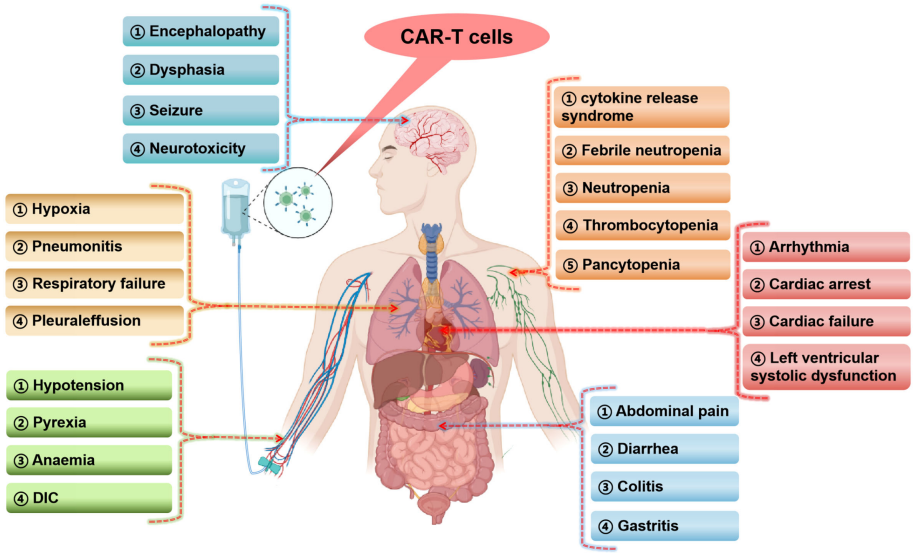

FIGURE 1
Occurrence of serious adverse events in various human systems in CAR-T cells clinical studies (The figure is produced using the BioRender online graphics website). DIC, disseminated intravascular coagulation.

CAR-T cells therapy in patients with R/R large B-cell lymphoma. There are a lot of neurologic adverse events associated with CAR-T cells therapy in the real world, which is a testament to the truthfulness of clinical trial reports. Although real data on CAR-T cells-associated neurotoxicity are limited, one study found an inverse association between grade 3-4 neurotoxicity and OS (43). According to these studies, neurological dysfunction is universal and important in the clinical application of CAR-T cells therapy.

2.1.3 Respiratory, thoracic and mediastinal toxicities

In this study, 103 patients (8.53%) developed respiratory, thoracic and mediastinal SAEs. The incidence of clinical symptoms from high to low were hypoxia (45 cases), respiratory failure (18 cases), dyspnea (12 cases), pleural effusion (10 cases), pulmonary edema (6 cases), ARDS (6 cases), pneumonitis (2 cases), etc (Table 2). The most common SAEs of the respiratory system is hypoxemia, and the disease can progress to respiratory failure. Common co-symptoms are dyspnea, pleural effusion, pulmonary edema, ARDS, and pneumonia.

Researchers have found that respiratory SAEs are a leading cause of death associated with CAR-T cells therapy. J. Pan et al. (44) evaluated the safety of anti-CD7 CAR-T cells in 20 patients with R/R T cells acute lymphoblastic leukemia (NCT04689659). The results of the study found that all adverse events were reversible, except for one patient who died from a related fungal pneumonia. Similarly, in the study of R. Benjamin et al. (45), two treatment-related deaths occurred. One was caused by neutropenic sepsis complicated by CRS, and the other by pulmonary hemorrhage with persistent cytopenia. K. Rejeski et al. (46) described the clinical course of a 59-year-old patient with R/R large B-cell lymphoma who received Axicabtagene-Ciloleucel. Severe pneumonia eventually leads to respiratory failure and death. Furthermore, respiratory adverse events may be affected by CRS. A. Goldman et al. (47) retrospectively analyzed adverse events in 2657 patients who received CD19-targeted CAR-T cells therapy. Cardiopulmonary adverse events occurred in 546 patients (20.5%). Ultimately, the mortality rate for cardiopulmonary adverse events was 30.9%. Studies have shown associations between CAR-T cells and various cardiopulmonary adverse events, including rapid respiratory failure, hypoxemia, arrhythmias, cardiomyopathy, pericardial and pleural diseases. In addition, the overlapping reports of cardiopulmonary adverse events and CRS were found in 68.3% of the cases. CRS may also be involved in the pathogenesis of severe cardiopulmonary adverse events, which should be considered in the multidisciplinary evaluation and monitoring of CAR-T cells recipients.

2.1.4 Cardiovascular toxicities

In this study, 116 patients (9.60%) had vascular SAEs, and the main clinical SAEs were hypotension (109 cases), thrombosis (3 cases), hypertension (3 cases), etc (Table 2). 68 patients (5.63%) had cardiac SAEs. The incidence of SAEs from high to low are sinus tachycardia (28 cases), atrial fibrillation (10 cases), cardiac arrest (8 cases), and supraventricular fibrillation

tachycardia (5 cases), left ventricular systolic dysfunction (5 cases), heart failure (5 cases), myocardial dysfunction (2 cases), etc (Table 2). Studies have found that the main SAEs of vascular complications is hypotension, the pathogenesis may be due to the occurrence of inflammation in the body produces a large number of inflammatory cytokines released into the blood, resulting in peripheral vascular dilatation (48, 49). Arrhythmias occur in the cardiovascular system to compensate for hypotension, so the most common arrhythmias are sinus tachycardia and atrial fibrillation. Severe arrhythmias can progress to cardiac arrest and eventually lead to heart failure (50). In addition, symptoms of left ventricular dysfunction have been seen in clinical studies (48, 51). Therefore, the occurrence of adverse cardiovascular events may be due to the massive cytokine release during CAR-T cells therapy.

Cardiovascular toxicity is not uncommon in patients receiving CAR-T cells therapy (52). Adam Goldman et al. (47) found that the occurrence of tachyarrhythmia was a major adverse effect of the heart. Atrial fibrillation is the main tachyarrhythmia, followed by ventricular arrhythmia. Studies have also shown an association between CAR-T cells and symptoms such as tachyarrhythmia, cardiomyopathy, pericardial and pleural disease. Additionally, 10-30% of patients also exhibit decreased left ventricular ejection function (48). R. M. Alvi et al. (53) also reported a new reduction in ejection fraction in 8 of 137 patients, 5 patients also experienced arrhythmias, and 6 patients experienced cardiovascular death. To examine cardiovascular adverse events associated with CAR-T cells, A. Guha et al. (54) used the U.S. Food and Drug Administration Adverse Event Reporting System (FAERS) to observe 996 cases in which the most commonly reported cardiovascular adverse event was arrhythmia (77.6%). This was followed by heart failure (14.3%) and myocardial infarction (0.5%). Cardiovascular adverse events associated with CAR-T cells therapy were also associated with higher mortality. Therefore, the use of CAR-T cells in tumor therapy should be vigilant for cardiovascular events.

2.1.5 Gastrointestinal toxicities

In this study, 48 patients (3.97%) had gastrointestinal SAEs. The incidence of SAEs from high to low were abdominal pain (13 cases), diarrhea (9 cases), nausea (5 cases), colitis (4 cases), dysphagia (4 cases), pancreatitis (3 cases), etc (Table 2). The adverse events of CAR-T cells on the digestive system are relatively less, and SAEs are mainly caused by gastroenteritis leading to abdominal pain, diarrhea and other clinical manifestations. A small number of adverse events of pancreatitis were also observed. These results suggest that CAR-T cells may be mainly through its cytokines acting on gastrointestinal mucosa, leading to impaired barrier function and the progression of mucositis (55). The incidence of SAEs in the digestive system is significantly less than that in the nervous, immune, cardiovascular and respiratory systems. Moreover, the severity of adverse effects is relatively mild, and no serious life-threatening adverse events have been reported.

2.1.6 Infections and infestations

Infection-related SAEs occurred in 116 patients (9.60%). The incidence of SAEs from high to low were lung infection (33 cases), upper respiratory infection(7 cases), sepsis (22 cases), bacteraemia(15 cases), Covid-19(4 cases), and Covid-19 pneumonia(3 cases), etc (Table 2). The most common infection is a respiratory tract infection, which can involve the lungs in severe cases. Telli Dizman et al. (56) conducted a systematic review and meta-analysis of the incidence of severe infections in hematological malignancies treated with CAR-T cells. The severe infection rate was 16.2%, with the respiratory tract being the most common site of infection. This also confirms the above views. The common pathogen is bacteria, but it can also be seen in clinical studies of COVID-19 infection. Besides, severe bacteremia and septicemia are often seen. The immune barrier function may be impaired during CAR-T cells therapy, allowing opportunistic pathogens to flourish (57).

Most infections after CAR-T cells therapy occur after neutropenia and/or severe CRS, indicating a greater degree of immune impairment (58, 59). Furthermore, most CAR-T cells recipients had previously received other antitumor therapies, including autologous and allogeneic hematopoietic cell transplants. Preexisting cytopenia and hypogammaglobulinemia increase the likelihood of infection (60, 61). The occurrence of CRS co-infection may lead to a greater impact on the body, which may not respond well to antimicrobial therapy. In the study conducted by J. A. Hill et al. (58), 80% of patients had their first infection within the first 10 days after CAR-T cells infusion, mainly with gram-negative bacterial infections. Besides, 42% of patients had predominantly viral infections within 30 days of infusion, including respiratory viral infections and cytomegaloviremia and pneumonia. Later infection may reflect a state of immunoglobulin deficiency and lymphocytopenia (58). These studies suggest that serious infection-related adverse events associated with CAR-T cells therapy are not only related to CRS, but also to the patient's immunocompromised physical condition, posing a serious threat to patient health.

2.1.7 Blood and lymphatic system toxicities

Blood and lymphatic system SAEs were found in 228 patients (18.87%). The incidence of SAEs from high to low is febrile neutropenia (187 cases), neutropenia (12 cases), anaemia (9 cases), pancytopenia (8 cases), thrombocytopenia (5 cases), and disseminated intravascular coagulation (DIC) (5 cases), etc (Table 2). The most common SAEs of hemolymph system is neutropenia. As an important immune cell, neutrophils play an important role in preventing the invasion of pathogenic microorganisms. However, neutrophil depletion during CAR-T

cells treatment may account for the susceptibility of the body to infection-related diseases. Besides, the study found that patients also had a decrease in various blood cells and platelets (62), which indicates that the blood system may be seriously damaged during the treatment.

When injected into the bloodstream to kill tumors, CAR-T cells have been shown to be hemotoxic (62). L. Wang et al. (63) retrospectively studied the characteristics and risk factors of new-onset severe cytopenia after CAR-T cells infusion in 76 patients with R/R acute lymphoblastic leukemia. A high incidence of new severe cytopenia was found, including severe neutropenia (56,70%), severe anemia (66,53%), and severe thrombocytopenia (64,48%). The study also found that people with higher levels of CRS had higher incidence and longer duration of severe cytopenia. Multivariate analysis showed that the occurrence of CRS and higher grade of CRS were risk factors for prolonged hematotoxicity. These observations lead to the conclusion that the occurrence of CRS is associated with the incidence of severe cytopenia, suggesting that CRS may be a direct or indirect cause of hemotoxicity.

2.1.8 General toxicities

General SAEs occurred in 133 patients (11.01%). The incidence of SAEs from high to low was pyrexia (116 cases), multi-organ failure (7 cases), fatigue (3 cases), etc (Table 2). The most common adverse effect of the body is pyrexia, which is mainly caused by the massive release of inflammatory factors into the blood during CRS, but the possibility of subsequent infection after the immune system is compromised cannot be ruled out (57). Therefore, it is difficult to distinguish CRS or infection from fever alone during CAR-T cell therapy.

2.2 SAEs of CAR-T in the treatment of solid tumors

In this study, nervous system SAEs occurred in 2 cases (2.17%) during the treatment of solid tumors. Confusion (1 case) and encephalopathy (1 case) were the SAEs (Table 4). There were 3 cases (3.26%) of SAEs in Immune system and the main SAEs was CRS (Table 4). The type of SAEs of CAR-T cells in the treatment of solid tumors is basically similar to that of the hematological tumors. However, no cardiovascular adverse events were found in the included studies. In addition, this study have found that the incidence of neurological SAEs and CRS in solid tumors is lower than that in hematological tumors (Figure 2). Similarly, a clinical study (NCT03874897) conducted by C. Qi et al. (64) evaluated the safety and efficacy of CAR-T cells targeting CLDN18.2 in the treatment of gastric cancer. Results of 37 patients treated, 94.6% had grade 1 or 2 CRS. However, no deaths have been reported. Besides, Y. Liu et al. (65) conducted a phase I trial (NCT01869166) to evaluate the safety and efficacy of autologous anti-EGFR CAR-T cells in patients with metastatic prostate cancer in 14 patients. No SAEs such as cardiovascular system, nervous system, blood system and CRS were found. Furthermore, Y. Zhang et al. (66) also evaluated the safety of EGFR-targeted CAR-T cells in the treatment of small cell lung cancer. The most common adverse events were grade 1 to 3 fever. No patients had grade 4 adverse events or severe CRS. The tumor-killing sites of CAR-T cells are different in hematological tumors than in solid tumors. Solid tumors are more limited to tumor tissues due to targeted guidance, while hematological tumors cover the entire blood system due to tumor cells dispersed in the blood system. Therefore, some SAEs of CAR-T cells in hematological tumors may be more severe than those in solid tumors.

In this study, Respiratory, thoracic and mediastinal SAEs, Infection-related SAEs, Blood and lymphatic system SAEs, General SAEs occurred in 13 cases (14.13%), 5 cases (5.43%), 8 cases (8.70%) and 33 cases (35.87%) respectively (Table 4). Similarly, Z. Zhao et al. (55) conducted a meta-analysis involving 10 studies (94 patients) that reported the occurrence of adverse events during the treatment of digestive system tumors with CAR-T cells. The study found that the five most common side effects were fever, lymphadenia, pain other than abdominal pain, thrombocytopenia and fatigue. The specific SAEs types were basically the same as those of hematological tumors. Interestingly, these findings suggest that CAR-T cells SAEs in solid tumors and hematological tumors are similar.

3 The pathological mechanism of SAEs in the treatment of malignant tumors by CAR-T cells

It has been established that CRS and ICANS are the two major causes of all complications associated with CAR-T cells therapy (31, 42, 67, 68). In light of this, understanding the pathological mechanism of CRS and ICANS is of theoretical importance when dealing with patients with severe complications.

CRS is a systemic inflammatory response, and current studies have shown that it can be induced by a variety of factors, including severe infection, followed by drugs, such as CAR-T cells and monoclonal antibodies (69–74). Severe viral infections such as influenza and COVID-19 can also trigger CRS through massive immune and non-immune cell stimulation (75). CRS is usually associated with tumor load and usually occurs between day 1 and week 2 after CAR-T cells infusion (76, 77). All systems of the body are affected by CRS, including fever, myalgia, anorexia, hypotension, tachycardia, arrhythmia, shortness of breath and hypoxia, coagulopathy, respiratory failure, shock and organ dysfunction etc (42, 46, 48, 57, 78).

Upon interaction of CAR-T cells with the corresponding target antigen, inflammatory cytokines and chemokines such as

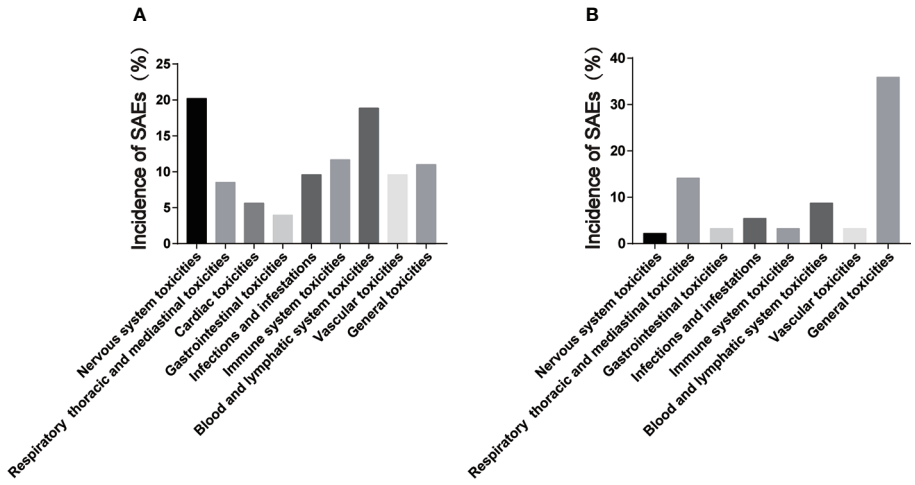

FIGURE 2
Incidence of serious adverse events of CAR-T cells in hematological and solid tumors. **(A)** is the incidence of serious adverse events of hematological tumors; **(B)** is the incidence of serious adverse events in solid tumors.

interferon (IFN) γ, tumor necrosis factor (TNF)α, granulocyte macrophage colony-stimulating factor (GM-CSF), interleukin (IL)-6, IL-10 are released (79–82). High secretion of these cytokines can lead to systemic inflammatory response-CRS. However, not all of these cytokines were secreted by activated CAR-T cells. Activating peripheral immune and non-immune cells such as monocytes, macrophages, dendritic cells, and endothelial cells is accomplished by CAR-T cells binding to antigens on tumor cells (83, 84). It has been shown that xenogeneic models emphasize the role of host immune cells in CRS pathogenesis, suggesting that IL-6 is primarily released by monocytes, macrophages, and dendritic cells, not CAR-T cells (82, 85, 86). Since IL-6 plays a key role in CRS, depleting macrophages (87) and eliminating monocytes (86) may reduce its severity. Further, inhibiting GM-CSF signaling alleviates symptoms of CRS (88, 89).

ICANS was another cause of SAEs during CAR-T cells therapy (40, 76, 90–92). In addition to CD19, CAR- T cells targeting CD22, BCMA, and other hematopoietic antigens have also been observed for neurotoxicity (11, 13, 93–95). Other treatments involving immune effector cells have also been reported to cause similar neurotoxic effects (96, 97). Therefore, the neurotoxicity of CAR-T cells was renamed ICANS (80, 98).ICANS can occur in conjunction with or independently of CRS (83, 99, 100). ICANS occurs independently and the general neurological symptoms tend to be mild (35). Typically, ICANS appear 4-5 days after CAR-T cells therapy, but delayed ICANS have also been reported after CAR-T cells therapy (26, 34, 98).

ICANS typically manifest as disturbances in attention and consciousness, and expressive aphasia is considered a fairly specific early sign of ICANS (26). ICANS can further develop into low levels of consciousness, coma, epilepsy, motor weakness, and cerebral edema. All cases of fatal cerebral edema are associated with CRS (34, 35), and severe CRS has been shown to be associated with severe ICANS (92, 101, 102). At present, relatively little is known about the pathophysiology of ICANS. ICANS have been associated with CAR-T cells transport in the central nervous system (98, 103, 104), passive diffusion of cytokines into the central nervous system (26, 34, 105), endothelial activation with impaired blood-brain barrier (26, 34), activation of microglia and myeloid cells in the central nervous system with secretion of IL-1 and IL-6 (85, 86).

4 Strategies to deal with SAEs of CAR-T cells therapy

The primary cause of CAR-T cells-associated SAEs is CRS and ICANS (31, 42, 67, 68), so treating SAEs involves preventing CRS and ICANS, as well as alleviating symptoms (67, 106). The specific measures were on one hand to optimize the CAR-T cells structure to reduce cytokine release. On the other hand, clinical management should be strengthened to find and correct CRS and ICANS in time to reduce the occurrence of related SAEs.

4.1 Optimization of CAR-T cells structure

Stable proliferation and activation of CAR-T cells in the tumor microenvironment are the prerequisite for tumor killing, but safety is also crucial (107). Endogenous non-effector

immune cells are also expanded during CAR-T cells therapy. In studies on CRS, monocytes and macrophages were found to be the major source of cytokines associated with severe manifestations (31, 108). A large number of preclinical studies have demonstrated that different CAR-T cells structures and scFv sequences can produce different tumor killing efficacy (17, 109–112). Additionally, CAR-T cells must be positively regulated by a large number of cytokines in order to kill tumors. Therefore, CAR-T cells constructs were designed to activate and maintain CAR-T cells while attenuating monocyte and macrophage activation. The structure of CAR-T cells is correlated with the incidence of CRS. To reduce the risk of CRS, newly designed next-generation CAR-T cells therapy is being developed for hematopoietic malignancies and solid tumors. S. Balagopal et al (113) have discussed Six interesting approaches to control cytokine production in CAR-T cells therapy: adaptor-based strategies, orthogonal cytokine–receptor pairs, regulation of macrophage cytokine activity, autonomous neutralization of key cytokines, kill switches and methods of reversible suppression of CARs. With these strategies, future CAR-T cells therapies will be designed to preemptively inhibit CRS, minimizing patient suffering and maximizing the number of patients who benefit.

Furthermore, the selection of different costimulatory domains by CAR-T cells affected the occurrence of ICANS. Approximately 45% of patients treated with CAR-T cells containing CD28 as a costimulatory domain develop high-grade ICANS (39, 91, 92, 114, 115). However, ICANS was less common during treatment with CAR-T cells using 4-1 BB as the co-stimulatory domain, with 13% of patients experiencing severe ICANS (76, 77). W. Luo et al. (116)conducted a meta-analysis involving 52 studies including 2,004 patients. Hematotoxicity analysis of CD19 CAR-T cells subsets demonstrated that 4-1BB, as a costimulatory domain, had less hematotoxicity than CD28. Therefore, it is of great significance to optimize the selection of co-stimulatory domain to avoid the occurrence of ICANS.

The development of relatively specific targets for solid tumors is also crucial. It is well known that specific targets have not been found in the treatment of solid tumors, and only tumor-associated targets are used in CAR-T cells (117, 118). This leads to the possibility that CAR-T cells targeting such targets may cause cytotoxicity outside the tumor. R. A. Morgan et al. (119) reported that CAR-T cells targeting HER-2 in the treatment of colorectal cancer, because CAR-T cells simultaneously targeted and killed the patient's pleural cells, the patient eventually died of respiratory failure. The above case report indicates that it is crucial to select relatively specific targets in the treatment of solid tumors with CAR-T cells. Therefore, the treatment of solid tumors with CAR-T cells should first optimize the selection of targets, and then design more optimal CAR frames to reduce the occurrence of CRS while killing tumors.

4.2 Clinical management and medication

The management of SAEs in CAR-T cells therapy is actually primarily about controlling CRS. Standardized grading of clinical adverse events was first required using the common terminology criteria for adverse events (CTCAE) (120) and CAR-T cells therapy-related toxicity (CARTOX) scoring systems. If CRS is suspected, the patient should be graded at least twice a day as the patient's condition changes (121). Management of CRS should be determined on a hierarchical basis, and low-grade CRS can be managed mainly through supportive care. The anti-IL-6 receptor antagonist tocilizumab and/or corticosteroids are considered when high-grade CRS and persistent refractory fever or fluid-refractory hypotension occur together (98).

The use of steroids for the suppression of excessive inflammatory responses and CRS has been proven in clinical experience (67). Several views exist regarding when and how corticosteroids should be administered. Some choose to use corticosteroids as a first-line agent, while others don't (83). It is important to recognize that corticosteroids have general effects on the immune system, which may also affect the antitumor efficacy and the amplification and persistence of CAR-T cells *in vivo* (122). Therefore, steroids should be avoided as first-line treatment, but used when ablating CAR-T cells is necessary in patients with severe CRS and who are resistant to other treatments. Furthermore, steroids are recommended for patients who are experiencing adverse neurological effects.

Tocilizumab is a humanized monoclonal antibody to the IL-6 receptor that inhibits the IL-6 signaling pathway (76, 123). It was approved by the FDA in 2017 as the first treatment for CRS-related toxicity following CAR-T cells infusion. Tocilizumab controlled CRS but did not significantly reduce CAR-T cells activity. The favorable effect of a single injection in patients with CRS induced by CAR-T cells therapy strongly suggests that IL-6 blocking may constitute a novel therapeutic approach for the treatment of severe systemic inflammatory responses. In patients who respond, fever and low blood pressure improve within a few hours, while in some patients supportive treatment is needed for several days. H. Liu et al. (124) evaluated the antitumor effect and safety of PD-L1-targeted CAR-T cells in patients with non-small cell lung cancer through a phase I clinical study. One patient in the trial developed severe CRS with symptoms of pneumonia and respiratory failure. The patient was given oxygen and treated with intravenous tocilizumab and methylprednisolone. The patient's symptoms improved quickly and the lung inflammation gradually subsided. Besides, K. Qi et al. (125) analyzed the adverse events after treatment in 126 patients with hematologic malignancies who received CAR-T cells therapy. The results showed that cardiac adverse events associated with CAR-T cells therapy were common and related to the development of CRS. For patients with grade 3-5 CRS,

timely administration of corticosteroids and/or tocilizumab can effectively prevent the occurrence and development of cardiac disease. However, a large number of patients are resistant to tocilizumab (98). Another therapeutic agent is a monoclonal antibody targeting IL-6, siltuximab, which has a higher affinity for IL-6 than tocilizumab for the IL6 receptor, making it a potential smoke screen for CRS treatment (126). Siltuximab is encouraged in patients who do not respond to tocilizumab and corticosteroids.

Clinically, because the clinical manifestations of infection and CRS are very similar (28, 127). Thus, diagnosis of infection becomes difficult when CRS are present. However, the treatment of CRS and infection is different (83, 98). CRS can be successfully improved with IL-6 receptor inhibitors and corticosteroids, whereas infection requires immediate initiation of antibiotic therapy (83). Therefore, it is necessary to distinguish between infections and CRS for appropriate treatment in CAR-T cells therapy. H. Luo et al. (49) selected 109 cases from three clinical trials (ChiCTR-OPN-16008526, ChiCTR-OPC-16009113, ChiCTR-OPN-16009847) to analyze the characteristics of infection events within 30 days after CAR-T cells infusion. The "IL-6 double peak" was found in most patients with life-threatening infections. Secondly, the prediction model constructed by IL-8, IL-1β and IFN-γ has high sensitivity and specificity for predicting life-threatening infections. This study indicates that the selection of effective markers during CAR-T cells therapy is very important for the diagnosis of life-threatening infections during CAR-T cells therapy and helps to reduce the risk of infection-induced death.

In addition, the classification and management of ICANS is also particularly important. It is recommended to have a neurological assessment prior to starting CAR-T cells therapy and to have one every day for the first 10 days following the infusion of CAR-T cells (128). Most commonly used tools for detecting and monitoring ICANS are the ICE score and ICANS grading system. The management of patients with grade 3 or greater ICANS should be conducted in the ICU, including the provision of airway support if the patient is not conscious (38, 128).

Corticosteroids are the mainstay of treatment for ICANS. While corticosteroids may reduce the antitumor effects of CD19 CAR-T cells (122, 129), they are appropriate for the treatment of moderate to severe ICANS due to their ICANS reversal effect. Generally, patients with low initial consciousness level are recommended to use dexamethasone for 1-3 days. The treatment for grade 4 ICANS includes 1000 mg of methylprednisolone, as the patient may not be able to wake up, may be epileptic, or may exhibit imaging characteristics of cerebral edema (128, 130). For patients with severe ICANS characterized by cerebral edema, some groups advocate supportive measures to manage elevated intracranial pressure, including the use of intracranial pressure monitors, decreasing intracranial pressure, etc (38, 128).

Tocilizumab can be used to treat ICANS, with the greatest benefit when ICANS occurs early and/or in conjunction with CRS (38, 98). It may be due to the increased permeability of the blood-brain barrier in the early stages, which facilitates tocilizumab 's entry into the brain (98). Studies have shown that tocilizumab may aggravate neurotoxicity, and the proposed mechanism is that blocking IL-6 receptors with tocilizumab may lead to increased circulating IL-6 in the central nervous system. Therefore, treatment with a monoclonal antibody (siltuximab) directly binding to IL-6 is recommended (38, 131, 132). Siltuximab directly bound to IL-6 may be more beneficial in isolated ICANS cases (38). Preclinical studies suggest that future therapies such as monoclonal antibodies targeting IL-1 may benefit ICANS, although clinical evidence is unproven for the time being (86, 130, 133). In early trials, when ICANS appeared, antiepileptic drugs were prophylactically administered to the clinic. The benefits of prophylactic use of antiepileptic drugs, which have not been proven to reduce epilepsy complications definitively, remain controversial (26, 38, 105). The use of benzodiazepines to treat sudden seizures is effective in most cases, although refractory or prolonged seizures may also occur (26, 105). Levetiracetam appears to be the preferred antiepileptic agent for ICANS patients, possibly because of its low incidence of drug interactions and good safety (38, 98).

Based on available evidence and clinical experience, the NCCN Guidelines for management of immunotherapy-related complications also provided recommendations on monitoring patients receiving CAR-T cells therapy (22). Patients with underlying organ dysfunction may have additional adverse events when receiving CAR-T cells therapy, and multidisciplinary intervention is particularly important for these patients when SAEs occur. Since SAEs caused by CAR-T cells can be seen in various organs of the body, the importance of multidisciplinary collaboration in CAR-T cells therapy is emphasized finally.

5 Discussion

CAR-T cells technology is a major breakthrough in the field of cancer, as the star of tumor immunotherapy has brought light to patients with advanced tumors, especially B cell-derived hematological tumors and multiple myeloma (134–136). More and more studies have shown its efficacy in a variety of cancers, and a large number of clinical studies on hematological tumors and solid tumors are ongoing. However, data from a growing number of clinical trials indicate that all CAR-T cells therapies have unique adverse events, such as CRS and ICANS (67, 137). Its adverse events can cause clinical symptoms in many systems of the whole body, manifested as a high incidence, serious can endanger life (68, 138). Therefore, it is important to pay attention to the occurrence of SAEs during CAR-T cells

therapy for advancing the treatment of advanced malignant tumors.

In this review, we summarize a subset of studies in the treatment of hematological malignancies and solid tumors and analyze the occurrence of clinical SAEs in the included studies. In combination with published clinical studies, CRS was found to be associated with SAEs in all major systemic systems. In addition, all cases of severe ICANS were found to be associated with CRS (34, 35).Thus, we found that CRS may be a major cause of life-threatening adverse events in the treatment of malignant tumors with CAR-T cells. In fact, cytokines play a dual role in CAR-T cells therapy. On the one hand, they activate CAR-T cells to kill tumor cells (110, 111, 139, 140). At the same time, it activates the non-effector immune cells and then produces a large number of negative cytokines, which leads to the damage of the body (81, 85, 141). Therefore, to be widely used in the treatment of malignant tumors in the future, CAR-T cells technology must be further optimized in the design process to activate CAR-T cells while reducing the impact on non-effector immune cells.

This review also provides an overview of the management and treatment of SAEs during CAR-T cells therapy. In view of the high incidence of SAEs in the clinical application of CAR-T cells (67, 142), it is necessary to closely monitor the vital signs of patients in clinical application, timely evaluate the CRS grade, and timely give standardized treatment according to the grade (67, 138). Most SAEs can be reversed (137), and patients will benefit most from timely multidisciplinary consultation.

In addition, the comparison of SAEs after CAR-T cells therapy for hematological and solid tumors included in this review may be different. Firstly, cardiac SAEs were not found in the solid tumor study. Secondly, the incidence of SAEs of nervous system and CRS in solid tumors is lower than that in hematological tumors (Figure 2). W. Lei et al. (143) included a total of 2592 patients in 84 studies for meta-analysis, and analyzed the differences in the incidence of CRS and ICANS of CAR-T cells in different tumor types. The results showed that the incidence of CRS and ICANS in hematologic malignancies was significantly higher than that in solid tumors. Our findings are confirmed by this study. CAR-T cells mainly exist in tumor tissues during the treatment of solid tumors because of the targeted guidance. Nevertheless, CAR-T cells need to be disseminated throughout the blood system in the treatment of hematological tumors, so the cytokines produced may be more readily disseminated in the body, which may be the reason for the difference in the incidence and severity of some adverse events during the treatment of hematologic and solid tumors with CAR-T cells therapy.

6 Conclusion

In conclusion, CAR-T cells technology can produce a variety of SAEs in the treatment of malignant tumors, which can occur in various systems of the body and can be life-threatening in severe cases. Studies have shown that CRS and ICANS may be the main causes of the above clinically SAEs. Therefore, through strict clinical grading and management of CRS and ICANS, most of the adverse events can be alleviated.

Author contributions

All authors conceptualized and wrote the manuscript.XC and XK additionally performed literature and data analysis. All authors contributed to the article and approved the submitted version.

Acknowledgments

Thanks to all the authors who participated in the design and data analysis of this paper, as well as the Xi 'an Honghui Hospital for providing convenience.

Conflict of interest

The authors declare that the research was conducted in the absence of any commercial or financial relationships that could be construed as a potential conflict of interest.

Publisher's note

References

1. Huo JL, Fu WJ, Liu ZH, Lu N, Jia XQ, Liu ZS. Research advance of natural products in tumor immunotherapy. *Front Immunol* (2022) 13:972345. doi: 10.3389/fimmu.2022.972345

2. Lesch S, Gill S. The promise and perils of immunotherapy. *Blood Adv* (2021) 5(18):3709–25. doi: 10.1182/bloodadvances.2021004453C

3. June CH, Sadelain M. Chimeric antigen receptor therapy. *N Engl J Med* (2018) 379(1):64–73. doi: 10.1056/NEJMra1706169

4. Feins S, Kong W, Williams EF, Milone MC, Fraietta JA. An introduction to chimeric antigen receptor (CAR) T-cell immunotherapy for human cancer. *Am J Hematol* (2019) 94(S1):S3–s9. doi: 10.1002/ajh.25418

5. Miao L, Zhang Z, Ren Z, Li Y. Reactions related to CAR-T cell therapy. *Front Immunol* (2021) 12:663201. doi: 10.3389/fimmu.2021.663201

6. Wang J, Mou N, Yang Z, Li Q, Jiang Y, Meng J, et al. Efficacy and safety of humanized anti-CD19-CAR-T therapy following intensive lymphodepleting chemotherapy for refractory/relapsed b acute lymphoblastic leukaemia. *Br J Haematol* (2020) 191(2):212–22. doi: 10.1111/bjh.16623

7. Geyer MB, Rivière I, Sénéchal B, Wang X, Wang Y, Purdon TJ, et al. Autologous CD19-targeted CAR T cells in patients with residual CLL following initial purine analog-based therapy. *Mol Ther* (2018) 26(8):1896–905. doi: 10.1016/j.ymthe.2018.05.018

8. Abramson JS. Anti-CD19 CAR T-cell therapy for b-cell non-Hodgkin lymphoma. *Transfus Med Rev* (2020) 34(1):29–33. doi: 10.1016/j.tmrv.2019.08.003

9. Gauthier J, Bezerra ED, Hirayama AV, Fiorenza S, Sheih A, Chou CK, et al. Factors associated with outcomes after a second CD19-targeted CAR T-cell infusion for refractory b-cell malignancies. *Blood* (2021) 137(3):323–35. doi: 10.1182/blood.2020006770

10. Zhang J, Hu Y, Yang J, Li W, Zhang M, Wang Q, et al. Non-viral, specifically targeted CAR-T cells achieve high safety and efficacy in b-NHL. *Nature* (2022) 609 (7926):369–74. doi: 10.1038/s41586-022-05140-y

11. Fry TJ, Shah NN, Orentas RJ, Stetler-Stevenson M, Yuan CM, Ramakrishna S, et al. CD22-targeted CAR T cells induce remission in b-ALL that is naive or resistant to CD19-targeted CAR immunotherapy. *Nat Med* (2018) 24(1):20–8. doi: 10.1038/nm.4441

12. Shalabi H, Wolters PL, Martin S, Toledo-Tamula MA, Roderick MC, Struemph K, et al. Systematic evaluation of neurotoxicity in children and young adults undergoing CD22 chimeric antigen receptor T-cell therapy. *J Immunother* (2018) 41(7):350–8. doi: 10.1097/cji.0000000000000241

13. Zhao WH, Liu J, Wang BY, Chen YX, Cao XM, Yang Y, et al. A phase 1, open-label study of LCAR-B38M, a chimeric antigen receptor T cell therapy directed against b cell maturation antigen, in patients with relapsed or refractory multiple myeloma. *J Hematol Oncol* (2018) 11(1):141. doi: 10.1186/s13045-018-0681-6

14. Raje N, Berdeja J, Lin Y, Siegel D, Jagannath S, Madduri D, et al. Anti-BCMA CAR T-cell therapy bb2121 in relapsed or refractory multiple myeloma. *N Engl J Med* (2019) 380(18):1726–37. doi: 10.1056/NEJMoa1817226

15. Cohen AD, Garfall AL, Stadtmauer EA, Melenhorst JJ, Lacey SF, Lancaster E, et al. B cell maturation antigen-specific CAR T cells are clinically active in multiple myeloma. *J Clin Invest* (2019) 129(6):2210–21. doi: 10.1172/jci126397

16. Staudt RE, Carlson RD, Snook AE. Targeting gastrointestinal cancers with chimeric antigen receptor (CAR)-T cell therapy. *Cancer Biol Ther* (2022) 23 (1):127–33. doi: 10.1080/15384047.2022.2033057

17. Zhao R, Cui Y, Zheng Y, Li S, Lv J, Wu Q, et al. Human hyaluronidase PH20 potentiates the antitumor activities of mesothelin-specific CAR-T cells against gastric cancer. *Front Immunol* (2021) 12:660488. doi: 10.3389/fimmu.2021.660488

18. Pang N, Shi J, Qin L, Chen A, Tang Y, Yang H, et al. IL-7 and CCL19-secreting CAR-T cell therapy for tumors with positive glypican-3 or mesothelin. *J Hematol Oncol* (2021) 14(1):118. doi: 10.1186/s13045-021-01128-9

19. Beatty GL, O'Hara MH, Lacey SF, Torigian DA, Nazimuddin F, Chen F, et al. Activity of mesothelin-specific chimeric antigen receptor T cells against pancreatic carcinoma metastases in a phase 1 trial. *Gastroenterology* (2018) 155 (1):29–32. doi: 10.1053/j.gastro.2018.03.029

20. You F, Jiang L, Zhang B, Lu Q, Zhou Q, Liao X, et al. Phase 1 clinical trial demonstrated that MUC1 positive metastatic seminal vesicle cancer can be effectively eradicated by modified anti-MUC1 chimeric antigen receptor transduced T cells. *Sci China Life Sci* (2016) 59(4):386–97. doi: 10.1007/s11427-016-5024-7

21. Zhou JT, Liu JH, Song TT, Ma B, Amidula N, Bai C. EGLIF-CAR-T cells secreting PD-1 blocking antibodies significantly mediate the elimination of gastric cancer. *Cancer Manag Res* (2020) 12:8893–902. doi: 10.2147/cmar.S260915

22. Thompson JA, Schneider BJ, Brahmer J, Achufusi A, Armand P, Berkenstock MK, et al. Management of immunotherapy-related toxicities, version 1.2022, NCCN clinical practice guidelines in oncology. *J Natl Compr Canc Netw* (2022) 20(4):387–405. doi: 10.6004/jnccn.2022.0020

23. Greenbaum U, Kebriaei P, Srour SA, Olson A, Bashir Q, Neelapu SS, et al. Chimeric antigen receptor T-cell therapy toxicities. *Br J Clin Pharmacol* (2021) 87 (6):2414–24. doi: 10.1111/bcp.14403

24. Turtle CJ, Hanafi LA, Berger C, Hudecek M, Pender B, Robinson E, et al. Immunotherapy of non-hodgkin's lymphoma with a defined ratio of CD8+ and CD4+ CD19-specific chimeric antigen receptor-modified T cells. *Sci Transl Med* (2016) 8(355):355ra116. doi: 10.1126/scitranslmed.aaf8621

25. Hay KA, Hanafi LA, Li D, Gust J, Liles WC, Wurfel MM, et al. Kinetics and biomarkers of severe cytokine release syndrome after CD19 chimeric antigen receptor-modified T-cell therapy. *Blood* (2017) 130(21):2295–306. doi: 10.1182/blood-2017-06-793141

26. Santomasso BD, Park JH, Salloum D, Riviere I, Flynn J, Mead E, et al. Clinical and biological correlates of neurotoxicity associated with CAR T-cell therapy in patients with b-cell acute lymphoblastic leukemia. *Cancer Discovery* (2018) 8(8):958–71. doi: 10.1158/2159-8290.Cd-17-1319

27. Lundh S, Maji S, Melenhorst JJ. Next-generation CAR T cells to overcome current drawbacks. *Int J Hematol* (2021) 114(5):532–43. doi: 10.1007/s12185-020-02923-9

28. Xu XJ, Tang YM. Cytokine release syndrome in cancer immunotherapy with chimeric antigen receptor engineered T cells. *Cancer Lett* (2014) 343(2):172–8. doi: 10.1016/j.canlet.2013.10.004

29. Wei Z, Cheng Q, Xu N, Zhao C, Xu J, Kang L, et al. Investigation of CRS-associated cytokines in CAR-T therapy with meta-GNN and pathway crosstalk. *BMC Bioinf* (2022) 23(1):373. doi: 10.1186/s12859-022-04917-2

30. Maus MV, Alexander S, Bishop MR, Brudno JN, Callahan C, Davila ML, et al. Society for immunotherapy of cancer (SITC) clinical practice guideline on immune effector cell-related adverse events. *J Immunother Cancer* (2020) 8(2): e001511. doi: 10.1136/jitc-2020-001511

31. Cosenza M, Sacchi S, Pozzi S. Cytokine release syndrome associated with T-Cell-Based therapies for hematological malignancies: Pathophysiology, clinical presentation, and treatment. *Int J Mol Sci* (2021) 22(14):7652. doi: 10.3390/ijms22147652

32. Zhang Z, Miao L, Ren Z, Tang F, Li Y. Gene-edited interleukin CAR-T cells therapy in the treatment of malignancies: Present and future. *Front Immunol* (2021) 12:718686. doi: 10.3389/fimmu.2021.718686

33. Ying Z, Song Y, Zhu J. Effectiveness and safety of anti-CD19 chimeric antigen receptor-T cell immunotherapy in patients with Relapsed/Refractory Large b-cell lymphoma: A systematic review and meta-analysis. *Front Pharmacol* (2022) 13:834113. doi: 10.3389/fphar.2022.834113

34. Gust J, Hay KA, Hanafi LA, Li D, Myerson D, Gonzalez-Cuyar LF, et al. Endothelial activation and blood-brain barrier disruption in neurotoxicity after adoptive immunotherapy with CD19 CAR-T cells. *Cancer Discovery* (2017) 7 (12):1404–19. doi: 10.1158/2159-8290.Cd-17-0698

35. Gust J, Ceppi F, Turtle CJ. Chapter 7 - neurotoxicities after CAR T-cell immunotherapy. In: Lee DW, Shah NN, editors. *Chimeric antigen receptor T-cell therapies for cancer*. Elsevier (2020) 83–105. doi: 10.1016/B978-0-323-66181-2.00007-X

36. Shao M, Yu Q, Teng X, Guo X, Wei G, Xu H, et al. CRS-related coagulopathy in BCMA targeted CAR-T therapy: a retrospective analysis in a phase I/II clinical trial. *Bone Marrow Transplant* (2021) 56(7):1642–50. doi: 10.1038/s41409-021-01226-9

37. Zhou J, Zhang Y, Shan M, Zong X, Geng H, Li J, et al. Cytopenia after chimeric antigen receptor T cell immunotherapy in relapsed or refractory lymphoma. *Front Immunol* (2022) 13:997589. doi: 10.3389/fimmu.2022.997589

38. Gust J, Taraseviciute A, Turtle CJ. Neurotoxicity associated with CD19-targeted CAR-T cell therapies. *CNS Drugs* (2018) 32(12):1091–101. doi: 10.1007/s40263-018-0582-9

39. Locke FL, Ghobadi A, Jacobson CA, Miklos DB, Lekakis LJ, Oluwole OO, et al. Long-term safety and activity of axicabtagene ciloleucel in refractory large b-cell lymphoma (ZUMA-1): a single-arm, multicentre, phase 1-2 trial. *Lancet Oncol* (2019) 20(1):31–42. doi: 10.1016/s1470-2045(18)30864-7

40. Schuster SJ, Bishop MR, Tam CS, Waller EK, Borchmann P, McGuirk JP, et al. Tisagenlecleucel in adult relapsed or refractory diffuse Large b-cell lymphoma. *N Engl J Med* (2019) 380(1):45–56. doi: 10.1056/NEJMoa1804980

41. Lv L, Wu Y, Shi H, Sun X, Deng Z, Huo H, et al. Efficacy and safety of chimeric antigen receptor T-cells treatment in central nervous system lymphoma: a PRISMA-compliant single-arm meta-analysis. *Cancer Immunol Immunother* (2022). doi: 10.1007/s00262-022-03246-w

42. Gajra A, Zettler ME, Phillips EGJr., Klink AJ, Jonathan KK, Fortier S, et al. Neurological adverse events following CAR T-cell therapy: a real-world

analysis. *Immunotherapy* (2020) 12(14):1077–82. doi: 10.2217/imt-2020-0161

43. Karschnia P, Jordan JT, Forst DA, Arrillaga-Romany IC, Batchelor TT, Baehring JM, et al. Clinical presentation, management, and biomarkers of neurotoxicity after adoptive immunotherapy with CAR T cells. *Blood* (2019) 133 (20):2212–21. doi: 10.1182/blood-2018-12-893396

44. Pan J, Tan Y, Wang G, Deng B, Ling Z, Song W, et al. Donor-derived CD7 chimeric antigen receptor T cells for T-cell acute lymphoblastic leukemia: First-in-Human, phase I trial. *J Clin Oncol* (2021) 39(30):3340–51. doi: 10.1200/jco.21.00389

45. Benjamin R, Graham C, Yallop D, Jozwik A, Mirci-Danicar OC, Lucchini G, et al. Genome-edited, donor-derived allogeneic anti-CD19 chimeric antigen receptor T cells in paediatric and adult b-cell acute lymphoblastic leukaemia: results of two phase 1 studies. *Lancet* (2020) 396(10266):1885–94. doi: 10.1016/s0140-6736(20)32334-5

46. Rejeski K, Kunz WG, Rudelius M, Bücklein V, Blumenberg V, Schmidt C, et al. Severe candida glabrata pancolitis and fatal aspergillus fumigatus pulmonary infection in the setting of bone marrow aplasia after CD19-directed CAR T-cell therapy - a case report. *BMC Infect Dis* (2021) 21(1):121. doi: 10.1186/s12879-020-05755-4

47. Goldman A, Maor E, Bomze D, Liu JE, Herrmann J, Fein J, et al. Adverse cardiovascular and pulmonary events associated with chimeric antigen receptor T-cell therapy. *J Am Coll Cardiol* (2021) 78(18):1800–13. doi: 10.1016/j.jacc.2021.08.044

48. Totzeck M, Michel L, Lin Y, Herrmann J, Rassaf T. Cardiotoxicity from chimeric antigen receptor-T cell therapy for advanced malignancies. *Eur Heart J* (2022) 43(20):1928–40. doi: 10.1093/eurheartj/ehac106

49. Luo H, Wang N, Huang L, Zhou X, Jin J, Li C, et al. Inflammatory signatures for quick diagnosis of life-threatening infection during the CAR T-cell therapy. *J Immunother Cancer* (2019) 7(1):271. doi: 10.1186/s40425-019-0767-x

50. Gill J. Cardiovascular toxicities with chimeric antigen receptor T-cell therapy. *Curr Cardiol Rev* (2022) 19(1):2023–11. doi: 10.2174/1573403x18666220623152350

51. Steiner RE, Banchs J, Koutroumpakis E, Becnel M, Gutierrez C, Strati P, et al. Cardiovascular events in patients treated with chimeric antigen receptor T-cell therapy for aggressive b-cell lymphoma. *Haematologica* (2022) 107(7):1555–66. doi: 10.3324/haematol.2021.280009

52. Hanna KS, Kaur H, Alazzeh MS, Thandavaram A, Channar A, Purohit A, et al. Cardiotoxicity associated with chimeric antigen receptor (CAR)-T cell therapy for hematologic malignancies: A systematic review. *Cureus* (2022) 14(8): e28162. doi: 10.7759/cureus.28162

53. Alvi RM, Frigault MJ, Fradley MG, Jain MD, Mahmood SS, Awadalla M, et al. Cardiovascular events among adults treated with chimeric antigen receptor T-cells (CAR-T). *J Am Coll Cardiol* (2019) 74(25):3099–108. doi: 10.1016/j.jacc.2019.10.038

54. Guha A, Addison D, Jain P, Gutierrez JM, Ghosh A, Roddie C, et al. Cardiovascular events associated with chimeric antigen receptor T cell therapy: Cross-sectional FDA adverse events reporting system analysis. *Biol Blood Marrow Transplant* (2020) 26(12):2211–6. doi: 10.1016/j.bbmt.2020.08.036

55. Zhao Z, Zhang J, Bian J, Lu X. The efficacy and safety of chimeric antigen receptor T cells in digestive system cancers: a systematic review and meta-analysis. *Ann Transl Med* (2022) 10(9):508. doi: 10.21037/atm-21-5019

56. Telli Dizman G, Aguado JM, Fernández-Ruiz M. Risk of infection in patients with hematological malignancies receiving CAR T-cell therapy: systematic review and meta-analysis. *Expert Rev Anti Infect Ther* (2022) 20 (11):1455–76. doi: 10.1080/14787210.2022.2128762

57. Fishman JA, Hogan JI, Maus MV. Inflammatory and infectious syndromes associated with cancer immunotherapies. *Clin Infect Dis* (2019) 69(6):909–20. doi: 10.1093/cid/ciy1025

58. Hill JA, Li D, Hay KA, Green ML, Cherian S, Chen X, et al. Infectious complications of CD19-targeted chimeric antigen receptor-modified T-cell immunotherapy. *Blood* (2018) 131(1):121–30. doi: 10.1182/blood-2017-07-793760

59. Park JH, Romero FA, Taur Y, Sadelain M, Brentjens RJ, Hohl TM, et al. Cytokine release syndrome grade as a predictive marker for infections in patients with relapsed or refractory b-cell acute lymphoblastic leukemia treated with chimeric antigen receptor T cells. *Clin Infect Dis* (2018) 67(4):533–40. doi: 10.1093/cid/ciy152

60. Maude SL, Barrett D, Teachey DT, Grupp SA. Managing cytokine release syndrome associated with novel T cell-engaging therapies. *Cancer J* (2014) 20 (2):119–22. doi: 10.1097/ppo.0000000000000035

61. Locke FL, Neelapu SS, Bartlett NL, Siddiqi T, Chavez JC, Hosing CM, et al. Phase 1 results of ZUMA-1: A multicenter study of KTE-C19 anti-CD19 CAR T cell therapy in refractory aggressive lymphoma. *Mol Ther* (2017) 25(1):285–95. doi: 10.1016/j.ymthe.2016.10.020

62. Nahas GR, Komanduri KV, Pereira D, Goodman M, Jimenez AM, Beitinjaneh A, et al. Incidence and risk factors associated with a syndrome of persistent cytopenias after CAR-T cell therapy (PCTT). *Leuk Lymphoma* (2020) 61 (4):940–3. doi: 10.1080/10428194.2019.1697814

63. Wang L, Hong R, Zhou L, Ni F, Zhang M, Zhao H, et al. New-onset severe cytopenia after CAR-T cell therapy: Analysis of 76 patients with relapsed or refractory acute lymphoblastic leukemia. *Front Oncol* (2021) 11:702644. doi: 10.3389/fonc.2021.702644

64. Qi C, Gong J, Li J, Liu D, Qin Y, Ge S, et al. Claudin18.2-specific CAR T cells in gastrointestinal cancers: phase 1 trial interim results. *Nat Med* (2022) 28 (6):1189–98. doi: 10.1038/s41591-022-01800-8

65. Liu Y, Guo Y, Wu Z, Feng K, Tong C, Wang Y, et al. Anti-EGFR chimeric antigen receptor-modified T cells in metastatic pancreatic carcinoma: A phase I clinical trial. *Cytotherapy* (2020) 22(10):573–80. doi: 10.1016/j.jcyt.2020.04.088

66. Zhang Y, Zhang Z, Ding Y, Fang Y, Wang P, Chu W, et al. Phase I clinical trial of EGFR-specific CAR-T cells generated by the piggyBac transposon system in advanced relapsed/refractory non-small cell lung cancer patients. *J Cancer Res Clin Oncol* (2021) 147(12):3725–34. doi: 10.1007/s00432-021-03613-7

67. Yáñez L, Alarcón A, Sánchez-Escamilla M, Perales MA. How I treat adverse effects of CAR-T cell therapy. *ESMO Open* (2020) 4(Suppl 4):e000746. doi: 10.1136/esmoopen-2020-000746

68. Schubert ML, Schmitt M, Wang L, Ramos CA, Jordan K, Müller-Tidow C, et al. Side-effect management of chimeric antigen receptor (CAR) T-cell therapy. *Ann Oncol* (2021) 32(1):34–48. doi: 10.1016/j.annonc.2020.10.478

69. Winkler U, Jensen M, Manzke O, Schulz H, Diehl V, Engert A. Cytokine-release syndrome in patients with b-cell chronic lymphocytic leukemia and high lymphocyte counts after treatment with an anti-CD20 monoclonal antibody (rituximab, IDEC-C2B8). *Blood* (1999) 94(7):2217–24. doi: 10.1182/blood.V94.7.2217.419k02_2217_2224

70. Freeman CL, Morschhauser F, Sehn L, Dixon M, Houghton R, Lamy T, et al. Cytokine release in patients with CLL treated with obinutuzumab and possible relationship with infusion-related reactions. *Blood* (2015) 126(24):2646–9. doi: 10.1182/blood-2015-09-670802

71. Wing MG, Moreau T, Greenwood J, Smith RM, Hale G, Isaacs J, et al. Mechanism of first-dose cytokine-release syndrome by CAMPATH 1-h: involvement of CD16 (FcgammaRIII) and CD11a/CD18 (LFA-1) on NK cells. *J Clin Invest* (1996) 98(12):2819–26. doi: 10.1172/jci119110

72. Alig SK, Dreyling M, Seppi B, Aulinger B, Witkowski L, Rieger CT. Severe cytokine release syndrome after the first dose of brentuximab vedotin in a patient with relapsed systemic anaplastic large cell lymphoma (sALCL): a case report and review of literature. *Eur J Haematol* (2015) 94(6):554–7. doi: 10.1111/ejh.12396

73. de Vos S, Forero-Torres A, Ansell SM, Kahl B, Cheson BD, Bartlett NL, et al. A phase II study of dacetuzumab (SGN-40) in patients with relapsed diffuse large b-cell lymphoma (DLBCL) and correlative analyses of patient-specific factors. *J Hematol Oncol* (2014) 7:44. doi: 10.1186/1756-8722-7-44

74. Rotz SJ, Leino D, Szabo S, Mangino JL, Turpin BK, Pressey JG. Severe cytokine release syndrome in a patient receiving PD-1-directed therapy. *Pediatr Blood Cancer* (2017) 64(12):e26642. doi: 10.1002/pbc.26642

75. Moore JB, June CH. Cytokine release syndrome in severe COVID-19. *Science* (2020) 368(6490):473–4. doi: 10.1126/science.abb8925

76. Maude SL, Laetsch TW, Buechner J, Rives S, Boyer M, Bittencourt H, et al. Tisagenlecleucel in children and young adults with b-cell lymphoblastic leukemia. *N Engl J Med* (2018) 378(5):439–48. doi: 10.1056/NEJMoa1709866

77. Schuster SJ, Svoboda J, Chong EA, Nasta SD, Mato AR, Anak Ö, et al. Chimeric antigen receptor T cells in refractory b-cell lymphomas. *N Engl J Med* (2017) 377(26):2545–54. doi: 10.1056/NEJMoa1708566

78. Liu YH, Zang XY, Wang JC, Huang SS, Xu J, Zhang P. Diagnosis and management of immune related adverse events (irAEs) in cancer immunotherapy. *BioMed Pharmacother* (2019) 120:109437. doi: 10.1016/j.biopha.2019.109437

79. Wang Z, Han W. Biomarkers of cytokine release syndrome and neurotoxicity related to CAR-T cell therapy. *biomark Res* (2018) 6:4. doi: 10.1186/s40364-018-0116-0

80. Lee DW, Santomasso BD, Locke FL, Ghobadi A, Turtle CJ, Brudno JN, et al. ASTCT consensus grading for cytokine release syndrome and neurologic toxicity associated with immune effector cells. *Biol Blood Marrow Transplant* (2019) 25 (4):625–38. doi: 10.1016/j.bbmt.2018.12.758

81. Frey N, Porter D. Cytokine release syndrome with chimeric antigen receptor T cell therapy. *Biol Blood Marrow Transplant* (2019) 25(4):e123–7. doi: 10.1016/j.bbmt.2018.12.756

82. Titov A, Petukhov A, Staliarova A, Motorin D, Bulatov E, Shuvalov O, et al. The biological basis and clinical symptoms of CAR-T therapy-associated toxicites. *Cell Death Dis* (2018) 9(9):897. doi: 10.1038/s41419-018-0918-x

83. Lee DW, Gardner R, Porter DL, Louis CU, Ahmed N, Jensen M, et al. Current concepts in the diagnosis and management of cytokine release syndrome. *Blood* (2014) 124(2):188–95. doi: 10.1182/blood-2014-05-552729

84. Liu Q, Zhou YH, Yang ZQ. The cytokine storm of severe influenza and development of immunomodulatory therapy. *Cell Mol Immunol* (2016) 13(1):3–10. doi: 10.1038/cmi.2015.74

85. Giavridis T, van der Stegen SJC, Eyquem J, Hamieh M, Piersigilli A, Sadelain M. CAR T cell-induced cytokine release syndrome is mediated by macrophages and abated by IL-1 blockade. *Nat Med* (2018) 24(6):731–8. doi: 10.1038/s41591-018-0041-7

86. Norelli M, Camisa B, Barbiera G, Falcone L, Purevdorj A, Genua M, et al. Monocyte-derived IL-1 and IL-6 are differentially required for cytokine-release syndrome and neurotoxicity due to CAR T cells. *Nat Med* (2018) 24(6):739–48. doi: 10.1038/s41591-018-0036-4

87. van der Stegen SJ, Davies DM, Wilkie S, Foster J, Sosabowski JK, Burnet J, et al. Preclinical *in vivo* modeling of cytokine release syndrome induced by ErbB-retargeted human T cells: identifying a window of therapeutic opportunity? *J Immunol* (2013) 191(9):4589–98. doi: 10.4049/jimmunol.1301523

88. Sachdeva M, Duchateau P, Depil S, Poirot L, Valton J. Granulocyte-macrophage colony-stimulating factor inactivation in CAR T-cells prevents monocyte-dependent release of key cytokine release syndrome mediators. *J Biol Chem* (2019) 294(14):5430–7. doi: 10.1074/jbc.AC119.007558

89. Sterner RM, Sakemura R, Cox MJ, Yang N, Khadka RH, Forsman CL, et al. GM-CSF inhibition reduces cytokine release syndrome and neuroinflammation but enhances CAR-T cell function in xenografts. *Blood* (2019) 133(7):697–709. doi: 10.1182/blood-2018-10-881722

90. Gardner RA, Finney O, Annesley C, Brakke H, Summers C, Leger K, et al. Intent-to-treat leukemia remission by CD19 CAR T cells of defined formulation and dose in children and young adults. *Blood* (2017) 129(25):3322–31. doi: 10.1182/blood-2017-02-769208

91. Park JH, Rivière I, Gonen M, Wang X, Sénéchal B, Curran KJ, et al. Long-term follow-up of CD19 CAR therapy in acute lymphoblastic leukemia. *N Engl J Med* (2018) 378(5):449–59. doi: 10.1056/NEJMoa1709919

92. Neelapu SS, Locke FL, Bartlett NL, Lekakis LJ, Miklos DB, Jacobson CA, et al. Axicabtagene ciloleucel CAR T-cell therapy in refractory Large b-cell lymphoma. *N Engl J Med* (2017) 377(26):2531–44. doi: 10.1056/NEJMoa1707447

93. Ali SA, Shi V, Maric I, Wang M, Stroncek DF, Rose JJ, et al. T Cells expressing an anti-b-cell maturation antigen chimeric antigen receptor cause remissions of multiple myeloma. *Blood* (2016) 128(13):1688–700. doi: 10.1182/blood-2016-04-711903

94. Brudno JN, Maric I, Hartman SD, Rose JJ, Wang M, Lam N, et al. T Cells genetically modified to express an anti-B-Cell maturation antigen chimeric antigen receptor cause remissions of poor-prognosis relapsed multiple myeloma. *J Clin Oncol* (2018) 36(22):2267–80. doi: 10.1200/jco.2018.77.8084

95. Ramos CA, Ballard B, Zhang H, Dakhova O, Gee AP, Mei Z, et al. Clinical and immunological responses after CD30-specific chimeric antigen receptor-redirected lymphocytes. *J Clin Invest* (2017) 127(9):3462–71. doi: 10.1172/jci94306

96. Topp MS, Gökbuget N, Stein AS, Zugmaier G, O'Brien S, Bargou RC, et al. Safety and activity of blinatumomab for adult patients with relapsed or refractory b-precursor acute lymphoblastic leukaemia: a multicentre, single-arm, phase 2 study. *Lancet Oncol* (2015) 16(1):57–66. doi: 10.1016/s1470-2045(14)71170-2

97. Bachanova V, Sarhan D, DeFor TE, Cooley S, Panoskaltsis-Mortari A, Blazar BR, et al. Haploidentical natural killer cells induce remissions in non-Hodgkin lymphoma patients with low levels of immune-suppressor cells. *Cancer Immunol Immunother* (2018) 67(3):483–94. doi: 10.1007/s00262-017-2100-1

98. Neelapu SS, Tummala S, Kebriaei P, Wierda W, Gutierrez C, Locke FL, et al. Chimeric antigen receptor T-cell therapy - assessment and management of toxicities. *Nat Rev Clin Oncol* (2018) 15(1):47–62. doi: 10.1038/nrclinonc.2017.148

99. Varadarajan I, Lee DW. Management of T-cell engaging immunotherapy complications. *Cancer J* (2019) 25(3):223–30. doi: 10.1097/ppo.0000000000000377

100. Maude SL, Frey N, Shaw PA, Aplenc R, Barrett DM, Bunin NJ, et al. Chimeric antigen receptor T cells for sustained remissions in leukemia. *N Engl J Med* (2014) 371(16):1507–17. doi: 10.1056/NEJMoa1407222

101. Teachey DT, Lacey SF, Shaw PA, Melenhorst JJ, Maude SL, Frey N, et al. Identification of predictive biomarkers for cytokine release syndrome after chimeric antigen receptor T-cell therapy for acute lymphoblastic leukemia. *Cancer Discovery* (2016) 6(6):664–79. doi: 10.1158/2159-8290.Cd-16-0040

102. Gofshteyn JS, Shaw PA, Teachey DT, Grupp SA, Maude S, Banwell B, et al. Neurotoxicity after CTL019 in a pediatric and young adult cohort. *Ann Neurol* (2018) 84(4):537–46. doi: 10.1002/ana.25315

103. Lee DW, Kochenderfer JN, Stetler-Stevenson M, Cui YK, Delbrook C, Feldman SA, et al. T Cells expressing CD19 chimeric antigen receptors for acute lymphoblastic leukaemia in children and young adults: a phase 1 dose-escalation trial. *Lancet* (2015) 385(9967):517–28. doi: 10.1016/s0140-6736(14)61403-3

104. Rheingold SR, Chen LN, Maude SL, Aplenc R, Barker C, Barrett DM, et al. Efficient trafficking of chimeric antigen receptor (CAR)-modified T cells to CSF and induction of durable CNS remissions in children with CNS/Combined Relapsed/Refractory ALL. *Blood* (2015) 126(23):3769. doi: 10.1182/blood.V126.23.3769.3769

105. Gust J, Finney OC, Li D, Brakke HM, Hicks RM, Futrell RB, et al. Glial injury in neurotoxicity after pediatric CD19-directed chimeric antigen receptor T cell therapy. *Ann Neurol* (2019) 86(1):42–54. doi: 10.1002/ana.25502

106. Landry K, Thomas AA. Neurological complications of CAR T cell therapy. *Curr Oncol Rep* (2020) 22(8):83. doi: 10.1007/s11912-020-00935-6

107. Gust J, Ponce R, Liles WC, Garden GA, Turtle CJ. Cytokines in CAR T cell-associated neurotoxicity. *Front Immunol* (2020) 11:577027. doi: 10.3389/fimmu.2020.577027

108. Liu P, Liu M, Lyu C, Lu W, Cui R, Wang J, et al. Acute graft-Versus-Host disease after humanized anti-CD19-CAR T therapy in relapsed b-ALL patients after allogeneic hematopoietic stem cell transplant. *Front Oncol* (2020) 10:573822. doi: 10.3389/fonc.2020.573822

109. Chen C, Gu YM, Zhang F, Zhang ZC, Zhang YT, He YD, et al. Construction of PD1/CD28 chimeric-switch receptor enhances anti-tumor ability of c-met CAR-T in gastric cancer. *Oncoimmunology* (2021) 10(1):1901434. doi: 10.1080/2162402x.2021.1901434

110. Adachi K, Kano Y, Nagai T, Okuyama N, Sakoda Y, Tamada K. IL-7 and CCL19 expression in CAR-T cells improves immune cell infiltration and CAR-T cell survival in the tumor. *Nat Biotechnol* (2018) 36(4):346–51. doi: 10.1038/nbt.4086

111. Hombach AA, Geumann U, Günther C, Hermann FG, Abken H. IL7-IL12 engineered mesenchymal stem cells (MSCs) improve a CAR T cell attack against colorectal cancer cells. *Cells* (2020) 9(4):873. doi: 10.3390/cells9040873

112. He C, Zhou Y, Li Z, Farooq MA, Ajmal I, Zhang H, et al. Co-Expression of IL-7 improves NKG2D-based CAR T cell therapy on prostate cancer by enhancing the expansion and inhibiting the apoptosis and exhaustion. *Cancers (Basel)* (2020) 12(7):1969. doi: 10.3390/cancers12071969

113. Balagopal S, Sasaki K, Kaur P, Nikolaidi M, Ishihara J. Emerging approaches for preventing cytokine release syndrome in CAR-T cell therapy. *J Mater Chem B* (2022) 10(37):7491–511. doi: 10.1039/d2tb00592a

114. Nastoupil LJ, Jain MD, Feng L, Spiegel JY, Ghobadi A, Lin Y, et al. Standard-of-Care axicabtagene ciloleucel for relapsed or refractory Large b-cell lymphoma: Results from the US lymphoma CAR T consortium. *J Clin Oncol* (2020) 38(27):3119–28. doi: 10.1200/jco.19.02104

115. Kochenderfer JN, Dudley ME, Kassim SH, Somerville RP, Carpenter RO, Stetler-Stevenson M, et al. Chemotherapy-refractory diffuse large b-cell lymphoma and indolent b-cell malignancies can be effectively treated with autologous T cells expressing an anti-CD19 chimeric antigen receptor. *J Clin Oncol* (2015) 33(6):540–9. doi: 10.1200/jco.2014.56.2025

116. Luo W, Li C, Zhang Y, Du M, Kou H, Lu C, et al. Adverse effects in hematologic malignancies treated with chimeric antigen receptor (CAR) T cell therapy: a systematic review and meta-analysis. *BMC Cancer* (2022) 22(1):98. doi: 10.1186/s12885-021-09102-x

117. Freitag F, Maucher M, Riester Z, Hudecek M. New targets and technologies for CAR-T cells. *Curr Opin Oncol* (2020) 32(5):510–7. doi: 10.1097/cco.0000000000000653

118. Wagner J, Wickman E, DeRenzo C, Gottschalk S. CAR T cell therapy for solid tumors: Bright future or dark reality? *Mol Ther* (2020) 28(11):2320–39. doi: 10.1016/j.ymthe.2020.09.015

119. Morgan RA, Yang JC, Kitano M, Dudley ME, Laurencot CM, Rosenberg SA. Case report of a serious adverse event following the administration of T cells transduced with a chimeric antigen receptor recognizing ERBB2. *Mol Ther* (2010) 18(4):843–51. doi: 10.1038/mt.2010.24

120. Freites-Martinez A, Santana N, Arias-Santiago S, Viera A. Using the common terminology criteria for adverse events (CTCAE - version 5.0) to evaluate the severity of adverse events of anticancer therapies. *Actas Dermosifiliogr (Engl Ed)* (2021) 112(1):90–2. doi: 10.1016/j.ad.2019.05.009

121. Adkins S. CAR T-cell therapy: Adverse events and management. *J Adv Pract Oncol* (2019) 10(Suppl 3):21–8. doi: 10.6004/jadpro.2019.10.4.11

122. Davila ML, Riviere I, Wang X, Bartido S, Park J, Curran K, et al. Efficacy and toxicity management of 19-28z CAR T cell therapy in b cell acute lymphoblastic leukemia. *Sci Transl Med* (2014) 6(224):224ra25. doi: 10.1126/scitranslmed.3008226

123. Fitzgerald JC, Weiss SL, Maude SL, Barrett DM, Lacey SF, Melenhorst JJ, et al. Cytokine release syndrome after chimeric antigen receptor T cell therapy for acute lymphoblastic leukemia. *Crit Care Med* (2017) 45(2):e124–e131. doi: 10.1097/CCM.0000000000002053

124. Liu H, Ma Y, Yang C, Xia S, Pan Q, Zhao H, et al. Severe delayed pulmonary toxicity following PD-L1-specific CAR-T cell therapy for non-small cell lung cancer. *Clin Transl Immunol* (2020) 9(10):e1154. doi: 10.1002/cti2.1154

125. Qi K, Yan Z, Cheng H, Chen W, Wang Y, Wang X, et al. An analysis of cardiac disorders associated with chimeric antigen receptor T cell therapy in 126 patients: A single-centre retrospective study. *Front Oncol* (2021) 11:691064. doi: 10.3389/fonc.2021.691064

126. Rose-John S, Scheller J, Elson G, Jones SA. Interleukin-6 biology is coordinated by membrane-bound and soluble receptors: role in inflammation and cancer. *J Leukoc Biol* (2006) 80(2):227–36. doi: 10.1189/jlb.1105674

127. Fried S, Avigdor A, Bielorai B, Meir A, Besser MJ, Schachter J, et al. Early and late hematologic toxicity following CD19 CAR-T cells. *Bone Marrow Transplant* (2019) 54(10):1643–50. doi: 10.1038/s41409-019-0487-3

128. Yakoub-Agha I, Chabannon C, Bader P, Basak GW, Bonig H, Ciceri F, et al. Management of adults and children undergoing chimeric antigen receptor T-cell therapy: best practice recommendations of the European society for blood and marrow transplantation (EBMT) and the joint accreditation committee of ISCT and EBMT (JACIE). *Haematologica* (2020) 105(2):297–316. doi: 10.3324/haematol.2019.229781

129. Brudno JN, Kochenderfer JN. Toxicities of chimeric antigen receptor T cells: recognition and management. *Blood* (2016) 127(26):3321–30. doi: 10.1182/blood-2016-04-703751

130. Azoulay E, Darmon M, Valade S. Acute life-threatening toxicity from CAR T-cell therapy. *Intensive Care Med* (2020) 46(9):1723–6. doi: 10.1007/s00134-020-06193-1

131. Santomasso B, Bachier C, Westin J, Rezvani K, Shpall EJ. The other side of CAR T-cell therapy: Cytokine release syndrome, neurologic toxicity, and financial burden. *Am Soc Clin Oncol Educ Book* (2019) 39:433–44. doi: 10.1200/edbk_238691

132. Neill L, Rees J, Roddie C. Neurotoxicity-CAR T-cell therapy: what the neurologist needs to know. *Pract Neurol* (2020) 20(4):285–93. doi: 10.1136/practneurol-2020-002550

133. Hunter BD, Jacobson CA. CAR T-cell associated neurotoxicity: Mechanisms, clinicopathologic correlates, and future directions. *J Natl Cancer Inst* (2019) 111(7):646–54. doi: 10.1093/jnci/djz017

134. Huang R, Li X, He Y, Zhu W, Gao L, Liu Y, et al. Recent advances in CAR-T cell engineering. *J Hematol Oncol* (2020) 13(1):86. doi: 10.1186/s13045-020-00910-5

135. Haslauer T, Greil R, Zaborsky N, Geisberger R. CAR T-cell therapy in hematological malignancies. *Int J Mol Sci* (2021) 22(16):8996. doi: 10.3390/ijms22168996

136. Han D, Xu Z, Zhuang Y, Ye Z, Qian Q. Current progress in CAR-T cell therapy for hematological malignancies. *J Cancer* (2021) 12(2):326–34. doi: 10.7150/jca.48976

137. Larson RC, Maus MV. Recent advances and discoveries in the mechanisms and functions of CAR T cells. *Nat Rev Cancer* (2021) 21(3):145–61. doi: 10.1038/s41568-020-00323-z

138. Rahman MM, Behl T, Islam MR, Alam MN, Islam MM, Albarrati A, et al. Emerging management approach for the adverse events of immunotherapy of cancer. *Molecules* (2022) 27(12):3798. doi: 10.3390/molecules27123798

139. Zhao Z, Li Y, Liu W, Li X. Engineered IL-7 receptor enhances the therapeutic effect of AXL-CAR-T cells on triple-negative breast cancer. *BioMed Res Int* (2020) 2020:4795171. doi: 10.1155/2020/4795171

140. Shum T, Omer B, Tashiro H, Kruse RL, Wagner DL, Parikh K, et al. Constitutive signaling from an engineered IL7 receptor promotes durable tumor elimination by tumor-redirected T cells. *Cancer Discovery* (2017) 7(11):1238–47. doi: 10.1158/2159-8290.Cd-17-0538

141. Pabst T, Joncourt R, Shumilov E, Heini A, Wiedemann G, Legros M, et al. Analysis of IL-6 serum levels and CAR T cell-specific digital PCR in the context of cytokine release syndrome. *Exp Hematol* (2020) 88:7–14.e3. doi: 10.1016/j.exphem.2020.07.003

142. Zettler ME, Feinberg BA, Phillips EGJr., Klink AJ, Mehta S, Gajra A. Real-world adverse events associated with CAR T-cell therapy among adults age ≥ 65 years. *J Geriatr Oncol* (2021) 12(2):239–42. doi: 10.1016/j.jgo.2020.07.006

143. Lei W, Xie M, Jiang Q, Xu N, Li P, Liang A, et al. Treatment-related adverse events of chimeric antigen receptor T-cell (CAR T) in clinical trials: A systematic review and meta-analysis. *Cancers (Basel)* (2021) 13(15):3912. doi: 10.3390/cancers13153912

frontiers | Frontiers in Immunology

TYPE Original Research
PUBLISHED 23 December 2022
DOI 10.3389/fimmu.2022.1054157

OPEN ACCESS

EDITED BY
Junjiang Fu,
Southwest Medical University, China

REVIEWED BY
Angela Rita Elia,
Institute of Oncology Research (IOR), Switzerland
Vinit C. Shanbhag,
University of Missouri, United States

*CORRESPONDENCE
Lei Sun
leisun@dmu.edu.cn

SPECIALTY SECTION
This article was submitted to Cancer Immunity and Immunotherapy, a section of the journal Frontiers in Immunology

RECEIVED 26 September 2022
ACCEPTED 12 December 2022
PUBLISHED 23 December 2022

CITATION
Shi C, Zhang L, Chen D, Wei H, Qi W, Zhang P, Guo H and Sun L (2022) Prognostic value of TMEM59L and its genomic and immunological characteristics in cancer.
Front. Immunol. 13:1054157.
doi: 10.3389/fimmu.2022.1054157

Prognostic value of TMEM59L and its genomic and immunological characteristics in cancer

Chang Shi[1,2], Lizhi Zhang[2], Dan Chen[2], Hong Wei[2], Wenjing Qi[2], Pengxin Zhang[2], Huiqi Guo[2] and Lei Sun[1]*

[1]Department of Pathology and Forensic Medicine, College of Basic Medical Sciences, Dalian Medical University, Dalian, Liaoning, China, [2]Department of Pathology, First Affiliated Hospital, Dalian, China

Background: TMEM59L is a newly discovered transmembrane protein; its functions in cancer remain unknown. This study was designed to reveal the prognostic value and the functional role of TMEM59L in cancer.

Methods: The gene expression profiles, methylation data, and corresponding clinical data of *TMEM59L* were retrieved from The Cancer Genome Atlas (TCGA) and the Genotype-Tissue Expression database. Survival analysis was employed to calculate the pan-cancer prognostic value of *TMEM59L*. The correlation between *TMEM59L* expression and tumor immune microenvironment, as well as DNA methylation dynamics and genomic heterogeneity across cancers were assessed based on data from TCGA.

Results: Our findings revealed that distinct differences of *TMEM59L* mRNA expression were observed in different cancer types and that higher *TMEM59L* expression was observed in the advanced pathological stage and associated with worse prognosis in kidney renal papillary cell carcinoma, bladder urothelial carcinoma, colon adenocarcinoma, and kidney renal clear cell carcinoma. Pathway analysis indicated that *TMEM59L* exerted a key influence in cancer development and in immune- and cancer-associated pathways such as epithelial–mesenchymal transition and TGF-β signaling. Moreover, correlation analysis hinted at a negative correlation of *TMEM59L* expression with CD8 T cells, activated CD4 T cells, and several immunomodulators, including IDO1, TIGIT, PD-L1, CTLA-4, and BTLA in various cancers. Survival analysis indicated that the hypermethylation of *TMEM59L* gene was associated with longer survival times. A significant correlation was also observed between *TMEM59L* expression and immunophenoscore, homologous recombination deficiency, loss of heterozygosity, tumor stemness score, and neoantigens in various cancers. Importantly, we also identified numerous potential agents that may target *TMEM59L*.

Conclusion: Our study revealed the prognostic value as well as the genomic and immunological characteristics of *TMEM59L* in cancers, highlighting the promising potential for TMEM59L as a prognostic cancer biomarker and a therapeutic target.

KEYWORDS

TMEM59L, pan-cancer, prognosis, tumor microenvironment, methylation

1 Introduction

The global incidence and mortality of cancer remain on the rise, with breast cancer, lung cancer, and colorectal cancer being the most common types of cancer with the highest mortality rates worldwide (1, 2). Cancer is a major cause of global mortality and a significant impediment to increasing life expectancy in the global population (3). Despite research efforts to improve cancer diagnosis and treatment, the associated clinical outcome and 5-year survival rate generally remain unfavorable, largely due to the complexity of this disease (4–8).

A large body of evidence has confirmed that the tumor microenvironment (TME) can determine abnormal tissue functions, alter the malignant behavior of tumor cells, and play vital roles in the consecutive evolution of malignant cancers and tumor resistance to anticancer drugs (9–11). The TME, characterized by hypoxia, oxidative stress, and abnormal levels of multiple cytokines and growth factors, induces dysplasia, which is defined as the emergence of heterogeneous tumor cell populations with distinct genetic and phenotypic characteristics (8, 12, 13). During cancer progression, tumor heterogeneity is exacerbated by the maturation of both cellular and acellular components of the TME (14, 15), enabling cancer stem cells (CSCs) to survive and proliferate – a principal attribute that underlies therapeutic resistance as well as tumor maintenance and recurrence (16–20). Multiple studies have indicated that genomic, epigenomic, and transcriptomic features are causally linked to the regulation of cancer pathways that support tumor cell growth and proliferation, and the phenomenon of cancer stemness (21–23). For these reasons, the outcome of current cancer chemotherapy, radiotherapy, and immunotherapy is far from satisfactory, and treatment regimens require further optimization.

DNA methylation signatures that are highly sensitive, specific, and analyzable have an enormous potential as clinical cancer biomarkers that play a non-negligible role in cancer diagnosis and prognosis, providing new technical means for early detection of different cancer types (24–27). Nevertheless, there is a need to explore new potential targets or cancer biomarkers to ensure that novel treatment regimens and appropriate combination therapy strategies can be specifically tailored to individual patients.

Transmembrane protein 59–like (TMEM59L), also known as brain-specific membrane-anchored protein BSMAP, was first discovered in 1999 (28). In 2006, using reverse transfection cell array technology, Mannherz et al. found that TMEM59L produced pro-apoptotic effects through an unknown mechanism (29). TMEM59L can regulate the N- and O-glycosylation steps that occur during Golgi maturation and is associated with glycosylation modifications of the amyloid precursor protein APP by inhibiting APP maturation, trafficking, and shedding (30). Recent studies have demonstrated that the downregulation of TMEM59L can protect neurons from oxidative stress, and that TMEM59L interacts with ATG5 and ATG16L1, partially activating LC3 and triggering autophagy (31, 32). Moreover, the homologue of TMEM59L, transmembrane protein 59 (TMEM59), is hypomethylated in late-onset Alzheimer's disease, and methylation is involved in the transcriptional regulation and thus protein expression of TMEM59 (33). However, there is currently a lack of in-depth reports on the functional mechanism of TMEM59L, especially in the context of cancer research.

In this study, we comprehensively explored TMEM59L gene expression signature, its prognostic value, as well as its association with immune cell infiltration and cancer-associated pathways in various cancer types. Moreover, our study underscores the importance of TMEM59L as a prognostic biomarker and a treatment target and identified in TMEM59L a molecule to be further explored.

2 Materials and methods

2.1 Datasets

The gene expression profiles, methylation data, and corresponding pan-cancer clinical data were downloaded from The Cancer Genome Atlas (TCGA) database (https://portal.gdc.cancer.gov/), the Genotype-Tissue Expression (GTEx) dataset was downloaded from UCSC-hosted genomics platform (https://xenabrowser.net/). The cancer type abbreviations are listed in Table 1.

TABLE 1 The cancer type abbreviations are as above.

ACC	Adrenocortical carcinoma
BLCA	Bladder Urothelial Carcinoma
BRCA	Breast invasive carcinoma
CESC	Cervical squamous cell carcinoma and endocervical adenocarcinoma
CHOL	Cholangiocarcinoma
COAD	Colon adenocarcinoma
COADREAD	Colon adenocarcinoma/Rectum adenocarcinoma Esophageal carcinoma
ESCA	Esophageal carcinoma
GBM	Glioblastoma multiforme
GBMLGG	Glioma
HNSC	Head and Neck squamous cell carcinoma
KICH	Kidney Chromophobe
KIPAN	Pan-kidney cohort (KICH+KIRC+KIRP)
KIRC	Kidney renal clear cell carcinoma
KIRP	Kidney renal papillary cell carcinoma
LAML	Acute Myeloid Leukemia
LGG	Brain Lower Grade Glioma
LIHC	Liver hepatocellular carcinoma
LUAD	Lung adenocarcinoma
LUSC	Lung squamous cell carcinoma
OV	Ovarian serous cystadenocarcinoma
PAAD	Pancreatic adenocarcinoma
PCPG	Pheochromocytoma and Paraganglioma
PRAD	Prostate adenocarcinoma
READ	Rectum adenocarcinoma
SARC	Sarcoma
STAD	Stomach adenocarcinoma
SKCM	Skin Cutaneous Melanoma
STES	Stomach and Esophageal carcinoma
TGCT	Testicular Germ Cell Tumors
THCA	Thyroid carcinoma
UCEC	Uterine Corpus Endometrial Carcinoma

2.2 Integrated network and enrichment analysis

Each patient was divided into a high-expression or a low-expression group based on the median of *TMEM59L* expression. We used the GSVA R package to conduct the gene set enrichment analysis (GSEA) to evaluate pathway enrichment for high- and low-*TMEM59L* expression groups (34). Hallmark gene sets (h.all.v7.2.symbols) were collected from GSEA database (http://www.gsea-msigdb.org/gsea/downloads.jsp). Reverse phase protein array (RPPA) data from TCPA database (https://www.tcpaportal.org/tcpa/index.html) were also used to assess pathway activity score (PAS). The evaluated pathways included apoptosis, cell cycle, DNA damage response, epithelial–mesenchymal transition (EMT),

as well as hormone androgen receptor (AR), hormone estrogen receptor (ER), tuberous sclerosis complex–mammalian target of rapamycin (TSC–mTOR), receptor tyrosine kinase (RTK), Ras/MAPK (mitogen-activated protein kinase), and PI3K/AKT signaling pathways, all of which are notably associated with cancer. The difference of PAS was evaluated using Student's *t*-test, and the resulting *p*-value was adjusted for false discovery rate (FDR), with FDR ≤ 0.05 being considered significant. When PAS (TMEM59L High expression) > PAS (TMEM59L Low expression), we considered TMEM59L to have an activating effect on a specific pathway; in the opposite case TMEM59L was considered to have an inhibitory effect on a pathway.

2.3 Estimation of immune cell infiltration

The correlation of *TMEM59L* expression with the immune infiltration level was assessed using the CIBERSORT algorithm (https://cibersort.stanford.edu) (35). The stromal, immune, and ESTIMATE scores for each patient were calculated using the ESTIMATE algorithm (36). The immunophenoscore (IPS) for each patient was calculated according to the method reported by Charoentong (37). We also extracted the expression data of 155 immunomodulators including chemokines, receptors, MHC, immune-inhibitors, and immune-stimulators from each patient based on the study of Charoentong et al. (37) as well, and correlation analyses were subsequently conducted to assess the association between immunological characteristics and *TMEM59L* across cancer types.

2.4 Methylation analysis

We downloaded the methylation data from TCGA database. In total, 14 cancer types were selected and analyzed including Colon adenocarcinoma (COAD), Colorectal carcinoma (COADREAD), Thyroid carcinoma (THCA), Cholangiocarcinoma (CHOL), Liver hepatocellular carcinoma (LIHC), Kidney renal papillary cell carcinoma (KIRP), Pan-kidney cohort (KIPAN), Adrenocortical carcinoma (ACC), Ovarian serous cystadenocarcinoma (OV), Uterine Corpus Endometrial Carcinoma (UCEC), Rectum adenocarcinoma (READ), Stomach and Esophageal carcinoma (STES), Breast invasive carcinoma (BRCA), Bladder Urothelial Carcinoma (BLCA), Kidney renal clear cell carcinoma (KIRC), Prostate adenocarcinoma (PRAD), Stomach adenocarcinoma (STAD), Lung squamous cell carcinoma (LUSC), Lung adenocarcinoma (LUAD), Pancreatic adenocarcinoma (PAAD), Glioma (GBMLGG), Esophageal carcinoma (ESCA), Kidney Chromophobe (KICH), and Head and Neck squamous cell carcinoma (HNSC). The cohort included more than 10 paired cancer and adjacent non-cancer samples. Spearman correlation analyses were performed to identify whether *TMEM59L* expression was associated with methylation levels.

2.5 Drug analysis

We recorded the drug sensitivity data from Genomics of Drug Sensitivity in Cancer (GDSC) database (38) and the Genomics of Therapeutics Response Portal (CTRP) database (39). Spearman correlation analysis was carried out to identify the association between gene mRNA expression and drug response.

2.6 Statistical analysis

We computed the statistical analyses in the R (version 4.1.1). Hazard analyses were carried out using Cox regression. Survival curves were analyzed by log-rank test. Correlation coefficients were obtained using the Spearman correlation method. Any *p*-value less than 0.05 was considered statistically significant.

3 Results

3.1 *TMEM59L* mRNA expression in human cancers

The TIMER online database (https://cistrome.shinyapps.io/timer/) was first used to identify the expression of *TMEM59L* mRNA transcripts in different types of cancer (Figure 1A). Compared with corresponding normal tissues, *TMEM59L* mRNA expression was significantly increased in six human cancers, specifically BRCA, CHOL, LIHC, LUAD, PRAD, and THCA. In contrast, *TMEM59L* expression was evidently lower in BLCA, COAD, KICH, KIRC, KIRP, and STAD than that in the normal tissues. Subsequently, a pan-cancer analysis demonstrated that *TMEM59L* expression was decreased across most cancer types, such as GBM, GBMLGG, KIRP, COAD, KICH, KIRC, LGG, KIPAN, COADREAD, STAD, UCEC, READ, STES, and BLCA (Figure 1B). Considering the small number of normal samples in TCGA database, we integrated the data of normal tissues from the GTEx database with the data of TCGA tumor tissues to determine the expression characteristics of TMEM59L across the pan-cancer cohort. The results were similar; compared with its expression in normal samples, *TMEM59L* was significantly downregulated in most cancer types (Figure 1C).

3.2 *TMEM59L* expression profile at different clinical stages or in different cancer subtypes

We further analyzed *TMEM59L* mRNA expression tendency at different clinical stages and in different cancer subtypes (Figure 2A). Distinct differences could be observed in varying

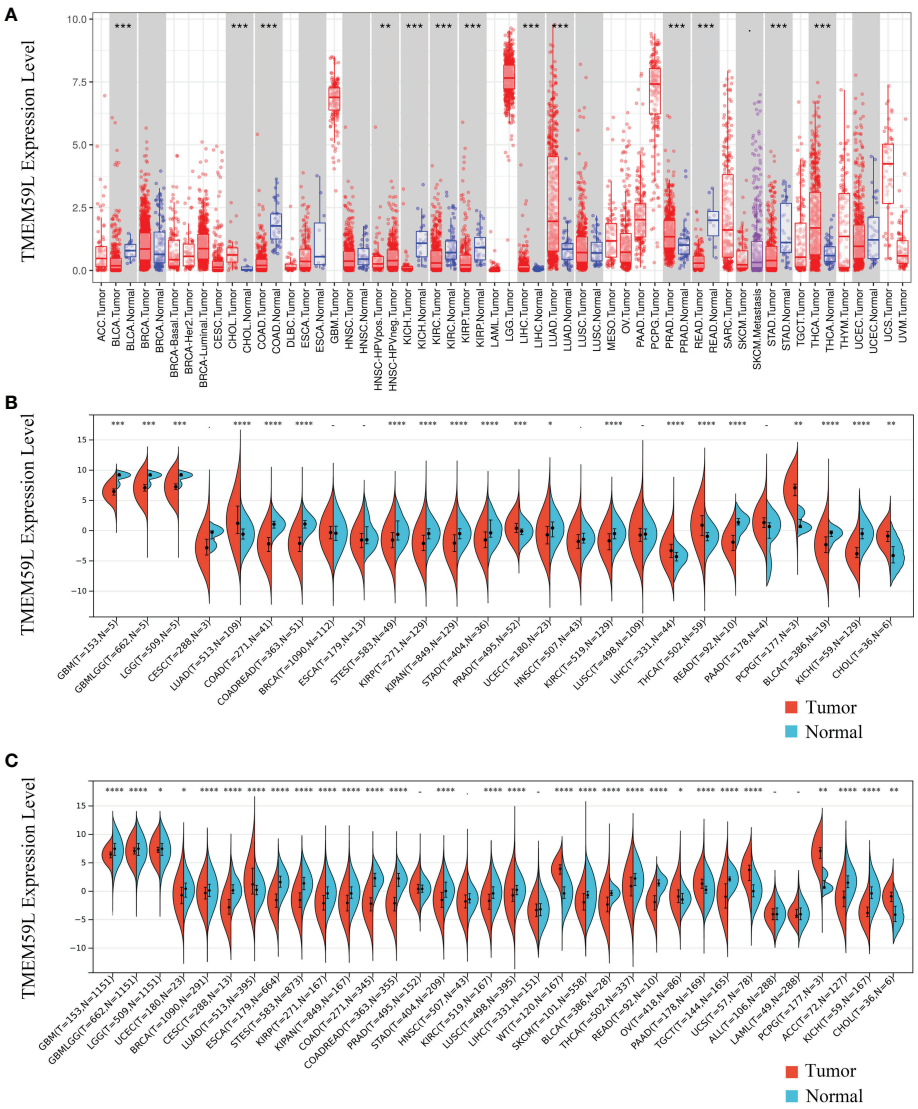

FIGURE 1
TMEM59L mRNA expression in different types of human cancers. **(A)** TMEM59L mRNA expression in different tumor types compared with normal tissues in the TIMER database. **(B)** TMEM59L mRNA expression in different tumor types compared with normal tissues from TCGA database. **(C)** mRNA expression of TMEM59L across tumor types using TCGA and GTEx data. (*P < 0.05, **P < 0.01, ***P < 0.001), ****p < 0.0001.

clinical stages in several cancer types, including KIRP, BLCA, COAD, and KIRC. Remarkably, in KIRP, BLCA, COAD, and KIRC, later pathological stage showed higher *TMEM59L* mRNA expression (Figures 2B–F). Furthermore, *TMEM59L* mRNA expression in LUAD, GBM, HNSC, BRCA, KIRC, and STAD was also significantly different based on the molecular specific subtype (Figures 2G–M). To increase the reliability of our study, we verified the protein expression level of TMEM59L. Based on the HPA database (https://www.proteinatlas.org/), we further explored the protein level of TMEM59L in normal tissues and human cancers. Figure S1A showed the protein expression level of TMEM59L in normal tissues. The immunohistochemical results showed that the expression level of TMEM59L is not high in most tissues except for the pituitary gland; Subsequently, we also explored the expression of TMEM59L in cancer tissues. As shown in Figure S1B, TMEM59L has a relatively high protein expression level in colorectal cancer, pancreatic cancer, kidney cancer, and liver cancer. These results were consistent with our previous results that the later the stage, the higher mRNA level of TMEM59L in COAD and KIRP. Figure S1C further showed the representative IHC images of TMEM59L in colorectal and renal cancer based on HPA database.

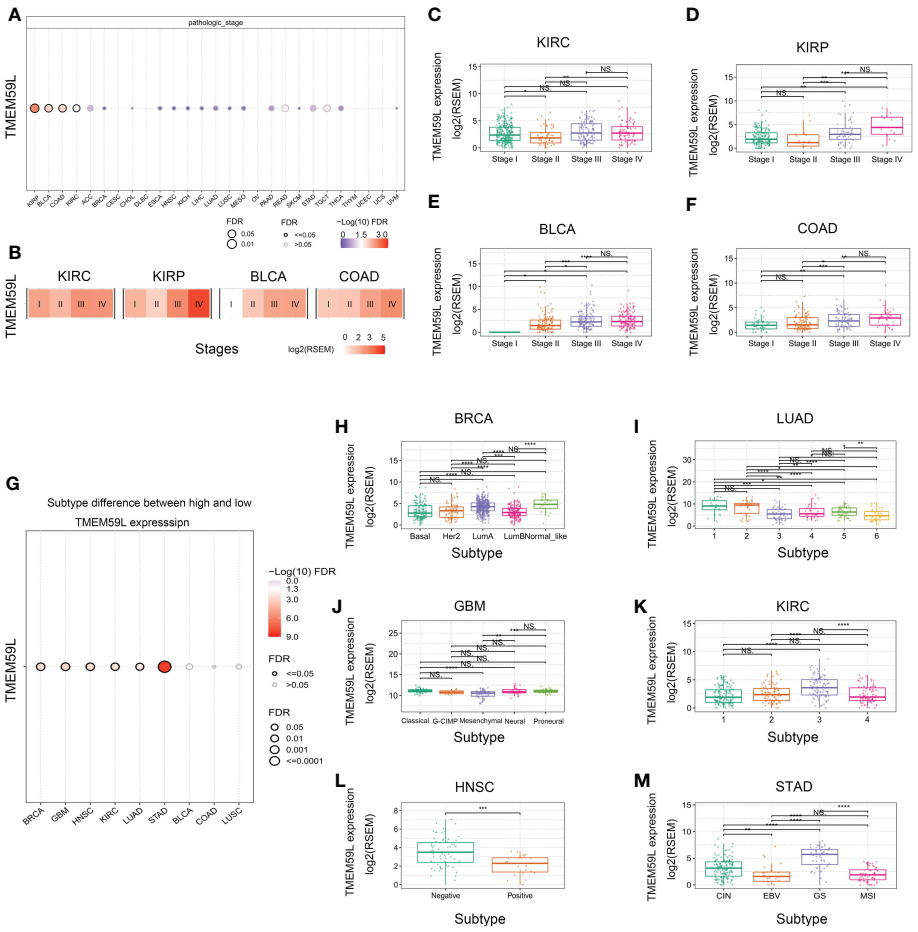

FIGURE 2
TMEM59L expression at different clinical stages or subtypes of different cancers. **(A)** The difference of TMEM59L mRNA expression between pathologic stages in the specific cancers. **(B)** Heatmap presents the TMEM59L mRNA expression profile among stages in the specific cancers. **(C–F)** TMEM59L mRNA expression in pathologic stage of KIRC, KIRP, BLCA, and COAD. **(G)** The associations between subtypes and TMEM59L expression. **(H–M)** TMEM59L mRNA expression in subtypes of BRCA, LUAD, GBM, KIRC, HNSC, and STAD. (ns: not significant, *P < 0.05, **P < 0.01, ***P < 0.001, ****p < 0.0001).

3.3 Prognostic value of *TMEM59L* mRNA expression

To further identify the prognostic value of *TMEM59L*, we then performed a survival analysis on the data retrieved from the TCGA database. Cox regression indicated that a high *TMEM59L* expression was associated with shorter overall survival (OS) and progression-free interval (PFI) of KIPAN, KIRP, BLCA, COAD, COADREAD, OV, ACC, HNSC, and STAD (Figures 3A, B). In contrast, higher *TMEM59L* expression predicted longer OS and PFI in GBMLGG, LGG, and PAAD (Figures 3A, B). Further survival curves also indicated that high *TMEM59L* expression was associated with worse OS (Figures 3C–F) and PFI in BLCA, COAD, KIRC, and KIRP (Figures 3G–J). Meanwhile, there was no significant association between *TMEM59L* expression and clinical outcome in other cancers.

3.4 Association between *TMEM59L* mRNA expression and cancer-related pathways

To better understand the relevance and potential functions of *TMEM59L* in cancer pathogenesis, we performed functional enrichment analysis on the low and high *TMEM59L* expression groups across several cancer types (Figure 4A). The results indicated that *TMEM59L* expression was closely correlated with cancer-related hallmarks, including epithelial-mesenchymal transition (EMT), P53 pathway, E2F target, cell cycle regulation at G2-M, KRAS signaling, WNT beta-catenin signaling, and immune-related pathways, such as TGF-β, IL2-STAT5, and TNFα signaling *via* NF-kB. Moreover, the pathway activity analysis suggested that *TMEM59L* was significantly involved in 10 salient cancer-related pathways, namely DNA

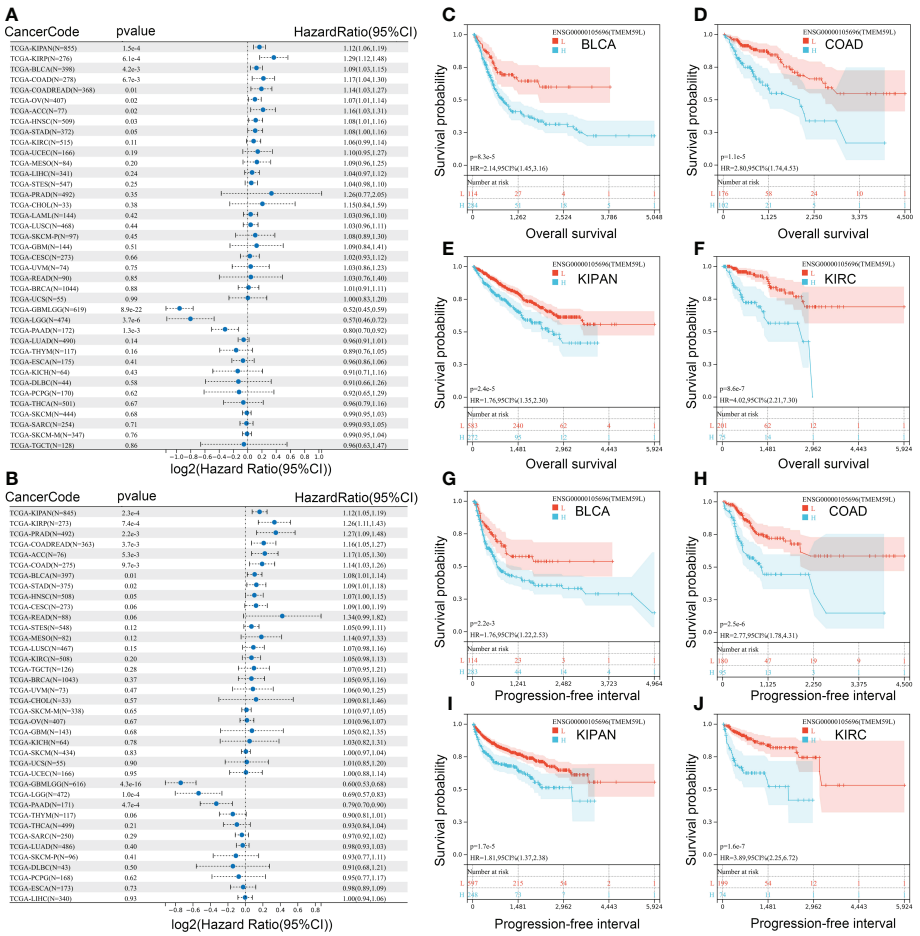

FIGURE 3
Correlation analysis between mRNA expression of TMEM59L and prognostic value. **(A)** The Overall survival (OS) difference between high and low TMEM59L expression groups. **(B)** The Progression-free interval (PFI) difference between high and low TMEM59L expression groups. **(C–J)** OS and PFI difference between high and low TMEM59L expression groups in BLCA, COAD, KIPAN, and KIRC.

damage response, apoptosis, RTK, cell cycle, Hormone AR, Hormone ER, TSC–mTOR, Ras/MAPK, EMT and PI3K/AKT signaling pathways (Figure 4B). The main pathway activated by *TMEM59L* was EMT (28% activation vs. 3% inhibition), especially in BLCA, BRCA, COAD, ESCA, OV, READ, STAD, TGCT, and THCA (Figure S2), whereas the pathways inhibited by *TMEM59L* included apoptosis (31% inhibition vs. 0% activation) and cell cycle (22% inhibition vs. 0% activation). When compared with low TMEM59L expression group, the activities of EMT and estrogen receptor (ER) pathways were also higher, whereas a lower pathway activity in cell cycle and DNA damage response was observed in the high *TMEM59L* expression group for patients with COAD (Figures 4C–F). The above results suggested that *TMEM59L* exerts a key influence on cancer pathogenesis and development.

3.5 Interaction network of *TMEM59L*

Based on the GeneMANIA database, the 20 proteins most closely correlated with TMEM59L expression, namely TMEM59, GABRA3, ITM2B, AK5, CAMK2B, HMGB4, BPIFB4, REEP2, ATP1B4, DNM1, RAB6B, GSTT1, PTPRN, CPLX2, MUC1, GDAP1L1, CORO2B, KCNS2, ASCL1, and KIF5A, were analyzed to construct a protein-protein interaction network (Figure 5A). Subsequently, these interacting genes were subjected to functional enrichment analysis, and consistently with the previous results, these genes were significantly enriched in the activation of EMT signaling pathway and in the inhibition of apoptosis and cell cycle signaling pathway (Figure 5B). Relative network analysis also indicated that *TMEM59L* and its interacting genes were involved

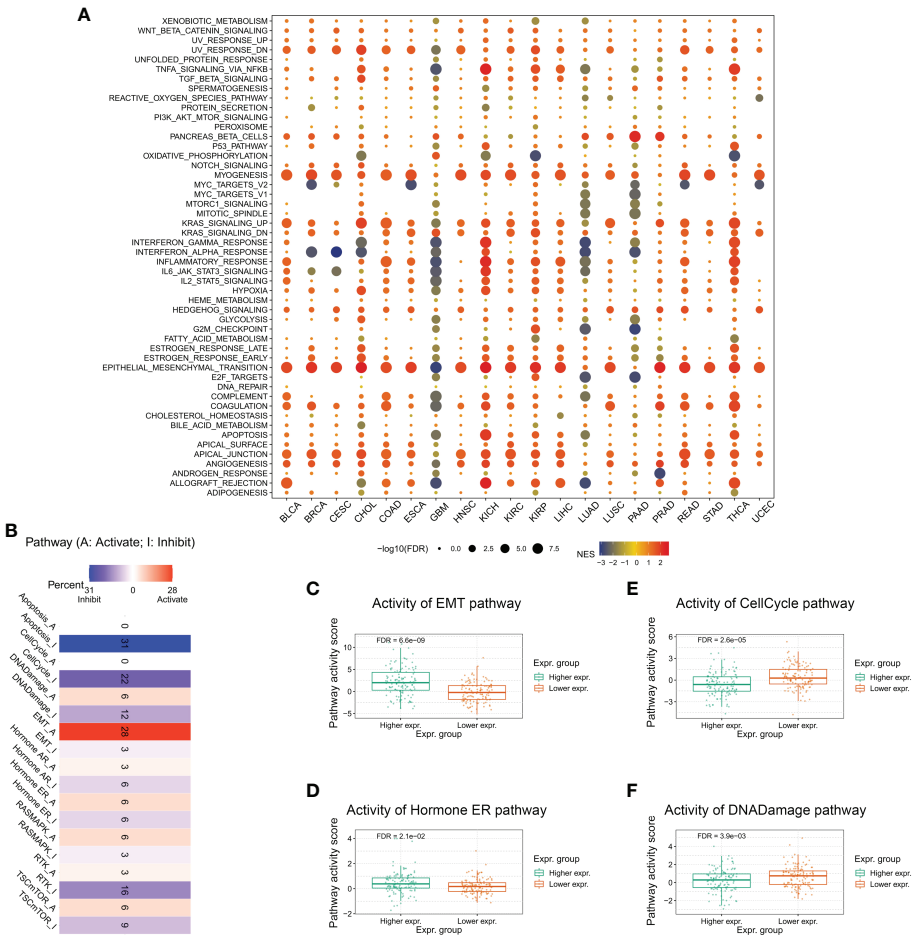

FIGURE 4
Association between TMEM59L and pathways in cancers. **(A)** Enrichment analysis for cancer signaling between high and low TMEM59L expression tumor tissues. NES is the normalized enrichment score in the GSEA algorithm. **(B)** The combined percentage of the effect of TMEM59L on pathway activity indifferent types of human cancers. **(C–F)** The differences of epithelial mesenchymal transition (EMT), Cell Cycle, Hormone estrogen receptor (ER), and DNA damage pathways activity between high and low TMEM59L expression groups in COAD.

in cancer-related pathways, such as TSC/mTOR, RTK, EMT, Ras/MAPK, and PI3K/AKT signaling, particularly in ACC, BLCA, COAD, READ, STAD, KIRP, KIRC, KICH, and PAAD (Figure 5C).

3.5.1 Association of *TMEM59L* expression with the tumor immune microenvironment

As the pathway enrichment analysis revealed that *TMEM59L* was closely related to inflammation and immune function, we further investigated the link between *TMEM59L* expression and immune cell infiltration levels using the CIBERSORT algorithm. The results demonstrated that *TMEM59L* expression was distinctly negatively correlated with immune infiltration levels in LUSC, SARC, COADREAD, LUAD, HNSC, CESC, BRCA, and TGCT, especially with the levels of CD8 T cell and activated CD4 T cells (Figure 6A and Table S1). We then further assessed Spearman's correlation coefficient of *TMEM59L* and immune scores across distinct cancer types using the ESTIMATE algorithm. A significantly positive correlation between *TMEM59L* and stromal scores was detected, yet a negative correlation with immune scores across many cancer types (Table S2). IPS has been shown to effectively predict the response rate to anti-CTLA-4 and anti-PD-1 therapy. For this reason, we investigated the link between *TMEM59L* expression and the IPS across various cancer types. Figure 6B showed that *TMEM59L* expression was evidently negatively correlated with IPS in several types of cancers, including GBMLGG, LGG, OV, CESC, KIRC, SKCM, KIRP, and KIPAN. Moreover, IPS analysis demonstrated that *TMEM59L* expression was positively associated with immune checkpoints (CP) and suppressor cells (SCs) but was negatively correlated with MHC, average Z-score (AZ), and effector cells (ECs) in most tumors, all the p-values are less than 0.05.

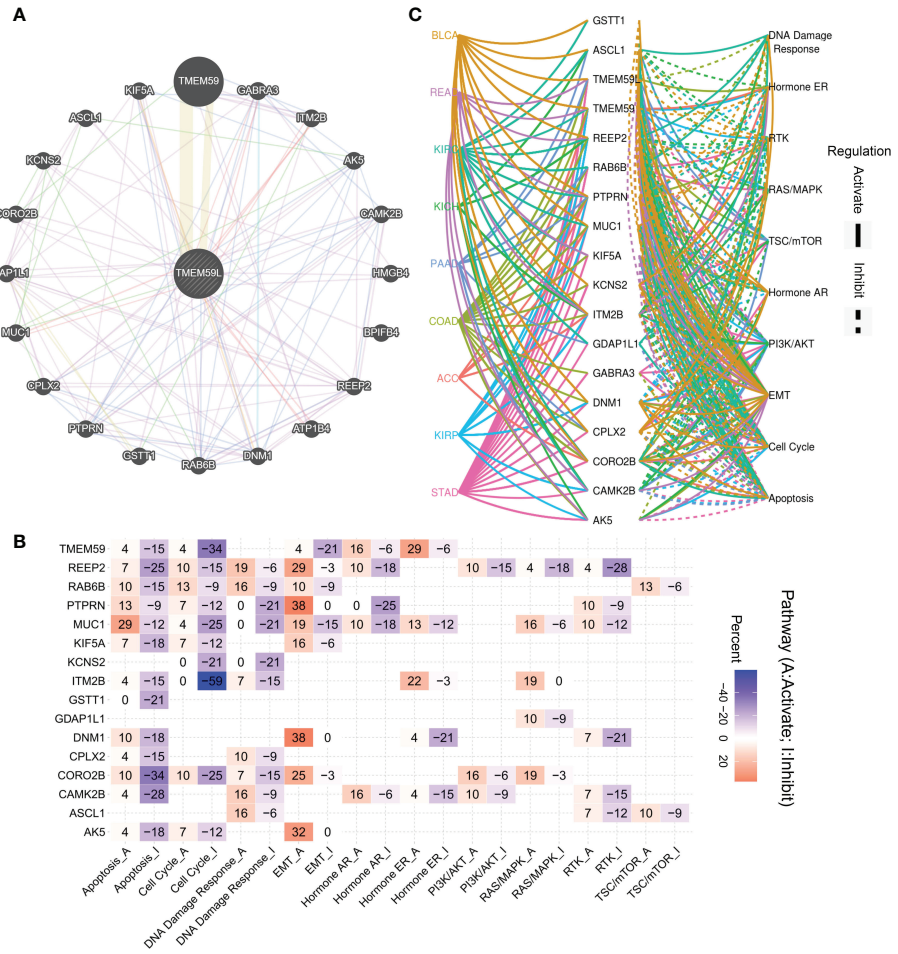

FIGURE 5
Association between interaction genes of TMEM59L and pathways in cancers. **(A)** Interaction Network of TMEM59L constructed by GeneMANIA. **(B)** The combined percentage of the effect of interaction genes of TMEM59L on pathway activity in different types of human cancers, the number in each cell means that the percentage of cancer types, in which TMEM59L showed significant association with the specific pathway, among the selected cancer types. **(C)** Association between interaction genes of TMEM59L and known pathways in ACC, BLCA, COAD, READ, STAD, KIRP, KIRC, KICH and PAAD. (solid line: activation; dashed line: inhibition), the different colors of the lines represent different types of cancer.

We also demonstrated that *TMEM59L* expression was negatively linked with the expression of many immune modulators, including PD-L1, IDO1, TIGIT, CTLA-4, and BTLA in various cancers (Figure 6C). *TMEM59L* also showed a negative correlation with tumor mutational burden (TMB) in many cancers, such as HNSC, LUAD, LIHC, KIRC, BRCA, THCA, BLCA, KIRP, LGG, ESCA, PAAD, UCEC, and STAD and a negative correlation with microsatellite instability (MSI) in UCEC, ACC, ESCA, LAML, and STAD, which suggest that *TMEM59L* may reflect cancer immunogenicity in these cancer types (Figures 6D–E and Table S3). Subsequently, based on the IMvigor210 cohort, we also found a link between the high expression of *TMEM59L* and poor clinical response to immune therapy (Figure 6F). These observations may hint at an intricate interplay between *TMEM59L* and the immune microenvironment, although more in-depth investigations are needed to unveil the specific molecular mechanisms.

To further clarify the possible role of TMEM59L in the tumor microenvironment, we analyzed single-cell sequencing data from BRCA-GSE148673 dataset through the TISCH database (a scRNA-seq database that provides extensive cell type annotations at the single-cell level, allowing TME exploration across various cancers). The results of UMAP showed that 28 clusters were identified in the BRCA-GSE148673 dataset (Figure S3A), and then the corresponding clusters were labeled into nine different cell subpopulations, including B cell, CD4 T conv, CD8 T cell, endothelial, epithelial, fibroblasts, malignant, mono/macro, and Tprolif (Figure S3B). For the BRCA-GSE148673 data set, TMEM59L is mainly expressed in fibroblasts (Figures S3C, D). Previous studies

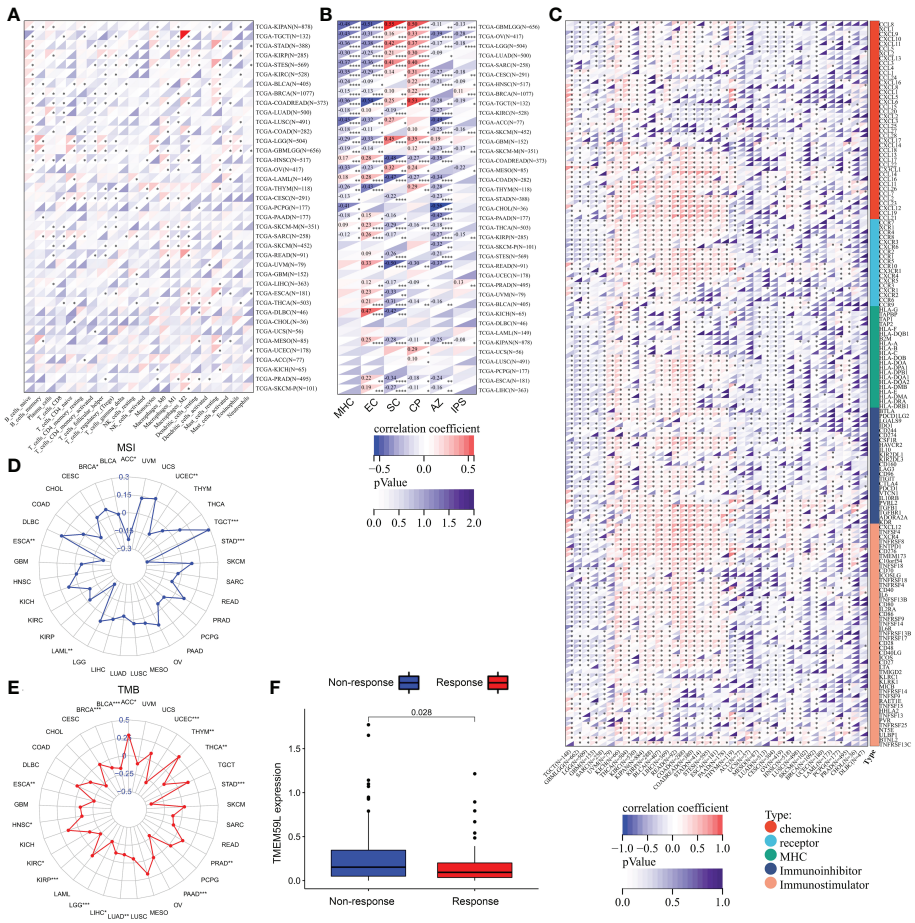

FIGURE 6
Relationship between TMEM59L expression and the tumor-immune microenvironment. **(A)** The correlation of TMEM59L expression with immune cell infiltration levels in pan-cancer. **(B)** The correlation between TMEM59L expression and the Immunophenoscore (IPS) across various cancer types. CP, immune checkpoints; SC, suppressor cells; EC, Effector cells; AZ, Average Z-score. **(C)** Correlation between TMEM59L and 155 immunomodulators, including chemokine, receptor, MHC, immuno-inhibitor, and immuno-stimulator across cancers. **(D, E)** Correlation of TMEM59L expression with tumor mutation burden (TMB) and microsatellite instability (MSI) in multiple cancer. **(F)** Patients with high TMEM59L expression have a worse clinical response to immune therapy in IMvigor210 cohort. (*p < 0.05, **p < 0.01, ***p < 0.001, ****p < 0.0001).

have shown that fibroblasts are mainly involved in the activation of the EMT pathway to promote metastasis (40–42), and functional enrichment analysis subsequently conducted further confirmed our speculation that the activity of the EMT and angiogenesis pathways in TMEM59L high-expressing cell cluster (fibroblasts) was significantly increased (Figures S3E, F). All the above results indicated that TMEM59L participates in tumor invasion and metastasis through the activity EMT pathway, which was consistent with our previous results.

We also performed GSEA analysis using TCGA-BRCA bulk RNA-seq data to compare the expression level of TMEM59L concerning related signaling pathways. The cancer-associated pathway signatures were extracted from Jiao Hu et al. (43), the cancer-immunity cycle reflects the anticancer immune response (44), and the activation levels cancer-immunity cycle were retrieved from tracking tumor immunophenotype (TIP) (45) (http://biocc.hrbmu.edu.cn/TIP/). And as shown, TMEM59L was significantly positively correlated with oncogenic pathways (such as Ta_pathway, EMT_differentiation, and Myofibroblasts pathway) (Figure S4A). Interestingly, we further found that TMEM59L is negatively correlated with cancer immunity cycle pathways which further confirmed that TMEM59L is related to the immunosuppressive microenvironment (Figure S4B).

3.6 DNA methylation alterations across *TMEM59L* gene across different human cancers

Epigenetic changes such as DNA methylation play key roles in modulating the behaviors of cancer cells and immune tolerance (46), thus we explored whether epigenetic regulation is involved in

TMEM59L mRNA expression. As shown in Figure 6A, the methylation levels of *TMEM59L* gene in distinct cancers were highly heterogeneous (Figure 7A). The *TMEM59L* gene was hypermethylated in most cancers, including COAD (Figure 7B), BRCA (Figure 7C), PAAD (Figure 7D), HNSC (Figure 7E), BLCA, UCEC, KIRC, and LUSC, whereas it was hypomethylated in KIRP, LUAD, and THCA ($P < 0.05$, Figure S5). Spearman correlation analysis indicated that *TMEM59L* expression correlated negatively with its gene methylation level in BLCA, BRCA, COAD, UCEC, HNSC, LUAD, PAAD, and THCA (FDR < 0.05; Figure 7F and Figure S6). Subsequently, survival analysis also showed that the hypermethylation of the *TMEM59L* gene correlated with longer survival times than the survival times associated with the hypomethylation of *TMEM59L* gene ($P < 0.05$, Figure 7G), especially in COAD, KIRC, and KIRP. The hypermethylation of *TMEM59L* was significantly correlated with longer OS and PFI (Figures 7H–M). No association was found between *TMEM59L* methylation and survival in other cancer types.

3.7 Correlation analysis of *TMEM59L* expression with stemness index and genomic heterogeneity across cancers

Stem cell–like characteristics have been established as the main cause of chemoresistance (47, 48) and the key drivers of tumor progression (49–51). In the present study, we conducted correlation analyses to identify the association between *TMEM59L* expression and tumor stemness scores (RNA and DNA stemness scores). A significant negative correlation between DNA stemness score and *TMEM59L* expression in most tumors was observed in LGG, ESCA, SARC, STES, GBMLGG, STAD, COAD, LIHC, BRCA, TGCT, COADREAD, BLCA, PRAD, and KICH (Figure 8A). Similar results were seen when assessing the correlation between RNA stemness score and *TMEM59L* expression in most cancers, except for GBM, GBMLGG, LGG, and PCPG (Figure 8B). Homologous recombination is a critical pathway for double-

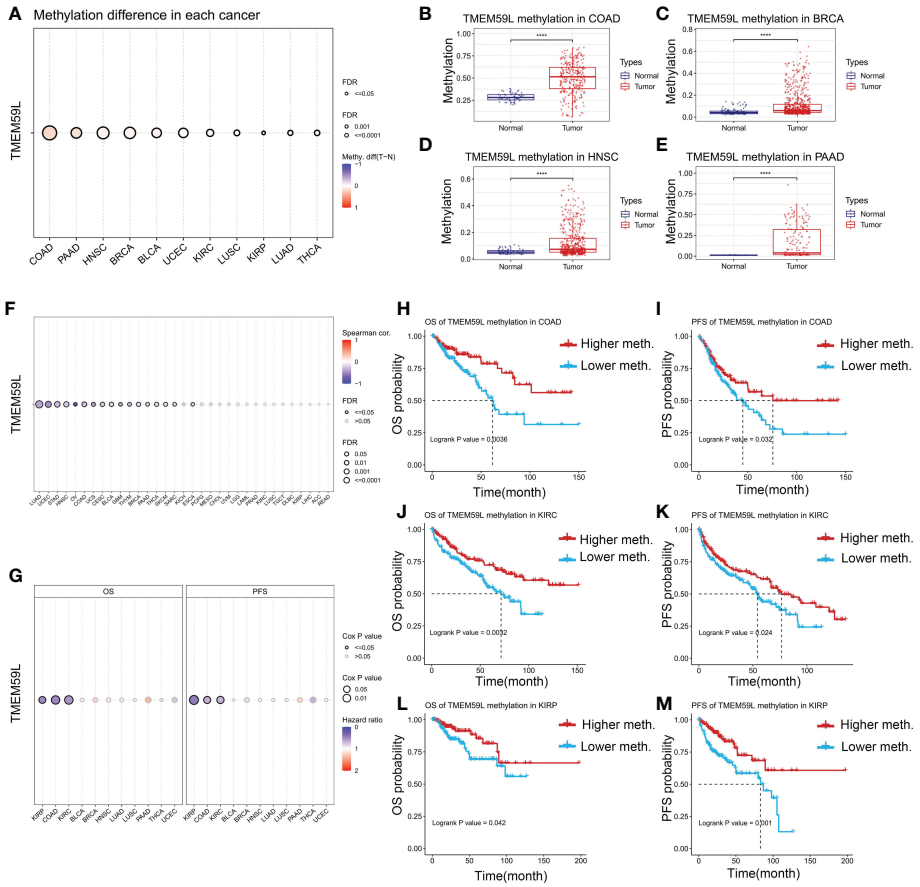

FIGURE 7
DNA methylation alterations of TMEM59L across different human cancers. **(A)** The methylation difference between tumor and normal samples of TMEM59L in different human cancers. **(B–E)** TMEM59L methylation in COAD, BRCA, HNSC, and PAAD. **(F)** The correlation between methylation and mRNA expression of TMEM59L in different human cancers. **(G)** The OS and PFS difference between higher and lower TMEM59L methylation groups in different human cancers. **(H–M)** The prognosis analysis of TMEM59L methylation in COAD, KIRC and KIRP.

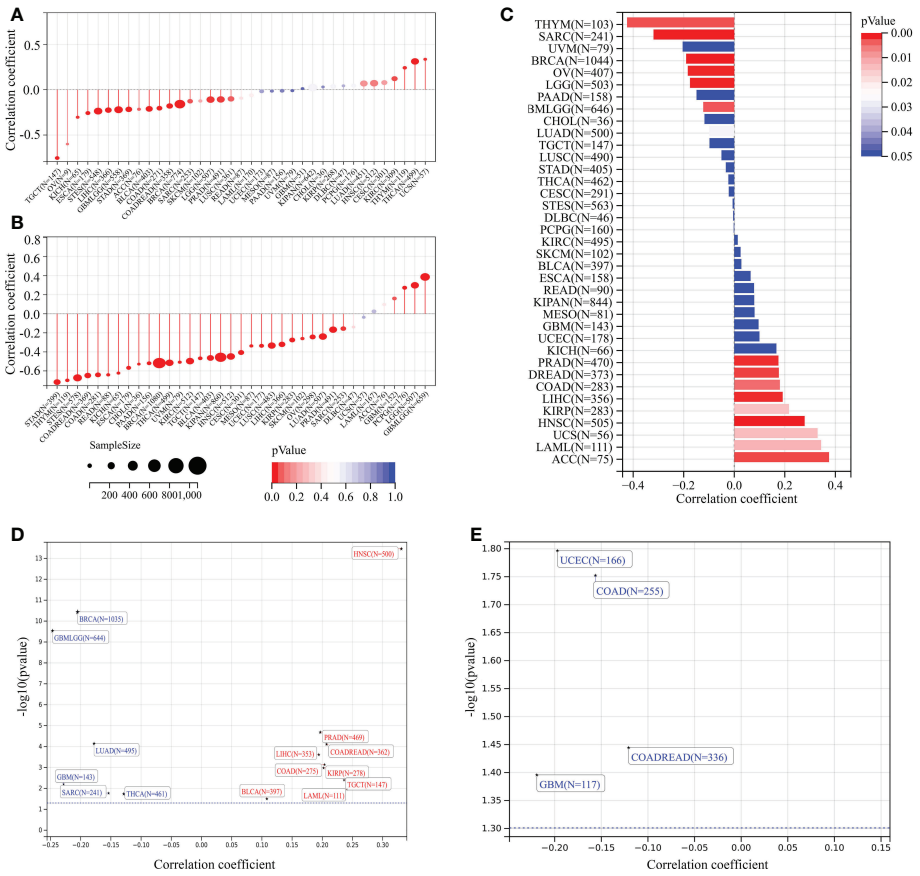

FIGURE 8
Correlation analysis of TMEM59L expression with stemness index and genomic heterogeneity across cancers. **(A, B)** The association between TMEM59L expression and tumor stemness score (DNAss and RNAss) in different cancers. **(C)** The association between TMEM59L expression and the homologous recombination deficiency (HRD) in different types of cancer. **(D, E)** The correlation of TMEM59L expression with heterozygosity (LOH) and Neoantigens (NEO) in different types of cancer.

strand break repairs (52, 53), thus homologous recombination deficiency would result in a high level of genomic instability, leading to a loss of heterozygosity and ultimately cell death (52, 54). Homologous recombination deficiency cancers have been shown to be markedly correlated with sensitivity to platinum-based chemotherapeutic drugs and PARP inhibitors (55, 56). In the current study, the expression of *TMEM59L* was closely related to homologous recombination deficiency status in most tumors (Figure 8C), and further loss of heterozygosity analysis showed a significantly positive association between loss of heterozygosity status and *TMEM59L* expression in several cancers, such as COAD, COADREAD, LAML, KIRP, PRAD, HNSC, LIHC, TGCT, and BLCA but a negative association with GBM, GBMLGG, LUAD, BRCA, SARC, and THCA (Figure 8D). Neoantigens were reported to be critical targets of immunotherapy and were correlated with improved clinical outcome and response rate to immune checkpoint blockade in several cancers, such as non-small cell lung cancer and melanoma (57–61). Our study discovered that *TMEM59L* expression was linked with neoantigens in only a limited number of cancers, such as COAD, COADREAD, GBM, UCEC, while no link was evident in other cancers (Figure 8E).

3.8 Drug sensitivity analysis

Genomic aberrations would impact the sensitivity of malignant tumors to drug therapy (including chemotherapy and targeted therapy) (62). Since *TMEM59L* expression was closely associated with the genomic heterogeneity of various cancers, we then performed the drug sensitivity analysis on the GDSC (38) and CTRP databases. The results indicated that patients with high *TMEM59L* expression were more susceptible to AG-01469, BMS-754807, SB 505124, CIL70, DBeQ, ML162, ML210, axitinib, alisertib, olaparib, PYR-41, GMX-1778, BMS-195614, and B52334 (negative correlation with IC50, $p < 0.05$; Figures 9A, B). This implied that the dysregulation of *TMEM59L* could lead to anti-tumor drug resistance.

4 Discussion

Transmembrane proteins (TMEMs) are proteins that span the entirety of the cell membranes (63), and many of such proteins play an important role in cancer development and cancer cell dissemination (64, 65), by mediating signal transduction between the cytoplasmic proteins and extracellular environment (66). Therefore, TMEMs represent attractive drug targets for cancer therapy (64). TMEM59L is a newly discovered brain-specific membrane-anchored protein that has been reported to act as a pro-apoptotic protein (29, 31). TMEM59L downregulation protects neurons from oxidative stress (31). Recent studies have also shown that *TMEM59L* can also regulate autophagy-related biological processes (32). However, there is currently a dearth of systematic studies in the literature on the TMEM59L regulation of tumor pathophysiology across cancer types.

In the present research, we assessed the pan-cancer expression of *TMEM59L* and the correlation of dysregulation of *TMEM59L* expression with clinical outcome of patients. The results indicated that *TMEM59L* expression was altered in different types of cancer and associated with the clinical outcome of cancer patients. *TMEM59L* expression was evidently downregulated across most cancer types compared to its expression in the corresponding normal tissues. Further analysis demonstrated that distinct differences was observed in different clinical stages of several cancer types, such as KIRP, BLCA, COAD, and KIRC, where advanced tumor stage correlated with higher *TMEM59L* mRNA expression. Therefore, in these specific cancer types *TMEM59L* may serve as a tumor promoting factor. Additionally, survival analysis confirmed that *TMEM59L* was a risk factor in patients with KIRP, BLCA, COAD, and KIPAN (KIRC+KIRP+KICH).

The mechanism by which *TMEM59L* regulates tumorigenesis and cancer pathophysiology remains unclear, but the relationship we observed between *TMEM59L* and the hallmarks of cancer could improve our understanding of the functional roles of *TMEM59L*. GSEA analysis demonstrated that *TMEM59L* expression was strictly linked with hallmarks of malignancy and immune-related pathways in most cancers, such as EMT, P53, apoptosis, cell cycle, WNT, IL-6-JAK-STAT3, IL2-STAT5 and TGF-β signaling pathways.

Genetic and epigenetic changes play key roles in immune tolerance and cancer development (46). In our study, the abnormal hypermethylation of *TMEM59L* was associated with decreased mRNA levels and better clinical outcomes for several cancers, such as KIRP, KIRC, and COAD, suggesting that hypermethylation of *TMEM59L* gene may be key regulatory mechanism for *TMEM59L* expression in these cancers. Interestingly, in line with our previous findings, high *TMEM59L* expression were associated with poor prognosis in COAD, KIRC, and KIRP. Thus, we speculated that the epigenetic changes of *TMEM59L* gene may promote the occurrence of KIRC, KIRP, and COAD in some cases.

Tumor immunotherapy has made remarkable achievements in cancer treatment (67). Immune checkpoint blockade therapy has significantly prolonged the survival in many cancers typically associated with poor prognosis, such as melanoma and non-small cell lung cancer (68). However, immunotherapy is still only available for a subset of patients, and immunotherapy response rates vary widely across cancer types (69, 70). Our study found that in addition to regulating pathways involved in cancer progression, *TMEM59L* was also involved in immune regulatory pathways such as IL6-JAK-STAT3, IL2-STAT5, and TGF-β signaling. Correlation analysis showed that *TMEM59L* expression negatively correlated with activated CD4 T cells and CD8 T cells in most cancer types, and further IPS analysis also replicated the same trend; *TMEM59L*

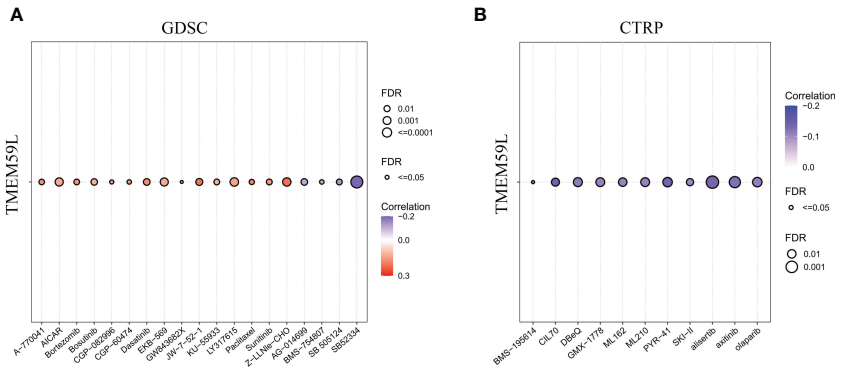

FIGURE 9
Drug sensitivity analysis. **(A)** The correlation between TMEM59L expression and the sensitivity of GDSC drugs in pan-cancer. **(B)** The correlation between TMEM59L expression and the sensitivity of CTRP drugs in pan-cancer. Blue bubbles represent negative correlations, red bubbles represent positive correlations, the deeper of color, the higher of the correlation. Bubble size is positively correlate with the FDR significance. Black outline border indicates FDR ≤ 0.05.

expression was negatively related to IPS score, AZ, and ECs, while being positively associated with SCs, indicating that TMEM59L could play a key role in the immunosuppressive microenvironment. At the same time, the close association of TMEM59L with most immunomodulators and immune checkpoints also implied that TMEM59L could predict the clinical response of patients to immune checkpoint blockade, and this was validated in the IMvigor210 cohort, as high expression of *TMEM59L* correlated with a worse clinical response to PD-L1 therapy. Taken together, all of the results presented above suggested that *TMEM59L* may exist in an 'immune-excluded' TME, consistent with higher stromal scores and activation of TGF-β signaling pathways. Despite the currently unclear role of *TMEM59L* in T cell suppression, our study indicated that *TMEM59L* could represent a potential novel immune target, and the application of anti-*TMEM59L* antibodies after other therapeutic interventions may be an effective therapeutic strategy.

The study bears few limitations. First, the bioinformatic analysis needs to be corroborated by experimental validation *via* immunostaining of the normal and tumor tissues. Then, mechanistic investigation is required to confirm the functional association between *TMEM59L* and cancer- and immune pathways, as well as the epigenetic regulation of *TMEM59L* expression in specific cancers.

In conclusion, by combining a multi-omics approach, we comprehensively explored *TMEM59L* gene expression signature, its prognostic value, as well as its association with immune cell infiltration and cancer-associated pathways in various cancer types. Our findings revealed that *TMEM59L* expression was correlated with poor prognosis across multiple tumor types, especially in COAD, KIRP, and KIRC. Moreover, our study also indicated that *TMEM59L* may represent a potential novel immune target and could play an immune-regulatory role in tumors. This study underscores the importance of *TMEM59L* as a prognostic biomarker and a treatment target and identified an area to be explored further in the future.

Data availability statement

The datasets presented in this study can be found in online repositories. The names of the repository/repositories and accession number(s) can be found in the article/Supplementary Material.

Author contributions

Conceptualization, CS, and LS; Data curation, analysis and validation, CS, LS, LZ, DC and HW, WQ, PZ, HG; Writing—original draft, CS, and LS; Writing—review and editing, CS, and LS. All authors contributed to the article and approved the submitted version.

Conflict of interest

The authors declare that the research was conducted in the absence of any commercial or financial relationships that could be construed as a potential conflict of interest.

Publisher's note

Supplementary material

The Supplementary Material for this article can be found online at: https://www.frontiersin.org/articles/10.3389/fimmu.2022.1054157/full#supplementary-material

FIGURE S1
The expression of TMEM59L in normal and cancer tissues based on the HPA database. (A) The expression of TMEM59L in healthy tissues. (B) The expression of TMEM59L in human cancer tissues. (C) The representative IHC images of TMEM59L in colorectal and renal cancer based on HPA database .(Scale bar: 100 μm).

FIGURE S2
The differences of EMT pathway activity between high and low TMEM59L mRNA expression in different types of cancer. (A) BRCA, (B) BLCA, (C) COAD, (D) ESCA, (E) READ, (F) OV, (G) TGCT, (H) THCA, (I) STAD.

FIGURE S3
The single-cell RNA sequencing analysis exhibits the expression pattern as well as the signal pathway of TMEM59L. (A, B) The UMAP projection of all clusters and cell subpopulations. (C, D) TMEM59L expression from BRCA-GSE148673; (E) GSEA showed the the activity of the hallmark EMT pathways in different cells based on TISCH database; (F) GSEA showed the enriched upregulated hallmark pathways in different cells based on TISCH database.

FIGURE S4
Correlations between TMEM59L and enrichment scores of cancer-associated pathways. (A) Correlations between TMEM59L and the enrichment scores of cancer-associated pathways. (B) Correlations between TMEM59L and the steps of the cancer immunity cycle. Solid lines represent a positive correlation, dashed lines represents a negative correlation, and the the colors represent significant P-values.

FIGURE S5
The methylation difference between tumor and normal samples of TMEM59L in different human cancers. (A) BLCA, (B) KIRC, (C) KIRP, (D) UCEC, (E) LUSC, (F) LUAD, (G) THCA.

FIGURE S6
The correlation between methylation and mRNA expression of TMEM59L in different human cancers. (A) BLCA, (B) BRCA, (C) COAD, (D) HNSC, (E) LUAD, (F) PAAD, (G) THCA, (H) UCEC.

References

1. Sung H, Ferlay J, Siegel RL, Laversanne M, Soerjomataram I, Jemal A, et al. Global cancer statistics 2020: GLOBOCAN estimates of incidence and mortality worldwide for 36 cancers in 185 countries. *CA: A Cancer J Clin* (2021) 71:209–49. doi: 10.3322/caac.21660

2. Cao W, Chen H, Yu Y, Li N, Chen W. Changing profiles of cancer burden worldwide and in China: a secondary analysis of the global cancer statistics 2020. *Chin Med J (Engl)* (2021) 134:783–91. doi: 10.1097/CM9.0000000000001474

3. Bray F, Laversanne M, Weiderpass E, Soerjomataram I. The ever-increasing importance of cancer as a leading cause of premature death worldwide. *Cancer* (2021) 127:3029–30. doi: 10.1002/cncr.33587

4. Malvezzi M, Carioli G, Bertuccio P, Negri E, La Vecchia C. Relation between mortality trends of cardiovascular diseases and selected cancers in the European union, in 1970–2017. focus on cohort and period effects. *Eur J Cancer* (2018) 103:341–55. doi: 10.1016/j.ejca.2018.06.018

5. Tahmasebi Birgani M, Carloni V. Data from: Tumor microenvironment, a paradigm in hepatocellular carcinoma progression and therapy. *Int J Mol Sci* (2017) 18(2):405. doi: 10.3390/ijms18020405

6. Zhang H, Grizzle WE. Exosomes: A novel pathway of local and distant intercellular communication that facilitates the growth and metastasis of neoplastic lesions. *Am J Pathol* (2014) 184:28–41. doi: 10.1016/j.ajpath.2013.09.027

7. Quail DF, Joyce JA. Microenvironmental regulation of tumor progression and metastasis. *Nat Med* (2013) 19:1423–37. doi: 10.1038/nm.3394

8. Catalano V, Turdo A, Di Franco S, Dieli F, Todaro M, Stassi G. Tumor and its microenvironment: A synergistic interplay. *Semin Cancer Biol* (2013) 23:522–32. doi: 10.1016/j.semcancer.2013.08.007

9. Roma-Rodrigues C, Mendes R, Baptista PV, Fernandes AR. Data from: Targeting tumor microenvironment for cancer therapy. *Int J Mol Sci* (2019) 20 (4):840. doi: 10.3390/ijms20040840

10. Hanahan D, Coussens LM. Accessories to the crime: Functions of cells recruited to the tumor microenvironment. *Cancer Cell* (2012) 21:309–22. doi: 10.1016/j.ccr.2012.02.022

11. Hanahan D, Weinberg RA. Hallmarks of cancer: The next generation. *Cell* (2011) 144:646–74. doi: 10.1016/j.cell.2011.02.013

12. Lyssiotis CA, Kimmelman AC. Metabolic interactions in the tumor microenvironment. *Trends Cell Biol* (2017) 27:863–75. doi: 10.1016/j.tcb.2017.06.003

13. Govaert KM, Emmink BL, Nijkamp MW, Cheung ZJ, Steller EJA, Fatrai S, et al. Hypoxia after liver surgery imposes an aggressive cancer stem cell phenotype on residual tumor cells. *Ann Surg* (2014) 259(4):750–9. doi: 10.1097/SLA.0b013e318295c160

14. Stanta G, Bonin S. Overview on clinical relevance of intra-tumor heterogeneity. *Front Med (Lausanne)* (2018) 5:85. doi: 10.3389/fmed.2018.00085

15. Wang M, Zhao J, Zhang L, Wei F, Lian Y, Wu Y, et al. Role of tumor microenvironment in tumorigenesis. *J Cancer* (2017) 8:761–73. doi: 10.7150/jca.17648

16. Assaraf YG, Brozovic A, Gonçalves AC, Jurkovicova D, Linē A, Machuqueiro M, et al. The multi-factorial nature of clinical multidrug resistance in cancer. *Drug Resist Update* (2019) 46:100645. doi: 10.1016/j.drup.2019.100645

17. Leonetti A, Wever B, Mazzaschi G, Assaraf YG, Rolfo C, Quaini F, et al. Molecular basis and rationale for combining immune checkpoint inhibitors with chemotherapy in non-small cell lung cancer. *Drug Resist Update* (2019) 46:100644. doi: 10.1016/j.drup.2019.100644

18. Chen Y, Tan W, Wang C. Tumor-associated macrophage-derived cytokines enhance cancer stem-like characteristics through epithelial-mesenchymal transition. *Onco Targets Ther* (2018) 11:3817–26. doi: 10.2147/OTT.S168317

19. Colak S, Medema JP. Cancer stem cells – important players in tumor therapy resistance. *FEBS J* (2014) 281:4779–91. doi: 10.1111/febs.13023

20. Rycaj K, Tang DG. Cancer stem cells and radioresistance. *Int J Radiat Biol* (2014) 90:615–21. doi: 10.3109/09553002.2014.892227

21. Eppert K, Takenaka K, Lechman ER, Waldron L, Nilsson B, van Galen P, et al. Stem cell gene expression programs influence clinical outcome in human leukemia. *Nat Med* (2011) 17:1086–93. doi: 10.1038/nm.2415

22. Kim J, Joo H, Moon H, Lee Y. A case of amblyomma testudinarium tick bite in a Korean woman. *Korean J Parasitol* (2010) 48:313–17. doi: 10.3347/kjp.2010.48.4.313

23. Ben-Porath I, Thomson MW, Carey VJ, Ge R, Bell GW, Regev A, et al. An embryonic stem cell–like gene expression signature in poorly differentiated aggressive human tumors. *Nat Genet* (2008) 40:499–507. doi: 10.1038/ng.127

24. Kang G, Chen K, Yang F, Chuai S, Zhao H, Zhang K, et al. Monitoring of circulating tumor DNA and its aberrant methylation in the surveillance of surgical lung cancer patients: protocol for a prospective observational study. *BMC Cancer* (2019) 19:579. doi: 10.1186/s12885-019-5751-9

25. Sina AAI, Carrascosa LG, Liang Z, Grewal YS, Wardiana A, Shiddiky MJA, et al. Epigenetically reprogrammed methylation landscape drives the DNA self-assembly and serves as a universal cancer biomarker. *Nat Commun* (2018) 9:4915. doi: 10.1038/s41467-018-07214-w

26. Micevic G, Theodosakis N, Bosenberg M. Aberrant DNA methylation in melanoma: biomarker and therapeutic opportunities. *Clin Epigenet* (2017) 9:34. doi: 10.1186/s13148-017-0332-8

27. Nakaoka T, Saito Y, Saito H. Data from: Aberrant DNA methylation as a biomarker and a therapeutic target of cholangiocarcinoma. *Int J Mol Sci* (2017) 18 (6):1111. doi: 10.3390/ijms18061111

28. Elson GCA, de Coignac AB, Aubry J, Delneste Y, Magistrelli G, Holzwarth J, et al. BSMAP, a novel protein expressed specifically in the brain whose gene is localized on chromosome 19p12. *Biochem Biophys Res Commun* (1999) 264:55–62. doi: 10.1006/bbrc.1999.1481

29. Mannherz O, Mertens D, Hahn M, Lichter P. Functional screening for proapoptotic genes by reverse transfection cell array technology. *Genomics* (2006) 87:665–72. doi: 10.1016/j.ygeno.2005.12.009

30. Ullrich S, Münch A, Neumann S, Kremmer E, Tatzelt J, Lichtenthaler SF. The novel membrane protein TMEM59 modulates complex glycosylation, cell surface expression, and secretion of the amyloid precursor protein. *J Biol Chem* (2010) 285:20664–74. doi: 10.1074/jbc.M109.055608

31. Zheng Q, Zheng X, Zhang L, Luo H, Qian L, Fu X, et al. The neuron-specific protein TMEM59L mediates oxidative stress-induced cell death. *Mol Neurobiol* (2017) 54:4189–200. doi: 10.1007/s12035-016-9997-9

32. Boada-Romero E, Letek M, Fleischer A, Pallauf K, Ramón-Barros C, Pimentel-Muiños FX. TMEM59 defines a novel ATG16L1-binding motif that promotes local activation of LC3. *EMBO J* (2013) 32:566–82. doi: 10.1038/emboj.2013.8

33. Bakulski KM, Dolinoy DC, Sartor MA, Paulson HL, Konen JR, Lieberman AP, et al. Genome-wide DNA methylation differences between late-onset alzheimer's disease and cognitively normal controls in human frontal cortex. *J Alzheimer's Dis* (2012) 29:571–88. doi: 10.3233/JAD-2012-111223

34. Hänzelmann S, Castelo R, Guinney J. GSVA: gene set variation analysis for microarray and RNA-seq data. *BMC Bioinf* (2013) 14:7. doi: 10.1186/1471-2105-14-7

35. Newman AM, Liu CL, Green MR, Gentles AJ, Feng W, Xu Y, et al. Robust enumeration of cell subsets from tissue expression profiles. *Nat Methods* (2015) 12:453–57. doi: 10.1038/nmeth.3337

36. Yoshihara K, Shahmoradgoli M, Martínez E, Vegesna R, Kim H, Torres-Garcia W, et al. Inferring tumour purity and stromal and immune cell admixture from expression data. *Nat Commun* (2013) 4:2612. doi: 10.1038/ncomms3612

37. Charoentong P, Finotello F, Angelova M, Mayer C, Efremova M, Rieder D, et al. Pan-cancer immunogenomic analyses reveal genotype-immunophenotype relationships and predictors of response to checkpoint blockade. *Cell Rep* (2017) 18:248–62. doi: 10.1016/j.celrep.2016.12.019

38. Yang W, Soares J, Greninger P, Edelman EJ, Lightfoot H, Forbes S, et al. Genomics of drug sensitivity in cancer (GDSC): a resource for therapeutic biomarker discovery in cancer cells. *Nucleic Acids Res* (2013) 41:D955–61. doi: 10.1093/nar/gks1111

39. Basu A, Bodycombe NE, Cheah JH, Price EV, Liu K, Schaefer GI, et al. An interactive resource to identify cancer genetic and lineage dependencies targeted by small molecules. *Cell* (2013) 154:1151–61. doi: 10.1016/j.cell.2013.08.003

40. Niu Z, Shi Q, Zhang W, Shu Y, Yang N, Chen B, et al. Caspase-1 cleaves PPAR纬 for potentiating the pro-tumor action of TAMs. *Nat Commun* (2017) 8:766. doi: 10.1038/s41467-017-00523-6

41. Fiaschi T, Marini A, Giannoni E, Taddei ML, Gandellini P, De Donatis A, et al. Reciprocal metabolic reprogramming through lactate shuttle coordinately influences tumor-stroma interplay. *Cancer Res* (2012) 72:5130–40. doi: 10.1158/0008-5472.CAN-12-1949

42. Giannoni E, Bianchini F, Masieri L, Serni S, Torre E, Calorini L, et al. Reciprocal activation of prostate cancer cells and cancer-associated fibroblasts stimulates epithelial-mesenchymal transition and cancer stemness. *Cancer Res* (2010) 70:6945–56. doi: 10.1158/0008-5472.CAN-10-0785

43. Hu J, Yu A, Othmane B, Qiu D, Li H, Li C, et al. Siglec15 shapes a non-inflamed tumor microenvironment and predicts the molecular subtype in bladder cancer. *Theranostics* (2021) 11:3089–108. doi: 10.7150/thno.53649

44. Chen DS, Mellman I. Oncology meets immunology: the cancer-immunity cycle. *Immunity* (2013) 39:1–10. doi: 10.1016/j.immuni.2013.07.012

45. Xu L, Deng C, Pang B, Zhang X, Liu W, Liao G, et al. TIP: A web server for resolving tumor immunophenotype profiling. *Cancer Res* (2018) 78:6575–80. doi: 10.1158/0008-5472.CAN-18-0689

46. Li B, Zhang B, Wang X, Zeng Z, Huang Z, Zhang L, et al. Expression signature, prognosis value, and immune characteristics of siglec-15 identified by pan-cancer analysis. *Oncoimmunology* (2020) 9:1807291. doi: 10.1080/2162402X.2020.1807291

47. Shibue T, Weinberg RA. EMT, CSCs, and drug resistance: the mechanistic link and clinical implications. *Nat Rev Clin Oncol* (2017) 14:611–29. doi: 10.1038/nrclinonc.2017.44

48. Seguin L, Desgrosellier JS, Weis SM, Cheresh DA. Integrins and cancer: regulators of cancer stemness, metastasis, and drug resistance. *Trends Cell Biol* (2015) 25:234–40. doi: 10.1016/j.tcb.2014.12.006

49. Zhang C, Chen T, Li Z, Liu A, Xu Y, Gao Y, et al. Depiction of tumor stemlike features and underlying relationships with hazard immune infiltrations based on large prostate cancer cohorts. *Brief Bioinform* (2021) 22:a211. doi: 10.1093/bib/bbaa211

50. Malta TM, Sokolov A, Gentles AJ, Burzykowski T, Poisson L, Weinstein JN, et al. Machine learning identifies stemness features associated with oncogenic dedifferentiation. *Cell* (2018) 173:338–54. doi: 10.1016/j.cell.2018.03.034

51. Friedmann-Morvinski D, Verma IM. Dedifferentiation and reprogramming: origins of cancer stem cells. *EMBO Rep* (2014) 15:244–53. doi: 10.1002/embr.201338254

52. Valieris R, Amaro L, Osório C, Bueno AP, Rosales MR, Carraro DM, et al. Deep learning predicts underlying features on pathology images with therapeutic relevance for breast and gastric cancer. *Cancers (Basel)* (2020) 12:3687. doi: 10.3390/cancers12123687

53. Moynahan ME, Jasin M. Mitotic homologous recombination maintains genomic stability and suppresses tumorigenesis. *Nat Rev Mol Cell Biol* (2010) 11:196–207. doi: 10.1038/nrm2851

54. Konstantinopoulos PA, Waggoner S, Vidal GA, Mita M, Moroney JW, Holloway R, et al. Single-arm phases 1 and 2 trial of niraparib in combination with pembrolizumab in patients with recurrent platinum-resistant ovarian carcinoma. *JAMA Oncol* (2019) 5:1141–49. doi: 10.1001/jamaoncol.2019.1048

55. Hoppe MM, Sundar R, Tan DSP, Jeyasekharan AD. Biomarkers for homologous recombination deficiency in cancer. *JNCI: J Natl Cancer Institute* (2018) 110:704–13. doi: 10.1093/jnci/djy085

56. Heeke AL, Baker T, Lynce F, Pishvaian MJ, Isaacs C. Prevalence of homologous recombination deficiency among all tumor types. *J Clin Oncol* (2017) 35:1502. doi: 10.1200/JCO.2017.35.15_suppl.1502

57. Sharma P, Barlow WE, Godwin AK, Pathak H, Isakova K, Williams D, et al. Impact of homologous recombination deficiency biomarkers on outcomes in patients with triple-negative breast cancer treated with adjuvant doxorubicin and cyclophosphamide (SWOG S9313). *Ann Oncol* (2018) 29:654–60. doi: 10.1093/annonc/mdx821

58. McGranahan N, Furness AJ, Rosenthal R, Ramskov S, Lyngaa R, Saini SK, et al. Clonal neoantigens elicit T cell immunoreactivity and sensitivity to immune checkpoint blockade. *Science* (2016) 351:1463–69. doi: 10.1126/science.aaf1490

59. Van Allen EM, Miao D, Schilling B, Shukla SA, Blank C, Zimmer L, et al. Genomic correlates of response to CTLA-4 blockade in metastatic melanoma. *Science* (2015) 350:207–11. doi: 10.1126/science.aad0095

60. Rizvi NA, Hellmann MD, Snyder A, Kvistborg P, Makarov V, Havel JJ, et al. Cancer immunology. mutational landscape determines sensitivity to PD-1 blockade in non-small cell lung cancer. *Science* (2015) 348:124–28. doi: 10.1126/science.aaa1348

61. Yap TA, Gerlinger M, Futreal PA, Pusztai L, Swanton C. Intratumor heterogeneity: seeing the wood for the trees. *Sci Transl Med* (2012) 4:110p–27p. doi: 10.1126/scitranslmed.3003854

62. Yang C, Huang X, Li Y, Chen J, Lv Y, Dai S. Prognosis and personalized treatment prediction in TP53-mutant hepatocellular carcinoma: an in silico strategy towards precision oncology. *Brief Bioinform* (2021) 22:a164. doi: 10.1093/bib/bbaa164

63. Zhang S, Dai H, Li W, Wang R, Wu H, Shen M, et al. TMEM116 is required for lung cancer cell motility and metastasis through PDK1 signaling pathway. *Cell Death Dis* (2021) 12:1086. doi: 10.1038/s41419-021-04369-1

64. Schmit K, Michiels C. TMEM proteins in cancer: A review. *Front Pharmacol* (2018) 9:1345. doi: 10.3389/fphar.2018.01345

65. Li B, Huang MZ, Wang XQ, Tao BB, Zhong J, Wang XH, et al. Erratum: TMEM140 is associated with the prognosis of glioma by promoting cell viability and invasion. *J Hematol Oncol* (2015) 8:101. doi: 10.1186/s13045-015-0199-0

66. Marx S, Dal Maso T, Chen J, Bury M, Wouters J, Michiels C, et al. Transmembrane (TMEM) protein family members: Poorly characterized even if essential for the metastatic process. *Semin Cancer Biol* (2020) 60:96–106. doi: 10.1016/j.semcancer.2019.08.018

67. Salmon H, Remark R, Gnjatic S, Merad M. Host tissue determinants of tumour immunity. *Nat Rev Cancer* (2019) 19:215–27. doi: 10.1038/s41568-019-0125-9

68. Cogdill AP, Andrews MC, Wargo JA. Hallmarks of response to immune checkpoint blockade. *Br J Cancer* (2017) 117:1–07. doi: 10.1038/bjc.2017.136

69. Pan C, Liu H, Robins E, Song W, Liu D, Li Z, et al. Next-generation immuno-oncology agents: current momentum shifts in cancer immunotherapy. *J Hematol Oncol* (2020) 13:29. doi: 10.1186/s13045-020-00862-w

70. Hamid O, Robert C, Daud A, Hodi FS, Hwu WJ, Kefford R, et al. Five-year survival outcomes for patients with advanced melanoma treated with pembrolizumab in KEYNOTE-001. *Ann Oncol* (2019) 30:582–88. doi: 10.1093/annonc/mdz011

frontiers | Frontiers in Immunology

TYPE Original Research
PUBLISHED 17 January 2023
DOI 10.3389/fimmu.2023.1084843

OPEN ACCESS

EDITED BY
Junjiang Fu,
Southwest Medical University, China

REVIEWED BY
Khalil Saleh,
Gustave Roussy Cancer Campus, France
Maria Serena Longhi,
Beth Israel Deaconess Medical Center and Harvard Medical School, United States

*CORRESPONDENCE
Xiaobo Yang
yangxiaobo67@pumch.cn
Haitao Zhao
zhaoht@pumch.cn

†These authors have contributed equally to this work

SPECIALTY SECTION
This article was submitted to Cancer Immunity and Immunotherapy, a section of the journal Frontiers in Immunology

RECEIVED 31 October 2022
ACCEPTED 02 January 2023
PUBLISHED 17 January 2023

CITATION
Wang Y, Zhang N, Xue J, Zhu C, Wang Y, Zhang L, Yang X, Wang H, Wang S, Chao J, Yang X and Zhao H (2023) Safety and feasibility of toripalimab plus lenvatinib with or without radiotherapy in advanced BTC. *Front. Immunol.* 14:1084843. doi: 10.3389/fimmu.2023.1084843

Safety and feasibility of toripalimab plus lenvatinib with or without radiotherapy in advanced BTC

Yunchao Wang†, Nan Zhang†, Jingnan Xue†, Chengpei Zhu†, Yanyu Wang, Longhao Zhang, Xu Yang, Hao Wang, Shanshan Wang, Jiashuo Chao, Xiaobo Yang* and Haitao Zhao*

Department of Liver Surgery, Peking Union Medical College Hospital, Chinese Academy of Medical Sciences and Peking Union Medical College (CAMS & PUMC), Beijing, China

Background: Toripalimab shows antitumor efficacy in cholangiocarcinoma. Radiotherapy (RT) may enhance systemic responses of PD-1 inhibitors and lenvatinib. This study was designed to assess the safety and feasibility of toripalimab plus lenvatinib with or without RT in advanced BTC.

Methods: This study involved 88 patients with advanced BTC receiving toripalimab plus lenvatinib with or without RT from the clinical trials (NCT03892577). Propensity score matching (PSM) (1:1) analysis was used to balance potential bias. The overall survival (OS), progression-free survival (PFS), objective response rate (ORR), and adverse events (AEs) were evaluated.

Results: After PSM, the final analysis included 40 patients: 20 receiving toripalimab plus lenvatinib without RT (NRT); 20 receiving toripalimab plus lenvatinib with RT. The AEs were more frequent in the RT group than in the NRT group without treatment-associated mortality. The addition of RT did not cause specific AEs. The median PFS was significantly longer with RT (10.8 versus 4.6 months, p<0.001). The median OS was 13.7 months with RT versus 9.2 months in the NRT group (p=0.008). The ORR was 35% (95% CI: 12.1-57.9) in the RT group versus 20% (95% CI: 0.8-39.2) in the NRT group.

Conclusions: The addition of RT may enhance the efficacy of toripalimab plus lenvatinib. Toripalimab plus lenvatinib with RT have a good safety profile without an increase in specific toxicities in advanced BTC patients.

KEYWORDS

advanced biliary tract cancer, PD-1 inhibitor, lenvatinib, radiotherapy, synergic effect

Abbreviations: PD-1, programmed cell death protein 1; PD-L1, programmed cell death ligand 1; BTCs, biliary tract cancers; ECC, extrahepatic cholangiocarcinoma; ICC, intrahepatic cholangiocarcinoma; GBC, gallbladder cancer; Lenvatinib, tyrosine kinase inhibitors; OS, overall survival; PFS, progression-free survival; ORR, objective response rate; DCR, disease control rate; SD, stable disease; PD, progressive disease; CR, complete response; PR, partial response; HR, hazard rate; RECIST, response evaluation criteria in solid tumors; AEs, adverse events; CTCAE, Common Terminology Criteria Coastocellular Group; RT, radiotherapy.

Introduction

Biliary tract carcinoma (BTC), including intrahepatic cholangiocarcinoma (ICC), extrahepatic cholangiocarcinoma (ECC), and gallbladder cancer (GBC), are aggressive malignancies (1). Most patients are diagnosed at an advanced stage with a poor prognosis (2, 3). Chemotherapy has been the mainstay of treatment for patients with advanced BTC (2, 4). However, conventional chemotherapy is often accompanied by side effects and the limited survival benefit, necessitating an evaluation of alternative drug combinations (5).

PD-1/PD-L1 inhibitors have exhibited encouraging therapeutic effects. However, the response rates of either PD-1/PD-L1 inhibitors alone or PD-1/PD-L1 inhibitors with targeted therapies remain less than ideal in BTC (6, 7). Continuous exploration has been made to improve the response of PD-1/PD-L1 inhibitors, including PD-1/PD-L1 inhibitors combined with chemotherapy (8) or locoregional treatment approaches (9–11). The phase III TOPAZ-1 study showed that the combination of durvalumab plus gemcitabine and cisplatin significantly improved the survival of patients with advanced BTC (12). Recently, durvalumab plus gemcitabine and cisplatin proved as first-line treatment by FDA and NCCN guidelines. New data have emerged that radiotherapy work in synergy with immunotherapies to increase patient response (13, 14). A study showed that adding RT into the combination of PD-1/PD-L1 inhibitors and targeted therapy was feasible and could improve treatment outcomes (15). However, combination of immunotherapy plus radiotherapy may lead to more AEs. Data on immunomodulatory effects of RT in BTC remains limited.

Toripalimab, a humanized programmed death-1 (PD-1) antibody, has shown a manageable safety profile and has promising antitumor activity in patients with advanced gastric cancer and metastatic mucosal melanoma (16, 17). Toripalimab shows antitumor efficacy in cholangiocarcinoma (18).

Considering the different anti-malignancy mechanisms of lenvatinib, toripalimab, and RT, combining these three modalities may show a potential synergic effect and promising preliminary efficacy results in advanced BTC. In this study, we assessed the safety and feasibility of RT plus toripalimab and lenvatinib in patients with advanced BTC.

Materials and methods

Patient characteristics and matched cohorts

This retrospective study assessed the safety and feasibility of non-first-line toripalimab plus lenvatinib with RT in advanced BTC. Advanced BTC was defined as initially diagnosed unresectable BTC (histologically confirmed ECC, ICC, or GBC by biopsy or surgical specimen). Other eligibility criteria included a good physical status with an Eastern Co-operative Oncology Group (ECOG) performance status score of 0–1, Child-Pugh A or B liver function status, at least one measurable or evaluable tumor lesion according to the Response Evaluation Criteria in Solid Tumors version 1.1 (RECIST 1.1). The study protocol was compliant with the Declaration of Helsinki and was approved by the Institutional Review Board and Ethics Committee at Peking Union Medical College Hospital.

A total of 113 patients were initially enrolled. Twenty-five patients have excluded: 2 patients received other target therapy; 14 patients received other PD-1/L1 inhibitors; 9 patients had no measurable lesion. Finally, 37 patients who received toripalimab plus lenvatinib with RT and 51 patients who received toripalimab plus lenvatinib without RT remained. Consecutive PSM was conducted by 1:1 matching with a caliper of 0.05 to balance potential bias. Finally, 40 patients with advanced BTC who received toripalimab plus lenvatinib with RT (RT group) or without RT (NRT group) were included for statistical analysis as a matched cohort (Figure 1).

Treatment

In the NRT group, lenvatinib was administered at a dosage of 12 mg (for patients with a body weight≥60 kg) or 8 mg (for patients with a body weight <60 kg) orally once a day. The PD-1 dose included a fixed dosage of 200 mg (240 mg for toripalimab) every three weeks or 3 mg/kg every three weeks.

In the RT group, patients received intensity-modulated radiation therapy (IMRT) plus lenvatinib and toripalimab. Lenvatinib plus toripalimab was not discontinued before or after each RT session. The radiation dose was prescribed to the isocenter or 95% planning target volume as 24.0–60.0 Gy in 6-25 fractions, a single dose between 1.8 and 6.0 Gy for tumor sites at the physician's discretion, no more than five times a week. RT was given during PD-1 inhibitors no later than six weeks (19).

Assessments

The overall response was assessed using enhanced computed tomography (CT) or magnetic resonance imaging (MRI) according to RECIST 1.1 after the patient's treatment. Professional radiologists evaluated the imaging examinations.

The therapeutic efficacy assessment included the objective response rate (ORR) [the percentage of patients with a confirmed complete/partial response (CR/PR)], progression-free survival (PFS) (the time from receiving toripalimab to disease progression at any site or death), the overall survival (OS) (the time from receiving toripalimab to the date of death), the disease control rate (DCR) (the proportion of patients who achieved an objective response or SD), and the safety. The adverse events (AEs) were collected and graded according to the National Cancer Institute Common Terminology Criteria for Adverse Events, version 4.0 (CTCAE 4.0).

Statistical analysis

The Data cut-off was June 1, 2022. We performed propensity score matching (PSM) in a 1:1 fashion to further reduce selection bias. We used a caliper (i.e., the maximum distance that two cases can be apart from each other based on their estimated propensity scores) of 0.05 to prevent matches with very dissimilar estimated propensity

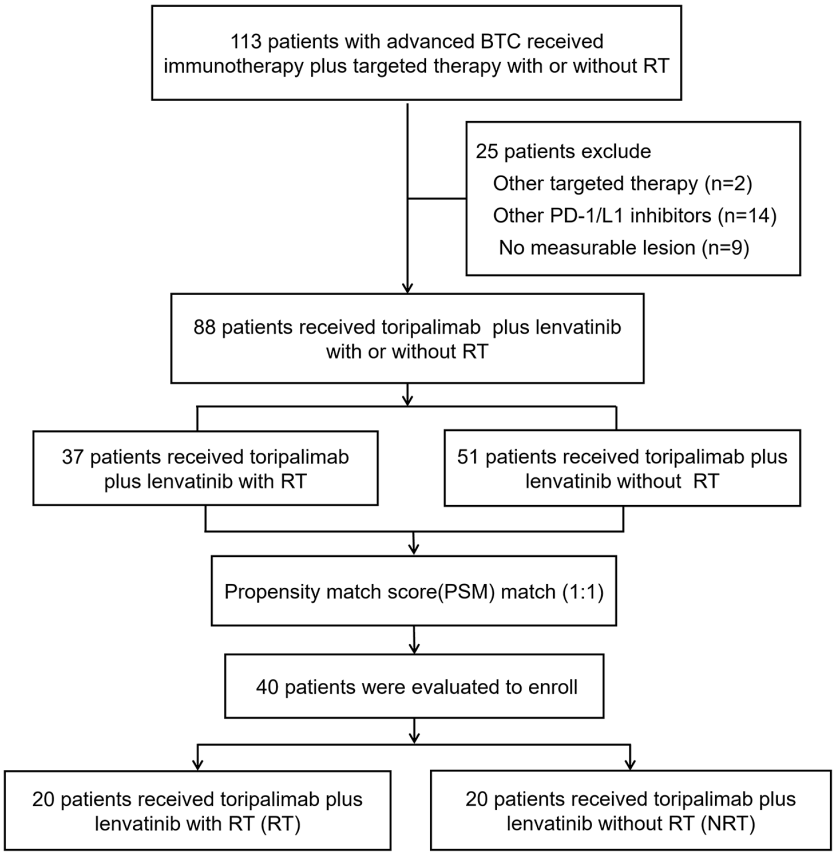

FIGURE 1
Study workflow.

scores. Variables used for PSM include age, sex, ECOG, subtype, and tumor stage. The Kaplan–Meier and bilateral log-rank tests were used to generate PFS and OS curves. The two treatment groups' baseline characteristics, efficacy, and AEs were compared using the chi-square test or Fisher's exact test. The hazard ratios of each clinicopathological feature for the OS were estimated by Cox proportional hazard modeling. All statistical analyses were undertaken using SPSS 22 (vision 22.0, SPSS, Inc., Chicago, IL) and R (version 4.0.3).

Results

The patient demographics and baseline characteristics

From March 19, 2019, to June 1, 2022, 40 patients with advanced BTC were included in this study: 20 in the NRT group and 20 in the RT group. The median duration of follow-up was 21.3 months. The demographics and baseline characteristics of the two groups are summarized in Table 1.

The two groups were well-balanced regarding demographics and characteristics. The median age of the patients was 61.5 years. Cholangiocarcinoma, including ICC and ECC, is the primary tumor type (75%). Most patients had a better ECOG performance status. The two groups did not differ significantly concerning differentiated histology, previous antitumor therapy, TNM stage, tumor diameter, or sites of metastases. The pathological differentiation types of 18 patients were unknown due to a lack of further pathological tissue analyses. The liver and lymph nodes were the common metastatic sites, and other metastatic lesions included uterine metastasis (one patient) and adrenal metastases (one patient).

The radiotherapy sites were mainly distributed in the liver (70%) and soft tissue or lymph nodes (60%). The median radiation dose delivered was 45 Gy (range 24 to 60 Gy) in 6–25 fractions with IMRT. 13 (65%) patients received one course, and 7 (35%) two courses.

Efficacy

At the time of analysis, 17 patients had disease progression, and 17 patients had died in the NRT group, while 12 patients had disease progression and 10 patients had died in the RT group. The median PFS was 10.8 months (95% CI: 6.2-15.4) in the RT group versus 4.6 months (95% CI: 3.3-5.8) in the NRT group (HR 0.21 [95% CI: 0.09-0.49], p<0.01, Figure 2A). Likewise, the median OS was significantly longer in the RT group (13.7 months, 95% CI: 7.8-19.6) than that in the NRT group (9.2 months, 95% CI: 6.5-11.8) (HR 0.36 [95% CI: 0.16-0.80]; p=0.008, Figure 2B).

No patient achieved a complete response (CR) in the two groups. In the RT group, 4 patients achieved a partial response (PR), 11 patients had SD, and 5 patients exhibited progressive disease (PD) (Table 2). The ORR was 20% (4/20; 95% CI: 0.8-39.2), and the DCR

10.3389/fimmu.2023.1084843

TABLE 1 Baseline characteristics.

Characteristics	Toripalimab plus lenvatinib with RT (n=20)	Toripalimab plus lenvatinib (n=20)	P-value
Age, years			1
≤ 65	13(65)	13(65)	
> 65	7(35)	7(35)	
Gender, n (%)			1
Male	10(50)	11(55)	
Female	10(50)	9(45)	
Tumor subtype, n (%)			0.76
Cholangiocarcinoma	14(70)	16(80)	
Gallbladder cancer	6(30)	4(20)	
ECOG performance status, n (%)			1
0	10	9	
1	10	11	
Differentiated histology, n (%)			0.08
Well	0	2(10)	
Moderately	1(5)	4(20)	
Poorly	6(30)	5(25)	
Moderately-poorly	4(20)	1(5)	
Well-moderately	0	1(5)	
Unsure	9(45)	7(35)	
Previous antitumor therapy, n (%)			
Radical surgery resection	7(35)	8(40)	1
Systemic chemotherapy	5(25)	6(30)	0.50
Targeted therapy	14(60)	14(70)	0.48
Site of metastases, n (%)			
Intrahepatic	17(85)	12(60)	0.08
Lymph nodes	18(90)	14(60)	0.12
Lung	2(10)	2(10)	1
Bone	4(20)	2(10)	0.69
Other (Uterus, adrenal glands, brain)	2(10)	1(5)	1
Radiotherapy dose (Gray)			
Median(range)	45(24-60)	–	–
Radiotherapy technique			
intensity-modulated radiation	20(100)	–	–
TNM stage, n(%)			0.33
III	10	14	
IV	10	6	
Tumor diameter, mean ± SD(cm)	4.7 ± 3.7	5.6 ± 3.7	0.90
Radiotherapy site			

(Continued)

TABLE 1 Continued

Characteristics	Toripalimab plus lenvatinib with RT (n=20)	Toripalimab plus lenvatinib (n=20)	P-value
Liver	14(70)	–	–
Bone	2(10)	–	–
Soft tissue or lymph nodes in the abdominal cavity	12(60)	–	–

was 75% (15/20; 95% CI: 54.2-95.8) in the NRT group. However, in the RT group, 7 patients achieved a partial response (PR), 10 patients had SD, and 3 patients exhibited progressive disease (PD), the ORR was 35% (7/20; 95% CI: 12.1-57.9), and the DCR was 85% (17/20; 95% CI: 67.9-102.1). The survival benefits in the RT group were observed. Among the two cohorts, the RT group showed a higher DCR than the NRT group but did not find a significant difference.

Univariate and multivariate analyses were performed to identify independent prognostic factors associated with OS. Potential predictors include age, sex, ECOG, method of treatment, and metastasis. Univariate and multivariate analyses found ECOG and treatment methods were associated with OS (Figure 3). Figure 4A shows a waterfall plot of the target lesions from baseline in the RT group: 13 of the 20 (65%) patients exhibited a decrease. In comparison, 7 of the 20 (35%) patients showed a decrease in the NRT group (Figure 4B). Three patients exhibited a decrease in tumor size from baseline after analysis of nine measurable non-target lesions in the RT group (Figure 4C).

In the RT group, one patient achieved a PR, who had been PD before radiotherapy; two patients had achieved PR, who had been SD before radiotherapy; five patients achieved SD, who was PD before radiotherapy.

Safety

All patients experienced ≥1 adverse event (AE), and no treatment-related deaths occurred in this study (Table 3). The adverse events were more frequent in the RT group than in the NRT group, especially hypothyroidism [8 (5.6%) versus 1, p = 0.008]. The most common AEs (any grade) in the RT group were fatigue (70%), ALT or AST elevation (60%), and bilirubin elevation (50%), while fatigue (65%), AST or ALT increased (50%) in NRT group. The RT group had a higher incidence of grade 3–4 AEs than the NRT group. The most frequent grade 3 AEs were rash, with an incidence of 20%. One patient experienced grade 4 severe AEs (SAEs) (gastrointestinal hemorrhage). All the recorded any-grade AEs were reversible.

Discussion

This is the first reported study that assessed the efficacy and safety of toripalimab plus lenvatinib with or without RT in advanced BTC patients and represents a potentially shifting approach to improve immunotherapy response. The combination of PD-1 inhibitor plus lenvatinib with RT was promising. Patients who received toripalimab plus lenvatinib with RT have significantly longer OS (13.7 versus 9.2 months, p=0.008) and PFS (10.8 versus 4.6 months, p<0.01) than patients who received toripalimab plus lenvatinib without RT. The risk of death was reduced by 64% in the RT group compared with the NRT group. Importantly, we found that toripalimab plus lenvatinib with RT were well tolerated.

In this study, patients accepting toripalimab plus lenvatinib with RT achieved approximately 35% ORR and 85% DCR, which were higher than the toripalimab plus lenvatinib regimen in our study and previous studies (7, 20, 21). The response rates of toripalimab with targeted therapies in BTC are not satisfactory. Previous studies showed that lenvatinib plus pembrolizumab has an ORR of 10% to 25% in advanced BTC (7, 20). Recently, a retrospective study of 74 patients who received PD-1 inhibitor plus lenvatinib revealed that the ORR was 20.27% (95% CI: 10.89%–29.65%), and the DCR was 71.62%

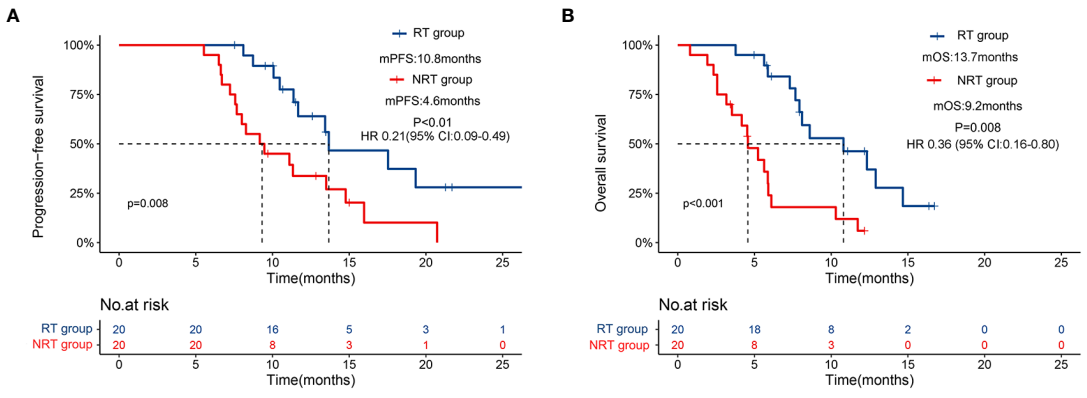

FIGURE 2
Kaplan–Meier curves for progression-free survival **(A)** and overall survival **(B)** for patients receiving PD-1 inhibitors plus lenvatinib with or without RT.

TABLE 2 Tumor response to treatment in each treatment group.

	Toripalimab plus lenvatinib with RT	Toripalimab plus lenvatinib	P	Effect size (95% CI)
	(n=20)	(n=20)		
Objective response rate (95% CI)	35(12.1-57.9)	20(0.8-39.2)	0.48	–
Complete response (n, %)	0	0	–	–
Partial response (n, %)	7	4	–	–
Stable disease (n, %)	10	11	–	–
Progressive disease (n, %)	3	5	–	–
DCR (n, %), 95% CI	85(67.9-102.1)	75(54.2-95.8)	0.70	–
Median progression-free survival, months (95% CI)	10.8(6.2-15.4)	4.6(3.8-5.3)	<0.01	HR:0.21(0.09-0.49)
Median overall survival, months (95% CI)	13.7(7.8-19.6)	9.2(6.5-11.8)	0.008	HR:0.36(0.16-0.80)

(21). A pool analysis showed that pembrolizumab plus RT significantly increased responses and outcomes in patients with metastatic non-small-cell lung cancer (22). A growing body of evidence suggests that the addition of RT to PD-1 inhibitor may improve the efficacy of immune checkpoint inhibitors (ICIs) (23, 24), where RT is administered before ICIs or concurrently with ICIs (25).

The addition of RT represented an encouraging response: one patient converted from PD to PR, two patients achieved PR from SD, and five from PD to SD. In addition, we observed that both target and non-target lesions in three patients were reduced, indicating that RT may have a synergistic effect with PD-1 inhibitors and lenvatinib. Evidence has revealed that radiation can exert potent immunomodulatory effects (26). Previous studies have demonstrated that radiation could induce immunogenic cell death (ICD), release tumor antigens and promote T-cell-mediated immune response against antigens derived from dying cells (23, 27–29).

The optimal radiotherapy dose, fractionation, timing, and target selection currently lack a consensus (30, 31). To choose the optimal radiation dose and fractionated dose, on the one hand, it is necessary to ensure that antitumor immunity is fully activated. On the other hand, the occurrence of adverse reactions should be minimized. Likewise, there is no clear framework for whether RT should be performed before or after PD-1/PD-L1 inhibitors (32). The sequence of radiotherapy and immunotherapy still needs further study and comparison.

Although the incorporation of RT into immunotherapy caused more AEs, they were generally manageable. The adverse events in the RT group were consistent with previous reports: fatigue was the most

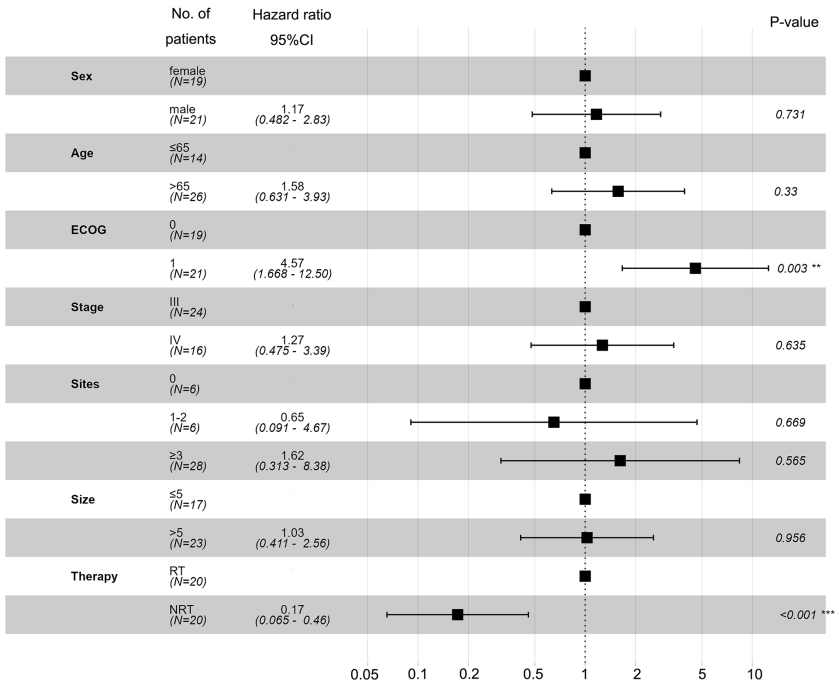

FIGURE 3
Univariate and multivariate analyses based on the Cox regression model were performed to identify independent prognostic factors associated with OS.

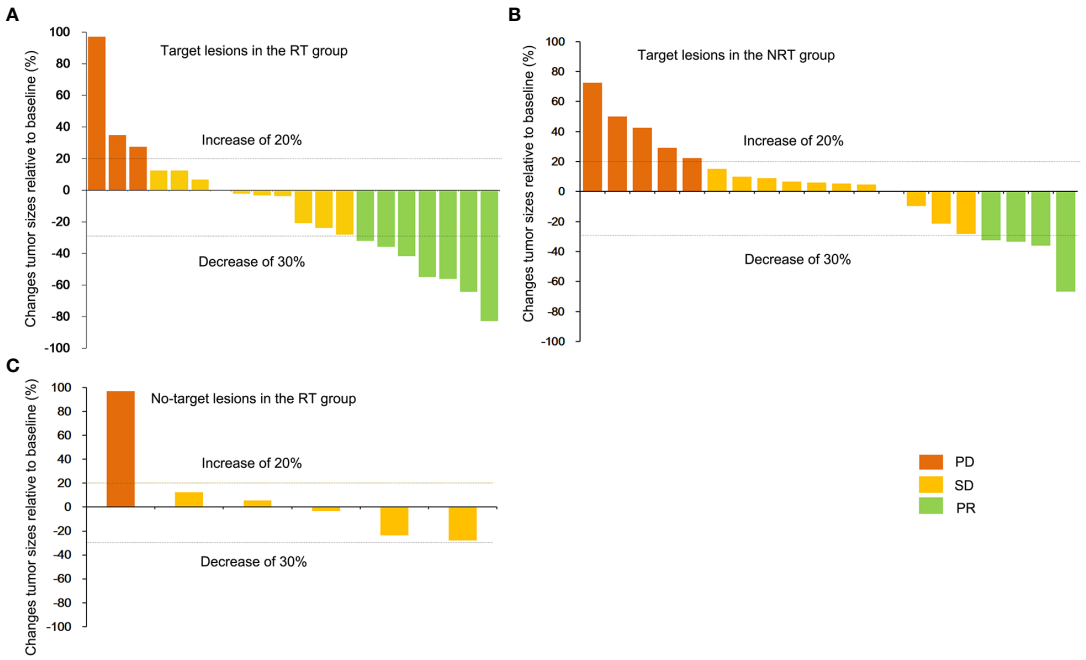

FIGURE 4
Best percentage change in the RT group. The best percentage change in the sum of the diameters of the target lesions from baseline **(A)** in the RT group and non-target lesions from baseline for nine patients in the RT group **(C)**. **(B)** shows the maximum percentage change in the sum of the diameters of the target lesions from baseline in the NRT group.

common all-grade adverse event (33). One patient experienced grade 4 severe AEs (SAEs) (gastrointestinal hemorrhage). Gastrointestinal hemorrhage was controlled after drug discontinuation and active management. No death-related adverse effects occurred. The combination of RT plus non-first-line toripalimab and lenvatinib could have a good safety profile.

We acknowledge that this study has some limitations. First, as a single-center retrospective study, the interpretation of the efficacy and safety of the combination of RT plus toripalimab and lenvatinib must be very cautious. Prospective studies are needed to validate the findings further. Second, some selection biases, including recall, observation, and selection biases, arose from the limited sample size and a retrospective study. A heterogeneous population of patients cannot be ruled out. Third, this study lacks evidence of synergy between radiation and immunotherapy, such as immune cell infiltration and transcriptional changes in tumor cells before and after radiotherapy. Although the study has certain limitations, these "real" data are still helpful for prospective follow-up studies.

TABLE 3 Safety summary.

	Toripalimab plus lenvatinib with RT (n=20)		Toripalimab plus lenvatinib (n=20)		P-value	
	Any grade	Grades 3-4	Any grade	Grades 3-4	Any grade	Grades 3-4
Fatigue	14(70)	1(5)	13(65)	1(5)	0.74	1
Nausea	8(40)	2(10)	6(30)	0	0.52	0.16
Vomiting	7(35)	2(10)	4(20)	0	0.30	0.16
Proteinuria	5(25)	0	6(30)	0	0.73	–
Stomatitis	4(20)	2(10)	1(5)	0	0.16	0.16
Arthralgia	3(15)	0	1(5)	0	0.31	–
Rash	10(50)	4(20)	5(25)	1(5)	0.11	0.16
Abdominal pain	9(45)	1(5)	8(40)	0	0.76	0.33
Diarrhea	4(20)	0	5(25)	0	0.71	–

(Continued)

TABLE 3 Continued

	Toripalimab plus lenvatinib with RT (n=20)		Toripalimab plus lenvatinib (n=20)		P-value	
	Any grade	Grades 3-4	Any grade	Grades 3-4	Any grade	Grades 3-4
Fever	2(10)	0	1(5)	0	0.56	–
Anorexia	4(20)	0	2(10)	0	0.39	–
Gastrointestinal hemorrhage	3(15)	2(10)	2(10)	1(5)	0.64	0.56
Epistaxis	3(15)	1(5)	1(5)	0	0.31	0.33
Hypertension	9(45)	2(10)	8(40)	1(5)	0.76	0.56
Headache	3(15)	0	1(5)	0	0.31	–
Myocarditis	0	0	1(5)	0	0.33	–
AST or ALT increased	12(60)	1(5)	10(50)	1(5)	0.54	1
Bilirubin elevation	10(50)	2(10)	5(25)	2(10)	0.108	1
Hypothyroidism	8(40)	1(5)	1(5)	0	0.008	0.33
Hypoproteinemia	2(10)	0	3(15)	0	0.64	–
Thrombocytopenia	7(35)	1(5)	4(20)	0	0.3	0.33
Leukopenia	3(15)	0	4(20)	0	0.69	–

Conclusions

Toripalimab plus lenvatinib with RT are safe and well tolerated in advanced BTC. Toripalimab plus lenvatinib with RT may prolong the survival of patients with previously treated advanced BTC. The addition of RT may enhance the efficacy of toripalimab and lenvatinib. Further research on prospective larger cohorts is needed.

Data availability statement

The original contributions presented in the study are included in the article/Supplementary Material. Further inquiries can be directed to the corresponding authors.

Ethics statement

The studies involving human participants were reviewed and approved by the institutional review board and ethics committee at Peking Union Medical College Hospital. The patients/participants provided their written informed consent to participate in this study.

Author contributions

YCW, NZ, and JX collected the data and wrote the manuscript. XBY and HZ designed and examined the study. YYW, LZ, and JC helped to collect the literature and participated in discussions. CZ, JX, and YYW performed the statistical analyses. All authors contributed to the article and approved the submitted version.

Funding

This work was supported by CAMS Innovation Fund for Medical Sciences (CIFMS) (2021-1-I2M-003 and 2021-I2M-1-061), CSCO-hengrui Cancer Research Fund (Y-HR2019-0239), CSCO-MSD Cancer Research Fund (Y-MSDZD2021-0213) and National Ten-thousand Talent Program.

Conflict of interest

The authors declare that the research was conducted in the absence of any commercial or financial relationships that could be construed as a potential conflict of interest.

Publisher's note

Supplementary material

The Supplementary Material for this article can be found online at: https://www.frontiersin.org/articles/10.3389/fimmu.2023.1084843/full#supplementary-material

References

1. Brindley PJ, Bachini M, Ilyas SI, Khan SA, Loukas A, Sirica AE, et al. Cholangiocarcinoma. *Nat Rev Dis Primers* (2021) 7(1):65. doi: 10.1038/s41572-021-00300-2

2. Valle J, Wasan H, Palmer DH, Cunningham D, Anthoney A, Maraveyas A, et al. Cisplatin plus gemcitabine versus gemcitabine for biliary tract cancer. *N Engl J Med* (2010) 362(14):1273–81. doi: 10.1056/NEJMoa0908721

3. Lamarca A, Palmer DH, Wasan HS, Ross PJ, Ma YT, Arora A, et al. Second-line folfox chemotherapy versus active symptom control for advanced biliary tract cancer (Abc-06): A phase 3, open-label, randomised, controlled trial.. *Lancet Oncol* (2021) 22 (5):690–701. doi: 10.1016/s1470-2045(21)00027-9

4. Kam AE, Masood A, Shroff RT. Current and emerging therapies for advanced biliary tract cancers. *Lancet Gastroenterol Hepatol* (2021) 6(11):956–69. doi: 10.1016/s2468-1253(21)00171-0

5. Wang Y, Yang X, Wang D, Yang X, Wang Y, Long J, et al. Lenvatinib beyond first-line therapy in patients with advanced biliary tract carcinoma. *Front Oncol* (2022) 12:785535. doi: 10.3389/fonc.2022.785535

6. Piha-Paul SA, Oh DY, Ueno M, Malka D, Chung HC, Nagrial A, et al. Efficacy and safety of pembrolizumab for the treatment of advanced biliary cancer: Results from the KEYNOTE-158 and KEYNOTE-028 studies. *Int J Cancer* (2020) 147(8):2190–8. doi: 10.1002/ijc.33013

7. Villanueva L, Lwin Z, Chung HCC, Gomez-Roca CA, Graham DM. Lenvatinib plus pembrolizumab for patients with previously treated biliary tract cancers in the multicohort phase 2 LEAP-005 study. *J Clin Oncol* (2021) 39(15_suppl):4080–0. doi: 10.1200/JCO.2021.39.15_suppl.4080

8. Jian Z, Fan J, Shi G-M, Huang X-Y, Wu D, Yang G-H, et al. Gemox chemotherapy in combination with anti-PD1 antibody toripalimab and lenvatinib as first-line treatment for advanced intrahepatic cholangiocarcinoma: A phase 2 clinical trial. *J Clin Oncol* (2021) 39(15_suppl):4094–4. doi: 10.1200/JCO.2021.39.15_suppl.4094

9. Yang X, Xu H, Zuo B, Yang X, Bian J, Long J, et al. Downstaging and resection of hepatocellular carcinoma in patients with extrahepatic metastases after stereotactic therapy. *Hepatobil Surg Nutr* (2021) 10(4):434–42. doi: 10.21037/hbsn-21-188

10. Franzese C, Bonu ML, Comito T, Clerici E, Loi M, Navarria P, et al. Stereotactic body radiotherapy in the management of oligometastatic and recurrent biliary tract cancer: single-institution analysis of outcome and toxicity. *J Cancer Res Clin Oncol* (2020) 146(9):2289–97. doi: 10.1007/s00432-020-03285-9

11. Taggar AS, Mann P, Folkert MR, Aliakbari S, Myrehaug SD, Dawson LA. A systematic review of intraluminal high dose rate brachytherapy in the management of malignant biliary tract obstruction and cholangiocarcinoma. *Radiother Oncol* (2021) 165:60–74. doi: 10.1016/j.radonc.2021.10.011

12. Oh D, He A, Qin S, Chen L, Okusaka T, Vogel A, et al. A phase 3 randomized, double-blind, placebo-controlled study of durvalumab in combination with gemcitabine plus cisplatin (Gemcis) in patients (Pts) with advanced biliary tract cancer (Btc): Topaz-1. *J Clin Oncol* (2022) 40(4_suppl):378–8. doi: 10.1200/JCO.2022.40.4_suppl.378

13. Chen D, Barsoumian HB, Fischer G, Yang L, Verma V, Younes AI, et al. Combination treatment with radiotherapy and a novel oxidative phosphorylation inhibitor overcomes PD-1 resistance and enhances antitumor immunity. *J Immunother Cancer* (2020) 8(1):e000289. doi: 10.1136/jitc-2019-000289

14. Geng Y, Zhang Q, Feng S, Li C, Wang L, Zhao X, et al. Safety and efficacy of PD-1/PD-L1 inhibitors combined with radiotherapy in patients with non-small-cell lung cancer: a systematic review and meta-analysis. *Cancer Med* (2021) 10(4):1222–39. doi: 10.1002/cam4.3718

15. Zhong L, Wu D, Peng W, Sheng H, Xiao Y, Zhang X, et al. Safety of PD-1/PD-L1 inhibitors combined with palliative radiotherapy and anti-angiogenic therapy in advanced hepatocellular carcinoma. *Front Oncol* (2021) 11:686621. doi: 10.3389/fonc.2021.686621

16. Sheng X, Yan X, Chi Z, Si L, Cui C, Tang B, et al. Axitinib in combination with toripalimab, a humanized IgG4 mAb against programmed death-1 (PD-1) in patients with metastatic mucosal melanoma: A non-randomized, open-label, dose-finding, and cohort-expansion phase 1b trial. *Journal of Clinical Oncology: Official Journal of the American Society of Clinical Oncology* (2019) 37(32):2987–99. doi: 10.1200/jco.19.00210

17. Wang F, Wei XL, Wang FH, Xu N, Shen L, Dai GH, et al. Safety, efficacy and tumor mutational burden as a biomarker of overall survival benefit in chemo-refractory gastric cancer treated with toripalimab, a PD-1 antibody in phase Ib/II clinical trial NCT02915432. *Ann Oncol* (2019) 30(9):1479–86. doi: 10.1093/annonc/mdz197

18. Jian Z, Fan J, Shi GM, Huang XY, Wu D, Liang F, et al. Lenvatinib plus toripalimab as first-line treatment for advanced intrahepatic cholangiocarcinoma: A single-arm, phase 2 trial. (2021) 39(15_suppl):4099–9. doi: 10.1200/JCO.2021.39.15_suppl.4099

19. Liniker E, Menzies AM, Kong BY, Cooper A, Ramanujam S, Lo S, et al. Activity and safety of radiotherapy with anti-PD-1 drug therapy in patients with metastatic melanoma. *Oncoimmunology* (2016) 5(9):e1214788. doi: 10.1080/2162402x.2016.1214788

20. Lin J, Yang X, Long J, Zhao S, Mao J, Wang D, et al. Pembrolizumab combined with lenvatinib as non-first-line therapy in patients with refractory biliary tract carcinoma. *Hepatobil Surg Nutr* (2020) 9(4):414–24. doi: 10.21037/hbsn-20-338

21. Shi C, Li Y, Yang C, Qiao L, Tang L, Zheng Y, et al. Lenvatinib plus programmed cell death protein-1 inhibitor beyond first-line systemic therapy in refractory advanced biliary tract cancer: A real-world retrospective study in China. *Front Immunol* (2022) 13:946861. doi: 10.3389/fimmu.2022.946861

22. Theelen W, Chen D, Verma V, Hobbs BP, Peulen HMU, Aerts J, et al. Pembrolizumab with or without radiotherapy for metastatic non-small-cell lung cancer: a pooled analysis of two randomised trials. *Lancet Respir Med* (2021) 9(5):467–75. doi: 10.1016/s2213-2600(20)30391-x

23. Mondini M, Levy A, Meziani L, Milliat F, Deutsch E. Radiotherapy-immunotherapy combinations - perspectives and challenges. *Mol Oncol* (2020) 14 (7):1529–37. doi: 10.1002/1878-0261.12658

24. Lan Y, Moustafa M, Knoll M, Xu C, Furkel J, Lazorchak A, et al. Simultaneous targeting of TGF-β/PD-L1 synergizes with radiotherapy by reprogramming the tumor microenvironment to overcome immune evasion. *Cancer Cell* (2021) 39(10):1388–1403.e1310. doi: 10.1016/j.ccell.2021.08.008

25. Mody K, Starr J, Saul M, Poorman K, Shields AF. Patterns and genomic correlates of PD-L1 expression in patients with biliary tract cancers. *J Gastrointest Oncol* (2019) 10 (6):1099–109. doi: 10.21037/jgo.2019.08.08

26. Yu WD, Sun G, Li J, Xu J, Wang X. Mechanisms and therapeutic potentials of cancer immunotherapy in combination with radiotherapy and/or chemotherapy. *Cancer Lett* (2019) 452:66–70. doi: 10.1016/j.canlet.2019.02.048

27. Wennerberg E, Vanpouille-Box C, Bornstein S, Yamazaki T, Demaria S, Galluzzi L. Immune recognition of irradiated cancer cells. *Immunol Rev* (2017) 280(1):220–30. doi: 10.1111/imr.12568

28. Cox MC, Lapenta C, Santini SM. Advances and perspectives of dendritic cell-based active immunotherapies in follicular lymphoma. *Cancer Immunol Immunother* (2020) 69 (6):913–25. doi: 10.1007/s00262-020-02577-w

29. Procureur A, Simonaggio A, Bibault JE, Oudard S, Vano YA. Enhance the immune checkpoint inhibitors efficacy with radiotherapy induced immunogenic cell death: A comprehensive review and latest developments. *Cancers (Basel)* (2021) 13(4):678. doi: 10.3390/cancers13040678

30. Pitroda SP, Chmura SJ, Weichselbaum RR. Integration of radiotherapy and immunotherapy for treatment of oligometastases. *Lancet Oncol* (2019) 20(8):e434–42. doi: 10.1016/s1470-2045(19)30157-3

31. Arina A, Gutiontov SI, Weichselbaum RR. Radiotherapy and immunotherapy for cancer: From "Systemic" to "Multisite". *Clin Cancer Res* (2020) 26(12):2777–82. doi: 10.1158/1078-0432.Ccr-19-2034

32. Chen Y, Gao M, Huang Z, Yu J, Meng X. SBRT combined with PD-1/PD-L1 inhibitors in NSCLC treatment: a focus on the mechanisms, advances, and future challenges. *J Hematol Oncol* (2020) 13(1):105. doi: 10.1186/s13045-020-00940-z

33. Abou-Alfa GK, Sahai V, Hollebecque A, Vaccaro G, Melisi D, Al-Rajabi R, et al. Pemigatinib for previously treated, locally advanced or metastatic cholangiocarcinoma: a multicentre, open-label, phase 2 study. *Lancet Oncol* (2020) 21(5):671–84. doi: 10.1016/s1470-2045(20)30109-1

frontiers | Frontiers in Immunology

TYPE Review
PUBLISHED 23 February 2023
DOI 10.3389/fimmu.2023.1111369

OPEN ACCESS

EDITED BY
Junjiang Fu,
Southwest Medical University, China

REVIEWED BY
Mauricio Díaz-Muñoz,
National Autonomous University of Mexico, Mexico
Saber Imani,
Affiliated Hospital of Southwest Medical University, China
Kenneth A. Jacobson,
National Institutes of Health, United States

*CORRESPONDENCE
Jingxin Liu
liujingxin@sztu.edu.cn
Rongsong Li
lirongsong@sztu.edu.cn
Bin Zeng
zengbin@sztu.edu.cn

†These authors have contributed equally to this work

SPECIALTY SECTION
This article was submitted to Cancer Immunity and Immunotherapy, a section of the journal Frontiers in Immunology

RECEIVED 29 November 2022
ACCEPTED 31 January 2023
PUBLISHED 23 February 2023

CITATION
Kang C, Liu L, Wu C, Li L, Jia X, Xie W, Chen S, Wu X, Zheng H, Liu J, Li R and Zeng B (2023) The adenosinergic machinery in cancer: In-tandem insights from basic mechanisms to therapy. *Front. Immunol.* 14:1111369. doi: 10.3389/fimmu.2023.1111369

The adenosinergic machinery in cancer: In-tandem insights from basic mechanisms to therapy

Chifei Kang[1,2†], Luyu Liu[3†], Chengyu Wu[4], Lingyun Li[1], Xiao Jia[1], Wendi Xie[1], Siyu Chen[1], Xinying Wu[1], Huaxiao Zheng[1], Jingxin Liu[1*], Rongsong Li[2*] and Bin Zeng[1*]

[1]College of Pharmacy, Shenzhen Technology University, Shenzhen, China, [2]College of Health Science and Environmental Engineering, Shenzhen Technology University, Shenzhen, China, [3]Guangdong Institute of Intelligence Science and Technology, Hengqin Guangdong-Macao In-Depth Cooperation Zone, Zhuhai, Guangdong, China, [4]Research Centre of Printed Flexible Electronics, School of Materials Science and Engineering, Harbin Institute of Technology, Shenzhen, China

Extracellular adenosine (eADO) signaling has emerged as an increasingly important regulator of immune responses, including tumor immunity. eADO is mainly produced from extracellular ATP (eATP) hydrolysis. eATP is rapidly accumulated in the extracellular space following cell death or cellular stress triggered by hypoxia, nutrient starvation, or inflammation. eATP plays a pro-inflammatory role by binding and activating the P2 purinergic receptors (P2X and P2Y), while eADO has been reported in many studies to mediate immunosuppression by activating the P1 purinergic receptors (A1, A2A, A2B, and A3) in diverse immune cells. Consequently, the hydrolysis of eATP to eADO alters the immunosurveillance in the tumor microenvironment (TME) not only by reducing eATP levels but also by enhancing adenosine receptor signaling. The effects of both P1 and P2 purinergic receptors are not restricted to immune cells. Here we review the most up-to-date understanding of the tumor adenosinergic system in all cell types, including immune cells, tumor cells, and stromal cells in TME. The potential novel directions of future adenosinergic therapies in immuno-oncology will be discussed.

KEYWORDS

adenosine, machinery and mechanisms, cancer, therapy, EADO

Introduction

Adenosine (ADO) is a metabolic intermediate involved in the ATP catabolism pathway and the synthesis of some important signaling molecules, such as cyclic adenosine monophosphate (cAMP) (1). Extracellular nucleotides, including purines and pyrimidines, have been unequivocally reported as signaling molecules involved in several systems such as blood pressure regulation, platelet activation, cardiovascular system remodeling, neurotransmission, anti-cell death, promotion of cell growth, and immunoregulation (2). Under physiological conditions, both ATP and ADO are usually at low levels in the

extracellular space (3). Several cell conditions and stresses like cell membrane damage, ischemia, inflammation, and cancer could trigger the massive release of endogenous ATP in controlled manners such as regulated vesicular exocytosis and ion channel/transporter-mediated release but also in a direct cell-lytic way through cell destruction (Figure 1) (4–6). Thus, the accumulation of extracellular ATP (eATP) actually functions as a danger sign or nominated Danger-Associated Molecular Pattern (DAMP) to attract phagocytic cells to immigrate to the inflammatory sites and caution the whole immune system about the presence of pathogen-associated molecules and cell/tissue damage (7, 8). The activation of inflammation achieved by eATP is notably mediated through P2 purinergic receptors, including ligand-gated receptors (P2X) and metabotropic nucleotide-selective receptors (P2Y) (9, 10). Most family members of P2Y receptors promote oncogenic processes directly in tumor cells, while P2Y receptors in immune cells regulate these processes indirectly (11). Recent studies suggested that eATP activates P2X purinoceptor 7 (P2X7) expressed on macrophages, dendritic cells (DCs), granulocytes, T cells, and B cells to promote the formation of the NLRP3 inflammasome and the release of inflammatory cytokines such as IL-1β and IL-18 to enhance anti-tumor immunity (12–14). However, eATP is rapidly hydrolyzed to extracellular adenosine (eADO) in the tumor microenvironment (TME) since solid tumors normally have higher levels of ectonucleotidases than non-tumor tissues (15, 16).

eADO is primarily derived from the sequential hydrolysis of eATP mediated by several established ectonucleotidases (5). In a canonical route, eATP is hydrolyzed to extracellular ADP and AMP sequentially by CD39, which is known as ectonucleoside triphosphate diphosphohydrolase 1, and AMP is finally hydrolyzed to eADO by CD73, which is known as 5′-nucleotidase (17). However, the fate of eAMP is not limited to producing eADO; eAMP can also be phosphorylated sequentially to eATP by secreted or membrane-associated adenylate kinase (ecto-AK) and nucleoside diphosphate kinase (NDPK) (18).

The non-classical eADO production pathway is mediated by CD38, which is known as NAD^+ ectohydrolase, and CD203a, which is known as ectonucleotide pyrophosphatase (19). Extracellular nicotinamide dinucleotide (NAD) released *via* gap junction protein connexin 43 (Cx43) regulation can be hydrolyzed to nicotinamide and ADP-ribose (ADPR) by CD38 (20, 21). Then CD203a consumes the ADPR to generate inorganic pyrophosphate and AMP, which are hydrolyzed by CD73 to eADO as mentioned above (19). In addition to CD73, prostatic acid phosphatase (22) and tissue-non-specific alkaline phosphatase (TNAP) were reported to hydrolyze eAMP to eADO (23, 24).

Analogous to eATP, in the extracellular space, the half-life of eADO is very short. The eADO molecule can be catalyzed directly into inosine by adenosine deaminase (ADA) and then into

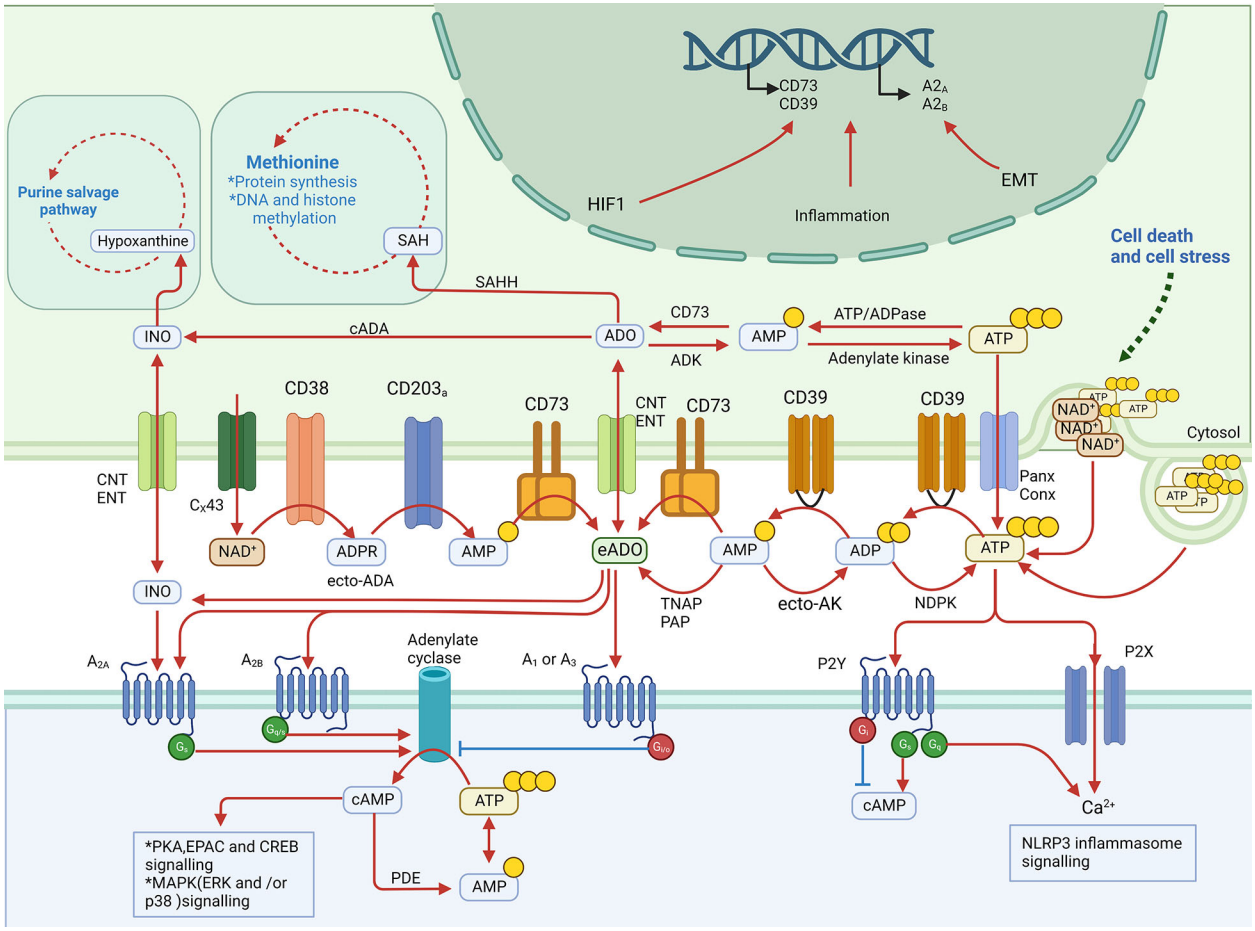

FIGURE 1
eADO metabolic pathways: production, degradation, and signaling.

hypoxanthine by purine nucleoside phosphorylase (PNP) on the cell surface (25). eADO could also be transported into cells *via* concentrative nucleoside transporters (CNT1/2) or equilibrative nucleoside transporters (ENT1/2) (26). Inside cells, adenosine also has several metabolic pathways. The fundamental route is that intracellular ADO is phosphorylated by cytosolic adenylate kinase (ADK) to AMP, followed by conversion to ATP (27). Intracellular ADO could also be converted by cytosolic ADA (cADA) into inosine or by S-adenosyl-homocysteine hydrolase (SAHH) into S-adenosyl-homocysteine (SAH) involved in the methionine cycle (28). In conclusion, the eATP–CD39–CD73 pathway is the fundamental factor determining the concentration of eADO, but alternative ecto-enzymes also regulate metabolism, counteracting ATP-regenerating regulation.

Although the half-life of eADO is short, the concentration of eADO could remain high in TME. Cancer cell death due to rapid growth or chemotherapy contributes to ATP release and then eADO accumulation in the extracellular space (29). In addition to cancer cells, Treg cell deaths also provide ATP and CD39/CD73 to supply eADO production for immunosuppression in TME (30). Other than immune cells, cancer-associated fibroblasts (CAFs) in TME were reported to highly express CD73 induced by A_{2B} receptor activation to sustain a high level of eADO concentration in colorectal cancer (31). Under physiological conditions, ADO plays a role in balancing the immune system's activation and overreaction. However, in TME, all cell types are also regulated by adenosine signaling and involved in eADO production, which ultimately builds up the role of eADO as a tumor cell growth supporter.

Adenosine receptor pathways

eADO has its own specific receptors, which are P1 purinergic receptors. The P1 receptor family is composed of four G protein-coupled receptors: A_1, A_{2A}, A_{2B}, and A_3 (15, 32). These four receptors have different affinities for eADO. According to affinity, they can be roughly divided into two groups: A_1, A_{2A}, and A_3 have affinities for eADO in the nanomolar range (100–310 nM), while A_{2B} has a comparatively low affinity for eADO in the micromolar range (15 μM) (33). The common primary function of P1 receptor family members is to regulate adenylate cyclase activity, which means modulating the intracellular cAMP concentration (34). A_1 and A_3, which are Gi/o(Gi/Go)-coupled adenosine receptors, implement inhibition of adenylate cyclase to decrease the intracellular level of cAMP. In contrast, A_{2A} and A_{2B}, as Gq/s(Gq/Gs)-coupled adenosine receptors, increase the intracellular level of cAMP, which could potently dampen the immune response in some immune cells (35). A_{2A} receptor is generally expressed on most immune cells—monocytes, macrophages, DCs, neutrophils, natural killer (NK) cells, T cells, and natural killer T (NKT) cells; meanwhile, A_{2B} receptor is primarily highly expressed on macrophages and DCs (7).

In T cells (Figure 2), the pioneering work that provided evidence on the role of A_{2A}-mediated immunosuppression in cancer can be traced to 20 years ago (36, 37). eADO binds to the A_{2A} receptor to stimulate the accumulation of cAMP, leading to the activation of the cAMP-dependent protein kinase A (38) signaling pathway, which negatively regulates the activation of T-cell receptor (TCR)-dependent transmembrane signaling *via* providing an OFF signal to

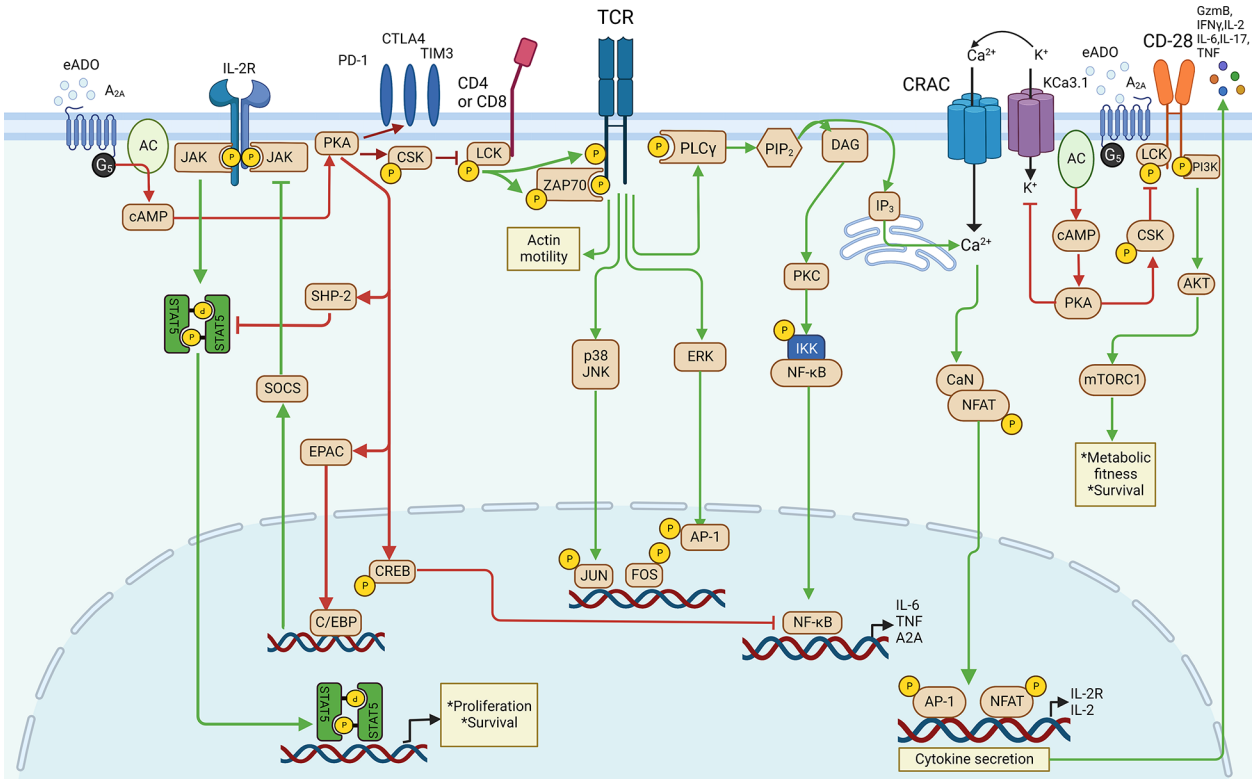

FIGURE 2
eADO/adenosine signaling in T cell.

activated immune cells (36). In addition to the cAMP/PKA pathway, eADO receptors can also function through cAMP-independent pathways such as DAG/PKC, MAPK (ERK and/or p38), and PI3K/AKT/mTOR pathways (39). In T cells, the eADO-activated A_{2A} receptor signaling-cAMP/PKA cascade triggers the direct inhibition of TCR activation *via* non-receptor tyrosine kinase (CSK). In addition, CSK inhibits CD28-mediated PI3K/AKT/mTORC pathways to decrease T cell protein synthesis, proliferation, and survival (40). PKA also phosphorylates the cAMP response element binding protein (CREB) to dampen the transcription activity of TCR downstream NF-κB (41, 42). In addition, PKA could activate SHP-2 and EPAC to impair T cell IL-2 receptor downstream signaling by inhibiting STAT5 and JAK, respectively, to suppress T-cell activation, survival, proliferation, and cytokine production (43–45). PKA inhibits KCa3.1 potassium channels, which causes extracellular Ca2 + cannot flux in through the calcium release-activated channels (CRAC) to suppress the upregulation of NFAT regulated genes which encode factors such as granzyme B (GzmB), IFNγ, TNF, IL-6, IL-17, IL-2, and IL-2R which are crucial to T-cell function and expansion (46). A_{2A} receptor activation was also reported to upregulate the expression of T-cell suppressive receptors such as programmed cell death protein 1 (PD-1), cytotoxic T lymphocyte antigen 4 (CTLA4), and T cell immunoglobulin and mucin domain-containing protein 3 (TIM3) so that T-cell immunosuppression is potentially enhanced (47, 48).

In other immune cells (Figure 3), such as B cells, NF-κB, the downstream factor of the B cell receptor (BCR), and Toll-like receptor 4 (TLR4), are suppressed by PKA from activated A_{2A} receptor signaling, hence disrupting B cell survival (49). PKA from A_{2A} receptor signaling decreases production of IFNγ and perforin, which is the Fas ligand, to dampen the maturation and activity of NK cells (50, 51). A_{2A} receptor activation reduces IFNγ production in NKT cells and inhibits NKT cell activation (52). In non-professional antigen-presenting cells (APCs), such as fibroblasts, A_{2B} receptor-induced cAMP can suppress IFNγ-stimulated STAT1 activity and inhibit CIITA through upregulating TGFβ. The combined effects of this A_{2B} receptor signaling lead to a decrease of MHC II transcription, which attenuates tumor immune response (53). In macrophages, the expression level of both A_{2A} and A_{2B} receptors is promoted by Toll-like receptor signaling (54, 55). Activation of both A_{2A} and A_{2B} receptor signaling favors the shift of macrophages towards a tolerogenic tumor-promoting "M2" phenotype polarization accompanied by increased production of immunosuppressive IL-10, IL-6, and VEGF as well as a decrease in pro-inflammatory IL-12 and

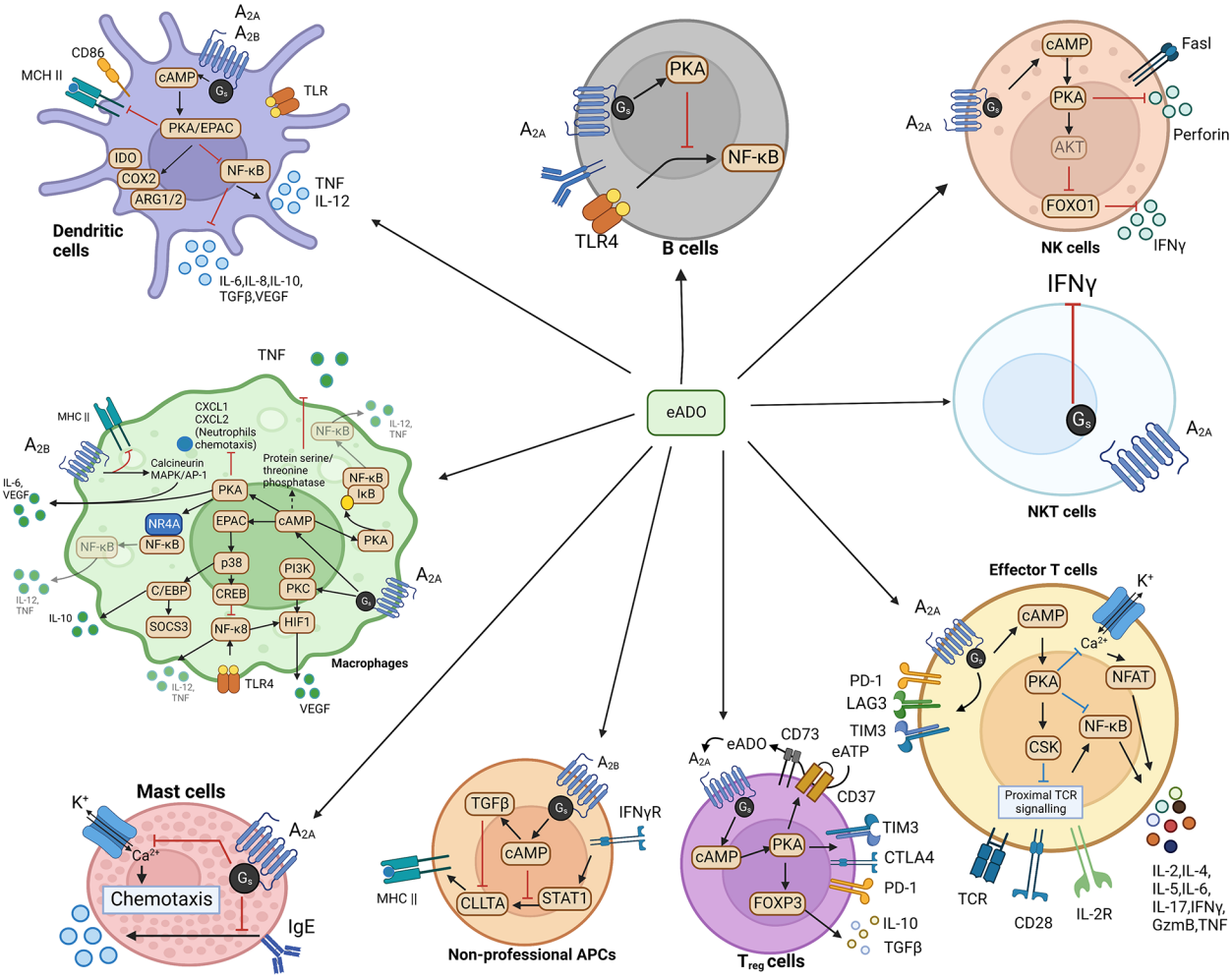

FIGURE 3
eADO/adenosine signaling in various immune cells.

THF (38, 56). Similarly, in dendritic cells (DCs), both A_{2A} and A_{2B}-mediated cAMP/PKA signaling enhance the production of IL-10, IL-6, VEGF, and TGFβ plus indoleamine 2,3-dioxygenase (IDO), cyclooxygenase 2 (COX2), and arginase 1/2 (ARG 1/2), which meanwhile dampen the expression of IL-12 and TNF (57). Based on most currently known data, in a sense, the A_{2A} receptor elicits immunosuppression in both lymphocytes and myeloid cells. In contrast, the A_{2B} receptor elicits immunosuppression mainly from myeloid cells.

In cancer cells: In the extracellular space of solid tumor TME, the concentration of eATP is considerably high due to both the passive release from tumor cell necrosis and the active secretion from tumor cells and other TME cells. Many factors, such as mechanical stress, starvation, hypoxia, and chronic inflammation, could induce this active secretion of ATP (12, 58). eATP binds to both P2X and P2Y, notably P2X7 expressed in immune cells in TME such as DCs, macrophages, B cells, and T cells (6, 12). The activation of P2X7 could promote calcium influx to enhance NLRP3 inflammasome formation, leading to antitumor immunity promotion (29, 59). In this regard, TME seems to provide a strategy to promote the inflammatory response, which could potentially contribute to antitumor activity. In fact, tumor cells express a higher level of ectonucleotidases such as CD39 and CD73 to execute the hydrolysis of eATP to eADO. In addition to the most reported transcription factor, hypoxia-inducible factor 1 (HIF1), several proteins such as TGFβ, TNF, IL-2, and IL-6 could enhance the expression of CD39 and CD73 (16, 60). As mentioned above, CD39 and CD73 are also generally expressed in immune cells; thus, ectonucleotidases from both tumor cells and immune cells together produce a large amount of eADO in the TME niche.

HIF1 as a transcription factor was found to increase the expression of CD39, CD73, A_{2A}, and A_{2B} as well as suppress the expression of both ENTs and adenylate kinase, leading to eADO accumulation in solid tumor TME, which is normally hypoxic (61–66). The upregulation of CD39, CD73, and A_{2B} in various cancers was reported to positively correlate with poor prognosis in patients (60, 67). In particular, there have already been tremendous studies showing that high expression of CD39 and CD73 consistently correlated with poor prognosis in patients with those high incidence rates and malignant cancers such as ovarian, gastric, rectal, breast cancers (including TNBC), hepatocellular carcinoma (HCC), and non-small-cell lung cancers (NSCLCs) (68–73). This is the rationale that supports many current and ongoing clinical trials targeting CD39 and CD73.

More studies uncovered the molecular mechanisms involved in CD73 upregulation in cancer cells in addition to the regulation of HIF1 and TGFβ. Epithelial-to-Mesenchymal Transition (EMT) factors such as WNT/β-catenin pathway activators and TWIST were found to upregulate the expression of CD73 in human tumors (74). Mutations or upregulation of TP53, KRAS, BRAF, and EGFR also positively correlated with increased expression of CD73 in various human tumors (73, 75–77). In tumor cells, especially those with an EMT phenotype, CD73 and some factors like TGFβ form a positive feedback loop in that TGFβ signaling increases CD73 expression and CD73 produces more eADO stimulating A_{2A} and A_{2B} receptor pathways to favor TGFβ production and secretion; thus, CD73/eADO receptor signaling contributes to EMT promotion in cancer cells (78). Since the high concentration of extracellular NAD^+ is present in the TME niche in some cancer types, probably due in part to the altered metabolism in cancer cells, the non-classical eADO production pathway mediated by CD38 also plays an influential role in eADO signaling in several solid tumors (22, 79).

The effects of eADO are not limited to immune cells to implement immunosuppression but also on cancer cells directly to regulate tumor proliferation, growth, anti-apoptosis, and metastasis. The PI3K/AKT/mTORC signaling pathway could be promoted upon eADO-mediated A_{2A} receptor signaling to promote cell proliferation, tumor progression, and metastasis in melanoma, hepatocellular carcinoma, and gastric cancer (80–82). The A_{2B} receptor was found to stimulate different downstream signaling compared to A_{2A} in cancer cells. In TNBC cells, activation of the A_{2B} receptor occurs notably *via* the ERK1/2-MAPK pathway. Knockdown of the A_{2B} receptor in TNBC cells suppresses cancer cell proliferation and lung metastasis (67). A_{2B} receptor signaling could activate FOS-related antigen 1 (FRA-1) and the small GTPase RAP1B to enhance TNBC cells' lung metastasis in mouse models (83, 84). An intriguing finding is that A_{2B} receptor signaling is constitutively activated in prostate cancer cells to promote cancer cell proliferation *in vitro*. However, activation is not dependent on the availability of the A_{2B} receptor ligand, eADO. This study suggested potential adenosine-independent signaling under the A_{2B} receptor in cancer cells (85). The EMT process has an unequivocal interaction with adenosine signaling. Enhancing EMT levels leads to increased CD73 expression and thus eADO receptor signaling, which in turn promotes the EMT process in ovarian cancer (68, 78). Cancer cells with an EMT phenotype usually exhibit cell stemness, which is suggested as a potential cancer stem cell. In breast cancer and glioblastoma, hypoxia-induced A_{2B} receptor activation results in the maintenance of self-renewing tumor cells in the mouse model (86, 87). In a hepatocellular carcinoma study, CD73 was found to be upregulated, leading to A_{2A} receptor activation, which results in cancer cells' EMT and stemness promotion through increasing SOX9 expression and activity (88).

Therapy for cancer targeting adenosine signaling pathway

Not surprisingly, drugs designed to target the adenosine signaling pathway have been blooming vigorously for the last decade. Strategies for targeting adenosine signaling pathway could generally be classified into two groups: ① inhibition of adenosine production and prevention of ATP degradation simultaneously in TME *via* targeting CD73 and/or CD39; and ② interruption of adenosine signaling through blocking A_{2A} and A_{2B} receptors. According to ongoing pre-clinical research and clinical trials, drugs targeting the CD73 and A_{2A} receptors are the mainstream adenosine pathway inhibitors. Most CD73 inhibitors are monoclonal antibodies for potential pharmacological application, whereas small-molecule inhibitors are currently the only available clinical drugs targeting A_{2A} and A_{2B} receptors since they are G protein-coupled receptors (GPCRs) with specific conformations notoriously difficult for antibody binding.

Targeting A2A and/or A2B in cancer: A_{2A} antagonists were initially developed for neurological disorders such as Parkinson's disease or adult attention deficit hyperactivity disorder (ADHD) (89, 90). Their evaluations in clinical trials suggested a great tolerability and safety profile. The available preliminary data of several A_{2A} antagonists in clinical trials with cancer patients showed good tolerability and exhibited some effects. They are CPI-444 (Corvus), PBF-509 (Novartis/Pablobiofarma), EOS100850 (iTeos), MK-3814 (Merck), AZD4635 (AstraZeneca/Heptares), and a dual A_{2A} and A_{2B} antagonist AB928 (Arcus) (91–96). PBF-1129 (Pablobiofarma), a selective A_{2B} antagonist, has also been developed and is being tested in a clinical trial involving NSCLC cancer patients. In two clinical trials, CPI-444 was administered alone and in combination with Atezolizumab (PD-L1 antibody, Genentech) in patients with renal and advanced metastatic castration-resistant prostate cancer (91). Most common adverse events are in grades 1–2, including fatigue, pruritus, nausea, diarrhea, rash, vomiting, and anemia as well as several in grades 3–4, such as decreased appetite, anemia, arthralgia, and peripheral edema. A better outcome (median progression-free survival of 5.8 months versus 4.1 months and overall survival of 90% versus 55% at 20 weeks) was observed with the A_{2A} antagonist CPI-444 plus the anti-PD-L1 antibody atezolizumab compared to CPI-444 alone in patients with advanced-stage renal cell carcinoma (91). Similar results have been reported in patients with mCRPC: 57% of patients (eight of 14) experienced disease control, with five partial responses and two stable disease responses.

Targeting CD73 and/or CD39: There are several anti-CD73 monoclonal antibodies in phase I/II clinical trials currently, including MEDI9447 (MedImmune), BMS-986179 (BMS), NZV930 (Novartis), and CPI-006 (Corvus), as well as a small molecule inhibitor, AB680 (Arcus) (97–99). In these clinical trials, CD73 inhibitors were administered alone and in combination with PD-1/PD-L1 monoclonal antibodies. Most adverse events were mild, and most outcomes indicated a decreased primary tumor expansion rate, less metastasis formation, and an improved survival rate (99). In addition to CD73, monoclonal antibodies and small-molecule antagonists to CD39 and CD38 are also under development (22, 99).

Targeting drugs are listed in Table 1.

Cautions in the adenosine targeting therapy

The existing controversial effects of adenosine blockage in cancer: The prevalent view is that eADO production and eADOA/ARs signaling activation are associated with poor clinical outcomes. However, it is not substantial for every type of cancer. A group found that in endometrial carcinoma, CD73 played a critical role in tumor suppression (100), whereas another group reported that in endometrial carcinoma, the loss of CD73 is essential for tumor progression (101). Although several studies found a link between A_{2A} expression or activation and poor outcomes in breast cancer, Vasiukov et al. revealed a positive correlation between A_{2A} receptor gene expression and better survival data in basal-type breast cancer and TNBC patients (102). In addition, adenosine receptors (ARs) also exhibit both stimulatory and inhibitory effects in melanoma (80). A similar contradictory effect of adenosine receptors on hepatocellular carcinoma progression has also been reported (103). More mechanisms and pre-clinical studies are necessary to provide fundamental knowledge for adenosine targeting therapy.

Specificity issue in adenosine receptor blockage: As mentioned, adenosine receptors are members of the GPCR family. The conformational complexity of GPCR gives rise to the difficulty of developing antibodies to target the receptors. The currently available pharmacological inhibitors of ARs are small molecules that have the notorious disadvantage of engaging of multiple targets (poly-pharmacology). Several compounds, which were previously confirmed as binding interactors of A_1, A_2, and A_3 receptors, were found to have intracellular binding targets (104, 105). In addition, the putative selective A_{2B} receptor agonist BAY 60-6583 was reported to have other binding molecules to increase CAR-T cell activity independently of the A_{2B} receptor (106).

TABLE 1 Representative eADO pathway-targeting drugs which were involved in the most recent clinical trials.

Target	Cancer Type	Drug Name	Company
A_{2A} receptor	Advanced solid tumors, non-Hodgkin lymphoma	CPI-444	Corvus
A_{2A} receptor	Non-small cell lung cancer	PBF-509	Novartis/Pablobiofarma
A_{2A} receptor	Adult solid tumor	EOS100850	iTeos
A_{2A} receptor	Advanced solid tumors	MK-3814A	Merck
A_{2A} receptor	Advanced solid tumors	AZD4635	AstraZeneca/Heptares
A_{2B} receptor	Non-small cell lung cancer	PBF-1129	Pablobiofarma
A_{2A} and A_{2B} receptors dual antagonist	Metastatic castrate resistant prostate cancer	AB928	Arcus
CD73	Solid tumors	MEDI9447	MedImmune
CD73	Advanced solid tumors	BMS-986179	BMS
CD73	Advanced solid tumors	NZV930	Novartis
CD73	Advanced solid tumors, non-Hodgkin lymphoma	CPI-006	Corvus
CD73	Healthy volunteers	AB680	Arcus
CD38	Lymphoma Prostate, Non-small cell lung cancer	Isatuximab/SAR650984	Sanofi

There is still a large amount of work to be done to pursue better safety and efficacy in adenosine signaling targeting therapy.

Conclusion

Both eATP and eADO are important signal molecules in the physiological processes of cells and tissues. Tissue damage or various cell stresses such as hypoxia, starvation, and mechanical stress, which are common in the TME niche, could stimulate eATP accumulation and rapid hydrolysis to eADO. This would lead to dramatically increased eADO. This eATP–eADO metabolic pathway is involved in pathological shifts in several aspects: rapid eATP degradation dampens the inflammatory response; accumulation of eADO triggers immunosuppression; and it promotes tumor cell proliferation and EMT.

In adenosine signaling, pre-clinical studies suggested the CD39–CD73–A_{2A} receptor pathway is an attractive and tractable therapeutic target for cancer treatment. Inhibitors targeting the CD73 and A_{2A} receptors exhibited good tolerability and achieved some therapeutic effects in some clinical trials. However, several knowledge gaps are worthy of exploring to assist further pre-clinical and clinical trial design (1): What are the potential compensation pathways for the inhibition of eADO signaling? They are probably not limited to intracellular ADO release and ADO-independent adenosine receptor activation. (2) More combined therapies, such as immune checkpoint blockers and adenosine signaling inhibitors, have shown better efficacy. (3) What are reliable biomarkers to indicate which patient subgroups have a higher chance of benefiting from treatments targeting eADO signaling? In conclusion, the adenosinergic system offers new therapeutic strategies aimed at limiting immunosuppression and potentiating antitumor immune responses.

Author contributions

BZ, RL, and JL, carried out the concepts, design, definition of intellectual content, literature search. CK and LLiu contributed writing and editing the manuscript. LLi, XJ, and HZ helped in formatting the manuscript. CW helped perform the manuscript with constructive discussions. WX, SC, and XW carried out the figures in manuscript. All authors contributed to the article and approved the submitted version.

Funding

This research received financial support by the Key Special Projects of National Key Research and Development Plan (2021YFA1301302), The Belt and Road Initiative and China-Africa Science and Technology Cooperation Project of Department of Science and Technology of Jiangxi Province (20202BDH80007), the National Natural Science Foundation of China (32200606), and the Natural Science Foundation of Top Talent of SZTU (GDRC202118), the Natural Science Foundation of Top Talent of SZTU (2020102), Shenzhen Natural Science Foundation (JCYJ20190813141001745, 20220718100823002).

Conflict of interest

The authors declare that the research was conducted in the absence of any commercial or financial relationships that could be construed as a potential conflict of interest.

Publisher's note

References

1. Moser GH, Schrader J, Deussen A. Turnover of adenosine in plasma of human and dog blood. *Am J Physiol* (1989) 256(4 Pt 1):C799–806. doi: 10.1152/ajpcell.1989.256.4.C799

2. Frankish A, Diekhans M, Ferreira AM, Johnson R, Jungreis I, Loveland J, et al. GENCODE reference annotation for the human and mouse genomes. *Nucleic Acids Res* (2019) 47(D1):D766–73. doi: 10.1093/nar/gky955

3. Blay J, White TD, Hoskin DW. The extracellular fluid of solid carcinomas contains immunosuppressive concentrations of adenosine. *Cancer Res* (1997) 57(13):2602–5.

4. Lazarowski ER. Vesicular and conductive mechanisms of nucleotide release. *Purinergic Signal* (2012) 8(3):359–73. doi: 10.1007/s11302-012-9304-9

5. Yegutkin GG. Nucleotide- and nucleoside-converting ectoenzymes: Important modulators of purinergic signalling cascade. *Biochim Biophys Acta* (2008) 1783(5):673–94. doi: 10.1016/j.bbamcr.2008.01.024

6. Kroemer G, Galluzzi L, Kepp O, Zitvogel L. Immunogenic cell death in cancer therapy. *Annu Rev Immunol* (2013) 31:51–72. doi: 10.1146/annurev-immunol-032712-100008

7. Cekic C, Linden J. Purinergic regulation of the immune system. *Nat Rev Immunol* (2016) 16(3):177–92. doi: 10.1038/nri.2016.4

8. Eltzschig HK, Sitkovsky MV, Robson SC. Purinergic signaling during inflammation. *N Engl J Med* (2012) 367(24):2322–33. doi: 10.1056/NEJMra1205750

9. Ralevic V, Burnstock G. Receptors for purines and pyrimidines. *Pharmacol Rev* (1998) 50(3):413–92.

10. Bours MJ, Swennen ELR, Di Virgilio F, Cronstein BN, Dagnelie PC. Adenosine 5'-triphosphate and adenosine as endogenous signaling molecules in immunity and inflammation. *Pharmacol Ther* (2006) 112(2):358–404. doi: 10.1016/j.pharmthera.2005.04.013

11. Woods LT, Forti KM, Shanbhag VC, Camden JM, Weisman GA. P2Y receptors for extracellular nucleotides: Contributions to cancer progression and therapeutic implications. *Biochem Pharmacol* (2021) 187:114406. doi: 10.1016/j.bcp.2021.114406

12. Di Virgilio F, Sarti AC, Falzoni S, De Marchi E, Adinolfi E. Extracellular ATP and P2 purinergic signalling in the tumour microenvironment. *Nat Rev Cancer* (2018) 18(10):601–18. doi: 10.1038/s41568-018-0037-0

13. Borges da Silva H, et al. The purinergic receptor P2RX7 directs metabolic fitness of long-lived memory CD8(+) T cells. *Nature* (2018) 559(7713):264–8. doi: 10.1038/s41586-018-0282-0

14. De Marchi E, Orioli E, Pegoraro A, Sangaletti S, Portararo P, Curti A, et al. The P2X7 receptor modulates immune cells infiltration, ectonucleotidases expression and extracellular ATP levels in the tumor microenvironment. *Oncogene* (2019) 38(19):3636–50. doi: 10.1038/s41388-019-0684-y

15. Chen JF, Eltzschig HK, Fredholm BB. Adenosine receptors as drug targets–what are the challenges? *Nat Rev Drug Discov* (2013) 12(4):265–86. doi: 10.1038/nrd3955

16. Allard B, Beavis PA, Darcy PK, Stagg J. Immunosuppressive activities of adenosine in cancer. *Curr Opin Pharmacol* (2016) 29:7–16. doi: 10.1016/j.coph.2016.04.001

17. Yegutkin GG, Henttinen T, Samburski SS, Spychala J, Jalkanen S. The evidence for two opposite, ATP-generating and ATP-consuming, extracellular pathways on endothelial and lymphoid cells. *Biochem J* (2002) 367(Pt 1):121–8. doi: 10.1042/bj20020439

18. Yegutkin GG, Henttinen T, Jalkanen S. Extracellular ATP formation on vascular endothelial cells is mediated by ecto-nucleotide kinase activities via phosphotransfer reactions. *FASEB J* (2001) 15(1):251–60. doi: 10.1096/fj.00-0268com

19. Horenstein AL, Chillemi A, Zaccarello G, Bruzzone S, Quarona V, Zito A. A CD38/CD203a/CD73 ectoenzymatic pathway independent of CD39 drives a novel adenosinergic loop in human T lymphocytes. *Oncoimmunology* (2013) 2(9):e26246. doi: 10.4161/onci.26246

20. Bruzzone S, Guida L, Zocchi E, Franco L, De Flora A. Connexin 43 hemi channels mediate Ca2+-regulated transmembrane NAD+ fluxes in intact cells. *FASEB J* (2001) 15 (1):10–2. doi: 10.1096/fj.00-0566fje

21. Malavasi F, Deaglio S, Funaro A, Ferrero E, Horenstein AL, Ortolan E. Evolution and function of the ADP ribosyl cyclase/CD38 gene family in physiology and pathology. *Physiol Rev* (2008) 88(3):841–86. doi: 10.1152/physrev.00035.2007

22. Chen L, Diao LX, Yang YB, Yi XH, Rodriguez L, Li YL, et al. CD38-mediated immunosuppression as a mechanism of tumor cell escape from PD-1/PD-L1 blockade. *Cancer Discovery* (2018) 8(9):1156–75. doi: 10.1158/2159-8290.CD-17-1033

23. Zylka MJ, Sowa NA, Taylor-Blake B, Twomey MA, Herrala A, Voikar V, et al. Prostatic acid phosphatase is an ectonucleotidase and suppresses pain by generating adenosine. *Neuron* (2008) 60(1):111–22. doi: 10.1016/j.neuron.2008.08.024

24. Street SE, Kramer NJ, Walsh PL, Taylor-Blake B, Yadav MC, King IF, et al. Tissue-nonspecific alkaline phosphatase acts redundantly with PAP and NT5E to generate adenosine in the dorsal spinal cord. *J Neurosci* (2013) 33(27):11314–22. doi: 10.1523/JNEUROSCI.0133-13.2013

25. Yegutkin GG. Enzymes involved in metabolism of extracellular nucleotides and nucleosides: functional implications and measurement of activities. *Crit Rev Biochem Mol Biol* (2014) 49(6):473–97. doi: 10.3109/10409238.2014.953627

26. Young JD. The SLC28 (CNT) and SLC29 (ENT) nucleoside transporter families: a 30-year collaborative odyssey. *Biochem Soc Trans* (2016) 44(3):869–76. doi: 10.1042/BST20160038

27. Boison D. Adenosine kinase: exploitation for therapeutic gain. *Pharmacol Rev* (2013) 65(3):906–43. doi: 10.1124/pr.112.006361

28. Zimmerman TP, Wolberg G, Duncan GS, Elion GB. Adenosine analogues as substrates and inhibitors of s-adenosylhomocysteine hydrolase in intact lymphocytes. *Biochemistry* (1980) 19(10):2252–9. doi: 10.1021/bi00551a040

29. Michaud M, Martins I, Sukkurwala AQ, Adjemian S, Ma YT, Pellegatti P, et al. Autophagy-dependent anticancer immune responses induced by chemotherapeutic agents in mice. *Science* (2011) 334(6062):1573–7. doi: 10.1126/science.1208347

30. Maj T, Wang W, Crespo J, Zhang HJ, Wang WM, Wei S, et al. Oxidative stress controls regulatory T cell apoptosis and suppressor activity and PD-L1-blockade resistance in tumor. *Nat Immunol* (2017) 18(12):1332–41. doi: 10.1038/ni.3868

31. Yu M, Guo G, Huang L, Deng LB, Chang CS, Achyut BR, et al. CD73 on cancer-associated fibroblasts enhanced by the A(2B)-mediated feedforward circuit enforces an immune checkpoint. *Nat Commun* (2020) 11(1):515. doi: 10.1038/s41467-019-14060-x

32. Borea PA, Gessi S, Merighi S, Varani K. Adenosine as a multi-signalling guardian angel in human diseases: When, where and how does it exert its protective effects? *Trends Pharmacol Sci* (2016) 37(6):419–34. doi: 10.1016/j.tips.2016.02.006

33. Müller CE, Jacobson KA. Recent developments in adenosine receptor ligands and their potential as novel drugs. *Biochim Biophys Acta* (2011) 1808(5):1290–308. doi: 10.1016/j.bbamem.2010.12.017

34. Borea PA, Gessi S, Merighi S, Vincenzi F, Varani K. Pharmacology of adenosine receptors: The state of the art. *Physiol Rev* (2018) 98(3):1591–625. doi: 10.1152/physrev.00049.2017

35. Kunzli BM, Bernlochner MI, Rath S, Kaser S, Csizmadia E, Enjyoji K, et al. Impact of CD39 and purinergic signalling on the growth and metastasis of colorectal cancer. *Purinergic Signal* (2011) 7(2):231–41. doi: 10.1007/s11302-011-9228-9

36. Ohta A, Sitkovsky M. Role of G-protein-coupled adenosine receptors in downregulation of inflammation and protection from tissue damage. *Nature* (2001) 414(6866):916–20. doi: 10.1038/414916a

37. Ohta A, Gorelik E, Prasad SJ, Ronchese F, Lukashev LD, Wong MKK, et al. A2A adenosine receptor protects tumors from antitumor T cells. *Proc Natl Acad Sci USA* (2006) 103(35):13132–7. doi: 10.1073/pnas.0605251103

38. Csoka B, Selmeczy Z, Koscso B, Nemeth ZH, Pacher P, Murray PJ, et al. Adenosine promotes alternative macrophage activation via A2A and A2B receptors. *FASEB J* (2012) 26(1):376–86. doi: 10.1096/fj.11-190934

39. Gessi S, Merighi S, Sacchetto V, Simioni C, Borea PA. Adenosine receptors and cancer. *Biochim Biophys Acta* (2011) 1808(5):1400–12. doi: 10.1016/j.bbamem.2010.09.020

40. Bjorgo E, Tasken K. Novel mechanism of signaling by CD28. *Immunol Lett* (2010) 129(1):1–6. doi: 10.1016/j.imlet.2010.01.007

41. Lukashev D, Ohta A, Apasov S, Chen JF. Cutting edge: Physiologic attenuation of proinflammatory transcription by the gs protein-coupled A2A adenosine receptor in vivo. *J Immunol* (2004) 173(1):21–4. doi: 10.4049/jimmunol.173.1.21

42. Sitkovsky MV. T Regulatory cells: hypoxia-adenosinergic suppression and re-direction of the immune response. *Trends Immunol* (2009) 30(3):102–8. doi: 10.1016/j.it.2008.12.002

43. Zhang H, et al. Adenosine acts through A2 receptors to inhibit IL-2-induced tyrosine phosphorylation of STAT5 in T lymphocytes: role of cyclic adenosine 3',5'-monophosphate and phosphatases. *J Immunol* (2004) 173(2):932–44. doi: 10.4049/jimmunol.173.2.932

44. Raskovalova T, Lokshin A, Huang XJ, Su YY, Mandic M, Zarour HM, et al. Inhibition of cytokine production and cytotoxic activity of human antimelanoma specific CD8+ and CD4+ T lymphocytes by adenosine-protein kinase a type I signaling. *Cancer Res* (2007) 67(12):5949–56. doi: 10.1158/0008-5472.CAN-06-4249

45. Csoka B, et al. Adenosine A2A receptor activation inhibits T helper 1 and T helper 2 cell development and effector function. *FASEB J* (2008) 22(10):3491–9. doi: 10.1096/fj.08-107458

46. Chimote AA, Balajthy A, Arnold MJ, Newton HS, Hajdu P, Qualtieri J, et al. A defect in KCa3.1 channel activity limits the ability of CD8(+) T cells from cancer patients to infiltrate an adenosine-rich microenvironment. *Sci Signal* (2018) 11(527). doi: 10.1126/scisignal.aaq1616

47. Leone RD, Sun IM, Oh MH, Sun IH, Wen JY, Englert J, et al. Inhibition of the adenosine A2a receptor modulates expression of T cell coinhibitory receptors and improves effector function for enhanced checkpoint blockade and ACT in murine cancer models. *Cancer Immunol Immunother* (2018) 67(8):1271–84. doi: 10.1007/s00262-018-2186-0

48. Ohta A, Kini R, Ohta A, Subramanian M, Madasu M, Sitkovsky M. The development and immunosuppressive functions of CD4(+) CD25(+) FoxP3(+) regulatory T cells are under influence of the adenosine-A2A adenosine receptor pathway. *Front Immunol* (2012) 3:190. doi: 10.3389/fimmu.2012.00190

49. Minguet S, Huber M, Rosenkranz L, Schamel WWA, Reth M, Brummer T, et al. Adenosine and cAMP are potent inhibitors of the NF-kappa b pathway downstream of immunoreceptors. *Eur J Immunol* (2005) 35(1):31–41. doi: 10.1002/eji.200425524

50. Raskovalova T, Lokshin A, Huang XJ, Jackson EK, Gorelik E. Adenosine-mediated inhibition of cytotoxic activity and cytokine production by IL-2/NKp46-activated NK cells: involvement of protein kinase A isozyme I (PKA I). *Immunol Res* (2006) 36(1-3):91–9. doi: 10.1385/IR:36:1:91

51. Raskovalova T, et al. Gs protein-coupled adenosine receptor signaling and lytic function of activated NK cells. *J Immunol* (2005) 175(7):4383–91. doi: 10.4049/jimmunol.175.7.4383

52. Lappas CM, Day YJ, Marshall MA, Engelhard VH, Linden J, et al. Adenosine A2A receptor activation reduces hepatic ischemia reperfusion injury by inhibiting CD1d-dependent NKT cell activation. *J Exp Med* (2006) 203(12):2639–48. doi: 10.1084/jem.20061097

53. Fang M, Xia J, Wu XY, Kong H, Wang H, Xie WP, et al. Adenosine signaling inhibits CIITA-mediated MHC class II transactivation in lung fibroblast cells. *Eur J Immunol* (2013) 43(8):2162–73. doi: 10.1002/eji.201343461

54. Cohen HB, Ward A, Hamidzadeh K, Ravid K, MossernDM . IFN-gamma prevents adenosine receptor (A2bR) upregulation to sustain the macrophage activation response. *J Immunol* (2015) 195(8):3828–37. doi: 10.4049/jimmunol.1501139

55. Ramanathan M, Luo W, Csóka B, Haskó G, Lukashev D, Sitkovsky MV, et al. Differential regulation of HIF-1alpha isoforms in murine macrophages by TLR4 and adenosine A(2A) receptor agonists. *J Leukoc Biol* (2009) 86(3):681–9. doi: 10.1189/jlb.0109021

56. Ferrante CJ, Pinhal-Enfield G, Elson G, Cronstein BN, Hasko G, Outram S, et al. The adenosine-dependent angiogenic switch of macrophages to an M2-like phenotype is independent of interleukin-4 receptor alpha (IL-4Ralpha) signaling. *Inflammation* (2013) 36(4):921–31. doi: 10.1007/s10753-013-9621-3

57. Novitskiy SV, Ryzhov S, Zaynagetdinov R, Goldstein AE, Huang YH, Tikhomirov OY, et al. Adenosine receptors in regulation of dendritic cell differentiation and function. *Blood* (2008) 112(5):1822–31. doi: 10.1182/blood-2008-02-136325

58. Aymeric L, Apetoh L, Ghiringhelli F, Tesniere A, Martins I, Kroemer G, et al. Tumor cell death and ATP release prime dendritic cells and efficient anticancer immunity. *Cancer Res* (2010) 70(3):855–8. doi: 10.1158/0008-5472.CAN-09-3566

59. Ma Y, Adjemian S, Mattarollo SR, Yamazaki T, Aymeric L, Yang H, et al. Anticancer chemotherapy-induced intratumoral recruitment and differentiation of antigen-presenting cells. *Immunity* (2013) 38(4):729–41. doi: 10.1016/j.immuni.2013.03.003

60. Allard B, Longhi MS, Robson SC, Stagg J. The ectonucleotidases CD39 and CD73: Novel checkpoint inhibitor targets. *Immunol Rev* (2017) 276(1):121–44. doi: 10.1111/imr.12528

61. Eltzschig HK, et al. Central role of Sp1-regulated CD39 in hypoxia/ischemia protection. *Blood* (2009) 113(1):224–32. doi: 10.1182/blood-2008-06-165746

62. Synnestvedt K, Kohler D, Eckle T, Kong T, Robson SC, Colgan SP, et al. Ecto-5'-nucleotidase (CD73) regulation by hypoxia-inducible factor-1 mediates permeability changes in intestinal epithelia. *J Clin Invest* (2002) 110(7):993–1002. doi: 10.1172/JCI0215337

63. Kong T, Westerman KA, Faigle M, Eltzschig HK, Colgan SP, et al. HIF-dependent induction of adenosine A2B receptor in hypoxia. *FASEB J* (2006) 20(13):2242–50. doi: 10.1096/fj.06-6419com

64. Ahmad A, Ahmad S, Glover L, Miller SM, Shannon JM, Guo XL, et al. Adenosine A2A receptor is a unique angiogenic target of HIF-2alpha in pulmonary endothelial cells. *Proc Natl Acad Sci USA* (2009) 106(26):10684–9. doi: 10.1073/pnas.0901326106

65. Morote-Garcia JC, Rosenberger P, Nivillac NMI, Coe MR, Eltzschig HK, et al. Hypoxia-inducible factor-dependent repression of equilibrative nucleoside transporter 2 attenuates mucosal inflammation during intestinal hypoxia. *Gastroenterology* (2009) 136 (2):607–18. doi: 10.1053/j.gastro.2008.10.037

66. Eltzschig HK, Abdulla P, Hoffman E, Hamilton KE, Daniels D, Schonfeld C, et al. HIF-1-dependent repression of equilibrative nucleoside transporter (ENT) in hypoxia. *J Exp Med* (2005) 202(11):1493–505. doi: 10.1084/jem.20050177

67. Mittal D, Sinha D, Barkauskas D, Young A, Kalimutho M, Stannard K, et al. Adenosine 2B receptor expression on cancer cells promotes metastasis. *Cancer Res* (2016) 76(15):4372–82. doi: 10.1158/0008-5472.CAN-16-0544

68. Turcotte M, Spring K, Pommey S, Chouinard G, Cousineau I, George J, et al. CD73 is associated with poor prognosis in high-grade serous ovarian cancer. *Cancer Res* (2015) 75(21):4494–503. doi: 10.1158/0008-5472.CAN-14-3569

69. Cai XY, Wang XF, Li J, Dong JN, Liu JQ, Li NP, et al. Overexpression of CD39 and high tumoral CD39(+)/CD8(+) ratio are associated with adverse prognosis in resectable gastric cancer. *Int J Clin Exp Pathol* (2015) 8(11):14757–64.

70. Zhang B, Pommey S, Haibe-Kains B, Beavis PA, Darcy PK, Smyth MJ, et al. The expression and clinical significance of CD73 molecule in human rectal adenocarcinoma. *Tumour Biol* (2015) 36(7):5459–66. doi: 10.1007/s13277-015-3212-x

71. Loi S, et al. CD73 promotes anthracycline resistance and poor prognosis in triple negative breast cancer. *Proc Natl Acad Sci U S A* (2013) 110(27):11091–6. doi: 10.1073/pnas.1222251110

72. Cai XY, Ni XC, Yi Y, He HW, Wang JX, Fu YP, et al. Overexpression of CD39 in hepatocellular carcinoma is an independent indicator of poor outcome after radical resection. *Med (Baltimore)* (2016) 95(40):e4989. doi: 10.1097/MD.0000000000004989

73. Inoue Y, Yoshimura K, Kurabe N, Kahyo T, Kawase A, Tanahashi M, et al. Prognostic impact of CD73 and A2A adenosine receptor expression in non-small-cell lung cancer. *Oncotarget* (2017) 8(5):8738–51. doi: 10.18632/oncotarget.14434

74. Spychala J, Kitajewski J. Wnt and beta-catenin signaling target the expression of ecto-5'-nucleotidase and increase extracellular adenosine generation. *Exp Cell Res* (2004) 296(2):99–108. doi: 10.1016/j.yexcr.2003.11.001

75. Lawrence RT, Hernandez D, Miller CP, Haas KM, Irie HY. The proteomic landscape of triple-negative breast cancer. *Cell Rep* (2015) 11(4):630–44. doi: 10.1016/j.celrep.2015.03.050

76. Sunaga N, Shames DS, Girard L, Peyton M, Larsen JE, Imai H, et al. Knockdown of oncogenic KRAS in non-small cell lung cancers suppresses tumor growth and sensitizes tumor cells to targeted therapy. *Mol Cancer Ther* (2011) 10(2):336–46. doi: 10.1158/1535-7163.MCT-10-0750

77. Reinhardt J, Landsberg J, Schmid-Burgk JL, Ramis BB, Bald T, Glodde N, et al. MAPK signaling and inflammation link melanoma phenotype switching to induction of CD73 during immunotherapy. *Cancer Res* (2017) 77(17):4697–709. doi: 10.1158/0008-5472.CAN-17-0395

78. Lupia M, Angiolini F, Bertalot G, Freddi S, Sachsenmeier KF, Chisci E, et al. CD73 regulates stemness and epithelial-mesenchymal transition in ovarian cancer-initiating cells. *Stem Cell Rep* (2018) 10(4):1412–25. doi: 10.1016/j.stemcr.2018.02.009

79. Horenstein AL, et al. Adenosine generated in the bone marrow niche through a CD38-mediated pathway correlates with progression of human myeloma. *Mol Med* (2016) 22:694–704. doi: 10.2119/molmed.2016.00198

80. Merighi S, Mirandola P, Milani D, Varani K, Gessi S, Klotz KN, et al. Adenosine receptors as mediators of both cell proliferation and cell death of cultured human melanoma cells. *J Invest Dermatol* (2002) 119(4):923–33. doi: 10.1046/j.1523-1747.2002.00111.x

81. Ma XL, Shen MN, Hu B, Wang BL, Yang WJ, Lv LH, et al. CD73 promotes hepatocellular carcinoma progression and metastasis via activating PI3K/AKT signaling by inducing Rap1-mediated membrane localization of P110beta and predicts poor prognosis. *J Hematol Oncol* (2019) 12(1):37. doi: 10.1186/s13045-019-0724-7

82. Shi L, Wu Z, Miao J, Du S, Ai S, Xu E, et al. Adenosine interaction with adenosine receptor A2a promotes gastric cancer metastasis by enhancing PI3K-AKT-mTOR signaling. *Mol Biol Cell* (2019) 30(19):2527–34. doi: 10.1091/mbc.E19-03-0136

83. Desmet CJ, Gallenne T, Prieur A, Reyal F, Visser NL, Wittner BS, et al. Identification of a pharmacologically tractable fra-1/ADORA2B axis promoting breast cancer metastasis. *Proc Natl Acad Sci U S A* (2013) 110(13):5139–44. doi: 10.1073/pnas.1222085110

84. Ntantie E, Gonyo P, Lorimer EL, Hauser AD, Schuld N, McAllister D, et al. An adenosine-mediated signaling pathway suppresses prenylation of the GTPase Rap1B and promotes cell scattering. *Sci Signal* (2013) 6(277):ra39. doi: 10.1126/scisignal.2003374

85. Vecchio EA, Tan CYR, Gregory KJ, Christopoulos A, White PJ, May LT, et al. Ligand-independent adenosine A2B receptor constitutive activity as a promoter of prostate cancer cell proliferation. *J Pharmacol Exp Ther* (2016) 357(1):36–44. doi: 10.1124/jpet.115.230003

86. Lan J, Lub H, Samantab D, Salmanb S, Gregg Lua Y, L. Hypoxia-inducible factor 1-dependent expression of adenosine receptor 2B promotes breast cancer stem cell enrichment. *Proc Natl Acad Sci U S A* (2018) 115(41):E9640–8. doi: 10.1073/pnas.1809695115

87. Liu TZ, Wang X, Bai YF, Liao HZ, Qiu SC, Yang YQ, et al. The HIF-2alpha dependent induction of PAP and adenosine synthesis regulates glioblastoma stem cell function through the A2B adenosine receptor. *Int J Biochem Cell Biol* (2014) 49:8–16. doi: 10.1016/j.biocel.2014.01.007

88. Ma XL, Hu B, Tang WG, Xie SH, Ren N, Guo L, et al. CD73 sustained cancer-stem-cell traits by promoting SOX9 expression and stability in hepatocellular carcinoma. *J Hematol Oncol* (2020) 13(1):11. doi: 10.1186/s13045-020-0845-z

89. Pinna A. Adenosine A2A receptor antagonists in parkinson's disease: progress in clinical trials from the newly approved istradefylline to drugs in early development and those already discontinued. *CNS Drugs* (2014) 28(5):455–74. doi: 10.1007/s40263-014-0161-7

90. Franco R, Navarro G. Adenosine A(2A) receptor antagonists in neurodegenerative diseases: Huge potential and huge challenges. *Front Psychiatry* (2018) 9:68. doi: 10.3389/fpsyt.2018.00068

91. Fong L, Hotson A, Powderly J, Sznol M, Heist RS, Choueiri TK. Adenosine 2A receptor blockade as an immunotherapy for treatment-refractory renal cell cancer. *Cancer Discovery* (2020) 10(1):40–53. doi: 10.1158/2159-8290.CD-19-0980

92. Chiappori AA, et al. Phase I study of taminadenant (PBF509/NIR178), an adenosine 2A receptor antagonist, with or without spartalizumab (PDR001), in patients with advanced non-small cell lung cancer. *Clin Cancer Res* (2022) 28(11):2313–20. doi: 10.1158/1078-0432.CCR-21-2742

93. Cortiula F, et al. Immunotherapy in unresectable stage III non-small-cell lung cancer: state of the art and novel therapeutic approaches. *Ann Oncol* (2022) 33(9):893–908. doi: 10.1016/j.annonc.2022.06.013

94. Cutler DL, Tendolkar A, Grachev ID. Safety, tolerability and pharmacokinetics after single and multiple doses of preladenant (SCH420814) administered in healthy subjects. *J Clin Pharm Ther* (2012) 37(5):578–87. doi: 10.1111/j.1365-2710.2012.01349.x

95. Lim EA, et al. Phase ia/b, open-label, multicenter study of AZD4635 (an adenosine A2A receptor antagonist) as monotherapy or combined with durvalumab, in patients with solid tumors. *Clin Cancer Res* (2022) 28(22):4871–84. doi: 10.1158/1078-0432.CCR-22-0612

96. Seitz L, Jin L, Leleti M, Ashok D, Jeffrey J, Rieger A, et al. Safety, tolerability, and pharmacology of AB928, a novel dual adenosine receptor antagonist, in a randomized, phase 1 study in healthy volunteers. *Invest New Drugs* (2019) 37(4):711–21. doi: 10.1007/s10637-018-0706-6

97. Herbst RS, et al. COAST: An open-label, phase II, multidrug platform study of durvalumab alone or in combination with oleclumab or monalizumab in patients with unresectable, stage III non-Small-Cell lung cancer. *J Clin Oncol* (2022) 40(29):3383–93. doi: 10.1200/JCO.22.00227

98. Lee DH. Update of early phase clinical trials in cancer immunotherapy. *BMB Rep* (2021) 54(1):70–88. doi: 10.5483/BMBRep.2021.54.1.242

99. Vigano S, Alatzoglou D, Irving M, Ménétrier-Caux C, Caux C, Romero P, et al. Targeting adenosine in cancer immunotherapy to enhance T-cell function. *Front Immunol* (2019) 10:925. doi: 10.3389/fimmu.2019.00925

100. Kurnit KC, Draisey A, Kazen RC, Chung C, Phan LH, Harvey JB, et al. Loss of CD73 shifts transforming growth factor-beta1 (TGF-beta1) from tumor suppressor to promoter in endometrial cancer. *Cancer Lett* (2021) 505:75–86. doi: 10.1016/j.canlet.2021.01.030

101. Bowser JL, Blackburn MR, Shipley GL, Molina JG, Dunner K, Broaddus RR, et al. Loss of CD73-mediated actin polymerization promotes endometrial tumor progression. *J Clin Invest* (2016) 126(1):220–38. doi: 10.1172/JCI79380

102. Vasiukov G, Novitskaya T, Zijlstra A, Owens P, Ye F, Zhao Z, et al. Myeloid cell-derived TGFbeta signaling regulates ECM deposition in mammary carcinoma via adenosine-dependent mechanisms. *Cancer Res* (2020) 80(12):2628–38. doi: 10.1158/0008-5472.CAN-19-3954

103. Ni S, Wei Q, Yang L. ADORA1 promotes hepatocellular carcinoma progression via PI3K/AKT pathway. *Onco Targets Ther* (2020) 13:12409–19. doi: 10.2147/OTT.S272621

104. Man S, Lu Y, Yin L, Cheng X, Ma L. Potential and promising anticancer drugs from adenosine and its analogs. *Drug Discovery Today* (2021) 26(6):1490–500. doi: 10.1016/j.drudis.2021.02.020

105. Jensen K, Johnson LAA, Jacobson PA, Kachler S, Kirstein MN, Lamba J, et al. Cytotoxic purine nucleoside analogues bind to A1, A2A, and A3 adenosine receptors. *Naunyn Schmiedebergs Arch Pharmacol* (2012) 385(5):519–25. doi: 10.1007/s00210-011-0719-6

106. Tang J, Zou Y, Li L, Lu F, Xu H, Ren P, et al. BAY 60-6583 enhances the antitumor function of chimeric antigen receptor-modified T cells independent of the adenosine A2b receptor. *Front Pharmacol* (2021) 12:619800. doi: 10.3389/fphar.2021.619800

frontiers | Frontiers in Immunology

TYPE Review
PUBLISHED 13 March 2023
DOI 10.3389/fimmu.2023.1135086

OPEN ACCESS

EDITED BY
Junjiang Fu,
Southwest Medical University, China

REVIEWED BY
Xue-Yan He,
Cold Spring Harbor Laboratory, United States
Nan Zhang,
Wistar Institute, United States

*CORRESPONDENCE
Meina Yan
ymn@njmu.edu.cn;
yanmeina2007@126.com

†These authors have contributed equally to this work

SPECIALTY SECTION
This article was submitted to Cancer Immunity and Immunotherapy, a section of the journal Frontiers in Immunology

RECEIVED 31 December 2022
ACCEPTED 28 February 2023
PUBLISHED 13 March 2023

CITATION
Yan M, Gu Y, Sun H and Ge Q (2023) Neutrophil extracellular traps in tumor progression and immunotherapy. *Front. Immunol.* 14:1135086. doi: 10.3389/fimmu.2023.1135086

Neutrophil extracellular traps in tumor progression and immunotherapy

Meina Yan[1*†], Yifeng Gu[2†], Hongxia Sun[3] and Qinghong Ge[1]

[1]Department of Laboratory Medicine, The Affiliated Suzhou Hospital of Nanjing Medical University, Suzhou Municipal Hospital, Gusu School, Nanjing Medical University, Suzhou, Jiangsu, China, [2]Department of Laboratory Medicine, Tumor Hospital Affiliated to Nantong University, Nantong, Jiangsu, China, [3]Department of Gynecology and Obstetrics, The Affiliated Suzhou Hospital of Nanjing Medical University, Suzhou Municipal Hospital, Gusu School, Nanjing Medical University, Suzhou, Jiangsu, China

Tumor immunity is a growing field of research that involves immune cells within the tumor microenvironment. Neutrophil extracellular traps (NETs) are neutrophil-derived extracellular web-like chromatin structures that are composed of histones and granule proteins. Initially discovered as the predominant host defense against pathogens, NETs have attracted increasing attention due to they have also been tightly associated with tumor. Excessive NET formation has been linked to increased tumor growth, metastasis, and drug resistance. Moreover, through direct and/or indirect effects on immune cells, an abnormal increase in NETs benefits immune exclusion and inhibits T-cell mediated antitumor immune responses. In this review, we summarize the recent but rapid progress in understanding the pivotal roles of NETs in tumor and anti-tumor immunity, highlighting the most relevant challenges in the field. We believe that NETs may be a promising therapeutic target for tumor immunotherapy.

KEYWORDS

neutrophil extracellular traps, anti-tumor immunity, immunotherapy, tumor microenvironment, tumor progression

1 Introduction

Recent studies have shown that strategies that increase anti-tumor immune responses play important roles in the fight against cancer (1, 2). Although neutrophils are the first line of defense in innate immunity, tumour-associated neutrophils (TANs) could promote tumor progression (3). Moreover, under certain circumstances, the tumor microenvironment (TME) can attract neutrophils to tumor tissue and functionally modulate them to release web-like structures to form neutrophil extracellular traps (NETs) (4). NETs are composed of DNA fragments coated with histones and toxic granule proteins, such as citrullinated histone H3 (H3Cit), myeloperoxidase (MPO), neutrophil elastase (NE), cathepsin G (CG), matrix metalloproteinase 9 (MMP-9), which

were first discovered by Volker Brinkmann (5). NETs can capture and kill pathogens such as bacteria (6), fungi (7), viruses (8) and parasites (9). However, dysregulated NETs are harmful to the host.

Extensive studies have confirmed that uncontrolled and excessive NETs are involved in the pathogenesis of autoimmune disease (10, 11), cardiovascular disease (12), inflammatory disease (13) and cancer (14). It is worth mentioning that the function of NETs in tumors is gradually expanding. NETs are related to detrimental outcomes in breast cancer, pancreatic cancer, and hepatocellular carcinoma (15–17). NETs can promote tumor growth, invasion, metastasis, and drug resistance (18–20). Although accumulating evidence has clarified how NETs contribute to tumor progression, the role of NETs in anti-tumor immune responses is less clear. Therefore, further studies are necessary to elucidate the effects of NETs on tumor immunity. This review primarily focuses on the function of NETs in tumor and anti-tumor immunity, and highlights their application in tumor immunotherapy.

2 NET structure and formation

NETs are large, extracellular, web-like structures composed of DNA fibers coated with histones and granule proteins. Various stimuli trigger NET formation, such as lipopolysaccharides (LPS), phorbol 12-myristate 13-acetate (PMA) (5), high mobility group box 1 [HMGB1] (21), tumor-associated stimuli (tumor-associated antigen, granulocyte-colony stimulating factor [G-CSF] (22), C-X-C motif chemokine ligands [CXCLs] (23), cathepsin C (24), amyloid β (18), tissue inhibitor of metalloproteinases-1 [TIMP1] (16)), different immunological stimuli (interleukin [IL]-8/CXCL8, interferon [IFN]-α/IFN-γ/C5a, granulocyte-macrophage [GM-CSF/C5a), IL-1β, IL-17, IL-18, IL-33, immune complex (5, 20, 25–30), and other pathogen-associated molecular pattern molecules(PAMPs) (31, 32), autoantibodies (33), activated platelets (34), bacteria (35, 36), viruses (37), fungi, calcium ionophores (38), cigarette smoke (39), free fatty acids (40), and bleomyci (41) (Table 1). These stimuli activate the cell surface receptors of neutrophils; for example, HMGB1 recognizes advanced glycation end products (RAGE) receptor and toll-like receptor 4 (TLR4) (42), C3a recognizes C3a receptor (C3aR) (43), C5a recognizes C5a receptor (C5aR) (44), CXC chemokines recognize CXC chemokine receptors (CXCRs) (23), immune complex activate the FcγRIIIb receptor (45), LPS and platelets activate the toll-like receptor (TLR) (46, 47), bacterial products recognize G protein-coupled receptors (48), fungi recognize the Dectin1 and Dectin 2 receptor (49, 50). After the stimuli activate the receptors of the neutrophils, different intracellular signaling mechanisms are further activated, leading to the formation of two types of NETs. The classical form is lytic NETosis, which is considered a type of slow cell death. Besides, this process depends on the NADPH oxidase-mediated generation of reactive oxygen species (ROS), as evidenced by chronic granulomatous disease patients with mutations in the NADPH oxidase that fail to form NETs (51). Many reactive oxygen species (ROS)-inducing factors, including PMA, C5a, LPS, TLR-4, immune complexes, IL-8, cathepsin C, calcium ionophores activate NOX *via* different molecular pathways that cause ROS generation (24, 25, 30, 52–55). Accumulation of ROS triggers the escape of MPO and NE from the granules (56). MPO first activates NE to degrade the cytoskeleton in the cytoplasm (57). Subsequently, NE translates to the nucleus to cleave histones that contributes to chromatin decondensation (56). Blocking NE by NE inhibitor or serum leukocyte protease inhibitor (SLPI) disrupts NET formation (56), suggest that NE is required for chromatin extrusion. Moreover, in the late stage of chromatin decondensation, MPO binds to chromatin to promote further decondensation (56). In parallel, ROS synthesis also leads to the activation of peptidyl arginine deiminase 4 (PAD4), a calcium-dependent enzyme, which catalyzes histone citrullination, thereby promoting chromatin decondensation (58). Further study showed that inhibition of PAD4 *in vitro* greatly reduced the process of NETosis, and PAD4 knockout mice failed to produce NETs *in vivo*, indicated that PAD4 is critical for NET formation (6). Recently, Amulic et al., have added on another critical step in NET formation: the activation of cyclin-dependent kinases (CDKs) 4 and 6 (59). Although the mechanism is still unclear, this study suggested CDK4/6 likely

TABLE 1 Stimuli that induce NET formation.

Stimuli	References
LPS	(5)
PMA	(5)
HMGB1	(21)
G-CSF	(22)
CXCLs	(23)
Cathepsin C	(24)
Amyloid β	(18)
TIMP1	(16)
CXCL8/IL-8	(5)
[IFN]-α/IFN-γ/C5a	(25)
GM-CSF/C5a	(25, 26)
IL-1β	(27)
IL-17	(20)
IL-18	(29)
IL-33	(28)
Immune complexes	(30)
Pathogen-associated molecular pattern molecules (PAMPs)	(31, 32)
Autoantibodies	(33)
Activated platelets	(34)
Bacteria	(35, 36)
Viruses	(37)
Fungi	(38)
Calcium ionophores	(38)
Cigarette smoke	(39)
Free fatty acids	(40)
Bleomyci	(41)

function downstream of MAPK and ROS, and CDK6 is required, while CDK4 is partially required for NET formation (59, 60). Finally, nuclear membrane breakage, nuclear DNA and proteins are released. Released DNA further decorated with NE, MPO and cytosolic proteins, followed by plasma membrane rupture and NET extrusion and eventually lysis (56, 58). Besides, there are also noncanonical signaling triggers NET formation independently of ROS and PAD4, which mediated by a pore-forming protein gasdermin D (GSDMD) (36, 61). The second type of NET is a non-cell-death form in which NET are rapidly released from live cells without nuclear membrane disruption or loss of membrane disruption, which accompanied by granule proteins; this is known as nonlytic NET formation (25, 32, 34, 62). In this process, NETs were also found to include mitochondria DNA (mtDNA) when neutrophils are stimulated with LPS or C5a (25). Besides, it has been confirmed that some pathogens, such as S. aureus and C. albicans induce a rapid nonlytic NET formation by activating TLR2 and C3 (62). Moreover, this type of nonlytic NET formation is critical to acute invasive infection (62). Additionally, LPS-stimulated platelets could also promote nonlytic NETosis by activating platelet TLR4 (31, 34). However, the molecular mechanisms of nonlytic NETosis are still poorly understood. It can be ROS dependent or independent. A summary of NETosis induced by various stimuli is shown in Figure 1.

Apart from the physiological roles in host defense against pathogens, uncontrolled NET formation has been found to play a pivotal role in atherosclerosis (63, 64), coronary artery disease (65), autoimmune disease (66, 67), sepsis (68), metabolic disease (69), coronavirus disease 19 (COVID-19) (37, 70), and cancer (71).

3 Evidence of NETs promoting tumor progression

Accumulating evidence suggests that the TME can induce NET formation in various types of cancer, including hematologic malignancy (72–74) and solid tumors, such as breast cancer (75), ovarian cancer (76), gastric cancer (77), hepatic carcinoma (78), lung cancer (79), and colon cancer (80, 81). In particular, studies have revealed that NETs are increased in the peripheral blood and tumor tissues of patients with cancer (16, 76, 82). To date, NET formation in tumors may be partly due to tumor cells interacting directly and indirectly with neutrophils *via* the production of cytokines, chemokines, proteases, extracellular vesicles. Recent studies have shown that NETs can promote tumor progression *via* different mechanisms (Table 2).

3.1 NETs in tumorigenesis and growth

NETs have been shown to participate in tumor initiation and growth. For instance, non-alcoholic steatohepatitis (NASH) is a risk

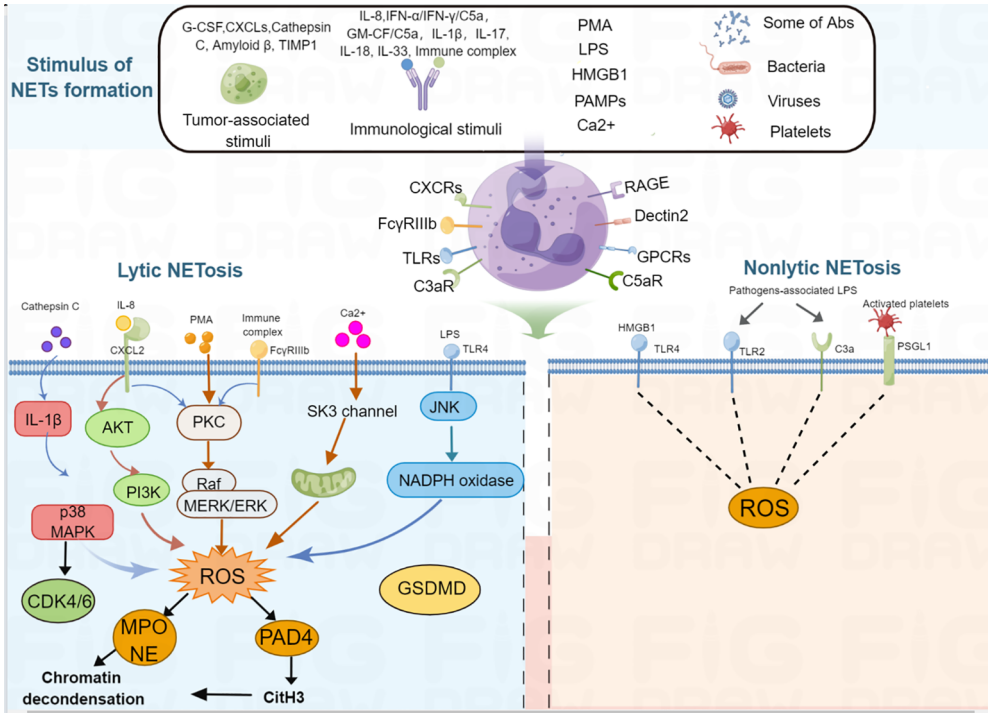

FIGURE 1
Schematic representation of NET formation. Different stimuli, such as PMA, tumor-associated stimuli, immunological stimuli, IL-1β, IL-17, IL-18, IL-33, LPS, PAMPs, some antibodies, activated platelets, bacteria, viruses, Ca2+ can induce NET formation. For lytic NETosis, external stimuli produce different kinds of ROS-inducing receptors, activating neutrophils to produce intracellular ROS, ROS further activates MPO and PAD4, then MPO activates NE and PAD4 citrullinates H3, therefore, leads to nuclear envelope disintegration, chromatin decondensation, cell membrane breakdown, NET formation. For non-lytic NETosis, some stimuli, such as *Staphylococcus aureus* and *Candida albicans*-associated LPS and HMGB1 can induce NET formation through a non-lytic manner.

TABLE 2 The roles of NETs in the cancer progression.

Cancer type	Detected NETs marker	NETs Formation Mechanism	Relevance to cancer progression	Potential Mechanisms	Ref.
Hepatocellular carcinoma (HCC)	MPO-DNA/ H3cit	Cancer cell-derived IL-8	Promote tumor invasiveness and metastasis; predict a poor prognosis	Activate TLR4/9-COX2; increase cathepsin G; oxidize mtDNA	(77, 83, 84)
Breast cancer	MPO-DNA/ H3cit	Cancer cell-derived cathepsin C	Promote tumor metastasis	Regulate CCDC25-ILK-β-parvin pathway; NF-κB pathway	(15, 24)
Pancreatic cancer	MPO-H3cit	Cancer cell-derived DDR1; TIMP1	Promote cancer cells migration and invasion; promote tumor metastasis; induce immunotherapy resistance	Activate IL-1β/EGFR/ERK pathway; inhibit CD8+ T cell function	(16, 19, 20, 85)
Ovarian cancer	MPO-H3cit	Cancer cell-derived inflammatory factors	Promote tumor metastasis and chemotherapy resistance	Unclear	(75)
Gastric cancer (GC)	MPO-DNA/ cfDNA/NE/ MPO-H3cit	Cancer cell-derived TME/Postoperative abdominal infectious complication	Promote tumor proliferation, invasion, migration, and metastasis	EMT, Activates TGF-β pathway	(76, 86)
Colon cancer	H3cit	Cancer cell-derived IL-8	Promote cancer proliferation and metastasis	EMT; Releases HMGB1 and activates TLR9 pathways	(79, 80)
Human melanoma	MPO-H3cit	Cancer-associated fibroblasts- derived Amyloid β	Promotes tumor proliferation	Unclear	(18)
Bladder cancer	NE-H3cit	Tumor immune microenvironment-derived HMGB1	Promotes tumor radioresistance	Unclear	(87)
Lung cancer	Unclear	Unclear	Promotes cancer invasion, metastasis	Interaction of TGF-β, IFN-β, and NE-pathways; trap CTCs	(78, 88)
Glioma	MPO-H3cit	IL-8	Promotes tumor proliferation and invasion	HMGB1/RAGE/IL-8 axis	(53)
Acute Promyelocytic Leukaemia (APL)	MPO-DNA/ H3cit	Activated platelets	Increases bleeding burden	Damage the integrity of endothelial cells	(71)
Hodgkin Lymphoma	H3cit	Unclear	Correlates with concurrent fibrosis and inflammation	Unclear	(72)
Diffuse large B-cell lymphoma (DLBCL)	MPO-DNA/ H3cit	IL-8	Promotes tumor proliferation and migration	TLR9-NFκB-STAT3-p38	(89)
Myeloproliferative neoplasms	H3cit	JAK2	Promotes thrombosis	Unclear	(73)

factor for hepatocellular carcinoma (HCC), and elevated levels of NETs contribute to the progression of NASH to HCC (90). Further study indicated that NASH-associated free fatty acids stimulate NET formation, which increased monocyte-derived macrophages and production of inflammatory cytokines, that contribute to HCC initiation (90). Furthermore, gut-derived LPS induced NET formation through activating TLR4 pathway, which further promoted alcohol-related HCC in mice model (91).Besides, Silvia Guglietta et al., demonstrated that C3aR-dependent NET formation induced protumorigenic neutrophils polarization, and promoted intestinal tumorigenesis (92). Subsequently, in a PAD4 knockout mouse model genetically incapable of NET formation, both subcutaneous tumors and hepatic metastases using murine colorectal (MC38) cells grew significantly more slowly than the WT mice (93). Similarly, human colorectal and hepatocellular cancer cell lines injected subcutaneously in the nu/nu mice treated with DNAse also grew slower (93), suggesting that inhibition of NETosis by preventing NET formation or degrading NETs is correlated with decreased tumor growth *in vivo*. Mechanistically, NETs-associated protein, NE, directly act TLR-4 on the cancer cells, leading to activation of the p38-PGC-1α pathway, followed by increased tumor mitochondrial function and increased tumor growth (93). The direct role of NETs in regulating the metabolism of cancer cells might provide a therapeutic opportunity to effectively halt tumor growth. Another study showed that subcutaneous injection of Lewis lung carcinoma

(LLC) cells reduced tumor growth while the B16 melanoma growth was not affected in PAD4-deficient mice (94). Further study showed that G-CSF released from LLC tumor increased more activated $CD11b^{high}$ neutrophils and NETs than B16 tumor, and B16 tumors in WT mice grew faster than the tumors in PAD4-deficient mice after G-CSF treatment (94). This highlights that, different tumors generate different TMEs, which affect the formation of NETs. In addition, it has been reported that increased NETs facilitated cell proliferation and tumor growth in diffuse large B-cell lymphoma (DLBCL) and were correlated with poor prognosis (89). The exact mechanism was that lymphoma cells secreted IL-8 induced NET formation, which depended on the Src and MAPK pathways, in turn, NETs directly activated of the TLR9-NFκB-STAT3-p38 pathway to promote tumor progression (89). In glioma, NETs-derived HMGB1 increased cell proliferation by binding to RAGE and activating the NF-κB signaling pathway (53). Moreover, a recent study demonstrated that DNA released from NETs enhances pancreatic tumor growth (95). And, the mechanism of the pro-tumorigenic effect was not directly through effects on cancer cells, but rather the through NET-DNA induced autophagy-dependent activation of pancreatic stellate cells, causing increased MMP-2 and -9 production to promote cancer progression (95). Hafsa et al. demonstrated that cancer-associated fibroblasts are important factors mediators of NET formation. They found that cancer-associated fibroblast-induced NETs contribute to tumor proliferation in Bladder cancer and pancreatic adenocarcinoma (18). Although further investigation is needed, there is a plenty of *in vitro* and *in vivo* evidence that inhibition of NETs decreased tumor growth in several different cancer types.

3.2 NETs in tumor metastasis

Metastasis is a hallmark of advanced stage cancer, which is the primary cause of cancer-related mortality. Moreover, metastasis is a multistep process, including the detachment of cancer cells from the primary tumor, the dissemination of tumor cells to surrounding tissues and distant organs (96). There is also evidence that NETs result in the metastasis cascade of animal and human tumors (97, 98). Epithelial–mesenchymal transition (EMT) is critical for tumor cells to physically disseminate from the primary site, which is the first step in distant metastasis (99). In breast cancer, after treatment with NETs, MCF7 cells gained a migratory and mesenchymal phenotype, accompanied by EMT induction (100). Moreover, the EMT program further upregulated the expression of cancer stem cells (CSCs) markers, such as CD44, and induced a pro-inflammatory response in breast cancer cells (100). These results show that NETs might contribute to breast cancer metastasis through the activation of EMT program. In another study, NETs promoted gastric cancer cells migration through EMT, inhibition of NETs by DNAse-1/GSK-484 upregulated the epithelial marker, E-cadherin, while downregulated the mesenchymal marker (77). Consistently, Jin et al. found that NETs facilitated cell migration and invasion, and EMT in pancreatic cancer. Besides, NETs-mediated EMT is dependent on the activation of IL-1β/EGFR/ERK pathway (85). Following this study, NETs decreased expression of epithelial markers E-cadherin (CDH1), epithelial cell adhesion molecule (EPCAM) and increased expression of mesenchymal markers vimentin (VIM), fibronectin (FN1), which initiates EMT transcriptional programs in colon cancer (80).This EMT-like phenotype increased cell motility and the migration of colorectal cancer cells, which further promoted local invasion and metastasis (80). In non-small cell lung cancer, NETs induced EMT through activating NF-κB/NLRP3 inflammasome pathway by downregulating the expression of long non-coding RNA MIR503HG, which further enhanced tumor cell metastasis (101). Additionally, one study showed that NETs could induce pancreatic cancer cells migration, invasion and EMT through activating the IL-1β/epidermal growth factor receptor (EGFR)/extracellular signal–regulated kinase (ERK) pathway (85). Taken together, there is increasing evidence that NETs can support tumor metastasis through inducing EMT program. In addition to EMT, NETs also increased cancer cell migration and invasion through other molecular signaling pathways. For example, NET markers, such as MPO-DNA and H3Cit were increased in patients with HCC and predicted a poor prognosis (83). Further studies revealed that NETs-associated Cathepsin G promoted HCC cell invasion through decreasing E-cadherin expression, which promoted HCC metastasis (83). Moreover, HCC cells not only stimulated NET formation, but also modified its composition by increasing the oxidized mitochondrial DNA, which increased HCC cells invasion and lung metastasis *in vitro* and vivo (84). In breast cancer, NETs could promote cell migration and invasion by activating nuclear factor (NF)-κB pathway (75). Another study found that NETs facilitate gastric cancer cell migration, invasion and metastasis by activating the transforming growth factor (TGF)-β pathway (86). Besides, recent research demonstrated that the receptor tyrosine kinase discoid domain receptor 1(DDR1) induces CXCL5 production to recruit neutrophils to stimulate NET formation, leading to pancreatic cancer cell invasion and metastasis (19). Taking into account the above findings, NETs might contribute to metastasis initiation that includes detachment of cancer cells from primary tumor, EMT and increased cell migration and invasion.

Primary cancer cells acquired the migration and invasion ability through EMT or other molecular signaling pathway, then invaded into the surrounding tissues. These cancer cells further intravasate to enter the circulation, where they are termed as circulating tumor cells (CTCs) (96). CTCs must overcome fluid shear stress, immune cells and oxidative stress to colonize distant organs (102). It has been reported that NETs can protect CTCs from cytotoxic immune cells with NETs-mediated physical barrier (103), thus increased metastatic seeding. Furthermore, localized degradation of NETs by photoregulated release of DNase I abolished the NET-mediated capture and colonization of metastasizing colorectal cancer cells in the liver (103). Besides, NETs were also found to promote adhesion of tumor cells to distant organ sites by trapping circulating lung carcinoma cells within DNA webs, which further increased formation of hepatic metastasis (88). Inhibition of NETs attenuated the development of hepatic metastases, suggest that NETs were responsible for lung cancer metastasis. In another study, NETs could interact with, trap (CTCs), which further

contributed to tumor metastasis in lung cancer *in vitro* and vivo (104).Moreover, both NETs and CTCs expressed β1-integrin protein, which acted as a bridge mediating the interactions between CTCs and NETs, then increased cancer cell adhesion to distant organs (104). These findings highlight the molecular mechanism by which NETs can trap CTCs *via* a protein–protein interaction. Whether NETs-derived proteins have other molecular mechanisms to protect CTCs from risks, such as anoikis and apoptosis, are still unclear now. Thus, it is important to explore the mechanism of CTCs adhesion to NETs, that might identify NETs as potential therapeutic targets. Recently, NETs were found to trap hepatocellular carcinoma cells, and trigger the cytotoxicity resistance, enhanced invasiveness and angiogenesis of the trapped HCC cells (78). Mechanically, NETs enhanced metastatic of the trapped HCC cells by activating TLR4/9-COX2 signaling, that induced an inflammatory response (78). Yang et al. (15) demonstrated that NET-DNA functions as a chemotactic factor to attract CTCs, then induces cancer cells migration, adhesion, and distant metastases in breast cancer. Further study revealed that NET-DNA interact with coiled-coil domain-containing 25 (CCDC25) to activate the ILK-β-parvin-RAC1-CDC42 pathway, which may further facilitate the metastasis of cancer cells (15). Furthermore, Xiao et al (24). found that the protease cathepsin C activates the PR3-IL-1β axis, induces NET formation, and contributed to the early stage of metastatic colonization in breast cancer lung metastasis. Similar studies have shown that complement 3 (C3) is increased in lung mesenchymal stromal cells, and C3-C3a receptor axis promotes neutrophil recruitment and NET formation, which facilitates breast cancer cell metastasis to the lungs (105). And this function of C3 in the regulation of NETs depends on Th2-drived IL-4/IL-13-STAT6 pathway (105). Taken together, these studies confirm that NETs promote cancer metastasis through regulating multiple steps of cancer metastasis.

3.3 NETs in tumor therapy resistance

In addition to tumor growth and metastasis, tumor therapy resistance remains a major challenge in current research. Resistance to tumor includes both primary and secondary resistance. Targeted therapy is frequently associated with acquired resistance (106), whereas immunotherapy is often associated with primary resistance (107). In the area of malignancy, tumor-associated neutrophils (TANs) have been shown to contribute to cancer resistance to therapies (108). Building on the function of TANs in cancer resistance to therapy, NET-dependent mechanisms of drug resistance are beginning to be recognized. For example, drug-resistant cancer cells are dormant during clinical remission and can be reactivated leading to cancer recurrence (109). It has been demonstrated that NETs are required for awakening dormant cancer (110). Mechanistic analysis revealed that NET-associated NE and MMP-9 proteins cleave laminin and activate integrin α3β1 signaling, which further induces focal adhesion kinase (FAK), ERK1/2, myosin light-chain kinase (MLCK), and yes-associated protein (YAP) signaling to reactivate dormant cancer cell proliferation (110). Moreover, NETs could trap doxorubicin (DOX) and inhibit its diffusion into ovarian cancer cells; the degradation of NETs could increase the DOX-induced apoptosis of ovarian cancer cells (111), suggested that NETs induced DOX chemotherapy resistance. Radiotherapy is an important component of cancer treatment, however, radioresistance can lead to tumor progression and mortality (112). One study revealed that radiation therapy could stimulate NET formation in bladder cancer; in turn, increased NETs contributed to tumor radioresistance (87). Researchers further found that HMGB1 was released by tumor cells after radiation therapy, and HMGB1 promoted NET formation by activating TLR4 signaling (87). Inhibition of HMGB1 and NETs significantly delayed tumor proliferation. Moreover, NET levels were significantly higher in radiation therapy non-responders than in radiation therapy responders, suggesting that NETs seem to have a pivotal influence on radioresistance (87). Additionally, another study indicated that NETs participated in the post-radiotherapy local recurrence of in breast cancer (113). NETs are increased in relapsed human breast cancer and are associated with poor prognosis, and inhibition of NETs might provide new opportunities to address post-radiotherapy resistance in clinical trials. Overall, NETs play important roles in tumor progression (Figure 2), further research on the molecular mechanism of NET-mediated tumor progression is warranted.

4 NETs in immune cells

Beyond the well-known functions of NETs in the diversified phases of tumor metastasis and tumor progression, NETs also play critical roles in tumor immune exclusion. The tumor-promoting function of NETs is mediated not only by diverse mechanisms, as described above, but also by attenuating the antitumor functions of the immune system. Accumulating evidence suggests that NETs are considerably involved in the regulation of immune cells (114, 115).Thus, interest in understanding how NETs interact with immune cells to modulate the tumor immune response of tumors is increasing.

4.1 Macrophages and DCs

Macrophages and Dendritic Cells (DCs), two major Antigen Presenting Cells (APCs), are pivotal innate immune cells that regulate the anti-tumour immune responses (116, 117). It has been shown that NETs activate macrophages and DCs through upregulating important costimulatory molecules (CD80, CD86) at early times (30 min), however, macrophages and DCs undergo apoptosis after prolonged incubation with NETs (118). Further study showed that NETs-derived histone H2A and to a lesser degree elastase caused mitochondrial morphological alterations, which further induced a caspase- and AIF-dependent apoptosis (118).These results indicated that NETs interact with macrophages and DCs for a long time might enhance tumor immunosuppression. Another study revealed that LPS induced significant upregulation of surface markers of activation and maturation on DCs, such as, CD80, CD83, and CD86 was significantly

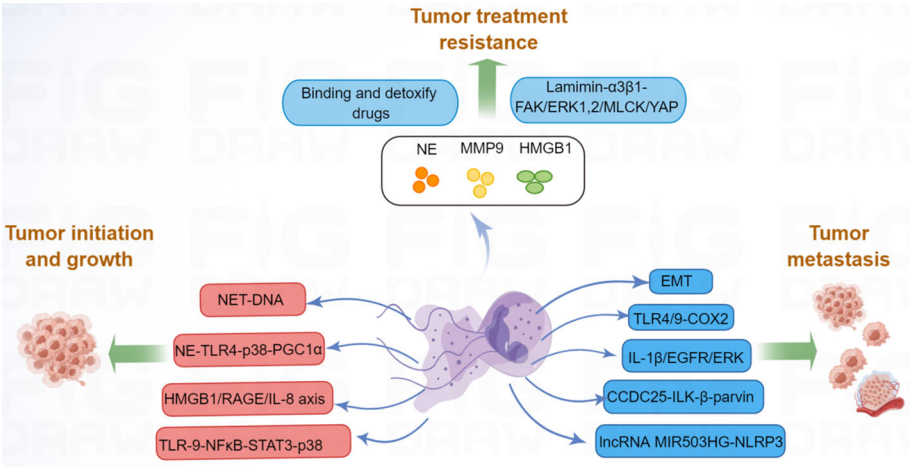

FIGURE 2
NETs promote tumor progression *via* many molecular pathways. NET can increase tumor cell proliferation by activating TLR9-NFκB-STAT3-p38 pathway; NET-DNA increased MMP-2 and -9 production, which increased tumor growth; NE released by NETs, can enhance tumor growth by activating TLR4-p38-PGC-1α pathway; HMGB1, released by NETs, can promote tumor growth by RAGE-IL-8 axis. Moreover, NETs promote tumor metastasis by promoting EMT, activating TLR4/9-COX2, IL-1β-EGFR-ERK, CCDC25-ILK-β-parvin, and lncRNA MIR503HG-NLRP3 pathway. Besides, NETs-associated NE, MMP-9, and HMGB1 contribute to tumor therapy resistance.

reduced when DCs were exposed to both NETs and LPS (119). Moreover, NETs plus LPS significantly promoted inflammasome activation though increased IL-1β secretion, and decreased LPS-induced IL-10, an immunomodulatory cytokine, and IL-12, a T cell stimulatory factor in both macrophages and DCs (119). In turn, both macrophages and DCs could also degrade NETs (119), suggesting that NETs acted as double-edged swords of innate immunity. Besides, the addition of NETs to IL-4/GM-CSF-treated monocytes downregulated the expression of the IL-4 receptor in monocytes and prevented monocytes from fully differentiating into DCs but induced them to differentiate into M2 macrophages (120). It has been reported that M2 macrophages such as tumor-associated macrophages (TAMs) promote tumor growth and invasion (121). Thus, NETs might contribute to tumor progression through promoting M2 polarization of macrophages. Moreover, DNA released from NETs also mediated pro-inflammatory macrophage polarization by activating the TLR-9 pathway (122). In addition, NETs induced the production of IL-8 by macrophages through activating the TLR9/NF-κB signaling pathway, which further aggravated atherosclerosis (123). Georgakis et al. found NETs from patients with systemic lupus erythematosus activate plasmacytoid DCs (pDCs) to secrete IFN-α, correlating with severe, active disease (124). Mechanistically, immunocomplexes stimulated neutrophils release IL-33-decorated NETs, which recognized the IL-33 receptor ST2L on pDCs, and further activating TLR9-IRF7 pathway, leading to IFN-α secretion (124). Similarly, cigarette smoke extract-induced NETs also promoted pDCs maturation and activation (125). The role of pDCs in TME is still ambiguous now (126). Thus, we hold the opinion that whether NETs-mediated pDCs activation display active immunity functions or involved in immune tolerance is determined by the specific tumor microenvironmental. In contrast, another recent study demonstrated that NETs induced by oleic acid stimulated DCs caused increased levels of CD40, CD86, and human leukocyte antigen DR (HLA-DR), indicating that oleic acid-induced NETs facilitated the maturation and activation of DCs (40). NE is an important component of NETs. A recent study indicated that NE could impair macrophage phagocytic function through the cleavage of cell surface receptors or opsonins (127). Furthermore, treatment of immature DCs with NE induced the generation of CD4+FOXP3 +Tregs, which showed suppressive activity *in vitro* (128). NETs regulate macrophages and DCs through different pathways, indicating that NETs might be an important indicator for antitumor immune response.

4.2 Natural killer cells

Natural killer (NK) cells are an important subset of innate immune cells that are found to be essential for tumor immunosurveillance (129). One study showed that NETs might inhibit the function of NK cells by upregulating *LGAS9* and *CEACAM1* genes, which are negative regulators for NK cells in patients with COVID-19 (130). Other groups have confirmed that NETs can accumulate decidual NK cells, which leads to immunological disorders in the placenta in patients with systemic lupus erythematosus (131). Moreover, CG, an important component of NETs, cleaves the NK cell-associated activating receptor NKp46, which further impairs NK cell function, including IFN-γ production and cell degranulation (132), suggesting that NETs might inhibit NK-cell based antitumor response. In turn, NK cells also induced NET formation *via* IFN-γ secretion, which further promotes thrombus formation (133).

4.3 T cells

T cells have long been regarded as a major subset of the immune cells involved in tumor immunity. Miranda et al. demonstrated that

Toxoplasma gondii-induced NETs promote CD4+ T cell recruitment and the secretion of IFN-γ, TNF, and IL-6, indicating that NETs contribute to the adaptive immune response (134). In addition, NET-stimulated DCs promote primary CD4+ T cell differentiation into T helper (Th) 1 and Th17 cells compared with DCs without stimulation by NETs (40). Consistent with this finding, it has been shown that NETs can directly promote naive T cell differentiation into Th17 cells (135). Further studies have shown that histones are involved in the NET-induced increase in Th17 cell differentiation, and this regulation is dependent on the TLR2/MyD88 pathway. Moreover, NETs could also activate Th17 cells, that enhanced immune cells recruitment in atherosclerotic plaques (136). These findings demonstrate that NETs may be acritical factor influencing the differentiation of Th17 cells. It has also been reported that increased infiltration of Th17 cells promoted tumor progression and was correlated with a poor prognosis (137, 138). By inducing Th17 cell differentiation, NETs might be important for Th17 cell-related cancer immunotherapy. Additionally, in patients with severe COVID-19, focal NETs were negatively associated with CD8+ T cell infiltration in lung tissues (139). Taken together, how to target NETs to improve Th helper-mediated anticancer immunity needs to be explored in the future.

4.4 B cells

B cells could inhibit tumor progression through secreting immunoglobulins, promoting T cell response, and killing cancer cells (140). In addition to macrophages, DCs, and NK cells, NETs are also associated with B cells. For example, IL-37-DNA complexes derived from NETs can trigger B cell proliferation and activation in lupus erythematosus (LE) patients (141). Further study showed that NET-derived LL37–DNA complexes gain access to endosomal compartments of B cells and activate TLR9 pathway (141). In addition, citrullinated histones in NETs are thought to act as a continuous source of fresh antigens for B cells, promoting the production of new immunoglobulin M pathogenic anti-citrullinated protein antibodies in rheumatoid arthritis (142).Another study showed that NETs might contribute to B cell activation and autoantibody secretion, which aggravates tissue damage in hidradenitis suppurativa (114). Moreover, elevated levels of NETs have been found to induce B-cell differentiation into plasma cells by activating the mitogen-activated protein kinases (MAPK) p38 pathway in bullous pemphigoid (143). These findings indicate that NETs might regulate tumor immune response. by acting on B cells. In summary, these studies suggest that NETs play an important but complicated role in immune cells (Figure 3).

5 Targeting NETs for tumor immunotherapy

Immunotherapy has provided new strategies for cancer therapy and has increased long-term survival in subsets of patients. The significant and wide-ranging effects of NETs in regulating tumor cells and immune cells have prompted the clinical investigation of additional therapies to improve the efficacy of tumor immunotherapy.

5.1 NETs in anti-tumor immunity

Given that there is much evidence for the participation of NETs in many types of immune cells, it is no surprise that NETs regulate tumor immunity. For instance, in non-small cell lung cancer, bladder cancer, and metastatic melanoma, NET density is inversely correlated with CD8+ T cell density, suggesting that NETs might impair CD8-mediated antitumor immunity (144). Furthermore, studies have shown that both CD4+ and CD8+ T cells in the NET-rich TME express significantly higher levels of T cell exhaustion-related markers, such as programmed cell death protein 1 (PD-1), T cell immunoglobulin domain and mucin domain 3 (Tim3), and lymphocyte-activation gene 3 (Lag3), indicating that increased NETs in the TME are responsible for the loss of T cell function (145). Further research demonstrated that both mouse and human neutrophil-derived NETs contained the immunosuppressive ligand programmed death-ligand 1 (PD-L1), blocking of PD-L1 in NETs obviously decreased tumor growth (145). In addition, NETs can obstruct contact between immune cells and the surrounding target tumor cells by wrapping and coating tumor cells and protecting them from CD8+ T cells and NK cell-mediated cytotoxicity, which further hamper immune-cell control of tumor metastases (23). Moreover, NETs inhibition sensitized tumors to PD-1+CTLA-4 dual checkpoint blockade (23). Another group reported that NETs participated in IL-17-associated immunosuppression in pancreatic cancer (20). Mechanistically, IL-17 recruited neutrophils, induced NETs formation, which favors tumor CD8+ T cell inactivation and spatial exclusion (20). Wang et al. recently demonstrated that NETs and regulatory T cells (Tregs) co-localized in NASH-associated HCC and that NETs could promote the differentiation of naïve $CD4^+$ T cells into Tregs which contributes to the initiation and progression of NASH-HCC (146). Further study showed that NETs activated TLR4 pathway in naive CD4+ T cells, leading to naive CD4+ T cells metabolic processes reprogram, tilting the balance toward mitochondrial oxidative phosphorylation (OXPHOS) to promote Treg differentiation (146). In addition, another study demonstrated that NETs lead to a hypercoagulable state in gastric cancer (147). Further studies revealed that NETs upregulated angiopoietin-2 (ANGPT2), and ANGPT2 was significantly correlated with macrophage M0, NK cell resting, and mast cell activation, suggesting that NETs might be involved in the regulation of the immune microenvironment in gastric cancer. Other studies have shown that NET-related long intergenic non-protein coding RNA 426 (LINC00426) contributes to the innate immune cyclic GMP-AMP synthase (cGAS)-stimulator of interferon genes (STING) signaling pathway in head and neck squamous cell carcinoma (148). Taken together, these observations suggest that the pro-tumorigenic activities of NETs are also mediated by the attenuation of antitumor functions of the immune system, which occurs by impairing the function of tumor-antagonizing immune cells and the maintenance of an immunosuppressive molecular signature in the TME.

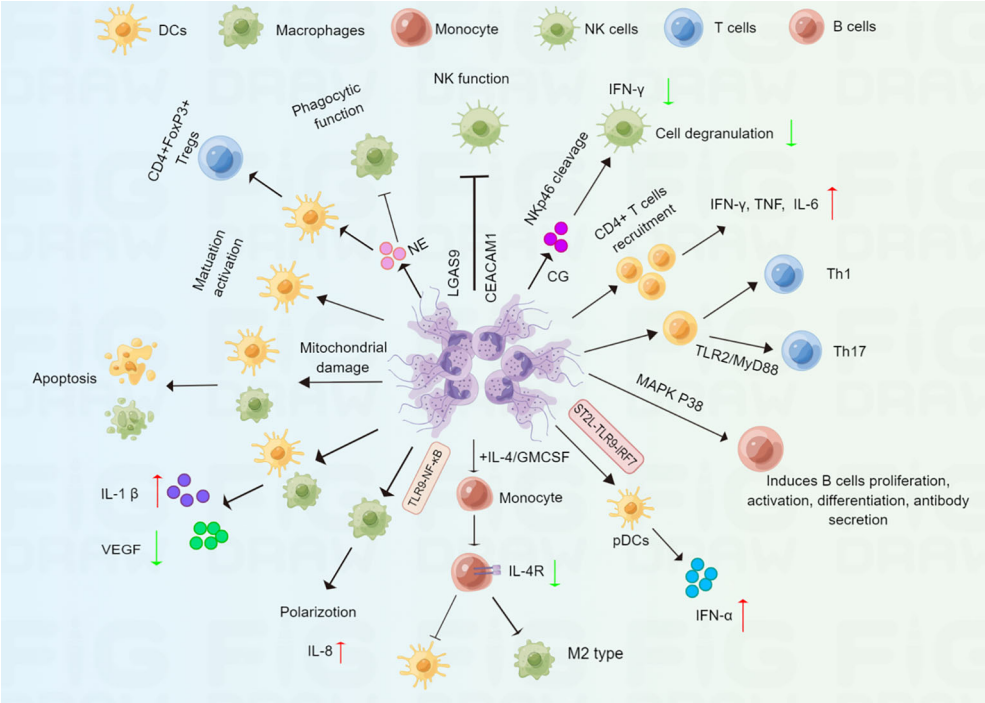

FIGURE 3
Schematic representation of NET in regulating immune cells. NETs can mediate immune response *via* complex regulations at multiple immune cells. Macrophages and DCs: NETs promote macrophages apoptosis, polarization, cytokine production, and impair macrophage phagocytic function; NETs can promote DCs apoptosis, maturation, activation and cytokine production. NK cells: NETs can impair NK cell function, including IFN-γ production and cell degranulation. T cells: NETs promote CD4+ T cell differentiation into Th1 and Th17 cell; NETs also promote immature DCs differentiation into CD4+FOXP3+Tregs.B cells: NETs can induce B cells proliferation, activation, differentiation and antibody secretion.

5.2 NETs in immunotherapy

As NETs are considerably involved in regulating the behavior of tumor cells and immune cells, thus affecting the efficacy of tumor immunotherapy in different ways. Therefore, targeting NETs is a relatively new option to inhibit tumor progression and boost the efficacy of immunotherapy, including decreasing NET formation and/or activity in tumors. Current trials targeting NETs are mainly based on interference with NETs formation or direct dismantling of their structure. For example, targeting of PAD4 with GSK484 inhibitor repressed NETs formation and prevented dormant cancer cell awakening in a breast cancer model (110); targeting PAD4 with the novel PAD4 inhibitor BMS-P5, delayed the appearance of symptoms and MM progression (149). In addition, targeting the tumor-associated induction of NETs formation is also a promising therapeutic strategy. ROS, TNF-α, IL-8, cathepsin C, amyloid β, and CXCR-1 and -2 are all responsible for NETs release, as mentioned above. Blocking these tumor-associated NET stimuli with antibodies or inhibitors might prevent metastatic colonization by abolishing NET-mediated capture of circulating tumor cells. Other groups have also focused on the interaction mediators present in NETs and cancer cells, such as integrin (104), TLR9 (94) and CCDC25 (15). Functional blocking of these mediators may also contribute to tumor treatment.

Recent report has demonstrated that NETs are associated with immunotherapy resistance (150). NET-mediated physical barriers inhibited contact between immune cytotoxic cells and tumor cells and influenced immune checkpoint therapy in primary colorectal cancer (88). Using photoregulated enzyme delivery for efficient release of DNase I for localized degradation of NETs destroyed the NET-mediated physical barrier, thereby enhancing the interaction of immune cytotoxic cells with tumor cells, and sensitized immune checkpoint therapy for primary colorectal cancer, and eliminating NET-mediated capture and colonization of metastasizing cells in the liver sinusoids (88). These results suggest inhibition of NETs by DNase I facilitate the removal of immunosuppressive NETs, and improve the efficacy of clinical treatment. Similarly, high levels of NETs inhibited the response to anti-PD-1 therapy in a mouse colorectal cancer model (150). Furthermore, degradation of NETs by DNase I reduced tumor cell-induced TAN infiltration within tumors, and increased CD8+ T cell infiltration and cytotoxicity, which further improved the efficacy of PD-1 blockade to inhibit tumor growth (150). In addition, NETs also mediated resistance to immune checkpoint blockade PD-1 and cytotoxic T-lymphocyte

associated protein 4 (CTLA4) by Ovarian cancer in pancreatic cancer (20). Besides, NETs could greatly counteract the efficacy of NK cell therapy and contribute to HCC recurrence (151). Inhibition of NETs enhanced NK cell infusion to kill cancer cells (151).These findings indicated that NET-mediated immunotherapy resistance is through protecting tumor cells from cytotoxic immune attack. Moreover, NET-associated T cell exhaustion was abrogated by DNase, which also supports the use of NET-targeting therapeutics to restore proper T cell antitumor activity. In addition, chimeric antigen receptor (CAR)-T therapy in solid tumors often resistance to immunotherapy, and NETs can prevent the interaction of CAR-T cells with tumor cells (152). Therefore, NET inhibition might overcome CAR-T resistance in the future. In addition, vaccination with DCs loaded with NETs reduced myeloproliferation in transgenic mice, and induced CD8+ T cell responses (153), suggesting that NETs might be used in the development of a leukemia vaccine. Taken together, NETs have the potential to enhance the efficacy of clinical immunotherapy by promoting T cell tumor infiltration and enhancing cytotoxic immune cells on tumor cells and could be used in tumor vaccines in the future (Figure 4).

6 Concluding remarks

While diverse studies have demonstrated the classic functions of NETs in promoting, tumor growth, metastatic spread and cancer therapy resistance, accumulating data in recent years have clearly shown that NETs play an important role in immune regulation. In this review, we summarized the functions of NETs in immune cells, anti-tumor immunity, and tumor immunotherapy. A better understanding of the crosstalk between NETs and anti-tumor immunity can help overcome cancer immunotherapy resistance. However, the role of NETs in anti-tumor immunity in other immune cells, including macrophages, DCs, myeloid-derived suppressor cells, B cells, and, has not been sufficiently evaluated. Moving forward, we believe that detailed analyses of the role of NETs in immune, tumor, and TME/stromal cells are required. Moreover, it should be noted that a number of proteins and potentially other NETs compounds may be detrimental for antitumor immune response. Thus, scientists need to carry out more research to identify the role of NETs-associated proteins in immunotherapy. These efforts would provide a substantial basis for targeting NETs as a new/alternative choice and a new approach for clinicians in cancer immunotherapy.

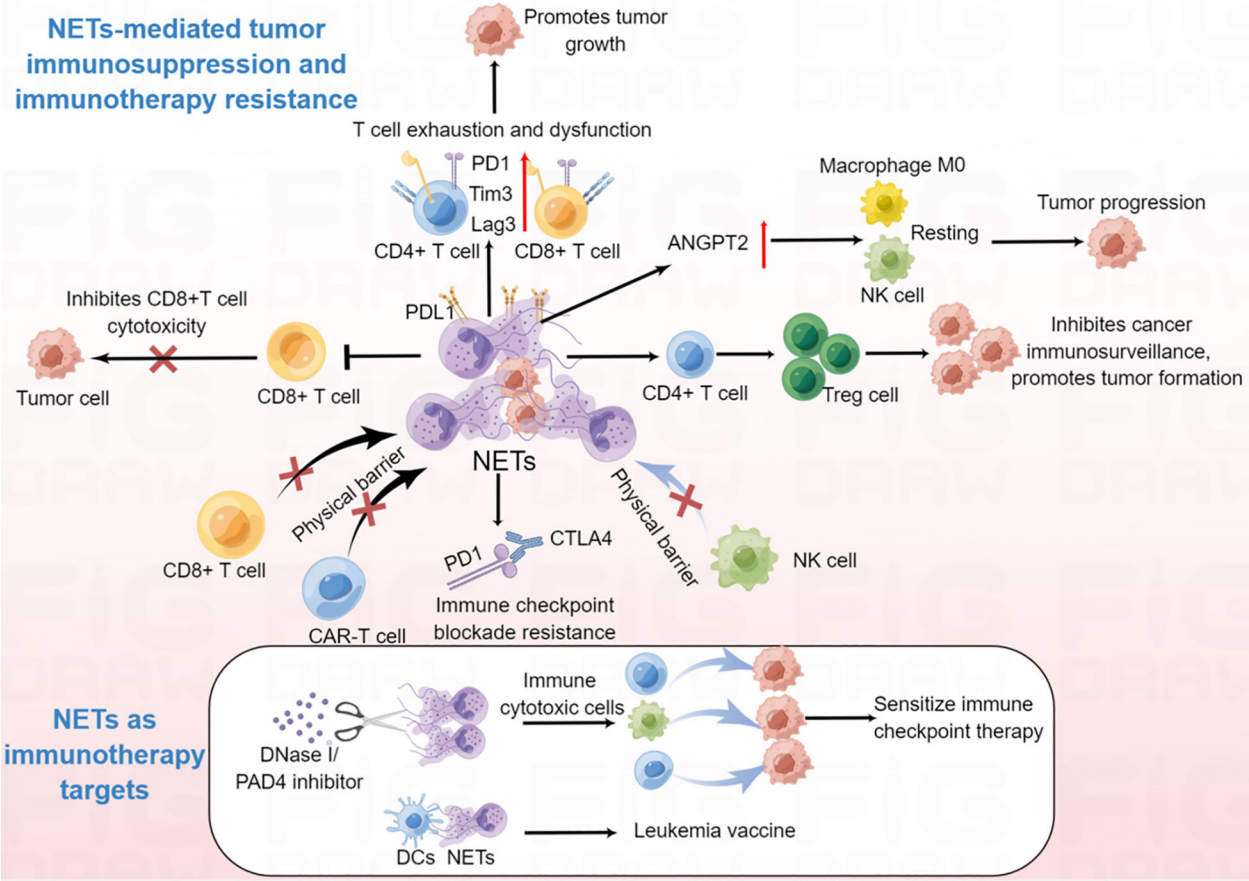

FIGURE 4
The emerging roles of NETs in the modulation of anti-tumor immunity and immunotherapy. NETs can promote CD4+ and CD8+ T cells exhaustion and dysfunction; NET-mediated physical barrier decreases the contact of immune cytotoxic cells (CD8+ T cell, NK cell and CAR-T cell) with tumor cells; NETs promote the differentiation of naïve CD4+ T cells into Tregs, which further contribute to tumor initiation and progression; NETs promote macrophage M0, NK cell resting. Degradation of NETs by DNase I can enhance the efficiency of tumor immunotherapy; NET/DC vaccine may be used for leukemia treatment.

Author contributions

MY: conception of the work, MY, YG, HS, and QG extensive literature search and manuscript drafting. MY and YG contributed to the editing and revising of this work. All authors contributed to the article and approved the submitted version.

Funding

This work was supported by Suzhou Science and Technology Development Plan Project (SYS2020166), Jiangsu Provincial Commission of Health and Family Planning (H2019064) and Suzhou Gusu Health talent Research Project (GSWS2021038).

Conflict of interest

The authors declare that the research was conducted in the absence of any commercial or financial relationships that could be construed as a potential conflict of interest.

Publisher's note

References

1. Poggio M, Hu T, Pai CC, Chu B, Belair CD, Chang A, et al. Suppression of exosomal PD-L1 induces systemic anti-tumor immunity and memory. *Cell* (2019) 177 (2):414–27.e13. doi: 10.1016/j.cell.2019.02.016

2. Banta KL, Xu X, Chitre AS, Au-Yeung A, Takahashi C, O'Gorman WE, et al. Mechanistic convergence of the TIGIT and PD-1 inhibitory pathways necessitates co-blockade to optimize anti-tumor CD8(+) T cell responses. *Immunity* (2022) 55(3):512–26.e9. doi: 10.1016/j.immuni.2022.02.005

3. Tian S, Chu Y, Hu J, Ding X, Liu Z, Fu D, et al. Tumour-associated neutrophils secrete AGR2 to promote colorectal cancer metastasis via its receptor CD98hc-xCT. *Gut* (2022) 71(12):2489–501. doi: 10.1136/gutjnl-2021-325137

4. Rayes RF, Mouhanna JG, Nicolau I, Bourdeau F, Giannias B, Rousseau S, et al. Primary tumors induce neutrophil extracellular traps with targetable metastasis promoting effects. *JCI Insight* (2019) 5(16). doi: 10.1172/jci.insight.128008

5. Brinkmann V, Reichard U, Goosmann C, Fauler B, Uhlemann Y, Weiss DS, et al. Neutrophil extracellular traps kill bacteria. *Science* (2004) 303(5663):1532–5. doi: 10.1126/science.1092385

6. Li P, Li M, Lindberg MR, Kennett MJ, Xiong N, Wang Y. PAD4 is essential for antibacterial innate immunity mediated by neutrophil extracellular traps. *J Exp Med* (2010) 207(9):1853–62. doi: 10.1084/jem.20100239

7. Urban CF, Reichard U, Brinkmann V, Zychlinsky A. Neutrophil extracellular traps capture and kill candida albicans yeast and hyphal forms. *Cell Microbiol* (2006) 8 (4):668–76. doi: 10.1111/j.1462-5822.2005.00659.x

8. Hong W, Yang J, Zou J, Bi Z, He C, Lei H, et al. Histones released by NETosis enhance the infectivity of SARS-CoV-2 by bridging the spike protein subunit 2 and sialic acid on host cells. *Cell Mol Immunol* (2022) 19(5):577–87. doi: 10.1038/s41423-022-00845-6

9. Guimarães-Costa AB, Nascimento MT, Froment GS, Soares RP, Morgado FN, Conceição-Silva F, et al. Leishmania amazonensis promastigotes induce and are killed by neutrophil extracellular traps. *Proc Natl Acad Sci U.S.A.* (2009) 106(16):6748–53. doi: 10.1073/pnas.0900226106

10. Chapman EA, Lyon M, Simpson D, Mason D, Beynon RJ, Moots RJ, et al. Caught in a trap? proteomic analysis of neutrophil extracellular traps in rheumatoid arthritis and systemic lupus erythematosus. *Front Immunol* (2019) 10:423. doi: 10.3389/fimmu.2019.00423

11. Apel F, Andreeva L, Knackstedt LS, Streeck R, Frese CK, Goosmann C, et al. The cytosolic DNA sensor cGAS recognizes neutrophil extracellular traps. *Sci Signal* (2021) 14(673). doi: 10.1126/scisignal.aax7942

12. Kim JK, Hong CW, Park MJ, Song YR, Kim HJ, Kim SG. Increased neutrophil extracellular trap formation in uremia is associated with chronic inflammation and prevalent coronary artery disease. *J Immunol Res* (2017), 8415179. doi: 10.1155/2017/8415179

13. Schroder AL, Chami B, Liu Y, Doyle CM, El Kazzi M, Ahlenstiel G, et al. Neutrophil extracellular trap density increases with increasing histopathological severity of crohn's disease. *Inflammation Bowel Dis* (2022) 28(4):586–98. doi: 10.1093/ibd/izab239

14. Li JC, Zou XM, Yang SF, Jin JQ, Zhu L, Li CJ, et al. Neutrophil extracellular traps participate in the development of cancer-associated thrombosis in patients with gastric cancer. *World J Gastroenterol* (2022) 28(26):3132–49. doi: 10.3748/wjg.v28.i26.3132

15. Yang L, Liu Q, Zhang X, Liu X, Zhou B, Chen J, et al. DNA Of neutrophil extracellular traps promotes cancer metastasis via CCDC25. *Nature* (2020) 583 (7814):133–8. doi: 10.1038/s41586-020-2394-6

16. Schoeps B, Eckfeld C, Prokopchuk O, Böttcher J, Häußler D, Steiger K, et al. TIMP1 triggers neutrophil extracellular trap formation in pancreatic cancer. *Cancer Res* (2021) 81(13):3568–79. doi: 10.1158/0008-5472.CAN-20-4125

17. Jiang ZZ, Peng ZP, Liu XC, Guo HF, Zhou MM, Jiang D, et al. Neutrophil extracellular traps induce tumor metastasis through dual effects on cancer and endothelial cells. *Oncoimmunology* (2022) 11(1):2052418. doi: 10.1080/2162402X.2022.2052418

18. Munir H, Jones JO, Janowitz T, Hoffmann M, Euler M, Martins CP, et al. Stromal-driven and amyloid β-dependent induction of neutrophil extracellular traps modulates tumor growth. *Nat Commun* (2021) 12(1):683. doi: 10.1038/s41467-021-20982-2

19. Deng J, Kang Y, Cheng CC, Li X, Dai B, Katz MH, et al. DDR1-induced neutrophil extracellular traps drive pancreatic cancer metastasis. *JCI Insight* (2021) 6 (17). doi: 10.1172/jci.insight.146133

20. Zhang Y, Chandra V, Riquelme Sanchez E, Dutta P, Quesada PR, Rakoski A, et al. Interleukin-17-induced neutrophil extracellular traps mediate resistance to checkpoint blockade in pancreatic cancer. *J Exp Med* (2020) 217(12). doi: 10.1084/jem.20190354

21. Zhang XL, Wang TY, Chen Z, Wang HW, Yin Y, Wang L, et al. HMGB1-promoted neutrophil extracellular traps contribute to cardiac diastolic dysfunction in mice. *J Am Heart Assoc* (2022) 11(4):e023800. doi: 10.1161/JAHA.121.023800

22. Park J, Wysocki RW, Amoozgar Z, Maiorino L, Fein MR, Jorns J, et al. Cancer cells induce metastasis-supporting neutrophil extracellular DNA traps. *Sci Transl Med* (2016) 8(361):361ra138. doi: 10.1126/scitranslmed.aag1711

23. Teijeira Á, Garasa S, Gato M, Alfaro C, Migueliz I, Cirella A, et al. CXCR1 and CXCR2 chemokine receptor agonists produced by tumors induce neutrophil extracellular traps that interfere with immune cytotoxicity. *Immunity* (2020) 52 (5):856–871.e8. doi: 10.1016/j.immuni.2020.03.001

24. Xiao Y, Cong M, Li J, He D, Wu Q, Tian P, et al. Cathepsin c promotes breast cancer lung metastasis by modulating neutrophil infiltration and neutrophil extracellular trap formation. *Cancer Cell* (2021) 39(3):423–437.e7. doi: 10.1016/j.ccell.2020.12.012

25. Yousefi S, Mihalache C, Kozlowski E, Schmid I, Simon HU. Viable neutrophils release mitochondrial DNA to form neutrophil extracellular traps. *Cell Death Differ* (2009) 16(11):1438–44. doi: 10.1038/cdd.2009.96

26. Martinelli S, Urosevic M, Daryadel A, Oberholzer PA, Baumann C, Fey MF, et al. Induction of genes mediating interferon-dependent extracellular trap formation during neutrophil differentiation. *J Biol Chem* (2004) 279(42):44123–32. doi: 10.1074/jbc.M405883200

27. Meher AK, Spinosa M, Davis JP, Pope N, Laubach VE, Su G, et al. Novel role of IL (Interleukin)-1β in neutrophil extracellular trap formation and abdominal aortic aneurysms. *Arterioscler Thromb Vasc Biol* (2018) 38(4):843–53. doi: 10.1161/ATVBAHA.117.309897

28. Jin R, Xu J, Gao Q, Mao X, Yin J, Lu K, et al. IL-33-induced neutrophil extracellular traps degrade fibronectin in a murine model of bronchopulmonary dysplasia. *Cell Death Discovery* (2020) 6:33. doi: 10.1038/s41420-020-0267-2

29. Kahlenberg JM, Carmona-Rivera C, Smith CK, Kaplan MJ. Neutrophil extracellular trap-associated protein activation of the NLRP3 inflammasome is enhanced in lupus macrophages. *J Immunol* (2013) 190(3):1217–26. doi: 10.4049/jimmunol.1202388

30. Behnen M, Leschczyk C, Möller S, Batel T, Klinger M, Solbach W, et al. Immobilized immune complexes induce neutrophil extracellular trap release by human neutrophil granulocytes via FcγRIIIB and mac-1. *J Immunol* (2014) 193(4):1954–65. doi: 10.4049/jimmunol.1400478

31. Pieterse E, Rother N, Yanginlar C, Hilbrands LB, van der Vlag J. Neutrophils discriminate between lipopolysaccharides of different bacterial sources and selectively release neutrophil extracellular traps. *Front Immunol* (2016) 7:484. doi: 10.3389/fimmu.2016.00484

32. Pilsczek FH, Salina D, Poon KK, Fahey C, Yipp BG, Sibley CD, et al. A novel mechanism of rapid nuclear neutrophil extracellular trap formation in response to staphylococcus aureus. *J Immunol* (2010) 185(12):7413–25. doi: 10.4049/jimmunol.1000675

33. Ali RA, Estes SK, Gandhi AA, Yalavarthi S, Hoy CK, Shi H, et al. Defibrotide inhibits antiphospholipid antibody-mediated neutrophil extracellular trap formation and venous thrombosis. *Arthritis Rheumatol* (2022) 74(5):902–7. doi: 10.1002/art.42017

34. Clark SR, Ma AC, Tavener SA, McDonald B, Goodarzi Z, Kelly MM, et al. Platelet TLR4 activates neutrophil extracellular traps to ensnare bacteria in septic blood. *Nat Med* (2007) 13(4):463–9. doi: 10.1038/nm1565

35. Pulavendran S, Prasanthi M, Ramachandran A, Grant R, Snider TA, Chow VTK, et al. Production of neutrophil extracellular traps contributes to the pathogenesis of francisella tularemia. *Front Immunol* (2020) 11:679. doi: 10.3389/fimmu.2020.00679

36. Chen KW, Monteleone M, Boucher D, Sollberger G, Ramnath D, Condon ND, et al. Noncanonical inflammasome signaling elicits gasdermin d-dependent neutrophil extracellular traps. *Sci Immunol* (2018) 3(26). doi: 10.1126/sciimmunol.aar6676

37. Middleton EA, He XY, Denorme F, Campbell RA, Ng D, Salvatore SP, et al. Neutrophil extracellular traps contribute to immunothrombosis in COVID-19 acute respiratory distress syndrome. *Blood* (2020) 136(10):1169–79. doi: 10.1182/blood.2020007008

38. Kenny EF, Herzig A, Krüger R, Muth A, Mondal S, Thompson PR, et al. Diverse stimuli engage different neutrophil extracellular trap pathways. *Elife* (2017) 6. doi: 10.7554/eLife.24437

39. Zou Y, Chen X, He B, Xiao J, Yu Q, Xie B, et al. Neutrophil extracellular traps induced by cigarette smoke contribute to airway inflammation in mice. *Exp Cell Res* (2020) 389(1):111888. doi: 10.1016/j.yexcr.2020.111888

40. Chen W, Chen H, Yang ZT, Mao EQ, Chen Y, Chen EZ. Free fatty acids-induced neutrophil extracellular traps lead to dendritic cells activation and T cell differentiation in acute lung injury. *Aging (Albany NY)* (2021) 13(24):26148–60. doi: 10.18632/aging.203802

41. Suzuki M, Ikari J, Anazawa R, Tanaka N, Katsumata Y, Shimada A, et al. PAD4 deficiency improves bleomycin-induced neutrophil extracellular traps and fibrosis in mouse lung. *Am J Respir Cell Mol Biol* (2020) 63(6):806–18. doi: 10.1165/rcmb.2019-0433OC

42. Abuelezz SA, Hendawy N. HMGB1/RAGE/TLR4 axis and glutamate as novel targets for PCSK9 inhibitor in high fat cholesterol diet induced cognitive impairment and amyloidosis. *Life Sci* (2021) 273:119310. doi: 10.1016/j.lfs.2021.119310

43. Gao S, Cui Z, Zhao MH. Complement C3a and C3a receptor activation mediates podocyte injuries in the mechanism of primary membranous nephropathy. *J Am Soc Nephrol* (2022) 33(9):1742–56. doi: 10.1681/ASN.2021101384

44. Kong LR, Chen XH, Sun Q, Zhang KY, Xu L, Ding L, et al. Loss of C3a and C5a receptors promotes adipocyte browning and attenuates diet-induced obesity via activating inosine/A2aR pathway. *Cell Rep* (2023) 42(2):112078. doi: 10.1016/j.celrep.2023.112078

45. Alemán OR, Mora N, Cortes-Vieyra R, Uribe-Querol E, Rosales C. Differential use of human neutrophil fcγ receptors for inducing neutrophil extracellular trap formation. *J Immunol Res* (2016) 2908034. doi: 10.1155/2016/2908034

46. Xiong T, Zheng X, Zhang K, Wu H, Dong Y, Zhou F, et al. Ganluyin ameliorates DSS-induced ulcerative colitis by inhibiting the enteric-origin LPS/TLR4/NF-κB pathway. *J Ethnopharmacol* (2022) 289:115001. doi: 10.1016/j.jep.2022.115001

47. Ren J, He J, Zhang H, Xia Y, Hu Z, Loughran P, et al. Platelet TLR4-ERK5 axis facilitates NET-mediated capturing of circulating tumor cells and distant metastasis after surgical stress. *Cancer Res* (2021) 81(9):2373–85. doi: 10.1158/0008-5472.CAN-20-3222

48. Thangaraju M, Cresci GA, Liu K, Ananth S, Gnanaprakasam JP, Browning DD, et al. GPR109A is a G-protein-coupled receptor for the bacterial fermentation product butyrate and functions as a tumor suppressor in colon. *Cancer Res* (2009) 69(7):2826–32. doi: 10.1158/0008-5472.CAN-08-4466

49. Reedy JL, Crossen AJ, Negoro PE, Harding HB, Ward RA, Vargas-Blanco DA, et al. The c-type lectin receptor dectin-2 is a receptor for aspergillus fumigatus galactomannan. *mBio* (2023) 14(1):e0318422. doi: 10.1128/mbio.03184-22

50. Herre J, Gordon S, Brown GD. Dectin-1 and its role in the recognition of beta-glucans by macrophages. *Mol Immunol* (2004) 40(12):869–76. doi: 10.1016/j.molimm.2003.10.007

51. Fuchs TA, Abed U, Goosmann C, Hurwitz R, Schulze I, Wahn V, et al. Novel cell death program leads to neutrophil extracellular traps. *J Cell Biol* (2007) 176(2):231–41. doi: 10.1083/jcb.200606027

52. Hakkim A, Fuchs TA, Martinez NE, Hess S, Prinz H, Zychlinsky A, et al. Activation of the raf-MEK-ERK pathway is required for neutrophil extracellular trap formation. *Nat Chem Biol* (2011) 7(2):75–7. doi: 10.1038/nchembio.496

53. Zha C, Meng X, Li L, Mi S, Qian D, Li Z, et al. Neutrophil extracellular traps mediate the crosstalk between glioma progression and the tumor microenvironment via the HMGB1/RAGE/IL-8 axis. *Cancer Biol Med* (2020) 17(1):154–68. doi: 10.20892/j.issn.2095-3941.2019.0353

54. Khan MA, Farahvash A, Douda DN, Licht JC, Grasemann H, Sweezey N, et al. JNK activation turns on LPS- and gram-negative bacteria-induced NADPH oxidase-dependent suicidal NETosis. *Sci Rep* (2017) 7(1):3409. doi: 10.1038/s41598-017-03257-z

55. Douda DN, Khan MA, Grasemann H, Palaniyar N. SK3 channel and mitochondrial ROS mediate NADPH oxidase-independent NETosis induced by calcium influx. *Proc Natl Acad Sci U.S.A.* (2015) 112(9):2817–22. doi: 10.1073/pnas.1414055112

56. Papayannopoulos V, Metzler KD, Hakkim A, Zychlinsky A. Neutrophil elastase and myeloperoxidase regulate the formation of neutrophil extracellular traps. *J Cell Biol* (2010) 191(3):677–91. doi: 10.1083/jcb.201006052

57. Metzler KD, Goosmann C, Lubojemska A, Zychlinsky A, Papayannopoulos V. A myeloperoxidase-containing complex regulates neutrophil elastase release and actin dynamics during NETosis. *Cell Rep* (2014) 8(3):883–96. doi: 10.1016/j.celrep.2014.06.044

58. Wang Y, Li M, Stadler S, Correll S, Li P, Wang D, et al. Histone hypercitrullination mediates chromatin decondensation and neutrophil extracellular trap formation. *J Cell Biol* (2009) 184(2):205–13. doi: 10.1083/jcb.200806072

59. Amulic B, Knackstedt SL, Abu Abed U, Deigendesch N, Harbort CJ, Caffrey BE, et al. Cell-cycle proteins control production of neutrophil extracellular traps. *Dev Cell* (2017) 43(4):449–462.e5. doi: 10.1016/j.devcel.2017.10.013

60. Albrengues J, Wysocki RW, Maiorino L, Egeblad M. Re-cyclin' cell-cycle components to make NETs. *Dev Cell* (2017) 43(4):379–80. doi: 10.1016/j.devcel.2017.11.002

61. Sollberger G, Choidas A, Burn GL, Habenberger P, Di Lucrezia R, Kordes S, et al. Gasdermin d plays a vital role in the generation of neutrophil extracellular traps. *Sci Immunol* (2018) 3(26). doi: 10.1126/sciimmunol.aar6689

62. Yipp BG, Petri B, Salina D, Jenne CN, Scott BN, Zbytnuik LD, et al. Infection-induced NETosis is a dynamic process involving neutrophil multitasking in vivo. *Nat Med* (2012) 18(9):1386–93. doi: 10.1038/nm.2847

63. Josefs T, Barrett TJ, Brown EJ, Quezada A, Wu X, Voisin M, et al. Neutrophil extracellular traps promote macrophage inflammation and impair atherosclerosis resolution in diabetic mice. *JCI Insight* (2020) 5(7). doi: 10.1172/jci.insight.134796

64. Sano M, Maejima Y, Nakagama S, Shiheido-Watanabe Y, Tamura N, Hirao K, et al. Neutrophil extracellular traps-mediated beclin-1 suppression aggravates atherosclerosis by inhibiting macrophage autophagy. *Front Cell Dev Biol* (2022) 10:876147. doi: 10.3389/fcell.2022.876147

65. Kluge KE, Langseth MS, Opstad TB, Pettersen A, Arnesen H, Tønnessen T, et al. Complement activation in association with markers of neutrophil extracellular traps and acute myocardial infarction in stable coronary artery disease. *Mediators Inflammation* (2020) p:5080743. doi: 10.1155/2020/5080743

66. Jeremic I, Djuric O, Nikolic M, Vlajnic M, Nikolic A, Radojkovic D, et al. Neutrophil extracellular traps-associated markers are elevated in patients with systemic lupus erythematosus. *Rheumatol Int* (2019) 39(11):1849–57. doi: 10.1007/s00296-019-04426-1

67. Wright HL, Lyon M, Chapman EA, Moots RJ, Edwards SW. Rheumatoid arthritis synovial fluid neutrophils drive inflammation through production of chemokines, reactive oxygen species, and neutrophil extracellular traps. *Front Immunol* (2020) 11:584116. doi: 10.3389/fimmu.2020.584116

68. Sun S, Duan Z, Wang X, Chu C, Yang C, Chen F, et al. Neutrophil extracellular traps impair intestinal barrier functions in sepsis by regulating TLR9-mediated endoplasmic reticulum stress pathway. *Cell Death Dis* (2021) 12(6):606. doi: 10.1038/s41419-021-03896-1

69. Bryk AH, Prior SM, Plens K, Konieczynska M, Hohendorff J, Malecki MT, et al. Predictors of neutrophil extracellular traps markers in type 2 diabetes mellitus: associations with a prothrombotic state and hypofibrinolysis. *Cardiovasc Diabetol* (2019) 18(1):49. doi: 10.1186/s12933-019-0850-0

70. Torres-Ruiz J, Absalón-Aguilar A, Nuñez-Aguirre M, Pérez-Fragoso A, Carrillo-Vázquez DA, Maravillas-Montero JL, et al. Neutrophil extracellular traps contribute to COVID-19 hyperinflammation and humoral autoimmunity. *Cells* (2021) 10(10). doi: 10.3390/cells10102545

71. Yang J, Jin L, Kim HS, Tian F, Yi Z, Bedi K, et al. KDM6A loss recruits tumor-associated neutrophils and promotes neutrophil extracellular trap formation in pancreatic cancer. *Cancer Res* (2022) 82(22):4247–60. doi: 10.1158/0008-5472.CAN-22-0968

72. Wang Y, Wang C, Zuo N, Yang H, Fang S, Shi J. Extracellular traps increase burden of bleeding by damaging endothelial cell in acute promyelocytic leukaemia. *Front Immunol* (2022) 13:841445. doi: 10.3389/fimmu.2022.841445

73. Francischetti IMB, Alejo JC, Sivanandham R, Davies-Hill T, Fetsch P, Pandrea I, et al. Neutrophil and eosinophil extracellular traps in Hodgkin lymphoma. *Hemasphere* (2021) 5(9):e633. doi: 10.1097/HS9.0000000000000633

74. Wolach O, Sellar RS, Martinod K, Cherpokova D, McConkey M, Chappell RJ, et al. Increased neutrophil extracellular trap formation promotes thrombosis in myeloproliferative neoplasms. *Sci Transl Med* (2018) 10(436). doi: 10.1126/scitranslmed.aan8292

75. Zhu B, Zhang X, Sun S, Fu Y, Xie L, Ai P. NF-κB and neutrophil extracellular traps cooperate to promote breast cancer progression and metastasis. *Exp Cell Res* (2021) 405(2):112707. doi: 10.1016/j.yexcr.2021.112707

76. Lee W, Ko SY, Mohamed MS, Kenny HA, Lengyel E, Naora H. Neutrophils facilitate ovarian cancer premetastatic niche formation in the omentum. *J Exp Med* (2019) 216(1):176–94. doi: 10.1084/jem.20181170

77. Zhu T, Zou X, Yang C, Li L, Wang B, Li R, et al. Neutrophil extracellular traps promote gastric cancer metastasis by inducing epithelial–mesenchymal transition. *Int J Mol Med* (2021) 48(1). doi: 10.3892/ijmm.2021.4960

78. Yang LY, Luo Q, Lu L, Zhu WW, Sun HT, Wei R, et al. Increased neutrophil extracellular traps promote metastasis potential of hepatocellular carcinoma via provoking tumorous inflammatory response. *J Hematol Oncol* (2020) 13(1):3. doi: 10.1186/s13045-019-0836-0

79. Lee J, Lee D, Lawler S, Kim Y. Role of neutrophil extracellular traps in regulation of lung cancer invasion and metastasis: Structural insights from a computational model. *PloS Comput Biol* (2021) 17(2):e1008257. doi: 10.1371/journal.pcbi.1008257

80. Stehr AM, Wang G, Demmler R, Stemmler MP, Krug J, Tripal P, et al. Neutrophil extracellular traps drive epithelial-mesenchymal transition of human colon cancer. *J Pathol* (2022) 256(4):455–67. doi: 10.1002/path.5860

81. Tohme S, Yazdani HO, Al-Khafaji AB, Chidi AP, Loughran P, Mowen K, et al. Neutrophil extracellular traps promote the development and progression of liver metastases after surgical stress. *Cancer Res* (2016) 76(6):1367–80. doi: 10.1158/0008-5472.CAN-15-1591

82. Rivera-Franco MM, Leon-Rodriguez E, Torres-Ruiz JJ, Gómez-Martín D, Angles-Cano E, de la Luz Sevilla-González M. Neutrophil extracellular traps associate with clinical stages in breast cancer. *Pathol Oncol Res* (2020) 26(3):1781–5. doi: 10.1007/s12253-019-00763-5

83. Guan X, Lu Y, Zhu H, Yu S, Zhao W, Chi X, et al. The crosstalk between cancer cells and neutrophils enhances hepatocellular carcinoma metastasis via neutrophil extracellular traps-associated cathepsin G component: A potential therapeutic target. *J Hepatocell Carcinoma* (2021) 8:451–65. doi: 10.2147/JHC.S303588

84. Yang LY, Shen XT, Sun HT, Zhu WW, Zhang JB, Lu L. Neutrophil extracellular traps in hepatocellular carcinoma are enriched in oxidized mitochondrial DNA which is highly pro-inflammatory and pro-metastatic. *J Cancer* (2022) 13(4):1261–71. doi: 10.7150/jca.64170

85. Jin W, Yin H, Li H, Yu XJ, Xu HX, Liu L. Neutrophil extracellular DNA traps promote pancreatic cancer cells migration and invasion by activating EGFR/ERK pathway. *J Cell Mol Med* (2021) 25(12):5443–56. doi: 10.1111/jcmm.16555

86. Xia X, Zhang Z, Zhu C, Ni B, Wang S, Yang S, et al. Neutrophil extracellular traps promote metastasis in gastric cancer patients with postoperative abdominal infectious complications. *Nat Commun* (2022) 13(1):1017. doi: 10.1038/s41467-022-28492-5

87. Shinde-Jadhav S, Mansure JJ, Rayes RF, Marcq G, Ayoub M, Skowronski R, et al. Role of neutrophil extracellular traps in radiation resistance of invasive bladder cancer. *Nat Commun* (2021) 12(1):2776. doi: 10.1038/s41467-021-23086-z

88. Cools-Lartigue J, Spicer J, McDonald B, Gowing S, Chow S, Giannias B, et al. Neutrophil extracellular traps sequester circulating tumor cells and promote metastasis. *J Clin Invest* (2013) 123(8):3446–58. doi: 10.1172/JCI67484

89. Nie M, Yang L, Bi X, Wang Y, Sun P, Yang H, et al. Neutrophil extracellular traps induced by IL8 promote diffuse Large b-cell lymphoma progression via the TLR9 signaling. *Clin Cancer Res* (2019) 25(6):1867–79. doi: 10.1158/1078-0432.CCR-18-1226

90. van der Windt DJ, Sud V, Zhang H, Varley PR, Goswami J, Yazdani HO, et al. Neutrophil extracellular traps promote inflammation and development of hepatocellular carcinoma in nonalcoholic steatohepatitis. *Hepatology* (2018) 68 (4):1347–60. doi: 10.1002/hep.29914

91. Liu Y, Zhang X, Chen S, Wang J, Yu S, Li Y, et al. Gut-derived lipopolysaccharide promotes alcoholic hepatosteatosis and subsequent hepatocellular carcinoma by stimulating neutrophil extracellular traps through toll-like receptor 4. *Clin Mol Hepatol* (2022) 28(3):522–39. doi: 10.3350/cmh.2022.0039

92. Guglietta S, Chiavelli A, Zagato E, Krieg C, Gandini S, Ravenda PS, et al. Coagulation induced by C3aR-dependent NETosis drives protumorigenic neutrophils during small intestinal tumorigenesis. *Nat Commun* (2016) 7:11037. doi: 10.1038/ncomms11037

93. Yazdani HO, Roy E, Comerci AJ, van der Windt DJ, Zhang H, Huang H, et al. Neutrophil extracellular traps drive mitochondrial homeostasis in tumors to augment growth. *Cancer Res* (2019) 79(21):5626–39. doi: 10.1158/0008-5472.CAN-19-0800

94. Demers M, Wong SL, Martinod K, Gallant M, Cabral JE, Wang Y, et al. Priming of neutrophils toward NETosis promotes tumor growth. *Oncoimmunology* (2016) 5(5): e1134073. doi: 10.1080/2162402X.2015.1134073

95. Miller-Ocuin JL, Liang X, Boone BA, Doerfler WR, Singhi AD, Tang D, et al. DNA Released from neutrophil extracellular traps (NETs) activates pancreatic stellate cells and enhances pancreatic tumor growth. *Oncoimmunology* (2019) 8(9):e1605822. doi: 10.1080/2162402X.2019.1605822

96. Chaffer CL, Weinberg RA. A perspective on cancer cell metastasis. *Science* (2011) 331(6024):1559–64. doi: 10.1126/science.1203543

97. Ortiz-Espinosa S, Morales X, Senent Y, Alignani D, Tavira B, Macaya I, et al. Complement C5a induces the formation of neutrophil extracellular traps by myeloid-derived suppressor cells to promote metastasis. *Cancer Lett* (2022) 529:70–84. doi: 10.1016/j.canlet.2021.12.027

98. Zhao H, Liang Y, Sun C, Zhai Y, Li X, Jiang M, et al. Dihydrotanshinone I inhibits the lung metastasis of breast cancer by suppressing neutrophil extracellular traps formation. *Int J Mol Sci* (2022) 23(23). doi: 10.3390/ijms232315180

99. Scheel C, Eaton EN, Li SH, Chaffer CL, Reinhardt F, Kah KJ, et al. Paracrine and autocrine signals induce and maintain mesenchymal and stem cell states in the breast. *Cell* (2011) 145(6):926–40. doi: 10.1016/j.cell.2011.04.029

100. Chen J, Hou S, Liang Q, He W, Li R, Wang H, et al. Neutrophil extracellular traps (NETs) promote pro-metastatic phenotype in human breast cancer cells through epithelial-mesenchymal transition. *Cancers (Basel)* (2020) 12(6). doi: 10.3390/cancers12061542

101. Wang Y, Liu F, Chen L, Fang C, Li S, Yuan S, et al. Neutrophil extracellular traps (NETs) promote non-small cell lung cancer metastasis by suppressing lncRNA MIR503HG to activate the NF-kappaB/NLRP3 inflammasome pathway. *Front Immunol* (2022) 13:867516. doi: 10.3389/fimmu.2022.867516

102. Massague J, Obenauf AC. Metastatic colonization by circulating tumour cells. *Nature* (2016) 529(7586):298–306. doi: 10.1038/nature17038

103. Chen J, Hou S, Liang Q, He W, Li R, Wang H, et al. Localized degradation of neutrophil extracellular traps by photoregulated enzyme delivery for cancer immunotherapy and metastasis suppression. *ACS Nano* (2022) 16(2):2585–97. doi: 10.1021/acsnano.1c09318

104. Najmeh S, Cools-Lartigue J, Rayes RF, Gowing S, Vourtzoumis P, Bourdeau F, et al. Neutrophil extracellular traps sequester circulating tumor cells via β1-integrin mediated interactions. *Int J Cancer* (2017) 140(10):2321–30. doi: 10.1002/ijc.30635

105. Zheng Z, Li YN, Jia S, Zhu M, Cao L, Tao M, et al. Lung mesenchymal stromal cells influenced by Th2 cytokines mobilize neutrophils and facilitate metastasis by producing complement C3. *Nat Commun* (2021) 12(1):6202. doi: 10.1038/s41467-021-26460-z

106. Yaeger R, Mezzadra R, Sinopoli J, Bian Y, Marasco M, Kaplun E, et al. Molecular characterization of acquired resistance to KRASG12C-EGFR inhibition in colorectal cancer. *Cancer Discovery* (2023) 13(1):41–55. doi: 10.1158/2159-8290.CD-22-0405

107. Kieffer Y, Hocine HR, Gentric G, Pelon F, Bernard C, Bourachot B, et al. Single-cell analysis reveals fibroblast clusters linked to immunotherapy resistance in cancer. *Cancer Discov* (2020) 10(9):1330–51. doi: 10.1158/2159-8290.CD-19-1384

108. Cheng Y, Mo F, Li Q, Han X, Shi H, Chen S, et al. Targeting CXCR2 inhibits the progression of lung cancer and promotes therapeutic effect of cisplatin. *Mol Cancer* (2021) 20(1):62. doi: 10.1186/s12943-021-01355-1

109. Bui TM, Yalom LK, Sumagin R. Tumor-associated neutrophils: orchestrating cancer pathobiology and therapeutic resistance. *Expert Opin Ther Targets* (2021) 25 (7):573–83. doi: 10.1080/14728222.2021.1954162

110. Albrengues J, Shields MA, Ng D, Park CG, Ambrico A, Poindexter ME, et al. Neutrophil extracellular traps produced during inflammation awaken dormant cancer cells in mice. *Science* (2018) 361(6409). doi: 10.1126/science.aao4227

111. Tamura K, Miyato H, Kanamaru R, Sadatomo A, Takahashi K, Ohzawa H, et al. Neutrophil extracellular traps (NETs) reduce the diffusion of doxorubicin which may attenuate its ability to induce apoptosis of ovarian cancer cells. *Heliyon* (2022) 8 (6):e09730. doi: 10.1016/j.heliyon.2022.e09730

112. Ma Y, Zhang H, Chen C, Liu L, Ding T, Wang Y, et al. TRIM32 promotes radioresistance by disrupting TC45-STAT3 interaction in triple-negative breast cancer. *Oncogene* (2022) 41(11):1589–99. doi: 10.1038/s41388-022-02204-1

113. Ruiz-Fernández de Córdoba B, Moreno H, Valencia K, Perurena N, Ruedas P, Walle T, et al. Tumor ENPP1 (CD203a)/Haptoglobin axis exploits myeloid-derived suppressor cells to promote post-radiotherapy local recurrence in breast cancer. *Cancer Discovery* (2022) 12(5):1356–77. doi: 10.1158/2159-8290.CD-21-0932

114. Byrd AS, Carmona-Rivera C, O'Neil LJ, Carlucci PM, Cisar C, Rosenberg AZ, et al. Neutrophil extracellular traps, b cells, and type I interferons contribute to immune dysregulation in hidradenitis suppurativa. *Sci Transl Med* (2019) 11(508). doi: 10.1126/scitranslmed.aav5908

115. Papadaki G, Kambas K, Choulaki C, Vlachou K, Drakos E, Bertsias G, et al. Neutrophil extracellular traps exacerbate Th1-mediated autoimmune responses in rheumatoid arthritis by promoting DC maturation. *Eur J Immunol* (2016) 46 (11):2542–54. doi: 10.1002/eji.201646542

116. Nixon BG, Kuo F, Ji L, Liu M, Capistrano K, Do M, et al. Tumor-associated macrophages expressing the transcription factor IRF8 promote T cell exhaustion in cancer. *Immunity* (2022) 55(11):2044–2058.e5. doi: 10.1016/j.immuni.2022.10.002

117. Wang C, Barnoud C, Cenerenti M, Sun M, Caffa I, Kizil B, et al. Dendritic cells direct circadian anti-tumour immune responses. *Nature* (2023) 614(7946):136–43. doi: 10.1038/s41586-022-05605-0

118. Donis-Maturano L, Sánchez-Torres LE, Cerbulo-Vázquez A, Chacón-Salinas R, García-Romo GS, Orozco-Uribe MC, et al. Prolonged exposure to neutrophil extracellular traps can induce mitochondrial damage in macrophages and dendritic cells. *Springerplus* (2015) 4:161. doi: 10.1186/s40064-015-0932-8

119. Lazzaretto B, Fadeel B. Intra- and extracellular degradation of neutrophil extracellular traps by macrophages and dendritic cells. *J Immunol* (2019) 203(8):2276–90. doi: 10.4049/jimmunol.1800159

120. Guimaraes-Costa AB, Rochael NC, Oliveira F, Echevarria-Lima J, Saraiva EM. Neutrophil extracellular traps reprogram IL-4/GM-CSF-Induced monocyte

differentiation to anti-inflammatory macrophages. *Front Immunol* (2017) 8:523. doi: 10.3389/fimmu.2017.00523

121. Jiang H, Ge H, Shi Y, Yuan F, Yue H. CAFs secrete CXCL12 to accelerate the progression and cisplatin resistance of colorectal cancer through promoting M2 polarization of macrophages. *Med Oncol* (2023) 40(3):90. doi: 10.1007/s12032-023-01953-7

122. Wei X, Zou S, Xie Z, Wang Z, Huang N, Cen Z, et al. EDIL3 deficiency ameliorates adverse cardiac remodelling by neutrophil extracellular traps (NET)-mediated macrophage polarization. *Cardiovasc Res* (2022) 118(9):2179–95. doi: 10.1093/cvr/cvab269

123. An Z, Li J, Yu J, Wang X, Gao H, Zhang W, et al. Neutrophil extracellular traps induced by IL-8 aggravate atherosclerosis via activation NF-κB signaling in macrophages. *Cell Cycle* (2019) 18(21):2928–38. doi: 10.1080/15384101.2019.1662678

124. Georgakis S, Gkirtzimanaki K, Papadaki G, Gakiopoulou H, Drakos E, Eloranta ML, et al. NETs decorated with bioactive IL-33 infiltrate inflamed tissues and induce IFN-α production in patients with SLE. *JCI Insight* (2021) 6(21). doi: 10.1172/jci.insight.147671

125. Qiu SL, Zhang H, Tang QY, Bai J, He ZY, Zhang JQ, et al. Neutrophil extracellular traps induced by cigarette smoke activate plasmacytoid dendritic cells. *Thorax* (2017) 72(12):1084–93. doi: 10.1136/thoraxjnl-2016-209887

126. Hernández SS, Jakobsen MR, Bak RO. Plasmacytoid dendritic cells as a novel cell-based cancer immunotherapy. *Int J Mol Sci* (2022) 23(19). doi: 10.3390/ijms231911397

127. Ma J, Kummarapurugu AB, Hawkridge A, Ghosh S, Zheng S, Voynow JA. Neutrophil elastase-regulated macrophage sheddome/secretome and phagocytic failure. *Am J Physiol Lung Cell Mol Physiol* (2021) 321(3):L555–l565. doi: 10.1152/ajplung.00499.2019

128. Tateosian NL, Reiteri RM, Amiano NO, Costa MJ, Villalonga X, Guerrieri D, et al. Neutrophil elastase treated dendritic cells promote the generation of CD4(+) FOXP3(+) regulatory T cells in vitro. *Cell Immunol* (2011) 269(2):128–34. doi: 10.1016/j.cellimm.2011.03.013

129. Beelen NA, Ehlers FAI, Kooreman LFS, Bos GMJ, Wieten L. An in vitro model to monitor natural killer cell effector functions against breast cancer cells derived from human tumor tissue. *Methods Cell Biol* (2023) 173:133–53. doi: 10.1016/bs.mcb.2022.05.001

130. Wang J, Li Q, Yin Y, Zhang Y, Cao Y, Lin X, et al. Excessive neutrophils and neutrophil extracellular traps in COVID-19. *Front Immunol* (2020) 11:2063. doi: 10.3389/fimmu.2020.02063

131. Jiang M, Shen N, Zhou H, Wang Y, Lin S, Wu J, et al. The enrichment of neutrophil extracellular traps impair the placentas of systemic lupus erythematosus through accumulating decidual NK cells. *Sci Rep* (2021) 11(1):6870. doi: 10.1038/s41598-021-86390-0

132. Valayer A, Brea D, Lajoie L, Avezard L, Combes-Soia L, Labas V, et al. Neutrophils can disarm NK cell response through cleavage of NKp46. *J Leukoc Biol* (2017) 101(1):253–9. doi: 10.1189/jlb.3AB0316-140RR

133. Bertin FR, Rys RN, Mathieu C, Laurance S, Lemarié CA, Blostein MD. Natural killer cells induce neutrophil extracellular trap formation in venous thrombosis. *J Thromb Haemost* (2019) 17(2):403–14. doi: 10.1111/jth.14339

134. Miranda FJB, Rocha BC, Pereira MCA, Pereira LMN, de Souza EHM, Marino AP, et al. Toxoplasma gondii-induced neutrophil extracellular traps amplify the innate and adaptive response. *mBio* (2021) 12(5):e0130721. doi: 10.1128/mBio.01307-21

135. Wilson AS, Randall KL, Pettitt JA, Ellyard JI, Blumenthal A, Enders A, et al. Neutrophil extracellular traps and their histones promote Th17 cell differentiation directly via TLR2. *Nat Commun* (2022) 13(1):528. doi: 10.1038/s41467-022-28172-4

136. Warnatsch A, Ioannou M, Wang Q, Papayannopoulos V. Inflammation. neutrophil extracellular traps license macrophages for cytokine production in atherosclerosis. *Science* (2015) 349(6245):316–20. doi: 10.1126/science.aaa8064

137. Peng DH, Rodriguez BL, Diao L, Gaudreau PO, Padhye A, Konen JM, et al. Th17 cells contribute to combination MEK inhibitor and anti-PD-L1 therapy resistance in KRAS/p53 mutant lung cancers. *Nat Commun* (2021) 12(1):2606. doi: 10.1038/s41467-021-22875-w

138. Tosolini M, Kirilovsky A, Mlecnik B, Fredriksen T, Mauger S, Bindea G, et al. Clinical impact of different classes of infiltrating T cytotoxic and helper cells (Th1, th2, treg, th17) in patients with colorectal cancer. *Cancer Res* (2011) 71(4):1263–71. doi: 10.1158/0008-5472.CAN-10-2907

139. Melero I, Villalba-Esparza M, Recalde-Zamacona B, Jiménez-Sánchez D, Teijeira Á, Argueta A, et al. Neutrophil extracellular traps, local IL-8 expression, and cytotoxic T-lymphocyte response in the lungs of patients with fatal COVID-19. *Chest* (2022) 162(5):1006–16. doi: 10.1016/j.chest.2022.06.007

140. Tokunaga R, Naseem M, Lo JH, Battaglin F, Soni S, Puccini A, et al. B cell and b cell-related pathways for novel cancer treatments. *Cancer Treat Rev* (2019) 73:10–9. doi: 10.1016/j.ctrv.2018.12.001

141. Gestermann N, Di Domizio J, Lande R, Demaria O, Frasca L, Feldmeyer L, et al. Netting neutrophils activate autoreactive b cells in lupus. *J Immunol* (2018) 200 (10):3364–71. doi: 10.4049/jimmunol.1700778

142. Karmakar U, Vermeren S. Crosstalk between b cells and neutrophils in rheumatoid arthritis. *Immunology* (2021) 164(4):689–700. doi: 10.1111/imm.13412

143. Fang H, Shao S, Xue K, Yuan X, Qiao P, Zhang J, et al. Neutrophil extracellular traps contribute to immune dysregulation in bullous pemphigoid via inducing b-cell differentiation and antibody production. *FASEB J* (2021) 35(7):e21746. doi: 10.1096/fj.202100145R

144. de Andrea CE, Ochoa MC, Villalba-Esparza M, Teijeira A, Schalper KA, Abengozar-Muela M, et al. Heterogenous presence of neutrophil extracellular traps in human solid tumours is partially dependent on IL-8. *J Pathol* (2021) 255(2):190–201. doi: 10.1002/path.5753

145. Kaltenmeier C, Yazdani HO, Morder K, Geller DA, Simmons RL, Tohme S. Neutrophil extracellular traps promote T cell exhaustion in the tumor microenvironment. *Front Immunol* (2021) 12:785222. doi: 10.3389/fimmu.2021.785222

146. Wang H, Zhang H, Wang Y, Brown ZJ, Xia Y, Huang Z, et al. Regulatory T-cell and neutrophil extracellular trap interaction contributes to carcinogenesis in non-alcoholic steatohepatitis. *J Hepatol* (2021) 75(6):1271–83. doi: 10.1016/j.jhep.2021.07.032

147. Yang S, Zou X, Li J, Yang H, Zhang A, Zhu Y, et al. Immunoregulation and clinical significance of neutrophils/NETs-ANGPT2 in tumor microenvironment of gastric cancer. *Front Immunol* (2022) 13:1010434. doi: 10.3389/fimmu.2022.1010434

148. He X, Xiao Y, Liu S, Deng R, Li Z, Zhu X. Predicting the immune microenvironment and prognosis with a NETosis-related lncRNA signature in head and neck squamous cell carcinoma. *BioMed Res Int* (2022), 3191474. doi: 10.1155/2022/3191474

149. Li M, Lin C, Deng H, Strnad J, Bernabei L, Vogl DT, et al. A novel peptidylarginine deiminase 4 (PAD4) inhibitor BMS-P5 blocks formation of neutrophil extracellular traps and delays progression of multiple myeloma. *Mol Cancer Ther* (2020) 19(7):1530–8. doi: 10.1158/1535-7163.MCT-19-1020

150. Zhang H, Wang Y, Onuma A, He J, Wang H, Xia Y, et al. Neutrophils extracellular traps inhibition improves PD-1 blockade immunotherapy in colorectal cancer. *Cancers (Basel)* (2021) 13(21). doi: 10.3390/cancers13215333

151. Cheng Y, Gong Y, Chen X, Zhang Q, Zhang X, He Y, et al. Injectable adhesive hemostatic gel with tumor acidity neutralizer and neutrophil extracellular traps lyase for enhancing adoptive NK cell therapy prevents post-resection recurrence of hepatocellular carcinoma. *Biomaterials* (2022) 284:121506. doi: 10.1016/j.biomaterials.2022.121506

152. Volkov DV, Tetz GV, Rubtsov YP, Stepanov AV, Gabibov AG. Neutrophil extracellular traps (NETs): Opportunities for targeted therapy. *Acta Naturae* (2021) 13 (3):15–23. doi: 10.32607/actanaturae.11503

153. Tripodo C, Bassani B, Jachetti E, Cancila V, Chiodoni C, Portararo P, et al. Neutrophil extracellular traps arm DC vaccination against NPM-mutant myeloproliferation. *Elife* (2022) 11. doi: 10.7554/eLife.69257

10.3389/fimmu.2023.1135086

Glossary

ANGPT2	angiopoietin-2
C3	complement 3
CAR	chimeric antigen receptor
CCDC25	coiled-coil domain-containing 25
CG	cathepsin G
COVID-19	coronavirus disease 2019
CSF	colony stimulating factor
CTLA4	cytotoxic T-lymphocyte associated protein 4
CXCLs	C-X-C motif chemokine ligand
CXCR	C-X-C motif chemokine receptor
DC	dendritic cell
DOX	doxorubicin
ERK	extracellular signal–regulated kinase
GM	granulocyte-macrophage
H3Cit	citrullinated histone H3
HCC	hepatocellular carcinoma
HMGB-1	high mobility group box 1
IFN	interferon
IL	interleukin
MM	multiple myeloma
MMP-9	matrix metalloproteinase 9
MPO	myeloperoxidase
NASH	non-alcoholic steatohepatitis
NE	neutrophil elastase
NET	neutrophil extracellular trap
NF	nuclear factor
NK	natural killer
NOX	NADPH-oxidase
PAD4	peptidyl arginine deiminase 4
PD-1	programmed cell death protein 1
PD-L1	programmed death-ligand 1
PMA	phorbol 12-myristate 13-acetate
ROS	reactive oxygen species
TAN	tumor-associated neutrophil
Th	T helper
TLR	toll-like receptor
TME	tumor microenvironment
Tregs	regulatory T cells
TIMP1	tissue inhibitor of metalloproteinases-1

frontiers | Frontiers in Immunology

TYPE Original Research
PUBLISHED 17 March 2023
DOI 10.3389/fimmu.2023.1098700

OPEN ACCESS

EDITED BY
Junjiang Fu,
Southwest Medical University, China

REVIEWED BY
Zhiming Li,
Sun Yat-sen University Cancer Center (SYSUCC), China
Shi-Jun Yue,
Shaanxi University of Chinese Medicine, China

*CORRESPONDENCE
Yinfeng Yang
yinfengyang@yeah.net
Jinghui Wang
jhwang_dlut@163.com

†These authors have contributed equally to this work

SPECIALTY SECTION
This article was submitted to Cancer Immunity and Immunotherapy, a section of the journal Frontiers in Immunology

RECEIVED 15 November 2022
ACCEPTED 07 March 2023
PUBLISHED 17 March 2023

CITATION
Yang W, Wei C, Cheng J, Ding R, Li Y, Wang Y, Yang Y and Wang J (2023) BTG2 and SerpinB5, a novel gene pair to evaluate the prognosis of lung adenocarcinoma. *Front. Immunol.* 14:1098700. doi: 10.3389/fimmu.2023.1098700

BTG2 and SerpinB5, a novel gene pair to evaluate the prognosis of lung adenocarcinoma

Wanting Yang[1†], Chunli Wei[2†], Jingliang Cheng[2†], Ran Ding[3], Yan Li[4], Yonghua Wang[5], Yinfeng Yang[3*] and Jinghui Wang[1*]

[1]School of Integrated Chinese and Western Medicine, Anhui University of Chinese Medicine, Hefei, Anhui, China, [2]Key Laboratory of Epigenetics and Oncology, the Research Center for Preclinical Medicine, Southwest Medical University, Luzhou, Sichuan, China, [3]School of Medical Informatics Engineering, Anhui University of Chinese Medicine, Hefei, Anhui, China, [4]Key Laboratory of Industrial Ecology and Environmental Engineering (MOE), Faculty of Chemical, Environmental and Biological Science and Technology, Dalian University of Technology, Dalian, Liaoning, China, [5]College of Life Sciences, Northwest University, Shaanxi, China

Introduction: Lung adenocarcinoma (LUAD), as the most frequent pathological subtype of non–small cell lung cancer, is often characterized by poor prognosis and low 5-year survival rate. Exploriton of new biomarkers and accurate molecular mechanisms for effectively predicting the prognosis of LUAD patients is still necessary. Presently, BTG2 and SerpinB5, which play important roles in tumors, are studied as a gene pair for the first time with the aim of exploring whether they can be used as potential prognostic markers.

Methods: Using the bioinformatics method to explore whether BTG2 and SerpinB5 can become independent prognostic factors, and explore their clinical application value and whether they can be used as immunotherapeutic markers. In addition, we also verify the conclusions obtained from external datasets, molecular docking, and SqRT-PCR.

Results: The results show that compared with normal lung tissue, BTG2 expression level was down-regulated and SerpinB5 was up-regulated in LUAD. Additionally, Kaplan–Meier survival analysis demonstrate that the prognosis of low expression level of BTG2 was poor, and that of high expression level of SerpinB5 was poor, suggesting that both of them can be used as independent prognostic factors. Moreover, the prognosis models of the two genes were constructed respectively in this study, and their prediction effect was verified by external data. Besides, ESTIMATE algorithm reveals the relationship between this gene pair and the immune microenvironment. Furthermore, patients with a high expression level of BTG2 and a low expression level of SerpinB5 have higher immunophenoscore for CTLA-4 and PD-1 inhibitors than patients with a low expression level of BTG2 and a high expression level of SerpinB5, indicating that such patients have a more obvious effect of immunotherapy.

Discussion: Collectively, all the results demonstrate that BTG2 and SerpinB5 might serve as potential prognostic biomarkers and novel therapeutic targets for LUAD.

KEYWORDS

BTG2, SerpinB5, LUAD, immunotherapeutic, tumor microenvironment

Introduction

Lung cancer is the third most common cancer in the world and the leading cause of cancer death worldwide. According to the histological classification of tumors, lung cancer can be divided into two types: small cell lung cancer, accounting for 15% of all lung cancer, and non-small cell lung cancer (NSCLC), accounting for about 85% of all lung cancer (1, 2). Among them, NSCLC can be divided into several histological subtypes: lung adenocarcinoma (LUAD), adenosquamous cell carcinoma, squamous cell carcinoma (LUSC) and large cell carcinoma (LCC) (3), in which LUAD is by far the most common subtype of NSCLC. The main reason for the high mortality of LUAD was the lack of early diagnosis methods that would find tumorigenesis at an early stage. So tumorigenesis can't be found in time in the early stage of cancer, leading to the diagnosis of most patients in the middle and late stages (4). At the same time, the tumor was prone to invasion and metastasis, resulting in poor curative effect (5).

Cisplatin is currently the first-line drug for the treatment of lung cancer, but the clinical application is limited due to drug resistance (6, 7). However, cisplatin is often used in combination with other drugs in the process of clinical medication. Although cisplatin has a strong tolerance to lung cancer, its basic pharmacological effect against lung cancer is still worthy of further study (8, 9). In this study, we use bioinformatics technology to predict the core targets during the development of LUAD, taking cisplatin as the main drug for the treatment of lung cancer to find the targets that could be used as prognostic markers. Through bioinformatics study of gene expression changes in LUAD patients after being treated by cisplatin that the data was downloaded from GEO dataset, it was found that cisplatin could regulate the abnormal decrease or increase of gene expression level of BTG2 and SerpinB5 in Lung cancer cells, and these two genes were related to the overall survival (OS) of the LUAD patients. Additionally, from the correlation of gene expression, which was calculated by Pearson's correlation test, it was found that there was a negative correlation between BTG2 and SerpinB5. Relevant studies have also found that both of them were related to p53 (10, 11). The expression level of BTG2 was related to the SerpinB5', and the two genes could interact through p53. Therefore, we took BTG2 and SerpinB5 as a new gene pair to study their clinical prognostic value.

Actually, BTG2 was the first gene found in the BTG/TOB gene family, which was involved in biological functions such as cell proliferation and differentiation, cell cycle regulation, and DNA damage repair (12). A large number of studies have shown that the expression level of BTG2 in tumors was closely related to the biological characteristics of tumors (12–15). The BTG2 was considered to be a tumor suppressor gene, and the expression level was significantly reduced or even not expressed in liver cancer, bladder cancer, breast cancer, ovarian cancer and other tumors (16). With respect to SerpinB5, it was one of the members of the serine protease inhibitor (Serpin) family, belonging to non-inhibitory subpins (17). SerpinB5 was expressed in normal breast epithelial cells, skin, prostate, testis, lung, tongue, intestine and thymus, but the expression level was abnormally lower in a variety of malignant tumors compared with the expression level in normal tissue. Previous studies have shown that SerpinB5 can inhibit the occurrence and development of tumors, including promoting tumor cell apoptosis, inhibiting tumor angiogenesis, and inhibiting tumor metastasis (18–20).

Presently, we performed a series of bioinformatics analyses on the gene expression level of BTG2 and SerpinB5 in LUAD, including transcriptional analysis, co-expression analysis, functional annotation enrichment analysis, protein-protein interaction (PPI) analysis, survival analysis, and constructed prognosis models. The increased levels of SerpinB5 and decreased BTG2 expression were observed in LUAD. Both a high expression level of SerpinB5 and a low expression level of BTG2 were associated with poor OS in LUAD. In addition, the expression level of BTG2 and SerpinB5 were related to macrophages in the immune microenvironment, which may be an important reason why these two genes can affect the immune microenvironment. Finally, we verified our research content through many methods, including external datasets, molecular docking, immunohistochemistry, and experiment which would make our findings more reliable. In our article, these two genes were studied together for the first time. We studied whether this gene pair could be a potential tumor prognostic marker and its potential mechanism. All these findings provide new insights for improving the prognosis of patients and may may promote the discovery and application of prognostic markers of LUAD.

Materials and methods

Data sources

The gene expression matrix of patients with LUAD samples was downloaded from the Gene Expression Omnibus (GEO) website (https://www.ncbi.nlm.nih.gov/), including GSE73302 datasets. The corresponding probe set GPL5175 of GSE73302 dataset was obtained from GEO website. Gene expression profile data of LUAD patients were downloaded from the TCGA database (https://portal.gdc.cancer.gov/repository), which included 59 samples of normal lung tissue and 539 LUAD tissues (Workflow Type: STAR-Counts). Four groups of samples were in GSE73302 dataset, including A549 cell samples that were not treated with cisplatin and cultured for 24 and 48 hours respectively as the experimental control group, and A549 cell samples treated with cisplatin for 24 and 48 hours respectively as the experimental group, each group repeated three times. Therefore, a total of 12 samples were analyzed in GSE73302 dataset. The pan-cancer analysis of genes in 33 kinds of cancers was obtained through Sangerbox (http://sangerbox.com/tool.html) database. Data on pan-cancer analysis in the Sangerbox were downloaded from UCSC XENA, which was from TCGA database and GTXs and the expression value was converted into Log2 (x+0.001).

Identification of DEGs in LUAD after treated with cisplatin

In order to obtain the differential expression genes (DEGs), the gene expression data need to be preprocessed, including the data correction and log2 (x+1) transformation. First, we corrected the gene expression data through the normalized BetweenArrays function of the "limma" package of R (4.2.0) and then calculated the log2 (x+1) of the corrected data. DEGs in GSE73302 were obtained by using the "limma" package. The gene expression level of DEGs in GSE73302 was visually displayed by heatmap and the volcano plot, which were drawn through the "ggplot2" package. The y-axis of the volcano plot is log2 fold change (log2FC) and the fold change represents the differential expression multiple. The expression of these genes that were increasing or decreasing can be judged by the positive and negative value of log2 fold change in the volcano plot.

The DEGs in normal tissues and tumor tissues were obtained by using the "limma" package. The screening criteria of DEGs were $P < 0.05$ and $|\log FC| \geq 1.0$. In order to obtain DEGs in tumor tissues after cisplatin interference, the overlapping DEGs of two gene expression profiles were obtained through the "Venn" package.

Protein-protein interaction network

In order to explore the interaction between DEGs, a PPI network was constructed. We obtained the gene interaction relationship among 17 DEGs through the online database STRING (https://cn.string-db.org/) and constructed a PPI network through Cytoscape (3.8.0). Meanwhile, the correlations of gene expression between the 17 DEGs were calculated by Pearson's correlation analysis and displayed by a heatmap.

Survival analysis of DEGs

To evaluate whether mRNA levels of DEGs affected the prognosis of LUAD, the correlation between the expression level of 17 DEGs and median OS were analyzed using the GEPIA database (http://gepia.cancer-pku.cn/). This database was used to assess the link between DEGs expression and patient prognosis in multiple cancer types and drew the survival curve plot between them. Enter DEGs one by one into "Gene" and "LUAD" in "Datasets". The prognosis-related genes could be got. Log-rank P-value <0.05 was considered statistically significant. DEGs with $P < 0.05$ were considered as genes that related to prognosis.

Moreover, receiver operating characteristic curves (ROC) were plotted to determine the sensitivity and specificity of these prognostic genes. Downloading clinical data, and analyzing the survival curve with the data through the TCGA database.

The ROC curves were drawn by the "pROC" package. The area covered under a curve is called the area under a curve (AUC). This is used to evaluate the performance of sensitivity and specificity. The higher the AUC, the better the effect by using the expression level to predict the survival time of cancer patients.

Evaluation of the independent prognostic factor and survival analysis of the gene pair

Correlations between core gene expression level and the clinicopathological and molecular features were analyzed by the "Complex Heatmap", "ggalluvial", and "ggpubr" packages (21). According to the median expression level of core genes, LUAD patients were divided into high-expression and low-expression groups. In order to accurately study the relationship between gene expression and patient survival time, the relationship between the two groups of BTG2 and SerpinB5 and OS and progression free survival (PFS) were calculated by using the "survival" package. The clinical data and the gene expression RNA-Seq (HTSeq-FPKM) were downloaded from the TCGA dataset.

Development and validation of the nomogram model

To establish the relationship between different clinical characteristics and patient survival, a prognosis model was constructed. Univariate and multivariate Cox regression analyses were used to determine whether core genes could be used as an independent prognostic factor in patients with LUAD without the influence of clinical characteristics.

The Cox regression model was constructed by the "RMS" (22) package and visualized the parameters related to the survival time of patients through nomogram. Nomogram is essentially a visual regression model. It sets the scoring criteria according to the regression coefficients of all independent variables and then gives the scoring values of each independent variable to calculate the total score of each patient. The conversion between occurrence probability and the prognosis were calculated to predict the survival time of each patient (22).

The concordance index (C-index) and a calibration curve plot were then used to evaluate the nomogram's predictive accuracy and discriminative ability. The nomogram's predictive accuracy was drawn by the "ggplot2" package. The x-axis represents the predicted survival rate of each patient, and the y-axis represents the actual survival rate of each patient. The correlations between core genes and co-expression genes were calculated by Pearson's correlation analysis in the cBioPortal database (https://www.cbioportal.org/), and genes with a correlation coefficient (absolute value) more than 0.5 were selected.

Enrichment in LUAD by GSEA and GO analysis

The GSEA is a computational analysis method used to judge whether an a priori-defined set of genes shows statistically significant differences between two biological states. In this study, the "clusterProfiler" package was used to perform GSEA between the high-expression and low-expression of core genes (23). Functional or pathway terms with adjusted P-values<0.05 and

False Discovery Rate (FDR) q-value <0.25 were considered statistically significant. The GO analysis and KEGG analysis were also used to obtain the pathway that these genes may participate.

Identification of potential mechanisms of lncRNA/miRNA/mRNA networks

In order to further study the possible mechanism of BTG2 and Serpinb5 in LUAD, the lncRNA/miRNA/mRNA network was used to reveal the mechanism. First, the miRNAs that were related to these two genes were screened through the "miRNA-mRNA" module in the StarBase v3.0 database (https://starbase.sysu.edu.cn/), and then the miRNAs that may be related to these two genes were obtained by the intersection of these two groups of genes. Then, the lncRNAs corresponding to the miRNAs were searched through the "miRNA-LncRNA" module. The screening condition was low stringency (>=1) in "CLIP Data", and "Pan-Cancer" was ≥ 4 cancer types (24). The miRNAs and lncRNAs obtained above were used to build a network through Cytoscape.

Infiltration patterns in the tumor microenvironment

The ESTIMATE algorithm (Estimation of Stromal and Immune cells in Malignant Tumors using Expression data) was applied to calculate the immune score, stromal score, estimate score, and tumor purity based on the expression level of mRNA of TCGA (25).

The ESTIMATE computational method in the "estimate" package was applied to calculate the "estimate score", "immune score", and "stromal score" in LUAD tissues. CIBERSORT computational method was used to compute cell components of the tissues. Twenty-two categories of TIICs (Tumor infiltrating immune cells), including plasma cells and natural killer cells were identified and the relative proportions were calculated by using the "CIBERSORT" package. Correlation analysis between different TIIC subpopulations was achieved by the "corrplot" package. The "vioplot" package was applied to visualize the TIICs between high-expression and low-expression groups. The association between the expression level of core genes and the TIICs was acquired by using "limma" "ggplot2" "ggpubr" and "ggExtra" packages.

Correlation analysis between different TIIC subpopulations was achieved by the "corrplot" package. For each tumor sample, the TMB was analyzed as the total count of somatic mutations (except silent mutations) detected in the tumor.

Immunotherapy

Next, we further predicted the response that the LUAD patients treated with anti-PD-1 and anti-CTLA-4 immunotherapy. To better predict the response to the immune checkpoint inhibitors (ICIs), the immune cell and immunophenotype data were downloaded from The Cancer Immunome Atlas (TCIA) (https://tcia.at/home). The immunophenogram was used to predict anti-PD1/PD-L1 therapy response in LUAD. The immunophenogram was used to calculate the immunophenoscore (IPS) among four types (CTLA4 positive + PD-1 positive, CTLA4 negative + PD-1 negative, CTLA4 positive + PD-1 negative, CTLA4 negative + PD-1 positive, CTLA4 negative + PD-1 positive) from the TCGA database. The IPS scale ranged from 0 to 10. A high IPS predicts a good response to anti-PD-1/PD-L1 therapy. In addition, the correlation between expression level of the gene pair with the other immune checkpoint was also analyzed by Pearson's correlation analysis and shown in a heatmap. The potential response of patients to immunotherapy was inferred by IPS and the tumor immune dysfunction and exclusion (TIDE) score. TIDE scores were calculated by the TIDE algorithm after normalizing the gene expression data (26). The tumor samples were divided into high-expression and low-expression according to the median value of expression level. Then, the TIDE score of the two groups were compared.

Immunohistochemistry

The protein expression of core genes in both LUAD and normal tissues was obtained from the Human Protein Atlas database (HPA) (https://www.proteinatlas.org/), which is a program to map all the human proteins in cells, tissues and organs by using an integration of various omics technologies, including antibody-based imaging, mass spectrometry-based proteomics, transcriptomics and systems biology. In this study, the HPA database was used to analyze the protein expression level and performed immunohistochemistry (IHC) analysis of core genes between normal lung tissues and LUAD tissues.

Molecular docking

To investigate the mechanism of the two genes binding with cisplatin, we made molecular docking between these two genes and cisplatin, respectively. We first obtained the molecular structure of the protein from the RCSB protein data bank (https://www.rcsb.org) and then the binding was obtained by Autodock software, which was used with default values for all parameters (27).

Semi-quantitation RT-PCR

A total of 7 pairs of LUAD tissues and paracancerous tissues were collected from LUAD patients in SWMU hospital. The study was approved by the Ethical Committee of Southwest Medical University/Anhui University of Chinese Medicine, and all patients signed the informed consent form. All surgically removed samples were immediately transferred to liquid nitrogen and stored at -80°C until further research and analysis. The Use RNAsimple Total RNA Kit which was purchased from TIANGEN (Catalog No. DP419) was used to extract total RNA from the sample. The ReverTra Ace® qRNA RT Master Mix which was purchased from TOYOBO (Code No. FSQ-201) was used to reversely transcribes RNA into cDNA. The procedure

of reverse transcription was 37°C for 15min, 50°C for 5min, 98°C for 5min, and 4°C for holding. Then the cDNA was used as a template to prepare the PCR reaction solution. Veriti Thermal Cycler 96 Well (Applied Biosystems AB) was used for the amplification reaction. *ACTB* was used as an internal control. The sequences of the primers *ACTB* were: RT-ACTB-5: 5'-CTCTTCCAGCCTTCCTTCCT-3' (forward primer), RT-ACTB-3: 5'-GTGGCCATCTGTGAGATCCT-3' (reverse primer). The expected product size of *ACTB* was 510 bp. The sequences of the primers SERPINB5 were: RT- SERPINB5 -5: 5'-TTCCTTTTCCACGCATTTTC -3' (forward primer), RT- SERPINB5 -3:5'- GTGGCCATCTGTGAGATCCT -3' (reverse primer). The expected product size of SerpinB5 was 476 bp. The standard procedure of three-step PCR amplification was used: pre-denaturing at 95 °C for 30s, annealling at 60°C for 30s, and extending at 72°C for 30s. *ACTB* has 25 cycles and *SerpinB5* has 33 cycles (28–30).

Statistical analysis

All statistical analyses and graphs were analyzed and displayed by R. $P < 0.05$ was considered to be statistically significant. $P<0.05$ is expressed by "*"; $P<0.01$ is expressed by "**"; $P<0.001$ is expressed by "***".

Results

Identification of DEGs for LUAD that treated by cisplatin

By unified processing of RNA-Seq data downloaded from the TCGA database, the mRNA gene expression levels in 59 normal samples were compared with 539 tumor samples and the results showed that 5169 genes were differentially expressed. There were 12 samples in the GSE73302 database, including 6 samples of the control group (lung cancer patients) and 6 samples of experimental groups (LUAD patients treated with cisplatin after 24h and 48h). The gene expression levels of the control group were compared with the experimental group and 107 genes were found to be differentially expressed. The change in gene expression level distribution in the GEO dataset can be seen in Figures 1A, B.

To obtain the DEGs that the LUAD patients were treated with cisplatin, the DEGs obtained from the TCGA dataset and DEGs obtained from the GEO dataset were intersected by the "Venn" package (Figure 1C). And a total of 17 DEGs were obtained. They were *ZNF677, TLR10, SPATA18, SESN1, SerpinB5, RTN4RL1, NPY5R, GPR87, GLIPR1L2, FUT9, FGF7, FGF5, CYP7A1, CYP2A13, BTG2, AQP9, ABCA12*. The changes in the expression level of 17 DEGs after being treated with cisplatin could be seen from the heatmap (Figure 1E).

PPI analysis in LUAD

The PPI of the 17 DEGs network was established based on the STRING database with 14 edges and 17 nodes. The four genes with the most nodes were *SESN1, SerpinB5, GPR87, and BTG2*. There were four genes, including *ZNF677, TLR10, GLIPR1L2* and *FUT9*, that had no direct relationship with other genes in the PPI network (Figure 1D).

After analysis of the PPI network, 17 genes will affect each other. But the genes that how influenced each other was still unknown. Therefore, we need to explore the correlation between 17 genes. In this study, a heatmap was used to study the correlation (Figure 1F). As depicted in Figure 1F, the expression level of *SerpinB5* was negatively correlated with *BTG2*, *GDR87* and *SESN1*, and positively correlated with *FGFG7*. The expression level of *GDR87* was positively correlated with *BTG2* and *ABCA12*. The expression level of *BTG2* was positively correlated with *SPATA18* and *AQP9*. The expression level of *CYP2A13* was negatively correlated with *SPATA18* and positively correlated with *CYP7A1*. *NYP5R* was positively correlated with *RTN4RL1*. *FGF7* was negatively correlated with *FGF5* (Figure 1F).

The mRNA expression of DEGs between LUAD tissue and Normal tissue.

By comparing the mRNA expression level in the TCGA database, the result showed that compared with normal tissues, the genes with higher expression level of DEGs were *TLR10*, *SerpinB5*, *GPR87*, *FUT9*, *FGF5* and *ABCA12*. The genes with lower expression level were *ZNF677, SPATA18, SESN1, RTN4RL1, NPY5R, GLIPR1L2, FGF7, CYP7A1, AQP9*, CYP2A13 and *BTG2* (Figure 2A).

Gene expression after cisplatin treatment

The DEGs with higher expression level after cisplatin treatment compared with the expression level of A549 were *TLR10, SPATA18, SESN1, RTN4RL1, NPY5R, GPR87, GLIPR1L2, FUT9, FGF5, BTG2, AQP9* and *ABCA12*. The genes with lower expression level after cisplatin treatment in LUAD were *ZNF677*, *SerpinB5*, *FGF7, CYP7A1 and CYP2A13* (Figure 2B). We sorted out the results of this part through a table

The mRNA expression level in normal lung tissue is expressed by "+". "++" respect the mRNA expression level was increased in LUAD tissue, "-" respect the mRNA expression level was decreased in LUAD tissue. Compared with tumor group,there was more "+" when the mRNA level increased after treated with cisplatin. The specific changes of gene expression are shown in Table 1.

From the above results, cisplatin could reduce the expression level of *CYP7A1, SerpinB5* which increased abnormally in LUAD and increase the mRNA expression level of *AQP9, BTG2, GLIPR1L2, NPY5R, RTN4RL1, SESN1, SPATA18* which decreased abnormally in LUAD. Therefore, the above genes may be the key genes of cisplatin in the treatment of LUAD. Next, the prognostic-related genes in DEGs were evaluated, and the results demonstrated that *TLR10, BTG2, FGF5, GPR87* and *SerpinB5* were significantly correlated with OS. Among them, the high-expression of *TLR10* and *BTG2* was significantly correlated with good OS. However, the low-expression of *FGF5, GPR87* and *SerpinB5* were significantly correlated with good OS

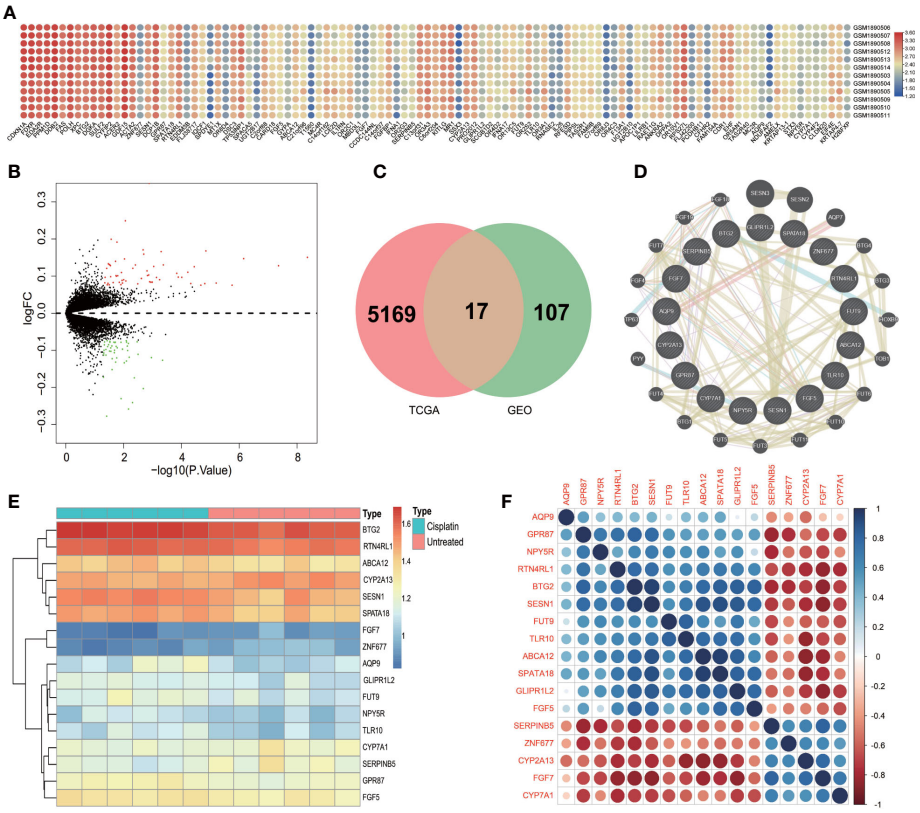

FIGURE 1
The differential expression genes. **(A)** Heatmap of the DEGs in GSE73302 according to the value of |log FC|>1 and P <0.01. The green color indicates lower expression and red color indicates high expression. **(B)** The volcano plots visualize the DEGs in GSE73302. The red nodes represent upregulated genes while the blue nodes represent downregulated genes. **(C)** Common DEGs in GSE73302 and TCGA data sets. A total of 17 commons in the intersection of two gene set. **(D)** Protein–protein interaction network of differentially expressed genes and the related genes from the STRING database. **(E)** Heatmap of the 17 DEGs in GSE73302 according to the value of |logFC|>1 and P<0.01. The green color indicates low expression and red color indicates high expression. **(F)** A heat map shows the correlations of 17 DEGs in LUAD.

(Figures 2C–G). Through the above research, *BTG2* and *SerpinB5* may play a therapeutic role in the treatment of LUAD with cisplatin and they were also mainly related to prognosis.

The mRNA expression of *BTG2* and *SerpinB5* in pan-cancers and LUAD

*BTG*2 is differentially expressed between various cancers and normal tissues. The mRNA expression level in tissues of GBM, GBMLGG, LGG, BRCA, CESC, LIHC, THCA, TGCT, ALL, LAML, and CHOL was higher than that in normal tissues. There was no difference between PCPG, READ tumor tissues and normal tissues. The mRNA expression level of *BTG2* in tissues of UCEC, LUAD, ESCA, STES, KIRP, KIPAN, COAD, COADREAD, PRAD, STAD, HNSC, KIRC, LUSC, WT, SKCM, BLCA, PAAD, OV, UCS, PCPG, ACC, KICH was significantly different from that in normal tissues, and the mRNA expression level in tumor tissues was lower than that in normal tissues (Figure 3A).

By comparing the mRNA expression level of *SerpinB5* in tumor tissues with that in normal tissues, there was no difference in the mRNA expression of SerpinB5 between KIRP, KIPAN, HNSC, KIRC, BLCA and PCPG in normal tissues. The genes with higher mRNA expression level in tumor tissues than that in normal tissues were UCEC, CESC, LUAD, ESCA, STES, COAD, COADREAD, STAD, LUSC, WT, OV, PAAD, UCS and CHO. The genes with lower mRNA expression level in tumor tissues include GBM, GBMLGG, LGG, BRCA, PRAD, LIHC, SKCM, BLCA, REA, TGCT, ALL, LAML, ACC and KICH (Figure 3B).

Compared with normal lung tissues, *BTG2* mRNA expression level was lower in the tissues of LUAD, while the *SerpinB5* higher in LUAD tissues (Figures 3C–F).

Survival analysis of *BTG2* and *SerpinB5*

The OS of patients with high *BTG2* expression was better than that of patients with low *BTG2* expression (P<0.05), and there was no significant difference in PFS between patients with high and low *BTG2* expression (P>0.05) (Figures 3G, I). The OS and PFS of patients with high *SerpinB5* expression were lower than those with low SerpinB5 expression (P<0.05) (Figures 3H, J).

10.3389/fimmu.2023.1098700

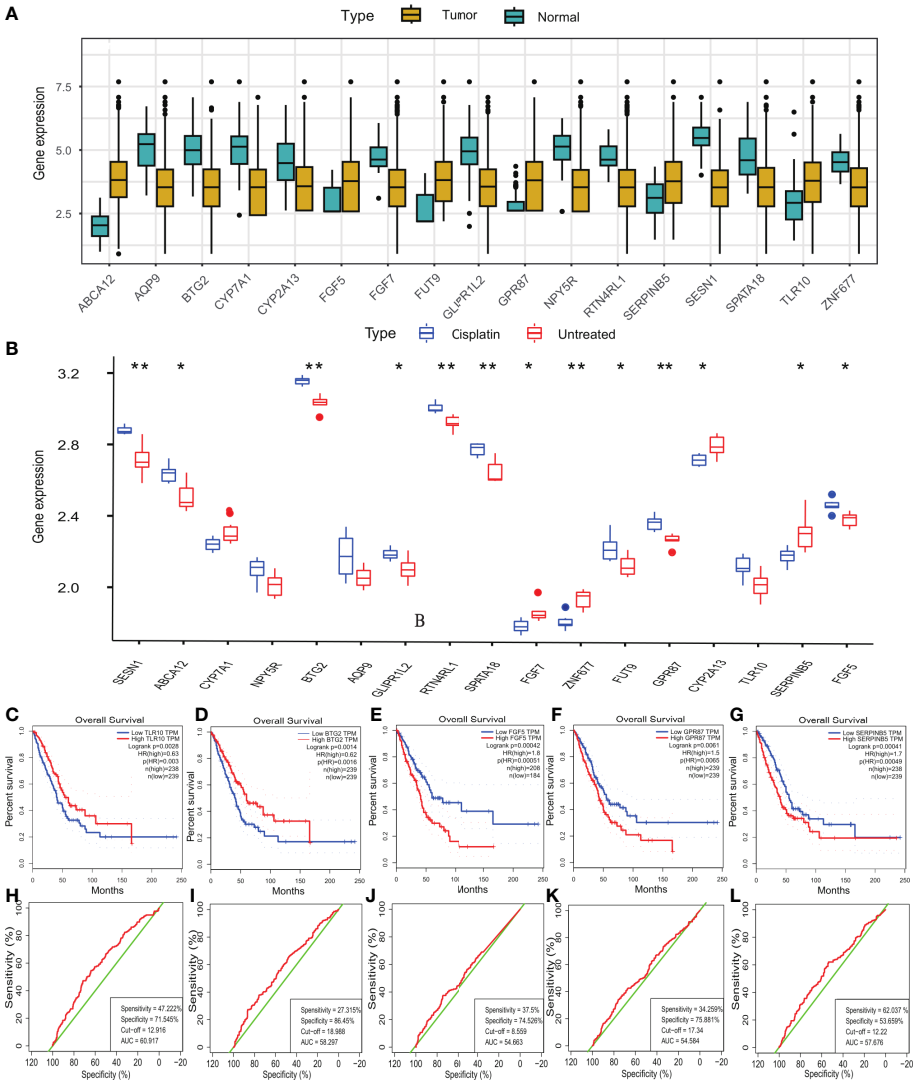

FIGURE 2
The mRNA expression level, survival analysis and ROC curve of DEGs. **(A)** The mRNA expression level of 17 DEGs in TCGA dataset. **(B)** The mRNA expression level of 17 DEGs in GSE73302 dataset. **(C-G)** The OS prognostic value of TLR10, BTG2, FGF5, GPR87, SerpinB5 in human cancer from GEPIA. **(H–L)** The ROC curve demonstrated the diagnostic value of TLR10, BTG2, FGF5, GPR87, SerpinB5 in LUAD patients. **(B)** *P <0.05, **P <0.01.

The relationship between *BTG2*, *SerpinB5* and the clinical characteristics of LUAD patients

BTG2 was differentially expressed in different N stages, M stages, pathological stages and different age groups (Figure 4G). The clinical baseline data was be shown in Table 2. There was no difference in the mRNA expression level of *BTG2* between different sexes (P>0.05) (Figure 4B), but it was differentially expressed between different age groups (P<0.019) (Figure 4A). The expression of *BTG2* in patients aged >=65 years was greater than that in patients aged <65 years (Figure 4A). It is also differentially expressed in different pathological stages. Stage I was differentially expressed with stage II and stage III respectively (P=0.0038, P=0.00019). Compared with Stage I, the gene expression of stage II and stage III are both down. There were significant differences in gene expression of *BTG2* between stage II, stage III and stage IV (P= 0.015, P= 0.0037). Compared with stage II and stage III, the gene expression of stage IV was relatively low (Figure 4C). It was differentially expressed between M0 and M1 (P=0.035), and the gene expression in M1 phase was lower than that in M0 (Figure 4D). N0 was differentially expressed with N1 and N2 (P=0.0023, P=0.0035), and N1 and N2 had lower gene expression than N0 (Figure 4E). It was differentially expressed among T1, T2 and T3 (P=0.0015, P=0.026), and the gene expression of T1 was higher than that of T2 and T3 (Figure 4F).

Overall, *SerpinB5* was differentially expressed in different T stages and different sexes (Figure 5G). The expression level of *SerpinB5* was not different in different age groups (P>0.05) (Figure 5A), but it was different between females and males (P=0.0023) (Figure 5B). Compared with female patients, the expression level of *SerpinB5* in male patients was higher (Figure 5B). In different pathological stages, *SerpinB5* was differentially expressed between stage I and stage III (P=0.016),

and the gene expression of stage I was lower than that of stage III (Figure 5C). There was no difference in N stages and M stages (Figures 5D, E). It was differentially expressed in different T stages. The gene expression levels of T1, T2 and T3 were differentially expressed (P=0.0058, P=0.0011). Compared with T1, the gene expression levels of T2 and T3 were both higher (Figure 5F).

The expression level of BTG2 and SerpinB5 impacted the prognosis of LUAD in patients with different clinicopathological status

Cox regression was used to analyze the potential relationship between *BTG2*, *SerpinB5* and the OS of patients. Univariate Cox

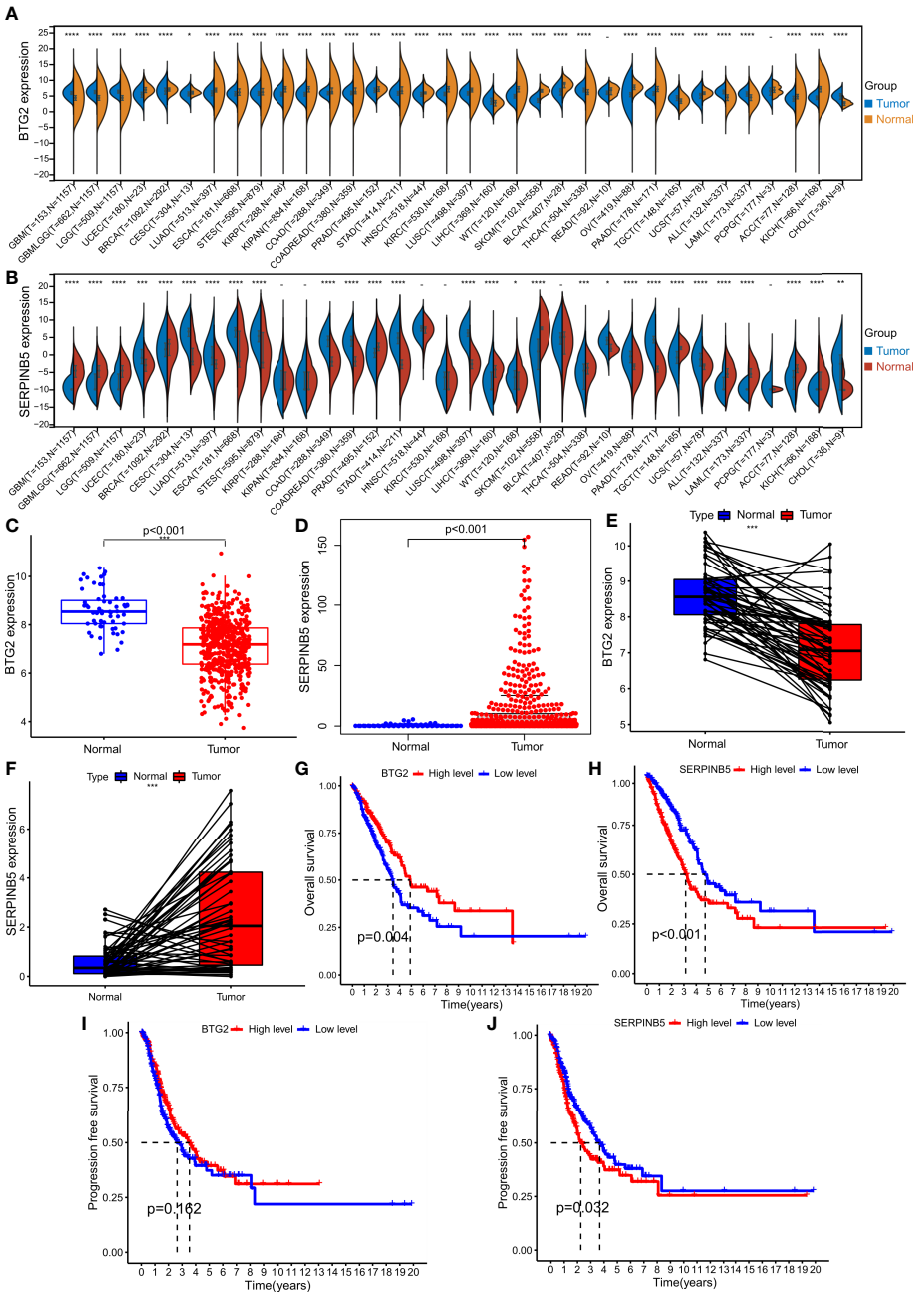

FIGURE 3
The expression levels in Pan cancer and LUAD and the survival analysis of BTG2 and SerpinB5. **(A)** BTG2 expression levels in multiple types of human cancers and adjacent normal tissues across TCGA (*P < 0.05, **P <0.01, ***P < 0.001). **(B)** SerpinB5 expression levels in multiple types of human cancers and adjacent normal tissues across TCGA. **(C, E)** The expression level of BTG2 in LUAD and normal lung tissues. BTG2 was more highly expressed in LUAD compared with normal lung tissues. **(D, F)** The expression level of SerpinB5 in LUAD and normal lung tissues. BTG2 was more highly expressed in LUAD compared with normal lung tissues. **(G–H)** The relationship between BTG2 and SerpinB5 expression and OS in LUAD patients. **(I-J)** The relationship between BTG2 and SerpinB5 expression and PFS in LUAD patients. **(A)** (*P < 0.05, **P <0.01, ***P < 0.001, ****P<0.0001, "-" respect P≥0.05).

TABLE 1 The change of mRNA expression level in LUAD tissue, normal lung tissue and treated with Cisplatin.

Gene symbol	Expression			Gene symbol	Expression		
	Normal	Tumor	Cisplatin		Normal	Tumor	Cisplatin
ABCA12	+	++	+++	GPR87	+	++	+++
AQP9	+	–	+	NPY5R	+	–	+
BTG2	+	–	+	RTN4RL1	+	–	+
CYP7A1	+	–	–	SERPINB5	+	++	+
CYP7A2	+	++	+	SESN1	+	–	+
FGF5	+	++	+++	SPATA18	+	–	+
FGF7	+	–	–	TLR10	+	++	+++
FUT9	+	++	+++	ZNF677	+	–	–
GLIPR1L2	+	–	+				

The mRNA expression level in normal lung tissue is expressed by "+". "++" respect the mRNA expression level was increased in LUAD tissue, "-" respect the mRNA expression level was decreased in LUAD tissue. Compared with tumor group,there was more "+" when the mRNA level increased after treated with cisplatin. "+++" respect the mRNA expression level was increased in LUAD tissue, which was increased compared with normal lung tissue, after treated with cisplatin.

proportional hazards regression was used to assess the factors influencing OS. The results of the univariate Cox analysis suggested that BTG2 was a predictive factor for LUAD (HR: 0.801, CI: 0.701-0.908, P <0.001) (Figure 6A). Using the forest plot to demonstrate the results of the multivariate Cox analysis, the results showed that *BTG2* was an independent prognostic factor for the prognosis of patients with LUAD (HR: 0.779, CI: 0.681-0.892, P <0.001) (Figure 6B). These results suggest that *BTG2* can be used as a diagnostic and prognostic marker for LUAD.

The results of the univariate Cox analysis suggested that *SerpinB5* was a high-risk factor for LUAD (HR:1.156, CI:1.085-1.233, P <0.001) (Figure 6E). Using the forest plot to demonstrate the results of the multivariate Cox analysis, *SerpinB5* was an independent risk factor for the prognosis of patients with LUAD (HR: 1.143, CI: 1.069-1.222, P <0.001) (Figure 6F). These results suggest that SerpinB5 can be also used as a diagnostic and prognostic marker for LUAD.

BTG2 and SerpinB5 co-expression in LUAD

In order to screen the core genes related to *BTG2* and *SerpinB5* and predict the regulatory relationship between genes, we constructed the co-expression network of *BTG2* and *SerpinB5*, respectively (Figure 6C). The results showed that *BTG2* has positive regulation with

TABLE 2 The clinical baseline data.

Characteristic	All patients [cases (%)]	Characteristic	All patients [cases (%)]
Gender		**Clinical T stage**	
female	265 (54.1)	T1	168 (34.3)
male	225 (45.9)	T2	257 (52.4)
Vital Status		T3	44 (9)
Alive	312 (63.7)	T4	18 (3.7)
Dead	178 (36.3)	Others	3 (0.6)
Age	NA	**Clinical Stage**	
<65	218 (46.2)	Stage_I	266 (54.3)
>65	254 (53.8)	Stage_II	118 (24.1)
Clinical N stage		Stage_III	80 (16.3)
N0	316 (64.5)	Stage_IV	26 (5.3)
N1	91 (18.6)	**Clinical M stage**	
N2	70 (14.3)	M0	323 (66.3)
N3	2 (0.4)	M1	25 (5.1)
others	11 (2.2)	others	139 (28.5)

CACNA2D2, FOS, CYFIP2, SFTPB, CGNL, EGR. It has negative regulation with *CENPA, SPC24, AUNIP, KIF2C and ANLN*. And the results showed that *SerpinB5* has positive regulation with *GJB4, KRT6B, GJB4, SH3PXD2A-AS1, ITGA6, ANXA8*. It has negative regulation with *CISH, PTCSC3, ST3GAL5, NKX2-1-AS1 and NKX2-1* (Figure 6G).

GSEA and GO Analysis of BTG2 and SerpinB5 in LUAD

In order to preliminarily explore the possible ways and pathways through which BTG2 and SerpinB5 function in the development of LUAD, the GSEA was used to perform enrichment analysis on BTG2 and SerpinB5. According to the p-value < 0.05, FDR < 0.05, significant enrichment pathways were screened. The results demonstrate that Aldosterone regulates sodium reabsorption, Neuroactivity, ligand receptor interaction and Vascular smooth muscle contraction were active when BTG2 was highly expressed. Olfactory conduction, Systemic lupus erythematosus were active when BTG2 was active at low BTG2 expression (Figure 6D).

The results demonstrate that Ascorbic acid and aldarate metabolism, Metabolism of xenobiotics by cytochrome P450, Porphyrin and chlorophyll metabolism, Retinol metabolism and Steroid hormone biosynthesis were active when SerpinB5 was highly expressed (Figure 6H).

The PPI network was made of genes related to BTG2 and SerpinB5, and the results show that FOS and EGR1 interact with

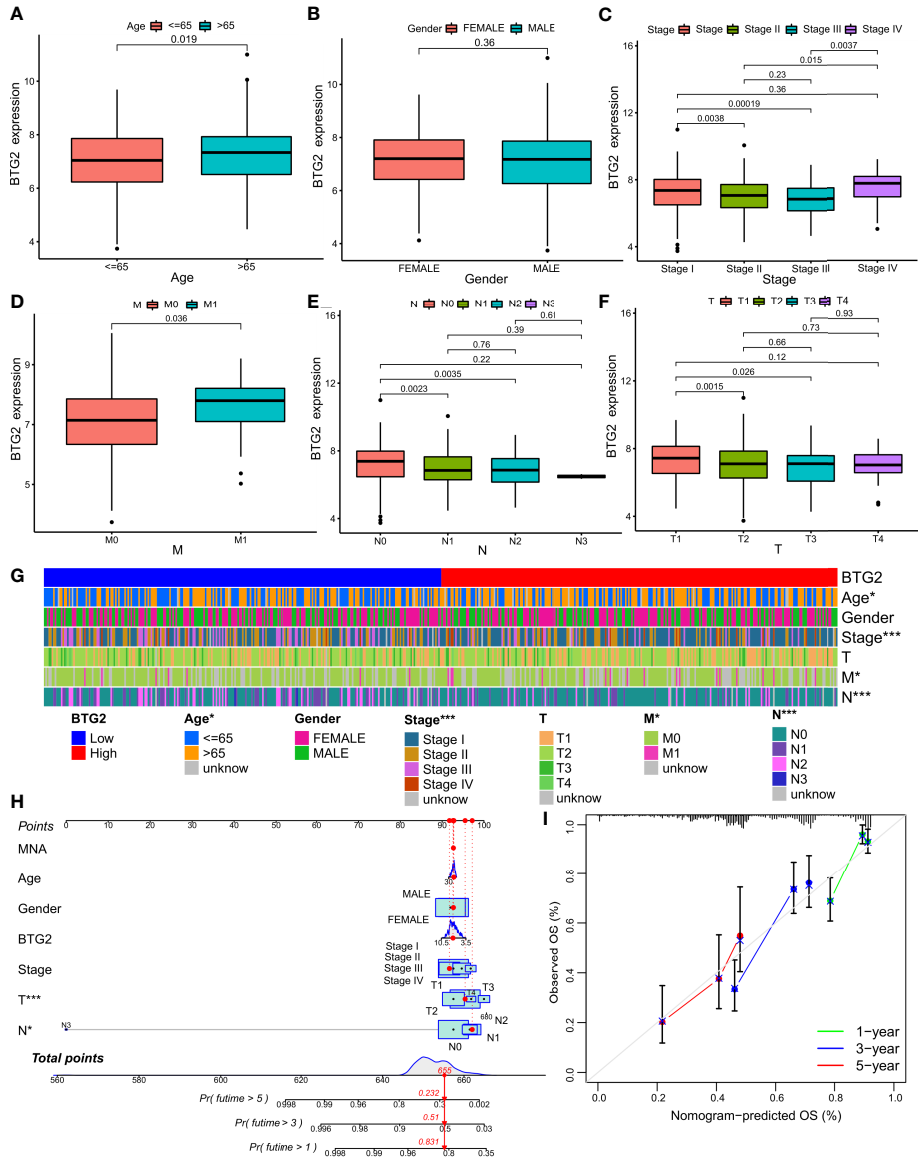

FIGURE 4
Relationship between the prognostic marker and clinicopathological factors of LUAD patients. **(A–F)** Correlation between BTG2 mRNA expression and clinical characteristics in patients with LUAD. P < 0.05 was considered significant. Age, Gender, Stage, M, N, T. **(G)** The heatmap shows the expression of the BTG2 and clinicopathological factors of LUAD patients in the high- and low-risk groups. **(H)** Construction BTG2-based nomogram for LUAD patients to predict OS. **(I)** The calibration curve and Hosmer–Lemeshow test of BTG2-based nomograms in the TCGA-LUAD cohort for OS. **(G)** (*P < 0.05, ***P < 0.001).

many other genes in the PPI network (Figure 7A). By the GO analysis, the above genes were found to be mainly enriched in wide pore channel activity, gap junction channel activity, contractile ring, NMS complex and other functions. This may be the potential mechanism of these two genes (Figure 7B).

Identification of lncRNA/miRNA/mRNA network

In order to study the mechanism, we also studied the potential lncRNA/miRNA/mRNA network. Searching for "BTG2" in the StarBase database, and a total of 218 miRNAs were obtained. Searching for "SerpinB5 ", and a total of 80 miRNAs were obtained. After the intersection of the two groups of miRNAs, 42 miRNAs were obtained (Figure 7C). Using these 42 miRNAs as keywords to search for relevant lncRNAs. These genes should be analyzed for correlation with BTG2 and SerpinB5 respectively, and a total of 31 lncRNAs were selected. The network results were shown in Figures 7F. NRAT1 was associated with more miRNAs and correlated with BTG2 and SerpinB5C (Figures 7D, E), so we speculate that these two genes may play a role through NRAT1.

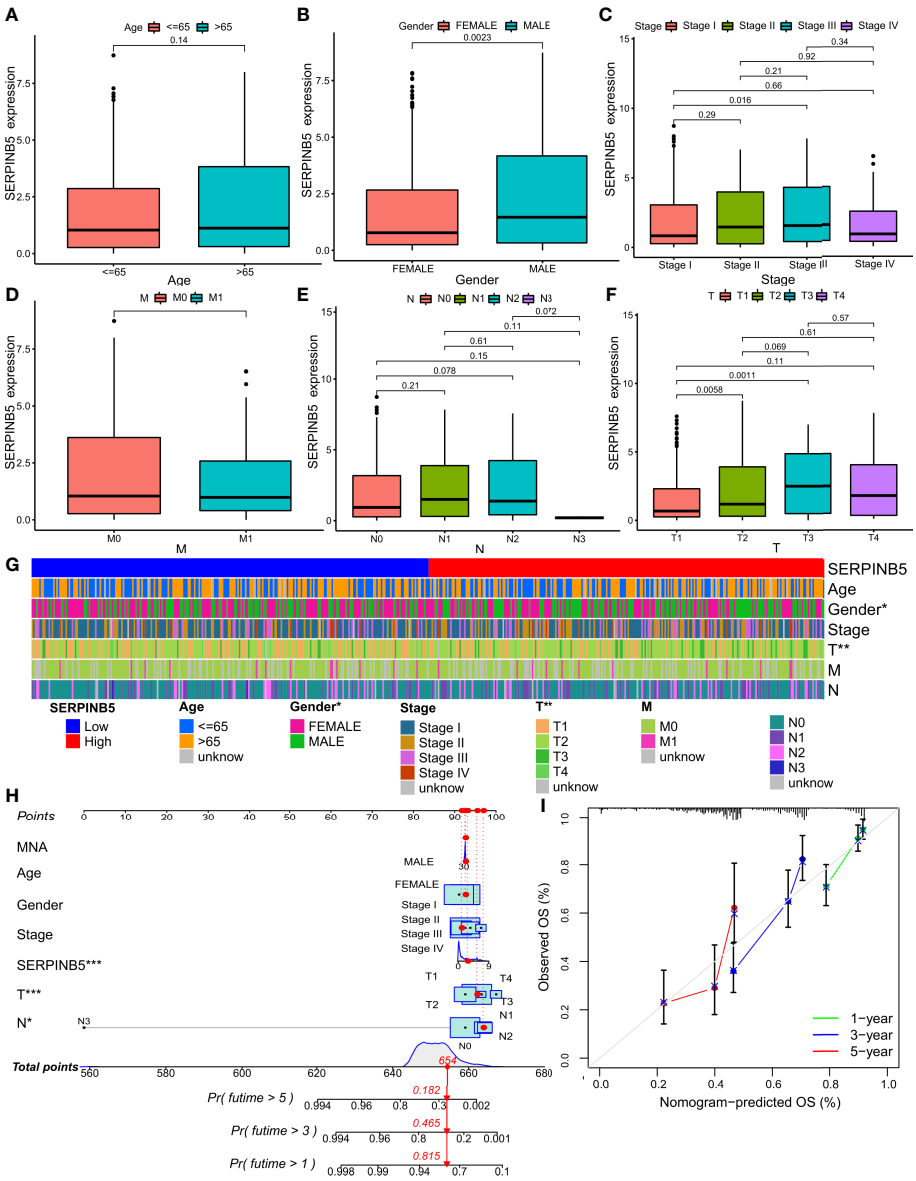

FIGURE 5
Relationship between the prognostic marker and clinicopathological factors of LUAD patients. **(A–F)** Correlation between SerpinB5 mRNA expression and clinical characteristics in patients with LUAD. P < 0.05 was considered significant. Age, Gender, Stage, M, N, T. **(G)** The heatmap shows the expression of the SerpinB5 and clinicopathological factors of LUAD patients in the high- and low-risk groups. **(H)** Construction SerpinB5-based nomogram for LUAD patients. predict OS. **(I)** The calibration curve and Hosmer–Lemeshow test of SerpinB5-based nomograms in the TCGA-LUAD cohort for OS. **(G)** (*P < 0.05, **P <0.01).

Relationship between mRNA expression of *BTG2* and *SerpinB5* and immune microenvironment and tumor mutational burden

The immune microenvironment influences cancer progression by immune cells. To understand whether immune cells contribute to tumor growth, tumor immune cell infiltra1. There were significant differences in the number of immune cells between high and low expression groups of *BTG2* (P<0.05) and *SerpinB5* (P<0.05) (Figures 8A, 9A). In the high-expression group of *BTG2* (Figure 8A) and the low-expression group of *SerpinB5* (Figure 9A), there were more immune cells in the immune microenvironment.

In order to further observe which immune cells are differentially expressed, the differentially expressed of *BTG2* in 22 immune cells was observed. The results showed that the *BTG2* in T cells CD8, T cells CD4 memory resetting, T cells CD4 memory activated, NK cells resting, Macrophages M0, Macrophages M1, Dendritic cells resting, Mast cells resting, Mast cells activated and Eosinophils were differentially expressed (Figure 8B). Besides, the correlation between gene expression and immune cells were also be studied (Figure 8C). The results suggest that mRNA expression level of *BTG2* were positively correlated with T cells CD4 memory resting (R = 0.25, p = 9.3e−08), Dendritic cells resting (R = 0.19, p = 5.8e−05), Mast cells resting (R = 0.19, p = 3.3e−05) and negatively correlated with Macrophages M1 (R = -0.16, p = 0.00079), T cells CD4 memory activated (R = -0.2, p = 1.2e−05), Macrophages M0 (R = -0.2, p = 2.3e−05), NK cells resting (R = - 0.14, p = 0.0036), Mast cells activated (R = - 0.1, p = 0.031), T cells regulatory (Tregs) (R = - 0.12, p = 0.011) (Figures 8D–L). The results showed that when the prognosis of patients with LUAD was poor, the expression level of *BTG2* was lower. Meanwhile, the immune cells which were

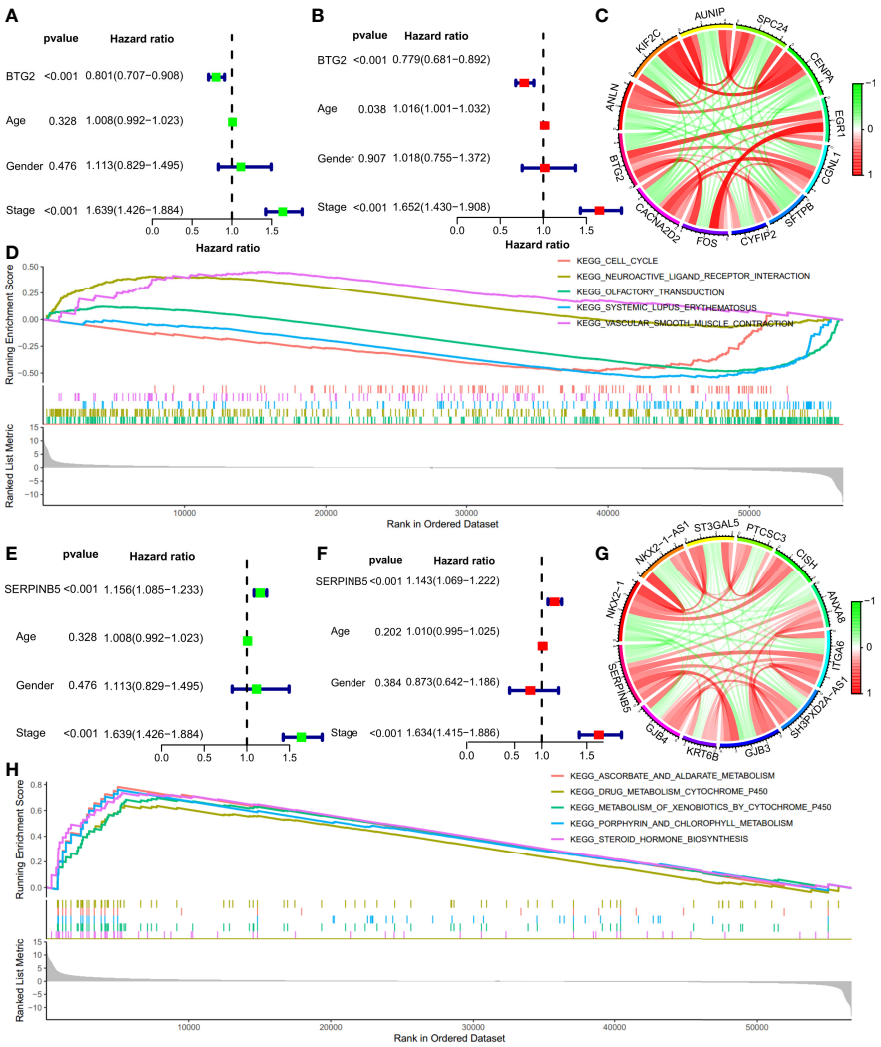

FIGURE 6
The Cox regression analyses, co-expression genes analyses, GSEA analyses of BTG2 and SerpinB5. **(A, B)** The univariate and multivariate Cox regression analyses of prognosis for BTG2 and clinicopathological factors. **(C)** The relationship of BTG2 and co-expression genes. The green color indicates negative correlation and red color indicates positive correlation. **(D)** The results of GSEA between high and low expression of BTG2 in LUAD patients. **(E, F)** The univariate and multivariate Cox regression analyses of prognosis for SerpinB5 and clinicopathological factors. **(G)** The relationship of BTG2 and co-expression genes. The green color indicates negative correlation and red color indicates positive correlation. **(H)** The results of GSEA between high and low expression of SerpinB5 in LUAD patients.

positively related to the expression of *BTG2* may play an anti-tumor role. However, the immune cells negatively related to the expression of *BTG2* may play a role in promoting the occurrence and development of tumors.

The two groups of *SerpinB5* were differentially expressed in T cells CD8, T cells CD4 memory resting, T cells CD4 memory activated, NK cells resting, Macrophages M0, Macrophages M1, Dendritic cells resting, Mast cells resting, Mast cells activated, Eosinophils among 22 immune cells (Figures 9B, C). The mRNA expression of *SerpinB5* were positively correlated with Macrophages M0 (R = 0.16, p = 0.00055), NK cells resting (R = 0.097, p = 0.04), T cells CD4 memory activated (R = 0.097, p = 0.04) (Figures 9D, G, H), and negatively correlated with Dendritic cells resting (R = -0.12, p = 0.012), Monocytes (R = - 0.11, p = 0.017) (Figures 9E, F). The mRNA expression level of *SerpinB5* was not correlated with TMB (P>0.05) (Figure 10B). The mRNA expression level of BTG2 was negatively correlated with TMB (R = - 0.29, P = 5.8e − 11) (Figure 10A).

The above results showed that when the gene expression of *BTG2* was low and the expression of *SerpinB5* was high, the prognosis of patients was poor when they were used as a gene pair as a prognostic marker. By analyzing the relationship between *BTG2*, *SerpinB5* and immune cells, the immune cells that were related to the changes of these two genes are Macrophages M0. At this time, the number of macrophages in the immune microenvironment increases, which indicates that the increase of Macrophages M0 may be a reason for the poor prognosis of LUAD patients.

Relationship between *BTG2*, *SerpinB5* and immunotherapy

In order to study the relationship between mRNA expression and immunotherapy, the IPS produced by the high-expression and low-expression groups under the four treatment methods would be compared. The higher the IPS, the better the effect of immunotherapy. The results show that in CTLA4_ negative+PD-1_ Negative type and CTLA4_ positive + PD-1_ negative type, there was a significant difference in IPS between high-expression and low-expression of *BTG2* (P<0.05) (Figures 10C, E), and in CTLA4_ positive + PD-1_ Positive type and CTLA4_ negative+ PD-1_ positive type (Figures 10D, F), there was no significant difference in IPS between the two groups (P>0.05). Interestingly, in CTLA4_

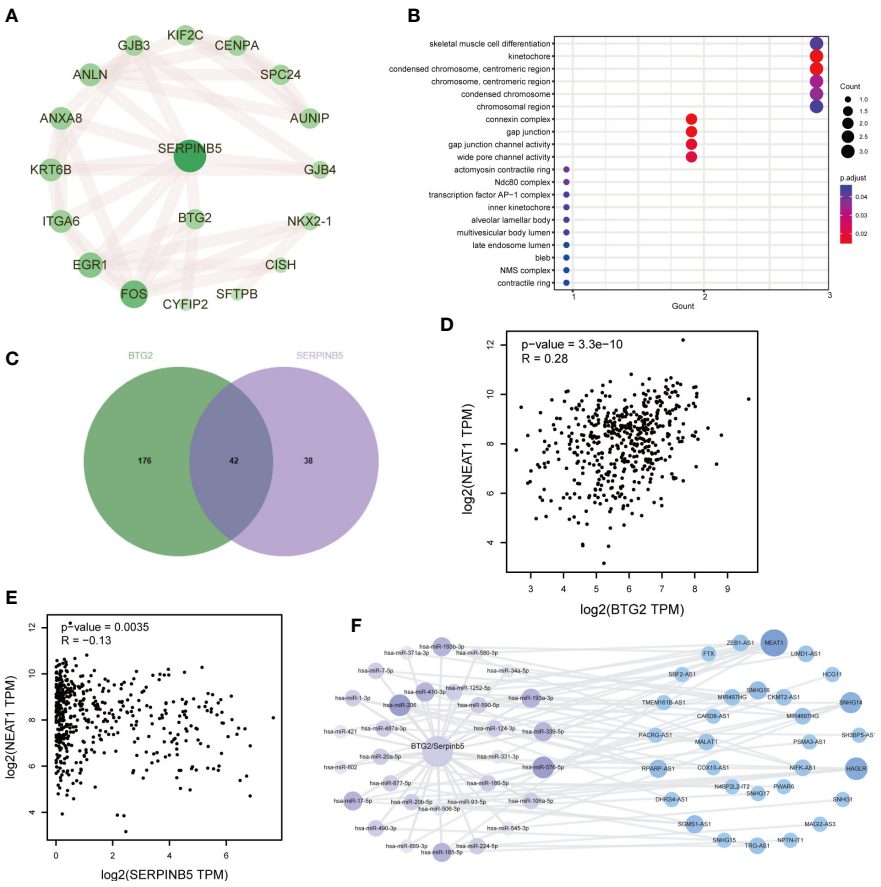

FIGURE 7
The potential mechanism of BTG2 and SerpinB5 in the LUAD. **(A)** PPI Network of BTG2, SerpinB5 and the co-expressed genes. **(B)** The GO enrichment analysis of BTG2, SerpinB5 and the co-expressed genes. **(C)** The counts of BTG2 related miRNAs, SerpinB5 related miRNAs and the intersection genes. **(D)** Correlation analysis of BTG2 and NEAT1 in LUAD. **(E)** Correlation analysis of SerpinB5 and NEAT1 in LUAD. **(F)** The LncRNA/miRNA/mRNA network.

negative+PD-1_ IPS of negative, *BTG2* high and low expression groups were higher than that of CTLA4_ positive + PD-1_ negative. The results showed that patients with high *BTG2* expression had a better therapeutic effect with the same immunotherapy. For patients with high expression, immunotherapy was better when CTLA-4 and PD-1 were inhibited at the same time.

By studying the relationship between the two groups of *SerpinB5* and immunotherapy methods, the results showed that in CTLA4_ negative+PD-1_ Negative and CTLA4_ positive + PD-1_ negative, IPS in the low-expression group was higher than that in high-expression group (P<0.005) (Figures 10H, J), and in CTLA4_ positive + PD-1_ Positive and CTLA4_ negative+ PD-1_ positive, there was no significant difference in IPS between high and low expression groups (Figures 10I, K). Interestingly, in CTLA4_ negative+PD-1_ Negative, IPS of high and low expression groups were higher than the IPS in CTLA4_ positive + PD-1_ negative. The results showed that patients with low *SerpinB5* expression had a better therapeutic effect with the same immunotherapy. For patients with low expression, CTLA4_ negative+PD-1_ Negative immunotherapy would be better.

In the TCGA LUAD cohort, the TIDE score of the high-expression group of *BTG2* was significantly lower than that of the low-expression group (Figure 10M). The TIDE score of the high-expression group of *SerpinB5* was significantly higher than that of the low-expression group (Figure 10N). By comparing the IPS and TIDE score of the high-expression group with the low-expression group of two genes, the potential immunotherapeutic effect of the high-expression group of *BTG2* would be better than that of the low-expression group, and the effect of the low-expression group of *SerpinB5* would be better than that of high-group.

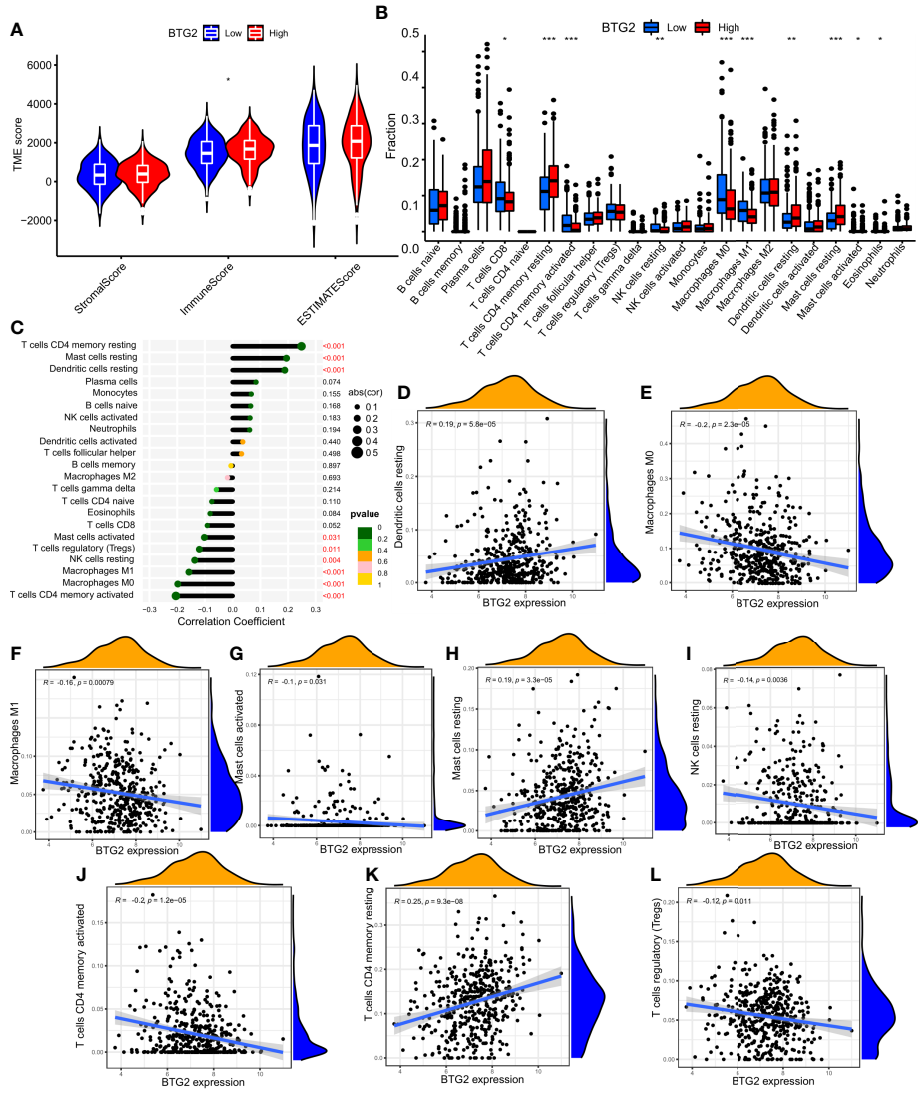

FIGURE 8
The expression of BTG2 was associated with immune infiltration in the LUAD microenvironment. **(A)** Composition of tumor microenvironment in high and low expression groups of BTG2. **(B)** Comparison of the infiltration of 22 leukocyte types between high and low BTG2 groups. **(C)** Correlation between the relative abundances of 22 immune cells and BTG2 expression level. **(D–L)** Correlation between BTG2 expression and immune cell infiltration in LUAD from TCGA sample. Dendritic cells resting, Macrophages M0, Macrophages M1, Mast cells activated, Mast cells resting, NK cells resting, T cells CD4 memory activated, T cells CD4 memory resting, T cells regulatory (Tregs). **(B)** [(*P < 0.05, **P <0.01, ***P < 0.001)].

Correlation between BTG2 and SerpinB5 gene expression levels and immune checkpoint gene expression levels

BTG2 was negatively correlated with immune checkpoint related gene *CD276*, and were positively correlated with *CD244*, *BTLA*, *ICOS*, *TNFRSF14*, *TNFSF14*, *TNFSF15*, *CD40LG*, *LGALS9*, *TNFSF18*, *CTLA4*, *CD27*, *CD200R1*, *CD28*, *CD48* (Figure 10G). Additionally, *SerpinB5* was negatively correlated with immune checkpoint-related genes *NRP1*, *TNFSF15*, *CD40LG*, *IDO2*, and positively correlated with *CD276* (Figure 10L). Both *BTG2* and *SerpinB5* were correlated with immune checkpoints *CD276* and *CD40LG*, while *BTG2* was negatively correlated with *CD276* and positively correlated with *CD40LG*. *SerpinB5* was positively correlated with *CD276* and negatively correlated with *CD40LG*. As a result, when *BTG2* was down-regulated and *SerpinB5* was up-regulated in LUAD, the expression of *CD276* increased and the expression of *CD40LG* decreased.

Multiple methods for validation

To verify the reliability of our analysis, we also investigated the changes in these two genes in other datasets. The GSE11969 database was downloaded, which was composed of 163 independent samples, including 158 lung samples and 5 normal lung tissue samples. We selected 90 LUAD patients from 158 patients and 5 normal patients as the study subjects. Differential analysis revealed that the two genes were differentially expressed in normal lung tissue and lung adenocarcinoma samples, with *BTG2* downregulated and *SerpinB5* upregulated compared with normal lung tissue, which is in agreement with the data we analyzed in the TCGA repository (Figures 11A, B).

In addition to these, we analyzed both genes in this dataset for survival analysis and correlation with clinical characteristics. The results showed that patients in the high expression group of *BTG2* had a better prognosis (Figure 11C). But showed no association of *SerpinB5* with patient outcome in this gene set. But there was no significant difference in *SerpinB5* by Survival analysis (Figure 11D).

Meanwhile, we analyzed the correlation between *SerpinB5* and clinical characteristics. The results showed that there were differences in mRNA expression level between different ages and different stages, but there was no difference between different genders (Figures 11E–G).

IHC staining images from HPA further validated the findings. IHC also indicated that SerpinB5 was remarkably overexpressed in the LUAD sample at the proteomic level, in

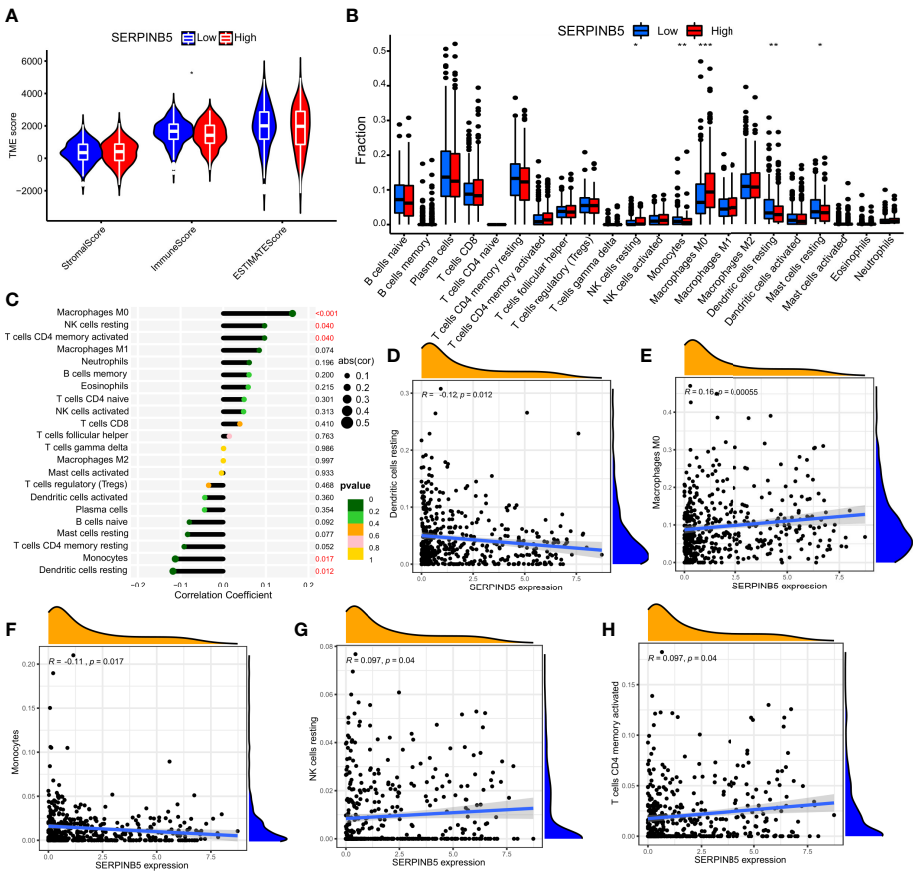

FIGURE 9
The expression of SerpinB5 was associated with immune infiltration in the LUAD microenvironment. **(A)** Composition of tumor microenvironment in high and low expression groups of SerpinB5. **(B)** Comparison of the infiltration of 22 leukocyte types between high and low SerpinB5 groups. **(C)** Correlation between the relative abundances of 22 immune cells and SerpinB5 expression level. **(D–H)** Correlation between BTG2 expression and immune cell infiltration in LUAD from TCGA sample. Dendritic cells resting, Macrophages M0, Monocytes, NK cells resting, T cells CD4 memory activated. **(B)** (*P < 0.05, **P <0.01, ***P < 0.001).

10.3389/fimmu.2023.1098700

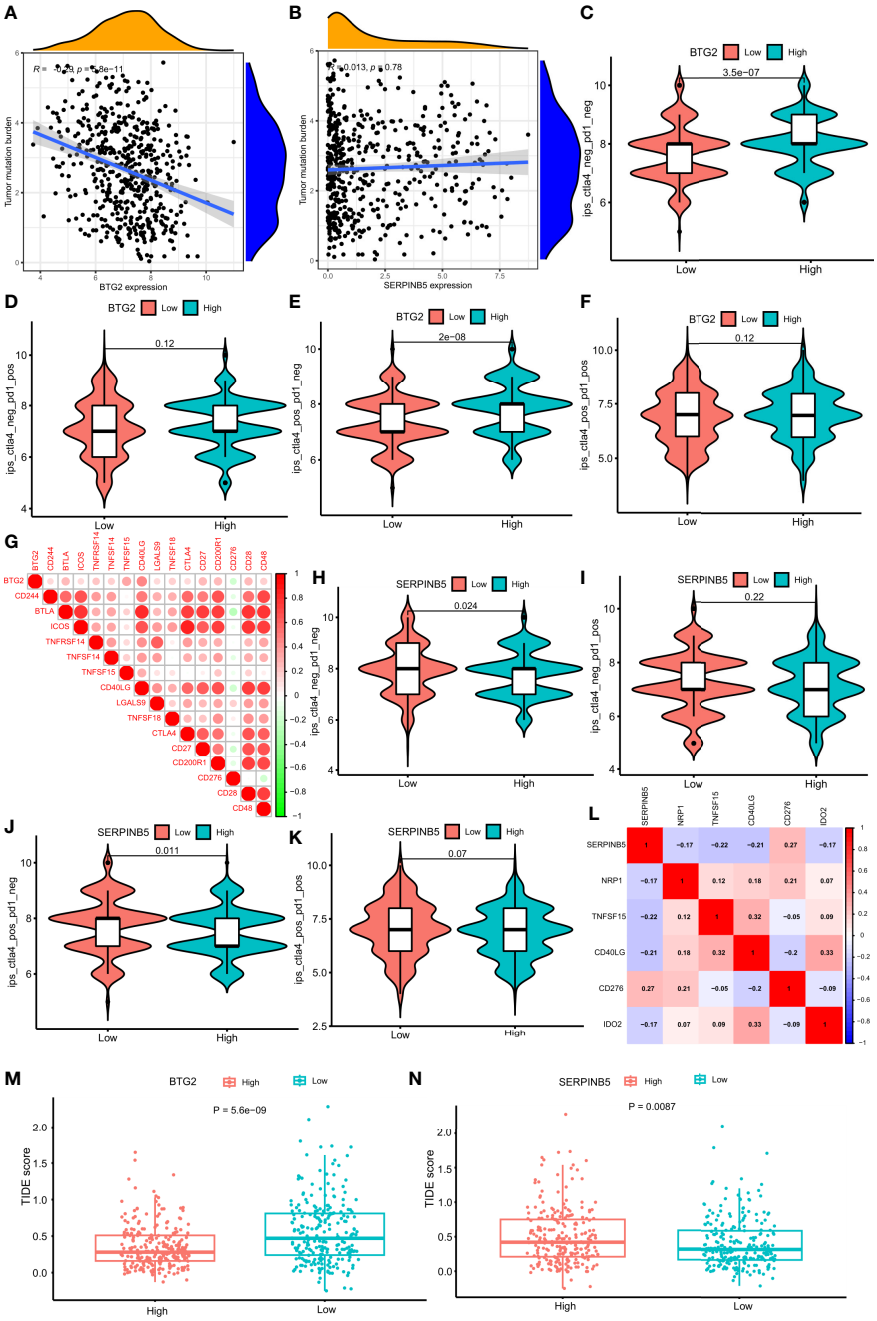

FIGURE 10
Comparison of the IPS in four groups and the relationship of the genes. **(A)** Correlation analysis of BTG2 expression and TMB in LUAD. **(B)** Correlation analysis of SerpinB5 expression and TMB in LUAD. **(C–F)** Comparison of the IPS between high- and low-expression groups of BTG2, IPS-CTLA4 negative + PD-1 negative, IPS-CTLA4 negative + PD-1 positive, IPS-CTLA4 positive + PD-1 negative, IPS-CTLA4 positive + PD-1 positive. **(G)** Correlations between BTG2 and Immune checkpoints associated with BTG2. Corr denotes Pearson correlation coefficient. The red nodes represent positive correlation with BTG2 while the green nodes represent negative correlation with BTG2. **(H–K)** Comparison of the IPS between high- and low-expression groups of SerpinB5, IPS-CTLA4 negative + PD-1 negative, IPS-CTLA4 negative + PD-1 positive, IPS-CTLA4 positive + PD-1 negative, IPS-CTLA4 positive + PD-1 positive. **(L)** Correlations between SerpinB5 and Immune checkpoints associated with the gene. Corr denotes Pearson correlation coefficient. The red nodes represent positive correlation with the gene while the green nodes represent negative correlation with the gene. **(M)** Boxplot representation of TIDE scores in the high-group versus low-group of BTG2 in TCGA LUAD cohort. **(N)** Boxplot representation of TIDE scores in the high-group versus low-group of SerpinB5 in TCGA LUAD cohort.

comparison with the expression of SerpinB5 in normal Lung gland tissue (Figure 11I) and BTG2 was an inadequate expression in LUAD tissues (Figure 11H). The results of the analysis by the two methods agree with the results analyzed in the TCGA database.

In addition to the above studies, we also compared the mRNA expression of *SerpinB5* in LUAD with paracancerous tissues through qRT-PCR, and the results showed that the gene expression of *SerpinB5* was higher in LUAD tissues compared with paracancerous tissues, which was consistent with the results

obtained by bioinformatics approach (Figure 11J). And the difference between *BTG2* was not significant. So we didn't do too much research about *BTG2*.

Molecular docking

We simulated the binding situation of cisplatin with BTG2 and SerpinB5 by molecular docking, and the results showed that the binding affinities of BTG2 and SerpinB5 with cisplatin were mainly affected by hydrogen bonding and hydrophobic bonds (Figures 12D–F). Cisplatin forms H-bond networks with BTG2 in His50, Asp76, Tyr66 (Figures 12D–F). And cisplatin forms H-bond interactions with SerpinB5 in Glu21, while forms hydrophobic bonds in Leu19, Val28, Lys371, Phe16, Lys17 (Figures 12D–F).

Discussion

NSCLC is the most common subtype of lung cancer, which can be divided into squamous cell carcinoma, large cell carcinoma and lung adenocarcinoma. Clinically, about 50% of patients were LUAD (31). Since most patients were diagnosed in the late stage of lung cancer, their 5-year survival time is difficult to exceed 15% after comprehensive treatment such as surgery, radiotherapy and chemotherapy (32). In recent years, the discovery of new molecular targets has promoted the development of new therapies such as targeted therapy and immunotherapy (25). For different treatment methods, there is an urgent need for stable and reliable prognostic biomarkers to identify subgroups with a high risk of death. Therefore, finding prognostic markers can effectively evaluate the survival probability of patients with LUAD and reasonably adjust the treatment methods.

Presently, in order to find appropriate tumor prognostic markers, we obtained DEGs in LUAD through bioinformatics technology. In addition, the cisplatin was used as the basic drug to study the genes whose gene expression changes when the drug acts. And the genes related to the OS of patients were also be studied. The genes that meet the above three conditions were regarded as genes that may become tumor prognostic markers. The results show that only BTG2 and SerpinB5 meet the above conditions. Compared with normal lung tissue, BTG2 was down-regulated in LUAD and *SerpinB5* was up-regulated in LUAD (Figure 3). After cisplatin treatment, cisplatin can increase the expression level of *BTG2* which was downregulated in LUAD compared with that in normal lung tissue, and decrease the expression level of *SerpinB5* which was upregulated in LUAD (Figure 2A) compared with that in normal lung tissue. At the same time, *BTG2* and *SerpinB5* were also related to the prognosis of patients. The prognosis was poor when *BTG2* was at low expression and poor when *SerpinB5* was at high expression (Figure 3). Therefore, we infer that *BTG2* and *SerpinB5* have the potential to become prognostic markers in patients with LUAD. Cox regression analysis showed that both of them were independent prognostic factors (Figures 6, 8). Moreover, the nomogram also confirmed that when both were used as prognostic factors, their prediction accuracy was also high (Figures 4, 5).

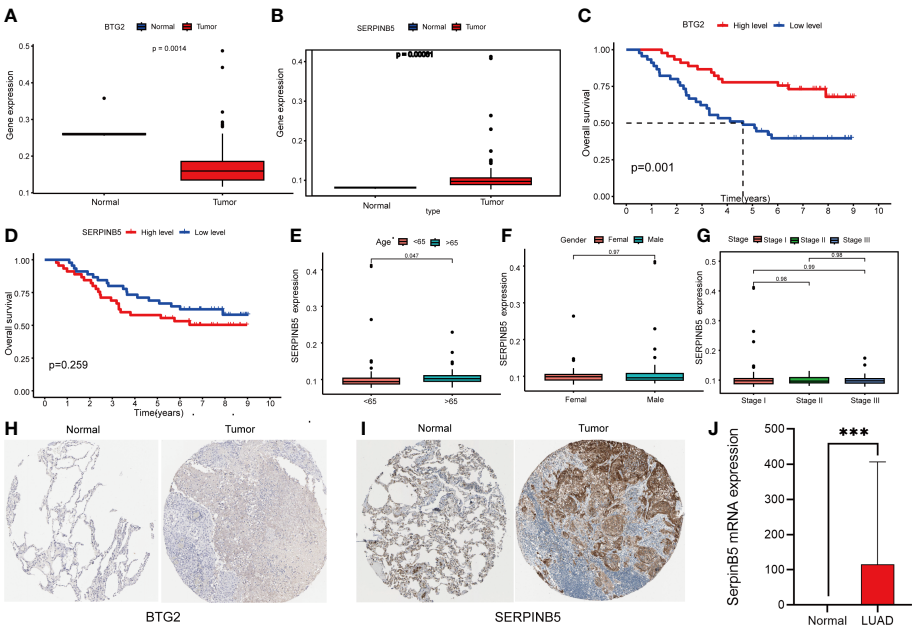

FIGURE 11
Analysis of BTG2 and SerpinB5 GSE11969 by dataset and Immunohistochemistry (IHC). **(A, B)** The expression level of *BTG2* and *SerpinB5* in LUAD and normal lung tissues in GSE11969 dataset. **(C, D)** The relationship between BTG2 and SerpinB5 expression and OS in LUAD patients. **(E–G)** Correlation between SerpinB5 mRNA expression and clinical characteristics in patients with LUAD. P< 0.05 was considered significant. Age, Gender, Stage. **(H, I)** Immunohistochemistry of BTG2 and SerpinB5 expression in LUAD tissues and corresponding normal tissues based on The Human Protein Atlas (HPA). **(J)** The results of SqRT-PCR of *SerpinB5*. Compared with paracancerous tissues, the mRAN expression were increasing in LUAD. **(J)** (***P < 0.001).

BTG2 was considered to be a tumor suppressor, which was highly expressed in a variety of normal tissues (33–36). It has been reported that BTG2 could play an anti-tumor role in a variety of ways. In the process of tumor occurrence and development, BTG2 played an important role in cell proliferation, differentiation, apoptosis and DNA damage repair. Wei found that overexpression of BTG2 can inhibit the proliferation and invasion of some tumors, including lung cancer cells (37). Zhang also found that BTG2 can promote or induce apoptosis of triple negative breast cancer cells and inhibit cell invasion (38).

SerpinB5 was first proposed as a tumor suppressor, and the mRNA expression level was downregulated in a variety of malignant tumors (39) compared with that in normal tissue. Some studies have found that SerpinB5 can inhibit tumor cell infiltration and metastasis, promote tumor cell apoptosis, and inhibit tumor vascular growth (40, 41). However, interestingly, our study found that *SerpinB5* expression level was up-regulated in LUAD (Figures 3E, F), and it may be used as a tumor inducer in the process of tumorigenesis. Lei found that SerpinB5 can promote the occurrence and development of gastric cancer in gastric cancer cell line HTB103 (42). However, there is no more in-depth study on SerpinB5 promoting the occurrence and development of gastric cancer. The results of this study showed that SerpinB5 has the potential to become an independent prognostic factor of LUAD (Figure 6), so it is necessary to further study the mechanism.

In addition to finding the relationship between the two genes, we reasoned the mechanism of the gene pair in LUAD from the perspective of lncRNA/miRNA/mRNA and finally deduced a pathway, which was NEAT1/miR-193b/SerpinB5 (BTG2) (Figure 7).

Besides, through correlation analysis, the mRNA expression of *BTG2* and *SerpinB5* was positively correlated (Figure 1F). This may be because both of them were p53 downstream regulatory genes. The recent study suggests that *BTG2* was originally identified as a p53-inducible gene. Expression of BTG2 was significantly increased in response to DNA damage, and this increase was a consequence of p53 induction since the expression of a loss-of-function p53 mutant does not lead to BTG2 accumulation in this context (41). Meanwhile, SerpinB5 has also been reported to be the target gene of tumor suppressor gene p53. There was a p53 binding site in the promoter region of 84~112 nucleotides of the SerpinB5, and p53 can bind to this site to activate the SerpinB5 promoter and control its mRNA transcription. When wild-type p53 binds to the p53 binding site in the promoter region, it can stimulate histone acetylation and increase the accessibility of chromatin in the promoter region, thus activating p53 expression. On the contrary, mutant p53 will inhibit SerpinB5 expression (43). The positive correlation between BTG2 and SerpinB5 gene expression may be due to both being regulated by p53. However, in-depth research is needed on its specific relationship. By constructing the prognosis model, both *BTG2* and *SerpinB5* can be used to evaluate the 1-year, 3-year and 5-year survival rates of patients, and the accuracy of the model was high.

Through the study, it was found that *BTG2* was low expression and *SerpinB5* was high expression, and the prognosis of LUAD patients was poor. At this time, the active biological function of BTG2 was Olfactory conduction, Systemic lupus erythematosus. Among them, some studies have found that patients with systemic lupus erythematosus were easy to be associated with lung cancer,

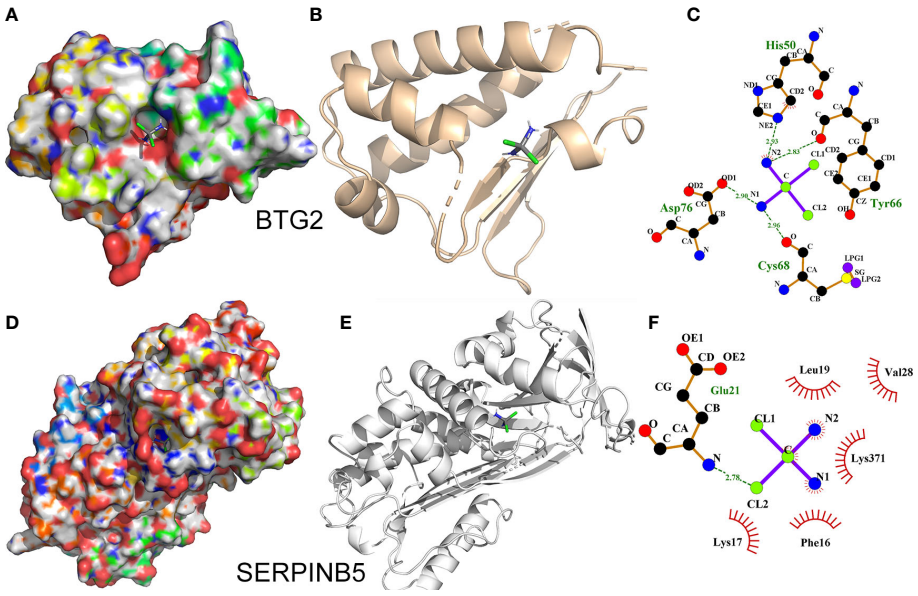

FIGURE 12
Interaction of BTG2 and SerpinB5 with cisplatin. **(A, D)** The binding mode of cisplatin to BTG2 and SerpinB5 in the active site. **(B, E)** Stereoview of binding mode for cisplatin with BTG2 and SerpinB5 in the binding site. **(C, F)** The detailed view of the 2-D ligand interaction among cisplatin with BTG2 and SerpinB5. The mRNA expression level in normal lung tissue is expressed by "+". "++" respect the mRNA expression level was increased in LUAD tissue, "-" respect the mRNA expression level was decreased in LUAD tissue. Compared with tumor group,there was more "+" when the mRNA level increased after treated with cisplatin.

and there was a positive correlation between them (44). *BTG2* was low expression in LUAD and systemic lupus erythematosus.

The results of our study showed that when *BTG2* was low expression and *SerpinB5* was high expression in LUAD, the macrophage M0 in the tumor microenvironment increases during tumorigenesis. Resting macrophages can be polarized into a variety of subpopulations. Classically activated macrophages (M1) and alternatively activated macrophages (M2) are the two main subpopulations of macrophages (45). In the process of tumorigenesis, primary tumor cells can recruit macrophages to infiltrate the tumor microenvironment and become tumor associated macrophages (TAMs). Clinical studies have found that the proportion of TAMs in the primary focus of lung cancer patients was high, and the prognosis was poor (45). The study found that in the animal model of lung cancer, knocking out or blocking CSF1/CSF1R will significantly reduce the number of TAMs, proving that blocking the survival signal of macrophages was one of the effective ways to prevent and treat lung cancer (46). Results showed that BTG2 was negatively correlated with macrophage M0, and SerpinB5 was positively correlated with macrophage M0 (Figures 8, 9). From the results of this study, when *BTG2* was low expression and *SerpinB5* was high expression, the macrophage infiltration level in tumor tissue increases, and the prognosis was poor. The results suggested that the increase of macrophages may be the main cause of poor prognosis in patients with LUAD (Figure 8, 9). This research result was also consistent with the above clinical research report, showing that these two genes can not only be used as tumor prognostic factors, but also as drug targets to play a therapeutic role.

Additionally, in recent years, immunotherapy has gradually become a new anti-tumor therapy, in which ICIs was a common tumor immunotherapy in the clinic (42). The immune checkpoint was the regulator of the immune system, which can inhibit the function of T cells under normal circumstances (47). However, some tumors can regulate immune checkpoints to protect themselves from the attack of the host immune system and form immune escape (48). At present, the ICIs that have been listed mainly include CTLA-4 inhibitors and PD-1/PD-L1 inhibitors. Our results indicate that when PD-1/PD-L1 and CTLA-4 were inhibited, the immunogenicity in tumor tissue was higher. However, the immunogenicity of high-expression group of *BTG2* and the low-expression group of *SerpinB5* was also higher (Figure 9). In addition, the same results were obtained by comparing the TIDE scores of the high and low groups of these two genes. This indicates that the mRNA expression level of *BTG2* and *SerpinB5* may be detected to judge the effect of immunotherapy, making BTG2 and SerpinB5 may become prognostic biomarkers of immunotherapy.

Besides, both the two genes are related to *CD276* and *CD40* (Figures 10G, L), which were other immune checkpoints. Previous studies showed that CD276 could promote tumor immune escape, thus promoting the occurrence and development of tumors (49). However, CD40 was an inhibitory immune checkpoint, which can inhibit the occurrence and development of tumors (50). Isn conclusion, BTG2 and SerpinB5 were correlated with the above immune checkpoints, which may further prove that BTG2 and SerpinB5 have the potential as biomarkers of immunotherapy.

BTG2 and *SerpinB5* were studied as a gene pair in our article to investigate their prognostic value in lung adenocarcinoma. This is the first time that the two genes were studied together to observe the prognostic value. Although there have been studies on the two genes separately, there was no one to report the combining of BTG2 and SerpinB5 (51–56). And we have also speculated the mechanism of how the gene pair influences the development of LUAD. By looking up the journal, we found that the two genes were p53-related genes (41, 43), and p53 was a key gene in tumor cell apoptosis (57, 58). It may also be the mechanism that this gene pair could become a prognostic marker for LUAD. In addition, we added the molecular dynamics simulation of BTG2 and SerpinB5 with cisplatin. Not only the molecular structure of the genes were displayed, but also the result demonstrated the genes could bind with cisplatin. And this is also the first time, the molecular structures of these two genes were presented in the article. At present, the common methods to find out prognostic markers were single gene analysis or constructing a prognostic model for prognostic analysis. Although the two methods are relatively common, the two methods are difficult to study the mechanism. However, it was found in our study that the gene pair were correlated about gene expression, and there may also be an interactive relationship in pathology. So it is easier to study the mechanism of the gene pair compared with other methods.

However, there are several limitations in this study. The present study mainly derived from public databases and was retrospective, but the sample size was small. Thus, to ensure greater reliability and representativeness of the findings and assumptions, the sample should be expanded for further research in the future. In addition, all data in this study were from public databases. Although the study included experimental verification, the sample size was small and the mechanism study could not be carried out.

Conclusion

In conclusion, the expression of *BTG2* decreased and *SerpinB5* increased in LUAD. Downregulation *BTG2* gene expression in LUAD tissue could be upregulated, and the up-regulation *SerpinB5* in LUAD tissue compared with normal lung tissue could be down-regulated after being treated with cisplatin. The correlation analysis of gene expression between the two genes showed that the expression of *BTG2* was negatively correlated with the *SerpinB5*, they were both P53 downregulated genes, which gave us a hypothesis that they could be studied as a gene pair. the survival analysis show that when the *BTG2* gene expression was low and the *SerpinB5* was high, the patient's prognosis was poor; Cox regression analysis showed that both *BTG2* and *SerpinB5* could be used as independent prognostic factors to evaluate the patient's prognosis. Morever, the relationship between the two genes and the immune microenvironment was studied and showed that both of them are related to macrophages. The macrophages increased when the prognosis was poor, which may be a reason for the poor prognosis of LUAD patients. We also studied the response of these two genes to immunotherapy and that they also have the potential to become markers of immunotherapy.

Take together, we proposed that *BTG2* and *SerpinB5* can be studied as a gene pair, but the common function of this gene pair has not been discussed in depth. In subsequent studies, it is necessary to conduct in-depth research and other experimental verification.

Data availability statement

The data could be download at https://portal.gdc.cancer.gov/, https://www.ncbi.nlm.nih.gov/ and the code used during the current study are available from the corresponding author on reasonable request.

Author contributions

JW and YY designed the study. JW performed data analysis and prepared figures. WY wrote the manuscript. CW, JC and WY did SqRT-PCR. RD, YL and YW scrutinized the data. JW and YY conceived the idea and coordinated the project. All authors contributed to the article and approved the submitted version.

Funding

Thanks for the Outstanding Youth Research Project of Anhui, Department of Education (No. 2022AH020042), National Science, Foundation for Young Scientists of China (Grant No. 81904062), the Natural Science Key Projects of Anhui University of Chinese, Medicine (Grant No. 2020zrzd15 and no. 2021zrzd12), the Research Foundation of Science and Technology Department of Sichuan Province(Grant No. 2022NSFSC1319) and the Natural Science Key Projects of Anhui universities (Grant No. KJ2020A0419, No. KJ2020A0394 and No. KJ2021A0577).

Conflict of interest

The authors declare that the research was conducted in the absence of any commercial or financial relationships that could be construed as a potential conflict of interest.

Publisher's note

References

1. Siegel R, Miller K, Jemal A. Cancer statistics,2018. *CA Cancer J Clin* (2018) 68:7–30. doi: 10.3322/caac.21442

2. Goldstraw P, Ball D, Jett J, Chevalier TL, Lim E, Nicholson A, et al. Non-small cell lung cancer. *Lancet* (2011) 378:1727–1740. doi: 10.1016/S0140-6736(10)62101-0

3. Chen Z, Fillmore CM, Hammerman PS, Kim CF, Wong K-K. Non-Small-Cell lung cancers: A heterogeneous set of diseases nat. *Rev Cancer* (2014) 14:535–46. doi: 10.1038/nrc3775

4. Yang X, Deng Y, He RQ, Li XJ, Ma J, Chen G, et al. Upregulation of HOXA11 during the progression of lung adenocarcinoma detected *via* multiple approaches. *Int J Mol Med* (2018) 42(5):2650–64. doi: 10.3892/ijmm.2018.3826

5. Zeng X, Liu Q, Yang Y, Jia W, Li S, He D, et al. Placenta-specific protein 8 promotes the proliferation of lung adenocarcinoma PC-9 cells and their tolerance to an epidermal growth factor receptor tyrosine kinase inhibitor by activating the ERK signaling pathway. *Oncol Lett* (2019) 18(5):5621–7. doi: 10.3892/ol.2019.10911

6. Makovec T. Cisplatin and beyond: molecular mechanisms of action and drug resistance development in cancer chemotherapy. *Radiol Oncol* (2019) 53(2):148–58. doi: 10.2478/raon-2019-0018

7. Ghosh S. Cisplatin: The first metal based anticancer drug. *Bioorg Chem* (2019) 88:102925. doi: 10.1016/j.bioorg.2019.102925

8. Teng JP, Yang ZY, Zhu YM, Ni D, Zhu ZJ, Li XQ. Gemcitabine and cisplatin for treatment of lung cancer *in vitro* and vivo. *Eur Rev Med Pharmacol Sci* (2018) 22 (12):3819–25. doi: 10.26355/eurrev_201806_15266

9. Liu M, Cui L, Li X, Xia C, Li Y, Wang R, et al. PD-0332991 combined with cisplatin inhibits nonsmall cell lung cancer and reversal of cisplatin resistance. *Thorac Cancer* (2021) 12(6):924–31. doi: 10.1111/1759-7714.13866

10. Tsui KH, Chiang KC, Lin YH, Chang KS, Feng TH, Juang HH. BTG2 is a tumor suppressor gene upregulated by p53 and PTEN in human bladder carcinoma cells. *Cancer Med* (2018) 7(1):184–95. doi: 10.1002/cam4.1263

11. Lin YH, Tsui KH, Chang KS, Hou CP, Feng TH, Juang HH. Maspin is a PTEN-upregulated and p53-upregulated tumor suppressor gene and acts as an HDAC1 inhibitor in human bladder cancer. *Cancers (Basel)* (2019) 12(1):10. doi: 10.3390/cancers12010010

12. Yuniati L, Scheijen B, van der Meer LT, van Leeuwen FN. Tumor suppressors BTG1 and BTG2: Beyond growth control. *J Cell Physiol* (2019) 234(5):5379–89. doi: 10.1002/jcp.27407

13. Chen Z, Chen X, Lu B, Gu Y, Chen Q, Lei T, et al. Up-regulated LINC01234 promotes non-small-cell lung cancer cell metastasis by activating VAV3 and repressing BTG2 expression. *J Hematol Oncol* (2020) 13(1):7. doi: 10.1186/s13045-019-0842-2

14. Mao B, Zhang Z, Wang G. BTG2: a rising star of tumor suppressors (review). *Int J Oncol* (2015) 46(2):459–64. doi: 10.3892/ijo.2014.2765

15. Zhang SJ, Ma J, Wu JC, Hao ZZ, Zhang YA, Zhang YJ. Circular RNA circCRIM1 suppresses lung adenocarcinoma cell migration, invasion, EMT, and glycolysis through regulating miR-125b-5p/BTG2 axis. *Eur Rev Med Pharmacol Sci* (2020) 24(7):3761–74. doi: 10.26355/eurrev_202004_20841

16. Huang CS, Zhai JM, Zhu XX, Cai JP, Chen W, Li JH, et al. BTG2 is down-regulated and inhibits cancer stemcell-like features of side population cells in hepato cellular carcinoma. *Dig Dis Sci* (2017) 62(12):3501–10. doi: 10.1007/s10620-017-4829-y

17. Gurzu S, Jung I. Subcellular expression of maspin in colorectal cancer: Friend or foe. *Cancers (Basel)* (2021) 13(3):366. doi: 10.3390/cancers13030366

18. Dzinic SH, Chen K, Thakur A, Kaplun A, Bonfil RD, Li X, et al. Maspin expression in prostate tumor elicits host anti-tumor immunity. *Oncotarget* (2014) 5 (22):11225–36. doi: 10.18632/oncotarget.2615

19. Zhu H, Mao Q, Liu W, Yang Z, Jian X, Qu L, et al. Maspin suppresses growth, proliferation and invasion in cutaneous squamous cell carcinoma cells. *Oncol Rep* (2017) 37(5):2875–82. doi: 10.3892/or.2017.5574

20. Lin K, Yang R, Zheng Z, Zhou Y, Geng Y, Hu Y, et al. Sulforaphane-cysteine-induced apoptosis *via* phosphorylated ERK1/2-mediated maspin pathway in human non-small cell lung cancer cells. *Cell Death Discovery* (2017) 3:17025. doi: 10.1038/cddiscovery.2017.25

21. Xie Q, Huang X, Huang W, Liu F. PD-L2 serves as a potential prognostic biomarker that correlates with immune infiltration and may predict therapeutic sensitivity in lower-grade gliomas. *Front Oncol* (2022) 12:860640. doi: 10.3389/fonc.2022.860640

22. Li K, Chen L, Zhang H, Wang L, Sha K, Du X, et al. High expression of COMMD7 is an adverse prognostic factor in acute myeloid leukemia. *Aging (Albany NY)* (2021) 13(8):11988–2006. doi: 10.18632/aging.202901

23. Chen Y, Lin X, Zheng J, Chen J, Xue H, Zheng X. APLN: A potential novel biomarker for cervical cancer. *Sci Prog* (2021) 104(2):368504211011341. doi: 10.1177/00368504211011341

24. Miao L, Yin RX, Zhang QH, Liao PJ, Wang Y, Nie RJ, et al. A novel circRNA-miRNA-mRNA network identifies circ-YOD1 as a biomarker for coronary artery disease. *Sci Rep* (2019) 9(1):18314. doi: 10.1038/s41598-019-54603-2

25. Yang X, Lei P, Huang L, Tang X, Wei B, Wei H. Prognostic value of LRRC4C in colon and gastric cancers correlates with tumour microenvironment immunity. *Int J Biol Sci* (2021) 17(5):1413–27. doi: 10.7150/ijbs.58876

26. Wang Q, Li M, Yang M, Yang Y, Song F, Zhang W, et al. Analysis of immune-related signatures of lung adenocarcinoma identified two distinct subtypes: implications for immune checkpoint blockade therapy. *Aging (Albany NY)* (2020) 12 (4):3312–39. doi: 10.18632/aging.102814

27. Wang X, Gao F, Xu W, Cao Y, Wang J, Zhu G. Depichering the effects of astragaloside IV on AD-like phenotypes: A systematic and experimental investigation. *Oxid Med Cell Longev* (2021) 2021:1020614. doi: 10.1155/2021/1020614

28. Cheng J, Fu J, Tan Q, Liu Z, Guo K, Zhang L, et al. The regulation of ISG20 expression on SARS-CoV-2 infection in cancer patients and healthy individuals. *Front Immunol* (2022) 13:958898. doi: 10.3389/fimmu.2022.958898

29. Wang K, Deng H, Song B, He J, Liu S, Fu J, et al. The correlation between immune invasion and SARS-COV-2 entry protein ADAM17 in cancer patients by bioinformatic analysis. *Front Immunol* (2022) 13:923516. doi: 10.3389/fimmu.2022.923516

30. Zhang L, Wei C, Li D, He J, Liu S, Deng H, et al. COVID-19 receptor and malignant cancers: Association of CTSL expression with susceptibility to SARS-CoV-2. *Int J Biol Sci* (2022) 18(6):2362–71. doi: 10.7150/ijbs.70172

31. Seguin L, Durandy M, Feral CC. Lung adenocarcinoma tumor origin: A guide for personalized medicine. *Cancers (Basel)* (2022) 14(7):1759. doi: 10.3390/cancers14071759

32. Goldstraw P, Chansky K, Crowley J, Rami-Porta R, Asamura H, Eberhardt WE, et al. The IASLC lung cancer staging project: Proposals for revision of the TNM stage groupings in the forthcoming (Eighth) edition of the TNM classification for lung cancer. *J Thorac Oncol* (2016) 11(1):39–51. doi: 10.1016/j.jtho.2015.09.009

33. Shen S, Zhang R, Guo Y, et al. A multi-omic study reveals BTG2 as a reliable prognostic marker for early-stage non-small cell lung cancer. *MolOncol* (2018) 12 (6):913–24. doi: 10.1002/1878-0261.12204

34. Bai Y, Qiao L, Xie N, Shi Y, Liu N, Wang J. Expression and prognosis analyses of the Tob/BTG antiproliferative (APRO) protein family inhuman cancers. *PloS One* (2017) 12(9):e0184902. doi: 10.1371/journal.pone.0184902

35. Chen Y, Chen C, Zhang Z, Xiao H, Mao B, Huang H, et al. Expression of b-cell translocation gene 2 is associated with favorable prognosis in hepatocellular carcinomapatients and sensitizes irradiation-induced hepatocellular carcinoma cell apoptosis in vitro and in nude mice. *Oncol Lett* (2017) 13(4):2366–72. doi: 10.3892/ol.2017.5685

36. Wagener N, Bulkescher J, Macher-Goeppinger S, Karapanagiotou-Schenkel I, Hatiboglu G, Abdel-Rahim M, et al. Endogenous BTG2 expression stimulates migration of bladder cancer cells andcorrelates with poor clinical prognosis for bladder cancer patients. *Br J Cancer* (2013) 108(4):973–82. doi: 10.1038/bjc.2012.573

37. Hirsch FR, Scagliotti GV, Mulshine JL, Kwon R, Curran WJJr, Wu YL, et al. Lung cancer: current therapies and new targeted treatments. *Lancet* (2017) 389:299–311. doi: 10.1016/S0140-6736(16)30958-8

38. Wang R, Wang R, Tian J, Wang J, Tang H, Wu T, et al. BTG2 as a tumor target for the treatment of luminal a breast cancer. *Exp Ther Med* (2022) 23(5):339. doi: 10.3892/etm.2022.11269

39. Zou Z, Anisowicz A, Hendrix MJ, Thor A, Neveu M, Sheng S, et al. Maspin, a serpin with tumor-suppressing activity in human mammary epithelial cells. *Science* (1994) 263(5146):526–9. doi: 10.1126/science.8290962

40. Bodenstine TM, Seftor RE, Khalkhali-Ellis Z, Seftor EA, Pemberton PA, Hendrix MJ. Maspin: molecular mechanisms and therapeutic implications. *Cancer Metastasis Rev* (2012) 31(3-4):529–51. doi: 10.1007/s10555-012-9361-0

41. McCarroll JA, Gan PP, Erlich RB, Liu M, Dwarte T, Sagnella SS, et al. TUBB3/βIII-tubulin acts through the PTEN/AKT signaling axis to promote tumorigenesis and anoikis resistance in non-small cell lung cancer. *Cancer Res* (2015) 75(2):415–25. doi: 10.1158/0008-5472.CAN-14-2740

42. Li K, Zhang A, Li X, Zhang H, Zhao L. Advances in clinical immunotherapy for gastric cancer. *Biochim Biophys Acta Rev Cancer* (2021) 1876(2):188615. doi: 10.1016/j.bbcan.2021.188615

43. Tsui KH, Chung LC , Feng TH, Chang PL, Juang HH. Upregulation of prostate- de-rived ets factor by luteolin causes inhibition of cell proliferation and cell invasion in prostate carcinoma cells. *Int J Cancer J Int du Cancer* (2012) 130(12):2812–2823. doi: 10.1002/ijc.26284

44. Peng H, Li C, Wu X, Wen Y, Lin J, Liang H, et al. Association between systemic lupus erythematosus and lung cancer: results from a pool of cohort studies and mendelian randomization analysis. *J Thorac Dis* (2020) 12(10):5299–302. doi: 10.21037/jtd-20-2462

45. Guilbaud E, Gautier EL, Yvan-Charvet L. Macrophage origin, metabolic reprogramming and IL-1 signaling: Promises and pitfalls in lung cancer. *Cancers (Basel)* (2019) 11(3):298. doi: 10.3390/cancers11030298

46. Lin W, Xu D, Austin CD, Caplazi P, Senger K, Sun Y, et al. Function of CSF1 and IL34 in macrophage homeostasis, inflammation, and cancer. *Front Immunol* (2019) 10:2019. doi: 10.3389/fimmu.2019.02019

47. Li B, Chan HL, Chen P. Immune checkpoint inhibitors: Basics and challenges. *Curr Med Chem* (2019) 26(17):3009–25. doi: 10.2174/0929867324666170804143706

48. Wei G, Zhang H, Zhao H, Wang J, Wu N, Li L, et al. Emerging immune checkpoints in the tumor microenvironment: Implications for cancer immunotherapy. *Cancer Lett* (2021) 511:68–76. doi: 10.1016/j.canlet.2021.04.021

49. Kontos F, Michelakos T, Kurokawa T, Sadagopan A, Schwab JH, Ferrone CR, et al. B7-H3: An attractive target for antibody-based immunotherapy. *Clin Cancer Res* (2021) 27(5):1227–35. doi: 10.1158/1078-0432.CCR-20-2584

50. Yuan M, Pei J, Li R, Tian L, He X, Li Y. CD40LG as a prognostic molecular marker regulates tumor microenvironment through immune process in breast cancer. *Int J Gen Med* (2021) 14:8833–46. doi: 10.2147/IJGM.S336813

51. Liang J, Cheng L, Gao H, Fu W, Zhang X, Zhang J, et al. B-cell translocation gene 2 upregulation is associated with favorable prognosis in lung adenocarcinoma and prolonged patient survival. *J Oncol* (2022) 2022:1892459. doi: 10.1155/2022/1892459

52. Nai A, Ma F, He Z, Zeng S, Bashir S, Song J, et al. Development and validation of a 7-gene inflammatory signature forecasts prognosis and diverse immune landscape in lung adenocarcinoma. *Front Mol Biosci* (2022) 9:822739. doi: 10.3389/fmolb.2022.822739

53. Zhang XZ, Chen MJ, Fan PM, Jiang W, Liang SX. BTG2 serves as a potential prognostic marker and correlates with immune infiltration in lung adenocarcinoma. *Int J Gen Med* (2022) 15:2727–45. doi: 10.2147/IJGM.S340565

54. Liu ZJ, Hou PX, Wang XX. An inflammation-related nine-gene signature to improve prognosis prediction of lung adenocarcinoma. *Dis Markers* (2021) 2021:9568057. doi: 10.1155/2021/9568057

55. Li YP, Liu GX, Wu ZL, Tu PH, Wei G, Yuan M, et al. A novel mitochondrial-related gene signature for the tumor immune microenvironment evaluation and prognosis prediction in lung adenocarcinoma. *J Immunol Res* (2022) 2022:5366185. doi: 10.1155/2022/5366185

56. Xiao L, Li Q, Huang Y, Fan Z, Qin W, Liu B, et al. Integrative analysis constructs an extracellular matrix-associated gene signature for the prediction of survival and tumor immunity in lung adenocarcinoma. *Front Cell Dev Biol* (2022) 10:835043. doi: 10.3389/fcell.2022.835043

57. Wang X, Simpson ER, Brown KA. p53: Protection against tumor growth beyond effects on cell cycle and apoptosis [published correction appears in cancer res. 2016 mar 15;76(6):1668]. *Cancer Res* (2015) 75(23):5001–7. doi: 10.1158/0008-5472.CAN-15-0563

58. Vazquez A, Bond EE, Levine AJ, Bond GL. The genetics of the p53 pathway, apoptosis and cancer therapy. *Nat Rev Drug Discovery* (2008) 7(12):979–87. doi: 10.1038/nrd2656

frontiers | Frontiers in Immunology

TYPE Original Research
PUBLISHED 20 March 2023
DOI 10.3389/fimmu.2023.1149986

OPEN ACCESS

EDITED BY
Wei-Lin Jin,
First Hospital of Lanzhou University, China

REVIEWED BY
Mazaher Maghsoudloo,
University of Tehran, Iran
Xiaoning Peng,
Hunan Normal University, China
Jun Hong,
Vanderbilt University Medical Center,
United States

*CORRESPONDENCE
Junjiang Fu
fujunjiang@swmu.edu.cn;
fujunjiang@hotmail.com
Chunli Wei
weichunli2015@swmu.edu.cn
Kai Wang
wangkai@swmu.edu.cn

†These authors have contributed equally to this work

SPECIALTY SECTION
This article was submitted to Cancer Immunity and Immunotherapy, a section of the journal Frontiers in Immunology

RECEIVED 23 January 2023
ACCEPTED 06 March 2023
PUBLISHED 20 March 2023

CITATION
Liu S, Yang L, Fu J, Li T, Zhou B, Wang K, Wei C and Fu J (2023) Comprehensive analysis, immune, and cordycepin regulation for SOX9 expression in pan-cancers and the matched healthy tissues. *Front. Immunol.* 14:1149986. doi: 10.3389/fimmu.2023.1149986

Comprehensive analysis, immune, and cordycepin regulation for SOX9 expression in pan-cancers and the matched healthy tissues

Shuguang Liu[1†], Lisha Yang[1,2†], Jiewen Fu[1†], Ting Li[1], Baixu Zhou[1,3], Kai Wang[1*], Chunli Wei[1*] and Junjiang Fu[1*]

[1]Key Laboratory of Epigenetics and Oncology, Research Center for Preclinical Medicine, Southwest Medical University, Luzhou, China, [2]Department of Obstetrics, The Affiliated Hospital of Southwest Medical University, Luzhou, China, [3]Department of Gynecology and Obstetrics, Guangdong Women and Children Hospital, Guangzhou, China

SRY-box transcription factor 9 (SOX9) (OMIM 608160) is a transcription factor. The expression of SOX9 in pan-cancers and the regulation by small molecules in cancer cell lines are unclear. In the current study, we comprehensively analyzed the expression of SOX9 in normal tissues, tumor tissues and their matched healthy tissues in pan-cancers. The study examined the correlation between immunomodulators and immune cell infiltrations in normal and tumor tissues. Cordycepin (CD), an adenosine analog for SOX9 expression regulation, was also conducted on cancer cells. The results found that SOX9 protein is expressed in a variety of organs, including high expression in 13 organs and no expression in only two organs; in 44 tissues, there was high expression in 31 tissues, medium expression in four tissues, low expression in two tissues, and no expression in the other seven tissues. In pan-cancers with 33 cancer types, SOX9 expression was significantly increased in fifteen cancers, including CESC, COAD, ESCA, GBM, KIRP, LGG, LIHC, LUSC, OV, PAAD, READ, STAD, THYM, UCES, and UCS, but significantly decreased in only two cancers (SKCM and TGCT) compared with the matched healthy tissues. It suggests that SOX9 expression is upregulated in the most cancer types (15/33) as a proto-oncogene. The fact that the decrease of SOX9 expression in SKCM and the increase of SOX9 in the cell lines of melanoma inhibit tumorigenicity in both mouse and human *ex vivo* models demonstrates that SOX9 could also be a tumor suppressor. Further analyzing the prognostic values for SOX9 expression in cancer individuals revealed that OS is long in ACC and short in LGG, CESC, and THYM, suggesting that high SOX9 expression is positively correlated with the worst OS in LGG, CESC, and THYM, which could be used as a prognostic maker. In addition, CD inhibited both protein and mRNA expressions of SOX9 in a dose-dependent manner in 22RV1, PC3, and H1975 cells, indicating CD's anticancer roles likely *via* SOX9 inhibition. Moreover, SOX9

might play an important role in tumor genesis and development by participating in immune infiltration. Altogether, SOX9 could be a biomarker for diagnostics and prognostics for pan-cancers and an emerging target for the development of anticancer drugs.

KEYWORDS

The SOX9 gene, pan-cancers, cordycepin (CD), immune, regulation, drug development

1 Introduction

SRY-box transcription factor 9 (SOX9) (OMIM 608160) is a transcription factor gene that maps to 17q24.3 and encodes 509 amino acids with a molecular mass of 56,137 Da (1). The SOX9 protein as a transcription factor recognizes the CCTTGAG motif along with other HMG-box class DNA-binding protein members, such as SRY (Sex-Determining Region Y) (2). SOX9 is involved in various developmental pathways, including differentiation and progenitor cell development (3, 4). During chondrocyte differentiation, SOX9 acts together with steroidogenic factor 1 to regulate the transcriptional expression of the anti-Muellerian hormone (AMH) gene. Mutations or defects with SOX9 are associated with skeletal malformation syndrome (campomelic dysplasia; OMIM 57 114290) or sex reversal (46,XY Sex Reversal 10; OMIM 57 616425) disorders (5, 6). Campomelic dysplasia is a severe form of autosomal dominant skeletal dysplasia with congenital short and curved long tubular bones. 46,XY Sex Reversal is an XY karyotype in which patients are born looking like normal females but fail to develop secondary sexual characteristics during puberty and have no menstruation.

Subsequently, the role of SOX9 in cancer growth and invasion was revealed. Wang et al. (7) first showed that overexpression of SOX9 promoted tumor growth in xenograft experiments using prostate cancer cells, whereas SOX9 knockdown repressed tumor growth (7). They also found that SOX9 expression was restricted to the basal epithelium of the adult prostate, which begins to be expressed at 19 weeks of gestation, ultimately concluding that SOX9 may allow prostate epithelial cells to grow toward the mesenchyme and then provide basal cellular support for the development and maintenance of ductal epithelial cells. However, SOX9 expression was weak or negative in melanoma specimens but positive in normal skin, and upregulation of SOX9 expression significantly inhibited tumorigenesis in both melanoma-bearing mice and human melanoma *ex vivo* models (8). In melanoma cell lines, treatment with PGD2 (176803) increased SOX9 expression and restored retinoic acid sensitivity. As a proto-oncogene or tumor suppressor gene, SOX9 can induce epithelial–mesenchymal transition (EMT) by regulating the tumor microenvironment (TME) to acquire stem cell characteristics, which are dependent on cancer type (9–11). Thus, activation of the SOX9 pathway may play crucial roles in cancer development and progression (10). Over the past decade, SOX9 has been intensively studied in the field of cancer.

Besides, SOX9 has been shown to be closely associated with tumor immunity. Yuan et al. found that SOX9 expression in thymoma was negatively correlated with target genes related to Th17 cell differentiation, primary immunodeficiency, PD-L1 expression, and T-cell receptor signaling pathways, suggesting that SOX9 may be associated with immune dysregulation in thymoma (12). In the progression of breast cancer, SOX9 triggers tumorigenesis by facilitating the immune escape of tumor cells (13). Ashkenazi et al. indicated that the downregulation of SOX9 contributed to reduced T-cell cytotoxicity (14). In our opinion, the immunopromotive and immunosuppressive effects of SOX9 on tumors may be attributed to the degree to which different tumor types act on the tumor microenvironment.

Cordycepin (CD) is an adenosine analog isolated from the traditional Chinese medicine cordyceps sinensis with a wide range of biological activities, including anti-inflammatory (15), anti-tumor (16), immunomodulatory (17), etc. In our previous studies, it was shown that CD downregulated transcription factors to inhibit the migration and invasion of triple-negative breast cancer cells as well as the progression of drug-resistant non-small cell lung cancer by regulating the AMPK signaling pathway (18, 19). In addition, we found that CD was also able to remarkably reduce the syncytium formation and fluorescence intensity of the SARS-CoV-2 spike pseudotyped virus that invaded 293-ACE2 cells, indicating its anti-COVID potential (20, 21). However, the expression and immunomodulation of SOX9 in pan-cancer and the regulation of the small-molecule drug CD in cancer cell lines are not clear.

In the current study, we thoroughly analyzed SOX9 expression in normal and tumor tissues, matched healthy tissues, and performed correlation analysis with immunomodulators and immune cell infiltration in pan-cancer. The regulation of SOX9 expression by the adenosine analog CD has also been studied in cancer cells, including prostate cancer cell lines.

2 Materials and methods

2.1 Online data collection

The Human Protein Atlas (HPA) database (https://www.proteinatlas.org/Ensembl ID: ENSG00000125398) was applied to search for mRNA and protein expression of SOX9 in normal

tissues. The immunohistochemical and immunofluorescence images of SOX9 in normal and tumor tissues were downloaded from HPA, too (22, 23). Gene expression profiles were obtained from the online Gene Expression Profile Interaction Analysis (GEPIA 2 dataset; http://gepia2.cancer-pku.cn/#index) (24–26) and were employed to compare SOX9 expression in tumors and corresponding healthy tissues. Mutational hot spot analysis of SOX9 as well as survival analysis were used in cBioPortal (27). Additionally, we downloaded the pan-cancer dataset from the UCSC (https://xenabrowser.net/) database: TCGA Pan-Cancer (PANCAN, N = 10,535; G = 60,499). The workflow of our study is shown in Figure 1.

2.2 HPA analysis

SOX9 mRNA and its protein expression in healthy and tumor tissues from HPA (https://www.proteinatlas.org/) were analyzed (23). *SOX9* mRNA expression levels in healthy tissues were found in HPA, GTEx, and FANTOM5, while normalized expression in tissues and distinct blood cells was obtained from the three databases mentioned above (v20.proteinatlas.org/about/assays+annotation#normalization_rna).

2.3 GEPIA and prognostic analysis of SOX9

SOX9 mRNA expression in 5,540 healthy and 9,663 tumor tissues and the relationship between SOX9 expression levels and median overall survival (OS) were analyzed by GEPIA (25). A correlation analysis of SOX9 expression and immune regulation was performed. Data for pan-cancer (PANCAN, N = 10,535; G = 60499) was downloaded from the UCSC database (http://xenabrowser.net/).

2.4 Cell culture and small molecular compound cordycepin treatment

Prostate cancer cells PC3 and 22RV1 and lung cancer cell H1975 were obtained from the Cell Bank of the Research Center for Preclinical Medicine, Southwest Medical University, and these cells were purchased from ATCC, USA. H1975 and PC3 cells were cultured in RPMI 1640 medium (Gibico, USA) containing 10% fetal bovine serum (FBS) and 1% penicillin/streptomycin. 22RV1 cells were cultured in DMEM medium (Gibico, USA), which contains 15% fetal bovine serum (FBS) and 1% penicillin/streptomycin. All cells were cultured in a 37°C incubator with 5% CO_2. CD was obtained from Chengdu Must Bio-Technology Co. Ltd. (Chengdu, Sichuan, China), which has been used previously (18, 28, 29). Cells were inoculated in 12-well plates and treated with CD at final concentrations of 0, 10, 20, and 40 μM for 24 h. Protein was collected, and expression levels were monitored by Western blot. Total RNA was extracted by reverse transcription (29, 30).

2.5 Western blot assays

Cells were lysed in EBC buffer and 2×SDS loading buffer to collect proteins. The protein samples were boiled at 100°C for 5 min and then electrophoresed in the Bio-Rad Mini PROTEAN Tetra

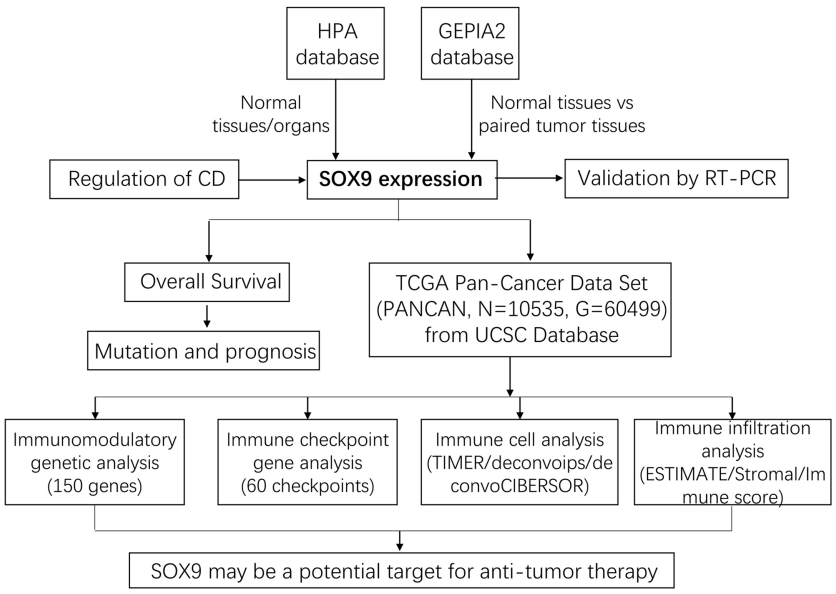

FIGURE 1
The workflow of our study. First, SOX9 expression in normal tissues and pan-cancer was analyzed using the HPA and GEPIA2 databases, which was further validated by RT-PCR. Subsequently, the overall survival analysis and mutation and prognosis analysis of tumor patients with SOX9 were performed comprehensively. The regulation of SOX9 by a small molecule compound, cordycepin **(CD)**, was explored. Finally, pan-cancer data were collected again from the UCSC database for immunomodulatory gene analysis, immune checkpoint gene analysis, immune cell analysis, and immune infiltration analysis, respectively.

System (Bio-Rad, USA). After electrophoresis, the proteins were transferred to the PVDF membrane under ice bath conditions, and then the membrane was washed twice with 1×TBST. The membrane was blocked with 5% free-fat milk for 2 h at room temperature. The primary antibodies to SOX9 (67439-1-Ig, Proteintech) and HSP90 (ab203126, Abcam) were diluted with 2% free-fat milk at ratios of 1:4,000 and 1: 10,000, respectively, and then incubated overnight at 4°C. Membrane was washed thrice for 15 min and incubated the secondary antibodies for 2 h at room temperature. After another three times washing, the bands were solarized and imaged using the Syngene G: BOX Imaging System (Cambridge, UK) (19, 31).

2.6 RT-PCR analysis

The total RNA was extracted using a TIANGEN kit (cat. no.: #DP419, TIANGEN, China), then reversely transcribed into cDNA using a reverse transcription kit (TOYOBO, China). The forward primer 5'-gaggaagtcggtgaagaacg-3' and the reverse primer 5'-atcgaaggtctcgatgttgg-3' for SOX9 were designed on the Primer3 online primer design website. The product size for SOX9 is 337 bp. ACTB was used as an internal control. PCR amplification was conducted using a Veriti 96-well thermal cycler (ABI, USA); it is worth noting that the amplification number for SOX9 did not exceed 30 cycles. After PCR reactions were completed, agarose electrophoresis for the amplified products was performed on 1.5% agarose gel (30).

For the LUSC samples' quantitative RT-PCR, the tumor samples and the matched healthy tissue samples were collected from Chinese individuals (seven pairs of samples) and the RT-PCR analysis was performed as mentioned above. This study was approved by the Ethical Committee of Southwest Medical University.

2.7 Immunomodulatory genetic analysis

The expression data of the *SOX9* gene and 150 marker genes of five immune pathways (chemokines (41), receptors (18), MHCs (21), immunoinhibitors (24) and immunostimulators (46)) in each tumor sample were extracted from the downloaded pan-cancer dataset (TCGA Pan-Cancer (PANCAN, N = 10,535; G = 60,499)), filtered all normal samples, and a log2(x + 0.001) transformation was performed for each expression value. Finally, a Pearson correlation was calculated between SOX9 and the five types of marker genes.

2.8 Immune checkpoint gene analysis

The expression data of the *SOX9* gene and 60 marker genes of two types of immune checkpoint pathway genes (inhibitory (24), stimulatory (36)) in pan-cancer were extracted from the downloaded pan-cancer dataset (TCGA Pan-Cancer (PANCAN, N = 10,535; G = 60,499)), and all normal samples were filtered. A log2(x + 0.001) transformation was performed for each expression value, and finally the Pearson correlation of SOX9 with marker genes of five types of immune pathways was calculated.

2.9 Immunocytometric analysis

Expression data of the *SOX9* gene in each sample were extracted from the downloaded pan-cancer dataset (TCGA Pan-Cancer (PANCAN, N = 10,535; G = 60,499)) and a log2(x + 0.001) transformation was performed for each expression value. The expression profile was mapped to GeneSymbol and reassessed separately using the R package IOBR (version 0.99.9) of the TIMER, deconvo_ips, and deconvo_CIBERSOR methods to reassess the immune cell infiltration score of each tumor in each patient based on gene expression.

2.10 Immune infiltration analysis

The expression data of the *SOX9* gene in each sample were extracted from the downloaded pan-cancer dataset (PANCAN, N = 10,535; G = 60,499); and a log2(x + 0.001) transformation was performed for each expression value, from which the gene expression profile of each tumor was extracted separately and the expression profile was mapped to GeneSymbol. Stromal, immune, and ESTIMATE scores were calculated for each tumor in each patient using the R package ESTIMATE (version 1.0.13).

2.11 Statistical analysis

The SOX9 expression levels of all individuals in the survival analysis were separated into high and low expression groups using the median expression of overall survival (OS). Logrank with $P < 0.05$ was considered a significant difference.

3 Results

3.1 SOX9 expression in human organs

SOX9 mRNA was expressed non-specifically in many human tissues. For example, it was highly expressed in the proximal digestive tract (salivary glands) and brain, moderately expressed in the gastrointestinal tract (stomach), pancreas, male tissues (prostate and testis), female tissues (breast), and skin, but lowly expressed in tissues such as the kidney and gallbladder (Figures 2A, B). The SOX9 protein was highly expressed in 13 organs and not expressed in only two organs (eye and skin) (Figure 2A); it was highly expressed in 31 tissues, expressed in four tissues, lowly expressed in two tissues, and not expressed in the other seven tissues (Figures 2A, C). This broad protein expression suggests an important role for SOX9 in multiple tissues/organs.

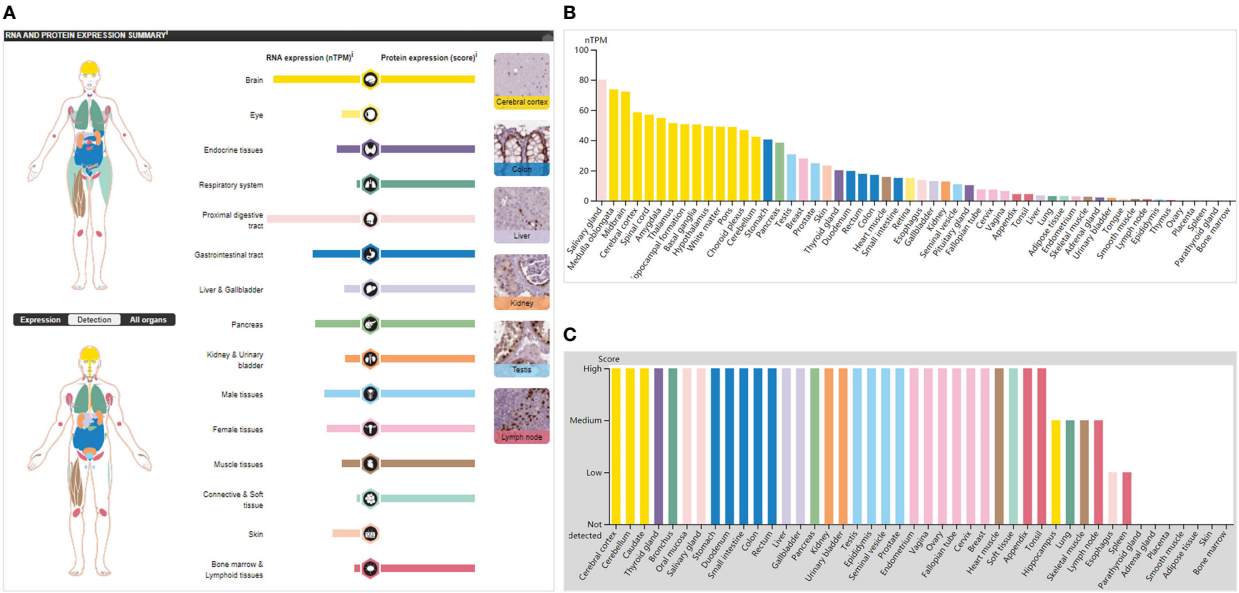

FIGURE 2
SOX9 expression in normal tissues/organs. **(A)** The general situation of SOX9 mRNA and protein expression. Color-coding lists are based on different tissue groups, and each group comprises tissues with similar functional characteristics. The image on the right shows the immunohistochemical (IHC) staining values of SOX9 in normal tissues. **(B)** mRNA expression of SOX9 in normal tissues, indicated by nTPM (normalized transcripts per million). **(C)** SOX9 protein expression levels in normal tissues by IHC score.

3.2 SOX9 expression in pan-cancers and the matched healthy tissues

In 33 cancer types, SOX9 expression was a significant increase in COAD (colon adenocarcinoma), CESC (cervical squamous cell carcinoma and endocervical adenocarcinoma), ESCA (esophageal carcinoma), GBM (glioblastoma multiforme), KIRP (kidney renal papillary cell carcinoma), LIHC (liver hepatocellular carcinoma), LGG (brain lower grade glioma), LUSC (lung squamous cell carcinoma), OV (ovarian serous cystadenocarcinoma), PAAD (pancreatic adenocarcinoma), READ (prostate adenocarcinoma), STAD (stomach adenocarcinoma), THYM (thymoma), UCES (uterine corpus endometrial carcinoma), and UCS (uterine carcinosarcoma), but significant decrease only in SKCM (skin cutaneous melanoma) and TGCT (testicular germ cell tumors) compared with the matched healthy tissues (Figures 3A, B). Higher expression of the *SOX9* gene in the LUSC tumor tissues was verified when compared with the matched normal tissues (Figure 3C). Thus, SOX9 expression was upregulated in most cancers.

3.3 Prognostic values for SOX9 expression in pan-cancer

Further analysis of the prognostic value of SOX9 expression in individuals with cancer revealed that overall survival was longer in ACC (Figure 3D) (adrenocortical carcinoma) and shorter in LGG (Figure 3E), CESC (Figure 3F), and THYM (Figure 3G) when SOX9 was highly expressed in pan-cancer compared with the matched healthy tissues. Consequently, the high expression of SOX9 was positively correlated with the poor prognosis of LGG, CESC, and THYM, which may be a prognostic factor.

3.4 SOX9 mutations and their prognostics

cBioPortal analysis in 26 cancer types revealed that SOX9 mutations are highest in COAD with 11.78%, including mutations at 10.77% in 64 cases, amplification at 0.67% in four cases, and deep deletion at 0.34% in two cases, and lowest in THCA (thyroid carcinoma) with 0.2% (amplification of 0.2% in one case) (Figure 4A). No SOX9 mutation was found in the other six cancer types, including ACC, KICH (kidney chromophobe), LAML (acute myeloid leukemia), DLBC (diffuse large B-cell lymphoma), CHOL (cholangiocarcinoma), and TGCT (Figure 4A). A total of 170 mutations (somatic mutation frequency: 1.4%) were found, including 89 missenses, 69 truncations, nine inframes, and three splices along the whole *SOX9* gene (Figure 4B).

Survivals for disease-specific, overall, disease-free, and progression-free conditions revealed no significant difference in the mutated group compared with the unaltered group of SOX9, although median months were much shorter (Figure 4C, $p > 0.05$). These data suggested that SOX9 was mutated in most cancers but did not have prognostic significance.

3.5 Treatment with CD inhibits SOX9 expression in both protein and mRNA in different cancer cells

We then analyzed the effect of CD on SOX9 expression levels in tumor cells and showed that CD dose-dependently decreased the protein of SOX9 and its mRNA expression levels in 22RV1 (Figures 5A, B), PC3 (Figures 5C, D), and H1975 (Figures 5E, F) cells, indicating that CD inhibited SOX9 expression in tumor cells, especially in prostate cancer cells.

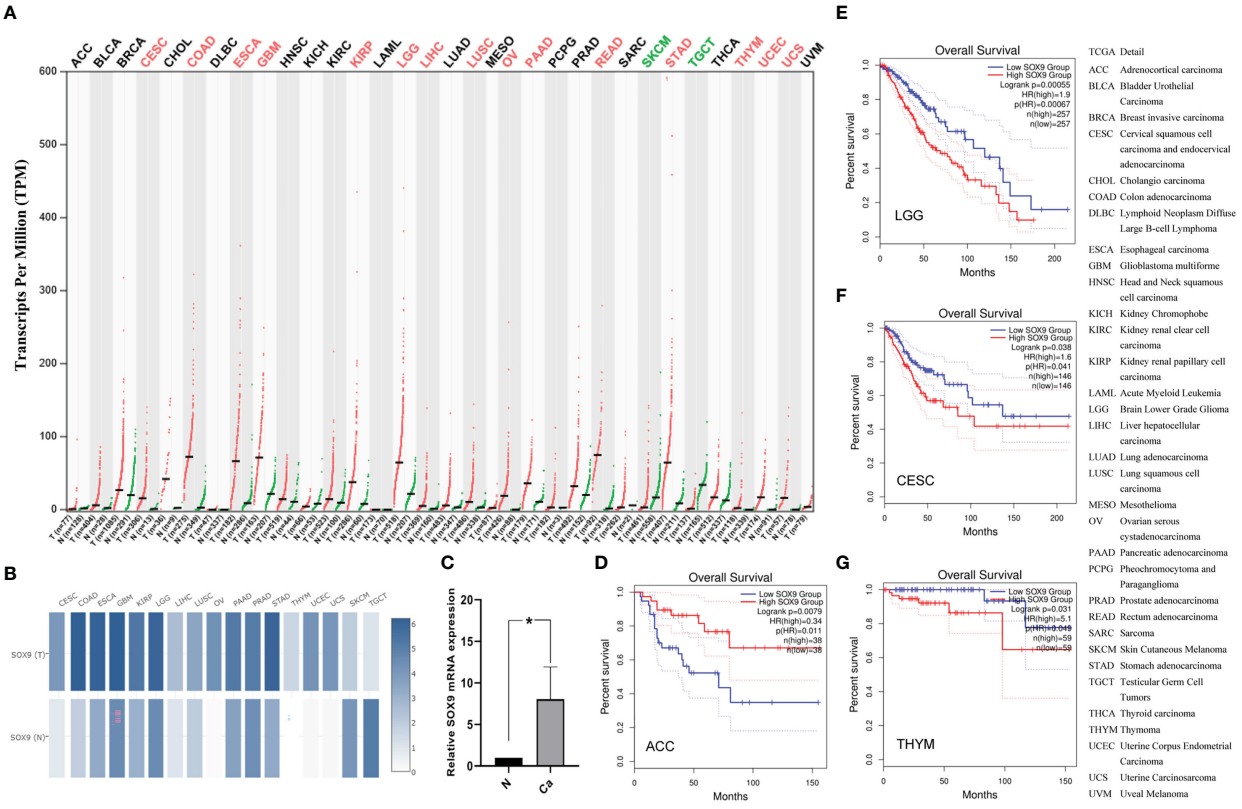

FIGURE 3
Expressions and prognostic values of SOX9 expression in pan-cancers and the matched healthy tissues. **(A)** The profiles of SOX9 in 33 types of cancer with dot plots. **(B)** The profiles of SOX9 with significant changes in 17 cancer types using heatmaps. "T" indicates tumors, and "N" indicates the matched healthy tissues. **(C)** Verification of LUSC samples by quantitative RT-PCR. *P <0.01. The prognostic values of SOX9 expressions in ACC **(D)**, LGG **(E)**, CESC **(F)**, and THYM **(G)**. The right panel provides a full description of all cancer types.

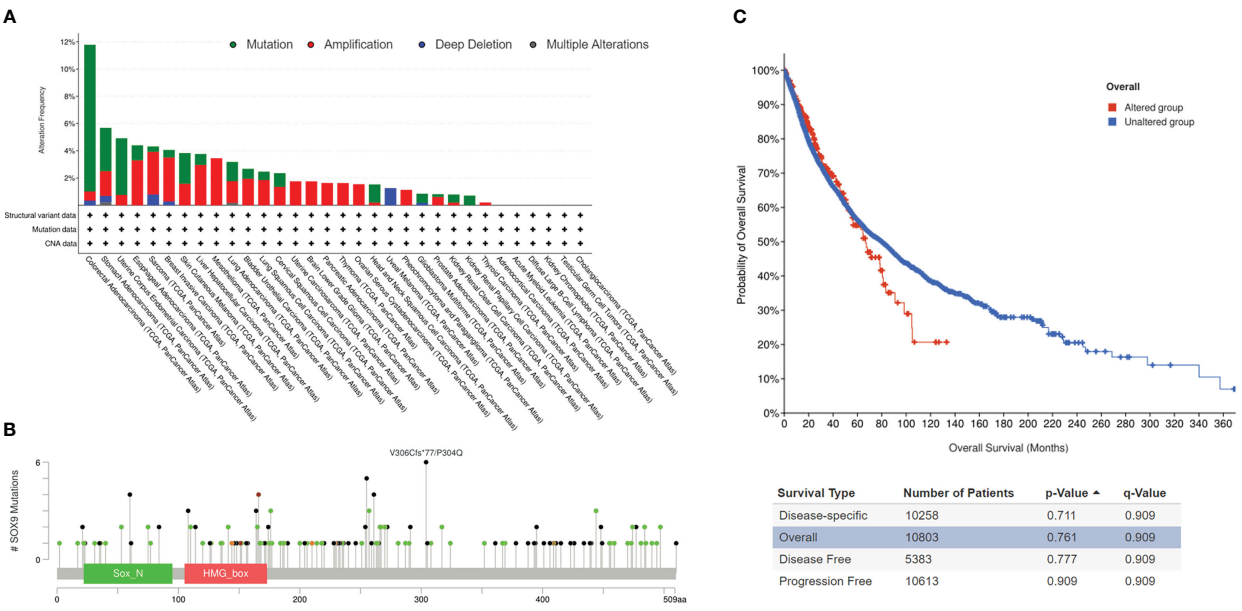

Survival Type	Number of Patients	p-Value	q-Value
Disease-specific	10258	0.711	0.909
Overall	10803	0.761	0.909
Disease Free	5383	0.777	0.909
Progression Free	10613	0.909	0.909

FIGURE 4
SOX9 mutations in pan-cancers. **(A)** Overview of SOX9 mutations in pan-cancers. Different colors indicate different types of mutations. **(B)** SOX9 mutations and locations in pan-cancers. **(C)** Correlation of survivals between the SOX9 mutated group (red) and unaltered group (blue) in pan-cancers.

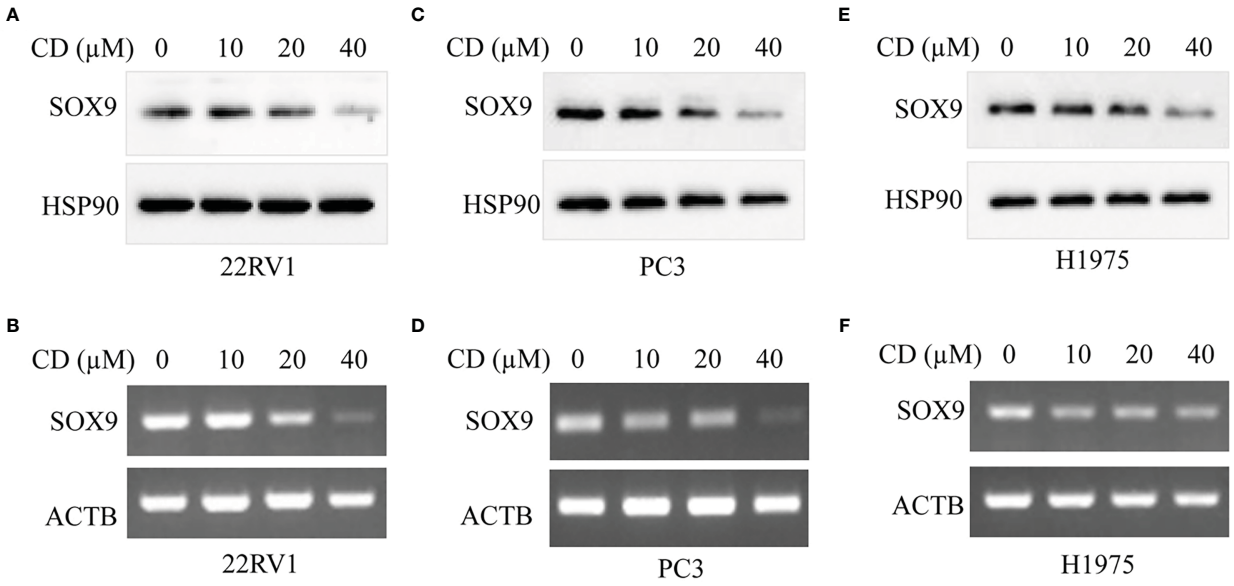

FIGURE 5
CD inhibits the expression of SOX9 in different tumor cells. **(A)** Protein expression levels of SOX9 in prostate cancer cell 22RV1 after CD treatment. **(B)** mRNA expression level of SOX9 in prostate cancer cell 22RV1 after CD treatment. **(C)** Protein expression levels of SOX9 in prostate cancer cell PC3 after CD treatment. **(D)** mRNA expression level of SOX9 in prostate cancer cell PC3 after CD treatment. **(E)** Protein expression level of SOX9 in lung cancer cell H1975 after CD treatment. **(F)** mRNA expression level of SOX9 in lung cancer cell H1975 after CD treatment.

3.6 SOX9 expression is associated with immune cell infiltration in pan-cancer

We first collected the *SOX9* gene and 60 genes of two immune checkpoint pathways and 150 genes of five immune pathways for analysis of immunoregulation genes, immune checkpoints, immunocytes, and immune infiltration. In the analysis, we detected that SOX9 expression had a positive association with lots of immune regulatory genes, including ADORA2A, TMIGD2, TGFB1, TMEM173, TNFRSF18, IL6R, IL10RB in THYM, CHOL, TGCT, PAAD, ESCA, ACC, LAML, and CESC (Figure 6A; Supplementary Table 1). In addition, SOX9 expression was reciprocally exclusive with several tumor immune checkpoints, such as CD27, CTLA4, LAG3, TIGIT, IL10, CSF1R, ADORA2A, CD244, etc. (Figure 6B; Supplementary Table 2).

Based on *SOX9* gene expression, we reappraised the invasion scores of six immune cells (lymphocyte T CD4, lymphocyte B, macrophage, lymphocyte T CD8, neutrophil, and dendritic cells) for 9,406 tumor samples in 36 cancer types and six immune cells (SC, MHC, EC, IPS, CP, and AZ) and 22 class immunocytes in 9,555 cancer specimens from 39 neoplasm types. Results showed that the SOX9 expression was sensibly related to immune infiltration in 26 tumor species (TCGA-BLCA (N = 405), TCGA-BRCA (N = 1,077), TCGA-CESC (N = 291), TCGA-CHOL (N = 36), TCGA-COAD (N = 282), TCGA-COADREAD (N = 373), TCGA-ESCA (N = 181), TCGA-GBM (N = 152), TCGA-GBMLGG (N = 656), TCGA-HNSC (N = 517), TCGA-KIRC (N = 528), TCGA-KIRP (N = 285), TCGA-LGG (N = 504), TCGA-LIHC (N = 363), TCGA-MESO (N = 85), TCGA-OV (N = 417), TCGA-PAAD (N = 177), TCGA-PCPG (N = 177), TCGA-PRAD (N = 495), TCGA-SARC (N = 258), TCGA-SKCM (N = 452), TCGA-STAD (N = 388), TCGA-TGCT (N = 132), TCGA-THCA (N = 503), TCGA-THYM (N = 118), TCGA-UVM (N = 79)) (Figures 7A–C; Supplementary Tables 3–5).

In addition, we detected the relevance between the state of immune invasion and SOX9 expression in cancer. We discovered that the *SOX9* gene expression was notably interrelated with immune invasion in 17 neoplasm species, indicating six significant positive correlations (TCGA-GBMLGG (N = 656, R = 0.20, P = 4.4e−7), TCGA-LGG (N = 504, R = 0.31, P = 7.8e−13), TCGA-LAML (N = 149, R = 0.30, P = 2.4e−4), TCGA-THYM (N = 118, R = 0.27, P = 2.9e−3), TCGA-TGCT (N = 132, R = 0.51, P = 6.3e−10), TCGA-BLCA (N = 405, R = 0.18, P = 3.5e−4)) and 11 significant negative associations (TCGA-GBM (N = 152, R = −0.34, P = 2.2e−5), TCGA-COADREAD (N = 373, R = −0.12, P = 0.02), TCGA-BRCA (N = 1,077, R = −0.12, P = 1.5e−4), TCGA-ESCA (N = 181, R = −0.28, P = 1.1e−4), TCGA-STES (N = 569, R = −0.32, P = 8.8e−15), TCGA-KIPAN (N = 878, R = −0.16, P = 1.4e−6), TCGA-STAD (N = 388, R = −0.42, P = 1.0e−17), TCGA-PRAD (N = 495, R = −0.09, P = 0.04), TCGA-READ (N = 91, R = −0.21, P = 0.05), TCGA-PAAD (N = 177, R = −0.36, P = 6.5e−7), TCGA-UCS (N = 56, R = −0.30, P = 0.02)) by assaying the connection among *SOX9* and immune infiltration marks in 9,555 tumor specimens from 39 cancers (Figure 8; Supplementary Table 6).

These results suggest that it is probable for SOX9 to be sensibly interrelated with immune infiltration of neoplasms and negatively associated with tumor immunosuppression. We know that tumor-related immune cells infiltrating tumor tissues affect TME and can help tumor cells escape immune surveillance, thus promoting the malignant progression of tumors (32–34). Additionally, our studies indicated that the expression of SOX9 was negatively correlated with multiple immunosuppressants, and many cancer species

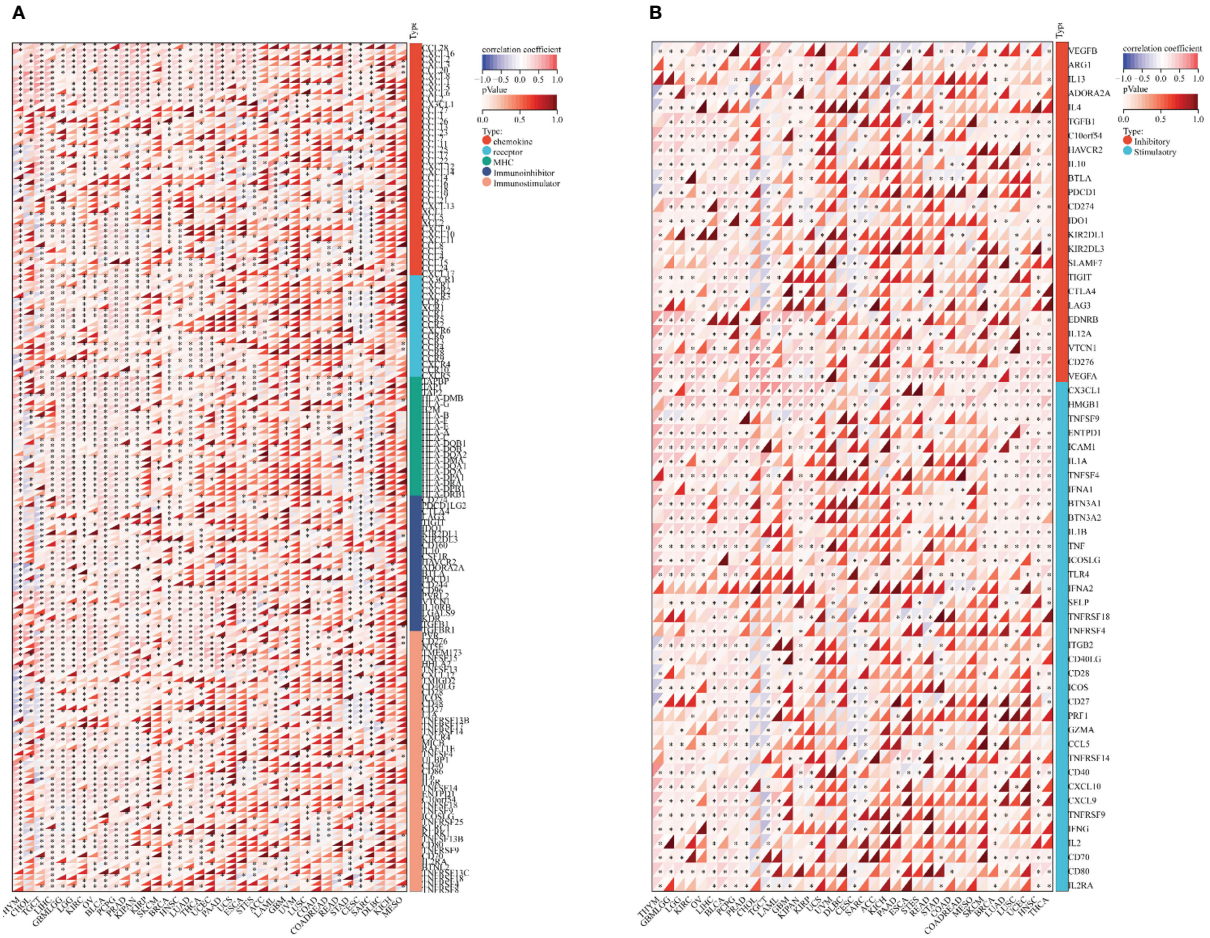

FIGURE 6
Bioinformatics analysis of the immunoregulatory actions of SOX9 in several cancer types. **(A)** Correlation between SOX9 and 150 genes of five classes of immune pathways (41 chemokines, 18 receptors, 21 MHCs, 24 immunoinhibitors, and 46 immunostimulators). *P <0.05. **(B)** Correlation between SOX9 and 60 genes of two types of immune checkpoint pathways.

related to the expression of SOX9 were highly malignant, such as COAD, LAML, ESCA, etc., implying that the correlation between SOX9 expression and immune cell infiltration in pan-cancer may be related to the malignancy of the tumor.

4 Discussion

In the current study, we revealed that SOX9 protein was expressed in multiple organs. For example, SOX9 was highly expressed in 13 organs and absent in only two organs (eye and skin); it was highly expressed in 31 of 44 tissues, expressed in four tissues, lowly expressed in two tissues, and absent in the other seven tissues, indicating an important role for SOX9 in multiple tissues/organs. This contrasts with the positive SOX9 expression results in healthy skin reported by Passeron et al. (8). In addition, we did not observe SOX9 protein expression but only saw significant SOX9 mRNA expression (23.3 nTPM), which implies that the IHC score may be inaccurate. We found that the *SOX9* gene was highly expressed in COAD, ESCA, CESC, GBM, KIRP, LGG, LIHC, LUSC, OV, PAAD, READ, STAD, THYM, UCES, and UCS, and lowly expressed in SKCM and TGCT, suggesting that SOX9 may be a pro-oncogene in most cancer types. It has also been reported in the literature that reduced expression of SOX9 in SKCM and overexpression of SOX9 in melanoma cell lines suppressed tumorigenesis in both mouse and human *in vitro* models (8), indicating that SOX9 may be a tumor suppressor gene in both cancer types. Prognostic analysis showed that SOX9 expression was positively correlated with the prognosis of ACC patients and negatively correlated with the prognosis of LGG, CESC, and THYM patients, which suggests that SOX9 is likely to be an oncogene, making it an important factor affecting the prognosis of LGG, CESC, and THYM patients.

The interaction between tumors and immunity is a hot and difficult point that has been studied but has never been deeply clarified (35). Many cancers use embryonic genes to grow wildly and escape the monitoring of the immune system. SOX9 is upregulated in many tumors, as described above in 15 cancers. However, the role of SOX9 in mediating an immunosuppressive

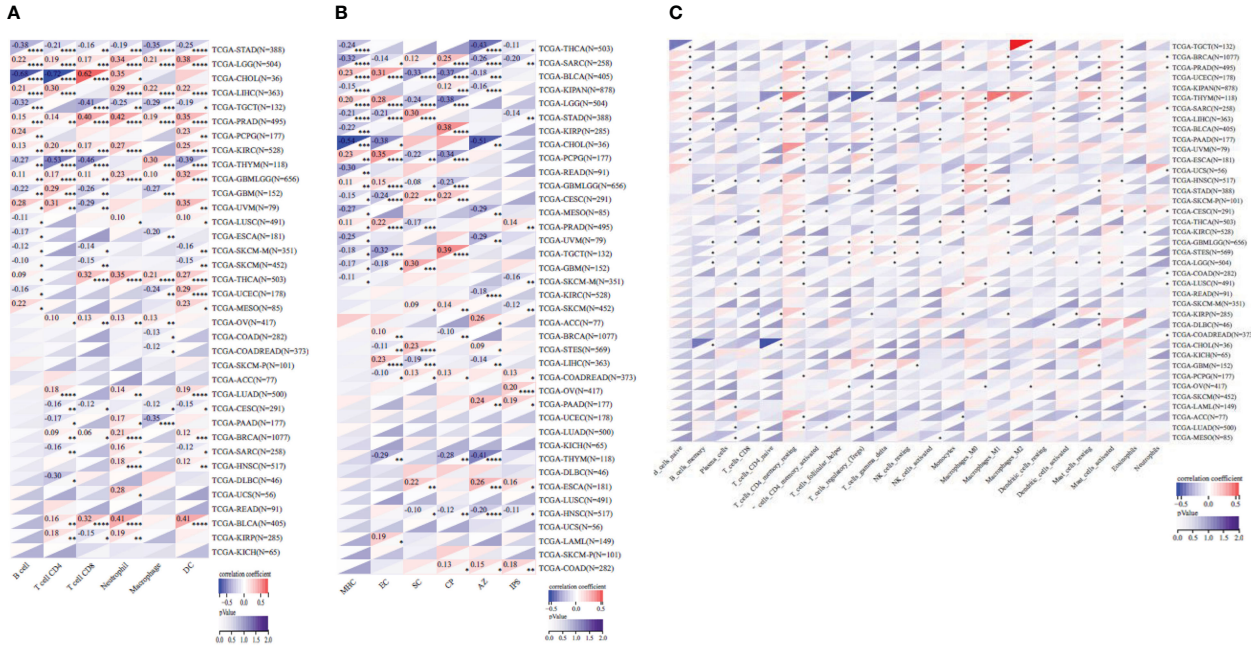

FIGURE 7
Pearson's correlation coefficient of the SOX9 expression with tumor-immune systems in several cancer types. **(A)** Correlation between SOX9 and six tumor-interrelated immune cells counted with TIMER. **(B)** Correlation between SOX9 and six tumor-related immune cells counted with deconvo_ips. **(C)** Correlation between SOX9 and 22 tumor-correlative immune cells calculated with the deconvo_CIBERSOR. *P <0.05; **P <0.005; ***P <0.001; ****P <0.0001. The full names of cancer types are shown in Figure 2.

tumor microenvironment is still unclear (36, 37). Next, we explored the immunomodulatory role of SOX9 in cancer. Bioinformatics results showed that SOX9 was positively associated with immunomodulatory genes such as ADORA2A, TMIGD2, TGFB1, TMEM173, TNFRSF18, IL6R, IL10RB in THYM, CHOL, TGCT, PAAD, ESCA, ACC, LAML, and CESC, indicating the immune-promoting role of SOX9. Because ADORA2A is an adenosine receptor distributed on the surface of immune cells (NK, CD4+ and CD8+ T cells, and macrophages) (38). In the tumor microenvironment (TME), ADORA2A promotes adenosine signal transduction, inhibits infiltration of CD8+ T cells and NK cells, and promotes tumor progression (39). TMIGD2 is widely expressed in T cells, B cell DCs, and monocytes and has been shown to promote angiogenesis and increase actin filament formation, leading to cell adhesion and inhibition of cell migration (40). PD-L1 is highly expressed in most cancers, and the PD-L1/PD-1 signaling pathway contributes to cancer evasion by T-cell immunity (41). We found that SOX9 negatively correlated with CD8+ T cells, activated NK cells, M2 macrophages, and other tumor-infiltrating immune cells. It is well known that TME is composed of vascular endothelial cells, fibroblasts, and immune cells, which promote oncogenic gene expression and block the immunomodulatory effects of distinct immune cells. Both CD8+ T cells and activated NK cells exhibit strong tumor-killing effects (42), and M2 macrophages play a role in suppressing immune responses in the tumor microenvironment (43). These results suggest that SOX9 expression may be able to regulate TME homeostasis by modulating various immune cells and immunomodulatory genes. The immune checkpoint pathway is a mechanism used by tumor cells to disguise themselves as normal components of the human body (44–46). In addition, SOX9 was mutually exclusive with a variety of tumor immune checkpoints (CD27, CTLA4, LAG3, TIGIT, IL10, CSF1R, ADORA2A, CD244, etc.), further suggesting that SOX9 may be a novel target with great potential in tumor immunotherapy. Thus, SOX9 may play an important role in tumor genesis and development by participating in immune infiltration. Moreover, the correlation between SOX9 expression and tumor immune cell infiltration may be related to the malignancy of the tumor. The bioinformatics approach we used in this study can rapidly predict the role of expected target molecules in disease progression and the potential association between molecules based on a large amount of sequencing data. However, the amount of sample size may also cause inconsistency between the prediction results and experimental results, thus generating errors.

CD is an adenosine analog with wide pharmacological effects and maybe resistance to a variety of tumors (18, 19, 47) and viruses (48–50), including SARS-CoV-2 (20, 29, 51, 52). We analyzed the role of CD in different tumor cells and found that CD concentration-dependently decreased SOX9 protein and mRNA expression in 22RV1, PC3, and H1975, suggesting that the anticancer effect of CD may be associated with SOX9 inhibition. CD has been shown to be an immunomodulator to suppress T-cell activity, reduce IL-2 levels, and to increase IL-10 levels, along with affecting the regulation of immune cells and cytokine networks (53). SOX9's tumor immunomodulatory role will be further elucidated in future experiments.

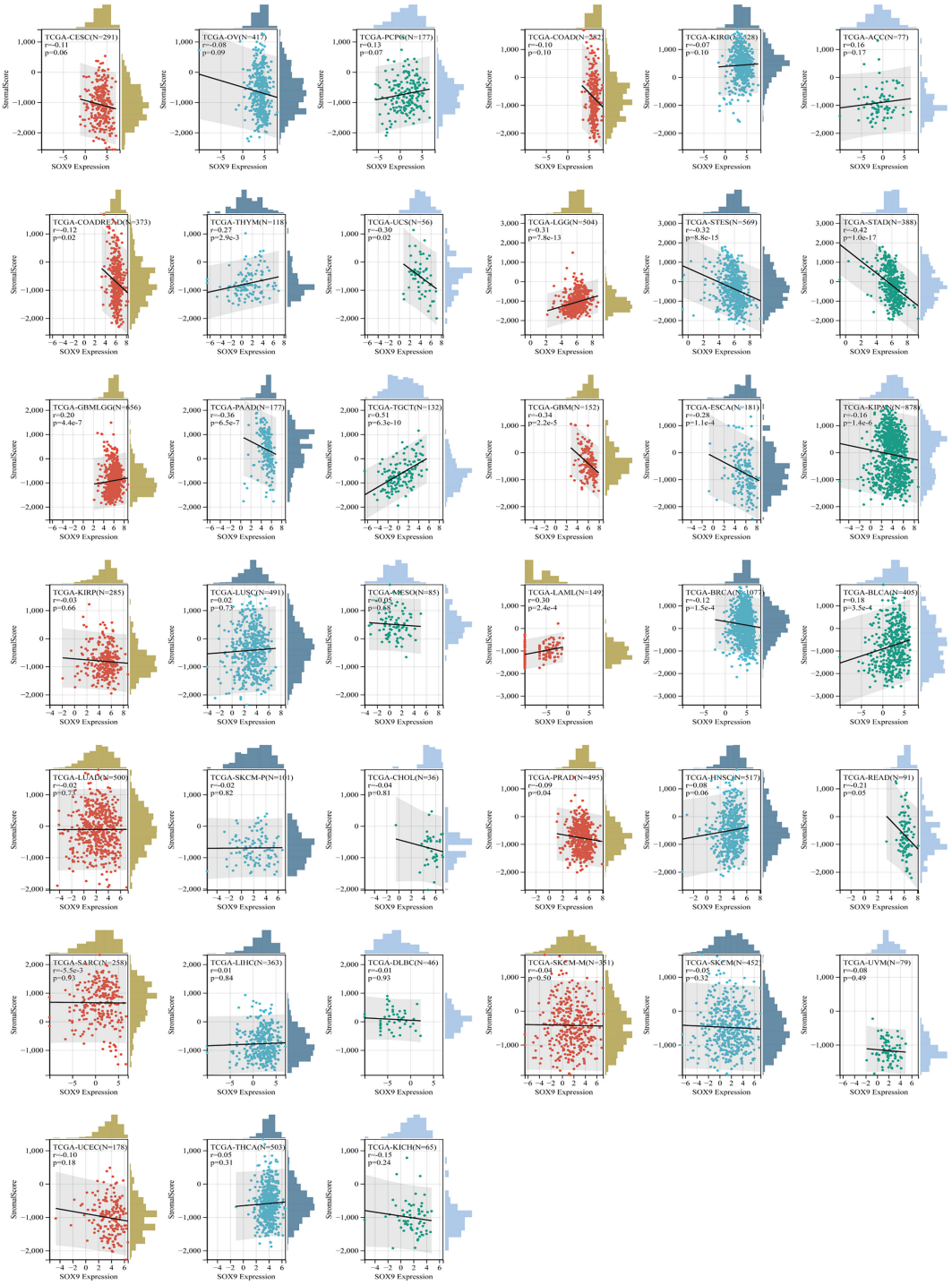

FIGURE 8
The correlation between SOX9 expression and the immune infiltration score indicated several cancer types.

Conclusions

Collectively, SOX9 can be used as a diagnostic and prognostic marker for many types of tumors. Notably, high SOX9 expression in pan-cancer may predict the tumor immunosuppressive microenvironment, suggesting an important role for SOX9 in tumor immune regulation. CD significantly inhibits SOX9 expression in a variety of tumor cells and targeting SOX9 with CD is more promising as a strategy for cancer therapy.

Data availability statement

The original contributions shown in the study are included in the article. Further inquiries can be directed to the corresponding authors.

Ethics statement

The study was approved by the Ethical Committee of Southwest Medical University.

Author contributions

JJF conceived and coordinated the study. SL, LY, JWF, TL, BZ, CW, KW, and JJF conducted experiments, analyzed and interpreted data. SL, KW, and JJF wrote and edited the manuscript. All authors contributed to the article and approved the submitted version.

Funding

This work was supported by the Foundation of Science and Technology Department of Sichuan Province (grant no. 2022NSFSC0737), the Joint Innovation Special Project of Science and Technology Plan of Sichuan Province (grant no. 2022YFS0623-C3), and the National Natural Science Foundation of China (grant nos. 82073263, 81672887).

Conflict of interest

The authors declare that the research was conducted in the absence of any commercial or financial relationships that could be construed as a potential conflict of interest.

Publisher's note

All claims expressed in this article are solely those of the authors and do not necessarily represent those of their affiliated organizations, or those of the publisher, the editors and the reviewers. Any product that may be evaluated in this article, or claim that may be made by its manufacturer, is not guaranteed or endorsed by the publisher.

Supplementary material

The Supplementary Material for this article can be found online at: https://www.frontiersin.org/articles/10.3389/fimmu.2023.1149986/full#supplementary-material

References

1. Tommerup N, Schempp W, Meinecke P, Pedersen S, Bolund L, Brandt C, et al. Assignment of an autosomal sex reversal locus (SRA1) and campomelic dysplasia (CMPD1) to 17q24.3-q25.1. *Nat Genet* (1993) 4:170–4. doi: 10.1038/ng0693-170

2. Sudbeck P, Schmitz ML, Baeuerle PA, Scherer G. Sex reversal by loss of the c-terminal transactivation domain of human SOX9. *Nat Genet* (1996) 13:230–2. doi: 10.1038/ng0696-230

3. Au TYK, Yip RKH, Wynn SL, Tan TY, Fu A, Geng YH, et al. Hypomorphic and dominant-negative impact of truncated SOX9 dysregulates hedgehog-wnt signaling, causing campomelia. *Proc Natl Acad Sci USA* (2023) 120:e2208623119. doi: 10.1073/pnas.2208623119

4. Kha M, Krawczyk K, Choong OK, De Luca F, Altiparmak G, Kallberg E, et al. The injury-induced transcription factor SOX9 alters the expression of LBR, HMGA2, and HIPK3 in the human kidney. *Am J Physiol Renal Physiol* (2023) 324:F75–90. doi: 10.1152/ajprenal.00196.2022

5. Foster JW, Dominguez-Steglich MA, Guioli S, Kwok C, Weller PA, Stevanovic M, et al. Campomelic dysplasia and autosomal sex reversal caused by mutations in an SRY-related gene. *Nature* (1994) 372:525–30. doi: 10.1038/372525a0

6. Cox JJ, Willatt L, Homfray T, Woods CG. A SOX9 duplication and familial 46,XX developmental testicular disorder. *N Engl J Med* (2011) 364:91–3. doi: 10.1056/NEJMc1010311

7. Wang H, Leav I, Ibaragi S, Wegner M, Hu GF, Lu ML, et al. SOX9 is expressed in human fetal prostate epithelium and enhances prostate cancer invasion. *Cancer Res* (2008) 68:1625–30. doi: 10.1158/0008-5472.CAN-07-5915

8. Passeron T, Valencia JC, Namiki T, Vieira WD, Passeron H, Miyamura Y, et al. Upregulation of SOX9 inhibits the growth of human and mouse melanomas and restores their sensitivity to retinoic acid. *J Clin Invest* (2009) 119:954–63. doi: 10.1172/JCI34015

9. Li T, Huang H, Shi G, Zhao L, Li T, Zhang Z, et al. TGF-beta1-SOX9 axis-inducible COL10A1 promotes invasion and metastasis in gastric cancer *via* epithelial-to-mesenchymal transition. *Cell Death Dis* (2018) 9:849. doi: 10.1038/s41419-018-0877-2

10. Panda M, Tripathi SK, Biswal BK. SOX9: An emerging driving factor from cancer progression to drug resistance. *Biochim Biophys Acta Rev Cancer* (2021) 1875:188517. doi: 10.1016/j.bbcan.2021.188517

11. Liang X, Duronio GN, Yang Y, Bala P, Hebbar P, Spisak S, et al. An enhancer-driven stem cell-like program mediated by SOX9 blocks intestinal differentiation in colorectal cancer. *Gastroenterology* (2022) 162:209–22. doi: 10.1053/j.gastro.2021.09.044

12. Yuan X, Huang L, Luo W, Zhao Y, Nashan B, Yu F, et al. Diagnostic and prognostic significances of SOX9 in thymic epithelial tumor. *Front Oncol* (2021) 11:708735. doi: 10.3389/fonc.2021.708735

13. Jana S, Madhu Krishna B, Singhal J, Horne D, Awasthi S, Salgia R, et al. SOX9: The master regulator of cell fate in breast cancer. *Biochem Pharmacol* (2020) 174:113789. doi: 10.1016/j.bcp.2019.113789

14. Ashkenazi S, Ortenberg R, Besser M, Schachter J, Markel G. SOX9 indirectly regulates CEACAM1 expression and immune resistance in melanoma cells. *Oncotarget* (2016) 7:30166–77. doi: 10.18632/oncotarget.7379

15. Tan L, Song X, Ren Y, Wang M, Guo C, Guo D, et al. Anti-inflammatory effects of cordycepin: A review. *Phytother Res* (2020) 35:1284–97. doi: 10.1002/ptr.6890

16. Liu Y, Guo ZJ, Zhou XW. Chinese Cordyceps: Bioactive components, antitumor effects and underlying mechanism-a review. *Molecules* (2022) 27:6576. doi: 10.3390/molecules27196576

17. Das G, Shin HS, Leyva-Gomez G, Prado-Audelo MLD, Cortes H, Singh YD, et al. Cordyceps spp.: A review on its immune-stimulatory and other biological potentials. *Front Pharmacol* (2020) 11:602364. doi: 10.3389/fphar.2020.602364

18. Wei C, Yao X, Jiang Z, Wang Y, Zhang D, Chen X, et al. Cordycepin inhibits drug-resistance non-small cell lung cancer progression by activating AMPK signaling pathway. *Pharmacol Res* (2019) 144:79–89. doi: 10.1016/j.phrs.2019.03.011

19. Wei C, Khan MA, Du J, Cheng J, Tania M, Leung EL, et al. Cordycepin inhibits triple-negative breast cancer cell migration and invasion by regulating EMT-TFs SLUG, TWIST1, SNAIL1, and ZEB1. *Front Oncol* (2022) 12:898583. doi: 10.3389/fonc.2022.898583

20. He J, Liu S, Tan Q, Liu Z, Fu J, Li T, et al. Antiviral potential of small molecules cordycepin, thymoquinone, and N6, N6-dimethyladenosine targeting SARS-CoV-2 entry protein ADAM17. *Molecules* (2022) 27:9044. doi: 10.3390/molecules27249044

21. Du J, Fu J, Zhang W, Zhang L, Chen H, Cheng J, et al. Effect of DPP4/CD26 expression on SARS–CoV–2 susceptibility, immune response, adenosine (derivatives m(6)(2)A and CD) regulations on patients with cancer and healthy individuals. *Int J Oncol* (2023) 62(3):41. doi: 10.3892/ijo.2023.5489

22. Uhlen M, Fagerberg L, Hallstrom BM, Lindskog C, Oksvold P, Mardinoglu A, et al. Proteomics. tissue-based map of the human proteome. *Science* (2015) 347:1260419. doi: 10.1126/science.1260419

23. Uhlen M, Zhang C, Lee S, Sjostedt E, Fagerberg L, Bidkhori G, et al. A pathology atlas of the human cancer transcriptome. *Science* (2017) 357:6352. doi: 10.1126/science.aan2507

24. Tang Z, Li C, Kang B, Gao G, Li C, Zhang Z. GEPIA: A web server for cancer and normal gene expression profiling and interactive analyses. *Nucleic Acids Res* (2017) 45:W98–W102. doi: 10.1093/nar/gkx247

25. Tang Z, Kang B, Li C, Chen T, Zhang Z. GEPIA2: An enhanced web server for large-scale expression profiling and interactive analysis. *Nucleic Acids Res* (2019) 47:W556–60. doi: 10.1093/nar/gkz430

26. Fu J, Wei C, He J, Zhang L, Zhou J, Balaji KS, et al. Evaluation and characterization of HSPA5 (GRP78) expression profiles in normal individuals and cancer patients with COVID-19. *Int J Biol Sci* (2021) 17:897–910. doi: 10.7150/ijbs.54055

27. Cerami E, Gao J, Dogrusoz U, Gross BE, Sumer SO, Aksoy BA, et al. The cBio cancer genomics portal: An open platform for exploring multidimensional cancer genomics data. *Cancer Discov* (2012) 2:401–4. doi: 10.1158/2159-8290.CD-12-0095

28. Li D, Liu X, Zhang L, He J, Chen X, Liu S, et al. COVID-19 disease and malignant cancers: The impact for the furin gene expression in susceptibility to SARS-CoV-2. *Int J Biol Sci* (2021) 17:3954–67. doi: 10.7150/ijbs.63072

29. Fu J, Liu S, Tan Q, Liu Z, Qian J, Li T, et al. Impact of TMPRSS2 expression, mutation prognostics, and small molecule (CD, AD, TQ, and TQFL12) inhibition on pan-cancer tumors and susceptibility to SARS-CoV-2. *Molecules* (2022) 27:7413. doi: 10.3390/molecules27217413

30. Fu J, Song B, Du J, Liu S, He J, Xiao T, et al. Impact of BSG/CD147 gene expression on diagnostic, prognostic and therapeutic strategies towards malignant cancers and possible susceptibility to SARS-CoV-2. *Mol Biol Rep* (2023) 50:2269–81. doi: 10.1007/s11033-022-08231-1

31. Zhou J, Imani S, Shasaltaneh MD, Liu S, Lu T, Fu J. PIK3CA hotspot mutations p. H1047R and p. H1047L sensitize breast cancer cells to thymoquinone treatment by regulating the PI3K/Akt1 pathway. *Mol Biol Rep* (2022) 49:1799–816. doi: 10.1007/s11033-021-06990-x

32. Kim R, Emi M, Tanabe K, Arihiro K. Tumor-driven evolution of immunosuppressive networks during malignant progression. *Cancer Res* (2006) 66:5527–36. doi: 10.1158/0008-5472.CAN-05-4128

33. Liu J, Zheng Z, Zhang W, Wan M, Ma W, Wang R, et al. Dysregulation of tumor microenvironment promotes malignant progression and predicts risk of metastasis in bladder cancer. *Ann Transl Med* (2021) 9:1438. doi: 10.21037/atm-21-4023

34. Kim SK, Cho SW. The evasion mechanisms of cancer immunity and drug intervention in the tumor microenvironment. *Front Pharmacol* (2022) 13:868695. doi: 10.3389/fphar.2022.868695

35. Li B, Severson E, Pignon JC, Zhao H, Li T, Novak J, et al. Comprehensive analyses of tumor immunity: implications for cancer immunotherapy. *Genome Biol* (2016) 17:174. doi: 10.1186/s13059-016-1028-7

36. Luo H, Wang C, Liu M, Yin B, Huang D, Ye L. Inhibition of SOX9 promotes inflammatory and immune responses of dental pulp. *J Endod* (2018) 44:792–9. doi: 10.1016/j.joen.2018.02.004

37. Fan Y, Li Y, Yao X, Jin J, Scott A, Liu B, et al. Epithelial SOX9 drives progression and metastases of gastric adenocarcinoma by promoting immunosuppressive tumour microenvironment. *Gut* (2022) 72:624–37. doi: 10.1136/gutjnl-2021-326581

38. Young A, Mittal D, Stagg J, Smyth MJ. Targeting cancer-derived adenosine: new therapeutic approaches. *Cancer Discov* (2014) 4:879–88. doi: 10.1158/2159-8290.CD-14-0341

39. Ohta A, Gorelik E, Prasad SJ, Ronchese F, Lukashev D, Wong MK, et al. A2A adenosine receptor protects tumors from antitumor T cells. *Proc Natl Acad Sci USA* (2006) 103:13132–7. doi: 10.1073/pnas.0605251103

40. Janakiram M, Shah UA, Liu W, Zhao A, Schoenberg MP, Zang X. The third group of the B7-CD28 immune checkpoint family: HHLA2, TMIGD2, B7x, and B7-H3. *Immunol Rev* (2017) 276:26–39. doi: 10.1111/imr.12521

41. Cha JH, Chan LC, Li CW, Hsu JL, Hung MC. Mechanisms controlling PD-L1 expression in cancer. *Mol Cell* (2019) 76:359–70. doi: 10.1016/j.molcel.2019.09.030

42. Wang W, Zhao J, Hao C, Hu S, Chen C, Cao Y, et al. The development of chiral nanoparticles to target NK cells and CD8(+) T cells for cancer immunotherapy. *Adv Mater* (2022) 34:e2109354. doi: 10.1002/adma.202109354

43. Pan Y, Yu Y, Wang X, Zhang T. Tumor-associated macrophages in tumor immunity. *Front Immunol* (2020) 11:583084. doi: 10.3389/fimmu.2020.583084

44. Li B, Chan HL, Chen P. Immune checkpoint inhibitors: Basics and challenges. *Curr Med Chem* (2019) 26:3009–25. doi: 10.2174/0929867324666170804143706

45. Wang K, Deng H, Song B, He J, Liu S, Fu J, et al. The correlation between immune invasion and SARS-COV-2 entry protein ADAM17 in cancer patients by bioinformatic analysis. *Front Immunol* (2022) 13:923516. doi: 10.3389/fimmu.2022.923516

46. Wang K, Yang C, Li H, Liu X, Zheng M, Xuan Z, et al. Role of the epigenetic modifier JMJD6 in tumor development and regulation of immune response. *Front Immunol* (2022) 13:859893. doi: 10.3389/fimmu.2022.859893

47. Zhang L, Wei C, Li D, He J, Liu S, Deng H, et al. COVID-19 receptor and malignant cancers: Association of CTSL expression with susceptibility to SARS-CoV-2. *Int J Biol Sci* (2022) 18:2362–71. doi: 10.7150/ijbs.70172

48. Richardson LS, Ting RC, Gallo RC, Wu AM. Effect of cordycepin on the replication of type-c RNA tumor viruses. *Int J Cancer* (1975) 15:451–6. doi: 10.1002/ijc.2910150311

49. Panya A, Songprakhon P, Panwong S, Jantakee K, Kaewkod T, Tragoolpua Y, et al. Cordycepin inhibits virus replication in dengue virus-infected vero cells. *Molecules* (2021) 26:3118. doi: 10.3390/molecules26113118

50. Cheng J, Fu J, Tan Q, Liu Z, Guo K, Zhang L, et al. The regulation of ISG20 expression on SARS-CoV-2 infection in cancer patients and healthy individuals. *Front Immunol* (2022) 13:958898. doi: 10.3389/fimmu.2022.958898

51. Bibi S, Hasan MM, Wang YB, Papadakos SP, Yu H. Cordycepin as a promising inhibitor of SARS-CoV-2 RNA dependent RNA polymerase (RdRp). *Curr Med Chem* (2022) 29:152–62. doi: 10.2174/0929867328666210820114025

52. Verma AK. Cordycepin: a bioactive metabolite of cordyceps militaris and polyadenylation inhibitor with therapeutic potential against COVID-19. *J Biomol Struct Dyn* (2022) 40:3745–52. doi: 10.1080/07391102.2020.1850352

53. Zhou X, Luo L, Dressel W, Shadier G, Krumbiegel D, Schmidtke P, et al. Cordycepin is an immunoregulatory active ingredient of cordyceps sinensis. *Am J Chin Med* (2008) 36:967–80. doi: 10.1142/S0192415X08006387

frontiers | Frontiers in Immunology

TYPE Review
PUBLISHED 28 April 2023
DOI 10.3389/fimmu.2023.1163585

OPEN ACCESS

EDITED BY
Luca Antonioli,
University of Pisa, Italy

REVIEWED BY
Chun Wai Mai,
UCSI University, Malaysia
Chang-il Hwang,
University of California, Davis, United States

*CORRESPONDENCE
Jennifer M. Bailey-Lundberg
Jennifer.M.Bailey@uth.tmc.edu

RECEIVED 11 February 2023
ACCEPTED 19 April 2023
PUBLISHED 28 April 2023

CITATION
Strickland LN, Faraoni EY, Ruan W, Yuan X, Eltzschig HK and Bailey-Lundberg JM (2023) The resurgence of the Adora2b receptor as an immunotherapeutic target in pancreatic cancer. *Front. Immunol.* 14:1163585. doi: 10.3389/fimmu.2023.1163585

The resurgence of the Adora2b receptor as an immunotherapeutic target in pancreatic cancer

Lincoln N. Strickland, Erika Y. Faraoni, Wei Ruan, Xiaoyi Yuan, Holger K. Eltzschig and Jennifer M. Bailey-Lundberg*

Department of Anesthesiology, Critical Care, and Pain Medicine, McGovern Medical School, The University of Texas Health Science Center at Houston, Houston, TX, United States

Pancreatic ductal adenocarcinoma (PDAC) is characterized by a dense desmoplastic stroma that impedes drug delivery, reduces parenchymal blood flow, and suppresses the anti-tumor immune response. The extracellular matrix and abundance of stromal cells result in severe hypoxia within the tumor microenvironment (TME), and emerging publications evaluating PDAC tumorigenesis have shown the adenosine signaling pathway promotes an immunosuppressive TME and contributes to the overall low survival rate. Hypoxia increases many elements of the adenosine signaling pathway, resulting in higher adenosine levels in the TME, further contributing to immune suppression. Extracellular adenosine signals through 4 adenosine receptors (Adora1, Adora2a, Adora2b, Adora3). Of the 4 receptors, Adora2b has the lowest affinity for adenosine and thus, has important consequences when stimulated by adenosine binding in the hypoxic TME. We and others have shown that Adora2b is present in normal pancreas tissue, and in injured or diseased pancreatic tissue, Adora2b levels are significantly elevated. The Adora2b receptor is present on many immune cells, including macrophages, dendritic cells, natural killer cells, natural killer T cells, γδ T cells, B cells, T cells, $CD4^+$ T cells, and $CD8^+$ T cells. In these immune cell types, adenosine signaling through Adora2b can reduce the adaptive anti-tumor response, augmenting immune suppression, or may contribute to transformation and changes in fibrosis, perineural invasion, or the vasculature by binding the Adora2b receptor on neoplastic epithelial cells, cancer-associated fibroblasts, blood vessels, lymphatic vessels, and nerves. In this review, we discuss the mechanistic consequences of Adora2b activation on cell types in the tumor microenvironment. As the cell-autonomous role of adenosine signaling through Adora2b has not been comprehensively studied in pancreatic cancer cells, we will also discuss published data from other malignancies to infer emerging therapeutic considerations for targeting the Adora2b adenosine receptor to reduce the proliferative, invasive, and metastatic potential of PDAC cells.

KEYWORDS

immunotherapy, pancreatic adenocarcinoma, hypoxia, Adenosine receptor 2B, CD8+ T cell response

Introduction

Pancreatic ductal adenocarcinoma (PDAC) is a lethal malignancy, with only a 3-13% 5-year survival rate, which is critically dependent on the stage at diagnosis. PDAC is characterized by a highly immunosuppressive and hypoxic tumor microenvironment. Risk factors include age, chronic pancreatitis, diabetes, genetic predisposition, obesity, and smoking (1, 2). Current therapeutic approaches including chemotherapy and radiation have not resulted in significant changes in overall survival, highlighting the continued need for testing new therapeutic strategies to treat PDAC patients. In this review, we will expand on an immune suppressive pathway in PDAC, the adenosine signaling pathway, with a focus on the role of the Adora2b receptor. Work from our lab and others has shown this pathway is elevated in a subset of patients with PDAC, and inhibition of extracellular adenosine generation augments anti-tumor immunity in several preclinical pancreatic cancer models (3–6). We will discuss the mechanistic consequences of elevated extracellular adenosine in the pancreatic cancer microenvironment and will emphasize emerging considerations for targeting the Adora2b receptor as a therapeutic target to improve outcomes for patients at high risk or who have been diagnosed with PDAC (7–9).

Heterocyclic aromatic molecules such as adenosine triphosphate (ATP), adenosine diphosphate (ADP), and adenosine are purines essential to life, indispensable for maintaining intracellular energy balance, cellular processes, and pathways (10). ATP is generated by glycolysis or oxidative phosphorylation and is commonly known as the principal molecule for storing and transferring energy in the cell (11). Within the cell, ATP molecules are transported by mitochondrial ADP/ATP carriers (AAC) proteins, major components of the inner mitochondrial membrane that regulate ATP synthesis by influencing ADP intake in the mitochondria. In the contexts of cellular injury, stress, hypoxia, or cell death, ATP can be secreted out of the cell in exosomes (exocytotic release), through connexin or pannexin channels, or by volume-regulated anion channels to the extracellular space, where it signals through purinergic receptors and participates in a broad range of cellular processes (12, 13). Some of the roles of extracellular ATP include the regulation of inflammation and fibrosis (14). Both ATP and extracellular ADP can be converted by an ectonucleotidase enzyme (CD39) into adenosine monophosphate (AMP), a molecule that can then be converted to adenosine by ecto-5'-nucleotidase (CD73) (Figure 1) (11, 15). Adenosine has been shown to participate in pro-inflammatory, anti-inflammatory, fibrotic, and immunosuppressive responses dependent on cell type activated, extracellular concentrations of ATP, ADP, and adenosine, degree of hypoxia, and availability and duration of binding to P1 receptors including Adora1, Adora3, Adora2a or Adora2b which can all be expressed on epithelial, stromal, or immune cells. Such responses vary depending on the P1 receptor involvement and intracellular signaling downstream of receptor activation (15–18). Extracellular adenosine signaling can be terminated through the uptake of adenosine into cells through two predominant equilibrative nucleoside transporters (ENTs), ENT1 and ENT2, which are bidirectional transport channels that allow transmembrane diffusion of nucleosides (19, 20). Termination of adenosine signaling can also occur when adenosine undergoes an irreversible termination process by the enzyme adenosine deaminase (ADA), which converts adenosine to inosine (21).

Hypoxia-mediated adenosine signaling in inflammatory and tumor microenvironments

Hypoxia is a hallmark of chronic inflammatory conditions including several solid tumors; yet hypoxic conditions can occur in the early stages of inflammation due to the oxygen requirements of neutrophils and other immune cells, causing nearby epithelial and stromal cells to become oxygen-depleted (22). Chronic inflammation exacerbates this response resulting in hypoxia-inducible factor (HIF) activation in immune, stromal, and epithelial cells. Hypoxia-inducible factor 1-alpha (HIF-1α) is a well-known regulator of hypoxic cellular processes, and its activity is mainly controlled by post-translational rather than transcriptomic modifications. During normoxic conditions, HIF-1α levels are kept low by the Von Hippel-Lindau (VHL) tumor suppressor which targets HIF-1α for ubiquitin-mediated proteasomal degradation. However, when oxygen levels become depleted, HIF-1α starts to accumulate and HIF-1α stabilizes and binds to HIF-1β forming a complex that enters the nucleus and binds to hypoxia response elements (HRE) to either promote or repress genes (23, 24). In a mouse model of caerulean-induced acute pancreatitis, injured tissues presented high expression of HIF-1α, and inhibition of HIF-1α, through intraperitoneal injections of HIF-1α small molecule inhibitor PX478, reduced RIP3/p-MLKL expression and ROS production, mitigating acinar cell injury and necrosis (25). In the context of pancreatic cancer, HIF-1α levels are elevated in part due to the desmoplastic stroma and HIF-1α staining and expression strongly associates with PDAC lymph node metastasis, high tumor stage, poor prognosis, and immune evasion (26). A recent study in an autochthonous mouse model of PDAC with pancreas-specific expression of $Kras^{G12D}$ implicates HIF-1α may have a protective role, as genetic deletion of the gene promotes neoplasia. Immunohistochemical staining and ELISA analysis revealed that HIF-1α genetic deletion significantly increases secretion of the B-cell chemoattractant CXCL13, which increases the intrapancreatic accumulation of B cells, as shown through flow cytometry analysis. These data indicate HIF-1α prevents B cell infiltration into hypoxic regions and when B cells were depleted in mice, PanIN development was decreased, implicating B cells promote tumorigenesis in PDAC (27). The expression of Adora2b and its subsequent activation was shown to be elevated by HIF-1α in hepatic ischemia-reperfusion injury mouse models, acute lung injury, liver cancer, and breast cancer (28). During pancreatic diseases, hypoxic conditions tend to develop and both HIF-1α and Adora2b are elevated and involved in the inflammatory process (4, 29), yet, further analysis is needed to

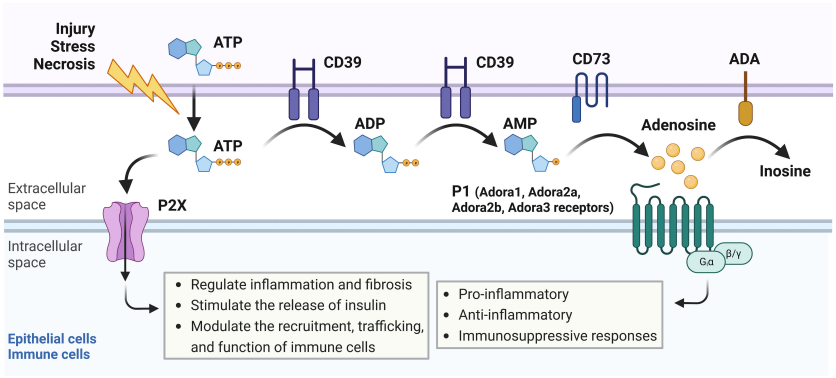

FIGURE 1
Adenosine signaling pathway overview. In response to cellular injury, stress, or necrosis, adenosine triphosphate (ATP) is released to the extracellular space, where it can signal through P2X receptors on epithelial or immune cells to regulate inflammation and fibrosis, stimulate the release of insulin, or modulate recruitment, trafficking, and function of immune cells. Extracellular ATP can also be converted by CD39, an ectonucleotidase enzyme, into adenosine diphosphate (ADP) or adenosine monophosphate (AMP). AMP can then be converted into adenosine by CD73, another ectonucleotidase enzyme. Adenosine binds to P1 receptors including Adora1, Adora3, Adora2a, or Adora2b, which can all be expressed on epithelial, stromal, or immune cells. Activation of the P1 receptors results in pro-inflammatory, anti-inflammatory, or immunosuppressive responses depending on which P1 receptor is involved and which intracellular signaling pathways are activated downstream. Adenosine can also be converted to inosine by adenosine deaminase (ADA) in an irreversible termination process.

fully uncover the potential link between both molecules and their participation in the development of these diseases.

Studies of hypoxia-induced changes in gene expression identified a transcriptional program that promotes CD73 expression in the extracellular vicinity of inflamed tissues (Figure 2). In these studies, Adora2b gene expression is also elevated resulting in an endogenous feedback loop critical for injury resolution and ischemia tolerance under oxygen-deprived conditions (30–32). Transcription of CD73 is regulated by an HRE on the promoter in hypoxic epithelial cells and transcription of CD39 is either upregulated through Sp1 or downregulated through the formation of a HIF-1α and AHR complex with ARNT which decreases AHR recruitment to the CD39 promoter that has three AHR response elements (33–35). HIF-1α inhibits adenosine kinase and ENTs resulting in increased accumulation of adenosine in the tumor microenvironment (19, 20, 36). Another ligand for Adora2b is Netrin-1, a neuronal guidance molecule essential for the proper development of neurons. In PDAC, perineural infiltration is present in early and late stages of the disease and neuronal infiltration by tumor cells may contribute to pain and tumor progression indicating Netrin-1/Adora2b signaling could be evaluated as a therapeutic strategy to reduce perineural infiltration. In addition,

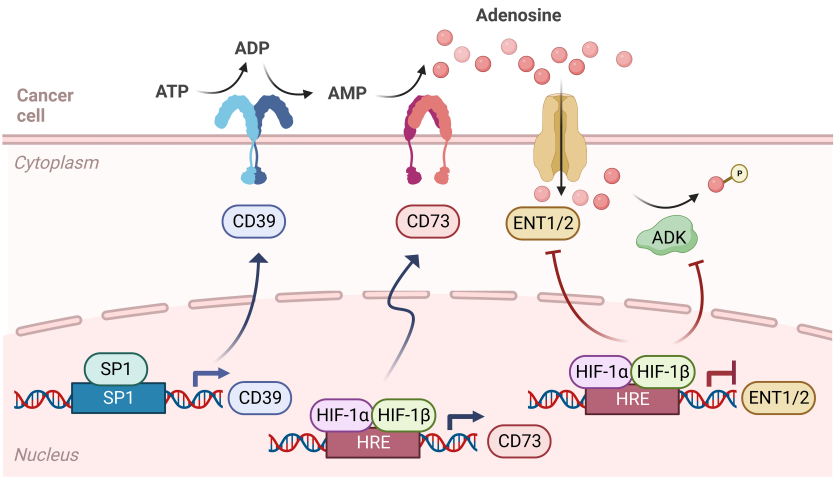

FIGURE 2
Adenosine signaling pathway during hypoxia. Adenosine signaling in hypoxia is similar to normoxia, as ATP is converted to ADP and AMP by CD39, then converted to adenosine by CD73. However, in hypoxic cancer cells, the transcription of CD39 is upregulated through Sp1, leading to more ADP and AMP in the tumor microenvironment (TME). Also, while levels of HIF-1α are kept low by the Von Hippel-Lindau (VHL) tumor suppressor in normoxic conditions, in hypoxia HIF-1α stabilizes and binds to HIF-1β, which forms a complex that enters the nucleus and binds to hypoxia response elements (HRE) on the gene promoter, therefore regulating the transcription of CD73 and equilibrative nucleoside transporters (ENT1/2). In hypoxia, CD73 transcription is upregulated, while ENT1 and ENT2 transcription is downregulated. HIF-1α also inhibits adenosine kinase and ENTs, leading to an accumulation of adenosine in the TME.

signaling of Netrin-1 through the Adora2b receptor also inhibits immune cell infiltration into organs under hypoxic and inflammatory conditions (37–39) indicating several mechanistic consequences for Adora2b in pancreatic and other solid tumors. In addition to Netrin, *in vitro* data have shown that stimulation and activation of Adora2b by adenosine and NECA promotes cell proliferation and secretion of chromogranin A, a protein that is widely accepted as a biomarker for neuroendocrine tumors. Such findings suggest inhibition of the adenosine pathway, specifically targeting Adora2b receptors, may be of high interest in the therapeutic management of neuroendocrine tumors (40).

Another component of the PDAC TME is the vasculature, which is characterized by high microvascular density yet poor perfusing in the vessels and decreased vascular integrity. In PDAC patients, the superior mesenteric vessels are commonly involved, especially when tumors arise in the head of the pancreas. These clinical features of PDAC are notable in the context of adenosine signaling as hypoxia-mediated adenosine signaling influences vascular responses. In the context of inflammation, neutrophils exit the bloodstream through transendothelial migration (TEM) and secrete ATP and ADP resulting in high adenosine concentrations (41–44). Studies exploring the role of adenosine receptors in vascular leakage were completed in mice that were deficient in either Adora1, Adora3, Adora2a, or Adora2b, then subjected to hypoxia. While the Adora1, Adora3, or Adora2a mice did not have an increase in hypoxia-induced vascular leakage, the Adora2b deficient mice showed a significant increase in hypoxia-induced vascular leakage. Furthermore, administration of the Adora2b antagonist PSB1115 to wild-type mice also significantly increased neutrophil infiltration through TEM and worsened vascular leakage while administration of Adora2b agonist BAY-60-6583 reversed the hypoxia-induced vascular leakage. These findings suggest Adora2b has a key role in controlling hypoxia-associated vascular leak by increasing endothelial cell intracellular levels of cAMP which promotes vasculature resealing (31, 45). These studies suggest adenosine signaling events can be targeted to dampen hypoxia-induced inflammation and prevent excessive tissue damage (13, 30). In solid tumors with a hypoxic TME, Adora2b antagonists may promote increased infiltration of immune cells and anti-tumor immunity.

Functional consequences of adenosine receptor signaling in inflammation and cancer

Adora1 and Adora3 receptors

The Adora1, or adenosine A_1 receptor, is a G protein-coupled receptor (GPCR) that, when bound to an agonist, causes $G_{i1,2,3}$ or G_0 protein binding. Adora1 is ubiquitously expressed in the body and, when $G_{i1,2,3}$ is bound, adenylate cyclase is inhibited, and cAMP concentrations are decreased. This has important consequences in several fundamental biological contexts including slowing heart rate (46, 47), reducing glucose-induced insulin secretion (48), reducing blood flow, and promoting edema during acute pancreatitis (49). In the context of cancer, Adora1 overexpression has been published to facilitate the malignant progression of colorectal, kidney, and breast cancers, as well as glioblastoma and leukemia (50). Inhibition of Adora1 in combination with immune checkpoint blockade (ICB) therapy targeting PD-1 has shown promising therapeutic effects in non-small cell lung cancer and melanoma (51). In contrast, studies evaluating the role of hypoxia in the pancreas reveal Adora1 is downregulated during hypoxia (52) and analysis of RNA-seq data from The Cancer Genome Atlas (TCGA) database indicated this receptor was not associated with PDAC prognosis (48). Thus, the role of Adora1 in response to hypoxia or other environmental triggers of adenosine is dependent on tumor type and organ of origin.

The Adora3 or adenosine A_3 receptor couples to Gi/Gq proteins. Like Adora1, Adora3 receptor activation promotes Gi protein binding and decreased adenylyl cyclase activity which reduces cAMP intracellular levels. Adenosine signaling through Adora3 has been shown to participate in the degranulation and activation of mast cells important in asthma pathogenesis (53–55). Adora3 also modulates cytokine release *via* T cell-mediated production of IL-10 which helps reverse neuropathic pain (56) and through down-regulation of nuclear factor-kappa B signaling results in the inhibition of inflammatory cytokine production in the colonic mucosa of patients with ulcerative colitis (57). Unlike the Adora1 receptor, hypoxic conditions do not affect Adora3 expression (52). In the context of the pancreas, low levels of Adora3 receptor expression have been reported and Adora3 is not associated with PDAC prognosis (48).

Adora2 receptors

Adora2 adenosine receptors consist of the adenosine $A2_A$ (Adora2a) and $A2_B$ (Adora2b) receptors, both of which are Gs-coupled GPCRs. In the pancreas, Adora2a and Adora2b have many similarities, as they both are present in the luminal membrane of ductal, insulin-positive beta, and PECAM-+ endothelial cells (11). Agonist binding to Adora2 receptors stimulates cAMP, a membrane-associated protein kinase A (type II PKA), and cAMP-activated Cl^- channels which mediate critical pancreatic ductal secretions (48). Adora2a is the most abundant adenosine receptor in the pancreas and it participates in endocrine pancreatic functions as well as water and bicarbonate secretion responses (48). Adora2a is also a potent anti-inflammatory regulator as its activation limits immune cell activity during an inflammatory response preventing additional tissue damage (16, 58, 59). In studies carried out in mice lacking Adora2a receptors, behavioral alterations are present, suggesting the participation of Adora2a in regulating neuronal populations (60). In caerulein-mediated mouse models of pancreatitis, inhibition of adenosine uptake using a pharmacologic inhibitor enhanced stimulation of the Adora2a receptor, and was capable of reducing the severity of pancreatitis (61). Specifically, in pancreatic cancer patients, studies show CD73

and Adora2a expression on neoplastic or tumor cells correlates with divergent immune cell populations in the tumor microenvironment. In a publication by Sweed et al, when Adora2a is overexpressed in human PDAC patients, there are correlative high levels of tumor-infiltrating mononuclear cells (TIMC), associated with larger tumor sizes (62). Moreover, in an immunohistochemical study performed on 48 human PDAC tissues, Adora2a was overexpressed, and high Adora2a PDAC expression was associated with more aggressive cases and later tumor stages at the time of diagnosis (62). While no functional experiments were reported in this manuscript, these data indicate both autocrine and paracrine adenosine signaling through Adora2a are important in the pathogenesis of pancreatic cancer.

The Adora2b receptor is the only low-affinity adenosine receptor [Adora2b EC_{50} = 24 μM, Adora2a EC_{50} = 0.7 μM, Adora1 EC_{50} = 0.31 μM, Adora3 EC_{50} = 0.29 μM (63)], requiring high levels of extracellular adenosine to become activated rather than existing in a resting state (64). Adora2b is present in myocardial cells, epithelial cells, fibroblasts, and several immune cell types (65) and in many disease models is a potent anti-inflammatory regulator. However, controversial findings exist around its role in disease, fibrosis, and tumor development. Across several mouse models of acute injury, Adora2b activation has shown protective effects, either by modulating IL-10 production on the intestinal epithelium (66), stabilization of circadian rhythm protein (67) or enhancing alveolar fluid clearance in mice (68). Additionally, studies in Adora2b deficient mice showed enhanced pulmonary recruitment of effector T cells and failed induction of regulatory T cells during endotoxin-induced inflammation resulting in increased severity of the disease. Similarly, in a pulmonary disease mouse model, induction of Adora2b signaling attenuated inflammation and edema only in wild-type mice but not in mice lacking expression of the receptor (69, 70). Contrarily, the absence of Adora2b in an ulcerative colitis mouse model ameliorated acute intestinal inflammation, suggesting this receptor plays a pro-inflammatory role in the development of this disease (71, 72).

In cancer, there are also conflicting studies related to the function of Adora2b in the progression of different malignant diseases. High Adora2b levels are associated with a better prognosis in patients with ovarian cancer. *In vitro* pharmacological activation of Adora2b in ovarian carcinoma cells reduced cell migration and actin stress fiber expression (7). However, detrimental effects were observed for mammary carcinoma, hepatocellular carcinoma, lung adenocarcinoma (LUAD), and PDAC. Adenosine signaling through Adora2b in breast cancer cells regulates the tumor microenvironment and enhances pro-tumorigenic actions in cancer-associated fibroblasts, effects correlated with increased metastatic potential and poor prognosis (73). In hepatocellular carcinoma, Adora2b receptor blockage enhanced the benefits of sorafenib treatment by suppressing the inhibitory effects of adenosine on $CD8^+$ T cells (74). Bioinformatic studies in LUAD and PDAC revealed Adora2b expression and associated signaling pathways predicted poor prognosis and significantly reduced overall survival (48, 75).

The function of Adora2b receptor on immune cells: implications for targeting to promote anti-cancer immunity

Adora2b in innate immunity

Comprised of many cell types including macrophages, dendritic cells, natural killer cells, natural killer T cells, γδ T cells, and more, the innate immune system provides a rapid response to foreign antigens, and the innate immunity antitumor response triggers effector mechanisms to contain the tumor. Adenosine binding to the Adora2b receptor has important functional consequences on innate immune cells (Figure 3). Macrophages impart critical functions in the resolution of inflammation and a return to normal tissue conditions. Their principal function is to clear dead cells from inflamed tissues through a process called efferocytosis, which also resolves inflammation by suppressing pro-inflammatory cytokines and stimulating anti-inflammatory cytokines. Adora2b on bone marrow-derived macrophages (BMDM) was discovered through flow cytometry experiments done in mice and functionality of the receptor was assessed by Adora2b agonist, 5'-N-ethylcarboxamidoadenosine (NECA), which resulted in increased cAMP levels in cultured BMDM (76, 77). Adora2b is upregulated on macrophages by IFN-γ and when Adora2b is activated, TNF production in infiltrating macrophages is suppressed, inhibiting their capacity to secrete cytokines important for anti-tumor immunity and promoting tumor growth (78).

Dendritic cells (DCs) are antigen-presenting cells and critical determinants of both innate and adaptive immunity. They dwell in peripheral tissues in an immature state and, when exposed to triggers, transform into differentiated and mature DCs. Stimulation of Adora2b on DCs stimulates maturation into a differentiated population with DC markers and monocyte or macrophage markers, allowing mature DCs to interact with T lymphocytes and promote CD4+ differentiation into Th1 cells through IL-12 production. DCs differentiated due to exposure to adenosine have decreased allostimulatory activity and express high levels of angiogenic, immune suppression, pro-inflammatory, and tolerogenic factors, such as COX-2, IDO, IL-6, IL-8, IL-10, TGF-β, and VEGF (79, 80).

Natural killer (NK) cells are critical in responses to stress and infections. Many types of NK cells have NK receptors (NKRs) that determine if a cell encountered by an NK cell becomes a target for destruction or is protected (81). When activated NK cells encounter adenosine through the Adora2b receptor, the cAMP pathway is activated and cytotoxic activity and cytokine production is blocked, contributing to reduced anti-tumor activity (82, 83). While NKs and natural killer T cells (NKTs) have many similarities, they are very different in the context of cancer. Both cell types display effector properties in early cancer stages and have impaired functionality in later stages. NKT cells become exhausted in advanced cancers and have an irregular metabolism. NKTs have exhaustion markers such

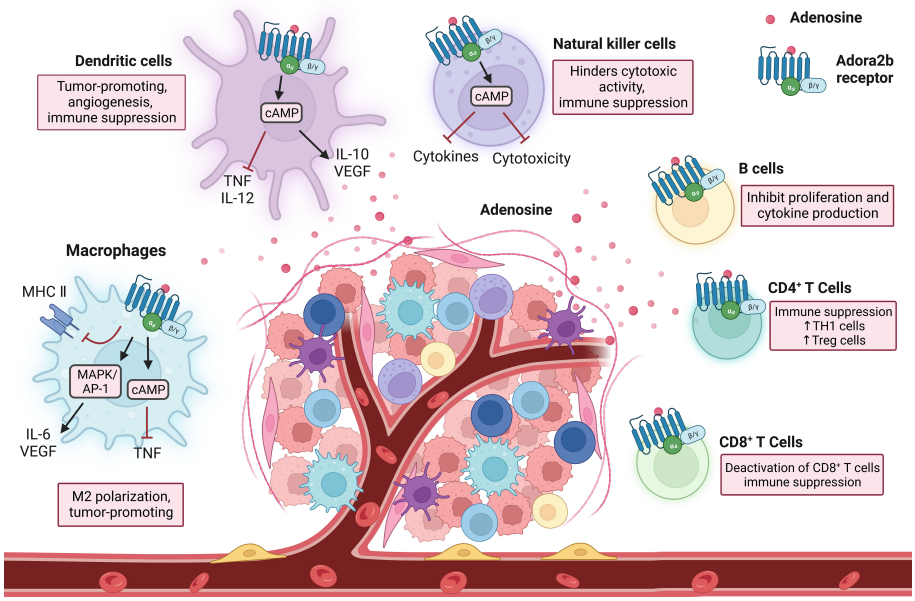

FIGURE 3
Immune cell interactions in response to Adora2b activation. As immune cells enter into the TME and encounter adenosine through the Adora2b receptor, they undergo changes resulting in immunosuppression. Adora2b activation on macrophages contributes to M2 polarization and tumorigenesis, as it inhibits MHC II expression, activates MAPK/AP-1 which increases IL-6 and vascular endothelial growth factor (VEGF) production, and increases cAMP levels which inhibits tumor necrosis factor (TNF) production. On dendritic cells, stimulation of Adora2b increases cAMP production which inhibits TNF and IL-12 production and increases IL-10 and VEGF release, resulting in tumorigenesis, angiogenesis, and immune suppression. Natural killer cells encounter adenosine through the Adora2b receptor and the cAMP pathway is activated resulting in blocked cytokine production and cytotoxicity, contributing to immunosuppression. On B cells, Adora2b activation results in the inhibition of proliferation and cytokine production. $CD4^+$ T cell activation of Adora2b increases TH1 cell and Treg cell levels, as well as contributes to immune suppression. On $CD8^+$ T cells, Adora2b activation results in the deactivation of CD8+ T cells and contributes to the suppression of the immune system.

as high CTLA4, PD1, and Tim3, as well as low granzyme B levels, and reduced cell numbers as cancer progresses further (84). Limited studies have been done assessing the role of the Adora2b receptor in NKT cells.

γδ T cells are a rare subtype of T cells, bridging the gap between the innate and adaptive immune system components, they possess both γ and δ T cell receptor chains. They have gained traction in the area of immunotherapy as they have an anti-tumor immune function and are critical in immune surveillance. Analysis of TCGA data has shown PDAC patients with high CD73 levels have lower amounts of γδ T cells (85). These cells are regulated by extracellular adenosine levels, and in mice treated with an Adora2b agonist, the DCs activate γδ T cells, elevating Th17 responses (86). When γδ T cells induce an elevated Th17 response, this contributes to the pathogenesis of autoimmune diseases and can be a target in inflammation-related diseases such as cancer. However, the specific role of the Adora2b receptor in this cell type is unknown and should be explored further.

Adora2b in adaptive immunity

Comprised of B cell and T cell subtypes, the adaptive immune system is responsible for recognizing and attacking specific antigens. B cells are lymphocytes that produce antibodies tagging specific antigens for destruction and play an important role in hypoxia and inflammation in the TME in PDAC. B cells express both CD73 and CD39, and the production of extracellular adenosine by B cells can inhibit T cell proliferation and the production of IL-10 cytokines. However, B cells have very low levels of the Adora2b receptor and few studies have been conducted to determine its role in B cell interactions (87).

T cells are a crucial group of cells in the immune system that generally express CD73, CD39, and the Adora2b receptor. The presence of Adora2b on T cells was confirmed through flow cytometry and the functionality of the receptor was determined by increased cAMP levels in the cells induced by an Adora2b agonist. Extracellular adenosine limits T cell mobility and increases cAMP levels in T cells, contributing to Adora2b-mediated immune suppression (87, 88). Helper T cells are $CD4^+$ T lymphocytes that stimulate other immune cells to respond to infection and when activated, Adora2b receptor levels increase on the $CD4^+$ T cell surface (88). In a model of endotoxin-induced pulmonary inflammation, mice with a genetic knockout of Adora2b had an enhanced $CD4^+$ T cell response, resulting in increased inflammation (69). Adora2b on $CD4^+$ T cells contributes to immunosuppression and could be a target in cancer, but additional studies are needed to learn more about the role of the receptor on $CD4^+$ T cells. Cytotoxic T cells are $CD8^+$ T cells that are important in protection against tumor growth, as they trigger apoptosis of pathogenic cells. In an *in vitro* experiment, activation of $CD8^+$ T cells through an unspecific activation signal (phytohemagglutinin) and by a specific activation signal (the anti-T cell receptor/CD3 complex mAb, OKT3) triggers increased

Adora2b levels and a decrease in IL-2 production (88). Through TCGA and The Cancer Immune Atlas analyses, PDAC patients with high CD73 levels had lower amounts of $CD8^+$ T cells (4, 85). In studies performed in mice with genetic deletion of *Adora2b*, when murine PDAC cell lines derived from *Pdx1:Cre; LsL-Kras^{G12D};LsL-Trp53$^{R172H/+}$* (KPC) mice, were implanted subcutaneously, tumor growth was significantly reduced compared to implanted cells in WT mice and there was a significant increase in Granzyme B (GZM+) and $CD8^+$ T cells in KPC-derived tumors implanted in *Adora2b$^{-/-}$* mice (4). These data indicate paracrine adenosine Adora2b signaling restrains cytotoxic $CD8^+$ T cell function. Also, in complimentary studies, wild-type mice treated with PSB1115, an Adora2b antagonist, had reduced KPC subcutaneous tumor growth compared to vehicle-treated KPC tumor-bearing mice. However, in wild-type mice without $CD8^+$ T cells, treatment with the PSB1115 did not inhibit the growth of the KPC subcutaneous tumors indicating paracrine adenosine signaling through Adora2b on $CD8^+$ T cells reduces their anti-tumor properties in PDAC (4). Future studies using genetic models or orthotopic implantation of KPC cells into the pancreas will aid in further delineating the role of Adora2b in pancreatic cancer.

Adora2b function in exocrine pancreatic diseases

The pancreas is comprised of both endocrine and exocrine cells. Specifically related to exocrine function, acinar cells organize into acini and constitute 70-90% of pancreatic cells while 5-25% of exocrine pancreatic cells are ducts. Acinar cells are responsible for releasing digestive enzymes and Cl^- rich fluid, while ducts release bicarbonate pancreatic juice to neutralize stomach acidity and deliver acinar cell-derived enzymes to the duodenum (89, 90). The characteristic zymogen granules in acini store intracellular ATP at 10uM concentrations (91, 92). In a healthy pancreas, ATP is secreted by acinar cells into the ducts where P2 receptors regulate Cl^- and K^+ ion channels, cAMP signaling, and transporters resulting in ductal secretion of $NaHCO_3$-rich fluid (93). Acini and ducts have both been shown to express CD39 and CD73 which generate luminal adenosine that signals through ductal P1 receptors Adora2a and Adora2b which stimulate the cystic fibrosis membrane conductance regulator Cl^- channels important for ductal function (94). While less numerous, accounting for approximately 3-5% of pancreatic parenchyma, endocrine-functioning islet cells are critical for glucose homeostasis, and pancreatogenic (Type3c) diabetes can occur in a subset of patients with acute or recurrent acute pancreatitis (48, 95, 96). Both human and rodent ducts express adenosine receptors, with Adora2a and Adora2b being the most prevalent in these cells. When these receptors are stimulated, Cl^- channels are opened and allow ductal secretions to occur indicating purinergic signaling is important for pancreas function and homeostasis (29, 48, 97, 98) (Figure 4, left panel).

In the pathophysiology of acute pancreatitis, the enzymes zymogen and trypsinogen are released due to premature activation of acinar cells resulting in local parenchymal destruction and activation of inflammatory pathways. When

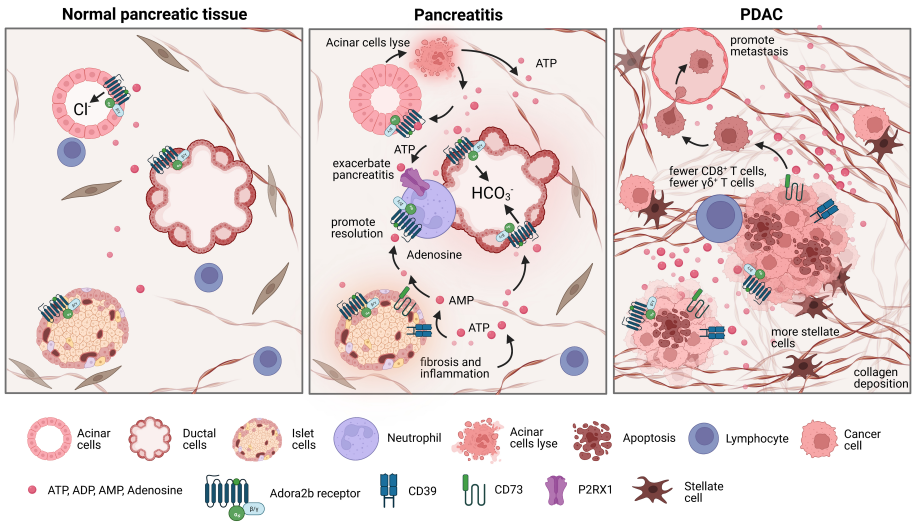

FIGURE 4
Changes in the pancreatic landscape in response to pancreatitis and pancreatic ductal adenocarcinoma (PDAC). Normal pancreas tissue is comprised of acinar cells that release digestive enzymes and Cl^- rich fluid, ductal cells that release bicarbonate pancreatic juice, and islet cells that maintain glucose homeostasis. However, during pancreatitis acinar cells lyse, releasing ATP into the extracellular environment, promoting elevated purinergic signaling which leads to altered bicarbonate secretion levels and exacerbates inflammation. In chronic pancreatitis, damage to islet cells contributes to increased fibrosis and inflammation, promoting high extracellular ATP levels and increased adenosine signaling. Neutrophils also contribute to exacerbating pancreatitis by expressing P2RX1 which promotes glycolytic metabolism. Contrarily, adenosine can inhibit the inflammatory function of neutrophils through Adora2b mediated deactivation, which partially promotes the resolution of pancreatitis. PDAC is characteristically immunosuppressive and possesses a dense desmoplastic stroma with a hypoxic necrotic core. In the necrotic core, there are high levels of extracellular ATP and higher levels of CD39 and CD73, which leads to an accumulation of adenosine in the TME which can then bind to Adora2b and contribute to immunosuppression. This also leads to fewer γδ+ T cells, more collagen deposition, and more stellate cells.

acinar cells prematurely secrete enzymes, they also secrete ATP and other inflammatory signals into the extracellular environment (99–101). High extracellular ATP levels promote elevated purinergic signaling which leads to altered bicarbonate secretion from pancreatic ducts, ductal dilation, infiltration of innate immune cells, and increased severity of pancreatitis (11). Purinergic receptors are expressed on neutrophils and are key chemoattracts for these cells, which elevate pancreatic inflammation and the severity of pancreatitis. Thus, the conversion of ATP by CD39 and CD73 to adenosine is an important anti-inflammatory mechanism to return the pancreas to normal homeostasis after acute injury (102). Recent studies using single-cell RNA sequencing reveal CD73 is expressed in T cells and ductal cells in murine and human models of chronic pancreatitis (103). During chronic pancreatitis, not only are acinar cells severely injured, but also islet cells, with increased fibrosis and inflammation. This causes an extreme accumulation of extracellular ATP and exacerbated purinergic signaling (11) as well as increased infiltration of P2RX1 expressing neutrophils (102). Anti-inflammatory adenosine Adora2b signaling on ducts, neutrophils, and insulin-producing beta cells is therefore critical to promote healing after acute and chronic pancreatic injury (Figure 4, middle panel). Adora2b signaling reduces netosis formation and reduces oxidative burst from neutrophils, critical functions that reduce neutrophil-mediated inflammation during pancreatitis (104, 105). Future studies to determine the exact role of Adora2b receptor signaling in acute and chronic pancreatitis are important for future therapeutic considerations.

PDAC has a characteristically immunosuppressive TME where tumor cells coexist with exhausted and deactivated immune cells within a dense hypoxic desmoplastic stroma and necrotic tumor core (27). Understanding and targeting mechanistic triggers of immune suppression is one therapeutic approach being testing in preclinical and clinical trials. In a recent immunohistochemical study on human PDAC tissues, Jacoberger-Foissac et al. found that worse prognosis occurred only when patients present with elevated expression of both CD39 and CD73. When CD39 levels are high but CD73 levels are low, there is an increase of $CD8^+$ T cells; however, this effect is not present when CD73 levels are also high, reaffirming that production of adenosine limits $CD8^+$ T cell infiltration into PDAC tumors (6). Elevated expression of CD39 and CD73 has also been associated with fewer γδ+ T cells, more collagen deposition, and more proliferation of stellate cells indicating adenosine signaling may also be a critical determinant of fibrosis and desmoplasia in pancreatitis and pancreatic cancer (85, 106, 107). Three recent publications have utilized preclinical mouse models to evaluate the role of adenosine signaling in pancreatic cancer and have collectively shown genetic deletion of CD73 or treatment with CD73 small molecule inhibitors in syngeneic or genetic mouse models significantly reduces the development and progression of pancreatic cancer and promotes increased anti-tumor immunity; however, there are some differences in the models and findings which we want to highlight (4–6). In a publication by King et al, the authors performed a metabolic screen and found elevated CD73 correlated with aggressiveness of disease. The authors genetically deleted Nt5e/CD73 in murine PDAC cells and used an orthotopic model to show deletion of CD73 significantly ablated tumor growth and reduced the abundance of infiltrating MDSCs. They further show the anti-tumor immune response in Nt5e depleted tumors was associated with $CD4^+$ and $CD8^+$ T cells expressing IFN γ and showed the response was dependent on $CD4^+$ T cells, but not $CD8^+$ T cells (5). In a second publication by Jacoberger-Foissac et al, CD39 expression on $CD8^+$ T cells was shown to suppress IFN γ production by T cells and transplantation of murine KPC tumors, myeloid expression of CD39 and CD73 and tumor expression of CD73 promoted polarization of myeloid cells to an M2 phenotype, which promoted PDAC growth and targeting both CD73 and CD39 significantly enhanced the anti-tumor T cell response. These findings were both done in the transplanted or orthotopic setting. Similarly, in the publication by Faraoni et al, inhibition of CD73 in murine genetic (spontaneous) models of pancreatic cancer, significantly reduced cancer development in spontaneous models with higher expression of CD73 in the neoplastic and cancer cells. Notably, pharmacologic inhibition of CD73 correlated with a significant increase in activated CD8+GZM+ T cells and F4/80+ cells in both genetic models. The authors then expanded these studies to a subcutaneous model to show inhibition of CD73 or the Adora2b receptor reduced the growth rate of murine KPC tumors. A limitation of the subcutaneous model is it does not recapitulate the microenvironment of the pancreas or the desmoplastic response in the pancreas. However, in this model, Faraoni et al. show the reduction in tumor growth using a small molecule inhibitor of Adora2b is dependent on $CD8^+$ T cells. These studies were conducted to expand beyond the findings using CD73 inhibitors in spontaneous, orthotopic and subcutaneous models as we show in the publication by Faraoni et al, that PDAC patients with high *ADORA2b* have reduced survival and poor prognosis. In addition, we have shown using Quantiseq and The Cancer Immune Atlas analysis that patients with high *ADORA2b* or high CD73 have decreased NK cells, $CD8^+$ T cells, B cells, and M2 macrophages (4). In studies using implantation of murine KPC tumors into WT or *Adora2b*$^{-/-}$ mice, we show a significant reduction in tumor growth in tumors arising in *Adora2b*$^{-/-}$ mice compared to WT mice. Pharmacologic inhibition of Adora2b also restrained tumor growth *in vivo*; however, the effect of the small molecule inhibitor was not present in tumor growth in CD8KO mice indicating adenosine signaling through Adora2b significantly restrains $CD8^+$ T cell anti-tumor activity in PDAC (4) (Figure 4, right panel). These data indicate that co-inhibition of CD73 and Adora2b may provide additional therapeutic targeting to activate anti-tumor immunity and improve outcomes for PDAC patients.

Adora2b function in metastasis

Greater than 90% of cancer-related deaths are due to metastasis, illustrating an urgent need for an improved understanding of mechanisms driving metastasis and ways to prevent metastases from forming. Traveling through the bloodstream, rogue cancer cells create metastatic cancer nodules that are highly resistant to therapies (108). In experimental mouse models of melanoma and triple-negative breast cancer metastasis, the incidence of metastasis

is significantly decreased when mice are treated with an Adora2b antagonist (109). Similarly, genetic deletion of the Adora2b receptor in mouse and human triple-negative breast cancer cells reduces their metastatic capability *in vivo* (109), suggesting an important role for Adora2b in cancer metastasis. Recently, it was also shown that antagonizing Adora2b expression in gastric cancer cells increased the efficacy of cisplatin treatment (110). However, despite these promising results in melanoma, breast cancer, and gastric cancer cells, the specific role of Adora2b in metastatic development remains unknown. Metastasis is especially common in PDAC patients, due to the unfortunate ability of PDAC tumor cells to evade the exhausted and suppressed immune system. Future studies will be needed to further demonstrate the potential role of Adora2b in pancreatic cancer metastasis as well as their potential impact on this and other diseases.

Experimental considerations for targeting autocrine and paracrine Adora2b signaling

PDAC organoids and cell lines

Organoid models are a highly translational model system and provide an *ex vivo* approach to studying healthy pancreas and PDAC. Derived most from human or murine tissues, they are 3D and capable of self-renewal as well as spontaneous self-organization, providing a unique opportunity to study therapeutic approaches to augment personalized medicine, therapeutics, and mechanisms of resistance (111–114). Pancreatic organoids can also be orthotopically implanted after cryopreservation or genetic manipulation allowing more rapid studies of mechanistic drivers of PDAC development and metastasis *in vivo*. Noteworthy, it is important to mention that although organoids offer an interesting platform to test therapeutic drugs and can be applied to many different cell types and diseases, they still lack a high-fidelity cell type composition, have limited maturation, and have an atypical physiology which does not always can recapitulate or mimic interactions between molecules when compared to the physiologically normal and/or tumor microenvironments, which limit their applicability and reliability for certain tumor studies (115). If organoid models are not available, human PDAC cell lines can also be used as an *in vitro* mechanistic approach to study cell autonomous and non-cell autonomous purinergic signaling. Established cell lines from human PDAC primary tumors are BxPC-3, Capan-2, HPAC, MIA PaCa-2, and Panc-1. BxPC-3 is the only cell line mentioned which is wild type for *KRAS* and does not represent the majority of PDAC tumors, which have somatic mutations in *KRAS* (116). For each of these human cell lines, experiments can be done with Adora2b agonists, Adora2b antagonists, siRNA, or CRISPR/Cas9 mediated genetic deletions, to study the cell-autonomous upstream and downstream effects of adenosine signaling through the Adora2b receptor. The KPC cell line is also a very common murine PDAC cell line with mutations in *Trp53* and *Kras*.

Mouse models

Mouse models are essential to studying pancreatic cancer and there are numerous models which would be useful to study the Adora2b receptor and its role in PDAC. First, there are syngeneic models utilizing subcutaneous or orthotopic implantation of KPC cells into the flank, pancreas, spleen, or any combination of these injection sites. These models are useful for studying treatment options using Adora2b antagonist compounds in primary tumors and metastatic sites (4). There are also genetically engineered mouse (GEM) models that can be used, such as the KPC and *Pdx : Cre;LsL-Kras^{G12D}* (KC) models. The KPC mice have mutations in *Kras, mutations or* genetic deletion of *Trp53*, and use Cre-Lox technology through Cre recombinase gene insertion into *Pdx-1* or *Ptf1a* (p48-Cre) coding exons. KPC mice begin to develop PDAC precursor lesions around 8-10 weeks of age and have PDAC by 4 months of age (117). KC mice are advantageous for prevention studies as they have slow development from PanIN to PDAC over a time frame of 12-15 months (118). Future studies in GEM models could also be used to test different Adora2b antagonist compounds *in vivo* and to study immune cell interactions in the preventive or therapeutic setting. Using cell-specific inducible CreER alleles crossed to an Adora2b floxed allele, genetically engineered mouse GEM models can be generated with genetic deletion of *Adora2b* in specific cells or tissues. Mice without Adora2b receptors in the defined immune cells, stromal cells, or vasculature could also be useful to study the role of the receptor in PDAC in the future.

Adora2b agonist and antagonist compounds

Selective adenosine agonists and antagonists have been described for the Adora2b receptor and support the protective and anti-inflammatory mechanistic consequences of Adora2b signaling. Particularly in pancreatic diseases, 5'-N-ethylcarboxamidoadenosine, commonly abbreviated as NECA, was recently administered in a model of pancreatitis and described as a suitable Adora2b agonist which may be involved in tissue regeneration and restraint of MPO accumulation and metaplasia during acute pancreatitis; however, no specific therapeutic applications of NECA have been described to date in the clinic (29). Though studies have shown short-term adenosine exposure is highly effective at reducing pain and inflammation, high levels of adenosine have been reported to increase tissue damage and may increase inflammation and potentiate protumor adenosine signaling (119). For these reasons, Adora2b antagonist compounds could be potential therapies in cancer (120). Notably, some of the Adora2b antagonists have been described to decrease the secretory rate of the pancreas by 25% and increase insulin production levels (48). Mice bearing KPC subcutaneous tumors treated with Adora2b antagonist PSB1115, presented with significantly decreased KPC tumor growth and significantly decreased fibrosis measured by IHC for α-SMA. These studies highlight the complex dynamics of this pathway and the urgent need for preclinical and clinical evaluation of targeting Adora2b receptor signaling to better deduce its role in immunity, fibrosis, and cancer (4) (Figure 5).

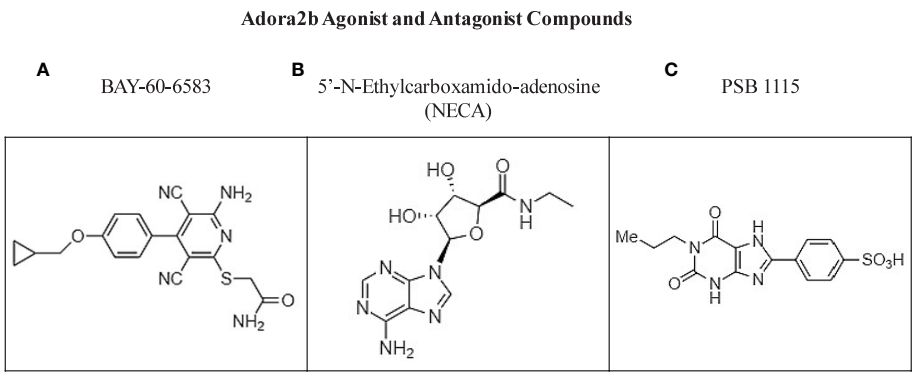

FIGURE 5
Commercially available compounds targeting Adora2b. **(A, B)** Chemical structures of Adora2b agonist compounds BAY-60-6583 and NECA. **(C)** Chemical structure of Adora2b antagonist compound PSB 1115.

Current therapeutic opportunities and clinical trials

Studies have shown there is an estimated time of 10 years between the moment at which a pancreatic epithelial cell undergoes an oncogenic hit and the time of diagnosis (121), which provides a wide window of opportunity for the detection and prevention of precancerous lesions including pancreatic intraepithelial neoplasia (PanIN). A recent study of healthy human pancreata has shown PanIN are present in individuals irrespective of age and these PanIN have transcriptional signatures that share similarities to cancer cells (122). Despite this recent finding, the lack of technology or systemic biomarkers available for performing early detection allows precursor lesions to progress to a point where, when detected, PDAC is diagnosed at advanced stages and is unresectable in 70-80% of patients diagnosed. Thus, there is a need to test and evaluate new approaches in patients with locally advanced or borderline resectable pancreatic cancer including the use of immunomodulators in the neoadjuvant setting. Considering recent publications showing Adora2b reduces the cytotoxic functionality of NKT and $CD8^+$ T cells, there is an increased premise to evaluate inhibiting Adora2b signaling in the prevention setting. Targeting the adenosine signaling pathway at the preclinical stage has been an intense area of study in recent years and future studies in GEM models of PanIN initiation and progression to PDAC would aid in determining if targeting this pathway has clinical promise. Preclinical studies utilizing checkpoint blockade combined with ectoenzyme blockade approach through inhibition of CD39, CD73, PD-1/PDL-1, and the various adenosine receptors may show enhanced antitumor immunity, decreased tumor initiation, and metastasis, but have not yet been evaluated. As a tightly balanced extracellular amount of both adenosine and ATP is needed to maintain an adequate immune response, therapeutic combinations of CD39 with PD1/PDL1 with and without chemotherapy are being studied (123, 124). There are also ongoing clinical trials targeting the Adora2a receptor in combination with CD73 or PDL-1 inhibitors (Table 1) (125–128). Adora2a blockade studies are also ongoing in combination with PD-1, PDL-1, or chemotherapy (11). However, there are no current clinical trials specifically targeting the Adora2b receptor. It is important to consider the complex interactions between purinergic receptors and ATP/ADP/adenosine signaling, because receptor blockade may impact unwanted cell types and promote unintended effects on other receptors (11). For clinical and therapeutic considerations, there is also a need to evaluate the role of the Adora2b receptor in regulating perineural infiltration, fibrosis, and vasculature as the PDAC microenvironment is dynamic and recent studies have shown multiple subtypes of PDAC can co-exist in patients with pancreatic cancer.

TABLE 1 Current clinical trials.

Target	Drug +/- combination therapy	Tumor	Identifier	Study Phase
Adora2a	Ciforadenant (A2A inhibitor) + atezolizumab (PD-L1 inhibitor)	Incurable Cancers	NCT02655822	Phase I/Ib
Adora2a	NIR178 (A2A inhibitor) + PDR001 (anti-PD-1 mAb)	Solid tumors and Non- Hodgkin Lymphoma	NCT03207867	Phase II
CD73 +/- Adora2a	CPI-006 (anti-CD73 mAb) +/- ciforadenant (A2A inhibitor) +/- pembrolizumab (anti-PD1 mAb)	Solid tumors, including PDAC	NCT03454451	Phase I/Ib
CD73 +/- Adora2a	NZV930 (anti-CD73 mAb) +/- PDR001 (anti-PD-1 mAb) +/- NIR178 (A2A inhibitor)	Solid tumors, including PDAC	NCT03549000	Phase I/Ib

Current ongoing clinical trials targeting adenosine receptors for treatment in pancreatic cancer and other tumors.

Challenges to the field

Pancreatic cancer is a particularly challenging field to study, as it is extremely complex, and tumor genetic and histologic heterogeneity is prominent when comparing patient tumor samples. The advent of sequencing human PDAC tumors has revealed PDAC subtypes (129–132) and Squamous and Basal subtypes have been reported to have the highest expression of CD73 (4) indicating they may have more pronounced intratumoral levels of adenosine. One of the challenges to this field is that most studies of adenosine receptor signaling, and interactions are performed in mouse models, which may not translate directly into humans. This limitation, while applicable to most, if not all preclinical studies, makes it difficult to accurately translate therapies targeting adenosine receptors into human patients, as there may be unintended side effects or limitations of small molecule inhibitor activity or delivery not observed in murine models. Another complication to using mouse models is the immense time requirement to breed genetically engineered mice that more accurately represent human PDAC progression. Despite these limitations, more preclinical and clinical studies need to be done to more accurately evaluate the role of adenosine signaling and possible resistance mechanisms to small molecular inhibitors targeting this pathway in cancer as most studies conducted on extracellular purinergic and adenosine signaling have been in diseases other than pancreatic cancer including acute lung disease, acute liver disease, asthma, diabetes, myocardial ischemia, sickle cell disease, and IBD. Another challenge related to the field of use of Adora2b small molecule inhibitors for immunotherapeutic consideration is that few studies have been performed exploring specifically the Adora2b receptor on individual tumor cells, fibroblasts, or immune cell types in the context of the tumor microenvironment. Studies using human or murine organoid cultures and genetic deletion of Adora2b or pharmacologic inhibition will aid in scientific understanding of the mechanistic consequences of Adora2b expression in pancreatic cancer and also help determine if different PDAC subtypes respond differently to Adora2b inhibition. In addition, the role of the gut microbiome or intrapancreatic bacteria or fungi may also elevate adenosine or inosine levels elevating the importance of targeting this pathway for cancer treatment (133, 134). Future studies evaluating the functional consequences of Adora2b receptor signaling in different innate and adaptive immune cell types and interactions are also desperately needed to advance immunotherapies in this field.

Discussion

Pancreatic ductal adenocarcinoma is aggressive, resistant to therapy, and successful treatments are desperately needed, as current options have not yet resulted in significant changes in overall survival. In this review, we discuss literature related to the function of Adora2b, a low-affinity adenosine receptor prominently known for its role in reducing inflammation. The hypoxic TME of PDAC creates a unique niche where CD73, CD39, and Adora2b are elevated resulting in dynamic changes in concentrations of ATP and extracellular adenosine. The ENT1 transporter promotes sensitivity to chemotherapy in PDAC patients and high expression has strong prognostic implications for improved outcomes in PDAC (135). ENT1 is critical for regulating nucleoside concentrations and under hypoxic conditions regulates adenosine receptor signaling (136) indicating another possible combination therapeutic approach, as ENT1 is important for the transport of nucleotides into and out of the cell. Future studies deducing the entire pathway in cancer development and metastasis will aid in determining the utility of targeting this pathway to improve patient outcomes.

Another important consideration is the four P1 adenosine receptors have divergent roles dependent on cell type expression and concentrations of ligands. Of the four receptors, Adora2a and Adora2b have been reported as high in PDAC and are overexpressed in the pancreas during pancreatic cancer; yet only high expression of Adora2b receptor was shown to correlate with significantly reduced survival in PDAC patients. We recently published that patients with high ADORA2B have reduced $CD8^+$ T cells and NK cells indicating inhibiting this receptor may have utility in recruiting activated $CD8^+$ T cells and NKT cells to target PDAC (4). However, these efforts are complicated by the fact that Adora2b is present on virtually all myeloid and lymphoid lineage cells, and activation of the receptor on these cells can alter their functionality and contribute to dynamic changes in immune cell function in the TME. A critical consideration for future trials is understanding patient-specific levels of CD73, Adora2b and ATP, ADP, and adenosine available to signal through P2 or P1 receptors. Adenosine is rapidly taken back into cells and converted to inosine by ADA, which has also been shown to have immunosuppressive consequences in cancer models (133). Thus, understanding the full context of this incredibly complex signaling pathway including Adora2b functionality warrants further consideration and research efforts. Clinical trials where patient samples are available pre and post-treatment are urgently needed to determine if targeting this pathway will improve overall survival. Trials in both the neoadjuvant and adjuvant setting should be conducted due to recent publications showing the Adora2 receptors can promote tumor growth, metastasis and reduce $CD8^+$ T cell anti-tumor immunity predominantly in preclinical models (3, 4, 11, 120, 123–126, 137–144).

Author contributions

LS wrote the original draft. EF, XY, WR, HE, and JB-L edited the manuscript. WR made the Figures and LS made the Table. All authors contributed to the article and approved the submitted version.

Funding

Natural Science Foundation of Hunan Province Grant 2018JJ3736, Young Talent Foundation of Hunan Province Grant 2021RC3034, and 2022 International Anesthesia Research Society Mentored Research Award to WR. National Institute of Health Grants R01HL155950, and Parker B. Francis Fellowship to XY.

National Institute of Health Grants R01HL154720, R01DK122796, R01HL133900, T32GM135118 and Department of Defense Grant W81XWH2110032 to HE; sponsored contract through Akebia Therapeutics, Inc. to HE. JB-L is funded by NIH grants Texas Medical Center Digestive Disease Center Pilot Award 2P30DK056338-16 and 1R21CA249924-01. The funder, Akebia Therapeutics Inc., was not involved in the study design, collection, analysis, interpretation of data, the writing of this article, or the decision to submit it for publication.

Acknowledgments

Figures were created with BioRender and Chemdraw software.

Conflict of interest

The authors declare that the research was conducted in the absence of any commercial or financial relationships that could be construed as a potential conflict of interest.

Publisher's note

References

1. Xiao A, Tan ML, Wu LM, Asrani VM, Windsor JA, Yadav D, et al. Global incidence and mortality of pancreatic diseases: a systematic review, meta-analysis, and meta-regression of population-based cohort studies. *Lancet Gastroenterol Hepatol* (2016) 1:45–55. doi: 10.1016/S2468-1253(16)30004-8

2. Hart PA, Conwell DL. Chronic pancreatitis: managing a difficult disease. *Am J Gastroenterol* (2020) 115:49–55. doi: 10.14309/ajg.0000000000000421

3. Faraoni EY, Strickland LN, O'Brien BJ, Barraza JF, Thosani NC, Wray CJ, et al. Radiofrequency ablation in combination with CD73 inhibitor AB680 reduces tumor growth and enhances anti-tumor immunity in a syngeneic model of pancreatic ductal adenocarcinoma. *Front Oncol* (2022) 12:995027. doi: 10.3389/fonc.2022.995027

4. Faraoni EY, Singh K, Chandra V, Le Roux O, Dai Y, Sahin I, et al. CD73-dependent adenosine signaling through Adora2b drives immunosuppression in ductal pancreatic cancer. *Cancer Res* (2023) 83(7):1111–27. doi: 10.1158/0008-5472.22361356.v1

5. King RJ, Shukla SK, He C, Vernucci E, Thakur R, Attri KS, et al. CD73 induces GM-CSF/MDSC-mediated suppression of T cells to accelerate pancreatic cancer pathogenesis. *Oncogene* (2022) 41(7):971–82. doi: 10.1038/s41388-021-02132-6

6. Jacoberger-Foissac C, Cousineau I, Bareche Y, Allard D, Chrobak P, Allard B, et al. CD73 inhibits cGAS-STING and cooperates with CD39 to promote pancreatic cancer. *Cancer Immunol Res* (2023) 11(1):56–71. doi: 10.1158/2326-6066.CIR-22-0260

7. Campos-Contreras ADR, González-Gallardo A, Díaz-Muñoz M, Vázquez-Cuevas FG. Adenosine receptor A2B negatively regulates cell migration in ovarian carcinoma cells. *Int J Mol Sci* (2022) 23(9):4585. doi: 10.3390/ijms23094585

8. Kitabatake K, Kaji T, Tsukimoto M. Involvement of CD73 and A2B receptor in radiation-induced DNA damage response and cell migration in human glioblastoma A172 cells. *Biol Pharm Bull* (2021) 44(2):197–210. doi: 10.1248/bpb.b20-00654

9. Wilkat M, Bast H, Drees R, Dünser J, Mahr A, Azoitei N, et al. Adenosine receptor 2B activity promotes autonomous growth, migration as well as vascularization of head and neck squamous cell carcinoma cells. *Int J Cancer* (2020) 147(1):202–17. doi: 10.1002/ijc.32835

10. Eltzschig HK. Extracellular adenosine signaling in molecular medicine. *J Mol Med (Berl)* (2013) 91(2):141–6. doi: 10.1007/s00109-013-0999-z

11. Faraoni EY, Ju C, Robson SC, EH K, Bailey-Lundberg JM. Purinergic and adenosinergic signaling in pancreatobiliary diseases. *Front Physiol* (2022) 13:849258. doi: 10.3389/fphys.2022.849258

12. Di Virgilio F, Sarti AC, Falzoni S, De Marchi E, Adinolfi E. Extracellular ATP and P2 purinergic signalling in the tumour microenvironment. *Nat Rev Cancer* (2018) 18:601–18. doi: 10.1038/s41568-018-0037-0

13. Eltzschig HK, Sitkovsky MV, Robson SC. Purinergic signaling during inflammation. *N Engl J Med* (2012) 367(24):2322–33. doi: 10.1056/NEJMra1205750

14. Le TT, Berg NK, Harting MT, Li X, Eltzschig HK, Yuan X. Purinergic signaling in pulmonary inflammation. *Front Immunol* (2019) 10:1633. doi: 10.3389/fimmu.2019.01633

15. Wang W, Chen NY, Ren D, Davies J, Philip K, Eltzschig HK, et al. Enhancing extracellular adenosine levels restores barrier function in acute lung injury through expression of focal adhesion proteins. *Front Mol Biosci* (2021) 8:2021 doi: 10.3389/fmolb.2021.636678

16. Hasko G, Cronstein BN. Adenosine: an endogenous regulator of innate immunity. *Trends Immunol* (2004) 25:33–9. doi: 10.1016/j.it.2003.11.003

17. Idzko M, Ferrari D, Eltzschig HK. Nucleotide signalling during inflammation. *Nature* (2014) 509(7500):310–7. doi: 10.1038/nature13085

18. Colgan SP. Neutrophils and inflammatory resolution in the mucosa. *Semin Immunol* (2015) 27(3):177–83. doi: 10.1016/j.smim.2015.03.007

19. Eltzschig HK, Abdulla P, Hoffman E, Hamilton KE, Daniels D, Schonfeld C, et al. HIF-1-dependent repression of equilibrative nucleoside transporter (ENT) in hypoxia. *J Exp Med* (2005) 202:1493–505. doi: 10.1084/jem.20050177

20. Aherne CM, Collins CB, Rapp CR, Olli KE, Perrenoud L, Jedlicka P, et al. Coordination of ENT2-dependent adenosine transport and signaling dampens mucosal inflammation. *JCI Insight* (2018) 3(20):e121521. doi: 10.1172/jci.insight.121521

21. Wiginton DA, Coleman MS, Hutton JJ. Purification, characterization and radioimmunoassay of adenosine deaminase from human leukaemic granulocytes. *Biochem J* (1981) 195(2):389–97. doi: 10.1042/bj1950389

22. Campbell EL, Bruyninckx WJ, Kelly CJ, Glover LE, McNamee EN, Bowers BE, et al. Transmigrating neutrophils shape the mucosal microenvironment through localized oxygen depletion to influence resolution of inflammation. *Immunity* (2014) 40(1):66–77. doi: 10.1016/j.immuni.2013.11.020

23. Eltzschig HK, Bratton DL, Colgan SP. Targeting hypoxia signalling for the treatment of ischaemic and inflammatory diseases. *Nat Rev Drug Discov* (2014) 13:852–69. doi: 10.1038/nrd4422

24. Semenza GL. The genomics and genetics of oxygen homeostasis. *Annu Rev Genomics Hum Genet* (2020) 21:183–204. doi: 10.1146/annurev-genom-111119-073356

25. Shen Q, Shi X, Tao L, Zhu Q, Xiao W, Ding Y, et al. Inhibition of hypoxia-inducible factor-1α alleviates acinar cell necrosis in a mouse model of acute pancreatitis. *Biochem Biophys Res Commun* (2021) 572:72–9. doi: 10.1016/j.bbrc.2021.07.043

26. Lu Y, Hu J, Sun W, Duan X, Chen X. Hypoxia-mediated immune evasion of pancreatic carcinoma cells. *Mol Med Rep* (2015) 11(5):3666–72. doi: 10.3892/mmr.2015.3144

27. Lee KE, Spata M, Bayne LJ, Buza EL, Durham AC, Allman D, et al. Hif1a deletion reveals pro-neoplastic function of b cells in pancreatic neoplasia. *Cancer Discovery* (2016) 6(3):256–69. doi: 10.1158/2159-8290.CD-15-0822

28. Zhang X, Du P, Luo K, Li Y, Liu Z, Wang W, et al. Hypoxia-inducible factor-1alpha protects the liver against ischemia-reperfusion injury by regulating the A2B adenosine receptor. *Bioengineered* (2021) 12(1):3737–52. doi: 10.1080/21655979.2021.1953217

29. O'Brien BJ, Faraoni EY, Strickland LN, Ma Z, Mota V, Mota S, et al. CD73-generated extracellular adenosine promotes resolution of neutrophil-mediated tissue injury and restrains metaplasia in pancreatitis. *FASEB J* (2023) 37(1):e22684. doi: 10.1096/fj.202201537R

30. Poth JM, Brodsky K, Ehrentraut H, Grenz A, Eltzschig HK. Transcriptional control of adenosine signaling by hypoxia-inducible transcription factors during ischemic or inflammatory disease. *J Mol Med* (2013) 91:183–93. doi: 10.1007/s00109-012-0988-7

31. Kong T, Westerman KA, Faigle M, Eltzschig HK, Colgan SP. HIF-dependent induction of adenosine A2B receptor in hypoxia. *FASEB J* (2006) 20:2242–50. doi: 10.1096/fj.06-6419com

32. Koeppen M, Eckle T, Eltzschig HK. Interplay of hypoxia and A2B adenosine receptors in tissue protection. *Adv Pharmacol* (2011) 61:145–86. doi: 10.1016/B978-0-12-385526-8.00006-0

33. Synnestvedt K, Furuta GT, Comerford KM, Louis N, Karhausen J, Eltzschig HK, et al. Ecto-5′-nucleotidase (CD73) regulation by hypoxia-inducible factor-1 mediates

permeability changes in intestinal epithelia. *J Clin Invest* (2002) 110:993–1002. doi: 10.1172/JCI0215337

34. Hart ML, Gorzolla IC, Schittenhelm J, Robson SC, Eltzschig HK. SP1-dependent induction of CD39 facilitates hepatic ischemic preconditioning. *J Immunol* (2010) 184:4017–24. doi: 10.4049/jimmunol.0901851

35. Mascanfroni ID, Takenaka MC, Yeste A, Patel B, Wu Y, Kenison JE, et al. Metabolic control of type 1 regulatory T cell differentiation by AHR and HIF1-α. *Nat Med* (2015) 21:638–46. doi: 10.1038/nm.3868

36. Morote-Garcia JC, Rosenberger P, Nivillac NM, Coe IR, Eltzschig HK. Hypoxia-inducible factor-dependent repression of equilibrative nucleoside transporter 2 attenuates mucosal inflammation during intestinal hypoxia. *Gastroenterology* (2009) 136:607–18. doi: 10.1053/j.gastro.2008.10.037

37. Yuan X, Mills T, Doursout M, Evans SE, Vidal Melo MF, Eltzschig HK. Alternative adenosine receptor activation: the netrin-Adora2b link. *Front Pharmacol* (2022) 13. doi: 10.3389/fphar.2022.944994

38. Stein E, Zou Y, Poo M, Tessier-Lavigne M. Binding of DCC by netrin-1 to mediate axon guidance independent of adenosine A2B receptor activation. *Science* (2001) 291:1976–82. doi: 10.1126/science.1059391

39. Rosenberger P, Schwab JM, Mirakaj V, Masekowsky E, Mager A, Morote-Garcia JC, et al. Hypoxia-inducible factor-dependent induction of netrin-1 dampens inflammation caused by hypoxia. *Nat Immunol* (2009) 10:195–202. doi: 10.1038/ni.1683

40. Kalhan A, Gharibi B, Vazquez M, Jasani B, Neal J, Kidd M, et al. Adenosine A2A and A2B receptor expression in neuroendocrine tumours: potential targets for therapy. *Purinergic Signal* (2012) 8(2):265–74. doi: 10.1007/s11302-011-9280-5

41. Kong T, Eltzschig HK, Karhausen J, Colgan SP, Shelley CS. Leukocyte adhesion during hypoxia is mediated by HIF-1-dependent induction of beta2 integrin gene expression. *Proc Natl Acad Sci USA* (2004) 101:10440–5. doi: 10.1073/pnas.0401339101

42. Lennon PF, Taylor CT, Stahl GL, Colgan SP. Neutrophil-derived 5 0 -adenosine monophosphate promotes endothelial barrier function *via* CD73-mediated conversion to adenosine and endothelial A2B receptor activation. *J Exp Med* (1998) 188:1433–43. doi: 10.1084/jem.188.8.1433

43. Eltzschig HK, Eckle T, Mager A, Kuper N, Karcher C, Weissmuller T, et al. ATP release from activated neutrophils occurs via connexin 43 and modulates adenosine-dependent endothelial cell function. *Circ Res* (2006) 99:1100–8. doi: 10.1161/01.RES.0000250174.31269.70

44. Cronstein BN. Adenosine, an endogenous anti-inflammatory agent. *J Appl Physiol* (1994) 76:5–13. doi: 10.1152/jappl.1994.76.1.5

45. Eckle T, Faigle M, Grenz A, Laucher S, Thompson LF, Eltzschig HK. A2B adenosine receptor dampens hypoxia-induced vascular leak. *Blood* (2008) 111:2024–35. doi: 10.1182/blood-2007-10-117044

46. Koeppen M ET, Eltzschig HK. Selective deletion of the A1 adenosine receptor abolishes heart-rate slowing effects of intravascular adenosine *in vivo*. *PloS One* (2009) 4:e6784. doi: 10.1371/journal.pone.0006784

47. Eltzschig H. Adenosine: an old drug newly rediscovered. *Anesthesiology* (2009) 111:904–15. doi: 10.1097/ALN.0b013e3181b060f2

48. Hayashi M. Expression of adenosine receptors in rodent pancreas. *Int J Mol Sci* (2019) 20(21):5329. doi: 10.3390/ijms20215329

49. Satoh A, Shimosegawa T, Satoh K, Ito H, Kohno Y, Masamune A, et al. Activation of adenosine A1-receptor pathway induces edema formation in the pancreas of rats. *Gastroenterology* (2000) 119:829–36. doi: 10.1053/gast.2000.16502

50. Lin X, Wang ZY, Xue G, Qin XJ, Wu JF, Zhang G. ADORA1 is a diagnostic-related biomarker and correlated with immune infiltrates in papillary thyroid carcinoma. *J Cancer* (2021) 12(13):3997–4010. doi: 10.7150/jca.50743

51. Liu H, Kuang X, Zhang Y, Ye Y, Li J, Liang L, et al. ADORA1 inhibition promotes tumor immune evasion by regulating the ATF3-PD-L1 axis. *Cancer Cell* (2020) 37(3):324–39.e8. doi: 10.1016/j.ccell.2020.02.006

52. Eltzschig HK, Ibla JC, Furuta GT, Leonard MO, Jacobson KA, Enjyoji K, et al. Coordinated adenine nucleotide phosphohydrolysis and nucleoside signaling in posthy- poxic endothelium: role of ectonucleotidases and adenosine A2B receptors. *J Exp Med* (2003) 198:783–96. doi: 10.1084/jem.20030891

53. Jin X, Shepherd RK, Duling BR, Linden J. Inosine binds to A3 adenosine receptors and stimulates mast cell degranulation. *J Clin Invest* (1997) 100:2849–57. doi: 10.1172/JCI119833

54. Zhong H, Shlykov SG, Molina JG, Sanborn BM, Jacobson MA, Tilley SL, et al. Activation of murine lung mast cells by the adenosine A3 receptor. *J Immunol* (2003) 171:338–45. doi: 10.4049/jimmunol.171.1.338

55. Gorzalczany Y, Akiva E, Klein O, Merimsky O, Sagi-Eisenberg R. Mast cells are directly activated by contact with cancer cells by a mechanism involving autocrine formation of adenosine and autocrine/paracrine signaling of the adenosine A3 receptor. *Cancer Lett* (2017) 397:23–32. doi: 10.1016/j.canlet.2017.03.026

56. Durante M, Squillace S, Lauro F, Giancotti LA, Coppi E, Cherchi F, et al. Adenosine A3 agonists reverse neuropathic pain *via* T cell-mediated production of IL-10. *J Clin Invest* (2021) 131(7):e139299. doi: 10.1172/JCI139299

57. Ren TH, Lv MM, An XM, Leung WK, Seto WK. Activation of adenosine A3 receptor inhibits inflammatory cytokine production in colonic mucosa of patients with ulcerative colitis by down-regulating the nuclear factor-kappa b signaling. *J Dig Dis* (2020) 21(1):38–45. doi: 10.1111/1751-2980.12831

58. Ohta A, Sitkovsky M. Role of G-protein-coupled adenosine receptors in downregulation of inflammation and protection from tissue damage. *Nature* (2001) 414:916–20. doi: 10.1038/414916a

59. Sitkovsky MV, Lukashev D, Apasov S, Kojima H, Koshiba M, Caldwell C, et al. Physiological control of immune response and inflammatory tissue damage by hypoxia- inducible factors and adenosine A2A receptors. *Annu Rev Immunol* (2004) 22:657–82. doi: 10.1146/annurev.immunol.22.012703.104731

60. Ledent C, Vaugeois JM, Schiffmann SN, Pedrazzini T, El Yacoubi M, Vanderhaeghen JJ, et al. Aggressiveness, hypoalgesia and high blood pressure in mice lacking the adenosine A2a receptor. *Nature* (1997) 388:674–8. doi: 10.1038/41771

61. Noji T, Nan-ya K, Mizutani M, Katagiri C, Sano J, Takada C, et al. KF24345, an adenosine uptake inhibitor, ameliorates the severity and mortality of lethal acute pancreatitis via endogenous adenosine in mice. *Eur J Pharmacol* (2002) 454:85–93. doi: 10.1016/S0014-2999(02)02476-7

62. Sweed D, Taha M, Abd Elhamed S, El Dein Mohamed AS. The prognostic role of CD73/A2AR expression and tumor immune response in periampullary carcinoma subtypes. *Asian Pac J Cancer Prev* (2022) 23(4):1239–46. doi: 10.31557/APJCP.2022.23.4.1239

63. Fredholm BB, Irenius E, Kull B, Schulte G. Comparison of the potency of adenosine as an agonist at human adenosine receptors expressed in Chinese hamster ovary cells. *Biochem Pharmacol* (2001) 61(4):443–8. doi: 10.1016/S0006-2952(00)00570-0

64. Feoktistov I, Biaggioni I. Adenosine A2B receptors. *Pharmacol Rev* (1997) 49:381–402.

65. Aherne CM, Kewley EM, Eltzschig HK. The resurgence of A2B adenosine receptor signaling. *Biochim Biophys Acta* (2011) 1808(5):1329–39. doi: 10.1016/j.bbamem.2010.05.016

66. Frick JS, MacManus CF, Scully M, Glover LE, Eltzschig HK, Colgan SP. Contribution of adenosine A2B receptors to inflammatory parameters of experimental colitis. *J Immunol* (2009) 182:4957–64. doi: 10.4049/jimmunol.0801324

67. Eckle T, Hartmann K, Bonney S, Reithel S, Mittelbronn M, Walker LA, et al. Adora2b-elicited Per2 stabilization promotes a HIF-dependent metabolic switch crucial for myocardial adaptation to ischemia. *Nat Med* (2012) 18:774–82. doi: 10.1038/nm.2728

68. Eckle T, Grenz A, Laucher S, Eltzschig HK. A2B adenosine receptor signaling attenuates acute lung injury by enhancing alveolar fluid clearance in mice. *J Clin Invest* (2008) 118(10):3301–15. doi: 10.1172/JCI34203

69. Ehrentraut H, Westrich JA, Eltzschig HK, Clambey ET. Adora2b adenosine receptor engagement enhances regulatory T cell abundance during endotoxin-induced pulmonary inflammation. *PloS One* (2012) 7(2):e32416. doi: 10.1371/journal.pone.0032416

70. Schingnitz U, Hartmann K, Macmanus CF, Eckle T, Zug S, Colgan SP, et al. Signaling through the A2B adenosine receptor dampens endotoxin-induced acute lung injury. *J Immunol* (2010) 184:5271–9. doi: 10.4049/jimmunol.0903035

71. Kolachala VL, Vijay-Kumar M, Dalmasso G, Yang D, Linden J, Wang L, et al. A2B adenosine receptor gene deletion attenuates murine colitis. *Gastroenterology* (2008) 135:861–70. doi: 10.1053/j.gastro.2008.05.049

72. Kolachala V, Ruble B, Vijay-Kumar M, Wang L, Mwangi S, Figler H, et al. Blockade of adenosine A2B receptors ameliorates murine colitis. *Br J Pharmacol* (2008) 155:127–37. doi: 10.1038/bjp.2008.227

73. Vasiukov G, Novitskaya T, Zijlstra A, Owens P, Ye F, Zhao Z, et al. Myeloid cell-derived TGFβ signaling regulates ECM deposition in mammary carcinoma *via* adenosine-dependent mechanisms. *Cancer Res* (2020) 80(12):2628–38. doi: 10.1158/0008-5472.CAN-19-3954

74. Liao J, Zeng DN, Li JZ, Hua QM, Xiao Z, He C, et al. Targeting adenosinergic pathway enhances the anti-tumor efficacy of sorafenib in hepatocellular carcinoma. *Hepatol Int* (2020) 14(1):80–95. doi: 10.1007/s12072-019-10003-2

75. Sui Y, Liu J, Zhang J, Zheng Z, Wang Z, Jia Z, et al. Expression and gene regulation network of adenosine receptor A2B in lung adenocarcinoma: a potential diagnostic and prognostic biomarker. *Front Mol Biosci* (2021) 8:663011. doi: 10.3389/fmolb.2021.663011

76. Xaus J, Valledor AF, Cardó M, Marquès L, Beleta J, Palacios JM, et al. Adenosine inhibits macrophage colony-stimulating factor-dependent proliferation of macrophages through the induction of p27kip-1 expression. *J Immunol* (1999) 163(8):4140–9. doi: 10.4049/jimmunol.163.8.4140

77. Xaus MM J, Lloberas J, Soler C, Lluis C, Franco R. A. celada. IFN-gamma up-regulates the A2B adenosine receptor expression in macrophages: a mechanism of macrophage deactivation. *J Immunol* (1999) 162:3607–14. doi: 10.4049/jimmunol.162.6.3607

78. Murphy PS, Wang J, Bhagwat SP, Munger JC, Janssen WJ, Wright TW, et al. CD73 regulates anti-inflammatory signaling between apoptotic cells and endotoxin-conditioned tissue macrophages. *Cell Death Differ* (2017) 24:559–70. doi: 10.1038/cdd.2016.159

79. Ben Addi A, Lefort A, Hua X, Libert F, Communi D, Ledent C, et al. Modulation of murine dendritic cell function by adenine nucleotides and adenosine: involvement of the A(2B) receptor. *Eur J Immunol* (2008) 38:1610–20. doi: 10.1002/eji.200737781

80. Novitskiy SV, Ryzhov S, Zaynagetdinov R, Goldstein AE, Huang Y, Tikhomirov OY, et al. Adenosine receptors in regulation of dendritic cell differentiation and function. *Blood* (2008) 112:1822–31. doi: 10.1182/blood-2008-02-136325

81. Victorino F, Sojka DK, Brodsky KS, McNamee EN, Masterson JC, Homann D, et al. Tissue-resident NK cells mediate ischemic kidney injury and are not depleted by anti-asialo-GM1 antibody. *J Immunol* (2015) 195:4973–85. doi: 10.4049/jimmunol.1500651

82. Bastid J, Regairaz A, Bonnefoy N, Déjou C, Giustiniani J, Laheurte C, et al. Inhibition of CD39 enzymatic function at the surface of tumor cells alleviates their immunosuppressive activity. *Cancer Immunol Res* (2015) 3(3):254–65. doi: 10.1158/2326-6066.CIR-14-0018

83. Raskovalova T, Huang X, Sitkovsky M, Zacharia LC, Jackson EK, Gorelik E. Gs protein-coupled adenosine receptor signaling and lytic function of activated NK cells. *J Immunol* (2005) 174:4383–91. doi: 10.4049/jimmunol.175.7.4383

84. Liu X, Li L, Si F, Huang L, Zhao Y, Zhang C, et al. NK and NKT cells have distinct properties and functions in cancer. *Oncogene* (2021) 40:4521–37. doi: 10.1038/s41388-021-01880-9

85. Chen Q, Pu N, Yin H, Zhang J, Zhao G, Lou W, et al. CD73 acts as a prognostic biomarker and promotes progression and immune escape in pancreatic cancer. *J Cell Mol Med* (2020) 24:8674–86. doi: 10.1111/jcmm.15500

86. Chen M, Liang D, Zuo A, Shao H, Kaplan HJ, Sun D. An A2B adenosine receptor agonist promotes Th17 autoimmune responses in experimental autoimmune uveitis (EAU) *via* dendritic cell activation. *PloS One* (2015) 10(7):e0132348. doi: 10.1371/journal.pone.0132348

87. Burnstock G, Boeynaems J. Purinergic signalling and immune cells. *Purinergic Signalling* (2014) 10:529–64. doi: 10.1007/s11302-014-9427-2

88. Mirabet M, Herrera C, Cordero OJ, Mallol J, Lluis C, Franco R. Expression of A2B adenosine receptors in human lymphocytes: their role in T cell activation. *J Cell Sci* (1999) 112:491–502. doi: 10.1242/jcs.112.4.491

89. Leung PS. Physiology of the pancreas. *Adv Exp Med Biol* (2010) 690:13–27. doi: 10.1007/978-90-481-9060-7_2

90. Grapin-Botton A. Ductal cells of the pancreas. *Int J Biochem Cell Biol* (2005) 37 (3):504–10. doi: 10.1016/j.biocel.2004.07.010

91. Sorensen CE, Novak I. Visualization of ATP release in pancreatic acini in response to cholinergic stimulus. use of fluorescent probes and confocal microscopy. *J Biol Chem* (2001) 276(35):32925–32. doi: 10.1074/jbc.M103313200

92. Novak I, Nitschke R, Amstrup J. Purinergic receptors have different effects in rat exocrine pancreas. calcium signals monitored by fura-2 using confocal microscopy. *Cell Physiol Biochem* (2002) 12(2-3):83–92. doi: 10.1159/000063784

93. Novak I. Purinergic signalling in epithelial ion transport: regulation of secretion and absorption. *Acta Physiol (Oxf)* (2011) 202(3):501–22. doi: 10.1111/j.1748-1716.2010.02225.x

94. Yegutkin GG, Samburski SS, Jalkanen S, Novak I. ATP-consuming and ATP-generating enzymes secreted by pancreas. *J Biol Chem* (2006) 281(40):29441–7. doi: 10.1074/jbc.M602480200

95. Burnstock G, Novak I. Purinergic signalling in the pancreas in health and disease. *J Endocrinology* (2012) 213(2):123–41. doi: 10.1530/JOE-11-0434

96. Ewald N, Bretzel RG. Diabetes mellitus secondary to pancreatic diseases (Type 3c)–are we neglecting an important disease? *Eur J Intern Med* (2013) 24(3):203–6. doi: 10.1016/j.ejim.2012.12.017

97. Novak I. Purinergic receptors in the endocrine and exocrine pancreas. *Purinergic Signalling* (2008) 4:237–53. doi: 10.1007/s11302-007-9087-6

98. Hansen MR, Krabbe S, Novak I. Purinergic receptors and calcium signalling in human pancreatic duct cell lines. *Cell Physiol Biochem* (2008) 22(1-4):157–68. doi: 10.1159/000149793

99. Sendler M, Weiss FU, Golchert J, Homuth G, van den Brandt C, Mahajan UM, et al. Cathepsin b-mediated activation of trypsinogen in endocytosing macrophages increases severity of pancreatitis in mice. *Gastroenterology* (2018) 154:704.e10–18.e10. doi: 10.1053/j.gastro.2017.10.018

100. Mayerle J, Sendler M, Hegyi E, Beyer G, Lerch MM, Sahin-Tóth M. Genetics, cell biology, and pathophysiology of pancreatitis. *Gastroenterology* (2019) 156:1951.e1–68.e1. doi: 10.1053/j.gastro.2018.11.081

101. Saluja A, Dudeja V, Dawra R, Sah RP. Early intra-acinar events in pathogenesis of pancreatitis. *Gastroenterology* (2019) 156:1937–40. doi: 10.1053/j.gastro.2019.03.050

102. Wang X, Liu D, Qin W, Liu Y, Yuan X, Zhang X, et al. P2RX1-involved glycolytic metabolism supports neutrophil activation in acute pancreatitis. *Front Immunol* (2020) 11:549179. doi: 10.3389/fimmu.2020.549179

103. Ma Z, Lytle NK, Chen B, Jyotsana N, Novak SW, Cho CJ, et al. Single-cell transcriptomics reveals a conserved metaplasia program in pancreatic injury. *Gastroenterology* (2021) 162(2):604–20.e20. doi: 10.1101/2021.04.09.439243

104. Barletta KE, Cagnina RE, Burdick MD, Linden J, Mehrad B. Adenosine A(2B) receptor deficiency promotes host defenses against gram-negative bacterial pneumonia. *Am J Respir Crit Care Med* (2012) 186(10):1044–50. doi: 10.1164/rccm.201204-0622OC

105. Wang X, Chen D. Purinergic regulation of neutrophil function. *Front Immunol* (2018) 9:399. doi: 10.3389/fimmu.2018.00399

106. Künzli BM, Nuhn P, Enjyoji K, Banz Y, Smith RN, Csizmadia E, et al. Disordered pancreatic inflammatory responses and inhibition of fibrosis in CD39-null mice. *Gastroenterology* (2008) 134:292–305. doi: 10.1053/j.gastro.2007.10.030

107. Shevchenko I, Mathes A, Groth C, Karakhanova S, Müller V, Utikal J, et al. Enhanced expression of CD39 and CD73 on T cells in the regulation of anti-tumor immune responses. *Oncoimmunology* (2020) 9(1):1744946. doi: 10.1080/2162402X.2020.1744946

108. Greten FR, Grivennikov SI. Inflammation and cancer: triggers, mechanisms, and consequences. *Immunity* (2019) 51(1):27–41. doi: 10.1016/j.immuni.2019.06.025

109. Mittal D, Sinha D, Barkauskas D, Young A, Kalimutho M, Stannard K, et al. Adenosine 2B receptor expression on cancer cells promotes metastasis. *Cancer Res* (2016) 76(15):4372–82. doi: 10.1158/0008-5472.CAN-16-0544

110. Wang H, Tan F, Xu Y, Ma Y, Li Y, Xiao H. Adenosine receptor A2B antagonist inhibits the metastasis of gastric cancer cells and enhances the efficacy of cisplatin. *Technol Cancer Res Treat* (2023) 22:15330338221150318. doi: 10.1177/15330338221150318

111. Casamitjana J, Espinet E, Rovira M. Pancreatic organoids for regenerative medicine and cancer research. *Front Cell Dev Biol* (2022) 10:886153. doi: 10.3389/fcell.2022.886153

112. Driehuis E, van Hoeck A, Moore K, Kolders S, Francies HE, Gulersonmez MC, et al. Pancreatic cancer organoids recapitulate disease and allow personalized drug screening. *Proc Natl Acad Sci USA* (2019) 116(52):26580–90. doi: 10.1073/pnas.1911273116

113. Boj SF, Hwang CI, Baker LA, Chio II, Engle DD, Corbo V, et al. Organoid models of human and mouse ductal pancreatic cancer. *Cell* (2015) 160(1-2):324–38. doi: 10.1016/j.cell.2014.12.021

114. Ponz-Sarvise M, Corbo V, Tiriac H, Engle DD, Frese KK, Oni TE, et al. Identification of resistance pathways specific to malignancy using organoid models of pancreatic cancer. *Clin Cancer Res* (2019) 25(22):6742–55. doi: 10.1158/1078-0432.CCR-19-1398

115. Andrews MG, Kriegstein AR. Challenges of organoid research. *Annu Rev Neurosci* (2022) 45:23–39. doi: 10.1146/annurev-neuro-111020-090812

116. di Magliano MP, Logsdon CD. Roles for KRAS in pancreatic tumor development and progression. *Gastroenterology* (2013) 144(6):1220–9. doi: 10.1053/j.gastro.2013.01.071

117. Hingorani SR, Wang L, Multani AS, Combs C, Deramaudt TB, Hruban RH, et al. Trp53R172H and KrasG12D cooperate to promote chromosomal instability and widely metastatic pancreatic ductal adenocarcinoma in mice. *Cancer Cell* (2005) 7 (5):469–83. doi: 10.1016/j.ccr.2005.04.023

118. Westphalen CB, Olive KP. Genetically engineered mouse models of pancreatic cancer. *Cancer J* (2012) 18(6):502–10. doi: 10.1097/PPO.0b013e31827ab4c4

119. Ingwersen J, Wingerath B, Graf J, Lepka K, Hofrichter M, Schröter F, et al. Dual roles of the adenosine A2a receptor in autoimmune neuroinflammation. *J Neuroinflammation* (2016) 13:48. doi: 10.1186/s12974-016-0512-z

120. Ohta A, Gorelik E, Prasad SJ, Ronchese F, Lukashev D, Wong MK, et al. A2A adenosine receptor protects tumors from antitumor T cells. *Proc Natl Acad Sci USA* (2006) 103(35):13132–7. doi: 10.1073/pnas.0605251103

121. Yachida S, Jones S, Bozic I, Antal T, Leary R, Fu B, et al. Distant metastasis occurs late during the genetic evolution of pancreatic cancer. *Nature* (2010) 467:1114–7. doi: 10.1038/nature09515

122. Carpenter ES, Elhossiny AM, Kadiyala P, Li J, McGue J, Griffith BD, et al. Analysis of donor pancreata defines the transcriptomic signature and microenvironment of early neoplastic lesions. *Cancer Discov* (2023). doi: 10.1158/2159-8290.CD-23-0013

123. Young A, Ngiow SF, Barkauskas DS, Sult E, Hay C, Blake SJ, et al. Co-Inhibition of CD73 and A2AR adenosine signaling improves anti-tumor immune responses. *Cancer Cell* (2016) 30(3):391–403. doi: 10.1016/j.ccell.2016.06.025

124. Moesta AK, Li XY, Smyth MJ. Targeting CD39 in cancer. *Nat Rev Immunol* (2020) 20(12):739–55. doi: 10.1038/s41577-020-0376-4

125. Hay CM, Sult E, Huang Q, Mulgrew K, Fuhrmann SR, McGlinchey KA, et al. Targeting CD73 in the tumor microenvironment with MEDI9447. *Oncoimmunology* (2016) 5(8):e1208875. doi: 10.1080/2162402X.2016.1208875

126. Beavis PA, Milenkovski N, Henderson MA, John LB, Allard B, Loi S, et al. Adenosine receptor 2A blockade increases the efficacy of anti-PD-1 through enhanced antitumor T-cell responses. *Cancer Immunol Res* (2015) 3(5):506–17. doi: 10.1158/2326-6066.CIR-14-0211

127. Mittal D, Young A, Stannard K, Yong M, Teng MW, Allard B, et al. Antimetastatic effects of blocking PD-1 and the adenosine A2A receptor. *Cancer Res* (2014) 74:3652–8. doi: 10.1158/0008-5472.CAN-14-0957

128. Allard B, Pommey S, Smyth MJ, Stagg J. Targeting CD73 enhances the antitumor activity of anti-PD-1 and anti-CTLA-4 mAbs. *J Clin Cancer Res* (2013) 19:5626–35. doi: 10.1158/1078-0432.CCR-13-0545

129. Collisson EA, Maitra A. Pancreatic cancer genomics 2. *0: Profiling Metastases Cancer Cell* (2017) 31(3):309–10. doi: 10.1016/j.ccell.2017.02.014

130. Collisson EA, Sadanandam A, Olson P, Gibb WJ, Truitt M, Gu S, et al. Subtypes of pancreatic ductal adenocarcinoma and their differing responses to therapy. *Nat Med* (2011) 17(4):500–3. doi: 10.1038/nm.2344

131. Bailey P, Chang DK, Nones K, Johns AL, Patch AM, Gingras MC, et al. Genomic analyses identify molecular subtypes of pancreatic cancer. *Nature* (2016) 531 (7592):47–52. doi: 10.1038/nature16965

132. Collisson EA, Bailey P, Chang DK, Biankin AV. Molecular subtypes of pancreatic cancer. *Nat Rev Gastroenterol Hepatol* (2019) 16(4):207–20. doi: 10.1038/s41575-019-0109-y

133. Mager LF, Burkhard R, Pett N, Cooke NCA, Brown K, Ramay H, et al. Microbiome-derived inosine modulates response to checkpoint inhibitor immunotherapy. *Science* (2020) 369(6510):1481–9. doi: 10.1126/science.abc3421

134. He B, Hoang TK, Wang T, Ferris M, Taylor CM, Tian X, et al. Resetting microbiota by lactobacillus reuteri inhibits T reg deficiency-induced autoimmunity *via* adenosine A2A receptors. *J Exp Med* (2017) 214(1):107–23. doi: 10.1084/jem.20160961

135. Farrell JJ, Elsaleh H, Garcia M, Lai R, Ammar A, Regine WF, et al. Human equilibrative nucleoside transporter 1 levels predict response to gemcitabine in patients with pancreatic cancer. *Gastroenterology* (2009) 136(1):187–95. doi: 10.1053/j.gastro.2008.09.067

136. Rose JB, Naydenova Z, Bang A, Ramadan A, Klawitter J, Schram K, et al. Absence of equilibrative nucleoside transporter 1 in ENT1 knockout mice leads to altered nucleoside levels following hypoxic challenge. *Life Sci* (2011) 89(17-18):621–30. doi: 10.1016/j.lfs.2011.08.007

137. Boison D, Yegutkin GG. Adenosine metabolism: emerging concepts for cancer therapy. *Cancer Cell* (2019) 36(6):582–96. doi: 10.1016/j.ccell.2019.10.007

138. Wang J, Lupo KB, Chambers AM, Matosevic S. Purinergic targeting enhances immunotherapy of CD73. *J Immunother Cancer* (2018) 6(1):136. doi: 10.1186/s40425-018-0441-8

139. Sek K, Mølck C, Stewart GD, Kats L, Darcy PK, Beavis PA. Targeting adenosine receptor signaling in cancer immunotherapy. *Int J Mol Sci* (2018) 19(12):3837. doi: 10.3390/ijms19123837

140. Ma SR, Deng WW, Liu JF, Mao L, Yu GT, Bu LL, et al. Blockade of adenosine A2A receptor enhances CD8+ T cells response and decreases regulatory T cells in head and neck squamous cell carcinoma. *Mol Cancer* (2017) 16(1):99. doi: 10.1186/s12943-017-0665-0

141. Allard B, Longhi MS, Robson SC, Stagg J. The ectonucleotidases CD39 and CD73: novel checkpoint inhibitor targets. *Immunol Rev* (2017) 276(1):121–44. doi: 10.1111/imr.12528

142. Allard D, Allard B, Gaudreau PO, Chrobak P, Stagg J. CD73-adenosine: a next-generation target in immuno-oncology. *Immunotherapy* (2016) 8(2):145–63. doi: 10.2217/imt.15.106

143. Leone RD, Lo YC, Powell JD. A2aR antagonists: next generation checkpoint blockade for cancer immunotherapy. *Comput Struct Biotechnol J* (2015) 13:265–72. doi: 10.1016/j.csbj.2015.03.008

144. Beavis PA, Divisekera U, Paget C, Chow MT, John LB, Devaud C, et al. Blockade of A2A receptors potently suppresses the metastasis of CD73+ tumors. *Proc Natl Acad Sci USA* (2013) 110(36):14711–6. doi: 10.1073/pnas.1308209110

frontiers | Frontiers in Oncology

TYPE Original Research
PUBLISHED 13 July 2023
DOI 10.3389/fonc.2023.1165257

OPEN ACCESS

EDITED BY
Luca Antonioli,
University of Pisa, Italy

REVIEWED BY
Todd Triplett,
Texas Tech University Health Sciences Center, United States
Bo Hu,
Zhejiang Chinese Medical University, China

*CORRESPONDENCE
Neslihan Cabioglu
neslicab@yahoo.com

RECEIVED 13 February 2023
ACCEPTED 22 June 2023
PUBLISHED 13 July 2023

CITATION
Cabioglu N, Bayram A, Emiroglu S, Onder S, Karatay H, Oner G, Tukenmez M, Muslumanoglu M, Igci A, Aydiner A, Saip P, Yavuz E and Ozmen V (2023) Diverging prognostic effects of CD155 and CD73 expressions in locally advanced triple-negative breast cancer.
Front. Oncol. 13:1165257.
doi: 10.3389/fonc.2023.1165257

Diverging prognostic effects of CD155 and CD73 expressions in locally advanced triple-negative breast cancer

Neslihan Cabioglu[1]*, Aysel Bayram[2], Selman Emiroglu[1], Semen Onder[2], Huseyin Karatay[2,3], Gizem Oner[1,4,5], Mustafa Tukenmez[1], Mahmut Muslumanoglu[1], Abdullah Igci[1,6], Adnan Aydiner[7], Pinar Saip[7], Ekrem Yavuz[2] and Vahit Ozmen[1,8]

[1]Department of General Surgery, Istanbul Faculty of Medicine, Istanbul University, Istanbul, Türkiye, [2]Department of Pathology, Istanbul Faculty of Medicine, Istanbul University, Istanbul, Türkiye, [3]Department of Pathology, Basaksehir Cam Sakura Hospital, Istanbul, Türkiye, [4]Multidisciplinary Oncologic Centre Antwerp (MOCA), Antwerp University Hospital, Edegem, Belgium, [5]Center for Oncological Research (CORE), University of Antwerp, Antwerp, Belgium, [6]Department of General Surgery, American Hospital, Istanbul, Türkiye, [7]Department of Medical Oncology, Institute of Oncology, Istanbul University, Istanbul, Türkiye, [8]Department of General Surgery, Istanbul Florence Nightingale Hospital, Istanbul, Türkiye

Background: Immune checkpoint inhibition, combined with novel biomarkers, may provide alternative pathways for treating chemotherapy-resistant triple-negative breast cancer (TNBC). This study investigates the expression of new immune checkpoint receptors, including CD155 and CD73, which play a role in T and natural killer (NK) cell activities, in patients with residual TNBC after neoadjuvant chemotherapy (NAC).

Methods: The expression of biomarkers was immunohistochemically examined by staining archival tissue from surgical specimens (n = 53) using specific monoclonal antibodies for PD-L1, CD155, and CD73.

Results: Of those, 59.2% (29/49) were found to be positive (>1%) for PD-L1 on the tumour and tumour-infiltrating lymphocytes (TILs), while CD155 (30/53, 56.6%) and CD73 (24/53, 45.3%) were detected on tumours. Tumour expressions of CD155 and CD73 significantly correlated with PD-L1 expression on the tumour (p = 0.004 for CD155, p = 0.001 for CD73). Patients with CD155 positivity ≥10% were more likely to have a poor chemotherapy response, as evidenced by higher MDACC Residual Cancer Burden Index scores and Class II/III than those without CD155 expression (100% vs 82.6%, p = 0.03). At a median follow-up time of 80 months (range, 24–239), patients with high CD73 expression showed improved 10-year disease-free survival (DFS) and disease-specific survival (DSS) rates compared to those with low CD73 expression. In contrast, patients with CD155 (≥10%) expression exhibited a decreasing trend in 10-year DFS and DSS compared to cases with lower expression, although statistical significance was not reached. However, patients with coexpression of CD155 (≥10%) and low CD73 were significantly more likely to have decreased 10-year DFS and DSS rates compared to others (p = 0.005).

Conclusion: These results demonstrate high expression of CD73 and CD155 in patients with residual tumours following NAC. CD155 expression was associated with a poor response to NAC and poor prognosis in this chemotherapy-resistant TNBC cohort, supporting the use of additional immune checkpoint receptor inhibitor therapy. Interestingly, the interaction between CD155 and CD73 at lower levels resulted in a worse outcome than either marker alone, which calls for further investigation in future studies.

KEYWORDS

CD155, CD73, chemotherapy response, prognosis, triple-negative breast cancer

Introduction

Triple-negative breast cancer (TNBC) is the most aggressive subtype, accounting for approximately 15–20% of all breast cancer cases (1). Recent studies in TNBC have indicated that high levels of stromal tumour-infiltrating lymphocytes (TILs) can serve as prognostic markers and may also predict patients' responses to chemotherapy (2, 3). Clinical trials have demonstrated some efficacy of targeted therapy against programmed death ligand 1 (PD-L1)/programmed cell death 1 (PD-1) and have shown improved survival outcomes for TNBC patients (4–6). Consequently, the existing literature emphasizes the need for new immunotherapeutic approaches for TNBC. CD155 (7–10) and CD73 (11–14) are targetable molecules that could modulate the anti-tumour immune response and serve as potential promising prognostic biomarkers for clinical outcomes in breast cancer.

T cell immunoglobulin and ITIM domain (TIGIT) is a member of the CD28 protein family and has emerged as a new target for immunotherapy (15–19). It is predominantly expressed on T and natural killer (NK) cells and inhibits their anti-tumour activities. In the tumour microenvironment, T cells often co-express TIGIT along with other immune checkpoint receptors, such as PD-1 (20). CD155, a type I transmembrane glycoprotein, belongs to the immunoglobulin superfamily and serves as one of the ligands for TIGIT alongside low affinity nectin-2/CD112 and nectin-3/CD113 (21). Originally identified as a poliovirus receptor (PVR), CD155 is involved in various physiological processes, including cell proliferation, adhesion, and potentially tumour invasion and migration (22–25). CD155 is highly expressed on endothelial cells, dendritic cells, and fibroblasts, and its overexpression has been observed in several cancer types, such as lung adenocarcinoma, colorectal cancer, pancreatic cancer, cutaneous melanoma, and hepatocellular carcinoma (26–30). Notably, CD155 interacts with regulatory receptors CD96 and CD226 expressed on NK cells, CD4+ T cells, and monocytes. The CD155-CD226 interaction stimulates the cytotoxicity of NK cells and T cell response, while the CD155-CD96 interaction inhibits NK cell function (31). Any imbalance in this interaction may result in tumour immunosuppression (23). Given its role as an immune checkpoint protein, CD155 represents a potential target for novel anti-tumour immunotherapy in TNBC, with its overexpression serving as an indicator of poor prognosis (7).

CD73 is a GPI-anchored ecto-nucleotidase that is crucial in limiting the breakdown of extracellular ATP to adenosine (32, 33). Adenosine acts as an immunosuppressive molecule, inhibiting the activity of CD8+ T cells and NK cells while promoting the proliferation of immunosuppressive cells (34, 35). Within the tumour microenvironment, adenosine levels increase, leading to a reduction in the anti-tumour immune response by promoting the stabilization of immunosuppressive regulatory cells and suppressing the functions of effector cells (36). Thus, the CD73-adenosine pathway contributes to creating an immunosuppressive microenvironment in various tumours (37). Overexpression of CD73 has been observed in infiltrating immune cells and stromal tumour cells (38). Moreover, CD73 is upregulated on regulatory T cells in response to adenosine signalling and hypoxia (38–40). Recent studies have shown that CD73 expression may be a better predictor of neoadjuvant chemotherapy (NAC) response than TILs in TNBC (13).

The significance of CD155 and CD73 expressions on tumours in TNBC remains controversial. Additionally, the potential interaction between CD155 and CD73 is unknown, considering the complex immunoregulatory mechanisms involving TIGIT and CD155 and adenosine and CD73 in modulating T and NK cell responses. Therefore, this study aims to investigate the immunohistochemical expressions of CD155 and CD73, along with PD-L1 expression, and to analyze the associations between their expression levels, response to chemotherapy, and prognosis in TNBC patients.

Materials and methods

Between September 2000 and May 2017, consecutive patients with TNBC diagnosed with locally advanced breast cancer, who underwent breast surgery at the Istanbul University, Istanbul Faculty of Medicine, Department of General Surgery, Breast Surgery Service after completing NAC, were included in the study. Patients with a pathologic complete response, male breast cancer, pregnancy-associated breast cancer, bilateral breast cancer, and distant metastases were excluded from the analysis. Patient and tumour characteristics were analyzed to evaluate the clinicopathological factors and outcomes in the study group. The American Joint

Committee on Cancer Staging System 8th edition was used in clinical and pathological evaluation of patients (41). Ethical committee approval was obtained from the Istanbul University, Istanbul Faculty of Medicine.

Immunohistochemical evaluation and scoring

Patients with TNBC were identified based on their previous pathology reports of the surgical specimen. All patients had negative estrogen and progesterone receptors and c-erb-B2 expressions, which were examined using immunochemistry (IHC). Immunological markers were retrospectively studied in archival tissue material of surgical specimens (n = 53) using immunohistochemistry. Tumour paraffin block sections containing TILs were chosen for immunostaining.

Immunohistochemical expressions of PD-L1, CD-73, and CD155 were detected using an automatic Ventana BenchMark slide staining device (Ventana Medical Systems, Tucson, AZ, USA). The 5-µm formalin-fixed paraffin-embedded sections were incubated with specific primary antibodies, including anti-CD73 rabbit mAb (D7F9A, Cell Signaling) at a 1:200 dilution, and anti-CD155 rabbit mAb (D8A5G, Cell Signaling) at a 1:200 dilution. PD-L1 expression was detected using the "rabbit monoclonal antibody, Ventana SP263 Clone kit" (Ventana Medical Systems, Tucson, AZ, USA). Placenta tissue was used as a control sample.

The staining percentage and intensity of tumour cells and TILs were recorded for each immune checkpoint receptor. The staining intensity was categorized as follows: no staining, weakly stained, moderately stained, or strongly stained. All immune checkpoint receptors, including PD-L1, CD73, and CD155, exhibited a membranous staining pattern. PD-L1 positivity was defined as membranous staining >1% on either tumour or TILs, or both, as previously described (42). Various staining percentages ranging from 1% to 20% (>1%, >5%, >10%, >20%), determined based on the median values for each biomarker, along with or without staining intensity, were tested to investigate significant associations with prognosis for CD73 and CD155. Furthermore, an expression score for CD73 and CD155 was calculated for each patient using the formula "staining intensity × percentage of positive cells" to evaluate its significance for the outcome. Stained tumour cells and TILs were assessed under a light microscope (Olympus BX51, Japan) at 40× magnification, equipped with an integrated digital camera (Olympus DP71, Japan).

The "MD Anderson Cancer Center Residual Cancer Burden Index" was calculated to assess the response to NAC based on the following residual tumour characteristics: a) The two largest dimensions of the residual tumour bed (including the largest tumour bed in multicentric cases), b) The histologic assessment of the percentage of the tumour bed area containing carcinoma, c) The histologic estimate of the percentage of carcinoma in the tumour bed that is *in-situ*, d) The number of metastatic lymph nodes, and e) The diameter of the largest lymph node metastasis. The "RCB" index was estimated using the MD Anderson Residual Cancer Calculator (www3.mdanderson.org/app/medcalc/index.cfm?pagename=jsconvert3) by incorporating these parameters. The residual cancer classification was determined based on this scoring system. A chemotherapy response was considered good if classified as Class 0 (pathologic complete response) or Class 1, and not as good if classified as Class 2 or 3 (chemotherapy resistant)

Statistical analysis

The study's statistical analysis was conducted using the SPSS 17 software program (Statistical Package for Social Sciences; SPSS, Inc, Chicago, IL). Categorical variables were assessed using the Pearson Chi-Square, Fisher's exact, or Continuity Correction tests. Differences between continuous variables were evaluated using the Mann-Whitney U test. The Spearman correlation test examined the expression associations between continuous variables, including the percentages of CD155, CD73, and PD-L1. Disease-free survival (DFS) rates were analyzed, considering locoregional and distant recurrences, while disease-specific survival (DSS) rates were analyzed considering breast cancer-associated mortality. Kaplan-Meier analyses were performed to calculate DFS and DSS rates and construct survival curves. The log-rank test was used to compare factors influencing the outcome. A p-value less than 0.05 was considered statistically significant.

Results

Of the 53 patients diagnosed with locally advanced TNBC, the mean age was 50 ± 13.3 (95% confidence interval (CI); 46.2–53.5), whereas the median age was 47 years (range, 24–76 years). Among them, 29 patients were clinically (= c) T3–4 (54.6%), while almost all of them had cN1-3 (96.2%) before NAC. All patients received NAC, including anthracyclines, followed by taxanes. Following completion of NAC, most patients (n = 39, 73.6%) underwent mastectomy and axillary dissection (n = 46, 86.8%). Breast-conserving surgery was performed in the remaining patients, and seven cases had only sentinel lymph node biopsy due to negative intraoperative pathological evaluation of the lymph nodes. In the definitive pathology evaluation of the surgical specimens, 16 cases (30.2%) showed axillary pathologic complete response (ypN0), while all patients had residual invasive cancer in the breast specimen. Histopathological examination revealed 43 tumours with invasive ductal carcinoma (81.1%), three tumours with invasive lobular carcinoma (5.7%), one tumour with mixed invasive ductal and lobular carcinoma (1.9%), and six tumours with metaplastic carcinoma (11.3%). The mean "MD Anderson Cancer Center Residual Cancer Burden Index" was 3.17 ± 1.2 (95%CI, 2.8–3.5).

Staining patterns and associations with clinicopathological characteristics

The mean values of PD-L1 expressions on tumours and TILs, as well as the expressions of CD73 and CD155 on the tumour (%), along with the CD73 and CD155 scores, are shown in Table 1.

TABLE 1 Immune check point expression levels.

Immune checkpoint receptor expression	Mean ± SD (95% Confidence Interval)
CD73 (%)	4.79 ± 8.22 (2.53-7.06)
CD73 score	8.17 ± 2.29 (3.59-12.76)
CD155 (%)	19.06 ± 3.05 (12.93-25.18)
CD155 score	28.11 ± 5.20 (17.67-38.55)
PD-L1$_{Tumour}$ (%)	5.33 ± 8.31 (2.94-7.71)
PD-L1$_{TIL}$ (%)	5.84 ± 9.12 (3.22-8.47)

Tumour expressions of CD155 and CD73 were found to have a significant correlation with PD-L1$_{tumors}$ (for CD73, r = 0.294, p = 0.040; and for CD155, r = 0.363, p = 0.010; Figure 1). However, the associations with PD-L1$_{TILs}$ expressions did not reach statistical significance (for CD73, r = 0.274, p = 0.057; and for CD155, r = 0.233, p = 0.108).

PD-L1 expression was observed on tumours or TILs in 29 cases (59.2%, Figure 2A). Additionally, tumoural staining for CD73 was observed in 24 patients (45.3%, Figure 2B), while 30 patients exhibited tumoural CD155 expression (56.6%, Figure 2C).

Low CD73 expression was considered if the tumour cells were weakly stained <20%. High CD73 expression was considered if the tumour cells were weakly stained ≥20% or any moderately/strongly staining. Patients with high CD73 expression (n = 11, 20.8%) were observed to have a higher likelihood of achieving an axillary pathologic complete response compared to those with low CD73 expression (54.6% vs 23.8%, p = 0.068); however, this difference did not reach statistical significance. In contrast, patients expressing CD155 were more likely to exhibit a poor chemotherapy response, as indicated by higher MD Anderson Cancer Center Residual Cancer Burden Index scores and Class II/III, compared to those without CD155 expression (100% vs 82.6%, p = 0.03; Table 2). Nevertheless, no significant associations were found between CD73 and CD155 expressions and other clinicopathological characteristics. Furthermore, no significant associations could be found in CD73 high-expression (n=11) among patients with CD155 ≥10% vs CD155 <10% expression (5/30, 16.7% vs 6/23, 26.1%, p=0.501, respectively). Patients with CD155 ≥10% were more likely to exhibit PD-L1$_{total}$ positivity compared to others (21/30, 70% vs. 8/19, 42.1%, p = 0.05, respectively). Similarly, patients with high CD73 expression were more likely to have PD-L1$_{total}$ positivity than those with low CD73 expression (9/10, 90% vs 20/39, 51.3%, p = 0.034, respectively).

Outcome

The median follow-up time was 80 months (range, 24–239 months). In univariate survival analyses (Figure 3), patients with

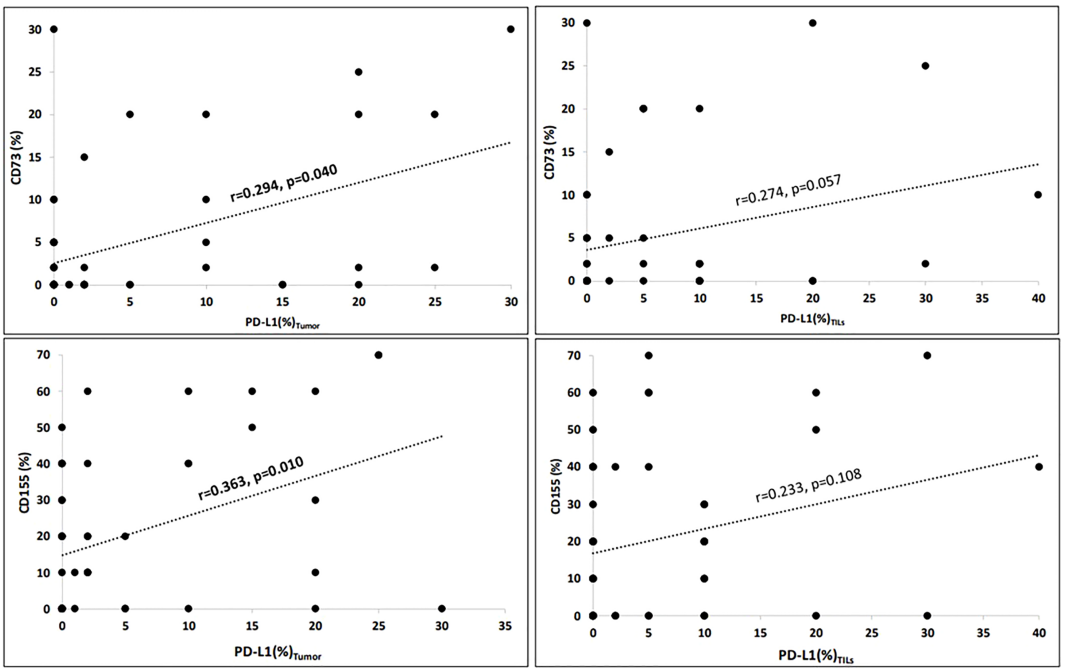

FIGURE 1
Correlations of immuncheckpoint receptors (Spearman's rho). Tumour expressions of CD155 (%) and CD73 (%) significantly correlated with PD-L1$_{tumour}$ (for CD73, r = 0.294, p = 0.040 and for CD155, r = 0.363, p = 0.010). However, the associations with PD-L1$_{TILs}$ expressions did not reach the statistical significance (for CD73, r = 0.274, p = 0.057 and for CD155, r = 0.233, p = 0.108). Correlation is significant at the 0.05 level (2-tailed).

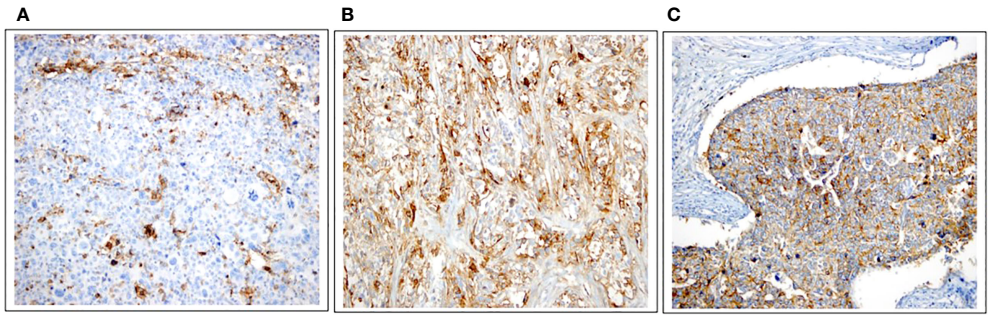

FIGURE 2
Immunohistochemical expressions of PD-L1, CD73, and CD155. **(A)** PD-L1 expression in the tumour with 25% strongly stained, in intratumoral lymphocytes with 5% -moderately stained (×20). **(B)** High expression of CD73 as membranous staining pattern on tumor cells (×20). **(C)** Positive CD155 expression (≥10%) as membranous staining pattern on tumor cells (×20).

TABLE 2 Associations of immune checkpoint receptor expression with clinicopathological factors.

Variables		CD73		*p-value*	CD155		*p-value*
	All (n = 53)	Low (n = 42)	High (n = 11)		<10% (n = 23)	≥10% (n = 30)	
	n	n(%)	n(%)		n(%)	n(%)	
Age				*0.735*[a]			*0.546*[b]
≤ 50	29 (54.7%)	22(52.4)	7(63.6)		11(47.8)	18(60)	
>50	24 (45.3%)	20(47.6)	4(36.4)		12(52.2)	12(40)	
				0.518[a]			*0.962*[b]
cT1-2	24 (45.3%)	18(42.9)	6(54.5)		11(47.8)	13(43.3)	
cT3-4	29 (54.7%)	24(57.1)	5(45.5)		12(52.2)	17(56.7)	
				0.999[a]			*0.639*[b]
cN0-1	33 (62.3%)	26(61.9)	7(63.6)		13(56.5)	20(66.7)	
cN2-3	20 (37.7%)	16(38.1)	4(36.4)		10(43.5)	10(33.3)	
				0.068[a]			*0.737*[b]
ypN0	16 (30.2%)	10(23.8)	6(54.5)		8(34.8)	8(26.7)	
ypN(+)	37 (69.8%)	32(76.2)	5(45.5)		15(65.2)	22(73.3)	
MDACC RCBI				*0.624*			*0.028*[c]*
Mean Score ± SD (95%CI)	3.2 ± 1.2 (2.8-3.5)	3.2 ± 1.2 (2.8-3.6)	3 ± 1.1 (2.2-3.7)		2.8 ± 1.3 (2.2-3.3)	3.5 ± 1.1 (1.6-5.1)	
MDACC RCBI				*0.569*[a]			*0.030*[a]*
Class I	4 (7.5%)	4(9.5)	0(0)		4(17.4)	0(0)	
Class II-III	49 (92.5%)	38(90.5)	11(100)		19(82.6)	30(100)	
				0.313[a]			*0.141*[b]
Class I-II	25 (47.2%)	18(42.9)	7(63.6)		14(60.9)	11(36.7)	
Class III	28 (52.8%)	24(57.1)	4(36.4)		9(39.1)	19(63.3)	

MDACC RCBI, MDACC Residual Cancer Burden Index.
*p<0.05, Chi-Square Tests ([a]Fisher's Exact Test, [b]Continuity Correction), [c]Mann Whitney U test
cT: clinical T size (determined by physical exam and imaging, AJCC 8th edition) (42);
cN: clinical nodal status (determined by physical exam and imaging, AJCC 8th edition) (42);
ypN0: pathological nodal complete response after neoadjuvan chemotherapy (AJCC 8th edition) (42);
ypN(+): pathological residual nodal disease after neoadjuvant chemotherapy (AJCC 8th edition) (42).
Low CD73 expression was considered if the tumour cells were weakly stained <20%. High CD73 expression was considered if the tumour cells were weakly stained ≥20% or any moderately/strongly staining.

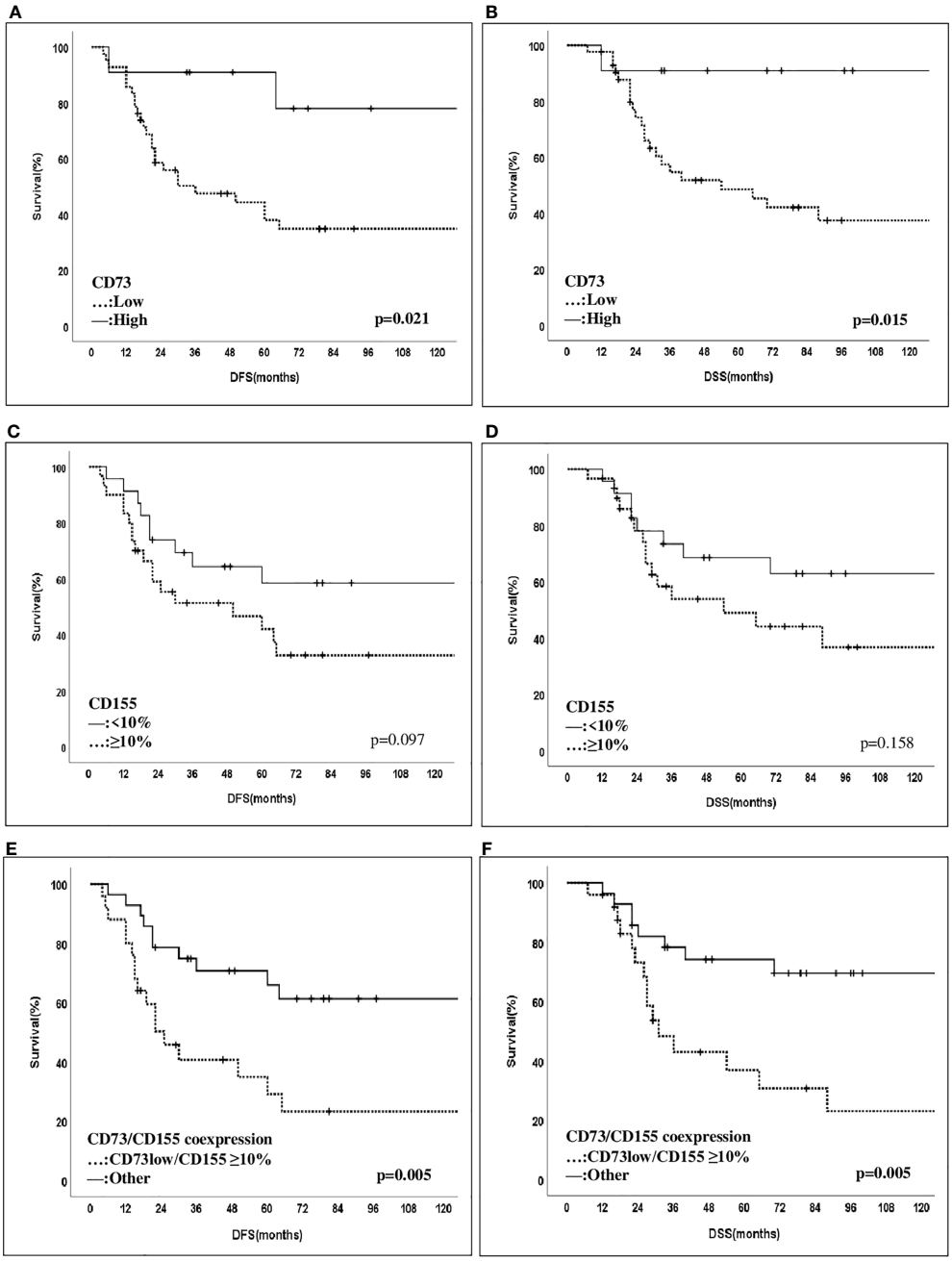

FIGURE 3
Disease-free and disease-spesific survival of patients with CD73 and CD155 expressions. Patients with CD73-high expression were found to have an improved 10-year DFS- and DSS rate compared to those with CD73-low expression (10-year DFS: 34.8% vs 77.9%, p = 0.021, and 10-year DSS: 37.3% vs 90.9%, p = 0.015) **(A, B)**. Those with a ≥10% CD155 expression have contrastly shown a decreased trend of 10-year-DFS and DSS compared to other cases with lower expression patterns (10-year DFS: 32.7% vs 58.3%, p = 0.097, and 10-year DSS: 36.7% vs 62.8%, p = 0.158) **(C, D)**. Notably, patients with coexpression of CD155 (>10%)/CD73-low were significantly more likely to have a decreased 10-year DFS and DSS rate compared to others (p = 0.005) **(E, F)**.

high CD73 expression showed an improved 10-year DFS and DSS rate compared to those with low CD73 expression. On the other hand, patients with CD155 expression (≥10%) demonstrated a decreasing trend in 10-year DFS and DSS rates, although it did not reach statistical significance. Notably, patients with coexpression of CD155 (≥10%)/CD73-low were significantly more likely to have a decreased 10-year DFS and DSS rate compared to others (p = 0.005). However, no other significant associations were found between the expression patterns of CD73, CD155, PD-L1, CD73PD-L1, or CD155PD-L1 and outcomes (Table 3). Furthermore, in multivariate Cox regression analysis, patients with a higher MD Anderson Cancer Center Residual Cancer Burden Index (RCBI) had an increased hazard ratio (HR) of DFS (HR = 1.941; 0.838–4.495) and DSS (HR = 2.904; 1.103–7.643) compared to those with better chemotherapy response. It is worth noting that patients with low CD73 expression had a higher HR of

10.3389/fonc.2023.1165257

TABLE 3 Outcome of patients according to biomarker expressions with different cut-off levels and staining patterns.

Biomarker expression	N (%)	10-year DFS (%)	*p-value*	10-year DSS (%)	*p-value*
CD73 (%, n = 53)					
CD73			0.303		0.490
<1%	29 (54.7%)	37.1		41.6	
≥1%	24 (45.3%)	54.0		59.9	
CD73			0.548		0.576
<5%	36 (67.9%)	40.2		43.4%	
≥5%	17 (32.1%)	52.8		62.7%	
CD73			0.475		0.324
<10%	42 (79.2%)	40.7		43.4%	
≥10%	11 (20.8%)	58.2		70.7%	
CD73			0.179		0.099
<20%	46 (86.8%)	39.8		42.0%	
≥20%	7 (13.2%)	68.6		85.7%	
CD73 expression*			0.021*		0.015*
Low (weakly stained <20%)	42 (79.2%)	34.8		37.3	
High (moderately/strongly staining &weakly stained if ≥20%)	11 (20.8%)	77.9		90.9	
CD73 score (n = 53)					
Score			0.548		0.576
<5	36 (67.9%)	40.2		43.4	
≥ 5	17 (32.1%)	52.8		62.7	
Score			0.293		0.199
<10	41 (77.4%)	39.0		41.5	
≥ 10	12 (22.6%)	62.5		73.3	
Score			0.123		0.070
<20	45 (84.9%)	39.1		41.3	
≥ 20	8 (15.1%)	70.0		87.5	
CD155 (%, n = 53)			0.097		0.158
<10%	23 (43.4%)	58.5		62.8	
≥10%	30 (56.6%)	32.7		36.7	
CD155			0.115		0.285
<20%	24 (46.1%)	56.4		59.7	
≥20%	28 (53.9%)	28.9		32.2	
CD155			0.218		0.446
<30%	30 (57.7%)	50.2		53.5	
≥30%	22 (42.3%)	31.4		41.0	
CD155 score (n = 53)					
Score			0.097		0.158
<10	23 (43.4%)	58.5		62.8	

(Continued)

TABLE 3 Continued

Biomarker expression	N (%)	10-year DFS (%)	*p-value*	10-year DSS (%)	*p-value*
≥ 10	30 (56.6%)	32.7		36.7	
Score			0.115		0.285
<20	29 (54.7%)	56.4		59.7	
≥ 20	24 (45.3%)	28.9		32.2	
Score			0.141		0.424
<40	32 (60.4%)	51.2		53.2	
≥ 40	21 (39.6%)	33.0		42.8	
Score			0.767		0.893
<50	40 (75.5%)	42.8		49.5	
≥ 50	13 (24.5%)	46.2		48.6	
PD-L1 (%)					
Tumour			0.687		0.878
–	24 (49%)	44.6		48.5	
+	25 (51%)	39.0		45.9	
TILs			0.405		0.255
–	24 (49%)	34.5		37.5	
+	25 (51%)	48.9		55.1	
Total			0.822		0.858
–	20 (40.8%)	43.1		47.6	
+	29 (59.2%)	41.2		46.6	
CD73/CD155 coexpression			0.005		0.005
CD73low/CD155 ≥10%	25 (47.2%)	23.2		23.0	
[a]Other (n = 28)	28 (52.8%)	61.2		69.5	
CD73/PD-L1$_{Total}$ coexpression			0.072		0.046*
CD73high/PD-L1$_{Total}$ (+)	9 (17.3%)	71.1		88.9	
[b]Other	43 (82.7%)	36.6		39.3	
CD155/PD-L1$_{Total}$ coexpression			0.289		0.209
CD155(≥10%)/PD-L1$_{Total}$ (+)	21 (39.6%)	34.9		36.3	
[c]Other	32 (60.4%)	50.9		58.0	

*: p<0.05; χ^2: Log-Rank (Mantel-Cox)
[a]Other: CD73high/PD-L1$_{Total}$ (-), CD73low/PD-L1$_{Total}$ (-), CD73low/PD-L1$_{Total}$ (+)
[b]Other: CD73high/PD-L1$_{Total}$ (-), CD73low/PD-L1$_{Total}$ (-), CD73low/PD-L1$_{Total}$ (+)
[c]Other: CD155(≥10%)/PD-L1$_{Total}$ (-), CD155(-)/PD-L1$_{Total}$ (-), CD155(-)/PD-L1$_{Total}$ (+).

DFS (HR = 3.979; 0.926–17.102) and DSS (HR = 6.45; 0.858–48.490) compared to those with high CD73 expression, although statistical significance was not reached (Table 4).

Discussion

There are currently no established molecular targets for TNBC patients, so chemotherapy remains the standard treatment approach. However, unlike patients with other subtypes, TNBC patients typically exhibit aggressive clinical behaviour and have an unfavourable prognosis. Consequently, novel systemic therapies, including immunotherapies, are being investigated for TNBC patients who are resistant to neoadjuvant chemotherapy or have only achieved a partial response to NAC. CD73 and CD155 have recently garnered significant attention as potential therapeutic targets for their immunoregulatory functions (18, 19, 21, 22, 43–45).

TABLE 4 Multivariate cox regression analysis.

Factors	Disease-free Survival HR (95%CI)	*p-value*	Disease-specific Survival HR (95%CI)	*p-value*
MDACC Residual Cancer Burden Index		0.122		0.031
Class I-II	Reference (1)		Reference (1)	
Class III	1.941 (0.838-4.495)		2.904(1.103-7.643)	
CD73		0.063		0.070
high (weakly stained <20%)	Reference (1)		Reference (1)	
low (moderately/strongly staining & weakly stained if ≥20%)	3.979(0.926-17.102)		6.451 (0.858-48.490)	
CD155		0.246		0.453
<10	Reference (1)		Reference (1)	
≥10%	1.636 (0.712-3.758)		1.407(0.577-3.430)	

Hazard ratio (HR) are presented with their 95% confidence interval (CI) and the p-value.

CD155 has emerged as a novel immune checkpoint protein highly expressed in many tumour cells (26–30). Its expression has been implicated in tumour immunosuppression (3), as its interaction with TIGIT or CD96-positive T lymphocytes and NK cells leads to immune exhaustion and reduced interferon-γ secretion (4, 5). Therefore, blocking CD155-TIGIT or CD96 signalling could enhance anti-tumour immune cell function, making it a potential marker for immunotherapy in breast cancer (43–45).

CD73, also known as ecto-5′-nucleotidase (NT5E), is the rate-limiting enzyme in the ATP to adenosine degradation pathway. It regulates the synthesis of adenosine through the catabolism of extracellular ATP (1, 2). Growing evidence suggests that the CD73-adenosine pathway plays a critical role in cancer progression and immune surveillance, exerting immunosuppressive effects on NK cells and CD8+ T cells, which can stimulate tumour escape mechanisms. Therefore, we investigated the potential interaction between these novel immune checkpoint expressions in response to NAC and the prognosis of patients with residual TNBC.

Our study found that CD155 was associated with poor chemotherapy response and outcome, whereas CD73 overexpression was conversely indicative of improved survival. Intriguingly, the interaction of CD155 with CD73 at lower levels resulted in a worse outcome than either protein alone. Furthermore, both CD73 and CD155 were found to be associated with PD-L1 expression in TNBC within our cohort.

There have been limited studies investigating the prognostic significance of CD155 immunohistochemical expression (IHC) in breast cancer (7, 10, 46, 47). In a study conducted by Yoshikawa et al. (7), CD155 expression was observed in 41% (25/61) of TNBC patients using IHC and tissue microarray. However, no associations were found between CD155 expression and pathological stage, histological grade, Ki-67 labelling index, or stromal tumour-infiltrating lymphocytes. Notably, only PD-L1 expression in tumour cells, as determined by the SP142 assay, exhibited a significant correlation with CD155 expression ($p = 0.035$). Our present study also found correlations between CD155 expression on tumour cells and PD-L1 expression on both tumour cells and tumour-infiltrating lymphocytes. However, unlike the current cohort, Yoshikawa et al. found no significant associations between CD155 expression and DFS or overall survival (OS).

Yong et al. conducted a study involving 216 patients and similarly found a significant association between CD155 expression, as determined by IHC, and primary tumour size, lymph node metastasis, TNM stage, Ki-67 expression, and CD163/CD8/CD68 expression (10). Among the cases, 117 had ER-negative tumours, and nearly half had HER2-positive cancer. Most of the cohort consisted of early-stage breast cancer patients who underwent upfront surgery. Importantly, patients with high CD155 expression were more likely to experience poor OS, as indicated by both univariate analysis (HR = 2.681, 95%CI = 1.458–4.928, $p < 0.001$) and multivariate analysis (HR = 2.029, 95%CI = 1.059–3.887, $P = 0.033$). Consistent with our findings, multivariate analysis further confirmed that CD155 expression level and TNM stage were independent risk factors for OS. These findings suggest an interaction between CD155 expression and TILs in breast cancer and highlight the potential utility of CD155 as a prognostic marker.

In a recent study conducted by Li et al. (46), CD155 overexpression was detected in 17%, 39%, 37%, and 62% of patients diagnosed with Luminal A, Luminal B, HER2-positive, and TNBC, respectively, in a cohort of 126 patients. Patients with CD155 overexpression exhibited a higher Ki-67 index and a greater presence of tumour-infiltrating lymphocytes and PD-1+ lymphocytes than those with low expression. Additionally, patients with CD155 overexpression experienced significantly poorer DFS and OS ($p < 0.05$), along with an increased risk of recurrence (HR = 13.93, 95%CI: 2.82, 68.91) and death (HR = 5.47, 95%CI: 1.42–20.9), consistent with the findings of our present study.

A recent meta-analysis (47) involving 26 studies and 4,325 cancer patients revealed that high CD155 expression was significantly associated with decreased OS compared to low CD155 expression (pooled HR = 1.772, 95%CI = 1.441–2.178, p <

0.001). Moreover, a subgroup analysis specifically focusing on breast cancer patients demonstrated a significant association between CD155 expression and decreased OS (pooled HR = 2.137, 95%CI = 1.448–3.154, $p < 0.001$). Consistent with previous studies (7), we observed a high expression of CD155 in 57% of TNBC patients within our cohort. Interestingly, in our cohort of patients with residual breast cancer after NAC, those with high CD155 expression were more likely to respond poorly to NAC. These findings, combined with our present report, suggest that CD155 may serve as a potential target for immunotherapy in breast cancer.

Moreover, our study revealed that more than half of the patients (59%) exhibited PD-L1 expression on both tumour cells and TILs, while CD73 expression on tumour cells was observed in 45% of the patients. In contrast to the findings of the study by Buisseret et al. (48), our study demonstrated correlations between CD73 expression on tumour cells and PD-L1 expression on both tumour cells and TILs. However, in our cohort of patients with residual tumours following NAC, no significant associations were found between CD73 expression and the response to NAC. Nevertheless, Cerbelli et al. demonstrated a higher likelihood of achieving a pathological complete response (pCR) in a cohort of 61 TNBC patients with low CD73 expression as determined by immunohistochemical staining (13).

Controversial findings have emerged regarding the prognostic significance of CD73 expression in breast cancer (11–14). Loi et al. analyzed gene expression data from over 6,000 TNBC patients and determined that CD73 expression was associated with poor prognosis (12). Additionally, high CD73 gene expression was significantly correlated with a lower rate of pathological complete response in TNBC patients treated with anthracycline-only preoperative chemotherapy. In *in vitro* assays utilizing breast cancer cell lines, it was demonstrated that doxorubicin treatment increased CD73 expression in tumour cells, potentially leading to chemoresistance in mouse models. However, blocking CD73 resulted in enhanced anti-tumour immune responses to doxorubicin and prolonged the survival of mice in an established metastatic mouse model.

A recent meta-analysis encompassing 2,951 patients from 14 publications explored the associations between CD73 expression, clinicopathological characteristics, and prognosis across different cancers (14). The analysis revealed that high CD73 expression was significantly associated with decreased OS in breast cancer (HR = 1.23) and ovarian cancer (HR = 1.14), while it correlated with favourable OS in lung cancer (HR = 0.80) and gastric cancer (HR = 0.71). High CD73 expression was also strongly linked to lymph node metastases (OR = 2.61, $p = 0.05$). Our study found that patients with high CD73 expression were more likely to achieve axillary pathologic complete response than those with low CD73 expression (54.6% vs 23.8%, $p = 0.068$); however, this difference did not reach statistical significance.

In contrast to studies reporting CD73 as a poor prognostic indicator, our findings revealed an intriguing observation. We demonstrated an improved 10-year DFS and DSS rate in patients with high CD73 expression, as determined by immunohistochemistry (IHC), compared to those with low CD73 expression. These results were obtained at a median follow-up time of 80 months. Interestingly, our findings align with a report by Supernat et al., which indicated that CD73 expression, as assessed by IHC on tissue microarrays, serves as a favourable prognostic marker in 136 stage I-III breast cancer patients (11).

Furthermore, we present a novel finding in this study: the interaction between CD155 and CD73 at lower expression levels resulted in a worse outcome than either protein alone. This observation warrants further investigation in future studies. Consequently, the precise role of CD73 and its interaction with CD155 in cancer progression remains unclear and should be elucidated through *in vitro* and clinical studies.

Conclusions

There is a critical need for novel targets in anti-cancer immunotherapy to improve the prognosis of TNBC patients. In this study, we demonstrated high expression of CD73 and CD155 in patients who had a partial response to NAC. Notably, CD155 expression was associated with a poor response to NAC and an unfavourable prognosis in this cohort of patients with residual TNBC, suggesting the potential benefit of additional immune checkpoint receptor inhibitor therapy. Consistent with other published studies (49–52), our findings also support the hypothesis that CD73 and CD155 could serve as promising therapeutic targets in TNBC, either alone or in combination with other immunotherapeutic agents targeting PD-L1. This opens avenues for developing personalized de-escalation or escalation strategies in patients with residual TNBC.

Data availability statement

The original contributions presented in the study are included in the article/supplementary material. Further inquiries can be directed to the corresponding author.

Ethics statement

The studies involving human participants were reviewed and approved by Istanbul University, Istanbul Faculty of Medicine, Ethical Committee. Written informed consent for participation was not required for this study in accordance with the national legislation and the institutional requirements.

Author contributions

The study was designed by NC. The initial search, literature organization, and analyses were performed by NC, SO, HK, GO and EY. Manuscript writing was performed by NC, AB, SE, SO and GO. Critical comments and typesetting corrections on the final version were made by MT, MM, AI, AA, PS, EY and VO. The manuscript was finalized by NC. All authors have read and revised the

manuscript critically. All authors contributed to the article and approved the submitted version.

Funding

This Project was supported by the Istanbul University, Department of Scientific Research Projects (ID26409/TTU-2017-26409 and ID27023/TOA-2017-27023) and Istanbul Breast Society.

Acknowledgments

The authors thank Mrs Fatma Yilmaz and Julide Hocaoğlu for their meticulous technical assistance in immunohistochemical staining and Atilla Bozdoğan for the statistical analyses.

Conflict of interest

The authors declare that the research was conducted in the absence of any commercial or financial relationships that could be construed as a potential conflict of interest.

Publisher's note

References

1. Lin NU, Vanderplas A, Hughes ME, Theriault RL, Edge SB, Wong YN, et al. Clinicopathologic features, patterns of recurrence, and survival among women with triple-negative breast cancer in the National Comprehensive Cancer Network. *Cancer* (2012) 118(22):5463–72. doi: 10.1002/cncr.27581

2. Loi S, Salgado R, Adams S, Pruneri G, Francis PA, Lacroix-Triki M, et al. Tumor infiltrating lymphocyte stratification of prognostic staging of early-stage triple negative breast cancer. *NPJ Breast Cancer* (2022) 8(1):3. doi: 10.1038/s41523-021-00362-1

3. Denkert C, Minckwitz G, Darb-Esfahani S, Lederer B, Heppner BI, Weber KE, et al. Tumour-infiltrating lymphocytes and prognosis in different subtypes of breast cancer: a pooled analysis of 3771 patients treated with neoadjuvant therapy. *Lancet Oncol* (2018) 19(1):40–50. doi: 10.1016/S1470-2045(17)30904-X

4. Adams S, Loi S, Toppmeyer D, Cescon DW, Laurentiis De M, Nanda R, et al. Pembrolizumab monotherapy for previously untreated, PD-L1-positive, metastatic triple-negative breast cancer: cohort B of the phase II KEYNOTE-086 study. *Ann Oncol* (2019) 30(3):405–11. doi: 10.1093/annonc/mdy518

5. Nanda R, Chow LQ, Dees EC, Berger R, Gupta S, Geva R, et al. Pembrolizumab in patients with advanced triple-negative breast cancer: phase Ib KEYNOTE-012 study. *J Clin Oncol* (2016) 34:2460–7. doi: 10.1200/JCO.2015.64.8931

6. Cortes J, Rugo HS, Cescon DW, Im SA, Yusof MM, Gallardo C, et al. Pembrolizumab plus chemotherapy in advanced triple-negative breast cancer. *New Engl J Med* (2022) 387(3):217–26. doi: 10.1056/NEJMoa2202809

7. Yoshikawa K, Ishida M, Yanai H, Tsuta K, Sekimoto M, Sugie T. Immunohistochemical analysis of CD155 expression in triple-negative breast cancer patients. *PLoS One* (2021) 16(6):e0253176. doi: 10.1371/journal.pone.0253176

8. Iguchi-Manaka A, Okumura G, Ichioka E, Kiyomatsu H, Ikeda T, Bando H, et al. High expression of soluble CD155 in estrogen receptor-negative breast cancer. *Breast Cancer* (2020) 27(1):92–9. doi: 10.1007/s12282-019-00999-8

9. Triki H, Charfi S, Bouzidi L, Ben Kridis W, Daoud J, Chaabane K, et al. CD155 expression in human breast cancer: clinical significance and relevance to natural killer cell infiltration. *Life Sci* (2019) 231:116543. doi: 10.1016/j.lfs.2019.116543

10. Yong H, Cheng R, Li X, Gao G, Jiang X, Cheng H, et al. CD155 expression and its prognostic value in postoperative patients with breast cancer. *BioMed Pharmacother* (2019) 115:108884. doi: 10.1016/j.biopha.2019.108884

11. Supernat A, Markiewicz A, Welnicka-Jaskiewicz M, Seroczynska B, Skokowski J, Sejda A, et al. CD73 expression as a potential marker of good prognosis in breast carcinoma. *Appl Immunohistochem Mol Morphol* (2012) 20(2):103–7. doi: 10.1097/pai.0b013e3182311d82

12. Loi S, Pommey S, Haibe-Kains B, Beavis PA, Darcy PK, Smyth MJ, et al. CD73 promotes anthracycline resistance and poor prognosis in triple negative breast cancer. *Proc Natl Acad Sci U.S.A.* (2013) 110(27):11091–6. doi: 10.1073/pnas.1222251110

13. Cerbelli B, Botticelli A, Pisano A, Pernazza A, Campagna D, De Luca A, et al. CD73 expression and pathologic response to neoadjuvant chemotherapy in triple negative breast cancer. *Virchows Arch* (2020) 476(4):569–76. doi: 10.1007/s00428-019-02722-6

14. Wang R, Zhang Y, Lin X, Gao Y, Zhu Y. Prognostic value of CD73-adenosinergic pathway in solid tumor: a meta-analysis and systematic review. *Oncotarget* (2017) 8(34):57327–36. doi: 10.18632/oncotarget.16905

15. Dougall WC, Kurtulus S, Smyth MJ, Anderson AC. TIGIT and CD96: new checkpoint receptor targets for cancer immunotherapy. *Immunol Rev* (2017) 276:112–20. doi: 10.1111/imr.12518

16. Stamm H, Wellbrock J, Fiedler W. Interaction of PVR/PVRL2 with TIGIT/DNAM-1 as a novel immune checkpoint axis and therapeutic target in cancer. *Mamm Genome* (2018) 29:694–702. doi: 10.1007/s00335-018-9770-7

17. Stamm H, Oliveira-Ferrer L, Grossjohann E-M, Muschhammer J, Thaden V, Brauneck F, et al. Targeting the TIGIT-PVR immune checkpoint axis as novel therapeutic option in breast cancer. *Oncoimmunology* (2019) 8:e1674605. doi: 10.1080/2162402X.2019.1674605

18. Chen X, Song X, Li K, Zhang T. FcγR-binding is an important functional attribute for immune checkpoint antibodies in cancer immunotherapy. *Front Immunol* (2019) 10:292. doi: 10.3389/fimmu.2019.00292

19. Boissière-Michot F, Chateau MC, Thézenas S, Guiu S, Bobrie A, Jacot W. Correlation of the TIGIT-PVR immune checkpoint axis with clinicopathological features in triple-negative breast cancer. *Front Immunol* (2022) 5:1058424(13). doi: 10.3389/fimmu.2022.1058424

20. Gros A, Robbins PF, Yao X, Li YF, Turcotte S, Tran E, et al. PD-1 identifies the patient-specific CD8(+) tumor-reactive repertoire infiltrating human tumors. *J Clin Invest* (2014) 124:2246–59. doi: 10.1172/JCI73639

21. Chiang EY, Mellman I. TIGIT-CD226-PVR axis: advancing immune checkpoint blockade for cancer immunotherapy. *J Immunother Cancer* (2022) 10:e004711. doi: 10.1136/jitc-2022-004711

22. Molfetta R, Zitti B, Lecce M, Milito ND, Stabile H, Fionda C, et al. CD155: a multi-functional molecule in tumor progression. *Int J Mol Sci* (2020) 21:922. doi: 10.3390/ijms21030922

23. Bowers JR, Readler JM, Sharma P, Excoffon KJDA. Poliovirus receptor: more than a simple viral receptor. *Virus Res* (2017) 242:1–6. doi: 10.1016/j.virusres.2017.09.001

24. Rikitake Y, Mandai K, Takai Y. The role of nectins in different types of cell-cell adhesion. *J Cell Sci* (2012) 125:3713–22. doi: 10.1242/jcs.099572

25. Nandi SS, Gohil T, Sawant SA, Lambe UP, Ghosh S, Jana S. CD155: a key receptor playing diversified roles. *Curr Mol Med* (2022) 22:594–607. doi: 10.2174/1566524021666210910112906

26. Nakai R, Maniwa Y, Tanaka Y, Nishio W, Yoshimura M, Okita Y, et al. Overexpression of Necl-5 correlates with unfavorable prognosis in patients with lung adenocarcinoma. *Cancer Sci* (2010) 101:1326–30. doi: 10.1111/j.1349-7006.2010.01530.x

27. Masson D, Jarry A, Baury B, Blanchardie P, Laboisse C, Lustenberger P, et al. Overexpression of the CD155 gene in human colorectal carcinoma. *Gut* (2001) 49:236–40. doi: 10.1136/gut.49.2.236

28. Nishiwada S, Sho M, Yasuda S, Shimada K, Yamato I, Akahori T, et al. Clinical significance of CD155 expression in human pancreatic cancer. *Anti-cancer Res* (2015) 35(4):2287–97.

29. Bevelacqua V, Candido S, Skarmoutsou E, Amoroso A, Guarneri C, et al. Nectin like-5 overexpression correlates with the malignant phenotype in cutaneous melanoma. *Oncotarget* (2012) 3(8):882–92. doi: 10.18632/oncotarget.594

30. Duan X, Liu J, Cui J, Ma B, Zhou Q, Yang X, et al. Expression of TIGIT/CD155 and correlations with clinical pathological features in human hepatocellular carcinoma. *Mol Med Rep* (2019) 20:3773–81. doi: 10.3892/mmr.2019.10641

31. Shibuya A, Campbell D, Hannum C, Yssel H, Franz-Bacon K, McClanahan T, et al. DNAM-1, a novel adhesion molecule involved in the cytolytic function of T lymphocytes. *Immunity* (1996) 4(6):573–81. doi: 10.1016/S1074-7613(00)70060-4

32. Jiang T, Xu X, Qiao M, Li X, Zhao C, Zhou F, et al. Comprehensive evaluation of NT5E/CD73 expression and its prognostic significance in distinct types of cancers. *BMC Cancer* (2018) 18(1):267. doi: 10.1186/s12885-018-4073-7

33. Allard D, Turcotte M, Stagg J. Targeting A2 adenosine receptors in cancer. *Immunol Cell Biol* (2017) 95(4):333–9. doi: 10.1038/icb.2017.8

34. Antonioli L, Yegutkin GG, Pacher P, Blandizzi C, Hasko G. Anti-CD73 in cancer immunotherapy: awakening new opportunities. *Trends Cancer* (2016) 2:95–109. doi: 10.1016/j.trecan.2016.01.003

35. Gao ZW, Dong K, Zhang HZ. The roles of CD73 in cancer. *BioMed Res Int* (2014) 2014:460654. doi: 10.1155/2014/460654

36. Cekic C, Linden J. Purinergic regulation of the immune system. *Nat Rev Immunol* (2016) 16:177–92. doi: 10.1038/nri.2016.4

37. Allard D, Allard B, Gaudreau PO, Chrobak P, Stagg J. CD73-adenosine: a next-generation target in immuno-oncology. *Immunotherapy* (2016) 8:145–63. doi: 10.2217/imt.15.106

38. Allard B, Longhi MS, Robson SC, Stagg J. The ectonucleotidases CD39 and CD73: novel checkpoint inhibitor targets. *Immunol Rev* (2017) 276:121–44. doi: 10.1111/imr.12528

39. Deaglio S, Dwyer KM, Gao W, Friedman D, Anny Usheva A, Erat A, et al. Adenosine generation catalyzed by CD39 and CD73 expressed on regulatory T cells mediates immune suppression. *J Exp Med* (2007) 204:1257–65. doi: 10.1084/jem.20062512

40. Leone RD, Emens LA. Targeting adenosine for cancer immunotherapy. *J Immunother Cancer* (2018) 6(1):57. doi: 10.1186/s40425-018-0360-8

41. Hortobagyi GN, Connolly JL, D'Orsi CJ, Edge SB, Mittendorf EA *AJCC Cancer Staging Manual. Eight Edition*. Chicago, Illionis: The American College of Surgeons 2017 (ACS), Part XI Breast (2017). doi: 10.1007/978-3-319-40618-3_48

42. Oner G, Önder S, Karatay H, Ak N, Tükenmez M, Müslümanoğlu M, et al. Clinical impact of PD-L1 expression in triple-negative breast cancer patients with residual tumor burden after neoadjuvant chemotherapy. *World J Surg Oncol* (2021) 19 (1):264. doi: 10.1186/s12957-021-02361-9

43. Kučan Brlić P, Lenac Rovis T, Cinamon G, Tsukerman P, Mandelboim O, Jonjić S. Targeting PVR (CD155) and its receptors in anti-tumor therapy. *Cell Mol Immunol* (2019) 16:40–52. doi: 10.1038/s41423-018-0168-y

44. Xu F, Sunderland A, Zhou Y, Schulick RD, Edil BH, Zhu Y. Blockade of CD112R and TIGIT signaling sensitizes human natural killer cell functions. *Cancer Immunol Immunother* (2017) 66:1367–75. doi: 10.1007/s00262-017-2031-x

45. He W, Zhang H, Han F, Chen X, Lin R, Wang W, et al. CD155T/TIGIT signaling regulates $CD8^+$ T-cell metabolism and promotes tumor progression in human gastric cancer. *Cancer Res* (2017) 77:6375–88. doi: 10.1158/0008-5472.CAN-17-0381

46. Li YC, Zhou Q, Song QK, Wang RB, Lyu S, Guan X, et al. Overexpression of an immune checkpoint (CD155) in breast cancer associated with prognostic significance and exhausted tumor-infiltrating lymphocytes: a cohort study. *J Immunol Res* (2020) 2020:1–9. doi: 10.1155/2020/3948928

47. Zhang D, Liu J, Zheng M, Meng C, Liao J. Prognostic and clinicopathological signifcance of CD155 expression in cancer patients: a meta-analysis. *World J Surg Oncol* (2022) 20:351. doi: 10.1186/s12957-022-02813-w

48. Buisseret L, Pommey S, Allard B, Garaud S, Bergeron M, Cousineau I, et al. Clinical significance of CD73 in triple-negative breast cancer: multiplex analysis of a phase III clinical trial. *Ann Oncol* (2018) 29(4):1056–62. doi: 10.1093/annonc/mdx730

49. Magagna I, Gourdin N, Kieffer Y, Licaj M, Mhaidly R, Andre P, et al. CD73-mediated immunosuppression is linked to a specific fibroblast population that paves the way for new therapy in breast cancer. *Cancers* (2021) 13:5878. doi: 10.3390/cancers13235878

50. Harjunpaa H, Guillerey C. TIGIT as an emerging immune checkpoint. *Clin Exp Immunol* (2020) 200:108–19. doi: 10.1111/cei.13407

51. Graeser M, Feuerhake F, Gluz O, Volk V, Hauptmann M, Jozwiak K, et al. Immune cell composition and functional marker dynamics from multiplexed immunohistochemistry to predict response to neoadjuvant chemotherapy in the WSG-ADAPT WSG-ADAPT-TN. *J Immunother Cancer* (2021) 9(5):e002198. doi: 10.1136/jitc-2020-002198

52. De Caluwé A, Buisseret L, Poortmans P, Van Gestel D, Salgado R, Sotiriou C, et al. Neo-CheckRay: radiation therapy and adenosine pathway blockade to increase benefit of immuno-chemotherapy in early stage luminal b breast cancer, a randomized phase II trial. *BMC Cancer* (2021) 21(1):899. doi: 10.1186/s12885-021-08601-1

frontiers | Frontiers in Immunology

TYPE Original Research
PUBLISHED 18 July 2023
DOI 10.3389/fimmu.2023.1179022

OPEN ACCESS

EDITED BY
Junjiang Fu,
Southwest Medical University, China

REVIEWED BY
Jia Li,
University of North Carolina at Charlotte, United States
Zheng Wang,
Jiao Tong University, China

*CORRESPONDENCE
Katri S. Selander
Katri.Selander@ppshp.fi

RECEIVED 03 March 2023
ACCEPTED 23 June 2023
PUBLISHED 18 July 2023

CITATION
Petruk N, Siddiqui A, Tadayon S, Määttä J, Mattila PK, Jukkola A, Sandholm J and Selander KS (2023) CD73 regulates zoledronate-induced lymphocyte infiltration in triple-negative breast cancer tumors and lung metastases.
Front. Immunol. 14:1179022.
doi: 10.3389/fimmu.2023.1179022

CD73 regulates zoledronate-induced lymphocyte infiltration in triple-negative breast cancer tumors and lung metastases

Nataliia Petruk[1], Arafat Siddiqui[1,2], Sina Tadayon[3,4], Jorma Määttä[1,5], Pieta K. Mattila[1,3,4,6], Arja Jukkola[7], Jouko Sandholm[6] and Katri S. Selander[8,9]*

[1]Institute of Biomedicine, University of Turku, Turku, Finland, [2]Western Cancer Centre FICAN West, Turku, Finland, [3]MediCity Research Laboratory, University of Turku, Turku, Finland, [4]InFLAMES Research Flagship Center, University of Turku, Turku, Finland, [5]Turku Center for Disease Modeling, University of Turku, Turku, Finland, [6]Turku Bioscience Centre, University of Turku and Åbo Akademi University, Turku, Finland, [7]Department of Oncology, Tampere University Hospital, Tays Cancer Center, Tampere, Finland, [8]Department of Oncology and Radiation Therapy, Oulu University Hospital, Oulu, Finland, [9]Cancer Research and Translational Medicine Research Unit, University of Oulu, Oulu, Finland

Introduction: Bisphosphonates (BPs) are bone-protecting osteoclast inhibitors, typically used in the treatment of osteoporosis and skeletal complications of malignancies. When given in the adjuvant setting, these drugs may also prevent relapses and prolong overall survival in early breast cancer (EBC), specifically among postmenopausal patients. Because of these findings, adjuvant nitrogen-containing BPs (N-BPs), such as zoledronate (ZOL), are now the standard of care for high-risk EBC patients, but there are no benefit-associated biomarkers, and the efficacy remains low. BPs have been demonstrated to possess anti-tumor activities, but the mechanisms by which they provide the beneficial effects in EBC are not known.

Methods: We used stably transfected 4T1 breast cancer cells together with suppression of CD73 (sh-CD73) or control cells (sh-NT). We compared ZOL effects on tumor growth and infiltrating lymphocytes (TILs) into tumors and lung metastases using two mouse models. B cell depletion was performed using anti-CD20 antibody.

Results: Sh-CD73 4T1 cells were significantly more sensitive to the growth inhibitory effects of n-BPs *in vitro*. However, while ZOL-induced growth inhibition was similar between the tumor groups *in vivo*, ZOL enhanced B and T lymphocyte infiltration into the orthotopic tumors with down-regulated CD73. A similar trend was detected in lung metastases. ZOL-induced tumor growth inhibition was found to be augmented with B cell depletion in sh-NT tumors, but not in sh-CD73 tumors. As an internal control, ZOL effects on bone were similar in mice bearing both tumor groups.

Discussion: Taken together, these results indicate that ZOL modifies TILs in breast cancer, both in primary tumors and metastases. Our results further demonstrate that B cells may counteract the growth inhibitory effects of ZOL. However, all ZOL-induced TIL effects may be influenced by immunomodulatory characteristics of the tumor.

KEYWORDS

CD73, TNBC, zoledronate, tumor growth, tumor-infiltrating lymphocytes

Introduction

Bisphosphonates (BPs) inhibit osteoclast-mediated bone resorption and thereby, effectively prevent osteoporotic bone fractures in osteoporosis and skeletal complications in bone metastasis (1). These drugs have also well documented anticancer effects (2–4). For example, BPs induce cancer cell apoptosis and prevent tumor growth *in vivo* (5–7). It has also been demonstrated in a large meta-analysis that BPs, when given in the adjuvant setting, provide survival advantage to a small fraction of breast cancer patients (8). This effect was detected with both pyrophosphate-like (p-BP) and N-BPs and was mostly due to prevention of bone metastasis. The protective effect was specifically detected among postmenopausal women (9, 10). Despite their well-characterized effects on the mevalonate pathway or on the production of ATP-like metabolites in cells (11), it remains unknown how adjuvant BPs prevent the outgrowth of microscopic disease into clinically detectable metastases (8). Furthermore, adjuvant BPs provide a survival effect for only 3% of breast cancer patients. Thus, the patient numbers needed to treat for one person to gain improved survival remains high. Although some prognostic biomarkers have been proposed, they are not yet in clinical use (12).

CD73 is a glycosylphosphatidylinositol-anchored membrane protein, which hydrolases AMP to adenosine and inorganic phosphate. A high CD73 expression has been reported in various cancer types, such as triple-negative breast cancer (TNBC) (13), pancreatic (14), gastric (15) cancer cells, renal cell carcinoma (16), esophageal squamous cell carcinoma (17) or lung adenocarcinoma (18). We and others showed that CD73 facilitates breast tumor growth in a pre-clinical model (19, 20). Low tumor CD73 expression is also associated with improved survival in TNBC. Moreover, a recent study demonstrated that low tumor CD73 expression levels were associated with higher pathologic complete response rates in TNBC patients receiving neo-adjuvant chemotherapy. These findings have raised interest in CD73 as a molecular target and currently, there are several active clinical trials investigating the effect of CD73 inhibition in cancer (21, 22).

Both BPs and CD73 regulate immune responses. Especially the newer, N-BPs are proinflammatory. They increase cytokine release and expand gamma-delta T cell populations, which are associated with cytotoxic effects against cancer cells (23). Furthermore, regulatory T cell expansion was suppressed in cell cultures using conditioned media from zoledronate pre-treated TNBC cells (24). CD73 and adenosine, on the other hand, have an immunosuppressive role in cancer progression (25). For example, blockage of adenosine production activated immune cells within the tumor microenvironment, along with sensitizing cancer cells to anti-cancer therapy (26). The correlation between elevated CD73 expression and unfavorable outcomes in TNBC may also be attributed to the impact on the immune system. Adenosine assists cancer cells in evading the immune system's attempts to target and eradicate them. As a result, TNBC tumors with high CD73 expression might be shielded from the body's inherent immune responses against tumors, ultimately resulting in a poorer prognosis for patients (21). The role of tumor infiltrating lymphocytes (TILs) is gaining importance in the pathophysiology and treatment of breast cancer (27). The aim of this study was to investigate whether zoledronate affects TILs. We also investigated whether CD73-dependent, tumor immunosuppressive characteristics affect N-BP responses in TNBC tumors.

Material and methods

Cells

Human MDA-MB-231 and mouse 4T1, representing TNBC cells and human T47-D cells, representing luminal A type breast cancer cells (all from ATCC, Manassas, VA, USA) were cultured as previously described (28). CD73 was downregulated in the 4T1 cells through stable small hairpin RNA (shRNA) transduction, using mouse-specific lentiviral particles, according to manufacturer's recommendations (Mission lentiviral transduction particles, Sigma-Aldrich) as described previously (20).

RNA sequencing

RNA-Seq (RNA sequencing) service was performed by LC Sciences (Houston, Texas) to analyze 4T1 sh-NT and 4T1 sh-CD73 cells. Poly(A) RNA sequencing library was prepared following Illumina's TruSeq-stranded-mRNA sample preparation protocol. RNA integrity was checked with Agilent Technologies 2100 Bioanalyzer. Poly(A) tail-containing mRNAs were purified using oligo-(dT) magnetic beads with two rounds of purification.

Cutadapt (29) and perl scripts in house were used to remove the reads that contained adaptor contamination, low quality bases and undetermined bases. The sequence quality was verified using FastQC (http://www.bioinformatics.babraham.ac.uk/projects/fastqc/). HISAT2 (30) was used to map reads to the genome of ftp://ftp.ensembl.org/pub/release-101/fasta/mus_musculus/dna/. StringTie (31) was used to perform expression level for mRNAs by calculating FPKM. mRNAs differential expression analysis was performed by R package DESeq2 (32) between two different groups (and by R package edgeR (33) between two samples). The mRNAs with the parameter of false discovery rate (FDR) below 0.05 and absolute fold change ≥ 2 were considered differentially expressed mRNAs. Database links presented in Supplementary Table 1.

Cell viability assay

Cancer cells were seeded in 96-well plates (2×10^3 cells/well) and left to attach overnight. IC_{50} of N-BPs (zoledronate = ZOL, alendronate = ALN, pamidronate = PAM) for sh-NT and sh-CD73 cells was measured using 6 technical replicates after 72 h of treatment. N-BP concentrations varied from 1 μM to 500 μM followed by 50% serial dilutions to lower doses. The IC50 values were obtained by non-linear regression analysis using GraphPad Prism version 7.0 (GraphPad Software Inc, San Diego, CA, USA). Obtained IC_{50} values for individual cell lines were used throughout the study. Additionally, cell viability was measured upon 100 μM Adenosine 5'-(α,β-methylene) diphosphate (APCP, Merck Life Science OY, Finland) treatment after 72h. Cell viability was measured by WST-8 assay (Dojindo, Biotop Oy, Denmark). The level of WST-formazan was quantified using a microplate Tecan ULTRA Reader (Tecan AG, Austria) at 450 nm.

CD73 analyses

For quantitative PCR, cells at the density of 10^4 cells were cultured with IC_{50} N-BP concentrations in 6-well plates (Corning, USA) for 72 h. Quantitative PCR was performed using SYBR Green qPCR kit (Bio-Rad) as previously described by us (20). For analysis of CD73 activity, cells were seeded onto 96-well flat bottom clear plates at a density of 1×10^4 cells/well and let to attach overnight. Cells were treated for 72h with N-BPs prior to addition of [^{3}H] AMP substrate. CD73 activity was determined by thin-layer chromatographic (TLC) analysis as was described before (34).

IncuCyte measurements

Cells were seeded onto 96-well plates (2×10^3 cells/well) and allowed to attach overnight. For proliferation studies, cell growth after N-BPs treatment was assessed for 72 h, to allow cells to reach confluency. For caspase3/7 measurement, ZOL and caspase 3/7 (4704, Sartorius) reporter red dye (ratio 1:8) were added for 72 h. Apoptotic cells showed cleaved caspase 3/7 staining in the nucleus, which was shown by the appearance of red fluorescence emission in IncuCyte S3. Cell density and the number of caspase3/7-positive cells were analyzed using IncuCyte S3 with IncuCyte 2020A software (Sartorius).

Flow cytometry analysis

Cell cycle assay was performed with Click-iT™ EdU Pacific Blue™ (ThermoFisher Scientific). Apoptosis assay was performed with Annexin V-FITC Apoptosis Staining/Detection Kit (ab14085, Abcam). Cells were seeded onto 6-well plates (3×10^4 cells/well) and allowed to attach overnight. Next, cells were treated with N-BPs and incubated for 72 h. Cell pellets were collected and stained according to the kit protocols. Samples were analyzed using BD LSRFortessa flow cytometer (BD Biosciences). The data was analyzed with Flowing Software 2.5.1 (Perttu Terho, Turku Bioscience Centre, Turku, Finland).

Western blotting

Cells were cultured in complete culture medium and harvested after 72 h of N-BPs treatment in RIPA buffer (Thermo Fisher Scientific). Protein amounts were measured using bicinchoninic acid (BCA) protein assay (Thermo Fisher Scientific). The membranes were incubated with 5'-Nucleotidase/CD73, Caspase-3, p27 and α-tubulin primary antibodies overnight at 4°C (Supplementary Table 2). Secondary detection was performed with anti-rabbit 800CW and anti-mouse 680CW antibodies (1:2000, IRDye, LI-COR). The emitted fluorescence was detected with Li-Cor Odyssey CLx imaging system.

In vivo experiments

Four-week-old female Balb/c mice (Balb/cOlaHsd) were obtained from Envigo (Netherlands). Animals were maintained under controlled pathogen-free environmental conditions with a 12h light/dark cycle. Mice were inoculated with sh-NT and sh-CD73 4T1cells (2×10^4 cells in 100 μl PBS per mouse) orthotopically into 4th mammary fat pads (n = 10/group) and followed for 31 days. For the metastasis models, the mice were inoculated intravenously with sh-NT and sh-CD73 4T1 cells (5×10^4 cells in 100 μl PBS per mouse) into tail vein (n = 6/group) and followed for 20 days. In the B cell depletion model, 100 μM/animal Ultra-leaf purified anti-mouse CD20 (BioLegend, 152104) and control IgG antibody (BioLegend, 400671) were injected intravenously in the tail vain, once cells were inoculated and followed for 34 days. Animals were treated intraperitoneally each 4th day with the dose of 6 μg ZOL/animal. Body weights and tumor dimensions (35) were measured once a week. The animals were sacrificed when weight loss was ≥ 10% (data not shown).

Analysis of the B cell depletion efficiency

After sacrifice, spleen and lung samples were mashed through 70 μm strainer (22363548, Fischer scientific) to a new well. The

strainer was washed with MAC buffer (2mM EDTA, 0,5% BSA, 1 x PBS). Isolated cells were incubated for 5 min RT with red blood lysis buffer (420301, Biolegend). The reaction was stopped with 1 x PBS. 1 x 10^6 cells were spined down (5 min, 500 x G) and resuspend in 2% BSA, 1 x PBS, 2 µL TruStain FcX (101320, Biolegend). Total cellular fraction isolated from lungs were analyzed from the presence of lymphocytes. Specifically, the isolated cells were incubated with anti-CD8 and anti-CD19 antibodies according to manufacturer's recommendations (Table S2). Isolated spleen cells were incubated with conjugated CD19/CD3 antibodies (Table S2) for 1 h at 4°C in dark. Blood was drawn with intracardiac punctures into anti-coagulated K2E tubes (BD Microtainer, 1307939). Whole blood was stained with conjugated anti-CD19 antibody for 1 h at 4° C in dark (Table S2). All samples were washed with cell staining buffer (BioLegend, 420201) and centrifugated for 5 min at 500 g. Cell pellet was resuspended in 500 µL of cell staining buffer. The presence of CD19-positive cells was analyzed using flow cytometry (BD LSRFortessa, BD Biosciences). The data was analyzed with Flowing Software 2.5.1 (Turku, Finland).

Histology and tissue staining

Dissected tumors and lungs were fixed with 10% paraformaldehyde for 24 h, after which they were processed into paraffin blocks and cut tissue sections with standard methods (20). Dissected lungs were stained with hematoxylin and eosin staining. For IHC staining, dissected tumors were stained immunohistochemically to analyze cleaved caspase-3 (cCas-3), phospho-histone H3 (pHH3), CD34, CD45R/B220 and CD4 cells (Table S2). Slides were scanned using Pannoramic 250 slide scanner (3DHISTECH Ltd, Hungary). For immunofluorescent staining, dissected tumors were stained with anti-CD8 AlexaFluor 488 and Ki-67 antibodies (Table S2). Secondary anti-rabbit AlexaFluor 488 antibody was applied for 1h at RT. DAPI was used as a nuclear counterstain. Slides were scanned using Pannoramic Midi fluorescence slide scanner (3DHISTECH Ltd, Hungary). Acquired digital slides were analyzed with QuPath-0.2.0 software (36). All stainings were evaluated blindly. QuPath scripts used for image analysis are presented in Table S3.

Bone analyses

For bone histology, tibiae were dissected and prepared into paraffin-blocks and cut sections, as previously described (37). Osteoclasts were stained for tartrate-resistant acid phosphatase (TRAP) (Merck, Germany). The number of osteoclasts were counted per area in the trabecular bone manually using Fiji-ImageJ (1.52p) software. Quantitative analysis of femurs was performed using a Skyscan 1272 X-ray computer tomography scanner (Bruker, Kontich, Belgium). Morphometric parameters including tissue volume (TV, mm^3), bone volume (BV, mm^3) and bone volume/tissue volume (%) were analyzed by CTan version 1.9.32 software from Skyscan. The parameters applied for scanning were the following: x 26.31 magnification, X-ray tube voltage 61 kV, tube current 148 µA, X-ray filtration with 0.25 mm aluminum filter. Trabecular bone morphometric region of interest was defined at metaphysis of the femur starting 11 layers (122µm) below an anatomic marker, showing lower surface of the growth plate and extending 50 layers (557µm).

Statistical analysis

Results are showed as the mean ± SD of independent experiments with parallels. All analyses were performed using GraphPad Prism version 7.0 (GraphPad Software Inc, San Diego, CA, USA). Data were analyzed for statistical significance using Mann-Whitney t-test, one-way and two-way analysis of variance (ANOVA). Differences for which P was <0.05 are reported as statistically significant. Original dataset is available in a publicly accessible repository. This data can be found here:

Ethical approval

All procedures involving animal studies were cared for in accordance with the Project Authorization Board of Finland (license No ESAVI/7015/2020) in accordance with the 2010/EU/63 EU Directive on the protection of animals used for scientific purposes and the ARRIVE guidelines (38).

Results

CD73 gene involvement in cell cycle and inflammatory pathways in 4T1 cancer cells

We have previously demonstrated that suppression of CD73 expression affects migration and viability of TNBC cells (20). To further characterize CD73 shRNA-induced changes in these cells, sh-NT and sh-CD73 cells were analyzed with RNA-seq. The analysis revealed 551 upregulated (log2 (fc) > 1, p < 0.05) and 886 downregulated (log2 (fc) < 1, p < 0.05) genes in sh-CD73 cells as compared with sh-NT cells (Figure 1A and Supplementary File 2). We then used k-means clustering to divide the top 1000 most variable genes from RNA-seq FPKM (fragments per kilobase of exon per million mapped fragments) data into clusters *via* iDEP tool (39). We identified 4 clusters based on GO Biological Process database. Three clusters were involved in inflammation and immune responses and one cluster in cell division and replication (Figure 1B and Figure S1). Additionally, we applied KEGG enrichment analysis on the most engaged pathways changed in sh-CD73 versus sh-NT cells (Figure 1C). The genes that passed the threshold level (log2 (fc) > 1.5 or log2 (fc) < –1.5, p > 0.05) in the pathways were associated with apoptosis, cell cycle and cytokine activity and are presented in Supplementary Table 4.

Suppression of CD73 expression sensitizes TNBC cells to bisphosphonates *in vitro*.

To begin our studies, we first wanted to define whether CD73 expression in TNBC alters direct cellular response to N-BPs. We

10.3389/fimmu.2023.1179022

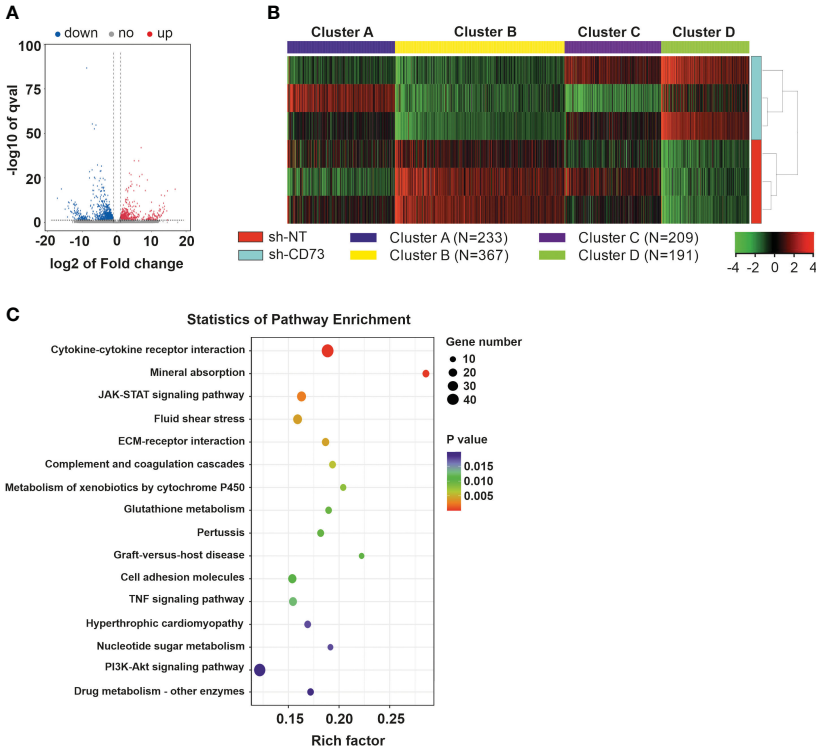

FIGURE 1
Gene expression in 4T1 sh-CD73 vs sh-NT cells. **(A)** Volcano map of the differential gene expression. **(B)** Differentially expressed gene clusters between sh-CD73 and sh-NT cells, using three replicates. The clusters were defined using the kmeans algorithm, using iDEP tool available online. **(C)** The KEGG diagram was made according to the gene pathway enrichment. The mRNAs with the parameter of false discovery rate (FDR) below 0.05 and absolute fold change ≥ 2 were considered differentially expressed mRNAs. The gene expression signature of 4T1 sh-NT and sh-CD73 cells were determined by RNA sequence (LC Sciences, Houston, Texas).

treated 4T1 sh-NT and sh-CD73 cells with ZOL, ALN and PAM, and determined the IC_{50} doses with cell viability assays (Table S5). Sh-CD73 cells were significantly more sensitive than sh-NT cells to ZOL and ALN IC_{50} doses after 48h, and to all selected N-BPs after 72h (Figures S2A, B). Thus, we selected ZOL and ALN for further experiments. N-BPs did not directly affect CD73 catalytic activity, mRNA or protein expression level (Figures S2C–E). We also tested the combined effects of APCP, a specific CD73 activity inhibitor and ZOL in parental cells. APCP did not augment ZOL effects on cell viability of any breast cancer cell lines (Figures S3A–C). Thus, our results suggest that suppression of CD73 expression, but not enzymatic activity sensitizes cells to N-BPs *in vitro*.

Suppression of CD73 expression delayed cell proliferation and induced apoptosis upon bisphosphonates

Further experiments were conducted with IC_{50} concentrations at 72h. In line with decreased viability, ZOL and ALN caused a significant decrease of proliferation in sh-CD73 cells compared to sh-NT cells after 72h of treatment (Figure 2A). Significantly higher percentage of sh-CD73 cells than sh-NT cells were at G1-phase after ZOL-treatment (Figure 2B). Compared with vehicle, ZOL also significantly increased the percentage of sh-NT cells at S-phase. No such effect was seen in sh-CD73 cells (Figure 2C). Both ZOL and ALN increased sh-NT cell population in G2-phase compared to 7vehicle. In sh-CD73 cells, no such effect was seen (Figure 2D). Cyclin-dependent kinase inhibitor, p27 is a marker of cell cycle transition. We showed that sh-CD73 cells increased expression of p27 upon ZOL and ALN (Figure 2E). There was a trend of increased the percentage of apoptotic cells in vehicle treated sh-CD73 cells compared to sh-NT cells (Figure 2F). Both ZOL and ALN induced a significantly higher fold-increase in apoptosis in sh-CD73 cells in comparison to sh-NT cells after 72h treatment (Figure 2G), an effect which was not seen in in vehicle treated sh-CD73 cells. Apoptotic marker, caspase-3 was increased upon ZOL- and ALN-treatments. Furthermore, sh-CD73 cells demonstrated increased expression of caspase-3 upon ZOL-treatment in comparison to sh-NT cells (Figure 2H). In agreement with this, ZOL significantly increased the number of caspase 3/7 positive cells (Figures 2I, J) in sh-CD73 cells, as compared to sh-NT cells. Taken together, these results indicate that the increased sensitivity of sh-CD73 cells to the growth inhibitory effects of ZOL or ALN is due to changes in cycle arrest and increased apoptosis.

ZOL increases tumor infiltrating lymphocytes in sh-CD73 tumors

As ZOL demonstrated the most effective growth inhibition of cells *in vitro*, we next compared effects of ZOL on sh-NT and sh-CD73 tumor growth *in vivo*, using an immune-competent,

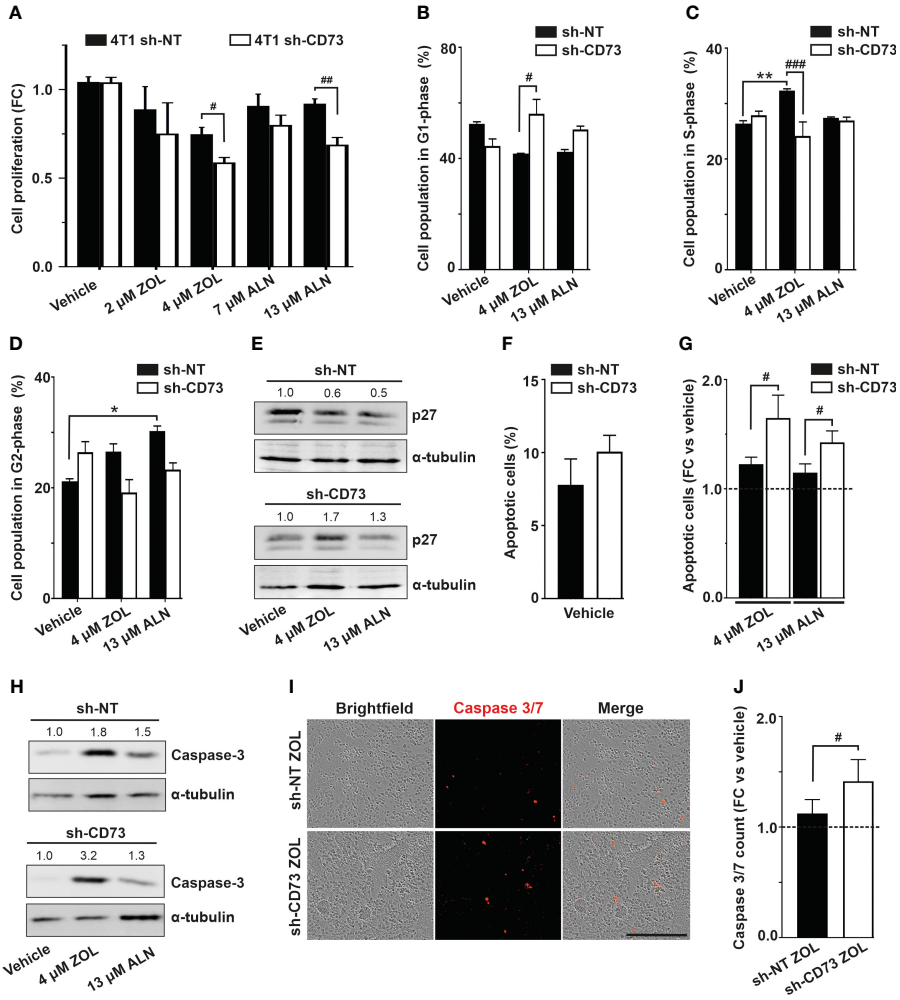

FIGURE 2
Suppression of CD73 causes cell cycle arrest and increases apoptosis upon N-BP treatment. **(A)** Cell proliferation of sh-NT and sh-CD73 4T1 cells upon N-BPs treatment for 72 h. Cell proliferation was assessed with confluence analysis using IncuCyte 2018B software (Essen Bioscience). The percentage of cells **(B)** in G1 phase, **(C)** S phase, **(D)** G2 phase of cell cycle upon N-BPs treatment for 72 h. **(E)** Representative dot plots of p27 protein expression upon N-BP treatment. **(F)** The percentage of apoptotic cells in vehicle and **(G)** N-BPs treated sh-NT and sh-CD73 groups. **(H)** Representative dot plots of caspase-3 protein expression upon N-BP treatment. **(I)** Representative images of caspase 3/7 staining. The images were generated by IncuCyte 2018B software (Essen Bioscience). **(J)** The number of caspase 3/7 positive 4T1 cells upon zoledronate treatment for 72 h. The bars represent fold-change in number of caspase3/7 in sh-NT ZOL-treated vs. sh-CD73 ZOL-treated cells. The results are expressed as mean ± SD, n = 3. * $P < 0.05$, ** $P < 0.01$, comparing within the same group upon different treatment; # $P < 0.05$, ## $P < 0.01$, ### $P < 0.001$, comparing sh-CD73 treated cells vs. sh-NT cells treated cells.

mammary fat pad mouse model of breast cancer (Figure 3A). As also seen previously (20), sh-CD73 cells formed significantly smaller tumors than sh-NT cells. Tumor growth was significantly suppressed in both ZOL-treated sh-NT (32%) and sh-CD73 (36%) groups compared to vehicle groups (Figure 3B). Unlike *in vitro*, ZOL-induced growth inhibition was similar in both tumor groups (Figures S4A, B). As an internal control for CD73 suppression throughout the experiment, significantly lower CD73 mRNA expression was maintained in the sh-CD73 tumors at sacrifice. In line with our *in vitro* results, ZOL did not influence CD73 mRNA expression in tumors either (Figure S4C). As an internal control for ZOL efficacy, we confirmed that ZOL significantly prevented bone resorption and decreased the number of osteoclasts in mice bearing either sh-NT or sh-CD73 tumors (Figures S4D–G).

There are several important characteristics, which implicate cancer progression, including proliferative status of tumor cells or their interaction with immune cells (40). Although, CD73 suppression in vehicle-treated tumors significantly decreased the number of $pHH3^+$ cells (mitotic marker) in comparison to vehicle-treated sh-NT tumors, it did not affect the number of cleaved-Caspase3 (apoptotic marker) cells or $CD34^+$ and $CYR61^+$ (angiogenesis markers) cells in vehicle-treated tumors (Figures S5B–E). ZOL significantly increased the number of cleaved-$Caspase3^+$ cells in sh-CD73 group compared to vehicle-treated sh-CD73 group. There was a trend of ZOL reducing pHH3+ cells in both groups (Figures S5B–E) and $CD34^+$ cells in sh-CD73 tumors (Figure S5C, D). However, the treatment did not alter the number of $CYR61^+$ cells (Figure S5E). Taken together, in agreement with the *in vitro* data,

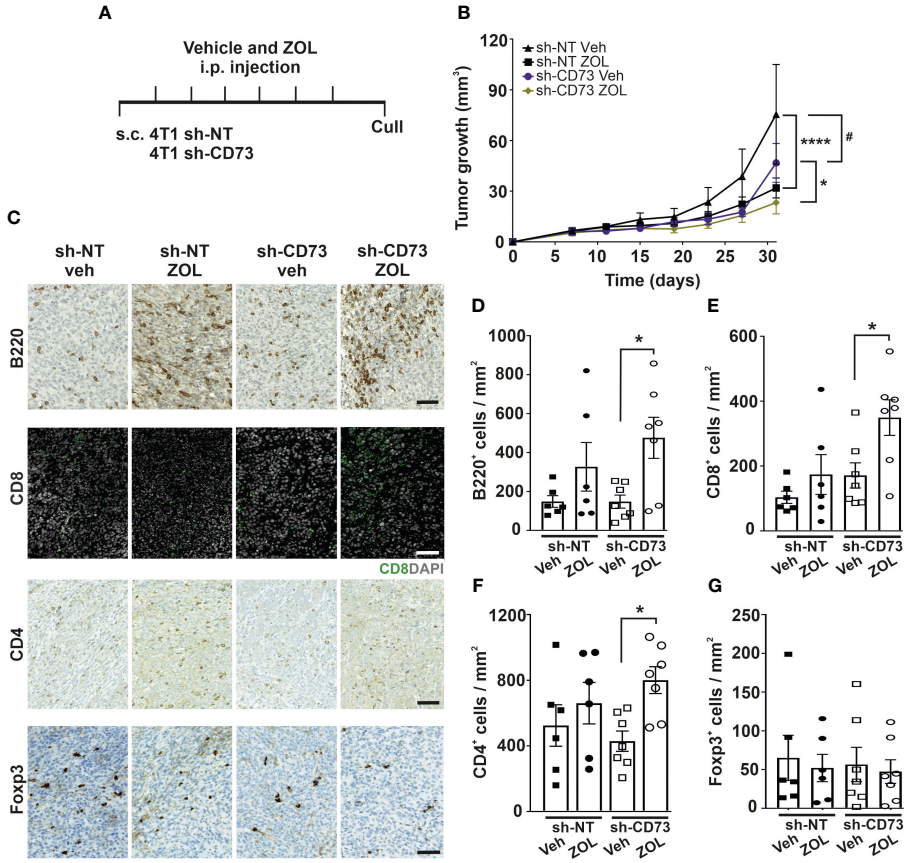

FIGURE 3
Zoledronate increases immune cell infiltration into CD73-suppressed tumors. **(A)** A schematic view of the in vivo experiment. Zoledronate was given at a dose of 6μg/animal for six times after tumors were formed. **(B)** sh-NT and sh-CD73 tumor growth demonstrated as a function of time. Tumor dimensions were measured with a caliper once a week. * $P < 0.05$, **** $P < 0.0001$, comparing within the same group upon different treatment; Data is expressed as mean ± SEM, by a two-tailed Student's t – test. # $P < 0.05$, comparing sh-CD73 tumors vs. sh-NT tumors. **(C)** Representative images of B220, CD8, CD4 and Foxp3 stainings in sh-NT and sh-CD73 tumors. Scale bar 100 μm. Number of **(D)** B220-positive cells, **(E)** CD4-positive cells, **(F)** CD8-positive and **(G)** Foxp3-positive cells from 4T1 sh-NT and sh-CD73 tumors. Data is expressed as mean ± SEM, by a two-tailed Student's t – test. * $P < 0.05$; sh-CD73 vs. sh-NT tumors.

sh-CD73 tumors had more apoptotic cells after ZOL treatment than after vehicle-treatment. A similar trend was seen in sh-NT tumors, but none of the differences were statistically significant.

Immune cell infiltration into tumors can promote or suppress tumor progression. The interplay of immune cells in this context is, however, very complex. For example, B cell infiltration demonstrated anti-tumor activity, resulting in better OS of cancer patients, but in the presence of effector T-cells (41). There are previous reports on BP effects on TILs, especially on T-cell (42, 43), but whether N-BPs affect B cell infiltration into tumors, is not known. The number of TILs was similar between vehicle-treated sh-NT and sh-CD73 tumors (Figures 3D–G). Compared with vehicle-treated sh-CD73 tumors, ZOL significantly increased $B220^+$ B cell, $CD4^+$ and $CD8^+$ T cell infiltration in sh-CD73 tumors. Only two tumors in the sh-NT group (n=6) showed increased numbers of B cells and $CD8^+$ T cells upon ZOL (Figures 3C–E). ZOL treatment had no effect on $FOXP3^+$ T helper cells in either group (Figure 3F). Thus, our results suggest that ZOL induces lymphocyte infiltration into primary tumors and that low CD73 expression in the tumor augments this effect.

ZOL increases TIL infiltration into lung metastases

We previously demonstrated that sh-CD73 cells formed significantly lower lung metastatic burden than sh-NT cells (20). ZOL had no obvious effects on the number and sizes of lung metastases in either group (Figures S5F, G). To investigate ZOL effects on TILs at lung metastases, we used an experimental lung metastasis model, which typically results in the formation of larger lung metastases without the engagement of primary tumors. With this model as well, there was a trend of fewer and smaller metastases formed by the sh-CD73 cells. ZOL, however, had no obvious effect on the number of metastases (Figures 4A–C). Similar to immune cell infiltration into mammary fat pad tumors, there was a trend towards ZOL-induced $B220^+$ B cell, $CD4^+$ and $CD8^+$ T cells infiltration into lung metastases. This effect appeared to be slightly more pronounced in the sh-CD73 than in the sh-NT tumors, but none of these changes reached statistical significance (Figures 4D–G).

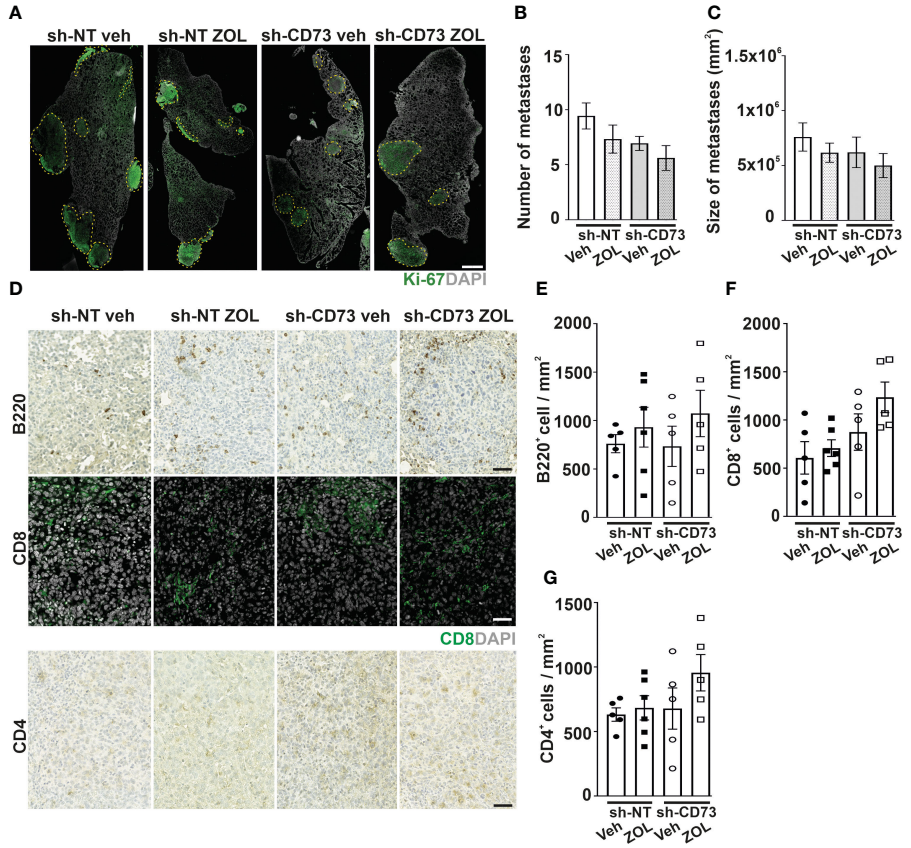

FIGURE 4
The effect of CD73 suppression on immune cell infiltration into lung metastases after zoledronate treatment. Cancer cells were injected intravenously into mouse tail veins (n = 6/group). Lung samples for staining were collected after 20 days. **(A)** Representative images of lung sections stained with antibody against Ki-67. Scale bar 500 µm. The number **(B)** and size **(C)** of lung metastases. **(D)** Representative images of B200, CD8 and CD4 immune cell stainings in lung metastases formed by sh-NT and sh-CD73 cells. Scale bar – 100 µm. Number of **(E)** B220-positive cells, **(F)** CD8-positive cells and **(G)** CD4-positive cells in lung metastases formed by sh-NT and sh-CD73 cells. Data is expressed as mean ± SEM.

B cell depletion augments ZOL effect on growth in CD73-expressing tumors

TNBC tumors have been suggested to have higher levels of B cell infiltration than other breast cancer subtypes, but their role in the disease pathophysiology is unclear (3, 9–21, 23–41). Therefore, we further explored the role of B-cells in our model in general, and also whether they contribute to ZOL effects in tumors (Figure 5A). We first determined an effective dose of B cell-depleting anti-CD20 antibody, by assaying its effect on circulating B cells using CD19 as a marker. A single dose of anti-CD20 IgG (100µM/animal) efficiently reduced the absolute number of $CD19^+$ lymphocytes in spleens, compared to control IgG group. Anti-CD20 treatment also slightly increased the absolute number of $CD3^+$ lymphocytes in spleen compared to control IgG group (Figure S6). This dose was used in further experiments. In the mouse orthotopic tumor model, both ZOL or anti-CD20 treatment alone significantly reduced tumor growth in sh-NT and sh-CD73 tumors, as compared with corresponding controls. The effect of anti-CD20 appeared to be slightly stronger in sh-CD73 tumors. No significant synergistic effects of ZOL and anti-CD20 were seen in sh-NT tumors. (Figures 5B, C). Notably however, whereas in sh-NT tumors there was a trend of anti-CD20 antibody further augmenting ZOL-induced growth inhibition, no such effect was detected in the sh-CD73 tumors (Figures 5B, C). Additionally, the post-mortem analysis suggested that ZOL significantly reduced tumor size in sh-CD73 group in comparison to sh-NT group. ZOL + anti-CD20 treatment could be more efficient that the individual treatments in sh-NT tumors, while in sh-CD73 tumors both ZOL and anti-CD20 seemed to have similar effect without further synergy (Figures 5D, E). The analysis of lung metastases showed the fewest and smallest metastases in the mice treated with anti-CD20, both with tumor cells expressing normal or reduced levels of CD73 and no clear synergy between ZOL and anti-CD20 was detected (Figures 5F–H). Taken together, the B cell depletion caused at least similar if not stronger growth inhibitory effects than ZOL in both tumor types and our data additionally suggested that sh-NT tumor could show some level of synergistic response, which was absent in sh-CD73 tumors.

The effect of B cell depletion upon ZOL on immune cell infiltration into tumors

In the orthotopic tumor model, ZOL significantly increased $B220^+$ B cell infiltration into both sh-NT and sh-CD73 tumors, in

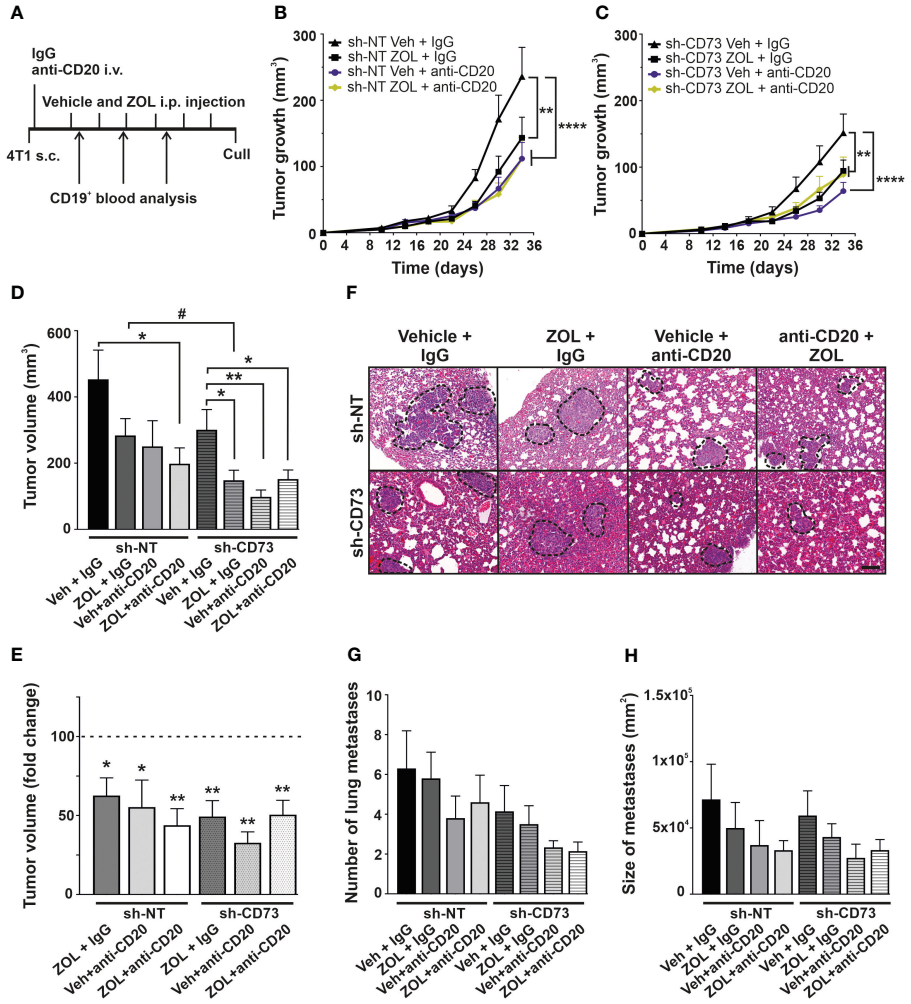

FIGURE 5
The effect of anti-CD20 and zoledronate treatment on tumor growth. **(A)** Schematic views of *in vivo* experiment. Animals were treatment with 100 µg/mouse anti-CD20 antibody after tumor cells were inoculated. Zoledronate was given at a dose of 6µg/animal for six times after tumors were formed. The number of circulating CD19-positive cells was analyzed throughout the experiment by Flow cytometry 3 times. **(B)** sh-NT and **(C)** sh-CD73 tumor growth upon treatment shown as a function of time. Tumor dimensions were measured with a caliper once a week. **(D)** Tumor volume and **(E)** fold-change of tumor volume at the sacrifice. **(F)** Representative images of H&E staining of lungs. Scale bar 200 µm. The number **(G)** and size **(H)** of lung metastases from 4T1 sh-NT and sh-CD73 cells. Data is expressed as mean ± SEM, by one-way ANOVA with a Sidak post-test. * $P < 0.05$, ** $P < 0.01$ and **** $P < 0.0001$, comparing within the same group upon different treatment. # $P < 0.05$, comparing sh-CD73 treated tumors vs. sh-NT cells treated tumors.

comparison to corresponding vehicle + IgG treatment (Figure 6A). Anti-CD20 treatment did not alter the baseline number of $B220^+$ B cells in sh-NT and sh-CD73 tumors in comparison to vehicle-treated groups. However, anti-CD20 treatment removed ZOL-induced $B220^+$ B cell infiltration in sh-NT tumors, but not in sh-CD73 tumors (Figure 6A). None of the treatments significantly affected $CD8^+$ T cell infiltration in the sh-NT group. However, the number of $CD8^+$ TILs was significantly suppressed by anti-CD20, with or without ZOL in sh-CD73 group (Figure 6B). ZOL seemed to increase $CD4^+$ T-cell infiltration in both groups, showing significant difference in the sh-CD73 tumors. The combination of anti-CD20 + ZOL significantly increased $CD4^+$ T-cell infiltration in comparison to anti-CD20 alone in the sh-NT group. This effect was not significantly affected by anti-CD20 in the sh-CD73 group (Figure 6C).

ZOL alone had no significant effect on the percentage of circulating $CD19^+$ cells in either mouse group. In mice bearing sh-NT tumors, anti-CD20 antibody decreased circulating $CD19^+$ cells, and this effect reached significance only upon anti-CD20 + ZOL. In mice bearing sh-CD73 tumors anti-CD20 and anti-CD20 + ZOL significantly decreased circulating $CD19^+$ cells (Figure 6D). Although neither treatment alone had a significant effect, the combination of anti-CD20 + ZOL significantly increased the number of circulating $CD8^+$ cells in comparison to corresponding vehicle in mice bearing sh-NT tumors. The effects were similar, but more pronounced in mice bearing sh-CD73 tumors (Figure 6E). We also investigated TILs in lung tissues with metastases, as our experimental metastases model demonstrated that lungs were a metastatic niche for 4T1 cells. The distribution of CD19+ cells in the total number of cells isolated from lungs mimicked those detected

10.3389/fimmu.2023.1179022

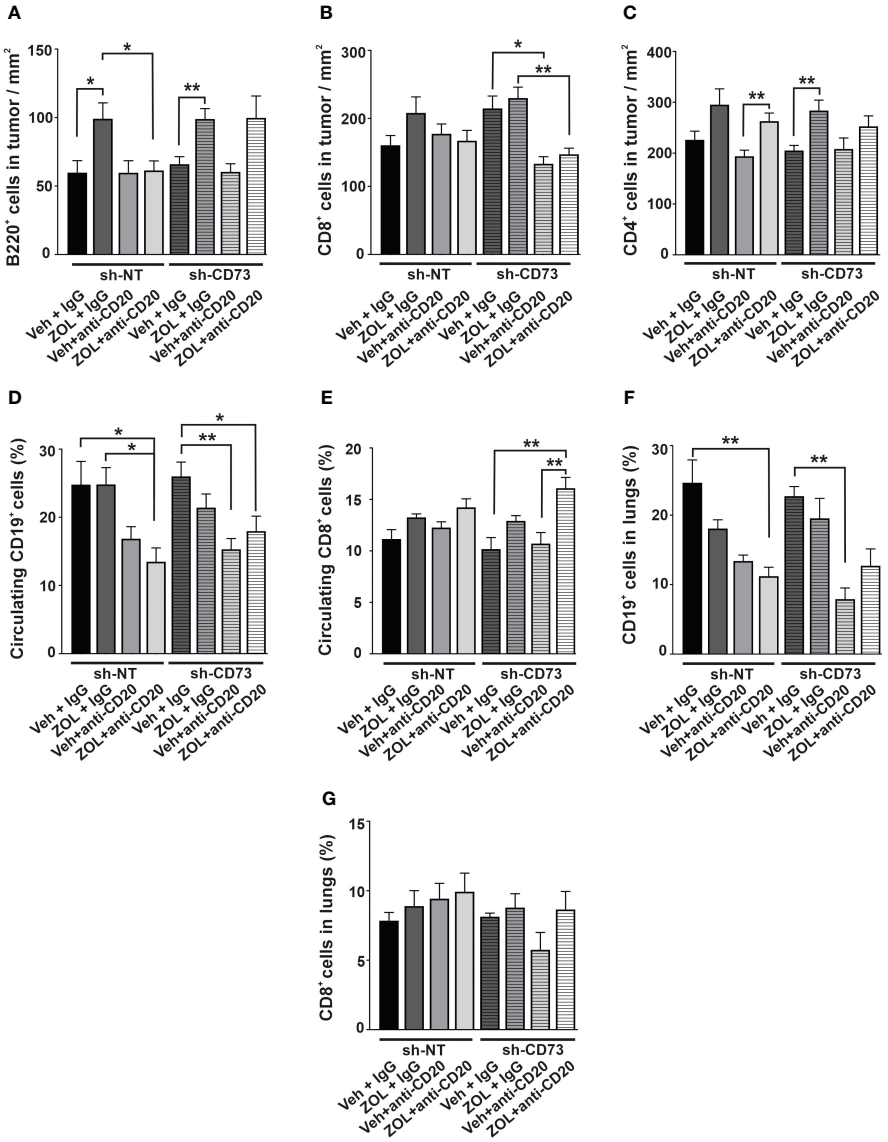

FIGURE 6
The effect of anti-CD20 treatment and zoledronate on circulating and tumor-infiltrating immune cells. The number of **(A)** B220-positive cells, **(B)** CD8-positive cells and **(C)** CD4-positive cells from 4T1 sh-NT and sh-CD73 tumors. The percentage of circulating **(D)** CD19-positive and **(E)** CD8-positive cells from 4T1 sh-NT and sh-CD73 tumor-bearing mice. The percentage of **(F)** CD19-positive and **(G)** CD8-positive cells in lungs from 4T1 sh-NT and sh-CD73 tumor-bearing mice. Data is expressed as mean ± SEM, by one-way ANOVA with a Sidak post-test. * $P < 0.05$, ** $P < 0.01$, comparing within the same group upon different treatment.

in blood (Figure 6F). Although, the changes were not significant, anti-CD20 + ZOL treatment resulted in highest $CD8^+$ infiltrating cells in the lungs of mice bearing sh-NT tumors. Anti-CD20 decreased CD8 + TILs in the lungs of mice bearing sh-CD73 tumors, but adding ZOL attenuated this effect (Figure 6G). Taken together, our data shows that anti-CD20 treatment alone significantly inhibits tumor growth in both sh-NT and sh-CD73 tumors, suggesting that B-cells regulate TNBC growth, regardless of tumor CD73 expression status. ZOL induces B cell infiltration into tumors, and this may counteract the growth inhibitory effects of this drug. However, tumor CD73 expression may interfere with this effect, making tumors less permissive for CD8 cells. The main immunological findings of this study are depicted in Figure 7.

Discussion

Adjuvant bisphosphonates increase the survival rate of postmenopausal women across different subtypes of breast cancer (44). The mechanism how this survival advantage is reached, is unclear and there are no predictive biomarkers for patient selection either. Especially N-BPs are pro-inflammatory and have been demonstrated to increase circulating immune cells both in pre-clinical and clinical studies (23). Less is known about their ability to affect tumor immunity. We studied here the effects of ZOL on tumor infiltrating lymphocytes. We further investigated whether immune system modulating tumor characteristics, namely CD73 expression, affects the growth inhibitory and inflammatory

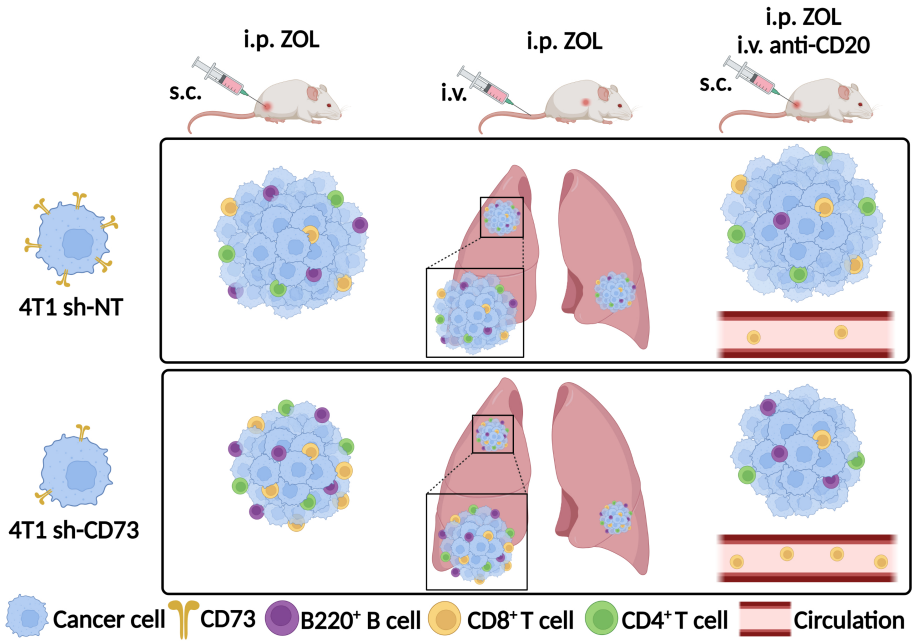

FIGURE 7
Zoledronate promotes B220+ B, CD8+ and CD4+ T cell infiltration into tumors or lung metastases with low CD73 expression. Depletion of B cells with anti-CD20 antibody led to reduced CD8+ T cell infiltration into tumors with low CD73 expression upon zoledronate-treatment. Zoledronate increased the number of CD8+ T cells in circulation when B cells were depleted in sh-CD73 tumor-bearing mice. ZOL, zoledronate; s.c., subcutaneously; i.v., intravenously; i.p., intraperitoneally; 4T1 sh-NT, cells were transfected with non-targeting particles; 4T1 sh-CD73, cells were transfected with a stable small hairpin RNA transduction, using mouse-specific lentiviral particles. Created with BioRender.com.

responses to N-BPs. Modulation of CD73 expression in the tumors was chosen, due to its prognostic significance and because it is a promising immunotherapeutic target especially in TNBC (21, 45, 46).

Our results demonstrate that CD73 suppression sensitizes 4T1 breast cancer cells to the growth inhibitory effects of N-BPs *in vitro*. These drugs, especially the most potent and clinically most frequently used N-BP, ZOL, paused the sh-CD73 4T1 cells at the G1-phase, delayed proliferation and increased apoptotic rate. These differences were not, however, reflected *in vivo*, as the tumor growth inhibitory responses to ZOL were similar regardless of the tumor CD73 expression rate.

N-BPs have well characterized pro-inflammatory effects. They have been shown to inhibit the migration of macrophages (47) and promote their polarization (48, 49), activate γδ T-cells, and increase the production of inflammatory mediators (43). It was also shown also that ZOL reduced infiltration of the immunosuppressive regulatory T cells (42). Here, we take these findings further and demonstrate, that ZOL also induces also B cell accumulation into the primary tumors and also into lung metastases. Our results also suggest that anti-CD20 antibody may weaken the growth inhibitory effects of ZOL in tumors with low CD73 expression. This suggests that under certain conditions, the infiltration of B-cells may oppose the growth inhibitory effects of this N-BP. This effect was partially regulated by tumor CD73 expression, suggesting that immunoregulatory characteristics of the tumor could modify the B-cell responses induced by ZOL. Anti-CD20 treatment, when given alone significantly inhibited tumor growth regardless of tumor CD73 expression, suggesting that eradication of B cells is a beneficial anti-tumor treatment approach in general. CD73 suppression made tumors less permissive for CD8 T cells upon ZOL treatment when B cells were depleted, without reducing CD8 T cells number in circulation or lungs. A previous study showed that inhibition of CD73 enzymatic activity did not influence CD8 T cells infiltration to tumors in mice with B cell depletion (50). Tumor sizes were assessed with caliper measurement in our experiments. This approach measures total tumors, including tumor infiltrating non-malignant cells, such as TILs. Thus, a possible explanation for the lack of difference in sensitivity to N-BPs between sh-NT and sh-CD73 cells, which was observed *in vitro*, but not *in vivo*, may partially be explained by differences in the immune cell responses that we detected. Furthermore, CD20 antibody could target not only CD20-positive B cells, but CD20-positive CD8 or CD4 T cells. This T cells subset showed the same activity as CD20-negative T cells (51), depletion of which could improve treatment for patients with multiple sclerosis (52). Given that cytotoxic activity of CD8 T cells against cancer cells, these CD20-posivite T cells could play role in cancer suppression as well, which requires further studies. Our finding is in agreement with previous publications demonstrating that anti-CD20 treatment decreases tumor growth in various cancer models (42, 43) and ZOL effects on B cell (53, 54).

There are several implications of our finding. First, immune surveillance plays a critical role in tumor progression (55). Thus, it could be, that it is the inflammatory, TIL promoting effects of adjuvant N-BPs that prevent the outgrowth of microscopic disease into macroscopic metastasis in post-menopausal women. This

hypothesis is supported also by the fact that the benefit is seen in post-menopausal women, who are not immunosuppressed by estrogen, like younger women (56). Second, breast cancers are considered immunologically "cold tumors", due to modest inflammatory infiltration (57). Converting immunologically cold tumors into hot is a major topic in immuno-oncology to improve responses to immunotherapy. Our results suggest that N-BPs should be further studied in this approach. Third, the role of B cells in tumor progression requires further analysis, since their role in cancer remains controversial (58, 59). B cells prevent tumor progression through releasing immunoglobulins and activation of T cells. However, the progression of tumor growth might also be promoted *via* B cell-induced immunosuppressive cytokines (60, 61). Further clinical studies are needed to examine N-BP treatment effects on TILs in breast and other cancers, and whether tumor baseline immunological features affect such outcomes.

Data availability statement

The dataset presented in this study can be found in online repository. This data can be found here: https://www.ncbi.nlm.nih.gov/sra/, PRJNA950306.

Ethics statement

The animal study was reviewed and approved by Project Authorization Board of Finland (license No ESAVI/7015/2020) in accordance with the 2010/EU/63 EU Directive.

Author contributions

NP and KS designed the study. NP, AS, ST performed investigation. NP analyzed data. JM and JS contributed to experiment performance. PM and AJ contributed to experiment design. NP, JS and KS wrote the original draft. NP, AS, ST, JM, JS, PM, AJ and KS wrote and edited the manuscript. All authors contributed to the article and approved the submitted version.

Funding

This study was supported by Academy of Finland (308375).

Acknowledgments

The authors thank Docent Gennady G. Yegutkin from the University of Turku for valuable help and providing equipment to perform thin-layer chromatographic analysis. We would also like to show our gratitude to the Adjunct Professor Tove Grönroos from the Preclinical Imaging Turku PET Centre at the University of Turku for support with the animal experiments. Turku Cell Imaging and Cytometry Core, Medisiina Imaging Core and Biocenter Finland are acknowledged for imaging equipment.

Conflict of interest

The authors declare that the research was conducted in the absence of any commercial or financial relationships that could be construed as a potential conflict of interest.

Publisher's note

Supplementary material

The Supplementary Material for this article can be found online at: https://www.frontiersin.org/articles/10.3389/fimmu.2023.1179022/full#supplementary-material

References

1. Yusuf AA, Cummings SR, Watts NB, Feudjo MT, Sprafka JM, Zhou J, et al. Real-world effectiveness of osteoporosis therapies for fracture reduction in post-menopausal women. *Arch Osteoporos* (2018) 13(1):33. doi: 10.1007/s11657-018-0439-3

2. Tripathi R, Singh P, Singh A, Chagtoo M, Khan S, Tiwari S, et al. Zoledronate and molecular iodine cause synergistic cell death in triple negative breast cancer through endoplasmic reticulum stress. *Nutr Cancer* (2016) 68(4):679–88. doi: 10.1080/01635581.2016.1158293

3. André Barrière D, Midavaine É, Doré-Savard L, Kirby K, Tremblay L, Beaudoin JF, et al. Dichotomic effects of clinically used drugs on tumor growth, bone remodeling and pain management. *Sci Rep* (2019) 9(1):20155.

4. Sandholm J, Lehtimäki J, Ishizu T, Velu SE, Clark J, Härkönen P, et al. Toll-like receptor 9 expression is associated with breast cancer sensitivity to the growth inhibitory effects of bisphosphonates *in vitro* and in vivo. *Oncotarget* (2016) 7 (52):87373–89. doi: 10.18632/oncotarget.13570

5. Wang L, Liu Y, Zhou Y, Wang J, Tu L, Sun Z, et al. Zoledronic acid inhibits the growth of cancer stem cell derived from cervical cancer cell by attenuating their stemness phenotype and inducing apoptosis and cell cycle arrest through the Erk1/2 and akt pathways. *J Exp Clin Cancer Res* (2019) 38(1):1–18. doi: 10.1186/s13046-019-1109-z

6. Rachner TD, Singh SK, Schoppet M, Benad P, Bornhäuser M, Ellenrieder V, et al. Zoledronic acid induces apoptosis and changes the TRAIL/OPG ratio in breast cancer cells. *Cancer Lett* (2010) 287(1):109–16. doi: 10.1016/j.canlet.2009.06.003

7. Gao X, Jiang B, Zou S, Zhang T, Qi X, Jin L, et al. Zoledronate can promote apoptosis and inhibit the proliferation of colorectal cancer cells. *Tumor Biol* (2015) 36 (7):5315–22. doi: 10.1007/s13277-015-3192-x

8. Wilson C, Bell R, Hinsley S, Marshall H, Brown J, Cameron D, et al. Adjuvant zoledronic acid reduces fractures in breast cancer patients; an AZURE (BIG 01/04) study. *Eur J Cancer* (2018) 94:70–8. doi: 10.1016/j.ejca.2018.02.004

9. Winter MC, Coleman RE. Bisphosphonates in the adjuvant treatment of breast cancer. *Clin Oncol* (2013) 25(2):135–45. doi: 10.1016/j.clon.2012.10.010

10. Strobl S, Wimmer K, Exner R, Devyatko Y, Bolliger M, Fitzal F, et al. Adjuvant bisphosphonate therapy in postmenopausal breast cancer. *Curr Treat Options Oncol* (2018) 19(4):18. doi: 10.1007/s11864-018-0535-z

11. Frith JC, Mönkkönen J, Auriola S, Mönkkönen H, Rogers MJ. The molecular mechanism of action of the antiresorptive and antiinflammatory drug clodronate: evidence for the formation in vivo of a metabolite that inhibits bone resorption and causes osteoclast and macrophage apoptosis. *Arthritis Rheumatol* (2001) 44(9):2201–10. doi: 10.1002/1529-0131(200109)44:9<2201::AID-ART374>3.0.CO;2-E

12. Westbrook JA, Cairns DA, Peng J, Speirs V, Hanby AM, Holen I, et al. CAPG and gipc1: breast cancer biomarkers for bone metastasis development and treatment. *J Natl Cancer Inst* (2016) 108(4). doi: 10.1093/jnci/djv360

13. Cerbelli B, Botticelli A, Pisano A, Pernazza A, Campagna D, De Luca A, et al. CD73 expression and pathologic response to neoadjuvant chemotherapy in triple negative breast cancer. *Virchows Arch* (2020) 476(4):569–76. doi: 10.1007/s00428-019-02722-6

14. Chen Q, Pu N, Yin H, Zhang J, Zhao G, Lou W, et al. CD73 acts as a prognostic biomarker and promotes progression and immune escape in pancreatic cancer. *J Cell Mol Med* (2020) 24(15):8674–86. doi: 10.1111/jcmm.15500

15. He X, Gu Y, Cao Y, Hu B, Fang H, Fei Y, et al. Impact of intratumoural CD73 expression on prognosis and therapeutic response in patients with gastric cancer. *Eur J Cancer* (2021) 157:114–23. doi: 10.1016/j.ejca.2021.08.006

16. Tripathi A, Lin E, Xie W, Flaifel A, Steinharter JA, Stern Gatof EN, et al. Prognostic significance and immune correlates of CD73 expression in renal cell carcinoma. *J Immunother Cancer* (2020) 8(2):e001467. doi: 10.1136/jitc-2020-001467

17. Chen YH, Lu HI, Lo CM, Li SH. Cd73 promotes tumor progression in patients with esophageal squamous cell carcinoma. *Cancers (Basel)* (2021) 13(16):3982. doi: 10.3390/cancers13163982

18. Rocha P, Salazar R, Zhang J, Ledesma D, Solorzano JL, Mino B, et al. CD73 expression defines immune, molecular, and clinicopathological subgroups of lung adenocarcinoma. *Cancer Immunol Immunother* (2021) 70(7):1965–76. doi: 10.1007/s00262-021-02893-9

19. Stagg J, Divisekera U, McLaughlin N, Sharkey J, Pommey S, Denoyer D, et al. Anti-CD73 antibody therapy inhibits breast tumor growth and metastasis. *Proc Natl Acad Sci* (2010) 107(4):1547–52. doi: 10.1073/pnas.0908801107

20. Petruk N, Tuominen S, Åkerfelt M, Mattsson J, Sandholm J, Nees M, et al. CD73 facilitates EMT progression and promotes lung metastases in triple-negative breast cancer. *Sci Rep* (2021) 11(1):6035. doi: 10.1038/s41598-021-85379-z

21. Buisseret L, Pommey S, Allard B, Garaud S, Bergeron M, Cousineau I, et al. Clinical significance of CD73 in triple-negative breast cancer: multiplex analysis of a phase III clinical trial. *Ann Oncol* (2018) 29(4):1056–62. doi: 10.1093/annonc/mdx730/4627685

22. De Caluwé A, Buisseret L, Poortmans P, Van Gestel D, Salgado R, Sotiriou C, et al. Neo-CheckRay: radiation therapy and adenosine pathway blockade to increase benefit of immuno-chemotherapy in early stage luminal B breast cancer, a randomized phase II trial. *BMC Cancer* (2021) 21(1):889. doi: 10.1186/s12885-021-08601-1

23. Dieli F, Gebbia N, Poccia F, Caccamo N, Montesano C, Fulfaro F, et al. Induction of γδ T-lymphocyte effector functions by bisphosphonate zoledronic acid in cancer patients *in vivo* [3]. *Blood* (2003) 102(6):2310–1. doi: 10.1182/blood-2003-05-1655

24. Liu H, Wang SH, Chen SC, Chen CY, Lin TM. Zoledronic acid blocks the interaction between breast cancer cells and regulatory T-cells. *BMC Cancer* (2019) 19(1):176. doi: 10.1186/s12885-019-5379-9

25. Hasmim M, Xiao M, Van Moer K, Kumar A, Oniga A, Mittelbronn M, et al. SNAI1-dependent upregulation of CD73 increases extracellular adenosine release to mediate immune suppression in TNBC. *Front Immunol* (2022) 13(September):982821. doi: 10.3389/fimmu.2022.982821

26. Vigano S, Alatzoglou D, Irving M, Ménétrier-Caux C, Caux C, Romero P, et al. Targeting adenosine in cancer immunotherapy to enhance T-cell function. *Front Immunol* (2019) 10(June):925. doi: 10.3389/fimmu.2019.00925

27. Stanton SE, Disis ML. Clinical significance of tumor-infiltrating lymphocytes in breast cancer. *J ImmunoTher Cancer* (2016) 4:59. doi: 10.1186/s40425-016-0165-6

28. Sandholm J, Kauppila JH, Pressey C, Tuomela J, Jukkola-Vuorinen A, Vaarala M, et al. Estrogen receptor-α and sex steroid hormones regulate toll-like receptor-9 expression and invasive function in human breast cancer cells. *Breast Cancer Res Treat* (2012) 132(2):411–9. doi: 10.1007/s10549-011-1590-3

29. Martin M. Cutadapt removes adapter sequences from high-throughput sequencing reads. *EMBnet.journal* (2011) 17(1). doi: 10.14806/ej.17.1.200

30. Kim D, Langmead B, Salzberg SL. HISAT: a fast spliced aligner with low memory requirements. *Nat Methods* (2015) 12(4):357–60. doi: 10.1038/nmeth.3317

31. Pertea M, Pertea GM, Antonescu CM, Chang TC, Mendell JT, Salzberg SL. StringTie enables improved reconstruction of a transcriptome from RNA-seq reads. *Nat Biotechnol* (2015) 33(3):290–5. doi: 10.1038/nbt.3122

32. Love MI, Huber W, Anders S. Moderated estimation of fold change and dispersion for RNA-seq data with DESeq2. *Genome Biol* (2014) 15(12):550. doi: 10.1186/s13059-014-0550-8

33. Robinson MD, McCarthy DJ, Smyth GK. edgeR: a bioconductor package for differential expression analysis of digital gene expression data. *Bioinformatics* (2009) 26(1):139–40. doi: 10.1093/bioinformatics/btp616

34. Yegutkin GG, Henttinen T, Jalkanen S. Extracellular ATP formation on vascular endothelial cells is mediated by ecto-nucleotide kinase activities *via* phosphotransfer reactions. *FASEB J* (2001) 15(1):251–60. doi: 10.1096/fj.00-0268com

35. Berrueta L, Bergholz J, Munoz D, Muskaj I, Badger GJ, Shukla A, et al. Stretching reduces tumor growth in a mouse breast cancer model. *Sci Rep* (2018) 8(1):1–7. doi: 10.1038/s41598-018-26198-7

36. Bankhead P, Loughrey MB, Fernández JA, Dombrowski Y, McArt DG, Dunne PD, et al. QuPath: open source software for digital pathology image analysis. *Sci Rep* (2017) 7(1):1–7. doi: 10.1038/s41598-017-17204-5

37. Yin JJ, Selander K, Chirgwin JM, Dallas M, Grubbs BG, Wieser R, et al. TGF-β signaling blockade inhibits PTHrP secretion by breast cancer cells and bone metastases development. *J Clin Invest* (1999) 103(2):197–206. doi: 10.1172/JCI3523

38. du Sert NP, Hurst V, Ahluwalia A, Alam S, Avey MT, Baker M, et al. The arrive guidelines 2.0: updated guidelines for reporting animal research. *PloS Biol* (2020) 18(7):e3000410. doi: 10.1371/journal.pbio.3000410

39. Ge SX, Son EW, Yao R. iDEP: an integrated web application for differential expression and pathway analysis of RNA-seq data. *BMC Bioinf* (2018) 19(1):534. doi: 10.1186/s12859-018-2486-6

40. Vasan N, Baselga J, Hyman DM. A view on drug resistance in cancer. *Nature* (2019) 575:299–309. doi: 10.1038/s41586-019-1730-1

41. Shi JY, Gao Q, Wang ZC, Zhou J, Wang XY, Min ZH, et al. Margin-infiltrating CD20+ b cells display an atypical memory phenotype and correlate with favorable prognosis in hepatocellular carcinoma. *Clin Cancer Res* (2013) 19(21):5994–6005. doi: 10.1158/1078-0432.CCR-12-3497

42. Maglioco A, Machuca DG, Badano MN, Nannini P, Camerano GV, Costa H, et al. B cells inhibit the antitumor immunity against an established murine fibrosarcoma. *Oncol Lett* (2017) 13(5):3225–32. doi: 10.3892/ol.2017.5810

43. Ren Z, Guo J, Liao J, Luan Y, Liu Z, Sun Z, et al. CTLA-4 limits anti-CD20-mediated tumor regression. *Clin Cancer Res* (2017) 23(1):1932–201. doi: 10.1158/1078-0432.CCR-16-0040

44. Rennert G, Pinchev M, Gronich N, Saliba W, Flugelman A, Lavi I, et al. Oral bisphosphonates and improved survival of breast cancer. *Clin Cancer Res* (2017) 23(7):1684–9. doi: 10.1158/1078-0432.CCR-16-0547

45. Xing Y, Ren Zq, Jin R, Liu L, Pei Jp, Yu K. Therapeutic efficacy and mechanism of CD73-TGFβ dual-blockade in a mouse model of triple-negative breast cancer. *Acta Pharmacol Sin* (2022) 43(9):2410–8. doi: 10.1038/s41401-021-00840-z

46. Jin F, Qi J, Liu D, You Y, Shu G, Du Y, et al. Cancer-cell-biomimetic upconversion nanoparticles combining chemo-photodynamic therapy and CD73 blockade for metastatic triple-negative breast cancer. *J Control Release* (2021) 337:90–104. doi: 10.1016/j.jconrel.2021.07.021

47. Hoefert S, Sade Hoefert C, Munz A, Northoff H, Yuan A, Reichenmiller K, et al. Altered macrophagic THP-1 cell phagocytosis and migration in bisphosphonate-related osteonecrosis of the jaw (BRONJ). *Clin Oral Investig* (2016) 20(5):1043–54. doi: 10.1007/s00784-015-1584-3

48. Kaneko J, Okinaga T, Hikiji H, Ariyoshi W, Yoshiga D, Habu M, et al. Zoledronic acid exacerbates inflammation through M1 macrophage polarization. *Inflammation Regen* (2018) 38(1):16. doi: 10.1186/s41232-018-0074-9

49. Zhu W, Xu R, Du J, Fu Y, Li S, Zhang P, et al. Zoledronic acid promotes TLR-4-mediated M1 macrophage polarization in bisphosphonate-related osteonecrosis of the jaw. *FASEB J* (2019) 33(4):5208–19. doi: 10.1096/fj.201801791RR

50. Forte G, Sorrentino R, Montinaro A, Luciano A, Adcock IM, Maiolino P, et al. Inhibition of CD73 improves B cell-mediated anti-tumor immunity in a mouse model of melanoma. *J Immunol* (2012) 189(5):226–33. doi: 10.4049/jimmunol.1200744

51. Schuh E, Berer K, Mulazzani M, Feil K, Meinl I, Lahm H, et al. Features of human CD3+CD20+ T cells. *J Immunol* (2016) 197(4):1111–7. doi: 10.4049/jimmunol.1600089

52. Von Essen MR, Ammitzbøll C, Hansen RH, Petersen ERS, McWilliam O, Marquart HV, et al. Proinflammatory CD20+ T cells in the pathogenesis of multiple sclerosis. *Brain* (2019) 142(1):120–32. doi: 10.1093/brain/awy301

53. Tonti E, JiménezdeOya N, Galliverti G, Moseman EA, DiLucia P, Amabile A, et al. Bisphosphonates target B cells to enhance humoral immune responses. *Cell Rep* (2013) 5(2):323–30. doi: 10.1016/j.celrep.2013.09.004

54. Ribeiro JM, Rodrigues-Alves ML, Oliveira E, Guimarães PPG, Maria Murta Santi A, Teixeira-Carvalho A, et al. Pamidronate, a promising repositioning drug to treat leishmaniasis, displays antileishmanial and immunomodulatory potential. *Int Immunopharmacol* (2022) 110(May):108952. doi: 10.1016/j.intimp.2022.108952

55. Zugazagoitia J, Guedes C, Ponce S, Ferrer I, Molina-Pinelo S, Paz-Ares L. Current challenges in cancer treatment. *Clin Ther* (2016) 38(7):1551–66. doi: 10.1016/j.clinthera.2016.03.026

56. Jansson L, Holmdahl R. Estrogen-mediated immunosuppression in autoimmune diseases. *Inflammation Res* 47(7):290–301. doi: 10.1007/s000110050332

57. Liu YT, Sun ZJ. Turning cold tumors into hot tumors by improving T-cell infiltration. *Theranostics* (2021) 11(11):5365–5386. doi: 10.7150/thno.58390

58. Bruno TC. B cells to the forefront of immunotherapy. *Nature* (2020) 577 (7791):474–6. doi: 10.1038/d41586-019-03943-0

59. Burger JA, Wiestner A. Targeting B cell receptor signalling in cancer: preclinical and clinical advances. *Nat Rev Cancer* (2018) 18(3):148–67. doi: 10.1038/nrc.2017.121

60. Tokunaga R, Naseem M, Lo JH, Battaglin F, Soni S, Puccini A, et al. B cell and B cell-related pathways for novel cancer treatments. *Cancer Treat Rev* (2019) 73:10–19. doi: 10.1016/j.ctrv.2018.12.001

61. Kuroda H, Jamiyan T, Yamaguchi R, Kakumoto A, Abe A, Harada O, et al. Tumor-infiltrating B cells and T cells correlate with postoperative prognosis in triple-negative carcinoma of the breast. *BMC Cancer* (2021) 21(1):286. doi: 10.1186/s12885-021-08009-x

frontiers | Frontiers in Immunology

TYPE Original Research
PUBLISHED 11 September 2023
DOI 10.3389/fimmu.2023.1201632

OPEN ACCESS

EDITED BY
Ali Hafez El-Far,
Damanhour University, Egypt

REVIEWED BY
Min Yang,
Chinese Academy of Medical Sciences and Peking Union Medical College, China
Shilei Hao,
Chongqing University, China

*CORRESPONDENCE
Abdallah Badou
abdallah.badou@univh2c.ma;
a.badou@cm6.ma

†These authors have contributed equally to this work

RECEIVED 06 April 2023
ACCEPTED 21 August 2023
PUBLISHED 11 September 2023

CITATION
Zohair B, Chraa D, Rezouki I, Benthami H, Razzouki I, Elkarroumi M, Olive D, Karkouri M and Badou A (2023) The immune checkpoint adenosine 2A receptor is associated with aggressive clinical outcomes and reflects an immunosuppressive tumor microenvironment in human breast cancer. *Front. Immunol.* 14:1201632. doi: 10.3389/fimmu.2023.1201632

The immune checkpoint adenosine 2A receptor is associated with aggressive clinical outcomes and reflects an immunosuppressive tumor microenvironment in human breast cancer

Basma Zohair[1], Dounia Chraa[2†], Ibtissam Rezouki[1†], Hamza Benthami[1], Ibtissam Razzouki[3], Mohamed Elkarroumi[4], Daniel Olive[2], Mehdi Karkouri[3] and Abdallah Badou[1,5*]

[1]Immuno-Genetics and Human Pathology Laboratory (LIGEP), Faculty of Medicine and Pharmacy, Hassan II University, Casablanca, Morocco, [2]Team Immunity and Cancer, The Cancer Research Center of Marseille (CRCM), Inserm, 41068, CNRS, UMR7258, Paoli-Calmettes Institute, Aix-Marseille University, UM 105, Marseille, France, [3]Department of Pathological Anatomy, Ibn Rochd University Hospital Center, Casablanca, Morocco, [4]Mohamed VI Oncology Center, Ibn Rochd University Hospital Center, Casablanca, Morocco, [5]Mohammed VI Center for Research & Innovation, Rabat, Morocco and Mohammed VI University of Sciences and Health, Casablanca, Morocco

Background: The crosstalk between the immune system and cancer cells has aroused considerable interest over the past decades. To escape immune surveillance cancer cells evolve various strategies orchestrating tumor microenvironment. The discovery of the inhibitory immune checkpoints was a major breakthrough due to their crucial contribution to immune evasion. The A2AR receptor represents one of the most essential pathways within the TME. It is involved in several processes such as hypoxia, tumor progression, and chemoresistance. However, its clinical and immunological significance in human breast cancer remains elusive.

Methods: The mRNA expression and protein analysis were performed by RT-qPCR and immunohistochemistry. The log-rank (Mantel-Cox) test was used to estimate Kaplan-Meier analysis for overall survival. Using large-scale microarray data (METABRIC), digital cytometry was conducted to estimate cell abundance. Analysis was performed using RStudio software (7.8 + 2023.03.0) with EPIC, CIBERSORT, and ImmuneCellAI algorithms. Tumor purity, stromal and immune scores were calculated using the ESTIMATE computational method. Finally, analysis of gene set enrichment (GSEA) and the TISCH2 scRNA-seq database were carried out.

Results: Gene and protein analysis showed that A2AR was overexpressed in breast tumors and was significantly associated with high grade, elevated Ki-67, aggressive molecular and histological subtypes, as well as poor survival. On tumor infiltrating immune cells, A2AR was found to correlate positively with PD-1

and negatively with CTLA-4. On the other hand, our findings disclosed more profuse infiltration of protumoral cells such as M0 and M2 macrophages, Tregs, endothelial and exhausted CD8+ T cells within A2ARhigh tumors. According to the Single-Cell database, A2AR is expressed in malignant, stromal and immune cells. Moreover, it is related to tumor purity, stromal and immune scores. Our results also revealed that CD8+T cells from A2ARhigh patients exhibited an exhausted functional profile. Finally, GSEA analysis highlighted the association of A2AR with biological mechanisms involved in tumor escape and progression.

Conclusion: The present study is the first to elucidate the clinical and immunological relevance of A2AR in breast cancer patients. In light of these findings, A2AR could be deemed a promising therapeutic target to overcome immune evasion prevailing within the TME of breast cancer patients.

KEYWORDS

A2AR, PD-1, CTLA-4, tumor and immune microenvironment, immunosuppression, immune checkpoint, immunotherapy, breast cancer prognosis

1 Introduction

Despite considerable progress in cancer management, breast cancer remains a major public health concern given its high morbidity and mortality rate, with an estimated 2.3 million new cases and 685,000 deaths worldwide in 2020 (1, 2). Breast cancer accurately reflects intratumoral heterogeneity conditioning therapeutic strategy. While chemotherapy remains the backbone of treatment for triple-negative breast cancer (TNBC), endocrine and human epidermal growth factor receptor 2 (HER2) targeted therapies provide the gold standard for hormone receptor-positive (HR+) and HER2-positive (HER2+) tumors, respectively (3, 4). In addition to TNBC and HER2+ tumors' propensity for recurrence, early metastasis, and poor survival, patients harboring these stubborn tumors are prone to build-up conventional therapy resistance (3–15). Although chemotherapy is widely perceived as the mainstay of TNBC treatment, this therapeutic approach reflects a detrimental aspect with some clinical drawbacks. One of the adverse effects of chemotherapy involves growth promotion and activity of cancer cell intravasation niches, called tumor microenvironment of metastasis (TMEM), which endows the tumor with aggressive features and dramatically affects the clinical outcome of patients (16, 17). The success of immunotherapy in patients with immune-sensitive tumors has brought this treatment strategy to the forefront of current oncology breakthroughs (18–20). Therefore, immune checkpoint inhibitors (ICIs), notably anti-PD-1 and anti-CTLA-4 mAbs have received widespread interest over the past decade. However, despite the clinical benefit of ICIs in some tumor contexts, these have not been proven to be highly effective in TNBC and HER2+ patients (5, 18–22). Indeed, tumors appear to be able to overcome effects of ICIs through various strategies, including synergistic engagement of several immunosuppressive pathways (23). Interestingly, recent studies have reported compensatory upregulation of inhibitory immune checkpoints in patients receiving ICI therapy (24–26). Among these regulatory molecules, A2AR represents one of the most prominent and essential pathways in the TME. Known as a member of the G protein-coupled receptor (GPCR) family, this adenosine (ADO) receptor is expressed on nearly all immune cells (27).

As is the case with most solid tumors, 25% to 40% of invasive breast carcinomas are hallmarked by hypoxic areas driving extracellular ATP release with an overexpression of hypoxia-inducible factor-1 alpha (HIF-1α) (27, 28). The latter serves as a potent enhancer of CD39 and CD73 ectonucleotidase expression, which in turn mediate ATP, ADP, and AMP hydrolysis and consequently extracellular ADO accumulation (27, 29–31). Under physiological conditions, A2AR signaling upholds immune homeostasis to safeguard tissues against the onset of autoimmune

Abbreviations: A2AR, Adenosine 2A receptor; ADO, Adenosine; APC, Antigen presenting cells; CAR, Chimeric antigen receptors; CTLA-4, Cytotoxic T-lymphocyte-associated protein 4; DC, Dendritic cell; EMT, Epithelial-mesenchymal transition; ER, Estrogen receptor; ES, Enrichment Score; GAL-1, Galectin-1; GPCR, G protein-coupled receptor; GSEA, Gene Set Enrichment Analysis; GZMA, Granzyme A; GZMB, Granzyme B; HER2, Human epidermal growth factor receptor 2; HIF-1α, Hypoxia-inducible factor-1 alpha; HR+, Hormone receptor positive; ICIs, Immune checkpoint inhibitors; IFNγ, Interferon gamma; IL, Interleukin; LAG-3, Lymphocyte-activation gene 3; MDSC, Myeloid-derived suppressor cells; NES, Normalized Enrichment Score; NK, Natural killer cell; NPI, Nottingham Prognostic Index; PD-1, Programmed cell death protein 1; PD-L1, Programmed death-ligand 1; PR, Progesterone receptor; PRF1, Perforin-1; TCR, T-cell receptor; Teff, Effector T cell; TGFβ, Transforming growth factor beta; TIM-3, T-cell immunoglobulin and mucin-domain containing-3; TISCH, Tumor Immune Single-cell Hub 2; TME, Tumor microenvironment; TMEM, Tumor microenvironment of metastasis; TNBC, Triple-negative breast cancer; TNF, Tumor necrosis factor; Treg, Regulatory T cell; UMAP, Uniform Manifold Approximation and Projection; VEGF, Vascular endothelial growth factor; VISTA, V-domain Ig suppressor of T cell activation.

disorder (32, 33). Nevertheless, in the cancer setting, the stimulation of this receptor via its ligand ADO triggers signal transduction of cAMP/PKA/CREB pathway while damping that of NFκB and JAK/STAT to inhibit the antitumor function of immune cells (27, 34). Thus, A2AR impairs the proliferative potential, effector and cytotoxic activity, as well as CD8+T cell infiltration within the TME (35–38). The attenuation of A2AR-mediated TCR and CD28 signaling drives CD8+T cells into an exhausted state marked by altered production of IFNγ, PRF and GZMB with upregulation of inhibitory immune checkpoints including PD-1, CTLA-4, LAG-3 and TIM-3 (27, 39–41). A2AR engagement also acts by preventing the maturation, proliferation and cytotoxicity of NK cells, while impairing the neoantigen presentation ability of dendritic cells (DC) (38, 42, 43). Otherwise, the A2AR pathway strengthens the immunosuppressive behavior of protumoral immune cells by hindering macrophage-induced phagocytosis, improving myeloid-derived suppressor cells (MDSC) function and promoting Tregs and M2-like macrophage polarization (38, 44–46). The A2AR receptor may also impinge on the non-immune axis of the TME, inducing tumor growth, epithelial-mesenchymal transition (EMT), and angiogenesis, thereby contributing to metastasis (36, 47–51).

Gastric, colorectal, and renal carcinomas have provided evidence of the link and involvement of A2AR in the poor prognosis of cancer patients (47, 48, 52, 53). Genetic and pharmacological inhibition of this immunosuppressive pathway has shown significant efficacy reflected by tumor burden decrease and metastasis prevention in experimental models (36, 54, 55). In renal cell carcinoma, phase I results from the first clinical trial of A2AR antagonist exhibited durable clinical improvement with immune response restoration even in patients resistant or refractory to PD-1/PD-L1 inhibitors (56). Given the complexity and heterogeneity of breast tumors and the large proportion of non-responders to currently available ICIs, the aim of the present study was to investigate the clinical and immunological relevance of A2AR in human breast cancer.

2 Materials and methods

2.1 Patients and specimen collection

Our study workflow is illustrated in (Figure 1). The present study includes 62 patients with invasive breast carcinoma who underwent surgical treatment between 2018 and 2021. The age of patients ranged from 32 to 89 years, with an average of 51 years. A total of 124 fresh specimens consisting of tumor tissues (n = 62) and matched adjacent tissues (n = 62) from the same patients were collected immediately after surgical resection at the Mohamed VI Oncology Center, Ibn Rochd University Hospital Center, Casablanca, Morocco. Tissue samples harvested from the uninvaded area adjacent to the tumor served as a control. Estrogen receptor (ER), Progesterone receptor (PR) and HER2 status were determined by the pathologists according to the American Society of Clinical Oncology/College of American Pathologists (ASCO/CAP) guidelines. Scarff-Bloom-Richardson (SBR) grading and histological subtyping were evaluated following standard recommendations.

Eligible patients were selected based on the following criteria: patients diagnosed with invasive breast carcinoma who underwent mastectomy or conservative surgery, free and informed consent, available formalin-fixed, paraffin-embedded tissue blocks and patients with defined molecular subtypes (Luminal A, Luminal B, HER2+ or TNBC). However, the exclusion criteria include male patients, unavailability of free and informed consent, unavailability of matched control tissue and incomplete medical records.

2.2 METABRIC dataset acquisition and preprocessing

Transcriptomic and clinicopathological data of 1904 primary invasive breast carcinoma tumors were collected from the large-scale METABRIC (Molecular Taxonomy of Breast Cancer International Consortium) cohort. For this purpose, we exported (METABRIC, Nature 2012 & Nat communication 2016) dataset using the cBioPortal for Cancer Genomics interface (https://www.cbioportal.org/). Clinicopathological parameters included in data_clinical_patient.txt and data_clinical_sample.txt files were merged and mapped to the corresponding gene expression data. The transcriptome file comprises mRNA expression levels of 24,368 genes measured by the Illumina Human v3 microarray, log2 transformed and normalized. To predict the 10-year survival rate, Nottingham Prognostic Index (NPI) scores were converted and categorized into 4 prognostic groups: Excellent, Good, Moderate and Poor.

Only patients with complete transcriptomic data were included in this study. In contrast, male patients or those with incomplete data were excluded. All analyses were repeated several times independently by two investigators.

2.3 Total RNA extraction, reverse transcription and quantitative real-time PCR

Total RNA was extracted from 124 fresh biopsies (breast carcinoma and matched control tissue) using TRIzol reagent (Invitrogen, France), according to the manufacturer's instructions. After the estimation of total RNA concentration and quality by a NanoVueTM Plus spectrophotometer (GE Healthcare, UK), cDNA was synthesized from 0.5 µg of RNA included in a reaction mixture containing RNase-Free Water and Random Hexamer Primer (Bioline, France) and incubated at 70°C for 5 min. Afterward, Tetro reverse transcriptase buffer, RNase-free water, RNase inhibitor (Invitrogen, France), dNTP (10 mM), and Tetro reverse transcriptase enzyme (Bioline, France) were added, followed by incubation at 25°C for 10 min, then at 45°C for 30 min, and finally at 85°C for 5 min.

Real-time PCR was performed using SYBR Green PCR Master Mix (Thermo Fischer) on the Bio-Rad CFX96 Real-Time PCR

System. Specific primer pairs targeting each gene were used at 10 µM concentration. All experiments were carried out according to the following schedule: holding stage at 95°C for 10 min, followed by 40 cycles of denaturation at 95°C for 15 s, then annealing and extension at 60°C for 1 min. The specificity control of PCR reaction was applied after each experiment by analyzing the amplicon melting curves. A second specificity-checking was implemented by submitting the PCR product (the amplified cDNA) to agarose gel electrophoresis. Data were assessed as a relative mRNA expression using the housekeeping gene ß-actin and matched control tissue as internal controls. The relative quantification was computed using the $2^{-\Delta\Delta Ct}$ approach. Only the comparative analysis of tumor and matched control tissues was conducted by applying the $2^{-\Delta Ct}$ method.

Primer pairs used in this study:

Gene	Forward sequence	Reverse sequence
β-actin	5′- GAGATGGCCACGGCTGCTT-3′	5′-GCCACAGGACTCCATGCCCA-3′
ADORA2A	5'-ATCGCCATTGACCGCTACAT3-'	5'-GCTGACCGCAGTTGTTCCA-3'

2.4 Immunohistochemistry

Formalin-fixed, paraffin-embedded (FFPE) specimens from 45 invasive breast carcinoma and 10 matched control tissues were sectioned at an optimal thickness of 3-4 µm. Histologic sections were oven-dried at 60°C for one hour and then left at 37°C overnight prior to any treatment. The sections were then deparaffinized and rehydrated prior to heat-induced epitope unmasking using the PT Link system (Dako, Denmark). This antigen retrieval step was performed with a (low or high pH) solution providing a 3-in-1 pretreatment (EnVision Flex target retrieval solution low/high PH (× 50), Dako, Denmark). Samples were incubated with peroxidase-blocking reagent (EnVision flex peroxidase-blocking reagent, Dako, Denmark) for 5 min at room temperature and then rinsed with wash buffer (EnVision flex wash buffer, Dako, Denmark).

Thereafter, sections were incubated with the primary antibodies (A2AR clone 7F6-G5-A2 (Santa Cruz Biotechnology Inc.) at a 1:50 dilution, PD-1 clone DBM15.5 (Diagnostic BioSystems) at a 1:100 dilution and CTLA-4 clone F-8 (Santa Cruz Biotechnology Inc.) at a 1:500 dilution for 1 hour at room temperature. Negative control sections were incubated with Isotype control antibodies (Mouse IgG2a Isotype Control clone PPV-04 (OriGene) at a 1:500 dilution and Mouse IgG1 Isotype Control clone MOPC-21 (LSBio) at a 1:200 dilution for each sample. Otherwise, different positive control tissues were added for each primary antibody used. After washing, the secondary antibody (EnVision Flex/HRP, Dako, USA) was added and slides were incubated for 20 min at room temperature. The latter were then rinsed and incubated with a DAB substrate-chromogen solution (EnVision DAB+chromogen, Dako, USA) for 10 min.

Subsequently, slides were immersed in a hematoxylin bath for counterstaining and dehydrated in 3 ethanol baths (70%, 96%, and 100%). Finally, they were cleared in toluene baths and then

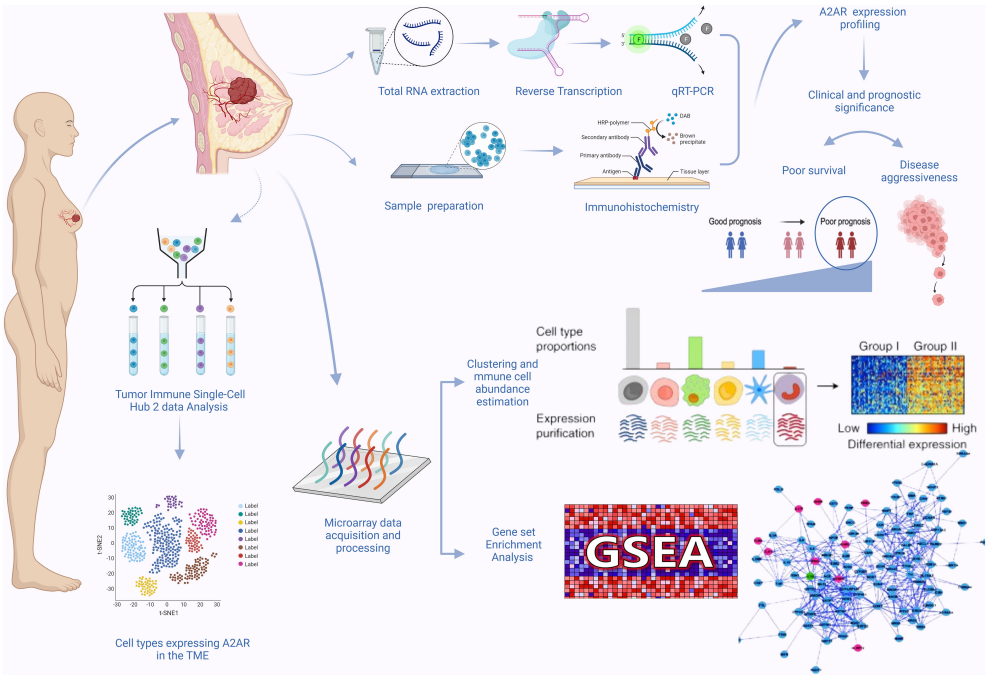

FIGURE 1
Graphical abstract.

mounted for reading under an Olympus light microscope (Olympus, Tokyo, Japan).

2.5 Immunostaining assessment and scoring system

Staining intensity, localization (membrane, cytoplasm, or nucleus), and percentage of labeled tumor, immune, and endothelial cells were evaluated by two independent pathologists. For gene expression analysis, a semi-quantitative assessment of immunostaining, presented as a Histoscore (H-score), was performed. This approach combines the intensity of staining and the percentage of labeled cells. Staining intensity was considered as negative (0), weak (1), intermediate (2) or strong (3). The H-score was calculated as follows: (1 x % of weak positive cells) + (2 x % of moderate positive cells) + (3 x % of strong positive cells). Thus, the expression level was ranged from 0 to 300.

2.6 Computational analysis of tumor-infiltrating immune cells

To assess the abundance of tumor infiltrating immune cells and to estimate tumor purity, stromal and immune scores, the computational deconvolution approach was performed using RStudio software version (7.8 + 2023.03.0) and four algorithms based on different immunological signatures: EPIC, CIBERSORT, ImmuneCellAI, and ESTIMATE. Prior to processing, the METABRIC transcriptomic dataset was standardized and converted into a non-log linear matrix. Then, according to A2AR gene expression and using the median as the cutoff, we stratified our cohort into two patient groups ($A2AR^{low}$ and $A2AR^{high}$).

2.7 Gene Set Enrichment Analysis (GSEA)

To investigate the key signaling pathways and biological processes linked to A2AR, we performed Gene Set Enrichment Analysis using RStudio software version (2023.03.0) and exploiting the three molecular signature databases: Hallmark, Curated and Ontology gene sets. Enriched terms with a false discovery rate (FDR) and a (p-nominal) < 0.05 are considered statistically significant.

2.8 A2AR exploration at single-cell resolution

The scRNA-seq Tumor Immune Single-cell Hub 2 (TISCH2) database is used to investigate the distribution of A2AR expression in different cell populations. The cell type annotation of three breast cancer datasets: BRCA_EMTAB8107, BRCA_GSE114727_10X and BRCA_Alex was arranged in two levels: Malignancy and Major Lineage. The manifold learning algorithm (UMAP) is adopted for dimension reduction. A2AR expression is explored in malignant, stromal and immune cells.

2.9 Statistical analysis

Statistical analysis, graphical representations and Heat map visualization were performedusing GraphPad Prism 8.0.1, RStudio software version 7.8, Morpheus (Broad Institute) and BioRender. For Overall survival, Kaplan–Meier analysis was estimated using the Log-rank (Mantel-Cox) test. To determine A2AR gene expression status, the median is used as a cutoff to stratify our METABRIC and experimental cohorts into $A2AR^{low}$ and $A2AR^{high}$ clusters. The non-parametric two-sided Wilcoxon signed rank test was applied for matched-pairs analysis. The Mann-Whitney rank test was conducted for unpaired analysis. Correlation coefficients were estimated with Pearson's r statistic. Analysis with a 2-sided P value less than 0.05 ($p < 0.05$) was considered statistically significant.

2.10 Study approval

All experiments were conducted in conformity with the principles set forth in the Helsinki declaration and approved by the Ethics Committee for Biomedical Research (CERB) of Ibn Rochd University Hospital Center, under the approval code (28/15). The free and informed consent form was signed by all subjects participating in this study. Medical records containing clinical and pathological data (age, stage, grade and histological and molecular subtypes) were obtained from the hospital pathology department.

METABRIC patients are anonymous and their data are publicly available. The authors of the original publication have obtained free informed consent from all participants (57), therefore, this part of the present study was exempt from Institutional Review Board approval requirements.

3 Results

3.1 Human breast tumor exhibit increased levels of A2AR compared to matched uninvaded control tissue

In order to highlight the clinical impact of A2AR and determine its eventual involvement in human breast tumorigenesis, a cohort of 62 invasive breast carcinoma patients with an average age of 51 years (ranging from 32 to 89 years) was included in this study. The mRNA relative expression of *ADORA2A* gene, encoding human A2AR was assessed by qRT-PCR in 124 fresh specimens. Comparative analysis of 62 tumor tissues and 62 matched control tissues revealed increased expression of A2AR in breast tumors (Figure 2A). To corroborate these findings, we evaluated A2AR expression at the protein level by performing immunohistochemical staining in tumor and matched control tissues from 10 patients. The IgG2a Isotype was used as a negative control, while the placenta and testis were included as positive control tissues (Figure 2C). Immunological labeling revealed membrane and cytoplasmic expression of A2AR protein in both immune and cancer cells (Figure 2D). Interestingly, quantification of A2AR H-score for

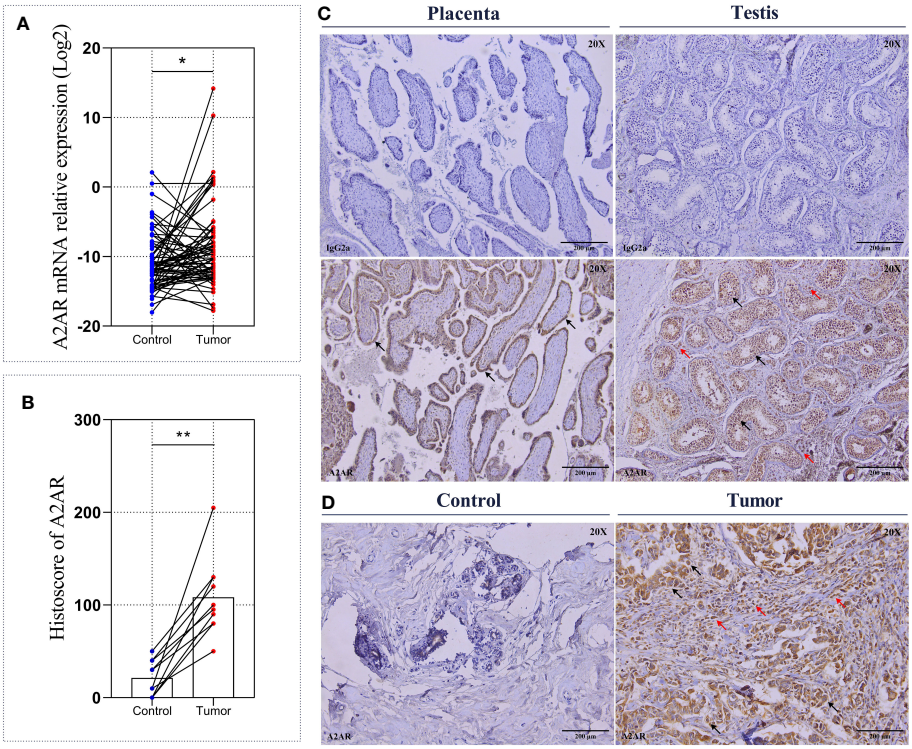

FIGURE 2
A2AR expression on breast tumors and matched control tissues. The A2AR expression level was measured by qRT-PCR and immunohistochemistry. **(A)** A2AR gene expression exhibits an elevated level in breast tumors compared to matched control tissues (p = 0.0176). **(C)** Representative immunohistochemical staining for A2AR and the IgG2a isotype (magnification20X, scale bar 200μm) in positive control tissues: Placenta (black arrows indicate tubular epithelial lining cells) and Testis (black arrows indicate germline cells at different development stages, and red arrows show Leydig cells). **(D)** A2AR staining showed membrane and cytoplasmic localization within both tumor and immune cells (black arrows indicate tumor cells, and red arrows show immune cells). **(B, D)** A2AR protein expression is more pronounced within tumors compared to matched control tissues (p = 0.0020). Significance was calculated using the Wilcoxon matched-pairs signed rank test. *p<0.05, **p<0.01.

each sample exhibited higher expression within the tumor compared to matched uninvaded control tissue (Figures 2B, D). These findings suggest that A2AR might potentially contribute to the pathogenesis of human breast cancer.

3.2 A2AR is associated with aggressive clinical features and predicts poor overall survival in breast cancer patients

Given the increased levels of A2AR within the mammary tumor, we aimed to explore its clinical value for our patients by investigating its association to well-established breast cancer prognostic features. The clinicopathological parameters of patients are summarized in (Table 1). In high-grade tumors (grade III), an overexpression of A2AR was detected by the transcriptional analysis (Figure 3A). Our findings further revealed an association with the most aggressive molecular subtypes, known for their poor prognosis, by showing a significant upregulation of our gene of interest in TNBC and HER2+ patients (Figure 3B). Estrogen and progesterone receptors and human epidermal growth factor status constitute independent risk factors which affect prognosis and predict response to immunotherapy. Consequently, the transcript-level study illustrated the association between A2AR and hormone receptor status with unfavorable prognosis (ER- and PR-) (Figures 3C, D). In contrast, analysis of HER2 status (Figure 3E) showed no significant difference in expression between groups. Ki-67 is another distinct parameter considered for decades as a prognostic marker related to disease aggressiveness (58). In order to evaluate A2AR expression according to the tumor proliferation index, we stratified our cohort into two groups, Ki-67^{low} (≤20%) and Ki-67^{high} (>20%). However, although Ki-67^{high} tumors seem to exhibit a strong A2AR transcript level trend (Figure 3F), the difference is not statistically significant.

The large-scale METABRIC dataset was also investigated to support the transcriptomic findings from our cohort. To this end, microarray expression data from 1904 patients with primary invasive breast carcinoma were explored. Patient clinicalpathological parameters are described in (Supplementary Table 1). Analysis of public data showed that A2AR is linked to ductal, lobular and mixed histological subtypes (Figure 4A). In accordance with the experimental cohort, High-grade tumors displayed increased A2AR expression (Figure 4B). As illustrated in (Figure 4D), the molecular subtyping of the METABRIC dataset included two additional subgroups (Normal and Claudin-low). In addition to its adverse prognosis, the latter represents a distinctly aggressive subgroup, related to stemness characteristics, downregulation of major cell junction components and activation of the EMT process during

TABLE 1 Clinicopathological parameters of the experimental cohort.

Clinicopathological parameters	Real-Time PCR		Immunohistochemistry	
	No.	(%)	No.	(%)
Histological grade				
Grade I	3	4.84	4	8.89
Grade II	31	50.00	17	37.78
Grade III	28	45.16	24	53.33
Molecular subtypes				
Luminal A	15	24.19	11	24.45
Luminal B	21	33.87	14	31.11
HER2+	12	19.36	10	22.22
TNBC	14	22.58	10	22.22
Estrogen receptor status (ER)				
ER+	36	58.06	24	53.33
ER-	26	41.94	21	46.67
Progesterone receptor status (PR)				
PR+	35	56.45	24	53.33
PR-	27	43.55	21	46.67
HER2 status				
HER2-	40	64.52	31	68.89
HER2+	22	35.48	14	31.11
Ki-67 proliferation index				
Ki-67 Low	11	24.44	14	31.11
Ki-67 High	34	75.56	31	68.89

HER-2, human epidermal growth factor receptor-2; TNBC, triple negative breast cancer; ER, estrogen receptor; PR, progesterone receptor.

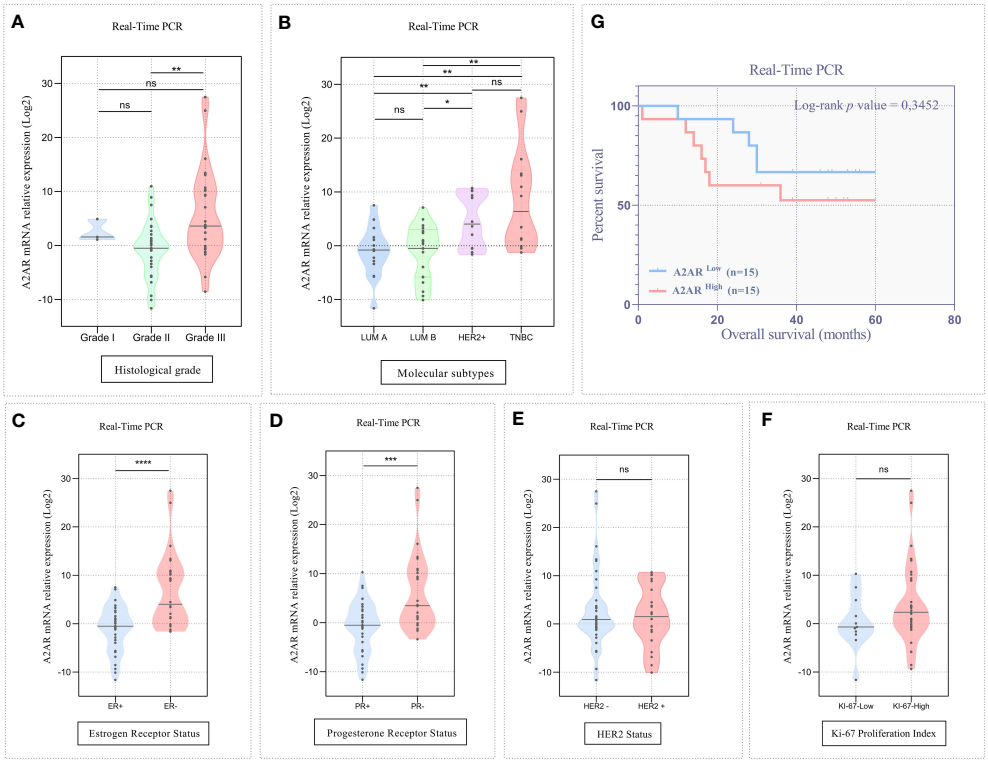

FIGURE 3
A2AR transcript level is linked to unfavorable clinicopathological outcomes. **(A, B)** The A2AR mRNA relative expression is significantly increased in high grade (grade II vs grade III: $p = 0.0019$), HER2+ (HER2+ vs LumA: $p = 0.0087$), (HER2+ vs LumB: $p = 0.0162$) and TNBC tumors (TNBC vs LumA: $p = 0.0011$), (TNBC vs LumB: $p = 0.0018$). **(C, D)** A2AR gene expression is strongly elevated in tumors with ER- ($p < 0,0001$), and PR- ($p = 0,0007$) status. **(E, F)** A2AR has no association with HER2 ($p = 0.9388$) status and KI-67 proliferation index ($p = 0.2130$). **(G)** Kaplan–Meier analysis reveals that A2AR gene expression is not related to survival ($p = 0.3452$). Significance was calculated using the Mann-Whitney and the Log-rank (Mantel-Cox) tests. *p<0.05, **p<0.01, ***p<0.001, ****p<0.0001, ns, not significant.

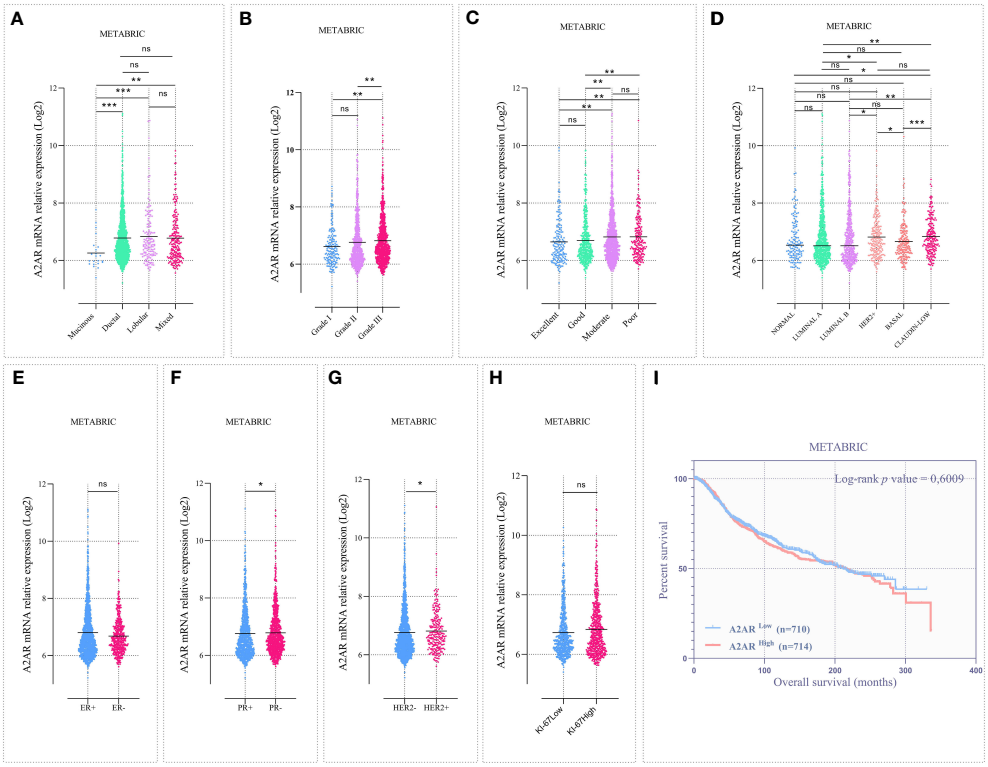

FIGURE 4
The A2AR gene expression is associated with aggressive clinical features in the METABRIC cohort. Microarray data from 1904 patients with invasive breast carcinoma were analyzed. **(A)** A2AR expression is downregulated in mucinous subtype tumors compared to ductal (p = 0.0002), lobular (p = 0.0005) and mixed (p = 0.0015). **(B)** A2AR is overexpressed in high-grade tumors compared to grade I (p = 0.0027) and grade II (p = 0.0064). **(C)** Patients presenting poor (poor vs excellent: p = 0.0067), (poor vs good: p = 0.0048) or moderate (moderate vs excellent: p = 0.0071), (moderate vs good: p = 0.0011) prognostic index exhibit high levels of A2AR transcripts. **(D)** Tumors with an aggressive subtype such as HER2+ (HER2+ vs. LumA: p = 0.0265), (HER2+ vs. LumB: p = 0.0204) and Claudin Low (Claudin Low vs. Normal: p = 0.0113), (Claudin Low vs. LumA: p = 0.0012), (Claudin Low vs. LumB: p = 0.0017) show increased A2AR expression. **(F, G)** A2AR gene level is linked to PR- (p = 0.0359) and HER2+ (p = 0.0160) status. **(E, H)** A2AR shows no association with ER (p = 0.6840) and Ki-67 (p = 0.0601) status. **(I)** Kaplan–Meier analysis reveals that A2AR gene expression is not related to survival (p = 0.6009). Significance was calculated using the Mann-Whitney and the Log-rank (Mantel-Cox) tests. *p<0.05, **p<0.01, ***p<0.001, ns, not significant.

tumor progression (59, 60). Interestingly, our data showed the association of A2AR with Claudin-low and HER2+ subtypes. Furthermore, A2AR mRNA levels was increased in patients exhibiting PR- and HER2+ status (Figures 4F, G), however, no significant difference was detected between groups of ER status and Ki-67 proliferation index (Figures 4E, H).

Although the management of breast cancer is mainly based on well-defined clinical features, this pathology is characterized by an extremely complex and heterogeneous molecular profile. Therefore, the NPI was established to predict the clinical outcome of patients (prediction of 10-year survival after surgery). This prognostic index is widely used in clinical practice and has undergone prospective validation after long-term follow-up in large multicentric studies. The NPI is computed by combining three histopathological criteria (grade and size of tumor and lymph node invasion). Consequently, we performed the NPI analysis by stratifying the cohort into 4 prognostic groups. Thus, we showed that A2AR was linked to patients with moderate to poor survival prediction (Figure 4C).

To substantiate these findings, we further analyzed the expression of our molecule of interest at the protein level by immunohistochemistry. Immunological staining was performed on tumor specimens from 45 patients. For each sample, H-score of cancer cells and tumor-infiltrating immune cells were estimated independently. Consistent with the transcriptomic data, A2AR expression on tumor-infiltrating immune cells was significantly associated with ER- and PR- status (Figures 5C, D), HER2+ and TNBC molecular subtypes (Figures 5A, G), as well as high tumor grade (Figures 6A, B). However, A2AR was not associated with HER2 status (Figure 5E). Furthermore, in contrast to the transcriptomic data, immunohistochemical staining revealed increased levels of A2AR protein in Ki-67^{high} tumors (Figures 5B, F). This discrepancy between gene and protein expression profiles could be ascribed to an eventual post-transcriptional regulation. Surprisingly, the analysis of tumor cells did not show any association between A2AR and clinicopathological parameters.

Finally, we evaluated the prognostic value of A2AR by estimating overall survival. Accordingly, patients were stratified into two groups, A2AR^{low} and A2AR^{high}. Clustering was performed according to A2AR expression using the median as a cutoff. At the transcriptomic level, Kaplan-Meier analysis estimated by the Log-rank (Mantel-Cox) test showed no significant difference between groups in the experimental (Figure 3G) and METABRIC (Figure 4I) cohorts. Interestingly, at the protein level, survival curves reflect the association of A2AR with a worse prognosis. In

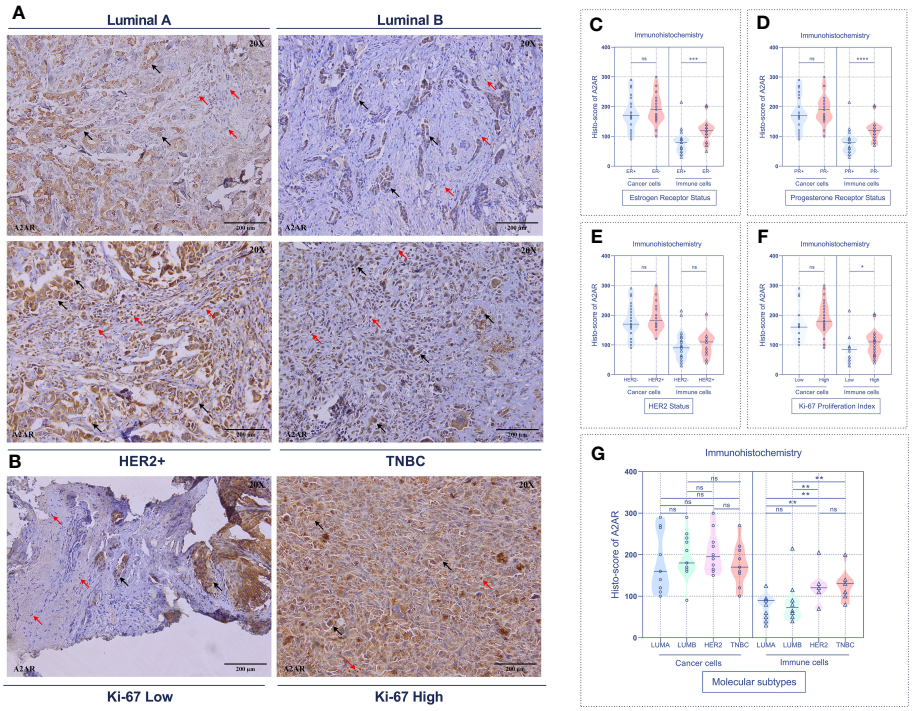

FIGURE 5
A2AR protein is associated with aggressive molecular subtypes and a high proliferation index. **(A, B)** Representative immunohistochemical staining (magnification 20X, scale bar 200μm) showing A2AR expression according to molecular subtypes and Ki-67 proliferation index status. **(C–F)** A2AR is overexpressed in immune cells from tumors with status: ER- ($p = 0.0003$), PR- ($p < 0.0001$) and high Ki-67 proliferation index ($p = 0.0473$). **(G)** A2AR is highly expressed in immune cells of HER2+ (HER2+ vs. LumA: $p = 0.0073$), (HER2+ vs. LumB: $p = 0.0054$) and TNBC (TNBC vs. LumA: $p = 0.0032$), (TNBC vs. LumB: $p = 0.0035$) tumors. Significance was calculated using the Mann-Whitney test. Black arrows indicate tumor cells. Red arrows show immune cells. *p<0.05, **p<0.01, ***p<0.001, ****p<0.0001, ns, not significant.

fact, $A2AR^{high}$ patients exhibit poor overall survival compared to the $A2AR^{low}$ group (Figure 6C). Therefore, our findings illustrate the prognostic impact of A2AR expression by predicting adverse clinical outcomes and negatively affecting the overall survival of breast cancer patients. In this regard, it should be emphasized that A2AR might be involved in breast cancer progression and aggressiveness mainly through the immunological process.

3.3 A2AR is remarkably correlated with PD-1 and CTLA-4 inhibitory immune checkpoints

Admittedly, in some tumor contexts, most notably melanoma, ICIs have proved to be considerably effective by achieving more durable antitumor responses than conventional therapies. Nevertheless, they have not been successful in breast cancer management, particularly for HER2+ and TNBC cancers, which are defined as immunogenic tumors. Indeed, only a restricted subset of metastatic TNBC is responsive to these immunotherapeutic agents with an overall response rate reaching 10%. Several studies have provided compelling evidence for the involvement of compensatory and synergistic immune checkpoint mechanisms in ICI monotherapy resistance. In this regard, we aimed to investigate the correlation of A2AR with PD-1 and CTLA-4 regulatory proteins to identify the potential interplay between these immunological pathways and consequently emphasize the relevance of combined therapy in human breast cancer. As a first result, our immunohistochemical analysis revealed that among these three regulators, A2AR protein exhibit the strongest expression in human breast tumor infiltrating immune cells (Figures 7A, B). Subsequently, Pearson's coefficient showed a positive correlation between A2AR and PD-1 protein (Figure 7C). However, as depicted in (Figure 7D), our protein of interest displays a negative correlation with CTLA-4. Taken together, these findings imply that the prevailing immunosuppression within the mammary TME may be more related to the immunosuppressive effect of A2AR and an eventual interplays with PD-1 and CTLA-4 checkpoints might exist. Therefore, we suggest that precision immunotherapy management in breast cancer requires a careful focus on the status of different immunological biomarker expression.

3.4 A2AR is closely linked to the biological processes underlying tumorigenesis and breast cancer progression

After shedding light on the clinical and prognostic relevance of A2AR in breast cancer, we attempted to assess its probable involvement in tumor pathogenesis. In this regard, we performed

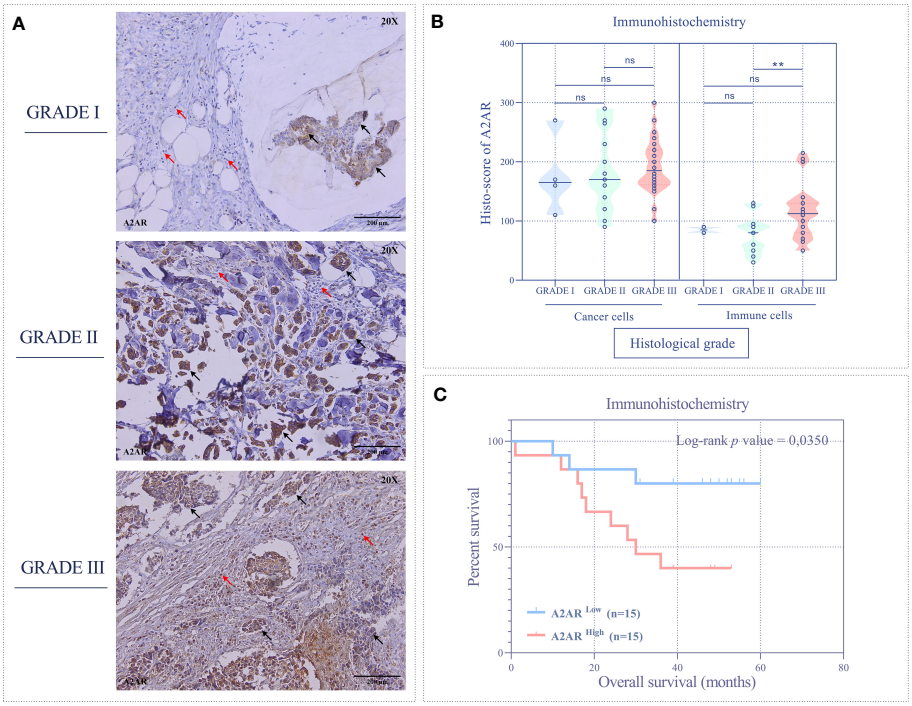

FIGURE 6
The A2AR protein is associated with high grade and predicts poor survival. **(A)** Representative immunohistochemical staining (magnification 20X, scale bar 200µm) of A2AR according to different histological grades. **(B)** A2AR shows high expression in immune cells from high-grade tumors (grade III) compared to those from grade II (p = 0.0054). **(C)** Patients overexpressing A2AR (A2AR^{high}) predict poor overall survival (p = 0.0350). Significance was calculated using the Mann-Whitney and the Log-rank (Mantel-Cox) tests. Black arrows indicate tumor cells. Red arrows show immune cells. **p<0.01, ns, not significant.

Gene Set Enrichment Analysis (GSEA) to decipher the biological functions and mechanisms implicated in cancer development and progression. According to the Normalized Enrichment Score (NES), analysis of three human molecular signature databases (Hallmark, Curated and Ontology) revealed that the A2AR^{high} phenotype is mainly concentrated in a panoply of gene sets related to oncogenesis and tumor progression (Figure 8C). As illustrated in (Figures 8A, B), the A2AR is linked to the invasive breast cancer signature, oncogenic and angiogenic signaling pathways (Myc, VEGF and IL6-JAK-STAT3) as well as proliferation, metastasis, hypoxia, adhesion and cell cycle processes (Rac1 GTPASE cycle). In light of these results, A2AR could be a key mediator in the development and progression of human breast cancer.

3.5 A2AR^{high} TME exhibits profuse infiltration of protumoral cells and an upregulation of immunosuppressive molecular mediators

In breast cancer, the immune profile of TME plays a critical role in the establishment of patient prognosis and response to immunotherapy. Mellman et al. have provided an overview of the immunologic background for each tumor phenotype. Indeed, tumors exhibiting an immune-inflamed profile testify to a pre-existing immune response marked by upregulation of inhibitory factors and protumoral cell infiltration. Therefore, patients harboring these tumors are more prone to respond to immunotherapy. Since our immunohistochemical analysis revealed an increased prevalence of A2AR in breast tumor infiltrating immune cells, we speculated that A2AR might represent a prominent mediator influencing the composition and abundance of the immune infiltrate. For this purpose, we performed a computational analysis to explore the immune profile of A2AR-related TME, by investigating the composition and abundance of several immune cell subsets in the 1904 patients of METABRIC cohort. To strengthen the validity of our results, the analysis is performed using four different deconvolution algorithms. First, the immune signature of the computational algorithm (EPIC) was used to estimate the proportions of immune and cancer cells (Figure 9A). The results show increased infiltration of B cells, CD4+ T cells, NK, macrophages and Endothelial cells within the A2AR^{high} TME. However, CD8+ T cells are significantly more abundant in A2AR^{low} tumors. Subsequently, we used the CIBERSORT (Figure 9B) and ImmuneCellAI (Figures 9C–E) algorithms to obtain a complete and integrated view of the different cell sub-populations and to identify which cell subsets CD4+, TCD8+, NK, DC and T macrophages infiltrate the A2AR^{high} TME. Interestingly, patients with A2AR^{high} TME displayed profuse infiltration of M0 and M2 macrophages, Treg, Tr1, nTreg, iTreg, T CD4+ memory resting cells, B cells, T γδ, T CD4+ naive, Th1, Th2, Th17, Tfh, Tcm and exhausted T CD8+ cells. However, DC, monocytes, activated

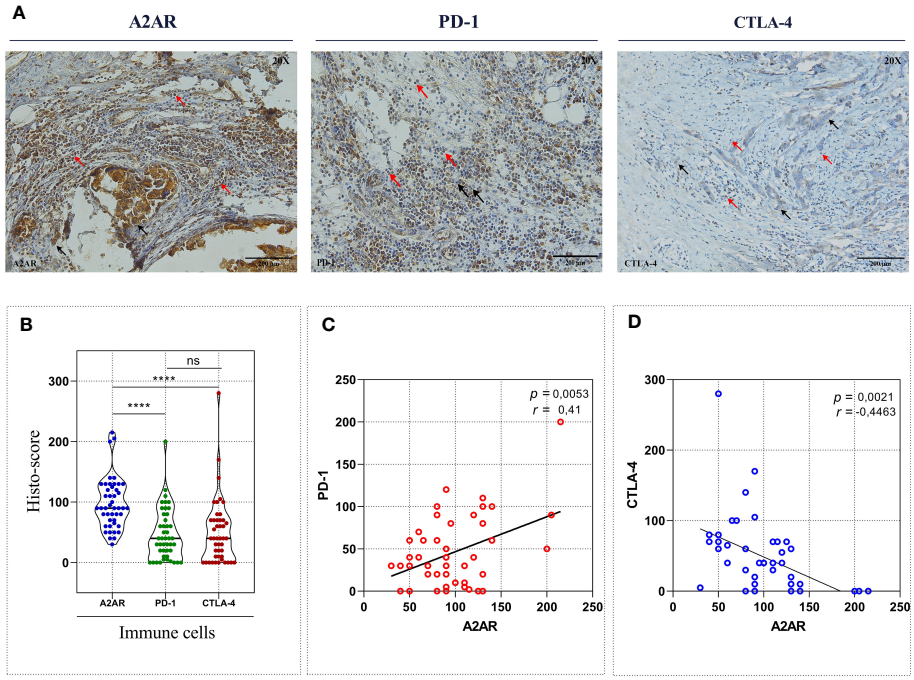

FIGURE 7
A2AR exhibits a significant correlation with PD-1 and CTLA-4 inhibitory immune checkpoint molecules. **(A)** Representative Immunohistochemical staining of A2AR, PD-1 and CTLA-4 (magnification 20X, scale bar 200μm). **(B)** A2AR protein seems to have the strongest expression compared to PD-1 ($p < 0.0001$) and CTLA-4 ($p < 0.0001$). **(C, D)** The expression of A2AR correlated positively with PD-1 ($p = 0.0053$, r = 0.41) and negatively with CTLA-4 ($p = 0.0021$, r = -0.44). Statistical difference was calculated using the Wilcoxon matched-pairs signed rank test. Pearson's rank coefficient was used for correlation. Black arrows indicate tumor cells. Red arrows show immune cells. ****p<0.0001, ns, not significant.

NK, NKT, neutrophils, MAIT, effector memory and naive CD8+ T cells appear to be more abundant in $A2AR^{low}$ tumors.

In order to estimate the stromal and immune score and to predict tumor purity, we applied the ESTIMATE enrichment test (Figures 9F, G). $A2AR^{hight}$ tumors exhibit high stromal and immune scores. The ESTIMATE score, which represents the non-tumoral component, was also found to be high in this group of patients. Meanwhile, $A2AR^{high}$ TME show lower tumor purity than $A2AR^{low}$ group.

After investigating the cellular components linked to A2AR, we attempted to pinpoint the functional state of CD8+T cells from patients overexpressing this gene ($A2AR^{high}$ CD8+T cells). Expression of effector and cytotoxic molecules (IFNγ, GZMA, GZMB, and PRF1) and inhibitory immune regulators (PD-1, PD-L1, CTLA-4, TIM-3, LAG-3, and VISTA) was assessed. As depicted in (Figure 9H), $A2AR^{high}$ CD8+T cells weakly express IFNγ, GZMA, GZMB and PRF1. In contrast, PD-1, CTLA-4, LAG-3, and VISTA exhibit an upregulation in the same group of cells (Figure 9I). Therefore, A2AR may also affect the functional state of intratumoral CD8+T cells.

To further elucidate the relevance of A2AR in TME regulation, we also investigated the pivotal molecular mediators involved in immunosuppression and tumor progression. We therefore assessed the correlation of A2AR with inhibitory immune checkpoints (Figures 10A, B) and chemokines (Figures 10C, D) involved in the attraction and polarization towards tolerogenic and protumoral cell sub-sets. Thus, A2AR was associated and positively correlated with these immunoregulatory molecules, including the immune checkpoints PD-1, CTLA-4, BTLA, LAG-3, TIGIT, VTCN-1, PD-L1, CD-47 and GAL-9, as well as the chemokines CCL-22, CXCL-13, CCL-5, CCL-17, CCR-4 and CCL-25.

In light of these results, this part of our work illustrates the potential involvement of A2AR in the establishment of the immunosuppressive TME, which is characterized by a pro-tumor cellular component, low tumor purity and an upregulation of major immunosuppressive molecular mediators.

3.6 A2AR tends to be prominently expressed on Tregs and exhausted CD8+ T cells

To decipher A2AR-expressing cells in the TME, we used the Tumor Immune Single-cell Hub 2 (TISCH2) database. For this purpose, three breast cancer datasets; BRCA_EMTAB8107 (Figures 11A, B), BRCA_GSE114727_10X (Figures 11C, D) and BRCA_Alex (Figures 11E, F), were analyzed. As a first result, A2AR seems to be expressed more in immune cells than in malignant and stromal cells. Subsequently, major lineage data showed that among the different cell populations analyzed, A2AR tends to be prominently expressed on Tregs and exhausted CD8+ T cells. These findings further underscore the potential contribution of A2AR to the immunosuppressive process.

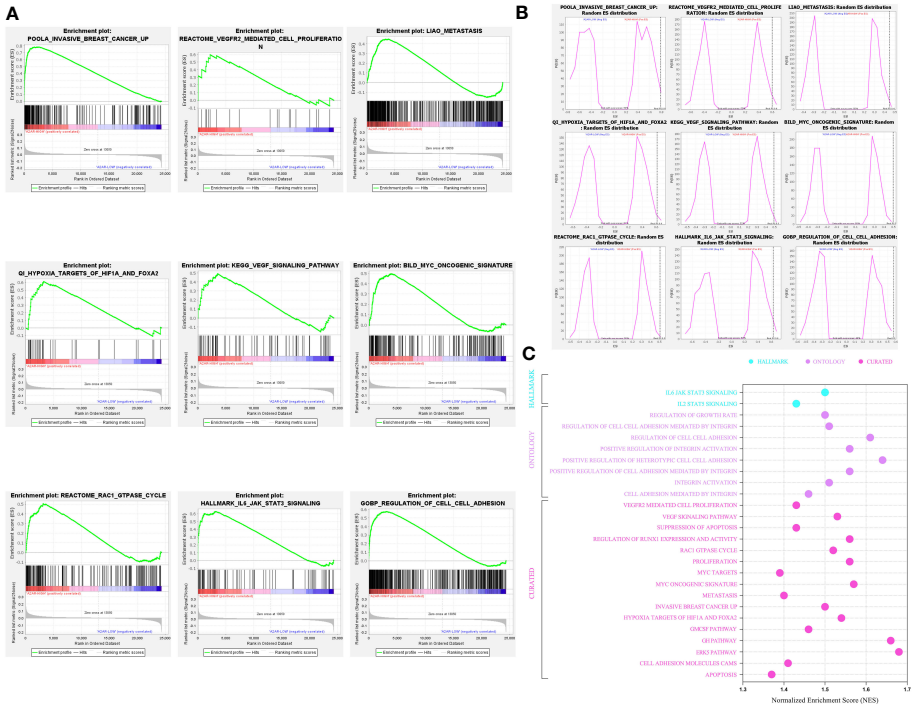

FIGURE 8
A2AR association with signaling pathways and biological functions involved in breast cancer pathogenesis revealed by Gene Set Enrichment Analysis. **(A)** Gene Set Enrichment Analysis (GSEA) plots illustrate statistically significant and concordant differences in an *a priori* defined set of genes reflecting various biological processes, between $A2AR^{Low}$ and $A2AR^{High}$ clusters. The Plots depict the key pathways implicated in breast cancer development and progression which are positively enriched in $A2AR^{High}$ patients. **(B)** Random ES (Enrichment Score) distribution based on the previous nine enrichment plots. **(C)** The major significant pathways involved in proliferation, invasion, angiogenesis, and metastasis are illustrated in the bubble plot. Hallmark, Ontology and Curated gene sets were exploited as molecular signatures. Enriched terms with a false discovery rate (FDR) and (p-nominal) < 0.05 are considered statistically significant. ES, Enrichment Score; NES, Normalized Enrichment Score.

3.7 A2AR is involved in immune tolerance and tumor escape processes

To further substantiate the protumoral aspect of $A2AR^{high}$ TME, we assessed their immunoregulatory impact using GSEA enrichment analysis. As illustrated in (Figure 12B), a wide range of immunosuppression and tumor escape-related gene-sets is positively enriched in $A2AR^{high}$ TME. These pathways mainly involve the dysfunction and downregulation of T cell proliferation, impaired antigen-specific response, reduced natural killer cell count, upregulation of IL-17 production, tumor escape and tolerogenicity (Figure 12A, Supplementary Figure 1).

Therefore we can suggest that A2AR represents a potent immunosuppression mediator and a promising target for immunotherapy to overcome the immune evasion prevalent in human breast cancer.

4 Discussion

The TME reflects a dynamic network wherein tumor and immune cells interplay is strictly mediated by molecular effectors promoting tumor progression (61, 62). The main constraint for breast cancer to elicit an effective antitumor response resides in its highly immunosuppressive profile. Immune evasion constitutes a critical step in breast tumor progression, where inhibitory immune checkpoint molecules represent a crucial protumoral mediator (63, 64). Thus, to overcome and defeat immune escape, the ICIs targeting PD-1 and CTLA-4 have been conceived as an emerging immunotherapeutic strategy. This treatment approach has proven promising, however, efficient and long-lasting responses occur among a restricted group of patients (65). In this regard, Atezolizumab (anti-PD-L1), the only FDA-approved immunotherapeutic agent for breast cancer is unfortunately limited to metastatic TNBC (66). The unresponsiveness to current ICIs could be ascribed to the post-therapeutic upregulation of other compensatory immune checkpoints such as A2AR (56, 67, 68). This mechanism is often adopted by tumors to counterbalance and offset the immunosuppressive effect of the blocked molecule (69). Furthermore, one third of invasive breast cancers exhibit hypoxic TME, which could promote the HIF-1α-A2A-adenosinergic pathway, and consequently the establishment of immunosuppression (70, 71). All these facts sparked our interest in bringing to light the clinical and prognostic relevance of A2AR and its related immunological profile in breast cancer. Accordingly, the first part of this work focused on transcriptomic and proteomic analysis in two distinct breast cancer cohorts. Our experimental study revealed that breast tumors exhibited increased levels of A2AR transcript compared to uninvaded control tissues. This overexpression was related to high grade, ER- and PR- status as

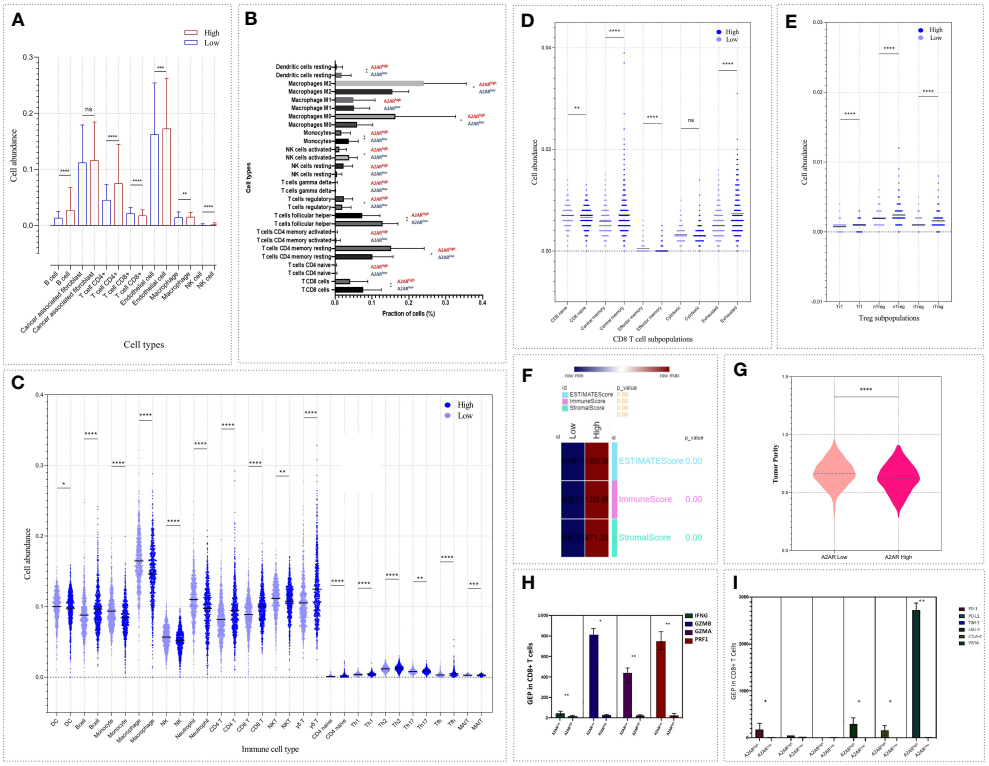

FIGURE 9
The abundance of cell populations infiltrating the TME reflects an immunosuppressive pattern of A2AR^{high} breast tumors. Four algorithms based on different immune signatures were exploited to analyze the differential distribution of immune cell fractions and tumor purity, ESTIMATE, stromal and immune scores between both groups of patients (A2AR^{low} and A2AR^{high}). **(A)** EPIC. **(B)** CIBERSORT. **(C–E)** ImmuneCellAI. **(F, G)** ESTIMATE. **(H)** Bar chart illustrating gene expression of IFNγ, GZMA, GZMB and PRF1 between CD8+ T cells from A2AR^{high} and A2AR^{low} patients. Cells from A2AR^{high} patients show decreased expression of effector and cytotoxic molecules. **(I)** Bar chart depicting the up-regulation of the inhibitory immune checkpoint molecules such as PD-1, LAG-3, CTLA-4 and VISTA on CD8+ T cells from A2AR^{high} patients. Significance was calculated using the Mann-Whitney rank test. *p<0.05, **p<0.01, ***p<0.001, ****p<0.0001, ns, not significant.

well as HER2+ and TNBC molecular subtypes. Protein analysis has supported the transcript level results with an additional association to the Ki-67 proliferation index. Nevertheless, this observation was noted exclusively in immune cells, hinting that A2AR severely affects patient clinical prognosis probably via the immune axis regulation. These findings were confirmed by METABRIC cohort, wherein A2AR expression was associated with high grade, aggressive histological subtypes, as well as PR- and HER2+ status. Interestingly, in addition to HER2+ molecular subtype, a strong expression of this inhibitory receptor was observed in Claudin-low tumors. The latter represents a group of patients who manifest poor survival (59). Moreover, the Nottingham Prognostic Index reported that patients predicting short 10-year survival displayed high levels of A2AR. Kaplan-Meier analysis further demonstrated the prognostic significance of A2AR by showing its association with worse survival in breast cancer patients. In gastric and colorectal cancers, A2AR protein appears to be overexpressed with a correlation to disease progression and reduced survival (48, 53). Head and neck squamous cell carcinoma samples also showed elevated expression of this protein, which was linked to advanced pathologic grade, larger tumor size, positive lymph node status, recurrence, and poor survival (47). Similar results were observed in renal cell carcinoma where A2AR was associated with metastatic profiles. It was also found that patients with A2AR^{high} status did not respond efficiently to anti-VEGF or anti-PD-1 monotherapy as well as to combined therapy with anti-PD-1 and anti-CTLA-4 (52). In agreement with our findings, all these observations testify to the aggressive clinical outcomes and poor prognosis of A2AR elevated expression in cancer.

Although ICIs monotherapy has emerged as an appealing strategy, the synergistic effect of multi-targeted blockade has brought considerably superior benefits (39, 67, 72–74). In fact, the relevance of combined therapy mirrors the cooperative interaction between negative regulators, which simultaneously collaborate to achieve immune tolerance (26, 52, 73, 75). Co-inhibition of A2AR and PD-1 or CTLA-4 has been investigated in several types of cancer and proven promising for the clinical application (39, 67, 72). However, the potential interplay between A2AR and PD-1 or CTLA-4 has not yet been elucidated in human breast cancer. In this regard, we have explored the correlation between A2AR and these two inhibitory receptors in the mammary TME. As a first observation, compared to PD-1 and CTLA-4, A2AR appears as the most highly expressed protein in breast cancer tumors. This could imply that the immunosuppression occurring in breast TME might be further orchestrated by A2AR pathway. As expected, our experimental

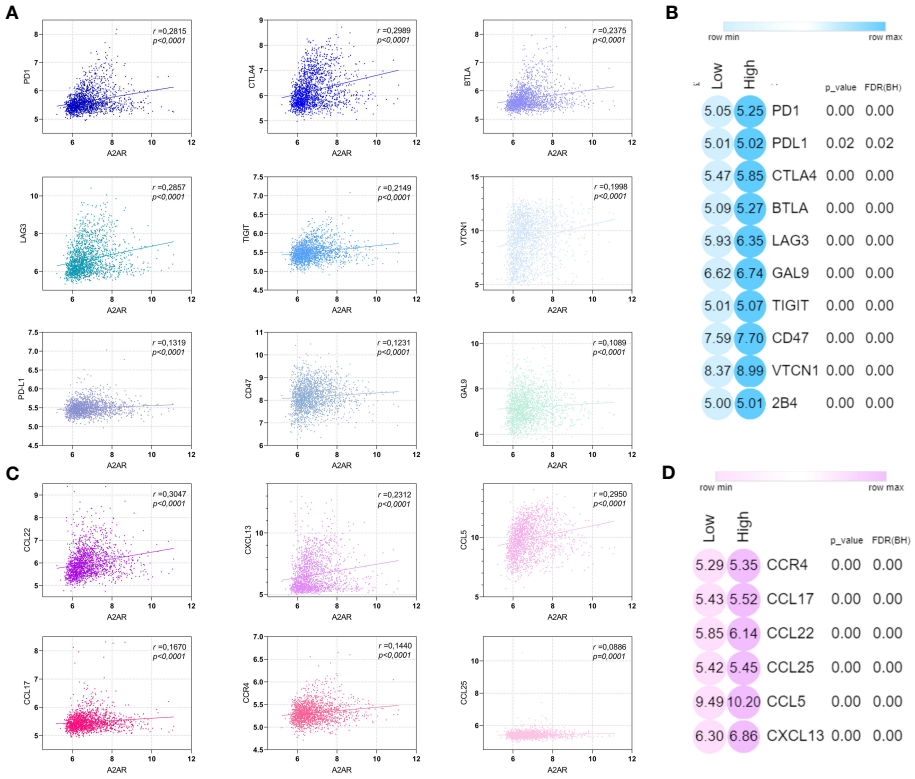

FIGURE 10
A2AR is positively correlated with immunosuppressive and protumoral molecular mediators. **(A, C)** A2AR exhibits a significant positive correlation with inhibitory immune checkpoint and immunosuppressive chemokines. **(B, D)** Heat maps illustrating the upregulation of inhibitory immune checkpoint and immunosuppressive chemokine in breast cancer patients overexpressing A2AR. Statistical difference was calculated using the Mann-Whitney rank test. Pearson's rank coefficient was used for correlation.

results also revealed the positive correlation between A2AR and PD-1. Therefore, we can speculate that inherent interdependence may exist between these two receptors to synergistically amplify immune escape. Compared to single agent treatment, dual blockade of A2AR and PD-1 pathways exhibited a significant improvement in immune response restoration, tumor growth inhibition and survival in preclinical models of breast and colorectal cancer (39, 67, 74, 76). In metastatic renal cell carcinoma patients treated with anti-PD-1, increased A2AR expression was associated with poor treatment response and reduced survival (52). Accordingly, the phase 1/1b clinical trials conducted on refractory renal and non-small cell lung cancer patients reported that A2AR antagonism showed antitumor activity with clinical responses, even in patients resistant or refractory to prior anti-PD-1/PD-L1 treatment (56, 77). Otherwise, CD73/A2AR and PD-1/PD-L1 signaling was found to induce immunosuppressive TME in diffuse large B-cell lymphoma (78). Indeed, patients whose CD8+T cells co-express both A2AR and PD-1 had shorter overall and progression-free survival than those whose CD8+T cells solely express either A2AR or PD-1 (75). Furthermore, studies have shown that A2AR stimulation would impact the regulation of PD-1/PD-L1 pathway, thereby supporting the interactive relationship between these two immune checkpoints. As a matter of fact, A2AR activation upregulates PD-1 on tumor-specific CD8+T and Treg cells, whereas its inhibition decreases the expression of PD-L1 on myeloid APCs and PD-1 on both tumor-associated CD8+T and Tregs cells (74, 79, 80).

In turn, concomitant blockade of A2AR and CTLA-4 also proved quite beneficial in various experimental models. A2AR antagonism was proven to significantly enhance the antitumor activity of anti-CTLA-4 in colorectal, renal, melanoma, prostate and metastatic breast cancer models (39, 72–74). It has been reported that co-targeting these two immunosuppressive pathways exhibited improved immune response with prolonged survival, whereas monotherapy showed partial efficacy (39, 72, 73). We therefore investigated the correlation between A2AR and CTLA-4 expression in our breast cancer patients. Surprisingly, in contrast to PD-1, we found that A2AR is negatively correlated with CTLA-4. Indeed, many studies have revealed that down-regulation of immune checkpoint molecules could induce the compensatory expression and stimulation of other immunosuppressive pathways. PD-1 deficient mice were found to overexpress the CTLA-4 protein (26, 81). Meanwhile, inhibition of CTLA-4 also results in upregulation of PD-1 and adenosinergic genes (72, 81). Consequently, we can suggest that the cooperative mechanism of immune checkpoints does not always rely on concomitant action, but also on compensatory feedback loops.

The composition of tumor-infiltrating immune cells is of major prognostic relevance, given its key role in disease growth and

10.3389/fimmu.2023.1201632

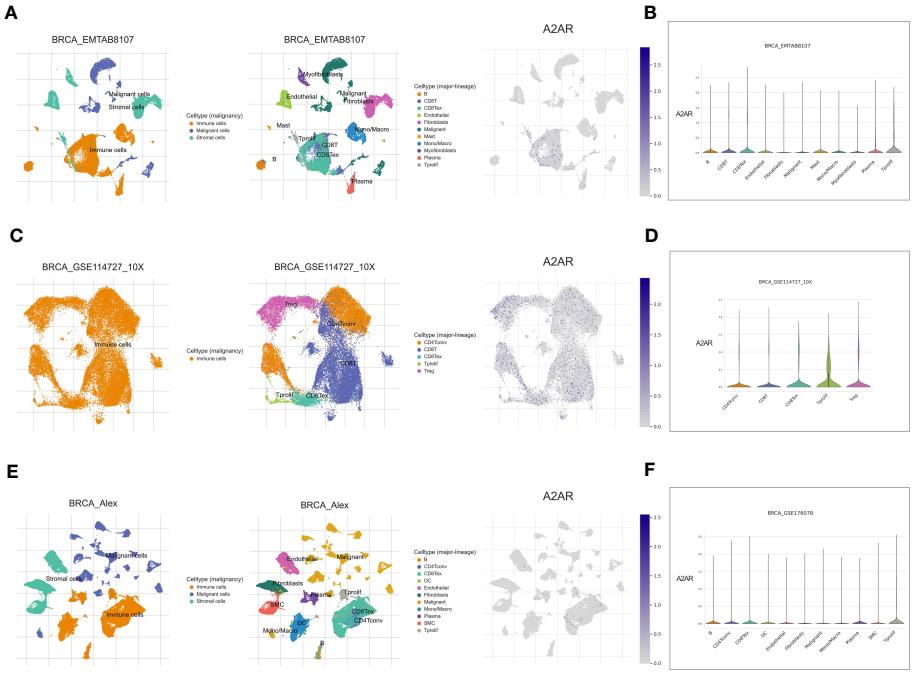

FIGURE 11
A2AR gene expression in breast TME at single-cell resolution. Analysis is performed using the Tumor Immune Single-cell Hub 2 (TISCH2) scRNA-seq database. Cell type annotation for three datasets: BRCA_EMTAB8107, BRCA_GSE114727_10X, and BRCA_Alex are curated according to two clusters: malignancy and major-lineage. **(A, C, E)** The Uniform Manifold Approximation and Projection (UMAP) dimension reduction learning algorithm was used for interactive visualization of A2AR expression and exploration of cellular landscapes. **(B, D, F)** Violin plot illustrating the distribution of A2AR in different populations of malignant, immune and stromal cells.

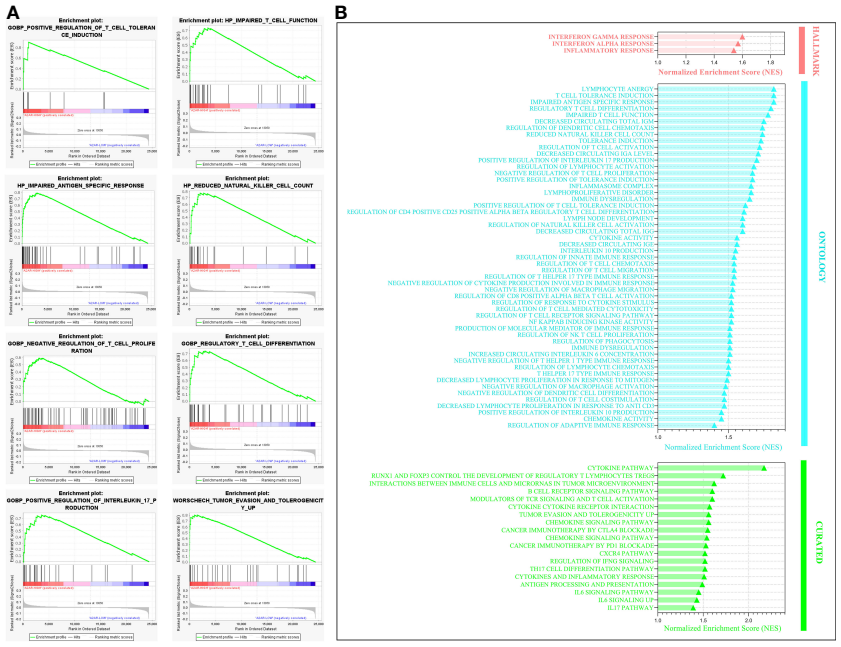

FIGURE 12
Gene set enrichment analysis illustrating the key immunosuppressive and tumor escape pathways enriched in A2AR^{high} patients. **(A)** Enrichment plot showing eight significant pathways involved in immune tolerance and key cellular effector dysfunction. **(B)** Bar chart of statistically significant immunoregulatory pathways that are positively enriched in A2AR^{High} patients. Hallmark, Ontology and Curated gene sets were exploited as molecular signatures. Enriched terms with a false discovery rate (FDR) and (p-nominal) < 0.05 are considered statistically significant. ES, Enrichment Score, NES, Normalized Enrichment Score.

development as well as response to treatment. The TME harbors different cell types, which can either favor tumor progression or conversely serve an antitumor function (62, 82). ESTIMATE, stromal and immune score computation revealed low tumor purity and abundant stromal and immune infiltration in $A2AR^{high}$ tumors. In fact, low tumor purity is an independent poor prognostic factor. Previous studies have shown the significant association of this tumor feature with short survival, early relapse, invasive and metastatic phenotype, EMT, upregulation of inhibitory immune checkpoints and immunosuppressive chemokines as well as high infiltration of protumoral cells, including M2 macrophages and Tregs (83, 84).

Subsequently, investigating the profile of tumor-infiltrating cell, we found that compared to the $A2AR^{low}$ phenotype, TME with a strong A2AR expression had an increased proportion of protumoral cells, including M0 and M2 macrophages, different subsets of Tregs (Tr1, nTreg and iTreg), exhausted T CD8+ cells and CD4+ memory resting T cells. The association between M0 macrophages and unfavorable patient prognosis has been illustrated in several tumor contexts. In breast cancer, a high fraction of this cell subset correlates positively with high grade, high Ki-67 proliferative index and poor overall and disease-free survival (85–89). Whereas the M2 phenotype has been shown to have proangiogenic activity promoting breast cancer metastasis and to be closely related to worse clinical outcomes (87, 89, 90). The polarization of monocytes into tolerogenic M2-like macrophages known for their weak proinflammatory effect could occur in response to A2AR stimulation. The protumoral behavior of this cell type lies in its high expression of IL-10, arginase 1, iNOS and VEGF with low expression of TNF and IL-12 cytokines (45, 91).

In turn, the frequency of Treg cells represents a useful hallmark for breast cancer prognosis. A higher fraction of Foxp3+ Tregs correlates positively with ER-, PR- and HER2+ status, nodal invasion and short survival (92, 93). However, the decrease in Treg abundance was associated with the complete pathological response in TNBC patients who underwent adjuvant chemotherapy (94). Taylor et al. reported that Tregs exhibit a substantial proportion of Claudin-low tumor-infiltrating lymphocytes. They have also shown that Tregs isolated from Claudin-low tumor-bearing mice display a strongly immunosuppressive function capable of inhibiting T cell proliferation and effector response (95). The activation of A2AR increases the intracellular rate of cAMP and HIF-1α in Tregs, which triggers the downstream signal transduction cascades leading to enhanced transcription of genes involved in Tregs development and function including; Foxp3, IL-10, TGFβ, GAL-1, PD-1, CTLA-4 and LAG-3 (46, 96–100). A2AR+Tregs are able to establish an immunosuppressed state of TME by upregulating CD39 and CD73 ectoenzymes, resulting in eADO release, which in turn induces inhibition of Teff lymphocytes (40, 46, 47, 97, 99). This eADO can also operate in an autocrine loop by feeding back to Tregs the transducing stimulus of rising intracellular cAMP via its A2AR receptor (97, 100). These observations were crowned by works of pharmacological blockade and gene silencing of A2AR in experimental models, highlighting the immunosuppressive impact of this receptor when expressed on Tregs (40, 47, 100).

Meanwhile, substantial abundance of CD4+ memory resting T cells is associated with unfavorable prognosis in gastric cancer (101). Nevertheless, prolonged survival and remarkable response to ICIs as well as increased tumor mutational burden and neoantigen load were observed in melanoma patients with a profuse infiltration of CD4+ memory activated T cells and a lower fraction of CD4+ memory resting T cells (102).

It is noteworthy that cell infiltrate analysis also portrays a reduced proportion of cells mediating antitumor activity, notably DC, activated NK, NKT and effector memory CD8+ T cells in $A2AR^{high}$ patients. It is clearly established that the presence of the above-mentioned cells within breast TME correlates positively with prolonged survival, prevention of metastatic progression and complete pathological response, consequently affording better prognosis for patients (103–109).

In NK cells, A2AR is regarded as an intrinsic negative regulator of the maturation and effective killing function of this cell type. Targeting this ADO-receptor results in reduced metastasis, improved tumor control and delayed tumor initiation in experimental models, by enhancing NK-mediated cytotoxic activity in a PRF1 and GZMB-dependent manner (42, 110). Furthermore, during infection and cancer, A2AR engagement seems to inhibit via IL-15 signaling blockade, the generation of human CD39+NK cells endowed with a potent degranulation capacity and overexpression of IFNγ and TNFα (111).

Several works have provided through *in vitro* systems and various murine models a clear evidence of A2AR-mediated CD8+T cell exhaustion (39–41, 68, 112). By impairing upstream TCR signaling, A2AR downregulates NOTCH1 pathway, leading to reduced production of IFNγ, PRF1 and GZMB (39–41). Moreover, restricted CD8+T cell proliferative potential has been described in A2AR-deficient mice (36). In this regard, our study aimed to investigate the expression impact of this ADO-receptor on the functional state of human breast tumor-infiltrating CD8+ T cells. Our digital cytometry analysis revealed a very weak expression of effector and cytotoxic molecules, including IFNγ, GZMA, GZMB and PRF1 within CD8+T cells from $A2AR^{high}$ patients. In contrast, an upregulation of negative regulators such as PD-1, CTLA-4, LAG-3 and VISTA was observed within this cell cluster. The inhibitory immune checkpoints included in the analysis are well established markers of CD8+T cell depletion (113–116). Based on these observations, our results provide some evidence of the impact of A2AR on the dysfunctional profile of CD8+T cells in breast cancer. Interestingly, Single-cell data corroborate these findings, showing that A2AR tends to be upregulated on exhausted CD8+ T cells and Tregs. As a matter of fact, recent study repoted that pharmacological and genetic targeting of A2AR substantially enhanced the clinical efficacy of CAR-T-cell therapy by promoting their activation, effector cytokine production and antitumor activity in breast tumor-bearing mice (68). A2AR antagonism has also improved melanoma patient-derived CAR-T-cell activity (68).

Admittedly, the cellular component has a major impact on cancer prognosis. However, molecular factors released by immunosuppressive TME cells and/or promoting their attraction and polarization towards a protumoral and tolerogenic phenotype play a pivotal role and reflect the aggressive tumor behavior. We

therefore studied the association of our gene of interest with a panel of inhibitory immune checkpoints, including PD-1, CTLA-4, BTLA, LAG-3, TIGIT, VTCN-1, PD-L1, CD-47 and GAL-9, as well as immunosuppressive chemokines such as CCL-22, CXCL-13, CCL-5, CCL-17, CCR-4 and CCL-25. Thus, A2AR was found to be positively correlated with these well-known mediators of immune evasion.

Finally, the last part of our work focused on enrichment analysis to provide further evidence for A2AR involvement in breast cancer pathogenesis. Thus, the present study revealed the close association of this inhibitory immune checkpoint with the invasive breast cancer signature as well as the mechanisms of immunosuppression, tumor escape, proliferation, hypoxia, angiogenesis and metastasis. In the light of these findings and to the best of our knowledge, this work is the first to elucidate the clinical and immunological relevance of A2AR in breast cancer. Considering its link to dismal clinical outcomes and unfavorable prognosis, we have provided compelling evidence for the involvement of this ADO-receptor in the aggressiveness of the disease. Furthermore, the present study underlines the link between A2AR and the mechanisms of immunosuppression and tumor development and progression.

Despite significant advances in the management of breast cancer, it remains a major public health problem. Although immunotherapy with current immune checkpoint inhibitors has attracted a great deal of interest, they remain ineffective in breast cancer. It is necessary to explore new potential biomarkers to improve patient prognosis. Accordingly, our work suggests that A2AR could be considered a promising therapeutic target for human breast cancer. Moreover, its use as part of a combination therapy might enhance the efficacy of currently available ICIs.

Data availability statement

The original contributions presented in the study are included in the article/Supplementary Materials, further inquiries can be directed to the corresponding author/s.

Ethics statement

The studies involving humans were approved by the Ethics Committee for Biomedical Research (CERB) of Ibn Rochd University Hospital Center, under the approval code (28/15). The studies were conducted in accordance with the local legislation and institutional requirements. The participants provided their written informed consent to participate in this study.

Author contributions

Study conception and design: BZ and AB. Data acquisition: BZ, IRe, ME, and MK. Technical support: DC, IRe, HB, and DO. Data analysis: BZ, DC, and AB. Data interpretation: BZ, IRa, MK, and AB. Manuscript drafting and editing: BZ and AB. All authors contributed to the article and approved the submitted version.

Funding

The present work was supported by the "PPR1" subvention from the Moroccan Ministry of Higher Education, Research and Innovation. The study was also funded by the "Al-Khawarizmi" grant awarded to Pr AB by the Moroccan Ministry of Higher Education, Research and Innovation and the Digital Development Agency "ADD". A Higher Education National Scholarship was granted to BZ.

Acknowledgments

The authors' sincere gratitude goes to patients who agreed to be included and participate in this study. We would like to thank all medical staff of the Mohamed VI Oncology Center, mainly gynecological surgeons Pr M. Benhessou and Pr M. Ennachit. We also appreciate the contribution of the Department of Pathological Anatomy team, notably R. Sairi, for her assistance in the access and collection of patients' clinicopathological records. Our deepest appreciation is extended to Dr. S. Stitou, from the Pathological Anatomy Laboratory, for her technical guidance and valuable advice.

Conflict of interest

The authors declare that the research was conducted in the absence of any commercial or financial relationships that could be construed as a potential conflict of interest.

Publisher's note

Supplementary material

The Supplementary Material for this article can be found online at: https://www.frontiersin.org/articles/10.3389/fimmu.2023.1201632/full#supplementary-material

SUPPLEMENTARY FIGURE 1
Random (ES) distribution plot of eight statistically significant pathways involved in immunosuppression and tumor evasion. Gene sets related to immune tolerance and immune cell dysfunction are enriched in the A2AR^{High} group. Hallmark, Ontology and Curated gene sets were exploited as molecular signatures. Enriched terms with a false discovery rate (FDR) and (p-nominal) < 0.05 are considered statistically significant. ES: Enrichment Score.

References

1. Sung H, Ferlay J, Siegel RL, Laversanne M, Soerjomataram I, Jemal A, et al. Global cancer statistics 2020: GLOBOCAN estimates of incidence and mortality worldwide for 36 cancers in 185 countries. *CA Cancer J Clin* (2021) 71:209–49. doi: 10.3322/caac.21660

2. Lei S, Zheng R, Zhang S, Wang S, Chen R, Sun K, et al. Global patterns of breast cancer incidence and mortality: A population-based cancer registry data analysis from 2000 to 2020. *Cancer Commun Lond Engl* (2021) 41:1183–94. doi: 10.1002/cac2.12207

3. Waks AG, Winer EP. Breast cancer treatment: A review. *JAMA* (2019) 321:288–300. doi: 10.1001/jama.2018.19323

4. Bianchini G, Balko JM, Mayer IA, Sanders ME, Gianni L. Triple-negative breast cancer: challenges and opportunities of a heterogeneous disease. *Nat Rev Clin Oncol* (2016) 13:674–90. doi: 10.1038/nrclinonc.2016.66

5. Loi S, Giobbie-Hurder A, Gombos A, Bachelot T, Hui R, Curigliano G, et al. Pembrolizumab plus trastuzumab in trastuzumab-resistant, advanced, HER2-positive breast cancer (PANACEA): a single-arm, multicentre, phase 1b–2 trial. *Lancet Oncol* (2019) 20:371–82. doi: 10.1016/S1470-2045(18)30812-X

6. Pestalozzi BC, Zahrieh D, Price KN, Holmberg SB, Lindtner J, Collins J, et al. Identifying breast cancer patients at risk for Central Nervous System (CNS) metastases in trials of the International Breast Cancer Study Group (IBCSG). *Ann Oncol Off J Eur Soc Med Oncol* (2006) 17:935–44. doi: 10.1093/annonc/mdl064

7. Kennecke H, Yerushalmi R, Woods R, Cheang MCU, Voduc D, Speers CH, et al. Metastatic behavior of breast cancer subtypes. *J Clin Oncol Off J Am Soc Clin Oncol* (2010) 28:3271–7. doi: 10.1200/JCO.2009.25.9820

8. Gonzalez-Angulo AM, Litton JK, Broglio KR, Meric-Bernstam F, Rakkhit R, Cardoso F, et al. High risk of recurrence for patients with breast cancer who have human epidermal growth factor receptor 2-positive, node-negative tumors 1 cm or smaller. *J Clin Oncol Off J Am Soc Clin Oncol* (2009) 27:5700–6. doi: 10.1200/JCO.2009.23.2025

9. Cazet AS, Hui MN, Elsworth BL, Wu SZ, Roden D, Chan C-L, et al. Targeting stromal remodeling and cancer stem cell plasticity overcomes chemoresistance in triple negative breast cancer. *Nat Commun* (2018) 9:2897. doi: 10.1038/s41467-018-05220-6

10. Farmer P, Bonnefoi H, Anderle P, Cameron D, Wirapati P, Wirapati P, et al. A stroma-related gene signature predicts resistance to neoadjuvant chemotherapy in breast cancer. *Nat Med* (2009) 15:68–74. doi: 10.1038/nm.1908

11. Kim C, Gao R, Sei E, Brandt R, Hartman J, Hatschek T, et al. Chemoresistance evolution in triple-negative breast cancer delineated by single-cell sequencing. *Cell* (2018) 173:879–93.e13. doi: 10.1016/j.cell.2018.03.041

12. Li X, Lewis MT, Huang J, Gutierrez C, Osborne CK, Wu M-F, et al. Intrinsic resistance of tumorigenic breast cancer cells to chemotherapy. *J Natl Cancer Inst* (2008) 100:672–9. doi: 10.1093/jnci/djn123

13. Su S, Chen J, Yao H, Liu J, Yu S, Lao L, et al. CD10+GPR77+ Cancer-associated fibroblasts promote cancer formation and chemoresistance by sustaining cancer stemness. *Cell* (2018) 172:841–56.e16. doi: 10.1016/j.cell.2018.01.009

14. Berns K, Horlings HM, Hennessy BT, Madiredjo M, Hijmans EM, Beelen K, et al. A functional genetic approach identifies the PI3K pathway as a major determinant of trastuzumab resistance in breast cancer. *Cancer Cell* (2007) 12:395–402. doi: 10.1016/j.ccr.2007.08.030

15. Ikink GJ, Boer M, Bakker ERM, Hilkens J. IRS4 induces mammary tumorigenesis and confers resistance to HER2-targeted therapy through constitutive PI3K/AKT-pathway hyperactivation. *Nat Commun* (2016) 7:13567. doi: 10.1038/ncomms13567

16. Karagiannis GS, Pastoriza JM, Wang Y, Harney AS, Entenberg D, Pignatelli J, et al. Neoadjuvant chemotherapy induces breast cancer metastasis through a TMEM-mediated mechanism. *Sci Transl Med* (2017) 9:eaan0026. doi: 10.1126/scitranslmed.aan0026

17. Plava J, Burikova M, Cihova M, Trnkova L, Smolkova B, Babal P, et al. Chemotherapy-triggered changes in stromal compartment drive tumor invasiveness and progression of breast cancer. *J Exp Clin Cancer Res* (2021) 40:302. doi: 10.1186/s13046-021-02087-2

18. Schmid P, Cortes J, Pusztai L, McArthur H, Kümmel S, Bergh J, et al. Pembrolizumab for early triple-negative breast cancer. *N Engl J Med* (2020) 382:810–21. doi: 10.1056/NEJMoa1910549

19. Schmid P, Adams S, Rugo HS, Schneeweiss A, Barrios CH, Iwata H, et al. Atezolizumab and nab-paclitaxel in advanced triple-negative breast cancer. *N Engl J Med* (2018) 379:2108–21. doi: 10.1056/NEJMoa1809615

20. Eggermont AMM, Chiarion-Sileni V, Grob J-J, Dummer R, Wolchok JD, Schmidt H, et al. Prolonged survival in stage III melanoma with ipilimumab adjuvant therapy. *N Engl J Med* (2016) 375:1845–55. doi: 10.1056/NEJMoa1611299

21. Chen L, Jiang Y-Z, Wu S-Y, Wu J, Di G-H, Liu G-Y, et al. Famitinib with camrelizumab and nab-paclitaxel for advanced immunomodulatory triple-negative breast cancer (FUTURE-C-plus): an open-label, single-arm, phase II trial. *Clin Cancer Res* (2022) 28:2807–17. doi: 10.1158/1078-0432.CCR-21-4313

22. Santa-Maria CA, Kato T, Park J-H, Flaum LE, Jain S, Tellez C, et al. Durvalumab and tremelimumab in metastatic breast cancer (MBC): Immunotherapy and immunopharmacogenomic dynamics. *J Clin Oncol* (2017) 35:3052–2. doi: 10.1200/JCO.2017.35.15_suppl.3052

23. Kim SK, Cho SW. The evasion mechanisms of cancer immunity and drug intervention in the tumor microenvironment. *Front Pharmacol* (2022) 13:868695. doi: 10.3389/fphar.2022.868695

24. Koyama S, Akbay EA, Li YY, Herter-Sprie GS, Buczkowski KA, Richards WG, et al. Adaptive resistance to therapeutic PD-1 blockade is associated with upregulation of alternative immune checkpoints. *Nat Commun* (2016) 7:10501. doi: 10.1038/ncomms10501

25. Shayan G, Srivastava R, Li J, Schmitt N, Kane LP, Ferris RL. Adaptive resistance to anti-PD1 therapy by Tim-3 upregulation is mediated by the PI3K-Akt pathway in head and neck cancer. *Oncoimmunology* (2017) 6:e1261779. doi: 10.1080/2162402X.2016.1261779

26. Huang R-Y, Francois A, McGray AR, Miliotto A, Odunsi K. Compensatory upregulation of PD-1, LAG-3, and CTLA-4 limits the efficacy of single-agent checkpoint blockade in metastatic ovarian cancer. *Oncoimmunology* (2017) 6:e1249561. doi: 10.1080/2162402X.2016.1249561

27. Allard B, Allard D, Buisseret L, Stagg J. The adenosine pathway in immuno-oncology. *Nat Rev Clin Oncol* (2020) 17:611–29. doi: 10.1038/s41571-020-0382-2

28. Lundgren K, Holm C, Landberg G. Hypoxia and breast cancer: prognostic and therapeutic implications. *Cell Mol Life Sci CMLS* (2007) 64:3233–47. doi: 10.1007/s00018-007-7390-6

29. Jarvis LB, Rainbow DB, Coppard V, Howlett SK, Georgieva Z, Davies JL, et al. Therapeutically expanded human regulatory T-cells are super-suppressive due to HIF1A induced expression of CD73. *Commun Biol* (2021) 4:1–14. doi: 10.1038/s42003-021-02721-x

30. Synnestvedt K, Furuta GT, Comerford KM, Louis N, Karhausen J, Eltzschig HK, et al. Ecto-5'-nucleotidase (CD73) regulation by hypoxia-inducible factor-1 mediates permeability changes in intestinal epithelia. *J Clin Invest* (2002) 110:993–1002. doi: 10.1172/JCI15337

31. Eltzschig HK, Köhler D, Eckle T, Kong T, Robson SC, Colgan SP. Central role of Sp1-regulated CD39 in hypoxia/ischemia protection. *Blood* (2009) 113:224–32. doi: 10.1182/blood-2008-06-165746

32. Welihinda A, Ravikumar P, Kaur M, Mechanic J, Yadav S, Kang GJ, et al. Positive allosteric modulation of A2AR alters immune cell responses and ameliorates psoriasis-like dermatitis in mice. *J Invest Dermatol* (2022) 142:624–32.e6. doi: 10.1016/j.jid.2021.07.174

33. Schmiel SE, Kalekar LA, Zhang N, Blankespoor TW, Robinson LJ, Mueller DL. Adenosine 2a receptor signal blockade of murine autoimmune arthritis via inhibition of pathogenic germinal center-follicular helper T cells. *Arthritis Rheumatol Hoboken NJ* (2019) 71:773–83. doi: 10.1002/art.40796

34. Sun C, Wang B, Hao S. Adenosine-A2A receptor pathway in cancer immunotherapy. *Front Immunol* (2022) 13:837230. doi: 10.3389/fimmu.2022.837230

35. Raskovalova T, Lokshin A, Huang X, Su Y, Mandic M, Zarour HM, et al. Inhibition of cytokine production and cytotoxic activity of human antimelanoma specific CD8+ and CD4+ T lymphocytes by adenosine-protein kinase A type I signaling. *Cancer Res* (2007) 67:5949–56. doi: 10.1158/0008-5472.CAN-06-4249

36. Young A, Ngiow SF, Barkauskas DS, Sult E, Hay C, Blake SJ, et al. Co-inhibition of CD73 and A2AR adenosine signaling improves anti-tumor immune responses. *Cancer Cell* (2016) 30:391–403. doi: 10.1016/j.ccell.2016.06.025

37. Ohta A, Ohta A, Madasu M, Kini R, Subramanian M, Goel N, et al. A2A adenosine receptor may allow expansion of T cells lacking effector functions in extracellular adenosine-rich microenvironments. *J Immunol* (2009) 183:5487–93. doi: 10.4049/jimmunol.0901247

38. Cekic C, Day Y-J, Sag D, Linden J. Myeloid expression of adenosine A2A receptor suppresses T and NK cell responses in the solid tumor microenvironment. *Cancer Res* (2014) 74:7250–9. doi: 10.1158/0008-5472.CAN-13-3583

39. Willingham SB, Ho PY, Hotson A, Hill C, Piccione EC, Hsieh J, et al. A2AR antagonism with CPI-444 induces antitumor responses and augments efficacy to anti–PD-(L)1 and anti–CTLA-4 in preclinical models. *Cancer Immunol Res* (2018) 6:1136–49. doi: 10.1158/2326-6066.CIR-18-0056

40. Shi L, Feng M, Du S, Wei X, Song H, Yixin X, et al. Adenosine generated by regulatory T cells induces CD8+ T cell exhaustion in gastric cancer through A2aR pathway. *BioMed Res Int* (2019) 2019:4093214. doi: 10.1155/2019/4093214

41. Sorrentino C, Hossain F, Rodriguez PC, Sierra RA, Pannuti A, Hatfield S, et al. Adenosine A2A receptor stimulation inhibits TCR-induced notch1 activation in CD8+T-cells. *Front Immunol* (2019) 10:162. doi: 10.3389/fimmu.2019.00162

42. Young A, Ngiow SF, Gao Y, Patch A-M, Barkauskas DS, Messaoudene M, et al. A2AR adenosine signaling suppresses natural killer cell maturation in the tumor microenvironment. *Cancer Res* (2018) 78:1003–16. doi: 10.1158/0008-5472.CAN-17-2826

43. Borodovsky A, Barbon CM, Wang Y, Ye M, Prickett L, Chandra D, et al. Small molecule AZD4635 inhibitor of A2AR signaling rescues immune cell function including CD103+ dendritic cells enhancing anti-tumor immunity. *J Immunother Cancer* (2020) 8:e000417. doi: 10.1136/jitc-2019-000417

44. Ingwersen J, Wingerath B, Graf J, Lepka K, Hofrichter M, Schröter F, et al. Dual roles of the adenosine A2a receptor in autoimmune neuroinflammation. *J Neuroinflamm* (2016) 13:48. doi: 10.1186/s12974-016-0512-z

45. Cekic C, Linden J. Purinergic regulation of the immune system. *Nat Rev Immunol* (2016) 16:177–92. doi: 10.1038/nri.2016.4

46. Ohta A, Kini R, Ohta A, Subramanian M, Madasu M, Sitkovsky M. The development and immunosuppressive functions of CD4+ CD25+ FoxP3+ regulatory T cells are under influence of the adenosine-A2A adenosine receptor pathway. *Front Immunol* (2012) 3:190. doi: 10.3389/fimmu.2012.00190

47. Ma S-R, Deng W-W, Liu J-F, Mao L, Yu G-T, Bu L-L, et al. Blockade of adenosine A2A receptor enhances CD8+ T cells response and decreases regulatory T cells in head and neck squamous cell carcinoma. *Mol Cancer* (2017) 16:99. doi: 10.1186/s12943-017-0665-0

48. Shi L, Wu Z, Miao J, Du S, Ai S, Xu E, et al. Adenosine interaction with adenosine receptor A2a promotes gastric cancer metastasis by enhancing PI3K-AKT-mTOR signaling. *Mol Biol Cell* (2019) 30:2527–34. doi: 10.1091/mbc.E19-03-0136

49. Allard B, Cousineau I, Allard D, Buisseret L, Pommey S, Chrobak P, et al. Adenosine A2a receptor promotes lymphangiogenesis and lymph node metastasis. *Oncoimmunology* (2019) 8:1601481. doi: 10.1080/2162402X.2019.1601481

50. Ahmad A, Ahmad S, Glover L, Miller SM, Shannon JM, Guo X, et al. Adenosine A2A receptor is a unique angiogenic target of HIF-2α in pulmonary endothelial cells. *Proc Natl Acad Sci* (2009) 106:10684–9. doi: 10.1073/pnas.0901326106

51. Liu Z, Yan S, Wang J, Xu Y, Wang Y, Zhang S, et al. Endothelial adenosine A2a receptor-mediated glycolysis is essential for pathological retinal angiogenesis. *Nat Commun* (2017) 8:584. doi: 10.1038/s41467-017-00551-2

52. Kamai T, Kijima T, Tsuzuki T, Nukui A, Abe H, Arai K, et al. Increased expression of adenosine 2A receptors in metastatic renal cell carcinoma is associated with poorer response to anti-vascular endothelial growth factor agents and anti-PD-1/Anti-CTLA4 antibodies and shorter survival. *Cancer Immunol Immunother* (2021) 70:2009–21. doi: 10.1007/s00262-020-02843-x

53. Wu Z, Yang L, Shi L, Song H, Shi P, Yang T, et al. Prognostic impact of adenosine receptor 2 (A2aR) and programmed cell death ligand 1 (PD-L1) expression in colorectal cancer. *BioMed Res Int* (2019) 2019:8014627. doi: 10.1155/2019/8014627

54. Masoumi E, Jafarzadeh L, Mirzaei HR, Alishah K, Fallah-Mehrjardi K, Rostamian H, et al. Genetic and pharmacological targeting of A2a receptor improves function of anti-mesothelin CAR T cells. *J Exp Clin Cancer Res CR* (2020) 39:49. doi: 10.1186/s13046-020-01546-6

55. Giuffrida L, Sek K, Henderson MA, Lai J, Chen AXY, Meyran D, et al. CRISPR/Cas9 mediated deletion of the adenosine A2A receptor enhances CAR T cell efficacy. *Nat Commun* (2021) 12:3236. doi: 10.1038/s41467-021-23331-5

56. Fong L, Hotson A, Powderly JD, Sznol M, Heist RS, Choueiri TK, et al. Adenosine 2A receptor blockade as an immunotherapy for treatment-refractory renal cell cancer. *Cancer Discovery* (2020) 10:40–53. doi: 10.1158/2159-8290.CD-19-0980

57. Curtis C, Shah SP, Chin S-F, Turashvili G, Rueda OM, Dunning MJ, et al. The genomic and transcriptomic architecture of 2,000 breast tumours reveals novel subgroups. *Nature* (2012) 486:346–52. doi: 10.1038/nature10983

58. Yerushalmi R, Woods R, Ravdin PM, Hayes MM, Gelmon KA. Ki67 in breast cancer: prognostic and predictive potential. *Lancet Oncol* (2010) 11:174–83. doi: 10.1016/S1470-2045(09)70262-1

59. Prat A, Parker JS, Karginova O, Fan C, Livasy C, Herschkowitz JI, et al. Phenotypic and molecular characterization of the claudin-low intrinsic subtype of breast cancer. *Breast Cancer Res* (2010) 12:R68. doi: 10.1186/bcr2635

60. Pommier RM, Sanlaville A, Tonon L, Kielbassa J, Thomas E, Ferrari A, et al. Comprehensive characterization of claudin-low breast tumors reflects the impact of the cell-of-origin on cancer evolution. *Nat Commun* (2020) 11:3431. doi: 10.1038/s41467-020-17249-7

61. Chen DS, Mellman I. Elements of cancer immunity and the cancer–immune set point. *Nature* (2017) 541:321–30. doi: 10.1038/nature21349

62. Chraa D, Naim A, Olive D, Badou A. T lymphocyte subsets in cancer immunity: Friends or foes. *J Leukoc Biol* (2019) 105:243–55. doi: 10.1002/JLB.MR0318-097R

63. Gil Del Alcazar CR, Huh SJ, Ekram MB, Trinh A, Liu LL, Beca F, et al. Immune escape in breast cancer during *in situ* to invasive carcinoma transition. *Cancer Discovery* (2017) 7:1098–115. doi: 10.1158/2159-8290.CD-17-0222

64. Kone A, Ait Ssi S, Sahraoui S, Badou A. BTN3A: A promising immune checkpoint for cancer prognosis and treatment. *Int J Mol Sci* (2022) 23:13424. doi: 10.3390/ijms232113424

65. Gaynor N, Crown J, Collins DM. Immune checkpoint inhibitors: Key trials and an emerging role in breast cancer. *Semin Cancer Biol* (2022) 79:44–57. doi: 10.1016/j.semcancer.2020.06.016

66. Narayan P, Wahby S, Gao JJ, Amiri-Kordestani L, Ibrahim A, Bloomquist E, et al. FDA approval summary: atezolizumab plus paclitaxel protein-bound for the treatment of patients with advanced or metastatic TNBC whose tumors express PD-L1. *Clin Cancer Res* (2020) 26:2284–9. doi: 10.1158/1078-0432.CCR-19-3545

67. Beavis PA, Milenkovski N, Henderson MA, John LB, Allard B, Loi S, et al. Adenosine receptor 2A blockade increases the efficacy of anti–PD-1 through enhanced antitumor T-cell responses. *Cancer Immunol Res* (2015) 3:506–17. doi: 10.1158/2326-6066.CIR-14-0211

68. Beavis PA, Henderson MA, Giuffrida L, Mills JK, Sek K, Cross RS, et al. Targeting the adenosine 2A receptor enhances chimeric antigen receptor T cell efficacy. *J Clin Invest* (2017) 127:929–41. doi: 10.1172/JCI89455

69. Qin S, Xu L, Yi M, Yu S, Wu K, Luo S. Novel immune checkpoint targets: moving beyond PD-1 and CTLA-4. *Mol Cancer* (2019) 18:155. doi: 10.1186/s12943-019-1091-2

70. Zhang Y, Zhang H, Wang M, Schmid T, Xin Z, Kozhuharova L, et al. Hypoxia in breast cancer-scientific translation to therapeutic and diagnostic clinical applications. *Front Oncol* (2021) 11:652266. doi: 10.3389/fonc.2021.652266

71. Vijayan D, Young A, Teng MWL, Smyth MJ. Targeting immunosuppressive adenosine in cancer. *Nat Rev Cancer* (2017) 17:709–24. doi: 10.1038/nrc.2017.86

72. De Velasco MA, Kura Y, Sako N, Ando N, Sakai K, Schuller A, et al. Abstract 1568: A2aR inhibition enhances the antitumor activity of CTLA4 blockade in mouse Pten-deficient prostate cancer. *Cancer Res* (2021) 81:1568. doi: 10.1158/1538-7445.AM2021-1568

73. Ho P, Hsieh M-Y, Hotson A, Miller R, McCaffery I, Willingham S. Abstract 5598: Adenosine signaling through A2AR limits the efficacy of anti-CTLA4 and chemotherapy in preclinical models. *Cancer Res* (2017) 77:5598. doi: 10.1158/1538-7445.AM2017-5598

74. Allard B, Pommey S, Smyth MJ, Stagg J. Targeting CD73 enhances the antitumor activity of anti-PD-1 and anti-CTLA-4 mAbs. *Clin Cancer Res* (2013) 19:5626–35. doi: 10.1158/1078-0432.CCR-13-0545

75. Zhang T, Liu H, Jiao L, Zhang Z, He J, Li L, et al. Genetic characteristics involving the PD-1/PD-L1/L2 and CD73/A2aR axes and the immunosuppressive microenvironment in DLBCL. *J Immunother Cancer* (2022) 10:e004114. doi: 10.1136/jitc-2021-004114

76. Willingham S, Hotson A, Ho P, Choy C, Laport G, McCaffery I, et al. Abstract PR04: CPI-444: A potent and selective inhibitor of A2AR induces antitumor responses alone and in combination with anti-PD-L1 in preclinical and clinical studies. *Cancer Immunol Res* (2016) 4:PR04. doi: 10.1158/2326-6066.IMM2016-PR04

77. Fong L, Forde PM, Powderly JD, Goldman JW, Nemunaitis JJ, Luke JJ, et al. Safety and clinical activity of adenosine A2a receptor (A2aR) antagonist, CPI-444, in anti-PD1/PDL1 treatment-refractory renal cell (RCC) and non-small cell lung cancer (NSCLC) patients. *J Clin Oncol* (2017) 35:3004–4. doi: 10.1200/JCO.2017.35.15_suppl.3004

78. Wang X, Zhang T, Liu H, Zhang S, Li L, Qiu L, et al. Immune checkpoints involving the PD-1/PD-L1/L2 and CD73/A2aR axes and the immunosuppressive microenvironment in DLBCL. *Blood* (2022) 140:6458–9. doi: 10.1182/blood-2022-165060

79. Cekic C, Linden J. Adenosine A2A receptors intrinsically regulate CD8+ T cells in the tumor microenvironment. *Cancer Res* (2014) 74:7239–49. doi: 10.1158/0008-5472.CAN-13-3581

80. Leone RD, Sun I-M, Oh M-H, Sun I-H, Wen J, Englert J, et al. Inhibition of the adenosine A2a receptor modulates expression of T cell coinhibitory receptors and improves effector function for enhanced checkpoint blockade and ACT in murine cancer models. *Cancer Immunol Immunother* (2018) 67:1271–84. doi: 10.1007/s00262-018-2186-0

81. Curran MA, Montalvo W, Yagita H, Allison JP. PD-1 and CTLA-4 combination blockade expands infiltrating T cells and reduces regulatory T and myeloid cells within B16 melanoma tumors. *Proc Natl Acad Sci U.S.A.* (2010) 107:4275–80. doi: 10.1073/pnas.0915174107

82. Ait Ssi S, Chraa D, El Azhary K, Sahraoui S, Olive D, Badou A. Prognostic gene expression signature in patients with distinct glioma grades. *Front Immunol* (2021) 12:685213. doi: 10.3389/fimmu.2021.685213

83. Gong Z, Zhang J, Guo W. Tumor purity as a prognosis and immunotherapy relevant feature in gastric cancer. *Cancer Med* (2020) 9:9052–63. doi: 10.1002/cam4.3505

84. Lou S, Zhang J, Yin X, Zhang Y, Fang T, Wang Y, et al. Comprehensive characterization of tumor purity and its clinical implications in gastric cancer. *Front Cell Dev Biol* (2022) 9:782529. doi: 10.3389/fcell.2021.782529

85. Zhang S, Zhang E, Long J, Hu Z, Peng J, Liu L, et al. Immune infiltration in renal cell carcinoma. *Cancer Sci* (2019) 110:1564–72. doi: 10.1111/cas.13996

86. Liu X, Wu S, Yang Y, Zhao M, Zhu G, Hou Z. The prognostic landscape of tumor-infiltrating immune cell and immunomodulators in lung cancer. *BioMed Pharmacother* (2017) 95:55–61. doi: 10.1016/j.biopha.2017.08.003

87. Ali HR, Chlon L, Pharoah PDP, Markowetz F, Caldas C. Patterns of immune infiltration in breast cancer and their clinical implications: A gene-expression-based retrospective study. *PLoS Med* (2016) 13:e1002194. doi: 10.1371/journal.pmed.1002194

88. Bense RD, Sotiriou C, Piccart-Gebhart MJ, Haanen JBAG, van Vugt MATM, de Vries EGE, et al. Relevance of tumor-infiltrating immune cell composition and functionality for disease outcome in breast cancer. *J Natl Cancer Inst* (2017) 109:djw192. doi: 10.1093/jnci/djw192

89. Zhang S-C, Hu Z-Q, Long J-H, Zhu G-M, Wang Y, Jia Y, et al. Clinical implications of tumor-infiltrating immune cells in breast cancer. *J Cancer* (2019) 10:6175–84. doi: 10.7150/jca.35901

90. Chen Y, Zhang S, Wang Q, Zhang X. Tumor-recruited M2 macrophages promote gastric and breast cancer metastasis via M2 macrophage-secreted CHI3L1 protein. *J Hematol OncolJ Hematol Oncol* (2017) 10:36. doi: 10.1186/s13045-017-0408-0

91. Ferrante CJ, Pinhal-Enfield G, Elson G, Cronstein BN, Hasko G, Outram S, et al. The adenosine-dependent angiogenic switch of macrophages to an M2-like phenotype is independent of Interleukin-4 receptor alpha (IL4Rα) signaling. *Inflammation* (2013) 36:921–31. doi: 10.1007/s10753-013-9621-3

92. Núñez NG, Tosello Boari J, Ramos RN, Richer W, Cagnard N, Anderfuhren CD, et al. Tumor invasion in draining lymph nodes is associated with Treg accumulation in breast cancer patients. *Nat Commun* (2020) 11:3272. doi: 10.1038/s41467-020-17046-2

93. Shou J, Zhang Z, Lai Y, Chen Z, Huang J. Worse outcome in breast cancer with higher tumor-infiltrating FOXP3+ Tregs : a systematic review and meta-analysis. *BMC Cancer* (2016) 16:687. doi: 10.1186/s12885-016-2732-0

94. Oshi M, Asaoka M, Tokumaru Y, Angarita FA, Yan L, Matsuyama R, et al. Abundance of regulatory T cell (Treg) as a predictive biomarker for neoadjuvant chemotherapy in triple-negative breast cancer. *Cancers* (2020) 12:3038. doi: 10.3390/cancers12103038

95. Taylor NA, Vick SC, Iglesia MD, Brickey WJ, Midkiff BR, McKinnon KP, et al. Treg depletion potentiates checkpoint inhibition in claudin-low breast cancer. *J Clin Invest* (2017) 127:3472–83. doi: 10.1172/JCI90499

96. Muhammad F, Wang D, Montieth A, Lee S, Preble J, Foster CS, et al. PD-1+ melanocortin receptor dependent-Treg cells prevent autoimmune disease. *Sci Rep* (2019) 9:16941. doi: 10.1038/s41598-019-53297-w

97. Sitkovsky MV. T regulatory cells: hypoxia-adenosinergic suppression and re-direction of the immune response. *Trends Immunol* (2009) 30:102–8. doi: 10.1016/j.it.2008.12.002

98. Jenabian M-A, Seddiki N, Yatim A, Carriere M, Hulin A, Younas M, et al. Regulatory T cells negatively affect IL-2 production of effector T cells through CD39/adenosine pathway in HIV infection. *PloS Pathog* (2013) 9:e1003319. doi: 10.1371/journal.ppat.1003319

99. Zarek PE, Huang C-T, Lutz ER, Kowalski J, Horton MR, Linden J, et al. A2A receptor signaling promotes peripheral tolerance by inducing T-cell anergy and the generation of adaptive regulatory T cells. *Blood* (2008) 111:251–9. doi: 10.1182/blood-2007-03-081646

100. Kinsey GR, Huang L, Jaworska K, Khutsishvili K, Becker DA, Ye H, et al. Autocrine adenosine signaling promotes regulatory T cell–mediated renal protection. *J Am Soc Nephrol JASN* (2012) 23:1528–37. doi: 10.1681/ASN.2012010070

101. Ning Z-K, Hu C-G, Huang C, Liu J, Zhou T-C, Zong Z. Molecular subtypes and CD4+ Memory T cell-based signature associated with clinical outcomes in gastric cancer. *Front Oncol* (2021) 10:626912. doi: 10.3389/fonc.2020.626912

102. Liu R, Yang F, Yin J-Y, Liu Y-Z, Zhang W, Zhou H-H. Influence of tumor immune infiltration on immune checkpoint inhibitor therapeutic efficacy: A computational retrospective study. *Front Immunol* (2021) 12:685370. doi: 10.3389/fimmu.2021.685370

103. Wang W-Q, Zhang L, Yang F, Zhou H-H, Zhang W, Zou Y, et al. Patterns of immune infiltration and survival in endocrine therapy-treated ER-positive breast cancer: A computational study of 1900 patients. *BioMed Pharmacother* (2022) 155:113787. doi: 10.1016/j.biopha.2022.113787

104. Mahmoud SMA, Paish EC, Powe DG, Macmillan RD, Grainge MJ, Lee AHS, et al. Tumor-infiltrating CD8+ lymphocytes predict clinical outcome in breast cancer. *J Clin Oncol Off J Am Soc Clin Oncol* (2011) 29:1949–55. doi: 10.1200/JCO.2010.30.5037

105. Hagerling C, Gonzalez H, Salari K, Wang C-Y, Lin C, Robles I, et al. Immune effector monocyte-neutrophil cooperation induced by the primary tumor prevents metastatic progression of breast cancer. *Proc Natl Acad Sci U.S.A.* (2019) 116:21704–14. doi: 10.1073/pnas.1907660116

106. Muntasell A, Rojo F, Servitja S, Rubio-Perez C, Cabo M, Tamborero D, et al. NK cell infiltrates and HLA class I expression in primary HER2+ Breast cancer predict and uncouple pathological response and disease-free survival. *Clin Cancer Res* (2019) 25:1535–45. doi: 10.1158/1078-0432.CCR-18-2365

107. Gu-Trantien C, Loi S, Garaud S, Equeter C, Libin M, de Wind A, et al. $CD4^+$ follicular helper T cell infiltration predicts breast cancer survival. *J Clin Invest* (2013) 123:2873–92. doi: 10.1172/JCI67428

108. Kini Bailur J, Gueckel B, Pawelec G. Prognostic impact of high levels of circulating plasmacytoid dendritic cells in breast cancer. *J Transl Med* (2016) 14:151. doi: 10.1186/s12967-016-0905-x

109. Ascierto ML, Idowu MO, Zhao Y, Khalak H, Payne KK, Wang X-Y, et al. Molecular signatures mostly associated with NK cells are predictive of relapse free survival in breast cancer patients. *J Transl Med* (2013) 11:145. doi: 10.1186/1479-5876-11-145

110. *Blockade of A2A receptors potently suppresses the metastasis of CD73+ tumors*. Available at: https://pubmed.ncbi.nlm.nih.gov/23964122/ (Accessed January 10, 2023).

111. Kang G, Zhao X, Sun J, Cheng C, Wang C, Tao L, et al. A2AR limits IL-15-induced generation of CD39+ NK cells with high cytotoxicity. *Int Immunopharmacol* (2023) 114:109567. doi: 10.1016/j.intimp.2022.109567

112. Borodovsky A, Wang Y, Ye M, Shaw JC, Sachsenmeier KF, Deng N, et al. Abstract 5580: Preclinical pharmacodynamics and antitumor activity of AZD4635, a novel adenosine 2A receptor inhibitor that reverses adenosine mediated T cell suppression. *Cancer Res* (2017) 77:5580. doi: 10.1158/1538-7445.AM2017-5580

113. Hashimoto M, Kamphorst AO, Im SJ, Kissick HT, Pillai RN, RaMalingam SS, et al. CD8 T cell exhaustion in chronic infection and cancer: opportunities for interventions. *Annu Rev Med* (2018) 69:301–18. doi: 10.1146/annurev-med-012017-043208

114. Ghouzlani A, Lakhdar A, Rafii S, Karkouri M, Badou A. The immune checkpoint VISTA exhibits high expression levels in human gliomas and associates with a poor prognosis. *Sci Rep* (2021) 11:21504. doi: 10.1038/s41598-021-00835-0

115. Ghouzlani A, Rafii S, Karkouri M, Lakhdar A, Badou A. The promising igSF11 immune checkpoint is highly expressed in advanced human gliomas and associates to poor prognosis. *Front Oncol* (2021) 10:608609. doi: 10.3389/fonc.2020.608609

116. Le Mercier I, Chen W, Lines JL, Day M, Li J, Sergent P, et al. VISTA regulates the development of protective antitumor immunity. *Cancer Res* (2014) 74:1933–44. doi: 10.1158/0008-5472.CAN-13-1506

Frontiers in Immunology

Explores novel approaches and diagnoses to treat immune disorders.

The official journal of the International Union of Immunological Societies (IUIS) and the most cited in its field, leading the way for research across basic, translational and clinical immunology.

Discover the latest Research Topics

See more →

Frontiers

Avenue du Tribunal-Fédéral 34
1005 Lausanne, Switzerland
frontiersin.org

Contact us

+41 (0)21 510 17 00
frontiersin.org/about/contact